Miguel Curto Rubio

Functional genomic approaches, proteomics and transcriptomics, to study legume responses to phytopathogenic fungi

Estudios de la interacción leguminosas-hongos fitopatógenos mediante una aproximación de genómica funcional (proteómica y transcriptómica)

ETSIAM

2014

TITULO: *Functional genomic approaches, proteomics and transcriptomics, to study legume responses to phytopathogenic fungi*

AUTOR: *Miguel Curto Rubio*

Campus de Rabanales
Ctra. Nacional IV, Km. 396 A
14071 Córdoba

www.uco.es/publicaciones
publicaciones@uco.es

TÍTULO DE LA TESIS: Estudios de la interacción leguminosas-hongos fitopatógenos mediante una aproximación de genómica funcional (proteómica y transcriptómica).

DOCTORANDO/A: Miguel Curto Rubio.

INFORME RAZONADO DEL/DE LOS DIRECTOR/ES DE LA TESIS

(se hará mención a la evolución y desarrollo de la tesis, así como a trabajos y publicaciones derivados de la misma).

Jesús V. Jorrín Novo, Catedrático del Departamento de Bioquímica y Biología Molecular de la Universidad de Córdoba.

Diego Rubiales Olmedo, Profesor de Investigación del Instituto de Agricultura Sostenible del Consejo Superior de Investigaciones Científicas.

Ana M. Maldonado Alconada, Profesora Titular del Departamento de Bioquímica y Biología Molecular de la Universidad de Córdoba.

INFORMAN: de que el trabajo titulado “Estudios de la interacción leguminosas-hongos fitopatógenos mediante una aproximación de genómica funcional (proteómica y transcriptómica); Functional genomic approaches, proteomics and transcriptomics, to study legume responses to phytopathogenic fungi”, realizado bajo nuestra dirección por D. Miguel Curto Rubio, reúne los requisitos exigidos para la obtención del grado de Doctor con mención internacional, así como para ser presentada bajo la modalidad de tesis como compendio de publicaciones a la que se refieren las normas reguladoras de los estudios de doctorado adaptadas al EEES de la Universidad de Córdoba.

Por todo ello, se autoriza la presentación de la tesis doctoral.

Córdoba, 27 de Octubre de 2014

Firma del/de los director/es

Fdo.: Dr. Jesús V. Jorrín Novo

Fdo.: Dr. Diego Rubiales Olmedo

Fdo.: Dra. Ana M. Maldonado Alconada

Financiación personal y de investigación

Este trabajo ha sido realizado gracias a la financiación de los proyectos de investigación y programas siguientes:

- Beca predoctoral de formación personal investigador (FPI), asociada al proyecto de investigación AGL2002-03248.

- Proyecto: "Aplicación de marcadores moleculares en la mejora genética del guisante por resistencia a enfermedades", AGL2002-03248.

- Proyecto: "Grain Legumes: New strategies for grain legume research", FP6-2002-FOOD-1-506223.

- Proyecto: "Mejora de guisantes, almortas y titarros por resistencia a estreses bióticos y abióticos", AGL2008-01239.

- Proyecto: "Identificación y caracterización de fuentes de resistencia a estreses bióticos y abióticos en guisante", AGL2011-22524.

Agradecimientos

Quiero dar mi agradecimiento a todos aquellos que han contribuido en la realización de esta tesis doctoral:

A mi director, Diego Rubiales Olmedo, por ofrecerme la oportunidad de realizar esta tesis y ayudarme en todo lo que he necesitado.

A mi director, Jesús V. Jorrín Novo, por haberme abierto las puertas de su grupo y haberme ofrecido su ayuda siempre que la he necesitado.

A mi directora, Ana María Maldonado Alconada, por su ayuda en los estudios de proteómica y la redacción de esta tesis doctoral.

A todos los coautores de los artículos que se incluyen en esta tesis.

A todos los compañeros que he conocido durante mi tesis, que han sido muchos, los cuales han contribuido en mi formación como investigador.

Esta tesis se la dedico a mis padres, en especial a mi madre que con su ejemplo de lucha y sacrificio me ha enseñado que no hay nada imposible, y a mi novia Susana Vega Chacón por su amor incondicional y apoyo constante.

Summary

The objectives pursued in this PhD thesis are to study the legume responses to phytopathogenic fungi by using a functional genomics approach (transcriptomics and proteomics). The pea (*Pisum sativum*) and the model legume *Medicago truncatula* were chosen to study their stress responses to *Erysiphe pisi* and *Mycosphaerella pinodes* pathogens. The pea crop constitutes an important source of protein for human consumption, being one of the most grown grain legume in the world, meanwhile *M. truncatula* is an important forage legume which is being used as a model plant for use in molecular and classical genetic studies. Moreover, within the phytopathogenic fungi, powdery mildew and ascochyta blight are one the most plant pathogenic fungi that seriously constrain crop production worldwide.

Within the functional genomics approaches carried out to study the defense mechanisms in legumes to phytopathogenic fungi infection, a differential expression proteomic approach was carried out in order to unveil which resistance mechanisms are involving in the defense response of the pea to *E. pisi* and *M. pinodes* infections. The results obtained from the application of this approach in both studies are presented. The changes observed reflect a metabolic adjustment performed by the pea in response to phytopathogen fungi infection.

To go deeper into the knowledge of the defence mechanism related to the response to *E. pisi* infection in legumes, two different transcriptomics approaches were performed using the model legume *M. truncatula*. Thus, *M. truncatula* - *E. pisi* pathosystem was analyzed by using microarray and quantitative real-time PCR platforms, respectively. These results revealed a wide variety of mechanisms and pathways involved in *M. truncatula* in response to *E. pisi* infection, including an important number of genes belonging to diverse functional groups, which will help to develop new genetic tools in the breeding program in legumes.

Resumen

Los objetivos planteados en esta tesis doctoral son analizar las respuestas de las leguminosas a la infección de hongos fitopatógenos mediante el uso de una aproximación de genómica funcional (transcriptómica y proteómica). El guisante (*Pisum sativum*) y la leguminosa modelo *Medicago truncatula* fueron elegidas para estudiar sus respuestas de estrés a los patógenos *Erysiphe pisi* y *Mycosphaerella pinodes*.

Dentro de las aproximaciones de genómica funcional llevadas a cabo para estudiar los mecanismos de defensa de las leguminosas a la infección de hongos fitopatógenos, una aproximación de proteómica diferencial fue llevada a cabo con el objetivo de revelar cuáles son los mecanismos de resistencia implicados en las respuestas de defensa del guisante a la infección de *E. pisi* y *M. pinodes*. Los resultados obtenidos de la aplicación de esta aproximación en ambos estudios son presentados. Los cambios observados reflejan un ajuste metabólico del guisante en respuesta a la infección de estos hongos fitopatógenos.

Para profundizar en el conocimiento de los mecanismos de defensa de las leguminosas en respuesta a la infección de *E. pisi*, dos aproximaciones transcriptómicas diferentes fueron realizadas usando la leguminosa modelo *M. truncatula*. En consecuencia, el patosistema *M. truncatula* - *E. pisi* fue analizado mediante dos plataformas, microarray y PCR cuantitativa en tiempo real, respectivamente. Estos resultados revelaron una amplia variedad de mecanismos y rutas implicadas en las respuestas de defensa de *M. truncatula* en respuesta a la infección de *E. pisi*, incluyendo un importante número de genes pertenecientes a diversos grupos funcionales, los cuales ayudaran en el desarrollo de nuevas herramientas genéticas en los programas de mejora vegetal en leguminosas.

Table of contents

1. Legumes

Legume family (*Fabaceae* or *Leguminosae*) is the third largest family of higher plants and second in agricultural importance (Doyle 2001; Lewis et al. 2005). It includes more than 650 genera and 18000 species ranging from herbs to trees (Doyle and Luckow 2003; Lewis et al. 2005). They are particularly interesting to fix atmospheric nitrogen through symbiotic relationships with rhizobial soil bacteria (Garg and Geetanjali 2009; Graham and Vance 2003; Udvardi and Poole 2013) playing a key role in crop rotation (Fig. 1). Among them, the subfamily *Papilionaceae* include cultivated species that provide the largest single source of vegetable protein in human diets and livestock feed (Evers 2011; Graham and Vance 2003; Rochon et al. 2004; Siddique et al. 2012).

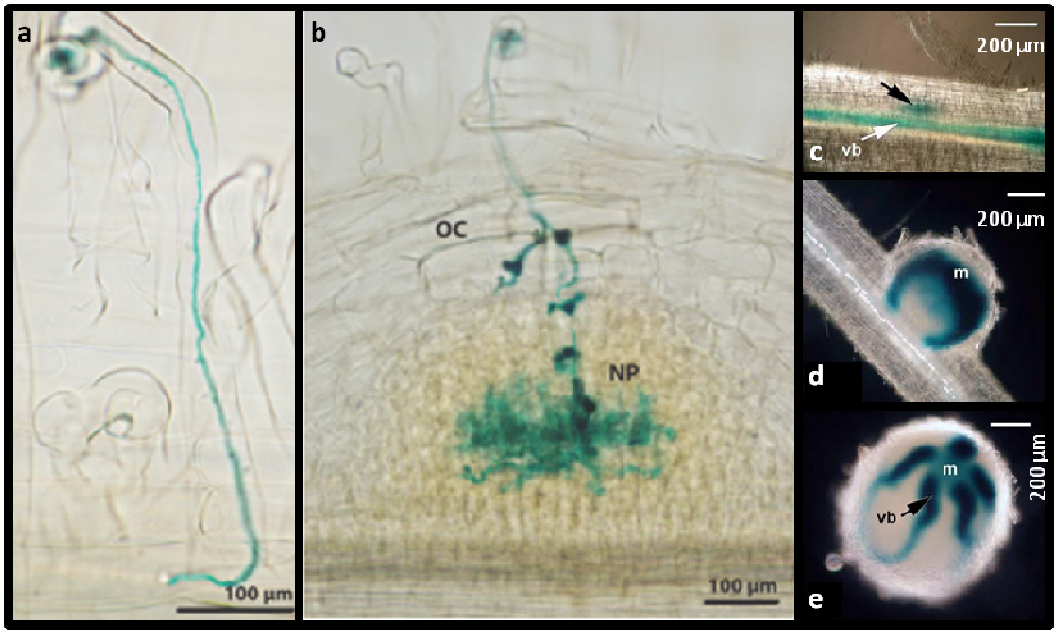

Figure 1. Root infection structures containing rhizobia. **(a)** Curled epidermal root hair with infection thread containing *LacZ*-expressing *rhizobia*. Histochemical X-gal staining highlights *rhizobia* in blue. **(b)** Infection threads traversing the outer cortical cell layers (OC) and ramifying through dividing cortical cells of a developing *Medicago* nodule; NP: nodule primordium. **(c)** Nodule primordium (black arrow) with *R. leguminosarum* bv. *viciae*. The white arrow points to a vascular bundle (vb); **(d)** Emergent nodule with GUS staining in the nodule meristem (m) and young vascular bundles; **(e)** Staining is apparent in the nodule meristem (m) and most recently developed vascular bundles (vb) (black arrow), (modified from Udvardi et. al, 2013 and Schwartz et. al, 2013).

Among them, cool season grain legumes (faba bean, chickpea, pea, lentil and lupin) play an important role in farming systems worldwide (Kelley et al. 1997). However, a wide number of biotic and abiotic stresses are severely affecting the yield and seed quality of these crops. Grain legumes are challenged by many pathogens (fungi, bacteria, nematodes, viruses, parasitic plants, insects), causing important economic losses (Fuchs et al. 2014; Rubiales et al. 2014).

Genetic resistance is one of the most desirable control method since it is more cost effective and environment friendly than the use of chemicals. Thus, many resistance sources (Sillero et al. 2006; Tivoli et al. 2006a) have been found in different grain legumes including pea (*Pisum sativum*) (Barilli et al. 2014; Castillejo et al. 2010a; Castillejo et al. 2011; Fondevilla et al. 2011; Fondevilla and Rubiales 2012; Fondevilla et al. 2008) and barrel medic (*Medicago truncatula*) (Ameline-Torregrosa et al. 2008; Castillejo et al. 2010a; Castillejo et al. 2009; Die et al. 2007; Dita et al. 2009; Foster-Hartnett et al. 2007; Lozano-Baena et al. 2007; Rubiales and Moral 2004). Several transcriptomics approaches, such as microarray and qPCR (Barilli et al. 2014; Curto et al. 2014; Fondevilla et al. 2011; Fondevilla et al. 2014), as well as proteomics (Castillejo et al. 2010a; Castillejo et al. 2010b; Curto et al. 2006) have been successful applied to these crops. These biotechnology approaches have increased the knowledge of the target species and the mechanism underlying resistance to these pathogens. However, molecular mechanisms involved in the legume defense against their pathogens are poorly understood. Biotechnology tools and specially the high throughput "omic" technologies promising strategies for understanding the molecular genetic basis of stress resistance, which is an important bottleneck for molecular breeding (Dita et al. 2006).

1.1. Pea (*Pisum sativum*)

Pea (*Pisum sativum* L.) plays a critical ecological role because it contributes to the development of low-input farming systems by fixing atmospheric nitrogen. Their seeds are rich in protein (around 25 %), starch (50%), sugar and others compounds such as fiber, mineral and vitamins (Bastianelli et al. 1998; Rubiales et al. 2011a; Smýkal et al. 2012). Pea was used in Mendel`s discovery of the laws inheritance, making in the

foundation of modern plant genetics (Bateson 1909) as well as model for experimental morphology and physiology (Tar'an et al. 2005). Spite of the pea genome size, several genomic resources such as, BAC libraries and transcriptome and proteome datasets already exist (Smýkal et al. 2012). Thanks to this knowledge several marker assisted selection programs have allowed to increase the precision and shortening the breeding cycle. The new "omic" methodologies are useful tools for the development of breeding tools for improved pea genotypes that are sustainable under current and future farming systems.

1.1.1. Origin and botanical description

Pea is considered one of the first domesticated plants in the world, together with chickpea, lentil, grass pea and several cereal species (Zohary and Hopf 2000). Prior to cultivation, pea together with vetches, vetchlings and chickpeas was part of the everyday diet of hunter-gatherers at the end of the last ice age in the Middle East and Europe (Smýkal et al. 2012). Hence, pea is one of the crops that played a significant role in the 'agricultural revolution' of the post-glacial Europe (Mikić et al. 2014; Smýkal et al. 2012). The earliest evidences of the use of pea for human consumption are the fossilized starch grains in calculus of the Neanderthal skeletons in Iraq about 46,000 years ago (Fig. 2) (Mikić et al. 2014). The archeological evidences establishes that pea is one of the founder grain crops of south-west-Asian Neolithic agriculture being a consistent crop in Neolithic and bronze ages. The domesticated pea belongs to *Pisum* genus, restricted, in the wild, to the Mediterranean basin and south-west Asia (Zohary et al. 2013). During centuries of selection and breeding thousands of pea varieties were developed and these are maintained in numerous germplasm collections worldwide (Smýkal et al. 2011). The range of wild representatives of *P. sativum* extends from Iran and Turkmenistan through Anterior Asia, northern Africa and southern Europe (Smýkal et al. 2012). However, due to the early cultivation of pea it is difficult to identify the precise location of the center of its diversity. The genus *Pisum* contains the wild species *P. fulvum* found in Jordan, Syria, Lebanon and Israel; the cultivated species *P. abyssinicum* from Yemen and Ethiopia, which was likely domesticated independently of *P. sativum*; and a large and loose aggregate of both wild (*P. sativum* subsp. *elatius*) and cultivated forms that comprise the species *P. sativum* in a broad sense (Smýkal et al. 2012).

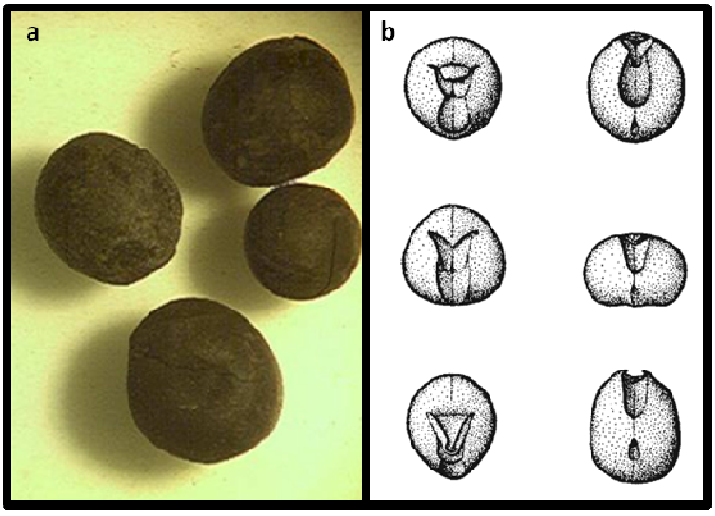

Figure 2. (a) Charred pea seed from Iron Age founded in southern Serbia. **(b)** Charred seed of domesticated pea, *Pisum sativum*, cotyledons only, no seed coat survived charring, late Neolithic (Dimini, Greece) (modified from Mikić et al, 2014 and Zohary et. al, 2013).

Pisum sativum is annual, diploid (2n=14) and mainly self-pollinated plants (Smýkal et al. 2011). Pea leaf type could be conventional, semi-leafless and leafless (Davies et al. 1985) and their size in most cases increases up to the first node bearing the first flower (Fig. 3). Stipules are large, leaf-like and up to 10 cm long and their inflorescence is a raceme arising from the axil of the leaf (Fig. 3). Corolla show color from white to purple; pods swollen or compressed, short-stalked, straight or curved, 4-15 cm long, 1.5-2.5 cm wide, 2-10 seeded, 2-valved, dehiscent on both sutures (Duke 1981; Gritton 1980). The node at which the first flower emerges is characteristic of a given variety; in temperate regions the number of nodes at which the first flower emerges is reported to vary from 4 in the earliest to about 25 in late maturing types under field conditions (Gritton 1980). Flowers borne on the same peduncle produce pods that mature at different times, the youngest being at the tip. On a whole plant basis, flowering is sequential and upwards from node to node. The main root, taproot, has many lateral branches and sub-branches, which allowed establishing the symbiotic nitrogen-fixing bacterium *Rhizobium leguminosarum* forming nodules (Fig. 1). Moreover, their stems are usually weak and internode length show height ranges from less than 50 cm to more 300 cm tall. Nonbearing (sterile) nodes occur on the main stem from the lowest node upward, with frequency correlated with time to flowering. Pod traits range from wide flattened to round and dehiscent on both structures, with color from yellow to dark green. Their seed mainly consists of two cotyledons, which provide initial growth support to the embry, with a primordial root or radical, stem tissue and an

embryonic growing point (also named plumule). In addition, the pea seed has an ilum, with which it was attached to the maternal pod tissue during developmental, and near this is a micropyle, where the germinating radical emerges. Pea seeds are globose or angled, smooth or wrinkled, exalbuminous, whitish, gray, green, or brownish and their size vary 10 to 36 g/100 seed being their germination cryptocotylar (Duke 1981).

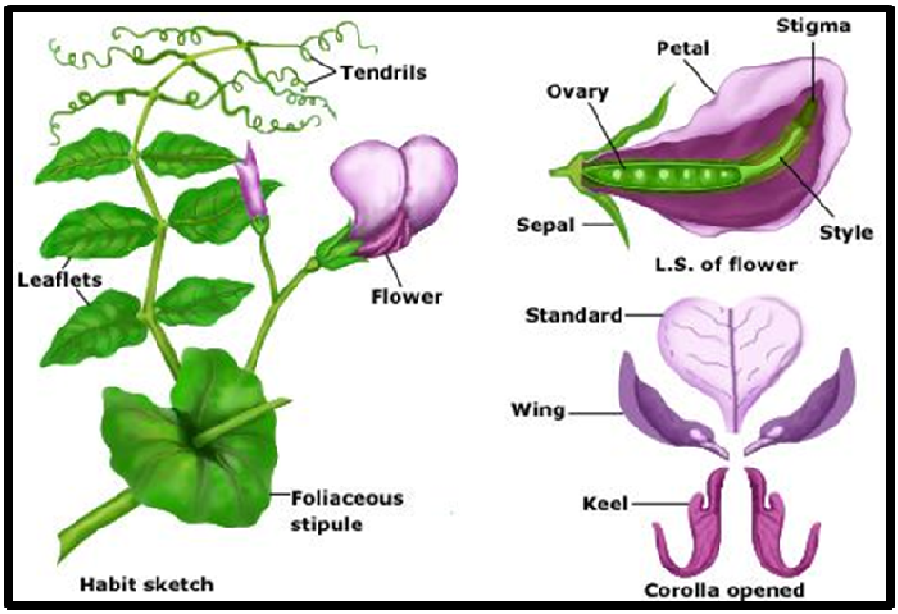

Figure 3. Detailed picture of leaf and flower in pea (*Pisum sativum*) (from tutorvista.com).

The genus *Pisum* is very diverse, showing a range of degrees of relatedness that reflect taxonomic identifiers, eco-geography and breeding gene pools (Smýkal 2014). Several pea germplasm pea collections, with over 1000 accessions are stored in national genbanks in more than 25 countries, with many other smaller collections worldwide (Smýkal et al. 2013). Thanks to the availability of these genetic resources numerous studies have investigated the genetic and trait diversity of *Pisum* germplasm, which might act as toolkits for association mapping (Smýkal et al. 2011). These studies have allowed to gain insight into genes underlying desired traits in the world pea collections (Smýkal 2014).

1.1.2. Importance of the crop

Pea is adapted to warm Mediterranean type as well as cool temperature conditions. Thus, this crop constitute an important source of protein for human

consumption in Mediterranean basin, temperate Europe, Ethiopia, south-west Asia and north-west India. Dry pea is one of the most grown grain legume in the world with a high primary production in temperate regions and registered 97 countries growing pea, whose cultivated area were 6.379 million hectares (FAOSTAT 2013). The most producers countries of dry pea in 2013, in million tons (MT) were Canada (3.85 MT), followed to Russian Federation (1.35 MT), China (1.38 MT) and USA (0.7 MT) (FAOSTAT 2013). In the last decade (2003-2013), Canada has remained the leading pea producing country (2.97 MT), followed to Russian Federation (1.29 MT), China (1.12 MT) and Ukraine (0.91 MT), respectively. Moreover, the average yield of dry pea during this period was around 4.000 Kg/Ha being Ireland the country that showed the highest yield (5,000 Kg/Ha), followed to Belgium-Luxembourg, Netherlands, France and Belgium (each ≈ 4.000 Kg/Ha) (FAOSTAT 2013). In the last decade Europe showed a gradual decrease in production from 2010 to 2013, while Canada, Russian Federation and USA showed a positive trend where production showed a slow increase.

1.2. *Medicago truncatula*

Annual medics (*Medicago* species) are widely used in low rainfall environments of the Mediterranean basin area, traditionally used as forage legumes providing nitrogen for rotational crops (Tivoli et al. 2006b; Walsh et al. 2001). *M. truncatula*, a close relative of alfalfa, naturally stands out as a model legume organism, with several unique characteristics, such as self-fertile, small diploid genome making a usefully tool for both genetics and genomics studies (Cook 1999; Young et al. 2005). *M. truncatula* is closely related to the cultivated tetraploid alfalfa (*M. sativa*) and to other legumes such as pea, chickpea, faba bean and lentil. This close phylogenic relationship increases the value of this model legumes as a resource for understanding the important agronomic traits of grain and forage legumes.

1.2.1. Model organism

In biology, the use of model species is necessary in order to better understand any biological process. Thus, in the last decade (2003-2013), particularly since the advent of the large-scale genomic scale genomic sequencing projects, the term *model organism* has become ubiquitous in contemporary biological discourse. Much of our knowledge

on heredity, development, physiology and the underlying cellular and molecular processes is derived from the studies of model, or reference, organisms (Müller and Grossniklaus 2010). The underlying concept of a *model organism* can be traced to a variety of sources, depending on how one defines it, as will be discussed in this essay (Ankeny and Leonelli 2011). Model organism can be defined as any experimental organism utilized to investigate a particular biological process or system, ranging wide organism such as *E. coli*, *S. cerevisiae*, *C. elegans*, *Drosophila*, *Xenopus*, *Arabidopsis* and *Medicago truncatula*. All model organisms have been used for use in molecular studies due to its ideal characteristic that are closely related to their power as genetic tools: they typically have small physical and genomic sizes, short generation times, short life cycles, high fertility rates, and often high mutation rates or high susceptibility to simple techniques for genetic modification. Therefore, it is now widely accepted that model organisms should be tractable using both forward-genetic approaches (identifying genes based on mutant phenotype), reverse-genetic approaches (functional analysis of a gene of known molecular identity) or both techniques (Ankeny and Leonelli 2011). Many of the core molecular mechanisms elucidated were found conserved in related species. Therefore, model organisms have uncovered the relatedness of life on this planet at the level of the blueprint, the beauty of which is hidden to the naked eye.

1.2.2. *M. truncatula* as a genetic model and their contribution to plant biology studies and functional genomics technologies.

Many agronomically important crops are legumes, such as faba bean, chickpea, pea, and alfalfa. However, the size and complexity of these genomes makes them unwieldy and has slowed progress on the genetic characterization of these crops. Several of these crop legumes are among the best characterized plant systems, including DNA marker maps and basic genomics tools (Cook 1999; Young et al. 2005). Nevertheless, despite the investment of resources from public and private sources, crop legumes have inconvenient features for genomics research, such as large genome size, abundant repetitive DNA, complex ploidy (Young and Bharti 2012).

M. truncatula is being used as a model plant for use in both molecular and classical genetic studies because of its ideal characteristics, such as its small, diploid genome, rapid generation time, self-fertility and ease of seed production (Cook 1999). This model plant has proven to be an easily transformed species, ensuring its role as an ideal model system for investigating and elucidating gene function in legume species. Hence, several large-scale international projects that have been initiated in relation to *M. truncatula* genomics, including the complete sequence description through an international consortium (http://www.medicagohapmap.org/). *M. truncatula* databases, including whole genome sequencing and annotation, expressed sequence tags (ESTs), structural genomics and comparative mapping, bacterial artificial chromosome (BAC) libraries and physical maps, gene expression, metabolic profiling and bioinformatic tools are available (http://www.medicago.org/). Thanks to closed phylogenetic relationship of *M. truncatula* to alfalfa (*M. sativa*) and other legumes, such as pea, chickpea, lentil or faba bean increases the attractiveness of utilizing this model legume (Dénarié 2002). The development of genetic and genomic tools in this model plant has propelled *M. truncatula* into the forefront of legume research as an ideal legume model. Hence, this model legume constitutes an ideal bridge between grain and forage legumes allowing to carry out comparative studies in these species. In addition, a wide availability of *M. truncatula* collections has allowed studying host–pathogen interactions at the histological, biochemical and physiological levels (Fernández-Aparicio et al. 2008; Prats et al. 2007; Rubiales et al. 2011b).

In the last decade, *M. truncatula* has emerged as an appropriate and agronomically relevant model plant for legumes, providing an excellent model upon which to dissect and to understand the mechanisms of resistance to pathogens of legumes in general (Rispail et al. 2010). Functional genomics technologies have been successfully applied in different *Medicago* pathosystems. Thus, an important number of transcriptomics (Curto et al. 2014; Dita et al. 2009; Foster-Hartnett et al. 2007; Gao et al. 2010; Madrid et al. 2010; Villegas-Fernández et al. 2014) and proteomics (Castillejo et al. 2009; Curto et al. 2006; Kiirika et al. 2014) approaches have allowing to identify the molecular pathways involved in the resistance to a wide variety of pathogens. This will undoubtedly help in the development of new forms of resistance in legumes to a variety of pathogens.

2. Plant pathogenic fungi.

2.1. The importance of phytopathogenic fungi.

The cool season food legumes (faba bean, chickpea, pea, lentil and lupin) play an important role in the farming systems worldwide, which are attacked by these phytopathogenic fungi that cause diseases such as grey mould, chocolate spot, ascochyta blight, anthracnose, rust, powdery mildew and downy mildew. These pathogens are major limiting factors in legume production and the most important of these are present in all areas where legumes are cultivated (Sillero et al. 2006).

Within legumes, pea is the most widely grown grain legume in Europe and the second-most in the world (FAOSTAT 2013). Significant efforts have been made in pea breeding for disease resistance in continental and oceanic conditions where it is mainly spring sown. Unfortunately, little efforts have been made so far in pea breeding for constraints typical of Mediterranean environments, such as rust, powdery mildew or broomrape (Rubiales D. et al. 2009) Several research works have reported levels of resistance in pea against ascochyta blight (Carrillo et al. 2013; Fondevilla et al. 2005), powdery mildew (Barilli et al. 2014; Curto et al. 2006; Fondevilla and Rubiales 2012) and rust (Barilli et al. 2009; Barilli et al. 2010). Control of these diseases is based on cultural management, the use of chemicals, genetic resistance or some combination of these approaches (Sillero et al. 2006). Disease resistance is currently a primary objective of most plant breeding programs. Procedures for screening and scoring germplasm and breeding lines for resistance have lacked uniformity among the various programs worldwide (Niks and Rubiales 2002).

2.1.1. Powdery mildew (*Erysiphe pisi*).

Powdery mildews (*Ascomycotina, Erysiphales*) are plant pathogenic fungi that seriously constrain crop production worldwide in many temperate regions (Belanger et al. 2002; Panstruga and Spanu 2014). The disease can cause important yield loses, reducing total yield biomass, number of pods per plant, number seeds per pod, plant height and number of nodes (Fondevilla and Rubiales 2012; Glawe 2008; Schulze-Lefert and Vogel 2000; Sillero et al. 2006). Pea powdery mildew is an air-borne disease

of worldwide distribution, which is caused by *Erysiphe pisi*, often reported as *E. communis* auct. p. p. or *E. polygoni* auct. p.p. (Braun 1987) differentiated *E. pisi* var. pisi infecting species in *Pisum*, *Medicago*, *Vicia*, *Lupinus* and *Lens*, and *E. pisi* var. *cruchetiana* infecting *Lathyrus* and *Ononis* species (Fondevilla and Rubiales 2012). Also, it has recently been reported that other fungi such as *E. trifolii* and *E. baeumleri* can also cause powdery mildew on pea (Fondevilla and Rubiales 2012).

These fungi are obligate biotrophic pathogens infecting aerial parts of higher plants (stems, leaves, flowers and fruits) owing to the profuse production of conidia that give them their common name (Fig. 4). Their life cycle is synchronized with host life cycles in order to develop an effective control strategy, which can involve both a sexual state (teleomorph) and asexual state (anamorph), or either can be lacking (Falloon and Viljanen-Rollinson 2001) (Fig. 5). In susceptible pea genotypes, *E. pisi* conidia germinate producing a germ tube with a lobed primary appressorium. A penetration peg emerges from this appressorium and penetrates the epidermal host cells through the cuticle and cell wall. Furthermore, a primary haustorium forms within the epidermal cell (Fig. 4 d). Nutrient uptake from the plant cell through the haustorium supports development of secondary hyphae that radiate across the host epidermis forming hyphal appressoria from which secondary haustoria are formed (Fig. 4 d). Finally, aerial conidiophores emerge from surface hyphae producing conidia capable of initiating a new cycle of infection (Fondevilla and Rubiales 2012). Moreover, several pea lines harboring genes for powdery mildew resistance have been described in *Pisum* germplasm (Fondevilla and Rubiales 2012). Thus, in pea lines harboring *er1* gene, the pathogen is stopped soon after, and no secondary hyphae are formed (Fondevilla et al. 2006), meanwhile the resistance provided by *er2* gene is governed at high temperatures is due to the occurrence of hypersensitive response in established colonies (Fig. 4c) (Fondevilla et al. 2006). In lines containing *Er3* gene, the growth of the established *E. pisi* colonies are stopped by a strong hypersensitive response (Fig. 4c) (Fondevilla et al. 2007a; Fondevilla et al. 2007b). Therefore, genetic resistance is an efficient, economic and environmentally friendly way of control. In spite of resistance conferred by these genes against to *E. pisi*, the identification of additional sources of resistance against these species is needed.

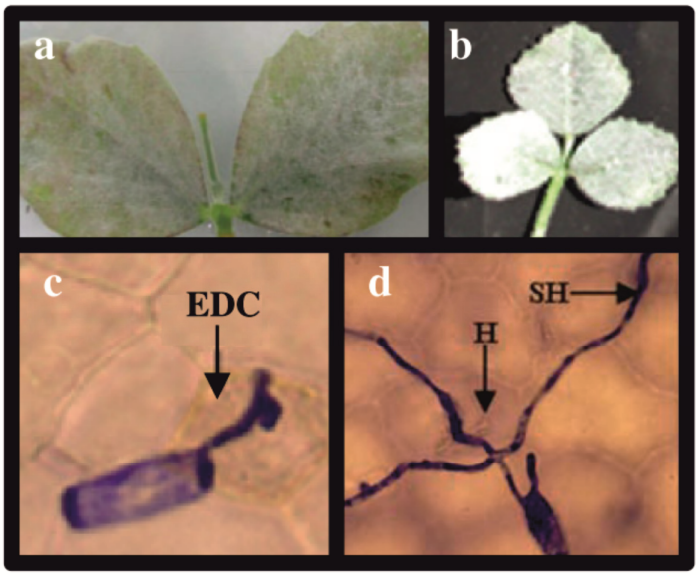

Figure 4. Representative symptoms of powdery mildews and their morphological features. **(a)** *Erysiphe pisi* f.sp. *pisi* development on pea leaf; **(b)** *Erysiphe pisi* f. sp. *medicaginis* development on *M. truncatula* leaf; **(c)** Microscope pictures of *Erysiphe pisi* f. sp. *medicaginis* on *M. truncatula* leaf epidermal cells (EDC: Epidermal Death Cell); **(d)** Differential interference microscopy of an *E. pisi* f. sp. *medicaginis* germling (H: haustorium; SH: secondary hyphae), (modified from Curto et al, 2006 and 2014)

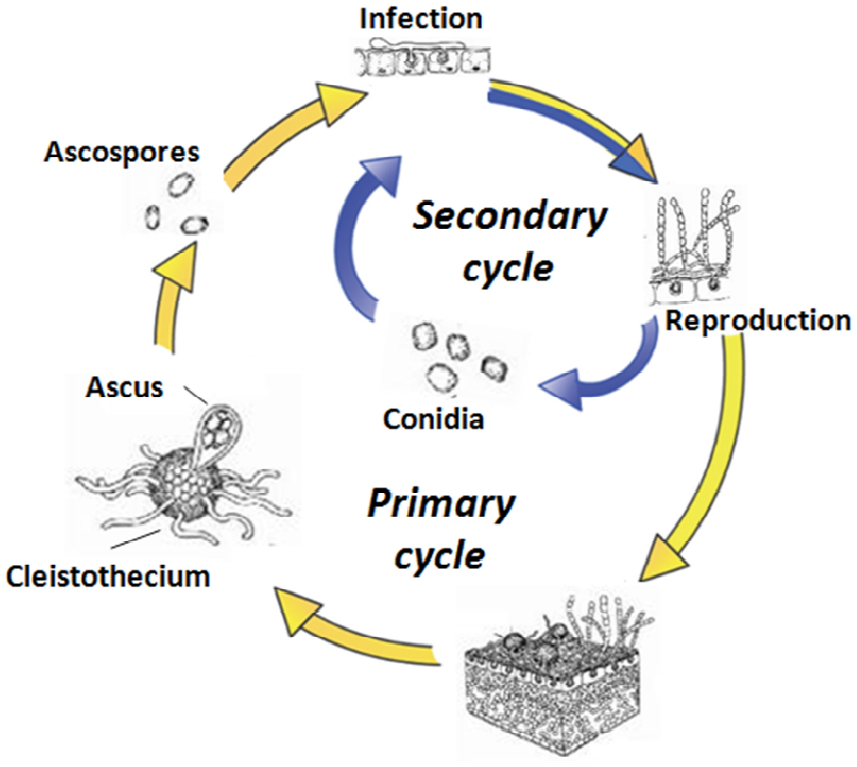

Figure 5. Diagram of powdery mildew life cycles. Primary (yellow and blue) and secondary (yellow) cycles are represented, (modified from González-Fernández et al. 2010).

2.1.2. Ascochyta blight (*Mycosphaerella pinodes*).

Ascochyta blight is a serious disease of cool-season grain legumes, including chickpea, faba bean, lentil and pea, caused by fungal species of the anamorphic genus *Ascochyta* (Fig. 6). Ascochyta blight has worldwide distribution, which is predominantly host-specific. Species of the coelomycete genus *Ascochyta* are all necrotrophic, killing plant cells in advance of mycelia development and the diseases they cause represent serious limitations to legume production worldwide (Rubiales and Fondevilla 2012). The disease in chickpea is caused by *Ascochyta rabiei* (teleomorph: *Didymella rabiei*); in lentil by *Ascochyta lentis* (*Didymella lentis*) and in faba beans by *Ascochyta fabae* (*Didymella fabae*) (Tivoli and Banniza 2007). The ascochyta blight complex of pea (*Pisum sativum*) is caused by three related fungal species, commonly referred to as the Ascochyta complex: *Ascochyta pisi*, *Ascochyta pinodes* (teleomorph: *Mycosphaerella pinodes*) and *Phoma medicaginis* var. *pinodella* (Jones 1927). Thus, in pea the disease is a complex because the three pathogens cause more or less similar symptoms and they frequently occur together. Ascochyta blight, caused by *Mycosphaerella pinodes* (also known as *Didymella pinodes*) the teleomorph of *Ascochyta pinodes*, is one of the most devastating pea pathogens (Khan et al. 2013). It is wide-spread throughout the major pea-growing areas, especially in temperate regions of Europe, North America, Australia and New Zealand (Bretag et al. 1995; Bretag and Ramsey 2001). Ascochyta blight is the most destructive disease affecting large areas in many countries, where pulses are cultivated and cause considerable losses in seed quality and quantity. Yield losses include both weight and quality losses due to seed infection. Average yield losses in commercial pea fields have been estimated at 10%, and losses of >50% have been measured in some trials (Xue et al. 1997).

Figure 6. Ascochyta blight on pea **(a)**, faba bean **(b)** and chickpea **(c)**. Disease symptoms on leaves **(a1, b1 and c1)**, fruits and seeds **(a2, b2 and c2)** and microscopic pictures of ascospores **(a1, c3)** and pycnidiospores **(b3)** are represented (modified from Koike et al. 2007 and Tivoli et al. 2007).

Ascochyta spp. cause well delineated lesions on all aerial organs of the plant (leaves, stems, flowers, pods) and consist of necrotic lesions, characterized by tan-coloured lesions on all above ground parts of the plant which contain concentric rings of black pycnidia exuding cirrhi of one or two-celled hyaline conidia (Bretag and Ramsey 2001). On the stems, these fungi cause deep necrotic lesions which can lead to breaking of stems and death of plant parts above the affected zone. *M. pinodes* and *P. medicaginis* var. *pinodella* causes blight starting with small purple to black spots, enlarging and turning brown to black spots. These lesions on stems, leaves, pods, foot rot and seeds appear as small, pinpoint and irregularly shaped flecks (Koike et al. 2007) (Fig. 6). Leaves with many lesions wither before the lesions become large, especially on the lower portion of the plants. Stem lesions are initiated at the bases of dead leaves and spread above and below that point. They coalesce to encircle the entire lower stem which generally does not break. All species cause necrosis on pods which results in seed infection. Heavily infected seeds have more or less severe discolourations and can shrivel in the most serious cases. The disease reduces number of seeds per stem and seed size (May et al. 2005; Tivoli and Banniza 2007; Tivoli et al. 1996) resulting in substantial yield throughout the major pea cropping regions worldwide (Bretag and Ramsey 2001).

Fungi responsible for ascochyta blights could be considered as hemibiotrophs characterised by an initial biotrophic phase that is followed by a necrotrophic phase. The epidemic caused by *M. pinodes* is based on both ascospores discharges as primary

and secondary inoculum, and successive pycnidiospore cycles (Fig. 7). The disease cycle of *M. pinodes* started with the dissemination of ascospores (primary inoculum) after which pycnidia developed rapidly in lesions on stipules, on green plant tissue or on senescent tissue (Roger and Tivoli 1996). However, the sexual fruiting structures pseudothecia are also formed alongside pycnidia during the cropping season; consequently ascospores are released during the entire season and constitute an important source of secondary inoculum. Rain-splashed pycnidiospores dispersed are responsible for secondary infections over short distances and further increases in disease severity accelerating tissue senescence. After rainfall, pseudothecia release ascospores which are dispersed over long distances by wind. In trials, pycnidiospores were principally trapped in the first 20 cm above the soil surface whereas ascospores were also trapped above the crop canopy. The formation of fruiting bodies progresses from the base to the top of the plants during crop development. Frequently, pycnidia and pseudothecia are simultaneously present on the same stipule. This is unusual because the sexual stage most commonly follows the asexual stage in plant pathogenic fungi (Agrios 2005).

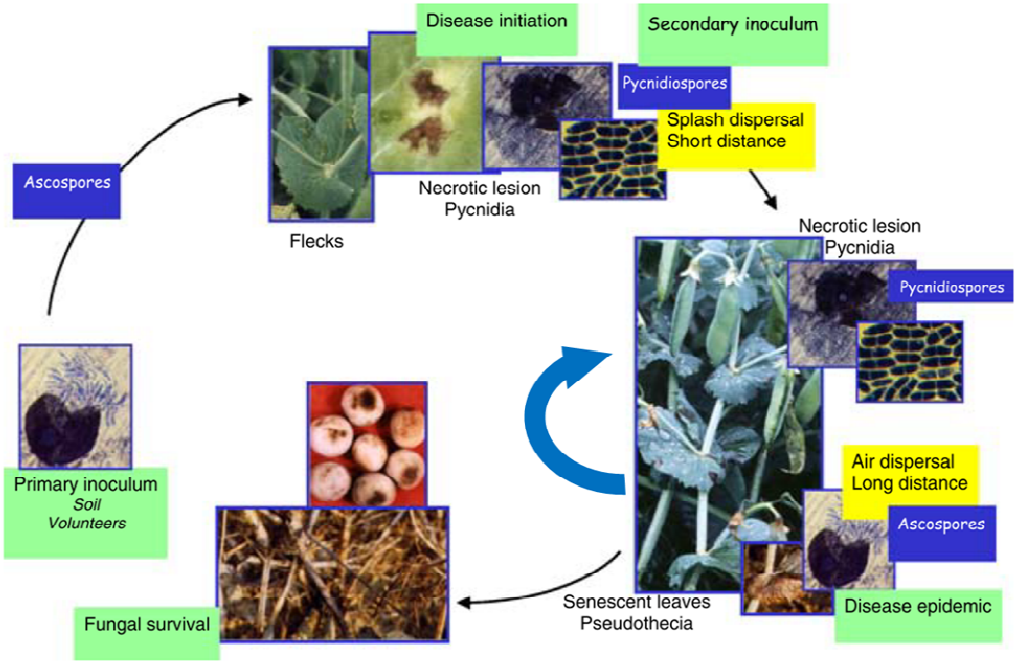

Figure 7. Disease cycle of *M. pinodes* on pea (modified from Tivoli et al. 2007).

2.2. Plant breeding for disease resistance

Although plants are exposed to a wide range of microorganisms in nature, their immune systems allow infection only by limited numbers of adapted pathogens (Boyd et al. 2013; Hartung and Schiemann 2014). Because plants lack a circulatory system, each plant cell must possess a preformed and/or inducible defense capability, so distinguishing plant defense from the vertebrate immune system (Walbot 1985). Biotrophic and necrotrophic fungal are a major constraint to plant production (Boyd et al. 2013). Pathogen and plants have interacting and they have given rise to a diverse array of exchanged signals and responses. The pathogen that elicit a host response can be met variously with hospitable acceptance (such as nitrogen-fixing *Rhizobium* bacteria), with tardy recognition and moderately effective defenses (as for most interactions that result in disease), or with a strong and rapid defense response that blocks further infection (Boyd et al. 2013; Dixon and Lamb 1990; Hammond-Kosack and Jones 1997; Ökmen and Doehlemann 2014). This latter form of disease resistance forms the subject of this review and is known variously as race-specific resistance, gene-for-gene resistance, or hypersensitive resistance. Considerable knowledge has since accumulated on the biochemical and genetic basis of disease resistance (Thakur and Sohal 2013), while the use of resistant cultivars has become a valuable strategy to control crop disease (Crute and Pink 1996).

2.2.1. Molecular genetics of plant disease resistance

Plants are constantly exposed to microbes and pathogens in nature that impair plant growth and reproduction. The immune system of an organism has been tailored through evolution by a long history of warfare with its invaders. Thus, plant pathogens have co-evoluted with their hosts developing diverse lifestyles and strategies of pathogenesis (Hammond-Kosack and Jones 1997). Pathogens deploy one of three main strategies to attack plants: necrotrophy, biotrophy or hemibiotrophy (Glazebrook 2005). Necrotrophic pathogens kill their hosts upon infection and feed on nutrients released from the dead cells, meanwhile in biotrophic and hemibiotrophic interactions, the pathogen depends on living host cells (De Wit et al. 2009). To be pathogenic, plant pathogen must access the plant interior, either by penetrating the leaf or root surface

directly or by entering through wounds or natural openings such as stomata, pores in the underside of the leaf used for gas exchange. Plants are sessile organisms and they lack a circulatory system whose cells are framed with a rigid cell wall. These evolutionary constraints have resulted in the evolution of a primary cell-autonomous immune system.

Currently, it is clear that the active defense responses of the plant are considered to operate at two levels (Jones and Dangl 2006). The first line of active plant defense involves the transmembrane pattern recognition receptors (PRRs) that respond to slowly evolving microbial- or pathogen-associated molecular patterns (MAMPS or PAMPs). The best-studied classes of plant PRRs are receptor-like kinases (RLKs), which feature an ectodomain of leucine-rich repeats (LRRs) involved in MAMP perception, and an intracellular kinase domain, involved in signal transduction relay via MAPK cascades, resulting in MAMP-triggered immunity (MTI) or PAMP-triggered immunity (PTI), which usually halts infection before the microbe gains a hold in the plant (Thomma et al. 2011) (Fig. 8a). Pathogens have developed mechanisms which have allowed evading or suppressing PRR-based plant defenses. They do so by deploying various effectors, determinants of virulence on susceptible hosts via MTI suppression, into the host cell. Successful pathogens are then faced with another hurdle, evolved by hosts to recognize the presence of their effectors and of intracellular MAMPs. PTI involve a series of defense reactions sufficient to repel most invading microbes. Several research works have reported significant advances in understanding PAMP–PRR interactions and the subsequent signaling event, such as bacterial PAMPs (*flg22, elf18*) and their PRRs (*FLS2*), which are leucine-rich repeat receptor-like kinases (LRR-RLKs) (Boyd et al. 2013). In addition, PRRs have also been found that can detect the peptides or cell wall fragments released during infection or wounding, referred to as damage-associated molecular patterns (DAMPs) (De Lorenzo et al. 2011). The pathogen is able to suppress the different components of PTI by ‘effector’ proteins delivered into the plant. Once pathogens acquired the capacity to suppress primary defenses, plants developed a more specialized mechanism to detect microbes, named as effector-triggered immunity (ETI). ETI involves the direct or indirect recognition of the very microbial proteins used to subvert PTI by plant resistance (R) proteins, which is mediated by nucleotide-binding domain LRR (NB-LRR) disease resistance proteins. Activation of R protein-mediated resistance also suppresses microbial growth, but not before the invader has had an opportunity for limited proliferation. Not surprisingly, pathogens seem to have adapted

effectors to interfere with ETI. PAMP recognition and PAMP-Triggered Immunity may be the plant's first active response to microbial perception. As will be outlined herein, PTI is initiated upon recognition of conserved microbial features by plant cell-surface receptors, and its induction is associated with MAP kinase signaling, transcriptional induction of pathogen-responsive genes, production of reactive oxygen species, and deposition of callose to reinforce the cell wall at sites of infection, all of which contribute to prevention of microbial growth (Nürnberger et al. 2004). Though the molecular mechanisms underlying PTI are not completely elucidated, much work has been done cataloguing microbial features that trigger PTI. PAMPs fulfill a function critical to the lifestyle of the organism, are highly structurally conserved across a wide range of microbes, and are not normally present in the host (Nürnberger et al. 2004).

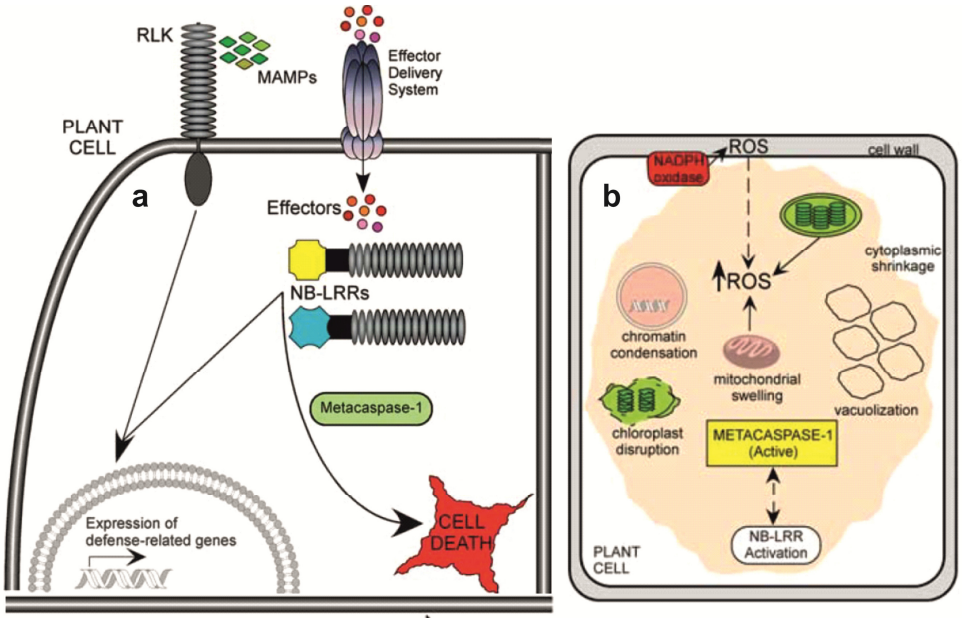

Figure 8. Innate immune pathways in plants. **(a)** Plants cells pathogen detection by membrane and intracellular innate immune receptors leads to signaling cascades that culminate in expression of defense-related genes. **(b)** Diagram representing programmed cell death in response to infection in plants (modified from Coll et al. 2011).

The second line acts largely inside the cell, using the polymorphic NB-LRR protein products encoded by most R genes (Jones and Dangl 2006). They are named after their characteristic nucleotide binding (NB) and leucine rich repeat (LRR) domains. Pathogen effectors from diverse kingdoms are recognized by NB-LRR proteins, and activate similar defence responses. NB-LRR-mediated disease resistance is effective against pathogens that can grow only on living host tissue (obligate biotrophs), or hemibiotrophic pathogens, but not against pathogens that kill host tissue

during colonization (necrotrophs) (Glazebrook 2005). Jones et al (Jones and Dangl 2006) has reported a model plant immune system which can be represented as a four phased. The first phase, PAMPs/MAMPs are recognized by PRRs, resulting in PAMP-triggered immunity (PTI) that can halt further colonization. The second phase successful pathogens deploy effectors that contribute to pathogen virulence. The third phase a given effector is 'specifically recognized' by one of the NB-LRR proteins, resulting in effector-triggered immunity (ETI). Recognition is either indirect, or through direct NB-LRR recognition of an effector. ETI is an accelerated and amplified PTI response, resulting in disease resistance and, usually, a hypersensitive cell death response (HR) at the infection site (Fig. 8b). The last fourth phase, natural selection drives pathogens to avoid ETI either by shedding or diversifying the recognized effector gene, or by acquiring additional effectors that suppress ETI.

2.2.2. The hypersensitive reaction in plants to pathogens

The hypersensitive response (HR) is a central component of plant resistance responses, form of programmed cell death localized to infection sites characterized by the formation of necrotic lesions at the attempted sites of infection, aiming to restrict pathogen growth and spread (Coll et al. 2011; Hammond-Kosack and Jones 1997). Its hallmarks include cytoplasmic shrinkage (whole-cell autofluorescence is clearly visible by fluorescence microscopy), vacuolization and chloroplast disruption (Mur et al. 2008).

Programmed cell death (PCD) is an important mechanism to regulate multiple aspects of growth and development, as well as to remove damaged or infected cells during responses to environmental stresses and pathogen attacks. HR is leading by a chain of events after effector recognition via NB-LRR receptors. Two separate signaling modules regulate NB-LRR proteins: non-race-specific disease resistance 1 (NDR1) regulates in most cases immune responses mediated by CC-NB-LRR proteins, whereas the enhanced disease susceptibility 1 (EDS1)/phytoalexin deficient 4 (PAD4)/senescence-associated gene 101 (SAG101) complex mediates TIR-NB-LRR signaling (Feys and Parker 2000). Both systems integrate redox signals downstream of NADPH oxidase leading to SA accumulation, which has a central role in defense

responses. ROS and SA act synergistically to drive HR (Durner et al. 1997). In addition, under pathogen infection plant cells exhibit a rapid synthesis of nitric oxide (NO) and a parallel accumulation of reactive oxygen species (ROS). Frequently, these responses trigger a PCD process leading to an intrinsic execution of plant cells. The accumulating evidence suggests that both NO and ROS play key roles in PCD. These redox active small molecules can trigger cell death either independently or synergistically. Several reviews have reported the progress on the cross-talk of NO and ROS signals in the hypersensitive response, leaf senescence, and other kinds of plant PCD caused by diverse cues (Choi et al. 2013; Iakimova et al. 2013). Both NO and ROS have been implicated in controlling the HR process (Fig. 8b). One of the key determinants for the HR is the balance between intracellular NO and ROS levels (Zaninotto et al. 2006). Following pathogen recognition, NO accumulation occurs concomitant with an oxidative burst, which consists of a biphasic production of apoplastic ROS at the site of attempted invasion (Lindermayr and Durner 2009). In this context, NO and H_2O_2 are thought to function in combination to promote HR cell death. Some key components of the defense signaling cascade that are known to be affected by ROS and NO activity include mitogen-activated protein kinases (MAPKs) and phosphatases. These local responses can, in turn, trigger a long lasting systemic response (systemic acquired resistance, SAR) that primes the plant for resistance against a broad spectrum of pathogens (Dong 2001).

Many plant pathogens have evolved strategies to inhibit different types of cell death further underscores its fundamental role in fighting infections. Specially, biotrophic/hemibiotrophic pathogen (i.e. powdery mildews) that feed on living cells, they have developed mechanisms to evade host detection and death of the invaded plant cells. Thus, they have evolved strategies to suppress HR using specific effectors delivered into the cell via diverse secretion systems. Moreover, necrotrophic pathogens have developed mechanisms to induce cell death in their hosts by secreting phytotoxins and cell wall degrading enzymes, resulting in the formation of expanding necrotic lesions in the infected plant tissue using the plant HR machinery as a strategy to promote virulence (Coll et al. 2011).

3. Plant functional genomics

Genetic and "omics" tools have revolutionized plant breeding increasing the knowledge of the genetic factors responsible for complex traits and developing a large amount of resources, which can be used in the selection of superior genotypes. The rapidly growing fields of "omics" tools, transcriptome, proteome and metabolome, have allowed studying the molecular biology of the responses of plants to experimental conditions (Kumpatla et al. 2012). However, bioinformatics is required for the analysis and interpretation of the data obtained. These efforts have provided huge databases of protein sequences, many of which are of unknown function. Hence, functional genomics approaches have allowed evaluating and studying the entire cell or organism as a system and understanding how different biological processes occur within this system, how they are controlled and how they are executed (Mittler and Shulaev 2013).

3.1. Structural and functional genomics

The cumulative utilization of "omics" technologies has advanced the fields of structural and functional genomics (Mittler and Shulaev 2013). The initial long-term goal of the structural genomics endeavor was to map all protein folds, so that the structures of virtually all proteins could be either found in the Protein Data Bank (PDB) or derived by computational methods. Thus, structural genomics studies have allowed delineating the total repertoire of protein folds, thereby providing three-dimensional portraits for all proteins in a living organism and to infer molecular function of the proteins (Grabowski et al. 2007). Hence, structural projects entail a conceptual shift from traditional structural biology in which structural information is obtained on known proteins to one in which the structure of a protein is determined first and the function assigned only later. Whereas the goal of converting protein structure into function can be accomplished by traditional sequence motif-based approaches, recent studies have shown that assignment of a protein's biochemical function can also be achieved by scanning its structure for a match to the geometry and chemical identity of a known active site. Importantly, this approach can use low-resolution structures provided by contemporary structure prediction methods. When applied to genomes, structural information (either experimental or predicted) is likely to play an important role in high-

throughput function assignment. In conclusion, structural genomics is a powerful tool that reveals to us a global view of the protein structure which complement the data obtained by proteomic and genomic technologies in providing molecular function of may proteins of unknown function (Rigden 2006).

Functional genomics approach seeks to decipher unknown gene function. Metabolomics, defined as the comprehensive analysis in which all the metabolites of an organism are identified and quantified, has emerged as a functional genomics methodology that contributes to our understanding of the complex molecular interactions in biological systems (Hall et al. 2002). Thus, metabolomics offers the unbiased ability to differentiate genotypes based on metabolite levels that may or may not produce visible phenotypes (Trethewey 2004). Furthermore, in those instances in which mutations or expression of trans-genes lead to measurable phenotypic changes, metabolomic approaches can be used to decipher the biochemical cause or consequence of the observed phenotypes. The functions of many genes, pathways and networks revealed in large scale sequencing projects can be inferred through nucleotide similarity with gene sequences of known function determined through traditional empirical methods. Moreover, systems biology although is related to functional genomics showed slightly different in its objectives. These approaches encompasses a holistic approach to the study of biology and the objective is to simultaneously monitor all biological processes operating as an integrated system, which allowed visualize how individual pathways or metabolic networks are interconnected (Oliver et al. 2002). Both, systems biology and functional genomics shared “omics” technologies in biological researches which have allowed predicting and explaining complex phenotypes in plants.

3.2. Transcriptomics techniques

The transcriptome encompasses the genes transcribed in any given organism, which include protein-coding mRNAs and non-coding small RNAs, such as ribosomal, tRNA, or miRNA. The transcriptome is a dynamic link between the genome, the proteome and the cellular phenotype (Rodrigues et al. 2014). The regulation of gene expression is one of the key processes for adapting to changes in environmental conditions and thus for survival. Hence, research in biology, biotechnology and medicine requires fast genome and transcriptome analysis technologies for the

investigation of cellular state, physiology and activity. Between the transcriptomics techniques, microarray technology, real-time quantitative PCR and the recently next generation sequencing of transcripts (RNA-Seq) have widely used in the plant molecular biology studies. Traditionally, transcriptome profiling has focused on quantifying gene expression (Curto et al. 2014; Fondevilla et al. 2014). With the advent of ultra high-throughput sequencing (UHTS) technologies, it is now possible to obtain highly resolved structural information of RNA populations on a high-throughput platform. This includes mapping transcript initiation and termination sites, splice junctions and post-transcriptional modifications (Pandey et al. 2003). Such information will lead to a better understanding of the functional elements within the genome and the discovery of novel developmental or environmental regulatory networks.

3.2.1. Microarray

Complete sequences of genomes and comprehensive sets of cDNA sequences open the way to a huge range of biological problems. Microarray technologies offer an approach to study the differential gene expression of different probes using complex populations of RNA (Charpe 2014; Schulze and Downward 2001). A microarray is a 2D arrangement of known biochemical constituent of a biological system on a solid substrate that is useful in high throughput screening of biological material. Refinements of these techniques have allowed analyzing of copy number imbalances and gene amplification of DNA and have recently been applied to the systematic analysis of expression at the protein level. Various types of microarrays using information have been developed such as, DNA microarrays (e.g. cDNA microarrays, SNP microarrays), MMChips, tissue microarrays, antibody microarrays and glycoarrays (Charpe 2014). Microarrays have become one of the revolutionary technologies enabling comprehensive and high through-put surveys of DNA or RNA molecules on a genome-wide scale (Lockhart and Winzeler 2000). Hence, this technique is a key element in today´s functional genomics toolbox, due to the method lies in miniaturization, automation and parallelism permitting large-scale and genome-wide acquisition of quantitative biological information from multiple samples.

DNA microarrays have been recognized as multiplex technology that either measure DNA as part of its detection system, which were gradually developed from

southern blotting (Southern 1996; Southern et al. 1992). Hybridization of probe with the blotted nucleic acid fragment results in separation of radioactivity or chromogenic substrate that can be detected by autoradiography or colorimeter. Currently, DNA microarray are manufactured by robotic plotting of picomoles range of specific DNA sequences known as probes or reports on a solid substrate like glass slide, silicon chip and microscope beads as Illumina. The probes are attached to the respective solid surface by surface engineering using a matrix, such as epoxy-silane, amino-silane, lysine or others that binds the probe to the surface by a covalent bond. Thanks to this technique thousands of probes can be fixed to each cm^2 area on the solid surface appearing like tiny dots known as features (Fig 9a). Thus, the arrays can contain several thousands of probes and several microarray platforms have been developed in plants (Wu et al. 2001), including crop species (Rensink and Buell 2005) and model plants, such as *Medicago truncatula* (Hohnjec et al. 2005; Küster et al. 2004), *Lotus* (Endo et al. 2002) and *Arabidopsis* (Zimmermann et al. 2004). Microarray probes might be prepared from available cDNA sequences from cDNA libraries developed by trapping expressed sequence tags (ESTs) those are usually 200–300 bp long; by in silico synthesis of 20–30 bp long non-overlapping oligonucleotide sequences or by using the nucleic acid sequences distinguishing the single nucleotide polymorphism (SNPs). The hybridization is performed using cDNA or cRNA target samples which are prepared from biological system under study that are subjected to a specific condition according the assay. For detection and quantification of hybridization of probe with the target, the target is labeled with the signal producing fluorophore, silver, or chemiluminescence labels (Fig 9b). Once the fluorescent sample is hybridised to a cDNA microarray, unbound material is washed away and the sample hybridized to each element is visualized by fluorescence detection. Both confocal scanning devices and CCD cameras are being used for this purpose. Fluorescence emission from the microarray is converted into a digital output for each dye, and is stored as separate image files. Next, image analysis software is used for quantification of individual array elements. Background fluorescence is then subtracted from the raw data. Although fluorescent signals measured (directly) on areas between the array elements are often employed for background, it is more appropriate to use signals from foreign, such as non-plant array elements that have been included on the array for plant microarray experiments (Kathleen Kerr 2003). Next, microarray data are normalized to correct for channel specific effects such as differences in quantum yield of the dyes and unequal labeling

efficiencies of the samples. Normalization also corrects for any unwanted differences in the amount of sample used. The use of housekeeping genes is a good an alternative. Thus, a set of these reference genes, included as probes on the array, could be used for channel normalization using a systematic validation procedure, such as geNorm software (Vandesompele et al. 2002). Subsequently, data exploration process must be carried out to interpret microarray data. Hence, several standard statistical techniques are currently being used to help interpret microarray data, including hierarchical clustering, principal component analysis (PCA) and self-organizing maps (SOM), which allowed grouping genes (or samples) together that show similar behavior. Hierarchical clustering of gene expression data in combination with false-colour coding of the expression levels has become a popular way of data analysis and presentation (Eisen et al. 1998). Thus, this technique allowed to group genes in clusters based on the similarity between their expression profiles. In a bottom-up approach genes are joined to form nodes, which in turn are then further joined.

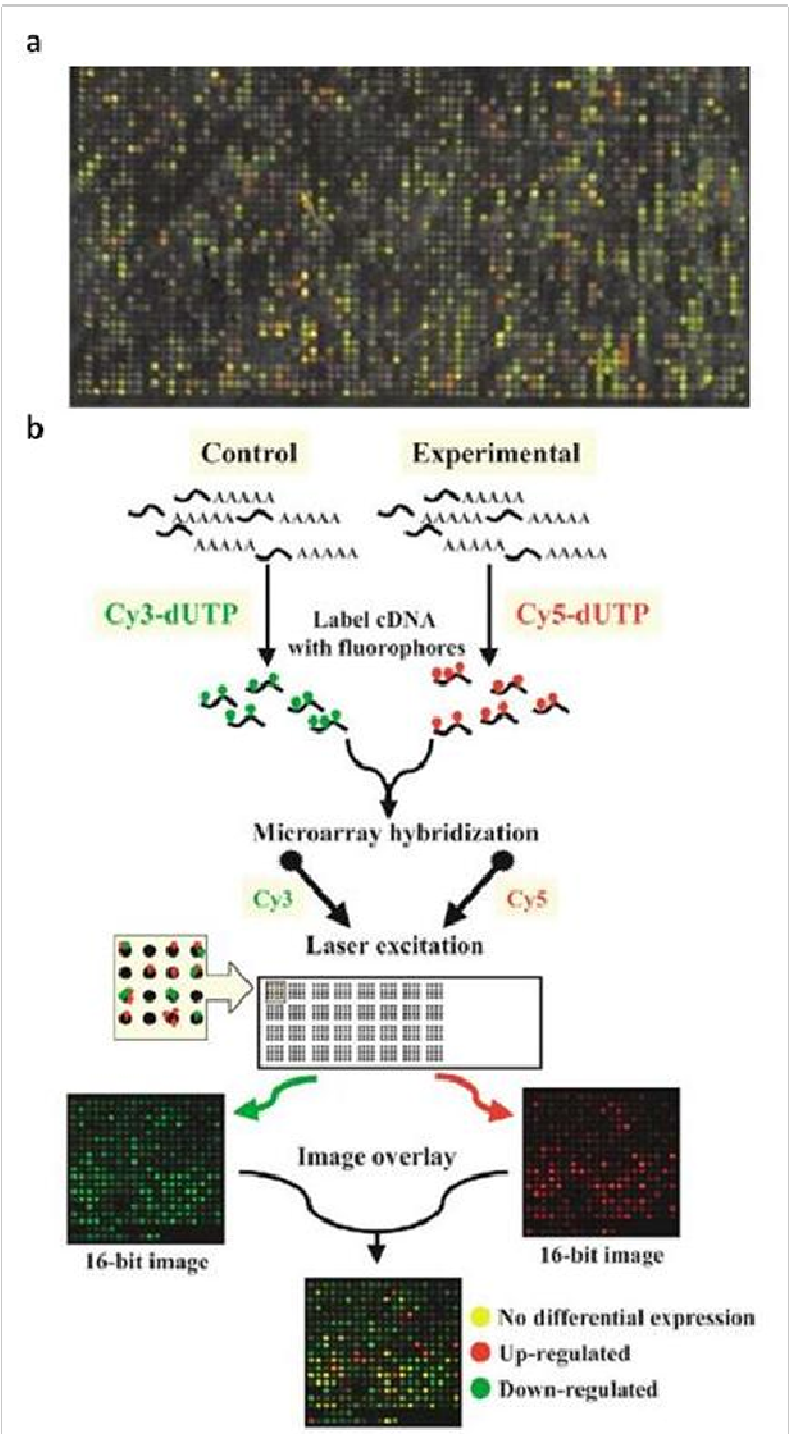

Fig. 9 cDNA array used in gene expression monitoring. **(a)** cDNA after hybridization of labeled samples. **(b)** DNA microarray hybridization and data acquisition**.** Two-colour hybridization strategy often used with cDNA microarrays. cDNA from two different conditions is labeled with two different fluorescent dyes (usually Cy3 and Cy5), and the two samples are co-hybridized to an array. After washing, the array is scanned at two different wavelengths to detect the relative transcript abundance for each condition (modified from Lockhart and Winzeler 2000 and Wu et al. 2001)

With respect to agricultural genomic research, group efforts have generated large amounts of sequence information, both as expressed sequence tags (EST) and as whole genome sequences. The full decoding of the model plant genomes, such as *Arabidopsis* and *M. truncatula* provides invaluable information for further understanding plant growth and development. A better understanding of these model plants can potentially be extrapolated to the improvement of other economically important plant species (Mittler and Shulaev 2013). In conclusion, the use of microarrays to explore gene expression on a global level is a rapidly evolving technology that seems set to become more powerful with the completion of the genomes. The biochemistry of the microarrays is proving very useful, and it seems likely that the significant advances in the next few years will come in the interpretation of the data sets generated. Currently, it seems that we may only be scratching the surface when it comes to extracting useful information from these large quantities of data. This will be improved by advances in bioinformatics, but will also require more thoughtful experimental design (Charpe 2014).

3.2.2. Quantitative real-time PCR

Microarray analysis, with all its comprehensive analytical power, is not without limitations (i.e. sensitivity). Gene expression analysis by quantitative real-time polymerase chain reaction (qPCR) has been a key enabling technology of the post-genome era (Taylor and Mrkusich 2014; VanGuilder et al. 2008). Hence, qPCR has become a routine and robust approach for measuring the expression of genes of interest, validating microarray experiments, and monitoring biomarkers (Canales et al. 2006). The current maturation of qPCR with fluorescent probes allows for rapid and easy confirmation of microarray results in a large number of samples. This methodology has been widely used for quantitation of RNA levels (Abbott et al. 1988; Bustin 2000). Hence, a number of early qPCR methods relying on end point analysis of PCR products were proposed soon after its development (Wang et al. 1989). Currently, qPCR represents the method of choice for analyzing gene expression of a moderate number of genes in anywhere from a small number to thousands of samples (Taylor and Mrkusich 2014).

qPCR technology allows quantification of PCR products in “real time” during each PCR cycle, yielding a quantitative measurement of PCR products accumulated during the course of the reaction. In practice, a video camera records the light emitted by a fluorochrome incorporated into the newly synthesized PCR product. Thus, real-time PCR allows the amplification to be followed in real-time during the exponential phase of the run, and thus allows the amount of starting material to be determined precisely. Contrary to end-point PCR techniques, the result is independent from the plateau corresponding to the saturation of the reaction, the latter leading to inaccurate quantification. Thus, qPCR allows the detection of a given nucleic acid target in a rapid, specific and very sensitive way. One of the relevant features of qPCR is its rapidity to provide reliable data. Typically, the time of a whole real-time PCR run ranges from 20 min to 2 h. Indeed, the time needed to shift temperature is a major limiting factor responsible for the duration of a classical PCR experiment. In addition, several machines can accommodate 384 well plates and can process queuing plates over 24 h non-stop , which might be a determining advantage for high throughput studies or if rapid sample processing is required (Ponchel et al. 2003). Moreover, qPCR provides a high sensitivity for the detection of DNA or RNA due to a combination of the amplification for double-stranded DNA. Thanks to intercalating agents bind regardless of the nucleotide nature, they can be used for any type of sequence and this is an economical advantage for a laboratory testing a large number of genes. The use of fluorescence-based technologies including: (i) probe sequences that fluoresce upon hydrolysis or hybridization; (ii) fluorescent hairpins; or (iii) intercalating dyes (i.e. SYBR Green). These approaches require less RNA than end point assays, possess a wider dynamic range than gel-based densitometry (five orders of magnitude vs. two orders of magnitude), and are more resistant to nonspecific amplification (Kim 2001). qPCR methodology also is noteworthy to show a high grade of specificity. Thus, in contrast to techniques requiring the hybridization of nucleic acids several hundred base pairs long, such as cDNA-based microarray and northern blotting, short oligonucleotide-mediated real-time PCR guarantees a high specificity in the detection of the target sequence. However, the specificity of the progress must be checked after completion of the PCR run, by testing the nature of the amplified product with gel electrophoresis, melting curves or sequencing data. The last and most relevant qPCR feature is its quantification, which is up to several orders of magnitude (Pabinger et al. 2009), and more recently in plants (Fletcher 2014; Li et al. 2014). This results from the

capacity of this technique to calculate, for every sample within an extremely low to high concentrations range, the number of cycles necessary to reach the threshold cycle (C_T), which is defined as the PCR cycle at which the fluorescent signal of the reporter dye crosses an arbitrarily placed threshold. The absolute amount of the target is calculated from a calibration curve. Moreover, qPCR methods require normalization of gene expression against stably expressed reference genes (also called housekeeping genes) (Guénin et al. 2009; Huggett et al. 2005). Thus, in qPCR experiments, reference genes are used as controls to normalize the data by correcting for differences in quantities of cDNA used as a template. Reference genes must therefore be carefully selected based on experimental data. It´s recommended extracting total RNA from at least one or two samples from each experimental condition or time point and confirm their purity and quality. Next, to normalize the sample concentration and perform reverse transcription PCR from the same volume of each sample using the same volume of each cDNA sample as a template. To evaluate and select the best reference genes several methods and programs can be used, such as geNorm method (Vandesompele et al. 2002), which allow calculating the target stability between the different conditions. In addition, geNorm also helps in the selection of the optimal number of reference genes.

Analysis of qPCR data has also reached a mature stage of development. Analyses can be either of absolute levels (i.e., numbers of copies of a specific RNA per sample) or relative levels (i.e., sample 1 has twice as much mRNA of a specific gene as sample 2). By far, the majority of analyses use relative quantitation as this is easier to measure and is of primary interest to researchers examining disease states. For absolute quantitation, an RNA standard curve of the gene of interest is required in order to calculate the number of copies. In this case, a serial dilution of a known amount (number of copies) of pure RNA is diluted and subjected to amplification. Like a protein assay, the unknown signal is compared with the curve so as to extrapolate the starting concentration. Alternatively, a computation method for absolute quantitation has been proposed that does not use standard curves (Alvarez et al. 2007). The most common method for relative quantitation is the $2^{-\Delta\Delta C}{}_T$ method (Livak and Schmittgen 2001) or $E^{-\Delta\Delta C}{}_T$ method, where E is the geometric mean of PCR efficiencies of PCR reactions (Fig. 10). However, the $2^{-\Delta\Delta C}{}_T$ method relies on two assumptions. First is that the reaction is occurring with 100% efficiency; in other words, with each cycle of PCR, the amount of product doubles, which can be ascertained through a simple experiment

as described in detail by Livak and Schmittgen (Livak and Schmittgen 2001). This assumption is also one of the reasons for using a low cycle number when the reaction is still in the exponential phase, due to in the initial exponential phase of PCR, substrates are not limiting and there is no degradation of products. Moreover, the $E^{-\Delta\Delta C}{}_T$ method allows selecting PCR reactions whose PCR efficiencies are higher (near 2). Hence, the $E^{-\Delta\Delta C}{}_T$ method is an accurate method of the $2^{-\Delta\Delta C}{}_T$ method where the real PCR efficiencies are used. Second assumption of the $2^{-\Delta\Delta C}{}_T$ method is that there are genes that are expressed at a constant level between the samples. This endogenous control will be used to correct for any difference in sample loading, which is critical to obtain the normalized gene expression values. Once the C_T value is collected for each reaction, it can be used to generate a relative expression level. The $2^{-\Delta\Delta C}{}_T$ and $E^{-\Delta\Delta C}{}_T$ methods are described in the figure 10. Michael Pfaffl and colleagues (Pfaffl 2001; Pfaffl et al. 2002) and others (Karlen et al. 2007) have also described several analysis methods. Overall, qPCR is an accurate, sensitive and reliable method for validating gene expression data.

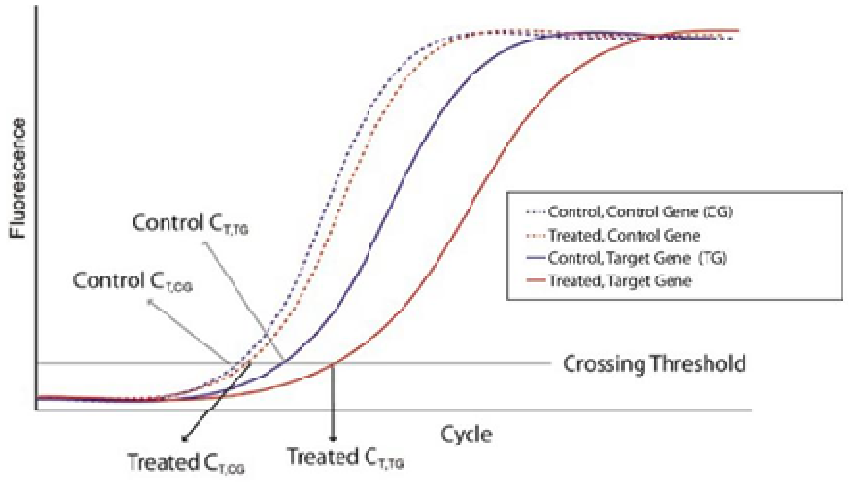

$$2^{-\Delta\Delta C_T} = 2^{-(C_{T,TG}-C_{T,CG})_{treated} - (C_{T,TG}-C_{T,CG})_{control}}$$

$$E^{-\Delta\Delta C_T} = \left(E_{CG}^{(CT_{CG})} / E_{TG}^{(C_{T,TG})}\right)_{treated} / \left(E_{CG}^{(C_{T,CG})} / E_{TG}^{(C_{T,TG})}\right)_{control}$$

Figure 10. Mathematical basis of $2^{-\Delta\Delta CT}$ and $E^{-\Delta\Delta CT}$ methods. Both methods enables relative quantitation (treated sample is X fold of control sample) through measurements of crossing thresholds (C_T). Formulas described allow calculating the differences between the gene of interest and an endogenous control for each sample enable a relative quantitative comparison between the samples (modified from VanGuilder et al. 2008).

3.2.3. Ultra high-throughput sequencing

Biological research has been revolutionized by the introduction of dideoxy DNA sequencing, developed by Frederick Sanger et al. in the late ‘70s (Sanger et al. 1977). Recent advances in DNA sequencing have revolutionized the field of genomics, making it possible for even single research groups to generate large amounts of sequence data very rapidly and at a substantially lower cost. The succeeding advent and rapid development of the so-called next-generation sequencing (NGS), second-generation sequencing, high-throughput next-generation sequencing (HT-NGS) or ultra-high-throughput sequencing (UHTS) technologies ushered in an era in which reading an organism’s genome has almost become a routine practice (Martin and Wang 2011; Wang et al. 2009). In addition to the sequencing of whole genomes, the development of different NGS methods and protocols has enabled a wide range of applications. To date, these technologies have been applied in a variety of contexts, including whole-genome sequencing, targeted resequencing, discovery of transcription factor binding sites, and non-coding RNA expression profiling. These technologies offer the potential to study the transcriptomes in detail that has traditionally been restricted to single gene surveys. For instance, it is now possible to globally define transcription start sites, polyadenylation signals, and alternative splice sites and generate quantitative data on gene transcript accumulation in single tissues or cell types. These technologies are thus paving the way for whole genome transcriptomics and will undoubtedly lead to novel insights into plant development and biotic and abiotic stress responses (Wang et al. 2010).

Two UHTS methods are mainly used to capture and sequence RNA pools. In both methods mRNA pools are enriched by capturing the molecules through the polyadenylated tails, and a ribosomal RNA removal step is often added before or after the mRNA purification. The first method captured mRNA-enriched pools, which are then fragmented into roughly equal lengths and then reverse-transcribed using random hexamers to generate a cDNA library. In the second method, RNA is reverse transcribed using an oligo-(dT)-adapter primer and the resulting cDNA is fractionated. The cDNAs are then fitted with adaptors at one or both ends through a ligation step(s). It is desirable to add these adaptors during the single-strand stage (RNA or cDNA) synthesis step in order to retain strand specificity in the final sequence reads (Simon et al. 2009). The

tagged cDNA library is subsequently amplified through PCR before being sequenced. Procedures of smRNA sequencing are very similar to those of smRNA-seq, substituting a size-selection step for small RNA molecules for the RNA fragmentation step (Simon et al. 2009). Moreover, other methods such as 'Digital gene expression (DGE)' also allow studying the transcript profiling (Linsen et al. 2009), which is qualitatively similar to serial analysis of gene expression analysis (SAGE), in that single transcripts are identified through a 30 end tag (Hu and Polyak 2006). However, this technique suffers a number of shortcomings including a dependence on a relatively small tag (21 and 20 bps when using NIaIII and DpnII, respectively) resulting in a large number of redundant placements in complex genomes, large differences in library populations if multiple restriction enzymes are used to generate the 30 tags, and low correlations between cDNA-based methods, where gene transcripts are represented by multiple alignments.

The most used UHTS platforms are currently commercialized by Roche 454 (GS FLX and GS Junior), Illumina (HiSeq, Genome Analyzer and MiSeq), and Life Technologies (SOLiD System and Ion Torrent sequencers). 454 *pyro*phosphate-based *sequencing*, also called "pyrosequencing", builds on a sequencing-by-synthesis approach. The latter involves determining the sequence of a DNA template by synthesizing the complementary DNA. A single-stranded DNA fragment is made double-stranded by the use of an enzyme (polymerase) that works its way along the fragment, starting at one end. This results in the release of inorganic pyrophosphate which – through a series of enzymatic reactions – produces visible light signals. The amount of light is recorded by a camera, and it is proportional to the number of nucleotides incorporated (Schuster 2008). Consecutive runs of the same nucleotide are referred to as homopolymer runs. Similarly to 454, also Illumina uses sequencing-by-synthesis, and a camera captures the fluorescently labeled nucleotides. DNA extensions occur one nucleotide at a time (as opposed to 454 sequencing where all nucleotides of a homopolymer run are represented by one light signal). Current read lengths are around 100-150 bp. A detailed description of the technology can be found in Bentley et al. (Bentley et al. 2008). The SOLiD platform differs from 454 and Illumina in that it does not rely on sequencing-by-synthesis, but uses DNA ligase and complementary probes to sequence the amplified fragments (Grada and Weinbrecht 2013). It reaches read lengths of around 75 bp. The technology is presented in Valouev et al. (Valouev et al. 2008). When HeliScope launched the first single-molecule sequencing technology in 2008, a

third generation of sequencers was born (Harris et al. 2008), and the term NGS was no longer referring to second-generation sequencers only. Schadt et al. (Schadt et al. 2010) and Blow (Blow 2008) provide an overview of HeliScope and nanopore (Venkatesan and Bashir 2011) sequencing.

To date, several groups have used UHTS for discovery-based studies of the mRNA populations in plants. Early analyses in crops (Emrich et al. 2007) and model plants, such as *Medicago* (Cheung et al. 2006) and *Arabidopsis* (Weber et al. 2007) used the 454-pyrosequencing platform. From their work, close to two million unique sequences were generated from pyrosequencing and over one third of these sequences were mapped to *Medicago* BACs (Bacterial Artificial Chromosomes) and over ten thousand novel transcripts were identified (Cheung et al. 2006). In a similar study by Weber and colleagues, over 5 million ESTs were generated from Arabidopsis seedlings (Weber et al. 2007). As a newly developed technology, UHTS transcriptomics faces many unique challenges. The most apparent obstacle arises from the complexity of the sequence data that is generated by the UHTS platforms. To process, interpret and visualize these large datasets, it is necessary to develop efficient and sophisticated algorithms and pipelines. Hence, several challenges exist to making this technology broadly accessible to the plant research community. These include the current need for a computationally intensive analysis of data sets, a lack of standardized alignment and formatting procedures and a relatively small number of analytical software packages to interpret UHTS outputs.

3.3. Proteomics techniques

Proteomics, the systematic analysis of the proteome, is a powerful tool in the post-genomic era and constitute a priority research for any organism (Breker and Schuldiner 2014; Jorrin-Novo 2014). Marc Wilkins was the first to coin the term “proteomics”, during the 1994 Siena Meeting, to simply refer to the “PROTein complement of a genOME” (Wilkins et al. 1995). The proteome can be defined as being the total set of protein species present in a biological unit (organule, cell, tissue, organ, individual, species and ecosystem) at any developmental stage and under specific environmental conditions. By using proteomics we aim to know how, where, when, and what for are

the several hundred thousands of individual protein species produced in a living organism, how they interact with one another and with other molecules to construct the cellular building, and how they work with each other to fit in with programmed growth and development, and to interact with their biotic and abiotic environment (Jorrín-Novo 2009). This methodology should be considered as part of a multidisciplinary integrative analysis at different levels, extending from the gene to the phenotype through proteins. Nowadays, proteomics has become more than just an appendix of genomics or an experimental approach but a complex scientific discipline dealing with the study of the cell proteome. Proteomics has expanded rapidly in recent years due to the completion genomes and the development of new techniques (Zhang et al. 2014). Different areas within proteomics can be defined (Jorrin-Novo 2014; Jorrín-Novo 2009):

i) Descriptive proteomics, including intracellular and subcellular proteomics, directed towards increasing proteome coverage of many plant species, rice (Kim et al. 2014; Komatsu et al. 2004), tomato (Ruiz May and Rose 2013; Xu et al. 2013), pine (Garcés et al. 2014; Valledor et al. 2008), wheat (Cao et al. 2014), pea (Schiltz et al. 2004), and specially model plant species such as Arabidopsis (Rödiger et al. 2014) and *M. truncatula* (Mathesius et al. 2001; Watson et al. 2003), among many others. In addition, subcellular fractionation techniques are key methods in plant proteomics which have allowed studying the proteomes of particular subcellular structures, especially chloroplast (Baginsky and Gruissem 2004; Gutierrez-Carbonell et al. 2014) and mitochondria (Huang et al. 2014).

ii) Differential expression proteomics have been widely used to study almost any process in plants, including growth and development, signalling, senescence, ripening, nutrition and stresses (Jorrín-Novo 2009; Jorrín-Novo et al. 2007; Jorrín-Novo et al. 2009).

iii) Post-translational modifications (PTMs) modulate the activity of most eukaryote proteins due to PTM generate tremendous diversity, complexity and heterogeneity of gene products, and their determination is one of the main challenges in proteomics research (Mann and Jensen 2003). However, PTMs in plants remains almost unexplored with the exception of the phosphoproteome (Kersten et al. 2009).

iv) Interactomics, with the aim of unveiled the complex relationship between proteins and other molecules for a system biology approach (Braun et al. 2013). Hence, one of the most important goals of post-genomic research for defining gene function and understanding the function of macromolecular complexes involves creating 'interactome' maps from empirical or inferred datasets. Some high-throughput technologies have been applied to plant systems to increase the knowledge in plant interactomes, especially within selected plant models (Geisler-Lee et al. 2007), for which large ORF collections of full-length cDNAs are already available. This knowledge will greatly improve our understanding of the mechanisms that control protein interaction and organize molecular structures in plants (Braun et al. 2013).

v) Proteinomics (targeted or hypothesis-driven proteomics), aimed at studying a particular protein using a multiapproach strategy, within the complex network of molecular machinery in a biological process. In plants, proteinomics and interactomics remain the main challenges.

Proteomics methodologies have become routine protocols in many plant laboratories worldwide in plant biology research during the last decade, ushering the "second-generation plant proteomics". Hence, plant proteomics has witnessed a substantive increase in online resources, tools and repositories (Jorrin-Novo 2014; Jorrín-Novo and Valledor 2013; Jorrín-Novo et al. 2007; Jorrín-Novo et al. 2009; Sakata and Komatsu 2014). Thus, recently plant research studies have moved towards the use of new platforms, such as DIGE (Vera-Estrella et al. 2014) as well as quantitative approaches (iTRAQ, SILAC and gel-free) (Martínez-Esteso et al. 2014; Matthes et al. 2014; Yin et al. 2014). In addition, multiple reaction monitoring mass spectrometry (MRM) have greatly enhanced the specificity and sensitivity of MS-based assays permitting the absolute quantification of analytes (proteins, peptides) within complex mixtures in plant research studies (Kitteringham et al. 2009; Yan et al. 2014). Plants proteomics is nowadays making practical contributions to applied fields, such as biomedicine, agronomy through studies of the equivalence of transgenic crop (Salekdeh and Komatsu 2007), studies of heterosis (Kristensen et al. 2010) and food science, through studies of food quality control and traceability (Cifuentes 2012), among others. Several multinational coordinated projects are currently carrying out, such as the "Green Proteome" that is one of the major challenges for plant proteomics. One of its benefits

has been the establishment of a searchable database of MS/MS reference spectra derived from wide organism, including model plants (Arabidopsis, and *Medicago truncatula*) and crops, such as potato (*Solanum tuberosum*) and tomato (*Solanum lycopersicum*), among other plants (Wienkoop et al. 2012). This database is an important tool that allows reliable protein identification through a genome-independent approach, since newly generated MS/MS spectra can be matched against previous experimental MS/MS spectra. In addition, other initiatives that deserve to be mentioned are the plant proteomics in Europe (COST Action FA0603).

Nevertheless, proteomics techniques have a number of limitations, such as sensitivity and speed of data capture. Thus, despite the continuous development and improvement of powerful proteomic techniques, protocols, instruments and bioinformatic tools, just a minimal fraction of the cell proteomes, and for only a few organisms, have been characterized. This is mainly due to the enormous diversity and complexity of proteomes, and to technical limitations in quantification, sensitivity, resolution, speed of data capture, and analysis. In addition, some recalcitrant proteomes, such as highly hydrophobic proteins and protein trafficking are still an unresolved issues (Jarvis 2008; Lunn 2007). Thus, some proteins have been identified at the "apparently wrong" location (Millar et al. 2006). Moreover, some questions are starting to be answered, including the potential number of protein species per gene as a result of posttranscriptional and posttranslational modifications, protein trafficking and interactions events.

A proteomic workflow includes the following steps: experimental design, sampling, sample preparation, protein extraction/fractionation/purification, labeling/modification, separation, MS analysis, protein identification, and statistical analysis of data and validation (Fig. 11). The protocols to be used depends on the objectives of the research (descriptive, comparative, PTMs, interactions, proteinomics) and must be optimized for the biological system (i.e. plant species, organ, tissue, cells) (Jorrin-Novo et al. 2008; Jorrín-Novo 2009; Jorrín-Novo et al. 2009). An appropriate experimental design, followed by decisive statistical methods is mandatory to extract all the information of any proteomic experiment (Lee and Cooper 2006; Valledor and Jorrín 2011; Valledor et al. 2014) and several tools have been developed for evaluating the success of current designs and for predicting the performance of future, better-

designed proteomics experiments (Eriksson and Fenyo 2007; Galetskiy et al. 2008). This simulation provides a holistic view of a general analytical experiment and attempts to identify the factors that affect the success rate. Thus, several parameters must be analyzed to simulate the steps of a proteome analysis: i) the distribution of protein amounts in the sample analyzed:; ii) the loss of analyte material and the maximal limit of the amount loaded at each step of sample manipulation (e.g. separation, digestion, and chemical modification); iii) the dynamic range, the detection limit and the losses associated with MS analysis. In addition, the establishment of an adequate number of replicates is crucial for any differential expression proteomics experiment, which should be set up while taking into account the dynamic nature of the proteome. This makes sense when searching for proteins that can be used as markers of disease or when looking for protein markers to develop plant breeding programmes.

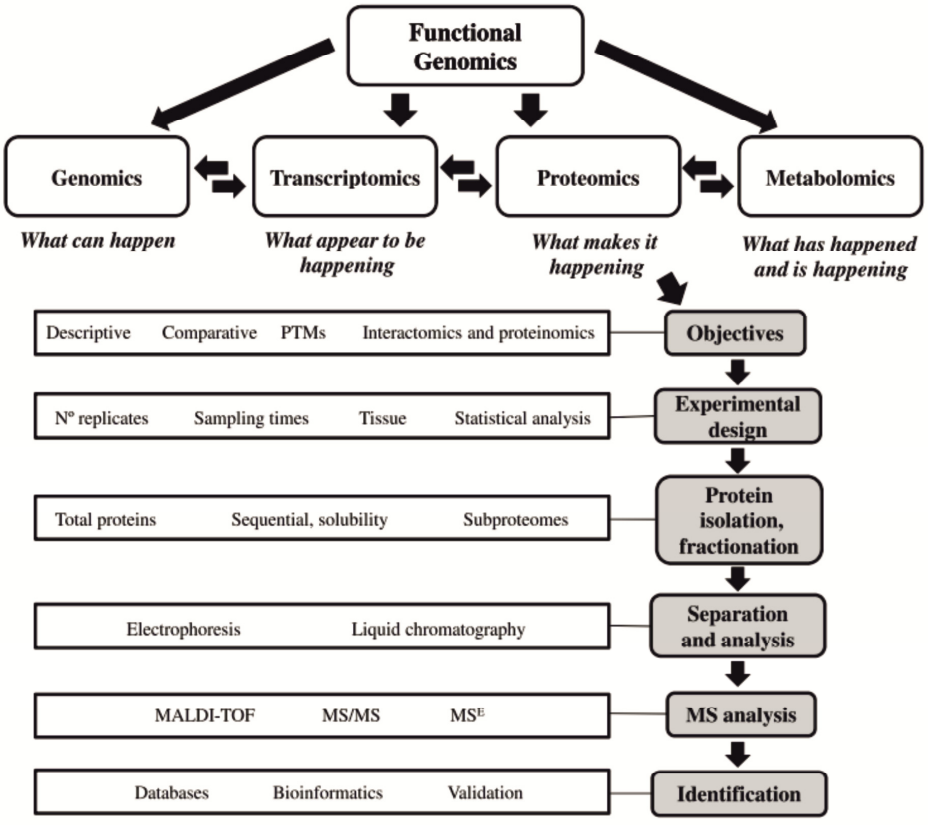

Figure 11. Interactions between the functional genomics approaches and standard workflow in a proteomic experiment. Proteomics have a central position in this scheme and several relevant steps are shown to analyze and characterize a biological system at the proteome level (modified from Jorrin-Novo et al., 2008; Baginsky 2009 and Dettmer et al. 2007).

Previously plant research works have analyzed plant proteomes determining the analytical and biological variability (Jorge et al. 2005; Valledor et al. 2008), as well as guidelines that described, in an understandable way, the current methodologies available to deal with all the stages of the experimental design, data processing and analysis (Valledor and Jorrín 2011).

The protein extraction protocol is a crucial step in a proteomic experiment. The following sentence summarized their importance: only if you can extract and solubilise a protein you have the chance to detect and identify it. In the plant proteomics is even more important, due to the low protein content relative to other systems, the presence of the cell wall and vacuoles that account for the majority of the cell mass, the presence of proteases and oxidative enzymes, and the accumulation of large quantities of polysaccharides, lipids, phenolics and other secondary metabolites (Isaacson et al. 2006; Martínez-Maqueda et al. 2013). An ideal extraction method should be highly reproducible and should extract the greatest number of protein species, while at the same time reducing the level of contaminants and minimizing artifactual protein degradation and modification (Maldonado et al. 2008; Wang et al. 2008). Two main types of extraction protocols have been used with plant material. First method involves tissue homogenisation in buffer-based media, while the second one uses organic solvent media (TCA-acetone, phenol, precipitation protocols), although both protocols can be combined. Since no single protein extraction protocol can capture the full proteome, the chosen protocol should be optimized for the particular plant tissue and research objective. In addition, due to the extreme complexity of the proteome and the large dynamic range in protein abundance, sample prefractionation is a good approach to solve these problems. In plant tissues one the major limitations is the great abundance of RuBisCO (ribulose-1,5-bisphosphate carboxylase/oxygenase), resulting in artifacts or false positives or impossibility to reach low abundance protein at worst. Hence, several research works have reported the applicability of RuBisCO depletion protocols, such as polyethylene glycol fractionation (Aryal et al. 2011; Xi et al. 2006), RuBisCO depletion columns for leaf proteomic analysis (Cellar et al. 2008) or specific precipitation (Kim et al. 2013).

The combination of SDS-PAGE, band cutting, trypsin digestion and LC separation of the resulting peptides remains the proteomic technique capable of providing the greatest protein coverage (Tribl et al. 2008). In addition, electrophoretic methods can be made compatible with chemical labeling in order to allow quantitative proteomics using such techniques as iTRAQ (Zieske 2006). Two-dimensional gel electrophoresis (2-DE) is by far the predominant separation technology, and it is continuously being evaluated and improved in the areas of separation of hydrophobic proteins (Braun et al. 2007), gel staining (Chakravarti et al. 2010; Wang et al. 2007), image capture and analysis (Grove et al. 2008; Komsta et al. 2011) and automation (Demianová et al. 2007). Recently, blue native polyacrylamide gel electrophoresis (BN-PAGE) has become very popular for analyzing membrane proteins and protein complexes (Wittig et al. 2006), which preserve the advantages of the technique and use it with in-gel fluorescent detection and in-gel catalytic activity assays. In BN-PAGE, coomassie dye in the cathode buffer can be replaced with non-coloured mixtures of anionic and neutral detergents (Van Leene et al. 2007). In addition, research works have reported have reported protocol for native 3-D electrophoresis that allows exhaustive separation and identification of membrane proteins (D'Amici et al. 2008).

Statistical analysis and validation of proteomic data is another issue in which proteomics has greatly evolved. First plant comparative proteomics research works have used arbitrary criteria (fold ratios) or univariate parametric and non-parametric statistical tests, namely Student's t-test or Mann–Whitney U-test to compare two groups and ANOVA or Kruskal–Wallis to compare more than two groups. However, these tests analyze individual spots instead of the complete set, omitting information about correlated variables. Multivariate data analysis methods, such as principal component analysis (PCA), are now used to pinpoint spots that differ between samples. These multivariate methods focus not only on differences in individual spots, but also on the covariance structure between proteins (Jacobsen et al. 2007). Nevertheless, the results of these methods are sensitive to data scaling, and they may fail to produce valid multivariate models due to the high number of spots in the gels that do not contribute to the discrimination process (Nedenskov Jensen et al. 2008). One of the limitations of PCA analysis is that it does not allow missing values, a problem that can be avoided by imputing them when possible (if enough replicates are available) (Albrecht et al. 2010). In contrast to these multivariate methods, univariate tests increase the number of false

positives, and for each species, a measure of significance reflecting rates of false discovery should be calculated. This measure of significance is called a q value (Karp et al. 2007). Moreover, proteomic data should be validated in order to go beyond description or speculation. Thus, HUPO's proteomic standard initiative has developed the "minimum information about a proteomics experiment" (MIAPE) documents (Taylor et al. 2007) to develop a guidance modules that to encourage the standardized collection, integration, storage and dissemination of proteomics data. The establishment of repositories containing MS/MS reference spectra will be very useful and will contribute to facilitate protein identification and quantification via a genome-independent approach, especially in the case of orphan species.

Despite the continuous development and improvement of powerful proteomic techniques, protocols, equipments and bioinformatic tools, just a minimal fraction of the cell proteome, and for only a few organisms, has been characterized so far. This is mainly related to the enormous diversity and complexity of proteomes, and to technical limitations in quantitation, sensitivity, resolution, speed of data capture and analysis. Specially, plant biology research is far from fully exploiting the potential of proteomics. Thanks to completion of plant genomes their annotation into plant databases and the new bioinformatic tools have allowed to grow the plant proteomics research, increasing confidence in protein identification and characterization.

3.3.1. One and two-dimensional electrophoresis

The proteome represents the array of proteins that are expressed in a biological compartment at a particular time, under a particular set of conditions. Because proteins are key structural and functional molecules, molecular characterization of proteomes is necessary for a complete understanding of biological systems. Hence, large-scale, comprehensive analysis of proteins is the main aim of proteomics. Electrophoresis separation proteins was introduced in the early 70s (Laemmli 1970) and soon became very widely used by protein biochemists. Two high-performance electrophoretic separations of proteins were available: i) zone electrophoresis of proteins in the presence of SDS, as described in its almost final form by Laemmli (Laemmli 1970), a technique that instantly became very popular, and still is, and ii) denaturing isoelectric

focusing, as described for example by Gronow and Griffith (Gronow and Griffiths 1971). In 1975, the first successful two-dimensional electrophoresis method that included both separation parameters (molecular weight and isoelectric point), was published (Macgillivray and Wood 1974). O'Farrell changed the situation dramatically one year later, with the seminal paper of O'Farrell (O'Farrell 1975), which coupled better technical choices increasing the resolution as, as expected, much greater than with other two-dimensional techniques separately. However, two core features of these early days had very strong consequences. The first is the rather poor reproducibility of isoelectric focusing with carrier ampholytes, which is prone to several problems such as cathodic drift (Righetti 1983). Hence, methods allowing to run several gels in parallel were developed to increase sample to sample reproducibility, and this parallelicity is still very widely used today (Anderson and Anderson 1978). The second one was the absence of techniques enabling to identify a specific protein spot on a 2D gel. In the 80´s the intense researches carried out overcoming these pitfalls, on the one hand with the introduction of immobilized pH gradients (Görg et al. 1988; Görg et al. 1987) and on the other hand with protein identification with Edman sequencing (Aebersold et al. 1987).

One-dimensional gel electrophoresis, in combination with appropriate software, is a powerful proteomics tool that provides information about the molecular size, amount, and purity of a protein sample (Fig. 12 b). This proteomic approach is a simple and reliable technique for finger-printing crude plant extracts (Supek et al. 2008), and is especially useful in the case of hydrophobic and low-molecular-weight proteins. Separated proteins can be recovered from polyacrylamide gels for subsequent characterization by a variety of secondary techniques, such as mass spectrometry to determine post-translational modifications and the amino acid sequence. Protein separations in vertical slab gels are performed in a variety of formats. Most recently, small format minigels are typical due to their ease of use, low relative cost, and ready commercial availability. Larger gels provide more separation area and thus better resolution for complex samples and continue to be in use for specialized analysis. This methodology have been applied successfully in plant protein extracts, including forest plant (Galván et al. 2011), crops (Gupta and Shepherd 1990; Krochko and Bewley 1990), among others. The combination of Sodium Dodecyl Sulfate-Polyacrylamide Gel Electrophoresis (SDS-PAGE), band cutting, trypsin digestion and LC separation of the

resulting peptides remains the proteomic technique capable of providing the greatest protein coverage (de Godoy et al. 2006; Han et al. 2001). In addition, electrophoretic methods can be made compatible with chemical labeling in order to allow quantitative proteomics using such techniques as iTRAQ (Lengqvist et al. 2007).

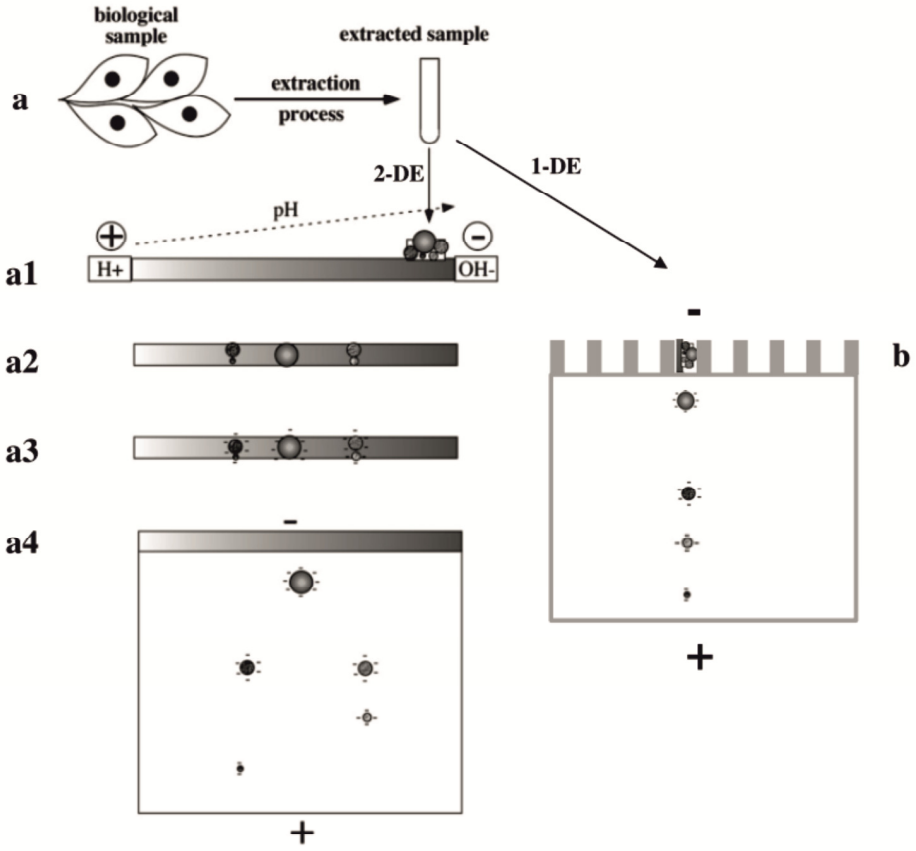

Figure 12. Scheme of principle of gel electrophoresis. **(a)** The total process starts with the extraction of proteins from the biological sample to get an extract compatible with electrophoretic methods. **(b)** In one-dimensional gel electrophoresis assays, the sample is loaded onto gel and the proteins are separated according to their molecular masses. In the case of two-dimensional gel electrophoresis experiments, the protein extracts is loaded onto a pH gradient **(a1)** oriented with the acidic side at the anode and the basic side at the cathode. **(a2)** After the IEF step, the proteins have reached their p*I* and thus have no remaining electrical charge. **(a3)** The strip is then equilibrated in a SDS-containing buffer, so that all proteins become strongly negatively charged. **(a4)** The IEF gel is then loaded on top of a SDS PAGE gel, and the proteins are separated according to their molecular masses. After this step, the proteins are detected directly on the gel (modified from Rabilloud and Lelong 2011).

Two-dimensional gel electrophoresis (2-DE) with immobilized pH gradients (IPGs) is by far the predominant separation technology (Rabilloud and Lelong 2011), and it is continuously being evaluated and improved in the areas of separation of hydrophobic proteins (Braun et al. 2007), gel staining (Harris et al. 2007; van den Broeck et al. 2008), image capture and analysis (Berth et al. 2008; Dunn et al. 2008; Maurer 2006) and automation (Demianová et al. 2007) (Fig. 12 a, a1 to a4). 2-DE is not without numerous technical difficulties and inadequacies. Thus, there are problems associated with reproducibility, resolution, proteins with extremes of p*I* (isoelectric point), recovery of hydrophobic proteins and large molecular weight proteins, poor representation of low abundance proteins, visualization methods, analysis and normalization of images and, finally, compatibility with mass spectrometric techniques that are generally employed in the identification of protein species of interest (Görg et al. 2000). Pre-electrophoretic subfractionation has proved a successful approach towards the simplification of protein mixtures (Butt et al. 2001). Specially, prefractionation of proteins with Triton-X114, chloroform/methanol or sodium carbonate washes, and sequential extraction by detergents can partly resolve the solubilization of protein (Santoni et al. 2000). From them, the most criticisms of 2-DE is its low precision, with relative standard deviations reported to fall in the range of 15–70%. The major source of variability for this technique can be attributed to the transfer between the first and the second dimension, the analyst's expertise and the detection of separated proteins (Valcu and Valcu 2007), as well as the irregular changes in the background signal from gel to gel, this can be solved using fluorescence labeling. To compare 2-DE maps between samples, which could be analytical or biological replicates, cells, tissues, organs or treatments, plant proteomic papers prior to the reviewed period used arbitrary criteria (fold ratios) or univariate parametric and non-parametric statistical tests, namely Student's t-test or Mann–Whitney U-test to compare two groups and ANOVA or Kruskal–Wallis to compare more than two groups. Nevertheless, these tests analyze individual spots instead of the complete set, omitting information about correlated variables. Multivariate data analysis methods, such as principal component analysis (PCA), are now used to pinpoint spots that differ between samples, which focus not only on differences in individual spots, but also on the covariance structure between proteins (Jacobsen et al. 2007). However, the results of these methods are sensitive to data scaling, and they may fail to produce valid multivariate models due to the high number of spots in the gels that do not contribute to

the discrimination process (Nedenskov Jensen et al. 2008). In contrast to these multivariate methods, univariate tests increase the number of false positives, and for each species, a measure of significance reflecting rates of false discovery should be calculated. This measure of significance is called a q value, which has been described by Karp et al. (Karp et al. 2007).

Blue native polyacrylamide gel electrophoresis (BN-PAGE) can be used for one-step isolation of protein complexes from biological membranes and total cell and tissue homogenates. In addition, BN-PAGE can also be used to determine native protein masses and oligomeric states and to identify physiological protein–protein interactions. By BN-PAGE, native complexes are recovered from gels by electroelution or diffusion and are used for 2D crystallization and electron microscopy or analyzed by in-gel activity assays or by native electroblotting and immunodetection (Wittig et al. 2006). This methodology has become very popular for analysing membrane proteins and protein complexes, but in some cases, as in the analysis of chloroplast light-harvesting complexes (LHC), it shows poor resolution, especially for proteins in the range of 22–25 kDa (Gómez et al. 2002). In order to preserve the advantages of the technique and use it with in-gel fluorescent detection and in-gel catalytic activity assays, Coomassie dye in the cathode buffer can be replaced with non-coloured mixtures of anionic and neutral detergents (Van Leene et al. 2007). In addition, new approaches in protein electrophoresis have been described, such as 3D native electrophoretic protocol proposed by D'Amici et al. (D'Amici et al. 2008), which allows exhaustive separation and identification of membrane proteins. This is based on native liquid phase isoelectrofocusing (N-LP-IEF) of protein complexes in the first dimension, followed by blue native polyacrylamide gel electrophoresis (BN-PAGE) in the second dimension, where both the p*I* and the molecular masses of protein complexes (2D N-LP-IEF-BN) were used to separate them in their native form. Finally, each single component can be resolved using denaturing electrophoresis (3D N-LP-IEF-BN-SDS-PAGE).

Despite the many advances and improvements in alternative separation technologies over the intervening years, 2-DE is still the method of choice to investigate a cell's/organism's proteome, as it is capable of resolving perhaps 3000 individual protein spots on a single gel (Lilley et al. 2002). This capability has led to its almost universal use to resolve the multitude of different proteins in a cell or tissue. Since the

spots (features) identified are now essentially pure, these spots can be picked (purified), proteolytically or chemically digested, and the resulting peptides used to identify the protein(s) present in the original spot using a mass spectrometric technique (Aebersold and Mann 2003). In all cases, the downstream processes rely absolutely on the ability to obtain maximum resolution of as many proteins as possible over the two-dimensional gel to reduce the possibility of cross-contamination with closely migrating protein spots.

3.3.2. Mass spectrometry

Mass spectrometry (MS)-based proteomics is the study of the entire complement of proteins and their modifications expressed by a given cell, subcellular compartment, tissue, or whole organism (Dettmer et al. 2007; Van Riper et al. 2013). MS has simplified protein analysis and characterization, and several important and recent innovations have extended their capabilities (Vaudel et al. 2014). Hence, MS has become the analytical technology of choice to analyze biological systems and to reveal their complex functions and interactions (Reinders et al. 2004). Nowadays, it is possible to measure the mass of proteins and peptides at the fmol level using MS with high accuracy, and to identify efficiently a number of proteins using software developed for proteome research. In addition, MS is also used frequently in the analysis of the protein expression, post-translational modification and protein–protein interaction. Thanks to the ability of mass spectrometry to identify and, increasingly, to precisely quantify thousands of proteins from complex samples can be expected to impact broadly on biology.

In spite of 2DE is an powerful proteomic tool, it`s an descriptive technique. Thus, a reliable technique for the identification of the separated protein species is necessary. At early 1990s two revolutionary techniques was developed, matrix-assisted laser desorption ionization (MALDI) time-of-flight (TOF) MS techniques, (Hillenkamp et al. 1991; Karas and Hillenkamp 1988) and electrospray ionization (ESI) (Dewald 1999; Fenn et al. 1989) MS and tandem mass spectrometry (MS/MS) replaced the slower and less sensitive chemical degradation methods (Aebersold et al. 1987; Lin et al. 1988) as the methods of choice for the identification of proteins separated by 2DE (Dunn and Corbett 1996; Shevchenko et al. 1996). Mass spectrometry has made rapid progress as an analytical technique, particularly over the last decade, with many new types of

instrumentation being introduced. Constant refinements to sensitivity, selectivity and mass measurement accuracy have transformed mass spectrometry, leading to its wide scale uptake by the life sciences community with many reviews being published on the method of mass spectrometry and its applications to biological sciences. Recent reviews have surveyed the type of instrumentation that is currently dedicated to proteomics research and the wide range of proteomes investigated (Van Riper et al. 2013; Vaudel et al. 2014).

The principles of mass spectrometry can be envisaged by four functions of the mass spectrometer, ionization, separation of ions by mass, measurement of mass and measurement of abundance. Mass spectrometers consist of three essential parts, ion source, mass spectrometer and ion detector. The first, an ionization source, converts molecules into gas-phase ions. Once ions are created, individual mass-to-charge ratios (m/z) are separated by a second device, a mass analyzer, and transferred to the third, an ion detector. Ionization is fundamental as the physics of mass spectrometry relies upon the molecule of interest being charged, resulting in the formation of either a positive ion or negative ion. Whilst this is a strength of the technique it is also a weakness, as the connection between ‘‘the ion’’ and the neutral moiety it must represent may be removed as ionization is a suprathermal process imparting internal energy to the ion which can lead to rearrangement and even fragmentation. Upon ionization a molecular ion species (generally an adduct ion) is formed and, depending on the ionization method, fragment ions may also be created. A range of ionization techniques are available (Table 1), together with their principal attributes and suitability for proteomic study. The most used methods in ionization of proteins and peptides, in the ion source, are matrix-assisted laser desorption ionization (MALDI) and electrospray ionization (ESI). MALDI creates ions by excitation of molecules that are isolated from the energy of the laser by an energy absorbing matrix. The laser energy strikes the crystalline matrix to cause rapid excitation of the matrix and subsequent ejection of matrix and analyte ions into the gas-phase. ESI creates ions by application of a potential to a flowing liquid causing the liquid to charge and subsequently spray. The electrospray creates very small droplets of solvent-containing analyte. Solvent is removed as the droplets enter the mass spectrometer by heat or some other form of energy (e.g. energetic collisions with a gas), and multiply-charged ions are formed in the process. ESI together with its low-flow variants, such as nanoflow-ESI, continues to dominate as one of the two preferred

ionization methods for proteomics (Griffiths et al. 2001). The method involves spraying the multiply charged ions into a specially designed charge reduction chamber placed at the entrance of the mass spectrometer. It is also well established that the sensitivity of electrospray increases as the flow rate of the spray reduces: miniaturization of spray devices (Shen et al. 2003) has been described and their improvement on signal intensity in LC/MS applications has shown sub attomol detection limits can be achieved. In addition, other ionization techniques, such as Fourier transform ion cyclotron resonance MS (FT-MS) (Liu et al. 2014b), which allows analyzing the sequence information and post-translational modification of proteins automatically without preparation by 2-DE and liquid chromatography (LC).

Table 1. Main ionization techniques and mass analyzers types used in mass spectrometry and features (modified from Newton et al. 2004).

Ionization			
Technique	***Typical ions***	***Upper limit of mass range*** [a]	***Usage***
Electrospray (ESI)/microspray/nanospray	Multiply protonated $[M + nH]^{n+}$	10^5–10^6 u	Wide
Matrix-assisted laser desorption/ ionization (MALDI)	Singly protonated, $[M + H]^+$	10^5–10^6 u	Wide
Atmospheric pressure chemical ionization (APCI)	$[M + H]^+$	<2000 u	Small chemicals; excellent for quantitation
Atmospheric pressure photoionization (APPI)	M^+	<2000 u	Extends the compound range of APCI
Electron impact ionization	M^+	<3000 u	Synthetic/organic chemistry
Chemical ionization	$M + NH_4^+$	<2000 u	Synthetic/organic chemistry
Mass analyzers			
Ttype	***Measures***	***Mass-to-charge (m/z) range***	***Mass measurement accuracy (ppm)*** [b]
Magnetic sector	Momentum-to-charge	10^4	2-5
Quadrupole	Path stability	10^4	≈100
Ion trap (IT)	Frequency	10^3-10^4	≈100
Time-of-flight (TOF)	Flight time	10^6	5-10
Fourier-transform ion cyclotron resonance (FTICR)	Cyclotron frequency	10^5	1-2

The mass analyzer is, literally and figuratively, central to the technology. In the context of proteomics, its key parameters are sensitivity, resolution, mass accuracy and the ability to generate information-rich ion mass spectra from peptide fragments (tandem mass or MS/MS spectra). The mass analyzer uses a physical property [e.g. electric or magnetic fields, or time-of-flight (TOF)] to separate ions of a particular m/z value that then strike the ion detector. Thus, the ion species are separated according to their mass-to-charge (m/z) ratio, and the masses assigned from the measurement of some physical parameter. Usually the mass is measured to better than 0.4 u so that a

nominal mass can be assigned and in certain cases the mass is measured to much higher accuracy so that an accurate mass measurement is made. The latter is usually necessary when the elemental composition is required and can be applied to molecules of MW <800 u (above this mass there are usually too many combinations of the elements, for any given mass, to assign a unique elemental formula). Five principal types of mass analyzer are most used (Table 1). The magnetic sector mass analyzer is included here on a historical basis; while not suitable for proteome study it is still a very good choice of analyzer for single sample analysis (MW <3000 u). The remaining four analyzers are: quadrupole; ion trap (IT) [either quadrupole ion trap (QIT) or linear quadrupole ion trap (LQIT)]; time-of-flight (TOF); and Fourier-transform ion cyclotron resonance (FTICR) (Table 1). These analyzers can be stand alone or, in some cases, put together in tandem to take advantage of the strengths of each. In ion-trap analyzers, the ions are first captured or 'trapped' for a certain time interval and are then subjected to MS or MS/MS analysis. Ion traps are robust, sensitive and relatively inexpensive, and so have produced much of the proteomics data reported in the literature. A disadvantage of ion traps is their relatively low mass accuracy, due in part to the limited number of ions that can be accumulated at their point-like centre before space-charging distorts their distribution and thus the accuracy of the mass measurement. In the 'linear' or 'two-dimensional ion trap' (Hager 2002; Schwartz et al. 2002) the ions are stored in a cylindrical volume that is considerably larger than that of sections are separated by a collision cell ('TOF-TOF instrument') (Medzihradszky et al. 1999), whereas in the second, the hybrid quadrupole TOF instrument, the collision cell is placed between a quadrupole mass filter and a TOF analyzer (Loboda et al. 2000). Ions of a particular m/z are selected in a first mass analyzer (TOF or quadrupole), fragmented in a collision cell and the fragment ion masses are 'read out' by a TOF analyzer. These instruments have high sensitivity, resolution and mass accuracy, and the quadrupole TOF instrument can be used interchangeably with an ESI ionization source. The resulting fragment ion spectra are often more extensive and informative than those generated in trapping instruments. Although TOF, ion-trap and hybrid TOF instruments dominate proteomics today, other configurations including linear ion traps and FT-MS instruments are also widespread in the mass spectrometry laboratories.

Proteomics would be impossible without software tools to correlate mass spectrometric data with sequence databases. Existing database searching programs have become both more sophisticated and (Web) accessible. Thus, automated protein identification is possible by database searching using several algorithms, such as Sequest (Eng et al. 1994), MASCOT (Perkins et al. 1999), PeptideSearch (Mann and Wilm 1994), PROWL (Qin et al. 1997), and Protein Prospector (Clauser et al. 1999). Each protein sequence from the database is virtually digested according to the specificity of the used protease and the resulting peptides that match the measured mass of the peptide ion are identified. In the next step, the experimentally derived tandem mass spectrum of the peptide ion is compared to the theoretical MS/MS spectra obtained by virtual fragmentation of candidate peptide sequences. Finally, a score is calculated for each peptide sequence by matching the predicted fragment ions to the ions observed in the experimental spectrum. When a preponderance of the fragment ions matches, it is considered a good fit.

In most MS analyses such as MALDI-TOF MS, ESI Q-TOF MS and ESI IT MS, the proteins are analyzed after digestion with protease into the peptides, because large molecular weight of proteins cannot be analyzed directly. This approaches are called ‘‘bottom-up proteomics’’. MALDI-TOF instruments have been used in numerous projects for large-scale protein identification by the peptide mass mapping technique. In this method, proteins are identified by matching a list of experimental peptide masses with the calculated list of all peptide masses of each entry in a database (for example, a comprehensive protein database). Because mass mapping requires an essentially purified target protein, the technique is commonly used in conjunction with prior protein fractionation using either one- or two-dimensional gel electrophoresis (1DE and 2DE, respectively). This technique has been particularly successful for the identification of proteins from species with smaller and completely sequenced genomes (Patterson and Aebersold 1995; Yates 2000). The addition of sequencing capability to the MALDI method should make protein identifications by MALDI-MS/MS more specific than those obtained by simple peptide-mass mapping. It should also extend the use of MALDI to the analysis of more complex samples, thereby uncoupling MALDI-MS from 2DE. However, if MALDI-MS/MS is to be used with peptide chromatography, the effluent of a liquid chromatography run must be deposited on a sample plate and mixed with the MALDI matrix, a process that has thus far proven difficult to automate. In

addition, shotgun proteomics techniques have allowed carrying out a rapid analysis of the entire protein complement of whole organelles, cells, and tissues (Kleffmann et al. 2004; Millar 2007; Wienkoop et al. 2004). This process fully automates the separation and identification of proteins from complex mixtures (Washburn et al. 2001). The method includes chemical or enzymatic (e.g. tryptic) digestion of proteins to generate a highly complex set of peptides that is well beyond the separation capacity of 1D separation techniques. This ‘‘bottom-up’’ approach takes advantage of the higher separation efficiency of chromatographic techniques on the peptide rather than the protein level. In addition, the use of highly accurate mass, such as FT-MS has been reported in the analysis of several plant proteomes, such as the citrus fruit proteome (Katz et al. 2007) or the chloroplast envelope of pea and maize (Bräutigam et al. 2008), among others.

3.3.3. Proteomics in the study of plant stresses

Plants have evolved to live in environments where they are often exposed to different stress factors in combination. Being sessile, they have developed specific mechanisms that allow them to detect precise environmental changes and respond to complex stress conditions, minimizing damage while conserving valuable resources for growth and reproduction. Plants activate a specific and unique stress response when subjected to a stresses (Mittler 2006; Rizhsky et al. 2004). Thus, plant responses to different stresses are highly complex and involve changes at the transcriptome, cellular, and physiological levels. Recent evidence shows that plants respond to multiple stresses differently from how they do to individual stresses, activating a specific programme of gene expression relating to the exact environmental conditions encountered (Kushalappa and Gunnaiah 2013; Liu et al. 2014a; Rodziewicz et al. 2014). Proteomics is a powerful tool that provides a more direct assessment of the biochemical processes of monitoring the actual proteins performing the signalling, enzymatic, regulatory and structural functions encoded by the genome and transcriptome. The improvements in high-resolution 2-DE (Görg et al. 2000; Görg et al. 1999; Rabilloud 2014; Zolla and Timperio 2005), an increase in the number of sequences of protein and nucleotides, increased capabilities for protein identification using modern mass spectrometry methods, such as matrix-assisted laser desorption ionization time-of-flight (MALDI-

TOF) mass spectrometry (Agrawal et al. 2013; Pappin et al. 1993) and valuable bioinformatic tools, have made the large-scale profiling and identification of proteins a dynamic area of renewed plant research.

Several studies have reported the plant responses at different extreme environmental conditions such as salinity (Kosová et al. 2013; Yan et al. 2005), drought (Jorge et al. 2006; Larrainzar et al. 2014; Larrainzar et al. 2007), cold (Shi et al. 2014), heat (Liu et al. 2014a), ozone (Agrawal et al. 2002; Vanzo et al. 2014), UV light (Casati et al. 2005; Zhang et al. 2013), heavy metals (Visioli and Marmiroli 2013), nutrient deficiencies (Kang et al. 2004), as well as biotic stress such as, fungal (Curto et al. 2006; Kroll et al. 2014), aphid (Carrillo et al. 2014), bacterial (Jorrín et al. 2006; Schmidt et al. 2014) and viral infections (Díaz-Vivancos et al. 2008). These studies all together have given rise to a specific field, 'environmental proteomics'. Now, there is a good amount of work to answer about the types of proteins under- and/or over-expressed during a particular or integrative stress, their impacts on cellular metabolism and the location of the proteins. The same is true regarding the organs on different plant organs (Dam et al. 2014; Watson et al. 2003) and on subcellular proteomes such as the chloroplast membrane (Gutierrez-Carbonell et al. 2014; Zolla et al. 2004), cell wall (Albenne et al. 2013; Minic et al. 2007) and nuclear envelope (Bae et al. 2003), whereas other researchers have focused on individual tissues, including seeds (Yacoubi et al. 2013), mitochondria (Huang et al. 2014), barrel medic roots (Abdallah et al. 2014; Mathesius et al. 2001), vacuoles (Jaquinod et al. 2007), chloroplasts (Kleffmann et al. 2004) and thylakoids (Aro et al. 2005; Zolla et al. 2003), among others.

In the field of plant stress research, the most common case is comparison of proteomes isolated from non-stressed (control) plants and the corresponding proteomes upon stress conditions by differential-expression proteomics. Other cases include comparison of proteomes from two different genotypes or plant species with contrasting levels of tolerance to a given stress factor. The studies aimed at comparison of several proteomes are mostly dominated by 2-DE followed by protein identification via MS analysis, although the sole use of MS techniques not only for protein identification, but also for protein quantitation is sometimes applied (Patterson et al. 2007) used iTRAQ for protein quantitation in two barley cultivars with different sensitivity to elevated concentrations of boron.

Two main protein categories are founded in differential-expression proteomic studies: (i) defense or stress-related proteins and (ii) enzymes associated with the metabolism of carbon and nitrogen, and secondary metabolism. The first group included wide protein families, including pathogenesis-related proteins (PR) (glucanases, chitinases, proteases and protease inhibitors), antioxidants (glutathione-S-transferases, catalases, superoxide-dismutase and peroxidases), chaperones and heat shock proteins (HSP), among others. Moreover, the second group included enzymes associated either with carbohydrate assimilation and primary metabolism (photosynthesis, glycolysis and Krebs cycle), nitrogen assimilation or secondary metabolism. Several review articles have reported that plants showed similar defence strategies against a broad range of pathogens, such as bacteria, fungi or parasitic plants responses (Dangl and Jones 2001; Kliebenstein 2014). Thus, as general rule the PR proteins, stress- related proteins and antioxidant enzymes increased in the resistant genotypes, while a decrease in enzymes of the photosynthesis and energetic metabolism is observed in the susceptible ones (Alam et al. 2010; Hajheidari et al. 2007). However, several studies have shown that primary metabolism could be reconfigured to support the increased demands of the resistance response (Berger et al. 2007; Bolton 2009). In addition, the PR and stress related proteins have been found well represented in plant tissues even in absence of stress, supporting the idea that they are part of the constitutive defence machinery of plants (Alvarez et al. 2006; Alvarez et al. 2008; Haslam et al. 2003; Jamet et al. 2008). Proteins involved in signal transduction and gene regulation, such as transcription factors, are also commonly found in stress studies, as they play an important role in the plant defence response (Gechev et al. 2006; González-Verdejo et al. 2007; Madrid et al. 2010; Singh et al. 2002). Hence, proteomics approaches on stress response even more complex.

4. References

Abbott MA, Poiesz BJ, Byrne BC, Kwok S, Sninsky JJ, Ehrlich GD (1988) Enzymatic gene amplification: Qualitative and quantitative methods for detecting proviral DNA amplified in vitro. J Infect Dis 158:1158-1169

Abdallah C, Valot B, Guillier C, Mounier A, Balliau T, Zivy M, van Tuinen D, Renaut J, Wipf D, Dumas-Gaudot E, Recorbet G (2014) The membrane proteome of *Medicago truncatula* roots displays qualitative and quantitative changes in response to arbuscular mycorrhizal symbiosis. J Proteomics 108:354-368

Aebersold R, Mann M (2003) Mass spectrometry-based proteomics. Nature 422:198-207

Aebersold RH, Leavitt J, Saavedra RA, Hood LE, Kent SB (1987) Internal amino acid sequence analysis of proteins separated by one- or two-dimensional gel electrophoresis after in situ protease digestion on nitrocellulose. Proc Natl Acad Sci USA 84:6970-6974

Agrawal GK, Rakwal R, Yonekura M, Kubo A, Saji H (2002) Proteome analysis of differentially displayed proteins as a tool for investigating ozone stress in rice (*Oryza sativa* L.) seedlings. Proteomics 2:947-959

Agrawal GK, Sarkar A, Righetti PG, Pedreschi R, Carpentier S, Wang T, Barkla BJ, Kohli A, Ndimba BK, Bykova NV, Rampitsch C, Zolla L, Rafudeen MS, Cramer R, Bindschedler LV, Tsakirpaloglou N, Ndimba RJ, Farrant JM, Renaut J, Job D, Kikuchi S, Rakwal R (2013) A decade of plant proteomics and mass spectrometry: Translation of technical advancements to food security and safety issues. Mass Spectrom Rev 32:335-365

Agrios GN (2005) Plant Pathology. (5th Ed). Elsevier Academic Press, ISBN: 13: 978-0120445653, San Diego, CA

Alam I, Sharmin S, Kim K-H, Yang J, Choi M, Lee B-H (2010) Proteome analysis of soybean roots subjected to short-term drought stress. Plant Soil 333:491-505

Albenne C, Canut H, Jamet E (2013) Plant cell wall proteomics: the leadership of Arabidopsis thaliana. Front Plant Sci 4

Albrecht D, Kniemeyer O, Brakhage AA, Guthke R (2010) Missing values in gel-based proteomics. Proteomics 10:1202-1211

Alvarez M, Vila-Ortiz G, Salibe M, Podhajcer O, Pitossi F (2007) Model based analysis of real-time PCR data from DNA binding dye protocols. BMC Bioinformatics 8:85

Alvarez S, Goodger JQD, Marsh EL, Chen S, Asirvatham VS, Schachtman DP (2006) Characterization of the maize xylem sap proteome. J Proteome Res 5:963-972

Alvarez S, Marsh EL, Schroeder SG, Schachtman DP (2008) Metabolomic and proteomic changes in the xylem sap of maize under drought. Plant Cell Environ 31:325-340

Ameline-Torregrosa C, Cazaux M, Danesh D, Chardon F, Cannon SB, Esquerré-Tugayé M-T, Dumas B, Young ND, Samac DA, Huguet T, Jacquet C (2008) Genetic dissection of resistance to anthracnose and powdery mildew in *Medicago truncatula*. Mol Plant-Microb Interact 21:61-69

Anderson NL, Anderson NG (1978) Analytical techniques for cell fractions: XXII. Two-dimensional analysis of serum and tissue proteins: Multiple gradient-slab gel electrophoresis. Analyt Biochem 85:341-354

Ankeny RA, Leonelli S (2011) What's so special about model organisms? Stud Hist Philos Sci Part A 42:313-323

Aro E-M, Suorsa M, Rokka A, Allahverdiyeva Y, Paakkarinen V, Saleem A, Battchikova N, Rintamäki E (2005) Dynamics of photosystem II: a proteomic approach to thylakoid protein complexes. J Exp Bot 56:347-356

Aryal UK, Krochko JE, Ross ARS (2011) Identification of phosphoproteins in *Arabidopsis thaliana* leaves using polyethylene glycol fractionation, immobilized metal-ion affinity chromatography, two-dimensional gel electrophoresis and mass spectrometry. J Proteome Res 11:425-437

Bae MS, Cho EJ, Choi E-Y, Park OK (2003) Analysis of the *Arabidopsis* nuclear proteome and its response to cold stress. Plant J 36:652-663

Baginsky S, Gruissem W (2004) Chloroplast proteomics: potentials and challenges. J Exp Bot 55:1213-1220

Barilli E, Sillero JC, Moral A, Rubiales D (2009) Characterization of resistance response of pea (*Pisum* spp.) against rust (*Uromyces pisi*). Plant Breed 128:665-670

Barilli E, Sillero JC, Rubiales D (2010) Induction of systemic acquired resistance in pea against rust (*Uromyces pisi*) by exogenous application of biotic and abiotic inducers. J Phytopathol 158:30-34

Barilli E, Rubiales D, Gjetting T, Lyngkjaer MF (2014) Differential gene transcript accumulation in peas in response to powdery mildew (*Erysiphe pisi*) attack. Euphytica 195:1-16

Bastianelli D, Grosjean F, Peyronnet C, Duparque M, Régnier JM (1998) Feeding value of pea (*Pisum sativum*, L.) 1. Chemical composition of different categories of pea. Animal Sci 67:609-619

Bateson W (1909) Mendel's principles of heredity. Cambridge University Press. doi:citeulike-article-id:13252468

Belanger RR, Dik AJ, Bushnell WR, Carver TLW (2002) The powdery mildews: A Comprehensive treatise PUBD American Phytopathological Society (APS) Press, St Paul, Minn.

Bentley DR, Balasubramanian S, Swerdlow HP, Smith GP, Milton J, Brown CG, Hall KP, Evers DJ, Barnes CL, Bignell HR, Boutell JM, Bryant J, Carter RJ, Keira Cheetham R, Cox AJ, Ellis DJ, Flatbush MR, Gormley NA, Humphray SJ, Irving LJ, Karbelashvili MS, Kirk SM, Li H, Liu X, Maisinger KS, Murray LJ, Obradovic B, Ost T, Parkinson ML, Pratt MR, Rasolonjatovo IMJ, Reed MT, Rigatti R, Rodighiero C, Ross MT, Sabot A, Sankar SV, Scally A, Schroth GP, Smith ME, Smith VP, Spiridou A, Torrance PE, Tzonev SS, Vermaas EH, Walter K, Wu X, Zhang L, Alam MD, Anastasi C, Aniebo IC, Bailey DMD, Bancarz IR, Banerjee S, Barbour SG, Baybayan PA, Benoit VA, Benson KF, Bevis C, Black PJ, Boodhun A, Brennan JS, Bridgham JA, Brown RC, Brown AA, Buermann DH, Bundu AA, Burrows JC, Carter NP, Castillo N, Chiara E. Catenazzi M, Chang S, Neil Cooley R, Crake NR, Dada OO, Diakoumakos KD, Dominguez-Fernandez B, Earnshaw DJ, Egbujor UC, Elmore DW, Etchin SS, Ewan MR, Fedurco M, Fraser LJ, Fuentes Fajardo KV, Scott Furey W, George D, Gietzen KJ, Goddard CP, Golda GS, Granieri PA, Green DE, Gustafson DL, Hansen NF, Harnish K, Haudenschild CD, Heyer NI, Hims MM, Ho JT, Horgan AM, Hoschler K, Hurwitz S, Ivanov DV, Johnson MQ, James T, Huw Jones TA, Kang G-D, Kerelska TH, Kersey AD, Khrebtukova I, Kindwall AP, Kingsbury Z, Kokko-Gonzales PI, Kumar A, Laurent MA, Lawley CT, Lee SE, Lee X, Liao AK, Loch JA, Lok M, Luo S, Mammen RM, Martin JW, McCauley PG, McNitt P, Mehta P, Moon KW, Mullens JW, Newington T, Ning Z, Ling Ng B, Novo SM, O/'Neill MJ, Osborne MA, Osnowski A, Ostadan O, Paraschos LL, Pickering L, Pike AC, Pike AC, Chris Pinkard D, Pliskin DP, Podhasky J, Quijano VJ, Raczy C, Rae VH, Rawlings SR, Chiva Rodriguez A, Roe PM, Rogers J, Rogert Bacigalupo MC, Romanov N, Romieu A, Roth RK, Rourke NJ, Ruediger ST, Rusman E, Sanches-Kuiper RM, Schenker MR, Seoane JM, Shaw RJ, Shiver MK, Short SW, Sizto NL, Sluis JP, Smith MA, Ernest Sohna Sohna J, Spence EJ, Stevens K, Sutton N, Szajkowski L, Tregidgo CL, Turcatti G, vandeVondele S, Verhovsky Y, Virk SM, Wakelin S, Walcott GC, Wang J, Worsley GJ, Yan J, Yau L, Zuerlein M, Rogers J, Mullikin JC, Hurles ME, McCooke NJ, West JS, Oaks FL, Lundberg PL, Klenerman D, Durbin R, Smith

AJ (2008) Accurate whole human genome sequencing using reversible terminator chemistry. Nature 456:53-59

Berger S, Sinha AK, Roitsch T (2007) Plant physiology meets phytopathology: plant primary metabolism and plant–pathogen interactions. J Exp Bot 58:4019-4026

Berth M, Moser F, Kolbe M, Bernhardt J (2008) The state of the art in the analysis of two-dimensional gel electrophoresis images. Appl Microbiol Biotechnol 79:329-329

Blow N (2008) DNA sequencing: generation next-next. Nat Meth 5:267-274

Bolton MD (2009) Primary metabolism and plant defense–fuel for the fire. Mol Plant-Microb Interact 22:487-497

Boyd LA, Ridout C, O'Sullivan DM, Leach JE, Leung H (2013) Plant–pathogen interactions: disease resistance in modern agriculture. Trends Genet 29:233-240

Braun P, Aubourg S, Van Leene J, De Jaeger G, Lurin C (2013) Plant protein interactomes. Annu Rev Plant Biol 64:161-187

Braun R, Kinkl N, Beer M, Ueffing M (2007) Two-dimensional electrophoresis of membrane proteins. Anal Bioanaly Chem 389:1033-1045

Braun U (1987) A monograph of the Erysiphales (powdery mildews). Nova Hedwigia, Suplement 89:195–196

Bräutigam A, Hoffmann-Benning S, Weber APM (2008) Comparative proteomics of chloroplast envelopes from C3 and C4 plants reveals specific adaptations of the plastid envelope to C4 photosynthesis and candidate proteins required for maintaining C4 metabolite fluxes. Plant Physiol 148:568-579

Breker M, Schuldiner M (2014) The emergence of proteome-wide technologies: systematic analysis of proteins comes of age. Nat Rev Mol Cell Biol 15:453-464

Bretag T, Keane P, Price T (1995) Effect of ascochyta blight on the grain yield of field peas (*Pisum sativum L.*) grown in southern Australia. Aus J Exp Agr 35:531-536

Bretag TW, Ramsey M (2001) Foliar diseases caused by fungi. *Ascochyta* spp. In J. M. Kraft, & F. L. Pfleger (Eds.), Compendium of pea diseases and pests. Second edition (pp. 24–28). St Paul, Minnesota, USA: APS Press, The American Phytopathological Society.

Bustin S (2000) Absolute quantification of mRNA using real-time reverse transcription polymerase chain reaction assays. J Mol Endocrinol 25:169-193

Butt A, Davison MD, Smith GJ, Young JA, Gaskell SJ, Oliver SG, Beynon RJ (2001) Chromatographic separations as a prelude to two-dimensional electrophoresis in proteomics analysis. Proteomics 1:42-53

Canales RD, Luo Y, Willey JC, Austermiller B, Barbacioru CC, Boysen C, Hunkapiller K, Jensen RV, Knight CR, Lee KY, Ma Y, Maqsodi B, Papallo A, Peters EH, Poulter K, Ruppel PL, Samaha RR, Shi L, Yang W, Zhang L, Goodsaid FM (2006) Evaluation of DNA microarray results with quantitative gene expression platforms. Nat Biotech 24:1115-1122

Cao H, Yan X, Chen G, Zhou J, Li X, Ma W, Yan Y (2014) Comparative proteome analysis of A- and B-type starch granule-associated proteins in bread wheat (*Triticum aestivum* L.) and *Aegilops crassa*. J Proteomics.in press

Carrillo E, Rubiales D, Pérez-de-Luque A, Fondevilla S (2013) Characterization of mechanisms of resistance against *Didymella pinodes* in *Pisum* spp. Eur J Plant Pathol 135:761-769

Carrillo E, Rubiales D, Castillejo MA (2014) Proteomic analysis of pea (*Pisum sativum* L.) response during compatible and incompatible interactions with the pea aphid (*Acyrthosiphon pisum H.*). Plant Mol Biol Rep 32:697-718

Casati P, Zhang X, Burlingame AL, Walbot V (2005) Analysis of leaf proteome after UV-B irradiation in maize lines differing in sensitivity. Mol Cell Proteomics 4:1673-1685

Castillejo MA, Maldonado A, Dumas-Gaudot E, Fernandez-Aparicio M, Susin R, Diego R, Jorrin J (2009) Differential expression proteomics to investigate responses and resistance to *Orobanche crenata* in *Medicago truncatula*. BMC Genomics 10:294

Castillejo MA, Curto M, Fondevilla S, Rubiales D, Jorrín JV (2010a) Two-dimensional electrophoresis based proteomic analysis of the pea (*Pisum sativum*) in response to *Mycosphaerella pinodes*. J Agric Food Chem 58:12822-12832

Castillejo MÁ, Susín R, Madrid E, Fernández-Aparicio M, Jorrín JV, Rubiales D (2010b) Two-dimensional gel electrophoresis-based proteomic analysis of the *Medicago truncatula*–rust (*Uromyces striatus*) interaction. Ann Appl Biol 157:243-257

Castillejo MÁ, Fernández-Aparicio M, Rubiales D (2011) Proteomic analysis by two-dimensional differential in gel electrophoresis (2D DIGE) of the early response of *Pisum sativum* to *Orobanche crenata*. J Exp Bot

Cellar NA, Kuppannan K, Langhorst ML, Ni W, Xu P, Young SA (2008) Cross species applicability of abundant protein depletion columns for ribulose-1,5-bisphosphate carboxylase/oxygenase. J Chromatogr B 861:29-39

Cifuentes A (2012) Food Analysis: present, future, and foodomics. ISRN Anal Chem 2012:16

Clauser KR, Baker P, Burlingame AL (1999) Role of accurate mass measurement (±10 ppm) in protein identification strategies employing MS or MS/MS and database searching. Anal Chem 71:2871-2882

Coll NS, Epple P, Dangl JL (2011) Programmed cell death in the plant immune system. Cell Death Differ 18:1247-1256

Cook DR (1999) *Medicago truncatula* — a model in the making!: Commentary. Curr Opin Plant Biol 2:301-304

Crute IR, Pink D (1996) Genetics and utilization of pathogen resistance in plants. Plant Cell 8:1747-1755

Curto M, Camafeita E, Lopez JA, Maldonado AM, Rubiales D, Jorrín JV (2006) A proteomic approach to study pea (*Pisum sativum*) responses to powdery mildew (*Erysiphe pisi*). Proteomics 6:S163-S174

Curto M, Krajinski F, Schlereth A, Rubiales D (2014) Plant defense responses in *Medicago truncatula* unveiled by microarray analysis. Plant Mol Biol Rep, in press

Chakravarti B, Fathy P, Sindicich M, Mallik B, Chakravarti DN (2010) Comparison of SYPRO Ruby and Flamingo fluorescent stains for application in proteomic research. Anal Biochem 398:1-6

Charpe A (2014) DNA Microarray. In: Ravi I, Baunthiyal M, Saxena J (eds) Advances in Biotechnology. Springer India, pp 71-104. doi:10.1007/978-81-322-1554-7_6

Cheung F, Haas B, Goldberg S, May G, Xiao Y, Town C (2006) Sequencing *Medicago truncatula* expressed sequenced tags using 454 Life Sciences technology. BMC Genomics 7:272

Choi HW, Kim NH, Lee YK, Hwang BK (2013) The pepper extracellular xyloglucan-specific endo-β-1,4-glucanase inhibitor protein gene, *CaXEGIP$_1$*, is required for plant cell death and defense responses. Plant Physiol 161:384-396

D'Amici GM, Timperio AM, Zolla L (2008) Coupling of native liquid phase isoelectrofocusing and blue native polyacrylamide gel electrophoresis: A potent

tool for native membrane multiprotein complex separation. J Proteome Res 7:1326-1340

Dam S, Dyrlund TF, Ussatjuk A, Jochimsen B, Nielsen K, Goffard N, Ventosa M, Lorentzen A, Gupta V, Andersen SU, Enghild JJ, Ronson CW, Roepstorff P, Stougaard J (2014) Proteome reference maps of the *Lotus japonicus* nodule and root. Proteomics 14:230-240

Dangl JL, Jones JDG (2001) Plant pathogens and integrated defence responses to infection. Nature 411:826-833

Davies DR, Berry GJ, Heath MC, Dawkins TCK (1985) Pea (*Pisum sativum L.*), pages 147-198. In: Grain legume crops, ed. R. J. Summerfield and E. H. Roberts (eds.). London: Collins Sons & Co. Ltd.

de Godoy L, Olsen J, de Souza G, Li G, Mortensen P, Mann M (2006) Status of complete proteome analysis by mass spectrometry: SILAC labeled yeast as a model system. Genome Biol 7:R50

De Lorenzo G, Brutus A, Savatin DV, Sicilia F, Cervone F (2011) Engineering plant resistance by constructing chimeric receptors that recognize damage-associated molecular patterns (DAMPs). FEBS Lett 585:1521-1528

De Wit PJGM, Mehrabi R, Van Den Burg HA, Stergiopoulos I (2009) Fungal effector proteins: past, present and future. Mol Plant Pathol 10:735-747

Demianová Z, Shimmo M, Pöysä E, Franssila S, Baumann M (2007) Toward an integrated microchip sized 2-D polyacrylamide slab gel electrophoresis device for proteomic analysis. Electrophoresis 28:422-428

Dénarié J (2002) Genomics and genetics of *Medicago truncatula*: resources for legume crop improvement. Grain Legumes 38:20-21

Dettmer K, Aronov PA, Hammock BD (2007) Mass spectrometry-based metabolomics. Mass Spectrom Rev 26:51-78

Dewald HD (1999) Electrospray ionization mass spectrometry: Fundamentals, Instrumentation and Applications (ed. Cole, Richard B.). J Chem Educ 76:33

Díaz-Vivancos P, Clemente-Moreno MJ, Rubio M, Olmos E, García JA, Martínez-Gómez P, Hernández JA (2008) Alteration in the chloroplastic metabolism leads to ROS accumulation in pea plants in response to plum pox virus. J Exp Botany 59:2147-2160

Die JV, Dita MA, Krajinski F, González-Verdejo CI, Rubiales D, Moreno MT, Román B (2007) Identification by suppression subtractive hybridization and expression analysis of *Medicago truncatula* putative defence genes in response to *Orobanche crenata* parasitization. Physiol Mol Plant Pathol 70:49-59

Dita M, Rispail N, Prats E, Rubiales D, Singh K (2006) Biotechnology approaches to overcome biotic and abiotic stress constraints in legumes. Euphytica 147:1-24

Dita MA, Die JV, Román B, Krajinski F, Küster H, Moreno MT, Cubero JI, Rubiales D (2009) Gene expression profiling of *Medicago truncatula* roots in response to the parasitic plant *Orobanche crenata*. Weed Res 49:66-80

Dixon RA, Lamb CJ (1990) Molecular communication in interactions between plants and microbial pathogens. Annu Rev Plant Physiol Plant Mol Biol 41:339-367

Dong X (2001) Genetic dissection of systemic acquired resistance. Curr Opin Plant Biol 4:309-314

Doyle J (2001) *Leguminosae*. In: *Encyclopedia of genetics*. Edited by Brenner S, Miller JH. San Diego: Academic Press; 2001:1081-1085.

Doyle JJ, Luckow MA (2003) The rest of the iceberg. Legume diversity and evolution in a phylogenetic context. Plant Physiol 131:900-910

Duke JA (1981) Hand book of legumes of world economic importance. Plenum Press, New York. p. 199-265.

Dunn MJ, Corbett JM (1996) Two-dimensional polyacrylamide gel electrophoresis. In: Barry L. Karger WSH (ed) Methods in Enzymology, vol Volume 271. Academic Press, pp 177-203. doi:http://dx.doi.org/10.1016/S0076-6879(96)71010-8

Dunn MJ, Gil C, Kleinhammer C, Lottspeich F, Pennington S, Sanchez JC, Albar JP, Bini L, Corrales F, Corthals GL, Fountoulakis MM, Hoogland C, James P, Jensen ON, Jiménez C, Jorrín-Novo J, Kraus HJ, Meyer H, Noukakis D, Palagi PM, Penque D, Quinn A, Rabilloud T (2008) EuPA achieves visibility — An activity report on the first three years. J Proteomics 71:11-18

Durner J, Shah J, Klessig DF (1997) Salicylic acid and disease resistance in plants. Trends Plant Sci 2:266-274

Eisen MB, Spellman PT, Brown PO, Botstein D (1998) Cluster analysis and display of genome-wide expression patterns. Proc Natl Acad Sci 95:14863-14868

Emrich SJ, Barbazuk WB, Li L, Schnable PS (2007) Gene discovery and annotation using LCM-$_{454}$ transcriptome sequencing. Genome Res 17:69-73

Endo M, Matsubara H, Kokubun T, Masuko H, Takahata Y, Tsuchiya T, Fukuda H, Demura T, Watanabe M (2002) The advantages of cDNA microarray as an effective tool for identification of reproductive organ-specific genes in a model legume, *Lotus japonicus*. FEBS Lett 514:229-237

Eng JK, McCormack AL, Yates JR (1994) An approach to correlate tandem mass spectral data of peptides with amino acid sequences in a protein database. J Am Soc Mass Spectrom 5:976-989

Eriksson J, Fenyo D (2007) Improving the success rate of proteome analysis by modeling protein-abundance distributions and experimental designs. Nat Biotech 25:651-655

Evers GW (2011) Forage legumes: Forage quality, fixed nitrogen, or both. Crop Sci 51:403-409

Falloon RE, Viljanen-Rollinson SLH (2001) Powdery mildew. Compendium of pea diseases and pests. APS Press, St. Paul, USA.

FAOSTAT (2013) Available online: http://faostat.fao.org (accessed on 05 August 2014).

Fenn J, Mann M, Meng C, Wong S, Whitehouse C (1989) Electrospray ionization for mass spectrometry of large biomolecules. Science 246:64-71

Fernández-Aparicio M, Pérez-de-Luque A, Prats E, Rubiales D (2008) Variability of interactions between barrel medic (*Medicago truncatula*) genotypes and *Orobanche* species. Ann Appl Biol 153:117-126

Feys BJ, Parker JE (2000) Interplay of signaling pathways in plant disease resistance. Trends Genet 16:449-455

Fletcher S (2014) qPCR for quantification of transgene expression and determination of transgene copy number. In: Fleury D, Whitford R (eds) Crop Breeding, vol 1145. Methods in Molecular Biology. Springer New York, pp 213-237. doi:10.1007/978-1-4939-0446-4_17

Fondevilla S, ÅVila CM, Cubero JI, Rubiales D (2005) Response to *Mycosphaerella pinodes* in a germplasm collection of *Pisum* spp. Plant Breed 124:313-315

Fondevilla S, Carver TLW, Moreno MT, Rubiales D (2006) Macroscopic and histological characterisation of genes *er1* and *er2* for powdery mildew resistance in pea. Eur J Plant Pathol 115:309-321

Fondevilla S, Carver TLW, Moreno MT, Rubiales D (2007a) Identification and characterization of sources of resistance to *Erysiphe pisi* Syd. in *Pisum* spp. Plant Breed 126:113-119

Fondevilla S, Torres AM, iacute, Moreno M, a T, Rubiales D (2007b) Identification of a new gene for resistance to powdery mildew in *Pisum fulvum*, a wild relative of pea. Breed Sci 57:181-184

Fondevilla S, Rubiales D, Moreno M, Torres A (2008) Identification and validation of RAPD and SCAR markers linked to the gene *Er3* conferring resistance to *Erysiphe pisi* DC in pea. Mol Breed 22:193-200

Fondevilla S, Küster H, Krajinski F, Cubero J, Rubiales D (2011) Identification of genes differentially expressed in a resistant reaction to *Mycosphaerella pinodes* in pea using microarray technology. BMC Genomics 12:28

Fondevilla S, Rubiales D (2012) Powdery mildew control in pea. A review. European Journal of Plant Pathology 32:401-409

Fondevilla S, Rotter B, Krezdorn N, Jüngling R, Winter P, Rubiales D (2014) Identification of genes involved in resistance to *Didymella pinodes* in pea by deepSuperSAGE transcriptome profiling. Plant Mol Biol Rep 32:258-269

Foster-Hartnett D, Danesh D, Peñuela S, Sharopova N, Endre G, Vandenbosch KA, Young ND, Samac DA (2007) Molecular and cytological responses of *Medicago truncatula* to *Erysiphe pisi*. Mol Plant Pathol 8:307-319

Fuchs JG, Thuerig B, Brandhuber R, Bruns C, Finckh MR, Fließbach A, Mäder P, Schmidt H, Vogt-Kaute W, Wilbois K-P, Lucius T (2014) Evaluation of the causes of legume yield depression syndrome using an improved diagnostic tool. App Soil Ecol 79:26-36

Galetskiy D, Susnea I, Reiser V, Adamska I, Przybylski M (2008) Structure and dynamics of Photosystem II light-harvesting complex revealed by high-resolution FTICR mass spectrometric proteome analysis. J Am Soc Mass Spectrom 19:1004-1013

Galván JV, Valledor L, Cerrillo RMN, Pelegrín EG, Jorrín-Novo JV (2011) Studies of variability in Holm oak (*Quercus ilex* subsp. *ballota* [Desf.] Samp.) through acorn protein profile analysis. J Proteomics 74:1244-1255

Gao L-L, Kamphuis LG, Kakar K, Edwards OR, Udvardi MK, Singh KB (2010) Identification of potential early regulators of aphid resistance in *Medicago truncatula* via transcription factor expression profiling. New Phytol 186:980-994

Garcés M, Le Provost G, Lalanne C, Claverol S, Barré A, Plomion C, Herrera R (2014) Proteomic analysis during ontogenesis of secondary xylem in maritime pine. Tree Physiol

Garg N, Geetanjali (2009) Symbiotic nitrogen fixation in legume nodules: Process and signaling: A review. In: Sust Agri. Springer Netherlands, pp 519-531. doi:10.1007/978-90-481-2666-8_32

Gechev TS, Van Breusegem F, Stone JM, Denev I, Laloi C (2006) Reactive oxygen species as signals that modulate plant stress responses and programmed cell death. BioEssays 28:1091-1101

Geisler-Lee J, O'Toole N, Ammar R, Provart NJ, Millar AH, Geisler M (2007) A predicted Interactome for Arabidopsis. Plant Physiol 145:317-329

Glawe DA (2008) The powdery mildews: A review of the world's most familiar (yet poorly known) plant pathogens. Annu Rev Phytopathol 46:27-51

Glazebrook J (2005) Contrasting mechanisms of defense against biotrophic and necrotrophic pathogens. Annu Rev Phytopathol 43:205-227

Gómez SM, Nishio JN, Faull KF, Whitelegge JP (2002) The chloroplast grana proteome defined by intact mass measurements from liquid chromatography mass spectrometry. Mol Cell Proteomics 1:46-59

González-Verdejo CI, Dita MA, Di Pietro A, Moreno MT, Barandiarán X, Rubiales D, González-Melendi P, Pérez-de-Luque A (2007) Identification and expression analysis of a MYB family transcription factor in the parasitic plant *Orobanche ramosa*. Ann App Biol 150:123-130

Görg A, Postel W, Weser J, Günther S, Strahler JR, Hanash SM, Somerlot L (1987) Horizontal two-dimensional electrophoresis with immobilized pH gradients in the first dimension in the presence of nonionic detergent. Electrophoresis 8:45-51

Görg A, Postel W, Gunther S (1988) Methodology of IPG-DALT for the analysis of cell lysates and tissue proteins. Electrophoresis:628

Görg A, Obermaier C, Boguth G, Weiss W (1999) Recent developments in two-dimensional gel electrophoresis with immobilized pH gradients: Wide pH gradients up to pH 12, longer separation distances and simplified procedures. Electrophoresis 20:712-717

Görg A, Obermaier C, Boguth G, Harder A, Scheibe B, Wildgruber R, Weiss W (2000) The current state of two-dimensional electrophoresis with immobilized pH gradients. Electrophoresis 21:1037-1053

Grabowski M, Joachimiak A, Otwinowski Z, Minor W (2007) Structural genomics: keeping up with expanding knowledge of the protein universe. Curr Opin Struct Biol 17:347-353

Grada A, Weinbrecht K (2013) Next-Generation Sequencing: Methodology and Application. J Invest Dermatol 133:e11

Graham PH, Vance CP (2003) Legumes: Importance and constraints to greater use. Plant Physiol 131:872-877

Griffiths WJ, Jonsson AP, Liu S, Rai DK, Wang Y (2001) Electrospray and tandem mass spectrometry in biochemistry. Biochem J 355:545-561

Gritton ET (1980) Field pea. Hybridization of crop plants. p. 347-356. In: W.R. Fehr and H.H. Hadley (eds.), American Society of Agronomy, Inc., and Crop Science Society of America, Inc., Wisconsin, USA.

Gronow M, Griffiths G (1971) Rapid isolation and separation of the non-histone proteins of rat liver nuclei. FEBS Lett 15:340-344

Grove H, Jørgensen BM, Jessen F, Søndergaard I, Jacobsen S, Hollung K, Indahl U, Færgestad EM (2008) Combination of statistical approaches for analysis of 2-DE data gives complementary results. J Proteome Res 7:5119-5124

Guénin S, Mauriat M, Pelloux J, Van Wuytswinkel O, Bellini C, Gutierrez L (2009) Normalization of qRT-PCR data: the necessity of adopting a systematic, experimental conditions-specific, validation of references. J Exp Bot 60:487-493

Gupta RB, Shepherd KW (1990) Two-step one-dimensional SDS-PAGE analysis of LMW subunits of glutelin. Theor App Genet 80:65-74

Gutierrez-Carbonell E, Takahashi D, Lattanzio G, Rodríguez-Celma J, Kehr J, Soll J, Philippar K, Uemura M, Abadía J, López-Millán AF (2014) The distinct functional roles of the inner and outer chloroplast envelope of pea (*Pisum sativum*) as revealed by proteomic approaches. J Proteome Res 13:2941-2953

Hager JW (2002) A new linear ion trap mass spectrometer. Rapid Commun Mass Spectrom 16:512-526

Hajheidari M, Eivazi A, Buchanan BB, Wong JH, Majidi I, Salekdeh GH (2007) Proteomics uncovers a role for redox in drought tolerance in wheat. J Proteome Res 6:1451-1460

Hall R, Beale M, Fiehn O, Hardy N, Sumner L, Bino R (2002) Plant metabolomics: The missing link in functional genomics strategies. Plant Cell 14:1437-1440

Hammond-Kosack KE, Jones JDG (1997) Plant disease resistance genes. Annu Rev Plant Physiol Plant Mol Biol 48:575-607

Han DK, Eng J, Zhou H, Aebersold R (2001) Quantitative profiling of differentiation-induced microsomal proteins using isotope-coded affinity tags and mass spectrometry. Nat Biotech 19:946-951

Harris LR, Churchward MA, Butt RH, Coorssen JR (2007) Assessing detection methods for gel-based proteomic analyses. J Proteome Res 6:1418-1425

Harris TD, Buzby PR, Babcock H, Beer E, Bowers J, Braslavsky I, Causey M, Colonell J, DiMeo J, Efcavitch JW, Giladi E, Gill J, Healy J, Jarosz M, Lapen D, Moulton K, Quake SR, Steinmann K, Thayer E, Tyurina A, Ward R, Weiss H, Xie Z (2008) Single-molecule DNA sequencing of a viral genome. Science 320:106-109

Hartung F, Schiemann J (2014) Precise plant breeding using new genome editing techniques: opportunities, safety and regulation in the EU. Plant J 78:742-752

Haslam RP, Downie AL, Raveton M, Gallardo K, Job D, Pallett KE, John P, Parry MAJ, Coleman JOD (2003) The assessment of enriched apoplastic extracts using proteomic approaches. Ann App Biol 143:81-91

Hillenkamp F, Karas M, Beavis RC, Chait BT (1991) Matrix-assisted laser desorption/Ionization mass spectrometry of biopolymers. Anal Chem 63:1193A-1203A

Hohnjec N, Vieweg MF, Pühler A, Becker A, Küster H (2005) Overlaps in the transcriptional profiles of *Medicago truncatula* roots inoculated with two different *Glomus* fungi provide insights into the genetic program activated during arbuscular mycorrhiza. Plant Physiol 137:1283-1301

Hu M, Polyak K (2006) Serial analysis of gene expression. Nat Protocols 1:1743-1760

Huang S, Jacoby R, Millar AH, Taylor N (2014) Plant mitochondrial proteomics. In: Jorrin-Novo JV, Komatsu S, Weckwerth W, Wienkoop S (eds) Plant proteomics, vol 1072. Methods in Molecular Biology. Humana Press, pp 499-525. doi:10.1007/978-1-62703-631-3_34

Huggett J, Dheda K, Bustin S, Zumla A (2005) Real-time RT-PCR normalisation; strategies and considerations. Genes Immun 6:279-284

Iakimova ET, Sobiczewski P, Michalczuk L, Węgrzynowicz-Lesiak E, Mikiciński A, Woltering EJ (2013) Morphological and biochemical characterization of *Erwinia amylovora*-induced hypersensitive cell death in apple leaves. Plant Physiol Biochem 63:292-305

Isaacson T, Damasceno CMB, Saravanan RS, He Y, Catala C, Saladie M, Rose JKC (2006) Sample extraction techniques for enhanced proteomic analysis of plant tissues. Nat Protocols 1:769-774

Jacobsen S, Grove H, Nedenskov Jensen K, Sørensen HA, Jessen F, Hollung K, Uhlen AK, Jørgensen BM, Færgestad EM, Søndergaard I (2007) Multivariate analysis of 2-DE protein patterns – Practical approaches. Electrophoresis 28:1289-1299

Jamet E, Albenne C, Boudart G, Irshad M, Canut H, Pont-Lezica R (2008) Recent advances in plant cell wall proteomics. Proteomics 8:893-908

Jaquinod M, Villiers F, Kieffer-Jaquinod S, Hugouvieux V, Bruley C, Garin J, Bourguignon J (2007) A proteomics dissection of *Arabidopsis thaliana* vacuoles isolated from cell culture. Mol Cell Proteomics 6:394-412

Jarvis P (2008) Targeting of nucleus-encoded proteins to chloroplasts in plants. New Phytologist 179:257-285

Jones JDG, Dangl JL (2006) The plant immune system. Nature 444:323-329

Jones LK (1927) Studies of the nature and control of blight, leaf and pod spot, and footrot of peas caused by species of *Ascochyta*. NY State Agricultural Experiment Station Bulletin, 547, 1–45.

Jorge I, Navarro RM, Lenz C, Ariza D, Porras C, Jorrín J (2005) The holm oak leaf proteome: Analytical and biological variability in the protein expression level assessed by 2-DE and protein identification tandem mass spectrometry *de novo* sequencing and sequence similarity searching. Proteomics 5:222-234

Jorge I, Navarro RM, Lenz C, Ariza D, Jorrín J (2006) Variation in the holm oak leaf proteome at different plant developmental stages, between provenances and in response to drought stress. Proteomics 6:S207-S214

Jorrin-Novo J, Calvete J, Maldonado A (2008) Proteómica: Conceptos y metodologías. In: Pallás, V.,Excobar, C., Rodriguez Palenzuela, P., Marcos, J., eds. Herramientas Biotecnológicas en Fitopatología. Madrid: Mundi-Prensa, 75-92.

Jorrin-Novo J (2014) Plant proteomics methods and protocols. In: Jorrin-Novo JV, Komatsu S, Weckwerth W, Wienkoop S (eds) Plant Proteomics, vol 1072. Methods in Molecular Biology. Humana Press, pp 3-13. doi:10.1007/978-1-62703-631-3_1

Jorrín-Novo J, Valledor L (2013) Special Issue: Translational plant proteomics. J Proteomics 93:1-4

Jorrín-Novo JV, Maldonado AM, Castillejo MA (2007) Plant proteome analysis: A 2006 update. Proteomics 7:2947-2962

Jorrín-Novo JV (2009) Plant Proteomics. J Proteomics 72:283-284

Jorrín-Novo JV, Maldonado AM, Echevarría-Zomeño S, Valledor L, Castillejo MA, Curto M, Valero J, Sghaier B, Donoso G, Redondo I (2009) Plant proteomics update (2007–2008): Second-generation proteomic techniques, an appropriate experimental design, and data analysis to fulfill MIAPE standards, increase plant proteome coverage and expand biological knowledge. J Proteomics 72:285-314

Jorrín JV, Rubiales D, Dumas-Gaudot E, Recorbet G, Maldonado A, Castillejo MA, Curto M (2006) Proteomics: a promising approach to study biotic interaction in legumes. A review. Euphytica 147:37-47

Kang JG, Pyo YJ, Cho JW, Cho MH (2004) Comparative proteome analysis of differentially expressed proteins induced by K^+ deficiency in *Arabidopsis thaliana*. Proteomics 4:3549-3559

Karas M, Hillenkamp F (1988) Laser desorption ionization of proteins with molecular masses exceeding 10,000 daltons. Anal Chem 60:2299-2301

Karlen Y, McNair A, Perseguers S, Mazza C, Mermod N (2007) Statistical significance of quantitative PCR. BMC Bioinformatics 8:131

Karp NA, McCormick PS, Russell MR, Lilley KS (2007) Experimental and statistical considerations to avoid false conclusions in proteomics studies using differential in-gel electrophoresis. Mol Cell Proteomics 6:1354-1364

Kathleen Kerr M (2003) Design considerations for efficient and effective microarray studies. Biometrics 59:822-828

Katz E, Fon M, Lee YJ, Phinney BS, Sadka A, Blumwald E (2007) The citrus fruit proteome: insights into citrus fruit metabolism. Planta 226:989-1005

Kelley TG, Parthasarathy RP, Grisko-Kelley H (1997) The pulse economy in the mid-1990s: A review of global and regional developments. In: R. Knight (Ed.), Proceedings IFLRC-III: Linking research and marketing opportunities for the 21st century (pp. 1–29). Dordrecht: Kluwer academic Publishers.

Kersten B, Agrawal GK, Durek P, Neigenfind J, Schulze W, Walther D, Rakwal R (2009) Plant phosphoproteomics: An update. Proteomics 9:964-988

Khan TN, Timmerman-Vaughan GM, Rubiales D, Warkentin TD, Siddique KHM, Erskine W, Barbetti MJ (2013) *Didymella pinodes* and its management in field pea: challenges and opportunities. Field Crop Res 148:61-77

Kiirika LM, Schmitz U, Colditz F (2014) The alternative *Medicago truncatula* defense proteome of ROS – defective transgenic roots during early microbial infection. Front Plant Sci 5

Kim DW (2001) Real time quantitative PCR. Exp Mol Med 33:101-109

Kim ST, Kim SG, Agrawal GK, Kikuchi S, Rakwal R (2014) Rice proteomics: A model system for crop improvement and food security. Proteomics 14:593-610

Kim YJ, Lee HM, Wang Y, Wu J, Kim SG, Kang KY, Park KH, Kim YC, Choi IS, Agrawal GK, Rakwal R, Kim ST (2013) Depletion of abundant plant RuBisCO protein using the protamine sulfate precipitation method. Proteomics 13:2176-2179

Kitteringham NR, Jenkins RE, Lane CS, Elliott VL, Park BK (2009) Multiple reaction monitoring for quantitative biomarker analysis in proteomics and metabolomics. J Chromatogr B 877:1229-1239

Kleffmann T, Russenberger D, von Zychlinski A, Christopher W, Sjölander K, Gruissem W, Baginsky S (2004) The *Arabidopsis thaliana* chloroplast proteome reveals pathway abundance and novel protein functions. Curr Biol 14:354-362

Kliebenstein DJ (2014) Orchestration of plant defense systems: genes to populations. Trends Plant Sci 19:250-255

Koike ST, Gladders P, Paulus AO (2007) Vegetable diseases, a colour handbook. Manson Publishing Ltd., UK. .

Komatsu S, Kojima K, Suzuki K, Ozaki K, Higo K (2004) Rice proteome database based on two-dimensional polyacrylamide gel electrophoresis: its status in 2003. Nucleic Acids Res 32:D388-D392

Komsta Ł, Cieśla Ł, Bogucka-Kocka A, Józefczyk A, Kryszeń J, Waksmundzka-Hajnos M (2011) The start-to-end chemometric image processing of 2D thin-layer videoscans. J Chromatogr A 1218:2820-2825

Kosová K, Vítámvás P, Urban MO, Prášil IT (2013) Plant proteome responses to salinity stress – comparison of glycophytes and halophytes. Funct Plant Biol 40:775-786

Kristensen TN, Pedersen KS, Vermeulen CJ, Loeschcke V (2010) Research on inbreeding in the 'omic' era. Trends Ecol Evol 25:44-52

Krochko JE, Bewley JD (1990) Identification and characterization of the seed storage proteins from alfalfa (*Medicago sativa*). J Exp Bot 41:505-514

Kroll K, Pähtz V, Kniemeyer O (2014) Elucidating the fungal stress response by proteomics. J Proteomics 97:151-163

Kumpatla SP, Abdurakhmonov IY, Mammadov JA, Buyyarapu R (2012) Genomics-assisted plant breeding in the 21st Century: Technological advances and progress. INTECH Open Access Publisher,

Kushalappa AC, Gunnaiah R (2013) Metabolo-proteomics to discover plant biotic stress resistance genes. Trends Plant Sci 18:522-531

Küster H, Hohnjec N, Krajinski F, El Yahyaoui F, Manthey K, Gouzy J, Dondrup M, Meyer F, Kalinowski J, Brechenmacher L, van Tuinen D, Gianinazzi-Pearson V, Pühler A, Gamas P, Becker A (2004) Construction and validation of cDNA-based Mt6k-RIT macro- and microarrays to explore root endosymbioses in the model legume *Medicago truncatula*. J Biotech 108:95-113

Laemmli UK (1970) Cleavage of structural proteins during the assembly of the head of bacteriophage T4. Nature 227:680-685

Larrainzar E, Wienkoop S, Weckwerth W, Ladrera R, Arrese-Igor C, González EM (2007) *Medicago truncatula* root nodule proteome analysis reveals differential plant and bacteroid responses to drought stress. Plant Physiol 144:1495-1507

Larrainzar E, Molenaar JA, Wienkoop S, Gil-Quintana E, Alibert B, Limami AM, Arrese-Igor C, GonzÁLez EM (2014) Drought stress provokes the down-regulation of methionine and ethylene biosynthesis pathways in *Medicago truncatula* roots and nodules. Plant Cell Env 37:2051-2063

Lee J, Cooper B (2006) Alternative workflows for plant proteomic analysis. Mol BioSyst 2:621-626

Lengqvist J, Uhlén K, Lehtiö J (2007) iTRAQ compatibility of peptide immobilized pH gradient isoelectric focusing. Proteomics 7:1746-1752

Lewis G, Schrirer B, Mackinder B, Lock M (2005) Legumes of the world; Royal Botanical Gardens: Kew, UK.

Li Y, Mao L, Yan D, Ma T, Shen J, Guo M, Wang Q, Ouyang C, Cao A (2014) Quantification of *Fusarium oxysporum* in fumigated soils by a newly developed real-time PCR assay to assess the efficacy of fumigants for Fusarium wilt disease in strawberry plants. Pest Manag Sci:n/a-n/a

Lilley KS, Razzaq A, Dupree P (2002) Two-dimensional gel electrophoresis: recent advances in sample preparation, detection and quantitation. Curr Opin Chem Biol 6:46-50

Lin CS, Aebersold RH, Kent SB, Varma M, Leavitt J (1988) Molecular cloning and characterization of plastin, a human leukocyte protein expressed in transformed human fibroblasts. Mol Cell Biol 8:4659-4668

Lindermayr C, Durner J (2009) S-Nitrosylation in plants: Pattern and function. J Proteomics 73:1-9

Linsen SEV, de Wit E, Janssens G, Heater S, Chapman L, Parkin RK, Fritz B, Wyman SK, de Bruijn E, Voest EE, Kuersten S, Tewari M, Cuppen E (2009) Limitations and possibilities of small RNA digital gene expression profiling. Nat Meth 6:474-476

Liu G-T, Ma L, Duan W, Wang B-C, Li J-H, Xu H-G, Yan X-Q, Yan B-F, Li S-H, Wang L-J (2014a) Differential proteomic analysis of grapevine leaves by iTRAQ reveals responses to heat stress and subsequent recovery. BMC Plant Biol 14:110

Liu X, Dekker LJM, Wu S, Vanduijn MM, Luider TM, Tolić N, Kou Q, Dvorkin M, Alexandrova S, Vyatkina K, Paša-Tolić L, Pevzner PA (2014b) *De novo* protein sequencing by combining top-down and bottom-up tandem mass spectra. J Proteome Res 13:3241-3248

Livak KJ, Schmittgen TD (2001) Analysis of relative gene expression data using real-time quantitative PCR and the $2^{-\Delta\Delta CT}$ Method. Methods 25:402-408

Loboda AV, Krutchinsky AN, Bromirski M, Ens W, Standing KG (2000) A tandem quadrupole/time-of-flight mass spectrometer with a matrix-assisted laser desorption/ionization source: design and performance. Rapid Commun Mass Spectrom 14:1047-1057

Lockhart DJ, Winzeler EA (2000) Genomics, gene expression and DNA arrays. Nature 405:827-836

Lozano-Baena MD, Prats E, Moreno MT, Rubiales D, Pérez-de-Luque A (2007) *Medicago truncatula* as a model for nonhost resistance in legume-parasitic plant Interactions. Plant Physiol 145:437-449

Lunn JE (2007) Compartmentation in plant metabolism. J Exp Bot 58:35-47

Macgillivray AJ, Wood DR (1974) The heterogeneity of mouse-chromatin nonhistone proteins as evidenced by two-dimensional polyacrylamide-gel electrophoresis and ion-exchange chromatography. Eur J Biochem 41:181-190

Madrid E, Gil J, Rubiales D, Krajinski F, Schlereth A, Millán T (2010) Transcription factor profiling leading to the identification of putative transcription factors involved in the *Medicago truncatula–Uromyces striatus* interaction. Theor Appl Genet 121:1311-1321

Maldonado AM, Echevarría-Zomeño S, Jean-Baptiste S, Hernández M, Jorrín-Novo JV (2008) Evaluation of three different protocols of protein extraction for *Arabidopsis thaliana* leaf proteome analysis by two-dimensional electrophoresis. J Proteomics 71:461-472

Mann M, Wilm M (1994) Error-tolerant identification of peptides in sequence databases by peptide sequence tags. Anal Chem 66:4390-4399

Mann M, Jensen ON (2003) Proteomic analysis of post-translational modifications. Nat Biotech 21:255-261

Martin JA, Wang Z (2011) Next-generation transcriptome assembly. Nat Rev Genet 12:671-682

Martínez-Esteso M, Casado-Vela J, Sellés-Marchart S, Pedreño M, Bru-Martínez R (2014) Differential plant proteome analysis by isobaric tags for relative and absolute quantitation (iTRAQ). In: Jorrin-Novo JV, Komatsu S, Weckwerth W, Wienkoop S (eds) Plant Proteomics, vol 1072. Methods in Molecular Biology. Humana Press, pp 155-169. doi:10.1007/978-1-62703-631-3_12

Martínez-Maqueda D, Hernández-Ledesma B, Amigo L, Miralles B, Gómez-Ruiz J (2013) Extraction/fractionation techniques for proteins and peptides and protein digestion. In: Toldrá F, Nollet LML (eds) Proteomics in Foods, vol 2. Food Microbiology and Food Safety. Springer US, pp 21-50. doi:10.1007/978-1-4614-5626-1_2

Mathesius U, Keijzers G, Natera SHA, Weinman JJ, Djordjevic MA, Rolfe BG (2001) Establishment of a root proteome reference map for the model legume *Medicago truncatula* using the expressed sequence tag database for peptide mass fingerprinting. Proteomics 1:1424-1440

Matthes A, Köhl K, Schulze W (2014) SILAC and alternatives in studying cellular proteomes of plants. In: Warscheid B (ed) Stable isotope labeling by amino acids in cell culture (SILAC), vol 1188. Methods in Molecular Biology. Springer New York, pp 65-83. doi:10.1007/978-1-4939-1142-4_6

Maurer MH (2006) Software analysis of two-dimensional electrophoretic gels in proteomic experiments. Curr Bioinformatics 1:255-262

May C, Schoeny A, Tivoli B, Ney B (2005) Improvement and validation of a pea crop growth model to simulate the growth of cultivars infected with ascochyta blight (*Mycosphaerella pinodes*). Eur J Plant Pathol 112:1-12

Medzihradszky KF, Campbell JM, Baldwin MA, Falick AM, Juhasz P, Vestal ML, Burlingame AL (1999) The characteristics of peptide collision-induced dissociation using a high-performance MALDI-TOF/TOF tandem mass spectrometer. Anal Chem 72:552-558

Mikić A, Medović A, Jovanović Ž, Stanisavljević N (2014) Integrating archaeobotany, paleogenetics and historical linguistics may cast more light onto crop domestication: the case of pea (*Pisum sativum*). Genet Resour Crop Evol 61:887-892

Millar AH, Whelan J, Small I (2006) Recent surprises in protein targeting to mitochondria and plastids. Curr Opin Plant Biol 9:610-615

Millar AH (2007) The plant mitochondrial proteome. In: Šamaj J, Thelen J (eds) Plant Proteomics. Springer Berlin Heidelberg, pp 226-246. doi:10.1007/978-3-540-72617-3_15

Minic Z, Boudart G, Albenne C, Canut H, Jamet E, Pont-Lezica R (2007) Cell Wall Proteome. In: Šamaj J, Thelen J (eds) Plant Proteomics. Springer Berlin Heidelberg, pp 169-185. doi:10.1007/978-3-540-72617-3_12

Mittler R (2006) Abiotic stress, the field environment and stress combination. Trends Plant Sci 11:15-19

Mittler R, Shulaev V (2013) Functional genomics, challenges and perspectives for the future. Physiol Plant 148:317-321

Müller B, Grossniklaus U (2010) Model organisms — a historical perspective. J Proteomics 73:2054-2063

Mur LAJ, Kenton P, Lloyd AJ, Ougham H, Prats E (2008) The hypersensitive response; the centenary is upon us but how much do we know? J Exp Bot 59:501-520

Nedenskov Jensen K, Jessen F, Jørgensen BM (2008) Multivariate data analysis of two-dimensional gel electrophoresis protein patterns from few Samples. J Proteome Res 7:1288-1296

Niks RE, Rubiales D (2002) Potentially durable resistance mechanisms in plants to specialised fungal pathogens. Euphytica 124:201-216

Nürnberger T, Brunner F, Kemmerling B, Piater L (2004) Innate immunity in plants and animals: striking similarities and obvious differences. Immunol Rev 198:249-266

O'Farrell PH (1975) High resolution two-dimensional electrophoresis of proteins. J Biol Chem 250:4007-4021

Ökmen B, Doehlemann G (2014) Inside plant: biotrophic strategies to modulate host immunity and metabolism. Curr Opin Plant Biol 20:19-25

Oliver DJ, Nikolau B, Wurtele ES (2002) Functional Genomics: High-Throughput mRNA, Protein, and Metabolite Analyses. Metabol Eng 4:98-106

Pabinger S, Thallinger G, Snajder R, Eichhorn H, Rader R, Trajanoski Z (2009) qPCR: Application for real-time PCR data management and analysis. BMC Bioinformatics 10:268

Pandey G, Paul D, Jain RK (2003) Branching of o-nitrobenzoate degradation pathway in *Arthrobacter protophormiae* RKJ100: identification of new intermediates. FEMS Microbiol Lett 229:231-236

Panstruga R, Spanu PD (2014) Powdery mildew genomes reloaded. New Phytol 202:13-14

Pappin DJC, Hojrup P, Bleasby AJ (1993) Rapid identification of proteins by peptide-mass fingerprinting. Curr Biol 3:327-332

Patterson J, Ford K, Cassin A, Natera S, Bacic A (2007) Increased abundance of proteins involved in phytosiderophore production in boron-tolerant barley. Plant Physiol 144:1612-1631

Patterson SD, Aebersold R (1995) Mass spectrometric approaches for the identification of gel-separated proteins. Electrophoresis 16:1791-1814

Perkins DN, Pappin DJC, Creasy DM, Cottrell JS (1999) Probability-based protein identification by searching sequence databases using mass spectrometry data. Electrophoresis 20:3551-3567

Pfaffl MW (2001) A new mathematical model for relative quantification in real-time RT–PCR. Nucleic Acids Res 29:e45

Pfaffl MW, Horgan GW, Dempfle L (2002) Relative expression software tool (REST©) for group-wise comparison and statistical analysis of relative expression results in real-time PCR. Nucleic Acids Res 30:e36

Ponchel F, Toomes C, Bransfield K, Leong F, Douglas S, Field S, Bell S, Combaret V, Puisieux A, Mighell A, Robinson P, Inglehearn C, Isaacs J, Markham A (2003) Real-time PCR based on SYBR-Green I fluorescence: An alternative to the TaqMan assay for a relative quantification of gene rearrangements, gene amplifications and micro gene deletions. BMC Biotechnol 3:18

Prats E, Llamas MJ, Rubiales D (2007) Characterization of resistance mechanisms to *Erysiphe pisi* in *Medicago truncatula*. Phytopathology 97:1049-1053

Qin J, Fenyö D, Zhao Y, Hall WW, Chao DM, Wilson CJ, Young RA, Chait BT (1997) A strategy for rapid, high-confidence protein identification. Anal Chem 69:3995-4001

Rabilloud T, Lelong C (2011) Two-dimensional gel electrophoresis in proteomics: A tutorial. J Proteomics 74:1829-1841

Rabilloud T (2014) How to use 2D gel electrophoresis in plant proteomics. In: Jorrin-Novo JV, Komatsu S, Weckwerth W, Wienkoop S (eds) Plant Proteomics, vol 1072. Methods in Molecular Biology. Humana Press, pp 43-50. doi:10.1007/978-1-62703-631-3_4

Reinders J, Lewandrowski U, Moebius J, Wagner Y, Sickmann A (2004) Challenges in mass spectrometry-based proteomics. Proteomics 4:3686-3703

Rensink WA, Buell CR (2005) Microarray expression profiling resources for plant genomics. Trends Plant Sci 10:603-609

Rigden DJ (2006) Understanding the cell in terms of structure and function: insights from structural genomics. Curr Opin Biotechnol 17:457-464

Righetti PG (1983) Isoelectric focusing: theory, methodology, and applications. Elsevier Biomedical Press,

Rispail N, Kaló P, Kiss GB, Ellis THN, Gallardo K, Thompson RD, Prats E, Larrainzar E, Ladrera R, González EM, Arrese-Igor C, Ferguson BJ, Gresshoff PM, Rubiales D (2010) Model legumes contribute to faba bean breeding. Field Crop Res 115:253-269

Rizhsky L, Liang H, Shuman J, Shulaev V, Davletova S, Mittler R (2004) When defense pathways collide. The response of Arabidopsis to a combination of drought and heat stress. Plant Physiol 134:1683-1696

Rochon JJ, Doyle CJ, Greef JM, Hopkins A, Molle G, Sitzia M, Scholefield D, Smith CJ (2004) Grazing legumes in Europe: a review of their status, management, benefits, research needs and future prospects. Grass Forage Sci 59:197-214

Rödiger A, Agne B, Baerenfaller K, Baginsky S (2014) Arabidopsis Proteomics: A simple and standardizable workflow for quantitative proteome characterization. In: Jorrin-Novo JV, Komatsu S, Weckwerth W, Wienkoop S (eds) Plant Proteomics, vol 1072. Methods in Molecular Biology. Humana Press, pp 275-288. doi:10.1007/978-1-62703-631-3_20

Rodrigues CM, Mafra VS, Machado MA (2014) Transcriptomics. In: Omics in Plant Breeding. John Wiley & Sons, Inc, pp 33-57. doi:10.1002/9781118820971.ch3

Rodziewicz P, Swarcewicz B, Chmielewska K, Wojakowska A, Stobiecki M (2014) Influence of abiotic stresses on plant proteome and metabolome changes. Acta Physiol Plant 36:1-19

Roger C, Tivoli B (1996) Spatio-temporal development of pycnidia and pseudothecia and dissemination of spores of *Mycosphaerella pinodes* on pea (*Pisum sativum*). Plant Pathol 45:518-528

Rubiales D, Moral A (2004) Prehaustorial resistance against alfalfa rust (*Uromyces striatus*) in *Medicago truncatula*. Europ J Plant Pathol 110:239-243

Rubiales D, Ambrose MJ, Domoney C, Burstin J (2011a) Pea. In: (Eds. M. Pérez de la Vega, A.M. Torres, J.I. Cubero & C. Kole). Genetics, genomics and breeding of cool season grain legumes. Science Publishers, Enfield, NH, pp. 1-49. ISBN 978-1-57808-765-5. In.

Rubiales D, Castillejo MA, Madrid E, Barilli E, Rispail N (2011b) Legume breeding for rust resistance: lessons to learn from the model *Medicago truncatula*. Euphytica 180:89-98

Rubiales D, Fondevilla S (2012) Future prospects for ascochyta blight resistance breeding in cool season food legumes. Front Plant Sci 3:27

Rubiales D, Fondevilla S, Chen W, Gentzbittel L, Higgins TJV, Castillejo MA, Singh KB, Rispail N (2014) Achievements and challenges in legume breeding for pest and disease resistance. Crit Rev in Plant Sci, in press

Rubiales D., Fernández-Aparicio M., Moral A., Barilli E., Sillero J.C., S. F (2009) Disease resistance in pea (*Pisum sativum* **L.**) types for autumn sowings in Mediterranean environments. Czech J Genet Plant Breed 45:135-142

Ruiz May E, Rose JKC (2013) Progress towards the tomato fruit cell wall proteome. Front Plant Sci 4

Sakata K, Komatsu S (2014) Plant proteomics: From genome sequencing to proteome databases and repositories. In: Jorrin-Novo JV, Komatsu S, Weckwerth W, Wienkoop S (eds) Plant Proteomics, vol 1072. Methods in Molecular Biology. Humana Press, pp 29-42. doi:10.1007/978-1-62703-631-3_3

Salekdeh GH, Komatsu S (2007) Crop proteomics: Aim at sustainable agriculture of tomorrow. Proteomics 7:2976-2996

Sanger F, Nicklen S, Coulson AR (1977) DNA sequencing with chain-terminating inhibitors. Proc Natl Acad Sci 74:5463-5467

Santoni V, Molloy M, Rabilloud T (2000) Membrane proteins and proteomics: Un amour impossible? Electrophoresis 21:1054-1070

Schadt EE, Turner S, Kasarskis A (2010) A window into third-generation sequencing. Hum Mol Genet 19:R227-R240

Schiltz S, Gallardo K, Huart M, Negroni L, Sommerer N, Burstin J (2004) Proteome reference maps of vegetative tissues in pea. An investigation of nitrogen mobilization from leaves during seed filling. Plant Physiol 135:2241-2260

Schmidt A, Trentini DB, Spiess S, Fuhrmann J, Ammerer G, Mechtler K, Clausen T (2014) Quantitative phosphoproteomics reveals the role of protein arginine phosphorylation in the bacterial stress response. Mol Cell Proteomics 13:537-550

Schulze-Lefert P, Vogel J (2000) Closing the ranks to attack by powdery mildew. Trends Plant Sci 5:343-348

Schulze A, Downward J (2001) Navigating gene expression using microarrays - a technology review. Nat Cell Biol 3:E190-E195

Schuster SC (2008) Next-generation sequencing transforms today's biology. Nat Meth 5:16-18

Schwartz JC, Senko MW, Syka JEP (2002) A two-dimensional quadrupole ion trap mass spectrometer. J Am Soc Mass Spectrom 13:659-669

Shen Y, Tolić N, Masselon C, Paša-Tolić L, Camp DG, Hixson KK, Zhao R, Anderson GA, Smith RD (2003) Ultrasensitive proteomics using high-efficiency on-line micro-SPE-nanoLC-nanoESI MS and MS/MS. Anal Chem 76:144-154

Shevchenko A, Jensen ON, Podtelejnikov AV, Sagliocco F, Wilm M, Vorm O, Mortensen P, Shevchenko A, Boucherie H, Mann M (1996) Linking genome and proteome by mass spectrometry: Large-scale identification of yeast proteins from two dimensional gels. Proc Natl Acad Sci 93:14440-14445

Shi H, Ye T, Zhong B, Liu X, Chan Z (2014) Comparative proteomic and metabolomic analyses reveal mechanisms of improved cold stress tolerance in bermudagrass (*Cynodon dactylon* (L). Pers.) by exogenous calcium. J Integr Plant Biol:in press

Siddique KM, Johansen C, Turner N, Jeuffroy M-H, Hashem A, Sakar D, Gan Y, Alghamdi S (2012) Innovations in agronomy for food legumes. A review. Agron Sustain Dev 32:45-64

Sillero JC, Fondevilla S, Davidson J, Patto MCV, Warkentin TD, Thomas J, Rubiales D (2006) Screening techniques and sources of resistance to rusts and mildews in grain legumes. Euphytica 147:255-272

Simon SA, Zhai J, Nandety RS, McCormick KP, Zeng J, Mejia D, Meyers BC (2009) Short-read sequencing technologies for transcriptional analyses. Annu Rev Plant Biol 60:305-333

Singh KB, Foley RC, Oñate-Sánchez L (2002) Transcription factors in plant defense and stress responses. Curr Opin Plant Biol 5:430-436

Smýkal P, Kenicer G, Flavell AJ, Corander J, Kosterin O, Redden RJ, Ford R, Coyne CJ, Maxted N, Ambrose MJ, Ellis NTH (2011) Phylogeny, phylogeography and genetic diversity of the *Pisum* genus. Plant Genet Resour 9:4-18

Smýkal P, Aubert G, Burstin J, Coyne CJ, Ellis NTH, Flavell AJ, Ford R, Hýbl M, Macas J, Neumann P, McPhee KE, Redden RJ, Rubiales D, Weller JL, Warkentin TD (2012) Pea (*Pisum sativum* L.) in the genomic era. Agronomy 2:74-115

Smýkal P, Coyne C, Redden R, Maxted N (2013) Peas. In: Singh M., Upadhyaya H. (eds): Genetic and genomic resources of grain legume improvement. Elsevier, Amsterdam, 41–80.

Smýkal P (2014) Pea (*Pisum sativum L.*) in biology prior and after Mendel's discovery. Czech J Genet Plant Breed, 50:52-64

Southern EM, Maskos U, Elder JK (1992) Analyzing and comparing nucleic acid sequences by hybridization to arrays of oligonucleotides: Evaluation using experimental models. Genomics 13:1008-1017

Southern EM (1996) DNA chips: analysing sequence by hybridization to oligonucleotides on a large scale. Trends Genet 12:110-115

Supek F, Peharec P, Krsnik-Rasol M, Šmuc T (2008) Enhanced analytical power of SDS-PAGE using machine learning algorithms. Proteomics 8:28-31

Tar'an B, Zhang C, Warkentin T, Tullu A, Vandenberg A (2005) Genetic diversity among varieties and wild species accessions of pea (*Pisum sativum* L.) based on molecular markers, and morphological and physiological characters. Genome 48:257-272

Taylor CF, Paton NW, Lilley KS, Binz P-A, Julian RK, Jones AR, Zhu W, Apweiler R, Aebersold R, Deutsch EW, Dunn MJ, Heck AJR, Leitner A, Macht M, Mann M, Martens L, Neubert TA, Patterson SD, Ping P, Seymour SL, Souda P, Tsugita A, Vandekerckhove J, Vondriska TM, Whitelegge JP, Wilkins MR, Xenarios I,

Yates JR, Hermjakob H (2007) The minimum information about a proteomics experiment (MIAPE). Nat Biotech 25:887-893

Taylor SC, Mrkusich EM (2014) The state of RT-quantitative PCR: First hand observations of implementation of Minimum Information for the publication of Quantitative real-time PCR Experiments (MIQE). J Mol Microbiol Biotechnol 24:46-52

Thakur M, Sohal BS (2013) Role of elicitors in inducing resistance in plants against pathogen infection: A review. ISRN Biochem 2013:10

Thomma BPHJ, Nürnberger T, Joosten MHAJ (2011) Of PAMPs and effectors: The blurred PTI-ETI dichotomy. Plant Cell 23:4-15

Tivoli B, Beasse C, Lemarchand E, Masson E (1996) Effect of ascochyta blight (*Mycosphaerella pinodes*) on yield components of single pea (*Pisum sativum*) plants under field conditions. Ann Appl Biol 129:207-216

Tivoli B, Baranger A, Avila C, Banniza S, Barbetti M, Chen W, Davidson J, Lindeck K, Kharrat M, Rubiales D, Sadiki M, Sillero J, Sweetingham M, Muehlbauer F (2006a) Screening techniques and sources of resistance to foliar diseases caused by major necrotrophic fungi in grain legumes. Euphytica 147:223-253

Tivoli B, Baranger A, Sivasithamparam K, Barbetti MJ (2006b) Annual *Medicago*: From a model crop challenged by a spectrum of necrotrophic pathogens to a model plant to explore the nature of disease resistance. Ann Bot 98:1117-1128

Tivoli B, Banniza S (2007) Comparison of the epidemiology of ascochyta blights on grain legumes. In: Tivoli B, Baranger A, Muehlbauer F, Cooke BM (eds) Ascochyta blights of grain legumes. Springer Netherlands, pp 59-76. doi:10.1007/978-1-4020-6065-6_7

Trethewey RN (2004) Metabolite profiling as an aid to metabolic engineering in plants. Curr Opin Plant Biol 7:196-201

Tribl F, Lohaus C, Dombert T, Langenfeld E, Piechura H, Warscheid B, Meyer HE, Marcus K (2008) Towards multidimensional liquid chromatography separation of proteins using fluorescence and isotope-coded protein labelling for quantitative proteomics. Proteomics 8:1204-1211

Udvardi M, Poole PS (2013) Transport and metabolism in legume-rhizobia symbioses. Annu Rev Plant Biol 64:781-805

Valcu C-M, Valcu M (2007) Reproducibility of two-dimensional gel electrophoresis at different replication levels. J Proteome Res 6:4677-4683

Valouev A, Ichikawa J, Tonthat T, Stuart J, Ranade S, Peckham H, Zeng K, Malek JA, Costa G, McKernan K, Sidow A, Fire A, Johnson SM (2008) A high-resolution, nucleosome position map of *C. elegans* reveals a lack of universal sequence-dictated positioning. Genome Res 18:1051-1063

Valledor L, Castillejo MA, Lenz C, Rodríguez R, Cañal MJ, Jorrín J (2008) Proteomic analysis of *Pinus radiata* needles: 2-DE map and protein Identification by LC/MS/MS and substitution-tolerant database searching. J Proteome Res 7:2616-2631

Valledor L, Jorrín J (2011) Back to the basics: Maximizing the information obtained by quantitative two dimensional gel electrophoresis analyses by an appropriate experimental design and statistical analyses. J Proteomics 74:1-18

Valledor L, Romero-Rodríguez MC, Jorrin-Novo J (2014) Standardization of data processing and statistical analysis in comparative plant proteomics experiment. In: Jorrin-Novo JV, Komatsu S, Weckwerth W, Wienkoop S (eds) Plant Proteomics, vol 1072. Methods in Molecular Biology. Humana Press, pp 51-60. doi:10.1007/978-1-62703-631-3_5

van den Broeck HC, America AHP, Smulders MJM, Gilissen LJWJ, van der Meer IM (2008) Staining efficiency of specific proteins depends on the staining method: Wheat gluten proteins. Proteomics 8:1880-1884

Van Leene J, Stals H, Eeckhout D, Persiau G, Van De Slijke E, Van Isterdael G, De Clercq A, Bonnet E, Laukens K, Remmerie N, Henderickx K, De Vijlder T, Abdelkrim A, Pharazyn A, Van Onckelen H, Inzé D, Witters E, De Jaeger G (2007) A tandem affinity purification-based technology platform to study the cell cycle interactome in *Arabidopsis thaliana*. Mol Cell Proteomics 6:1226-1238

Van Riper S, de Jong E, Carlis J, Griffin T (2013) Mass spectrometry-based proteomics: Basic principles and emerging technologies and directions. In: Leszczynski D (ed) Radiation Proteomics, vol 990. Advances in Experimental Medicine and Biology. Springer Netherlands, pp 1-35. doi:10.1007/978-94-007-5896-4_1

Vandesompele J, De Preter K, Pattyn F, Poppe B, Van Roy N, De Paepe A, Speleman F (2002) Accurate normalization of real-time quantitative RT-PCR data by geometric averaging of multiple internal control genes. Genome Biol 3:research0034.0031 - research0034.0011

VanGuilder H, Vrana K, Freeman W (2008) Twenty-five years of quantitative PCR for gene expression analysis. Biotechniques 44:619-626

Vanzo E, Ghirardo A, Merl-Pham J, Lindermayr C, Heller W, Hauck SM, Durner J, Schnitzler J-P (2014) S-nitroso-proteome in poplar leaves in response to acute ozone stress. PLoS ONE 9:e106886

Vaudel M, Sickmann A, Martens L (2014) Introduction to opportunities and pitfalls in functional mass spectrometry based proteomics. BBA Proteins and Proteomics 1844:12-20

Venkatesan BM, Bashir R (2011) Nanopore sensors for nucleic acid analysis. Nat Nano 6:615-624

Vera-Estrella R, Barkla BJ, Pantoja O (2014) Comparative 2D-DIGE analysis of salinity responsive microsomal proteins from leaves of salt-sensitive *Arabidopsis thaliana* and salt-tolerant *Thellungiella salsuginea*. J Proteomics:in press

Villegas-Fernández AM, Krajinski F, Schlereth A, Madrid E, Rubiales D (2014) Characterisation by transcription factor expression profiling of the interaction *Medicago truncatula – Botrytis spp*. Plant Mol Biol Rep, in press

Visioli G, Marmiroli N (2013) The proteomics of heavy metal hyperaccumulation by plants. J Proteomics 79:133-145

Walbot V (1985) On the life strategies of plants and animals. Trends Genet 1:165-169

Walsh MJ, Delaney RH, Groose RW, Krall JM (2001) Performance of annual medic species (*Medicago spp.*) in southeastern Wyoming. Agron J 93:1249-1256

Wang AM, Doyle MV, Mark DF (1989) Quantitation of mRNA by the polymerase chain reaction. Proc Natl Acad Sci 86:9717-9721

Wang L, Li P, Brutnell TP (2010) Exploring plant transcriptomes using ultra high-throughput sequencing. Brief Funct Genomic 9:118-128

Wang W, Tai F, Chen S (2008) Optimizing protein extraction from plant tissues for enhanced proteomics analysis. J Sep Sci 31:2032-2039

Wang X, Li X, Li Y (2007) A modified Coomassie Brilliant Blue staining method at nanogram sensitivity compatible with proteomic analysis. Biotech Lett 29:1599-1603

Wang Z, Gerstein M, Snyder M (2009) RNA-Seq: a revolutionary tool for transcriptomics. Nat Rev Genet 10:57-63

Washburn MP, Wolters D, Yates JR (2001) Large-scale analysis of the yeast proteome by multidimensional protein identification technology. Nat Biotech 19:242-247

Watson BS, Asirvatham VS, Wang L, Sumner LW (2003) Mapping the proteome of barrel medic (*Medicago truncatula*). Plant Physiol 131:1104-1123

Weber APM, Weber KL, Carr K, Wilkerson C, Ohlrogge JB (2007) Sampling the Arabidopsis transcriptome with massively parallel pyrosequencing. Plant Physiol 144:32-42

Wienkoop S, Glinski M, Tanaka N, Tolstikov V, Fiehn O, Weckwerth W (2004) Linking protein fractionation with multidimensional monolithic reversed-phase peptide chromatography/mass spectrometry enhances protein identification from complex mixtures even in the presence of abundant proteins. Rapid Commun Mass Spectrom 18:643-650

Wienkoop S, Staudinger C, Hoehenwarter W, Weckwerth W, Egelhofer V (2012) ProMEX – a mass spectral reference database for plant proteomics. Front Plant Sci 3, Article 125

Wilkins MR, Sanchez J-C, Gooley A, Appel R, Humphery-Smith I, Hochstrasser D, Williams K (1995) Progress with proteome projects: why all proteins expressed by a genome should be identified and how to do it. Biotechnol Genet Eng 13:19-50

Wittig I, Braun H-P, Schagger H (2006) Blue native PAGE. Nat Protocols 1:418-428

Wu S-H, Ramonell K, Gollub J, Somerville S (2001) Plant gene expression profiling with DNA microarrays. Plant Physiol Biochem 39:917-926

Xi J, Wang X, Li S, Zhou X, Yue L, Fan J, Hao D (2006) Polyethylene glycol fractionation improved detection of low-abundant proteins by two-dimensional electrophoresis analysis of plant proteome. Phytochemistry 67:2341-2348

Xu J, Pascual L, Aurand R, Bouchet J-P, Valot B, Zivy M, Causse M, Faurobert M (2013) An extensive proteome map of tomato (*Solanum lycopersicum*) fruit pericarp. Proteomics 13:3059-3063

Xue AG, Warkentin TD, Kenaschuk EO (1997) Effects of timings of inoculation with *Mycosphaerella pinodes* on yield and seed infection of field pea. Can J Plant Sci 77:685-689

Yacoubi R, Job C, Belghazi M, Chaibi W, Job D (2013) Proteomic analysis of the enhancement of seed vigour in osmoprimed alfalfa seeds germinated under salinity stress. Seed Sci Res 23:99-110

Yan S, Tang Z, Su W, Sun W (2005) Proteomic analysis of salt stress-responsive proteins in rice root. Proteomics 5:235-244

Yan Z, Lin G, Ye Y, Wang Y, Yan R (2014) A generic multiple reaction monitoring based approach for plant flavonoids profiling using a triple quadrupole linear ion trap mass spectrometry. J Am Soc Mass Spectrom 25:955-965

Yates JR (2000) Mass spectrometry: from genomics to proteomics. Trends Genet 16:5-8

Yin X, Sakata K, Nanjo Y, Komatsu S (2014) Analysis of initial changes in the proteins of soybean root tip under flooding stress using gel-free and gel-based proteomic techniques. J Proteomics 106:1-16

Young ND, Cannon SB, Sato S, Kim D, Cook DR, Town CD, Roe BA, Tabata S (2005) Sequencing the genespaces of *Medicago truncatula* and *Lotus japonicus*. Plant Physiol 137:1174-1181

Young ND, Bharti AK (2012) Genome-enabled Insights into legume biology. Annu Rev Plant Biol 63:283-305

Zaninotto F, Camera SL, Polverari A, Delledonne M (2006) Cross talk between reactive nitrogen and oxygen species during the hypersensitive disease resistance response. Plant Physiol 141:379-383

Zhang L, Li X, Zheng W, Fu Z, Li W, Ma L, Li K, Sun L, Tian J (2013) Proteomics analysis of UV-irradiated *Lonicera japonica*Thunb. with bioactive metabolites enhancement. Proteomics 13:3508-3522

Zhang Z, Wu S, Stenoien DL, Paša-Tolić L (2014) High-throughput proteomics. Annu Rev Anal Chem 7:427-454

Zieske LR (2006) A perspective on the use of iTRAQ™ reagent technology for protein complex and profiling studies. J Exp Bot 57:1501-1508

Zimmermann P, Hirsch-Hoffmann M, Hennig L, Gruissem W (2004) GENEVESTIGATOR. Arabidopsis microarray database and analysis toolbox. Plant Physiol 136:2621-2632

Zohary D, Hopf M (2000) Domestication of plants in the old world: the origin and spread of cultivated plants in west Asia. Oxford University Press, Oxford.

Zohary D, Hopf M, Ehud W (2013) Domestication of plants in the old world: The origin and spread of domesticated plants in southwest Asia, Europe, and the Mediterranean basin. Oxford University Press, Oxford.

Zolla L, Timperio A-M, Walcher W, Huber CG (2003) Proteomics of light-harvesting proteins in different plant species. Analysis and comparison by liquid chromatography-electrospray ionization mass spectrometry. Photosystem II. Plant Physiol 131:198-214

Zolla L, Rinalducci S, Timperio AM, Huber CG, Righetti PG (2004) Intact mass measurements for unequivocal identification of hydrophobic photosynthetic photosystems I and II antenna proteins. Electrophoresis 25:1353-1366

Zolla L, Timperio AM (2005) Involvement of active oxygen species in protein and oligonucleotide degradation induced by nitrofurans. Biochem Cell Biol 83:166-175

Objectives

As already stated, the objectives pursued in this PhD thesis are to study the legume responses to phytopathogenic fungi by using a functional genomics approach (transcriptomics and proteomics). Thus, according to the actual trends in biosciences research, a multidisciplinary *omic* approach was used to carry out the studies of this PhD thesis.

Legumes are the third largest family of higher plants and they are second in agricultural importance. The pea (*Pisum sativum*) and the model legume *Medicago truncatula* were chosen to study their stress responses to *Erysiphe pisi* and *Mycosphaerella pinodes* pathogens. The pea crop constitutes an important source of protein for human consumption, being one of the most grown grain legume in the world, meanwhile *M. truncatula* is an important forage legume which is being used as a model plant for use in molecular and classical genetic studies. Moreover, within the phytopathogenic fungi, powdery mildew and ascochyta blight are one the most plant pathogenic fungi that seriously constrain crop production worldwide. Up to date very little is known about the molecular aspects of the defense and resistance responses of legumes to powdery mildew and ascochyta blight diseases. For a better understanding of such relationships, the study of the stress responses of these legumes to these phytopathogenic fungi is recommended.

Thus, the specific objectives pursued in this PhD thesis were:

- The detection of proteins and molecular mechanisms triggered by *P. sativum* in response to *E. pisi* and *M. pinodes* infections. These studies were attempted by applying a differential expression proteomic approach. The proteins found can be classified according to cellular processes to give a metabolic explanation for the adjustments performed by *P. sativum* in response to these phytopathogenic fungi.

- The elucidation of molecular mechanisms involved in *E. pisi* resistance by *M. truncatula*. This pathosystem was analyzed using two transcriptomics platforms,

microarray and quantitative real-time PCR, respectively. The sequences found in these experiments can be classified according to cellular processes to unveil the molecular mechanism and the regulatory network that controls the expression of genes involved in resistance to *E. pisi*.

Chapter 1: A proteomic approach to study pea (*Pisum sativum*) responses to powdery mildew (*Erysiphe pisi*)

Proteomics 2006, *6*, S163–S174 DOI 10.1002/pmic.200500396

RESEARCH ARTICLE

A proteomic approach to study pea (*Pisum sativum*) responses to powdery mildew (*Erysiphe pisi*)

Miguel Curto[1, 2], *Emilio Camafeita*[3], *Juan A. Lopez*[3], *Ana M. Maldonado*[1], *Diego Rubiales*[2] *and Jesús V. Jorrín*[1]

[1] Agricultural and Plant Biochemistry Research Group, Departamento de Bioquímica y Biología Molecular, Universidad de Córdoba, Córdoba, Spain
[2] Instituto de Agricultura Sostenible, IAS-CSIC, Córdoba, Spain
[3] Unidad de Proteómica, Centro Nacional de Investigaciones Cardiovasculares (CNIC), Madrid, Spain

As a global approach to gain a better understanding of the mechanisms involved in pea resistance to *Erysiphe pisi*, changes in the leaf proteome of two pea genotypes differing in their resistance phenotype were analyzed by a combination of 2-DE and MALDI-TOF/TOF MS. Leaf proteins from control non-inoculated and inoculated susceptible (Messire) and resistant (JI2480) plants were resolved by 2-DE, with IEF in the 5–8 pH range and SDS-PAGE on 12% gels. CBB-stained gels revealed the existence of quantitative and qualitative differences between extracts from: (i) non-inoculated leaves of both genotypes (77 spots); (ii) inoculated and non-inoculated Messire leaves (19 spots); and (iii) inoculated and non-inoculated JI2480 leaves (12 spots). Some of the differential spots have been identified, after MALDI-TOF/TOF analysis and database searching, as proteins belonging to several functional categories, including photosynthesis and carbon metabolism, energy production, stress and defense, protein synthesis and degradation and signal transduction. Results are discussed in terms of constitutive and induced elements involved in pea resistance against *Erysiphe pisi*.

Received: May 31, 2005
Revised: September 9, 2005
Accepted: October 3, 2005

Keywords:
Erysiphe pisi / Pea leaf proteome / *Pisum sativum* / Plant responses to pathogens / Powdery mildew

1 Introduction

Pea powdery mildew disease is caused by *Erysiphe pisi*, an obligate biotrophic ascomycete infecting different parts of the plant including seeds, leaves, stems and pods [1]. This disease causes important crop damage and yield losses, especially in semiarid regions [2]. The biological cycle of the parasite includes very well-defined stages from conidia infection to colony formation and conidia production: germination, appressorium development, host leaf cuticle penetration, haustoria, mycelium, and colony formation [1, 3]. Breeding for resistance, although being the most desirable control strategy, is a difficult task. Since resistance has proven to be a quantitative multigenic character [4], research is at present focused on new sources of resistance. To date there are only two known genes involved in resistance to powdery mildew in *Pisum sativum*, namely *er1* and *er2* [5]; however, little is known about their function and coding proteins, and there is a total absence of published reports dealing with molecular approaches of resistance to powdery mildew in legumes. In contrast, a number of histological

Correspondence: Dr. Jesús V. Jorrín, Departamento de Bioquímica y Biología Molecular, Universidad de Córdoba, Campus de Rabanales, Ed. Severo Ochoa (C6), 14071 Córdoba, Spain
E-mail: bf1jonoj@uco.es
Fax: +34-957-218592

Abbreviations: DIC, differential interference contrast microscopy; **FNR**, ferredoxin-NADP+(oxido) reductase; **HSP**, heat shock protein; **NBS-LRR**, nucleotide binding site-leucine-rich repeat; **PHGP**, phospholipid-hydroperoxide glutathione peroxidase; **PR**, pathogenesis-related; **ROS**, reactive oxygen species; **SA**, salicylic acid

studies have been published [6–8], showing that resistance operates during fungal haustoria formation and is associated with host epidermal cell necrosis [9].

Consequently, we have initiated research directed at investigating the molecular bases of pea-powdery mildew interaction and those underlying resistance using proteomics, an approach that is gaining interest for plant biology studies [10]. Proteomics has been successfully used for the study of different pathosystems and symbiotic interactions involving legumes [11]. In addition, a number of papers dealing with the mitochondrial, chloroplast, root and symbiosome pea proteome have been previously published [12–16].

The aim of the present study was to identify proteins/genes implicated in powdery mildew resistance. For that purpose, the 2-DE protein profile of inoculated and non-inoculated leaves from two pea cultivars displaying different degrees of resistance to *E. pisi* has been compared. Spots showing qualitative and quantitative changes between genotypes or treatments were subjected to MS analysis and a number of them identified by searching against protein databases. Results are discussed in terms of the functional implications of the proteins identified, with special emphasis on their putative defense role.

2 Material and methods

2.1 Plant and fungal material, growth conditions and inoculation

The pea JI2480 accession (John Innes Centre, Norwich, UK), carrying the *er2* gene, and the cultivar Messire were used as resistant and susceptible control genotypes, respectively [17]. The *E. pisi* isolate CO-01 was collected from pea-infected fields at Córdoba, and were maintained and propagated by infecting Messire plants.

The petri dish infection bioassay with leaves detached from adult plants (six-leaf developmental stage) was used [18]. Pea seeds were germinated and grown in a climatic chamber under controlled conditions until inoculation [17]. Leaves detached from the second to fifth node from individual plants were deposited on the surface of square Petri dishes (12 cm) containing agar (4 g/L, 62.5 mg/L benzimidazole), and inoculated using a setting tower to give an inoculum density of about 5 conidia/mm^2. Petri dishes were placed in a growth chamber (25°C, 12-h photoperiod, 250 μmol/m^2 light intensity, 80% relative humidity). Four independent replicates per genotype and treatment were performed, each replicate consisting of two leaves from two different plants.

Microscopic observations were carried out on one leaflet from each plant. The remaining leaflets were sampled, abundantly washed with water, blot dried with filter paper, weighed, frozen in liquid nitrogen and stored at −80°C until protein extraction.

2.2 Microscopy

One leaflet per plant was processed for microscopic observations at 48 and 72 h after inoculation, before disease symptoms were visible to the naked eye in susceptible plants. Leaflets were bleached with acetic acid:ethanol (1:3), washed with water, and fixed with lactoglycerol [19]. For light microscope examination of fungal development, fungal structures were first stained so as to avoid displacing ungerminated spores, by spraying leaves lightly with a solution of 0.2% methyl blue in 95% ethanol [20]. For every leaf, the germination percentage was calculated by scoring each of 100 conidia for the presence of a germ tube. To assess further development, another 100 germinated sporelings were examined and classified according to whether they had each formed a simple germ tube but no appressorium, had formed an appressorium but no secondary hyphae, or a colony had established as indicated by secondary hyphae emerging from the appressorial germ tube or mother conidium. As a measurement of colony size, the number of hyphal tips produced by each colony (indicating the total number of hyphae) was counted in 20 randomly selected colonies. To assess host cell death, indicating a hypersensitive response as a result of pathogen attack, 20 established colonies (sporelings with secondary hyphae) were examined on every leaf fixed after 48 h incubation. Leaves were observed using bright field and differential interference contrast (DIC) microscopy. Under bright field, the walls and contents of dead cells were discolored yellow or brown, while under DIC the cell contents appeared granular and disorganized.

2.3 Protein extraction and 2-DE

Leaf tissue (2 g fresh weight) was crushed in a precooled mortar with liquid nitrogen until a fine powder was formed. Proteins were extracted by TCA-acetone (10% TCA in acetone containing 0.07% DTT) precipitation [21]. The homogenate was sonicated for 5 min, kept at −20°C for 1 h, and centrifuged (Beckman Model J2–21 centrifuge) at 48 000 × *g* for 30 min at 4°C. The recovered pellet was washed twice with acetone-DTT, and once only with acetone, and dried at room temperature before solubilization in 8 M urea, 2% CHAPS, 0.5% IPG buffer, 20 mM DTT and 0.001% bromophenol blue. The protein content was quantified with the RC-DC protein assay (Bio-Rad), using BSA as standard. Samples were stored at −20°C until electrophoresis.

Three replicates were performed for each treatment and genotype, each consisting of an independent protein extraction from different plant samples. Precast 17 cm, pH 5–8 linear gradient (Bio-Rad) strips, were rehydrated for 12 h with 300 μL buffer containing 8 M urea, 2% CHAPS, 20 mM DTT, 0.5% Bio-Lyte (Bio-Rad) and bromophenol blue. About 500 μg protein were loaded at the cathodic end of the strips and electrofocussed (Bio-Rad Protean IEF Cell system) at 20°C with a gradually increasing voltage: 250 V for 20 min,

4 000 V for 150 min and 4 000 V/h to complete 10 000 V. After IEF, IPG strips were equilibrated according to Görg *et al.* [22]. The strips were then transferred onto vertical slab 12% SDS-polyacrylamide gels (Bio-Rad PROTEAN Plus Dodeca Cell) and electrophoresis run at 50 mA/gel until the dye front reached the bottom of the gel. Gels were stained with CBB G-250 according to the procedure reported by Mathesius *et al.* [23]. Gel images were captured with a GS-800 imaging densitometer (Bio-Rad), and analyzed with PD-Quest™ software (Bio-Rad) using tenfold over background as a minimum criterion for presence/absence. The analysis was re-evaluated by visual inspection, focusing on those spots most drastically altered between treatments and plant genotypes, and consistent in all replicates. Normalized spot volumes (individual spot intensity/normalization factor, calculated for each gel based on total quantity in valid spots) were determined for each spot, these values were used to designate the significant differentially expressed spots (at least twofold increase/decrease and statistically significant as calculated by Student's *t*-test, $p<0.05$), and further transformed into the protein amount using the ε value of 8.5192/ng [24]. For each spot, the average protein amount, SD, and CV were determined.

2.4 MS and protein identification

Spots from CBB-stained gels were manually excised and stored in milli-Q water at −20°C until MALDI-TOF/TOF analysis. The excised protein spots were automatically digested by using a Proteineer DP protein digestion station (Bruker-Daltonics). The digestion protocol used was that of Schevchenko *et al.* [25] with minor variations: gel plugs were subjected to reduction with 10 mM DTT in 50 mM ammonium bicarbonate and alkylation with 55 mM iodoacetamide in 50 mM ammonium bicarbonate. Gel pieces were then rinsed with 50 mM ammonium bicarbonate and ACN, and dried under a stream of nitrogen. Modified porcine trypsin (sequencing grade; Promega) at a final concentration of 13 ng/μL in 50 mM ammonium bicarbonate was added to the dry gel pieces and the digestion proceeded at 37°C for 6 h; peptides were extracted with 0.5% TFA. For PMF and peptide fragmentation fingerprinting (PFF) spectra acquisition, an aliquot of the above digestion solution was mixed with an aliquot of CHCA (Bruker-Daltonics) in 33% aqueous ACN and 0.1% TFA. This mixture was deposited onto a 600-mm AnchorChip MALDI probe (Bruker-Daltonics) and allowed to dry at room temperature. MALDI PMF and PFF were measured on a Bruker Ultraflex TOF/TOF MALDI mass spectrometer (Bruker-Daltonics). Mass measurements were performed in a positive ion reflector mode using 140-ns delayed extraction and a nitrogen laser (337 nm). The laser repetition rate was 50 Hz and the ion acceleration voltage was 25 kV. Mass measurements were performed automatically through fuzzy logic-based software to accumulate 100 single laser shot spectra or manually to accumulate ca. 200 single laser shot spectra. Each spectrum was internally calibrated with the mass signals of two trypsin autolysis ions: $[VATVSLPR+H]^+$ (m/z = 842 510) and $[LGEHNIDVLEGNEQFINAAK+H]^+$ (m/z = 2211.105) to reach a typical mass measurement accuracy of ±30 ppm. Known trypsin and keratin mass signals, as well as potential sodium adducts (+21.982 Da) or signals arising from methionine oxidation (+15.995 Da) were removed from the peak list. The measured tryptic peptide masses were transferred through the MS BioTools program (Bruker-Daltonics) as inputs to search the NCBInr database using MASCOT (Matrix Science) [26]. A detailed analysis of peptide mass mapping data was performed using flexAnalysis software (Bruker-Daltonics). When available, MS/MS data from LIFT TOF/TOF spectra were combined with MS PMF data for database searching.

3 Results

3.1 Development of *E. pisi* on leaves of Messire and JI2480 genotypes

The petri dish bioassay revealed the existence of differences in resistance to *E. pisi* between Messire and JI2480 genotypes (Fig. 1). Disease symptoms started to be visible all over the leaf as early as 48 h after inoculation in Messire but not in JI2480 leaflets (Fig. 1B, E). Furthermore, Messire leaf tissue was completely covered by powdery mildew and collapsed by day 12 post infection, while only punctual necrotic lesions

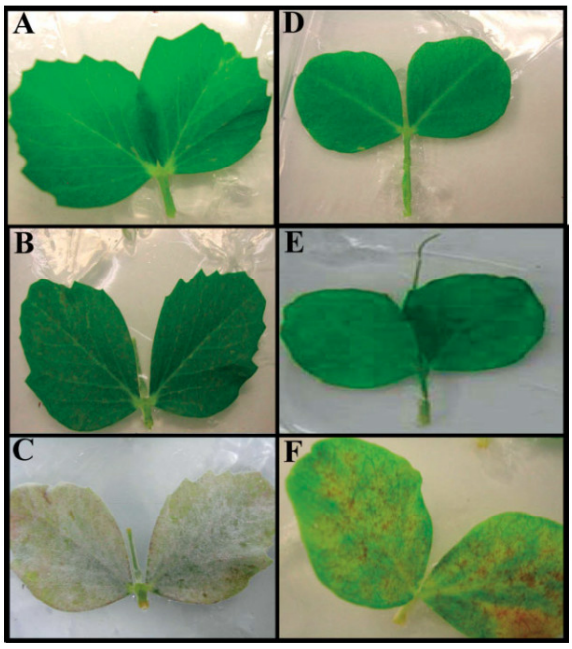

Figure 1. *E. pisi* development on pea leaves from Messire (A–C) and JI2480 (D–F) genotypes. Pictures correspond to 0 h (A, D), 48 h (B, E) and 12 days (C, F) after inoculation with spores of *E. pisi*.

were observed in leaves of JI2480 (Fig. 1C, F). Microscopic evaluation of fungal progress revealed no quantitative differences between either genotype for spore germination and appresorium formation (Table 1). Nevertheless, a slight reduction in the percentage of spores forming haustoria, together with a significant decrease in the number of colonies forming hyphal tips, were assessed in the resistant genotype. In addition, a significantly higher percentage of colonies was associated with epidermal cell necrosis in the resistant plants (Table 1). The phenotypic differences between genotypes described above occurred 48 h after inoculation. Accordingly, we selected this time as the tissue sampling instance for protein analysis, expecting the proteins responsible for such phenotypes to be present in the extracts.

3.2 2-DE, spot analysis and protein identification

The protein profile of *P. sativum* leaf tissue was analyzed by 2-DE in healthy as well as in inoculated leaves 48 h post infection. Previous experiments (data not shown) revealed that most of the pea leaf proteins resolved were in the 5–8 pH and 8–98-kDa range. Accordingly, IEF was carried out within the 5–8 pH range and SDS-PAGE using 12% polyacrylamide. Following CBB staining of the gels, the number of spots resolved was of about 450 (Fig. 2). The protein pattern was quite reproducible among technical replicates of the same sample and replicates from independent extractions (average value for the biological CV, 20.3 ± 15.6; Suppl. Table 1). Analysis of the 2-D gels using the PD-Quest™ software, followed by visual confirmation, revealed the existence of at least 106 spots showing qualitative or quantitative differences between genotypes or treatments (Fig. 3; Suppl. Table 1). Spot differences were only considered if they were consistently manifested in all the replicates proven to be statistically significant (Student's *t*-test; $p<0.05$) and displaying higher differences than the biological variability for the spot. Thus, 77 spots were present in different amounts in gels from non-infected Messire and JI2480 leaf tissue. Significantly, only 19 and 12 spots were differentially expressed between control and inoculated leaf extracts from Messire and JI2480 plants (Fig. 3; Suppl. Table 1).

Table 1. *E. pisi* development on pea leaves from Messire and JI2480 plants, as determined by the petri dish bioassay. Fungal progress was evaluated microscopically. Data correspond to percentage of germinated spores and spores forming haustoria and colonies, as well as percentage of colonies associated with epidermal cell death and number of hyphal tips per established colony

Fungal developmental stage	Plant genotype	
	Messire	JI2480
% Spore germination[a), b)]	90.7	83.8
% Appressoria formation[c), b)]	99.6	98.9
% Colony establishment[d), b)]	92.1	85.2[e)]
% Colonies associated with epidermal cell death[f)]	0.7	33.9[e)]
Number of hyphal tips per colony[f)]	8.3	2.3[e)]

a) % of spores that germinated producing a germtube longer than the spore.
b) 100 individual spores were visualized.
c) % of germtubes forming an appressorium over an epidermal cell.
d) % of colonies established out of the appressoria formed.
e) Indicates that means of Messire and JI2480 are significantly different (Student's *t*-test $p<0.05$).
f) 20 established colonies were visualized.

Protein identification was accomplished by PMF combined with PFF of selected peptides by MALDI-TOF/TOF, resulting in 67 matches out of the 106 differences observed. Table 2 shows the accession numbers and putative names of proteins that correspond to specific spots shown in Fig. 3, along with their experimental and theoretical p*I* and molecular mass values and relative protein amount. Proteins were clustered according to their putative function, and the proteins with no assigned function were classified as unnamed or hypothetical.

Thus, the 44 identified spots differentiating genotypes (non-inoculated, JI2480 *vs.* Messire) corresponded to proteins involved in several cellular functions (Table 2): (i) photosynthesis and carbohydrate metabolism, 10 spots; (ii) Krebs cycle, 3 spots: 2 of them, spots 12 and 14, correspond to the same protein displaying different p*I* values and might account for posttranslational forms of the enzyme; (iii) proteins involved in diverse functions but related to plant stress and defense responses, 15 spots; (iv) secondary metabolism, 1 spot; (v) protein synthesis and degradation, 4 spots, including spots 31 and 69, corresponding to a proteasome iota subunit displaying a different size; (vi) signal transduction, 1 spot; (vii) vesicle trafficking, 1 spot; and finally, (viii) unnamed or hypothetical proteins, 9 spots.

When comparing inoculated and non-inoculated JI2480 plants, 7 proteins were identified that belong to the following functional categories: (i) phothosynthesis and carbohydrate metabolism, 4 spots; spots 103 and 106 correspond to the same protein, a chloroplast translation elongation factor, displaying a slight shift in their p*I* value; (ii) proteins involved in stress and defense responses, 2 spots: these spots, 22 and 60, were previously identified in this study as differentiating genotypes; and finally (iii) a putative protein.

When comparing inoculated and control, non-inoculated, Messire plants, 19 differentially expressed spots were observed; 16 of them were identified and participate in the following processes: (i) photosynthesis and carbohydrate metabolism, 6 spots; (ii) Krebs cycle, 3 spots; (iii) stress response, 1 spot; (iv) secondary metabolism and other metabolic pathways, 4 spots; (v) protein degradation, 1 spot; and finally, (vi) one unnamed protein.

Table 2 shows the organism from which the identified proteins proceed, together with the sequence coverage and the values for the experimental and theoretical p*I* and mo-

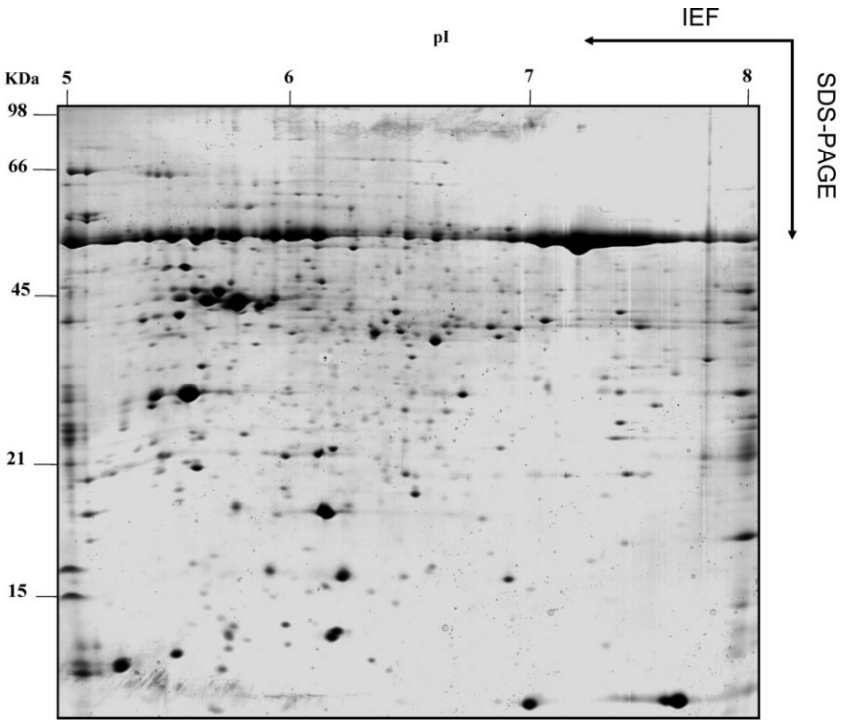

Figure 2. 2-DE protein profile of CBB-stained leaf proteins from *P. sativum*. Proteins, 500 μg, were loaded and resolved on first-dimension, pH 5–8 linear gradient, and second dimension, SDS-PAGE on a 12% gel. The gel corresponds to leaf extracts from non-infected JI2480 plants. Molecular mass is given on the left, while the p*I* is given at the top of the figure.

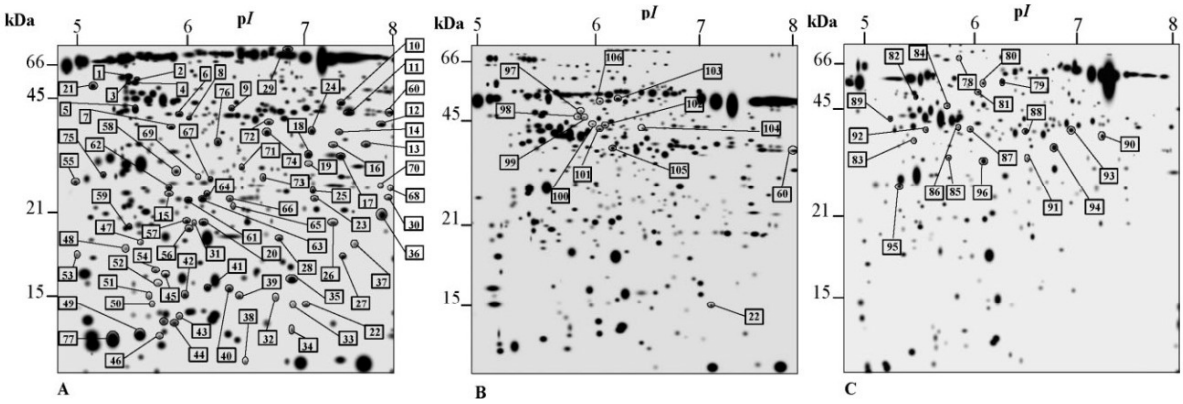

Figure 3. Master gels corresponding to leaf extracts of: (A) control, non-infected, leaf tissue from JI2480 and Messire; (B) non-infected and infected JI2480 leaf tissue; (C) non-infected and infected Messire leaf tissue. Circled and numbered spots correspond to those showing changes among genotypes or treatments (Table 2, Suppl. Table 1). Molecular mass (on the left) and p*I* (on the top) were calculated using the PD-Quest software and standard molecular weight markers.

lecular mass. The 22 spots identified by matching against *P. sativum* sequences showed a good correlation between experimental and theoretical p*I*/molecular mass. The number of matched peptides was between 5 and 13, with 16–71% of sequence coverage when PMF analysis was used to identify the protein, while 10–17 amino acid peptides were used for PFF analyses. Similar results were found for proteins identified by homology to sequences from very closely related species such as *Medicago sativa* (4 spots) and garden pea (2 spots). The remaining proteins (37 spots) were identified by comparison with sequences from different organisms, showing more variable score results and bigger differences between theoretical and experimental p*I* and molecular mass values.

Table 2. List of identified proteins

Spot[a]	Protein/function[b]	R.P.A.[c]	Accession no.[d]	Organism[e]	Mol. mass; p*I*[f] experimental/ theoretical	Matched peptides/ sequence[g]	% sequence coverage[h]
JI2480 *vs.* Messire[i]	**Photosynthesis and carbohydrate metabolism**						
1	Rubisco activase	nd-JI	nr gi|13430334	*Zantedeschia aethiopica*	52.4;5.4/37.0;6.6	8	31
2	Ribulose-1,5-bisphosphate carboxylase/ oxygenase activase	nd-ME	nr gi|415852	*Malus domestica*	51.3;5.5/48.0;7.6	6	16
15	Chloroplast ribosomal protein L1	nd-ME	nr gi|577089	*Pisum sativum*	24.0;5.8 /23.5;5.5	VAVLTQGERFDEAK	7
16	Flavoenzyme ferredoxin-NADP+(oxido) reductase, chain B	nd-ME	nr gi|4930124	*Pisum sativum*	32.9;7.2 /34.8;6.5	8	34
24	Carbonate dehydratase precursor	nd-ME	nr gi|100078	*Garden pea*	35.2;7.1/35.3;7.0	11	55
25	Carbonic anhydrase	nd-ME	nr gi|8569257	*Pisum sativum*	23.7;7.0/23.9;6.7	AQHGDAPFAELCTHCEK	64
30	Chloroplast Rieske FeS protein	nd-ME	nr gi|20832	*Pisum sativum*	23.0;8.0/24.2;8.6	GDPTYLVVEKDR	20
37	Ribulose bisphosphate carboxylase	nd-ME	nr gi|20855	*Pisum sativum*	19.0;7.5/20.0;8.3	KGWVPCLEFELEK	43
61	Putative triosephosphate isomerase	nd-ME	nr gi|21593477	*Arabidopsis thaliana*	23.0;6.0/33.3;7.6	8	26
68	Plastoquinol-plastocyanin reductase	nd-ME	nr gi|280397	*Pisum sativum*	25.1;8.0/24.6;8.6	7	43
	Krebs cycle						
3	Isocitrate dehydrogenase	nd-ME	nr gi|1708402	*Nicotiana tabacum*	51.1;5.4 /47.0;6.0	8	24
12	Putative malate dehydrogenase	nd-ME	nr gi|37725953	*Pisum sativum*	36.0;7.7/37.0;7.1	6	29
14	Putative malate dehydrogenase	nd-ME	nr gi|37725953	*Pisum sativum*	35.2;7.3/37.0;7.1	GGAEEIYQLGPLNEYER	5
	Stress and defense responses						
20	Phospholipid-hydroperoxide glutathione peroxidase	nd-ME	nr gi|7433104	*Spinach*	20.5;6.0/19.2;5.9	9	18
21	Resistance protein RGC2	nd-ME	nr gi|34485235	*Lactuca sativa*	46.5;5.2/47.7;5.5	7	11
22	Disease resistance	nd-ME	trm Q9FI14_ARATH	*Arabidopsis thaliana*	14.7;7.0/13.6;6.5	10	32
29	Probable disease resistance protein At1g58390	nd-ME	nr gi|29839584	*Arabidopsis thaliana*	69.5;6.8/71.1;6.0	6	14
42	Superoxide dismutase [Cu-Zn],	nd-ME	nr gi|134683	*Pisum sativum*	15.5;6.0/15.6;5.9	5	31
45	ABA-responsive protein	nd-ME	nr gi|20633	*Pisum sativum*	16.5;5.8/17.0;5.5	8	71
48	Lysozyme	nd-ME	nr gi|2781278	*Medicago sativa*	17.6;5.4/17.2;5.4	FESNFNTQATNR	51
52	Kunitz-trypsin inhibitors A/C precursor	nd-ME	nr gi|125020	*Glycine max*	15.9;5.7/24.0;4.9	7	28
53	Ripening-related protein	nd-ME	nr gi|34452233	*Pisum sativum*	17.5;5.2/18.2;5.1	6	43
55	Pathogenesis-related protein 5 precursor	nd-ME	nr gi|135915	*Arabidopsis thaliana*	24.1;5.0/25.2;4.7	5	31
57	Extensin-like protein (Ext1)	nd-ME	nr gi|18138038	*Lycopersicon esculentum*	20.6;6.0/45.2;9.2	6	16
60	Exopolygalacturonase	nd-ME	nr gi|1346701	*Arabidopsis thaliana*	41.5;8.0/41.3;8.2	7	22
65	Fruit-ripening gene	nd-ME	nr gi|7580480	*Lycopersicon esculentum*	22.1;6.4/22.0;6.1	AEEYHQQYLEK	35
70	PR1-like protein	nd-ME	nr gi|50908387	*Oryza sativa*	26.7;7.9/24.3;11.0	5	26
72	Peroxidase 21 precursor	nd-ME	nr gi|25453196	*Arabidopsis thaliana*	35.9;6.6/36.7;7.0	4	13
	Protein synthesis and degradation						
31	Proteasome IOTA subunit	nd-ME	nr gi|3377794	*Glycine max*	20.2;6.0/27.0;5.8	7	36
33	E2, ubiquitin-conjugating enzyme, putative	nd-ME	nr gi|21553737	*Arabidopsis thaliana*	14.6;6.9/16.5;6.3	5	36
51	Eukaryotic translation initiation factor 5A-2	nd-ME	nr gi|15866587	*Medicago sativa*	15.1;5.6/17.2;5.4	KLEDIVPSSHNCDV PHVNR	26
69	Proteasome IOTA subunit	nd-ME	nr gi|3377794	*Glycine max*	26.9;6.0/27.0;5.8	6	32
	Signal transduction						
13	G protein beta subunit-like	nd-ME	nr gi|2385376	*Medicago sativa*	33.0;7.5/36.0;7.1	9	36
	Vesicle trafficking						
71	Ras-related protein Rab-2-B	nd-ME	nr gi|1346957	*Zea mays*	28.5;6.4/23.2;6.9	5	27

Table 2. Continued

Spot[a)]	Protein/function[b)]	R.P.A.[c)]	Accession no.[d)]	Organism[e)]	Mol. mass; p*I*[f)] experimental/ theoretical	Matched peptides/ sequence[g)]	% sequence coverage[h)]
	Secondary metabolism						
54	Probable strictosidine synthase	nd-ME	nr gi|25335893	*Arabidopsis thaliana*	16.8;5.7/44.5;6.3	5	14
	Hypothetical proteins						
5	Hypothetical protein	nd-ME	nr gi|50908465	*Oryza sativa*	41.3;5.5/23.0;4.3	EGAVAAISTAPRR	6
23	Hypothetical protein	nd-ME	nr gi|7487885	*Arabidopsis thaliana*	23.3;7.1/89.3;5.0	8	14
27	Hypothetical protein	nd-ME	nr gi|50936897	*Oryza sativa*	17.8;7.3/14.6;8.9	5	9
35	Unnamed protein	nd-ME	nr gi|12149	*Pisum sativum*	16.4;6.6/15.1;6.5	8	31
47	Hypothetical protein	nd-ME	nr gi|7486947	*Arabidopsis thaliana*	18.0;5.6/21.0;5.5	GGGPYGQGVTR	6
58	Unnamed protein product	nd-ME	nr gi|20617	*Pisum sativum*	27.4;5.8/28.0;5.5	QYYNISVLTR	24
73	Hypothetical protein	nd-ME	nr gi|25405727	*Arabidopsis thaliana*	26.8;6.6/26.6;5.1	4	18
74	Unnamed protein product	nd-ME	nr gi|20673	*Pisum sativum*	34.4;6.8/35.3;7.0	13	51
76	Unnamed protein product	nd-JI	nr gi|20621	*Pisum sativum*	33.4;6.3/34.9;6.2	9	36
JI2480 I *vs.* C[i)]	**Photosynthesis and carbohydrate metabolism**						
101	Putative rubisco activase	nd-JI-C	nr gi|19387266	*Oryza sativa*	44.1;5.9/48.5;5.5	TFQTELIFR	2
103	Choloroplast translation elongation factor	nd-JI-C	nr gi|2330655	*Pisum sativum*	53.0;6.0/53.0;6.6	KYDEIDAAPEER	19
105	Fructose-bisphosphate aldolase 1	nd -JI-C	nr gi|399024	*Pisum sativum*	40.8;6.0/39.0;5.8	12	44
106	Choloroplast translation elongation factor	nd -JI-C	nr gi|2330655	*Pisum sativum*	52.0;5.9/53.0;6.6	KYDEIDAAPEER	8
	Stress and defense						
22	Disease resistance	5 -JI-Inf	trm Q9FI14_ARATH	*Arabidopsis thaliana*	14.7;7.0/13.6;6.5	10	9
60	Exopolygalacturonase	3.93-JI-Inf	nr gi|1346701	*Arabidopsis thaliana*	41.5;8.0/41.3;8.2	7	22
	Unnamed protein						
104	Putative protein	nd -JI-C	nr gi|7270317	*Arabidopsis thaliana*	44.3;6.3/46.6;6.3	THVVTTPGSGFG PGGEGFVR	5
Messire I *vs.* C[i)]	**Photosynthesis and carbohydrate metabolism**						
82	Ribulose-bisphosphate carboxylase activase	nd-ME-C	nr gi|100616	*Hordeum vulgare*	50.8;5.5/47.4;7.5	14	36
83	Putative fructokinase	nd-ME-C	nr gi|20258778	*Arabidopsis thaliana*	38.8;5.5/36.0;5.5	TALAFVTLR	10
87	ADP-glucose synthase	nd-ME-C	nr gi|1707939	*Beta vulgaris*	40.9;5.9/54.1;5.6	10	20
92	Aldolase	3.86 -ME-Inf	nr gi|169039	*Pisum sativum*	41.6;5.6/38.0;5.4	SPNPWHVSFSYAR	38
93	Malate dehydrogenase precursor	nd-ME-C	nr gi|2827080	*Medicago sativa*	42.2;6.8/35.8;8.8	ALEGADVVIIPAGVPR	21
95	N-Glyceraldehyde-2-phosphotransferase	nd-ME-C	nr gi|8885622	*Arabidopsis thaliana*	32.8;5.4/32.0;5.1	ENPGCLFIATNR	7
96	Putative triosephosphate isomerase	3.13 -ME-Inf	nr gi|34908172	*Oryza sativa*	34.9;6.0/27.2;5.5	VIACIGETLEQR	5
	Krebs cycle						
86	Pyruvate dehydrogenase E1 beta subunit isoform 1	nd-ME-C	nr gi|3850999	*Zea mays*	41.7;5.8/40.0;5.5	VLAPYSAEDAR	10
90	Nodule-enhanced malate dehydrogenase	nd-ME-C	nr gi|3377762	*Pisum sativum*	40.9;7.2/41.8;7.4	7	23
93	Malate dehydrogenase precursor	nd-ME-C	nr gi|2827080	*Medicago sativa*	42.2;6.8/35.8;8.8	ALEGADVVIIPAGVPR	21
	Secondary metabolism						
81	S-Adenosyl methionine synthetase	nd-ME-C	nr gi|497900	*Populus balsamifera*	53.0;6.0/44.0;5.6	8	25
85	2′-Hydroxyisoflavone reductase	nd-ME-C	nr gi|1084375	*Garden pea*	35.0;5.7/35.4;5.3	21	68
89	O-Acetylserine (thiol)-lyase	nd-ME-C	nr gi|17944	*Capsicum annuum*	42.9;5.3/40.0;5.5	LIAVVFPSFGER	3
91	Putative isoflavone reductase	nd-ME-C	nr gi|19310585	*Arabidopsis thaliana*	35.0;6.4/34.0;6.6	FFPSEFGNDVDR	8
	Stress and defense responses						
78	HSP70	nd-ME-C	nr gi|20835	*Pisum sativum*	73.1;5.8/72.3;5.8	9	16

Table 2. Continued

Spot[a)]	Protein/function[b)]	R.P.A.[c)]	Accession no.[d)]	Organism[e)]	Mol. mass; p*I*[f)] experimental/ theoretical	Matched peptides/ sequence[g)]	% sequence coverage[h)]
	Protein degradation						
84	DegP protease precursor	nd-ME-C	nr gi|2565436	*Arabidopsis thaliana*	45.9;5.7/46.0;5.5	VVGFDQDKDVAVLR	19
	Unnamed protein						
88	Unnamed protein product	3.17 -ME-Inf	nr gi|20751	*Pisum sativum*	40.8;6.4/39.2;6.1	HKEHIAAYGEGNER	34

a) Assigned spot number as indicated in Fig. 3.
b) Identified protein of *Pisum sativum* or homologous protein from other organism.
c) Relative protein amount. Values are mean of three independent replicates. Fold change between the protein amount of JI2480 and Messire genotypes, JI2480 infected and control plants, and between Messire infected and control plants. The plants that overexpress the spot are indicated (-JI, indicates the spot is overexpressed in JI2480; -ME-Inf and –JI-Inf, indicates the spot is overexpressed in the infected plants. nd-ME and nd-JI, non-detected in Messire and JI2480, respectively; and nd-ME-C and nd-JI-C, non-detected in control conditions in Messire and JI2480, respectively.
d) Database accession numbers according to: NCBInr (nr); trEMBL (trm).
e) Organism from which the identified protein proceeds.
f) Experimental and theoretical mass (kDa) and p*I* of identified proteins. Experimental values were calculated with PD-Quest software and standard molecular mass markers. Theoretical values were retrieved from the protein database.
g) Number of matched peptides with PMF data and peptide sequences matched with PFF data.
h) Amino acid sequence coverage for the identified proteins. Identified proteins corresponding to spots showing differences between genotypes (JI2480 *vs.* Messire) or treatments (infected, I *vs.* control, C)
i) Identified proteins corresponding to spots showing differences between genotypes (JI2480 *vs.* Messire) or treatments (infected, I *vs.* control, C).

4 Discussion

We report changes in the leaf proteome of two pea genotypes, JI2480 and Messire, differing in their resistance to *E. pisi* (powdery mildew), as previously shown by field experiments [17]. Using a proteomic approach we aimed at a better understanding of the molecular bases of this plant-pathogen interaction and that of the resistance.

The petri dish bioassay showed that the pathogen completed its biological cycle in the susceptible cultivar Messire. In resistant JI2480 plants, by contrast, the development of the pathogen was blocked after germination and appressoria formation, most colonies being associated with epidermal cell necroses (Fig. 1; Table 1). We have consistently found that resistance in JI2480 plants occurs after appressorium formation, at about 48 h after inoculation, the sampling time chosen for proteome analysis.

According to our experimental conditions, changes observed in the leaf proteome in this study were limited to just a small fraction of the total leaf proteome. These include major (those visible after CBB staining) soluble proteins (at least soluble in the IEF buffer), and within the p*I* 5–8 and 8–98-kDa range. Even so, a considerable number of differentially expressed spots, 106, about 23% of resolved spots, were observed. Only 2 of them (spots 22 and 60) were common differences between genotypes (unique to the resistant plants) and treatments (further induced in these plants upon pathogen challenge).

Interestingly, most of the spot changes (77) were in differentiated genotypes, with a much lower figure obtained when comparing inoculated and non-inoculated Messire (19 spots) and JI2480 (12 spots) leaf extracts (Fig. 3a; Suppl. Table 1). This is in agreement with the ability of the 2-DE technique to successfully detect genetic diversity within plant species [27], and to the protein signature information that can be ascribed to the protein profile in different genetic backgrounds [28]. Although not all the observed differences are necessarily related to resistance, our data suggest that resistance in JI2480 plants could be based on defense elements constitutively present in these plants, rather than on those induced after pathogen challenge.

The combination of PMF and PFF analyses allowed the identification of 67 out of the 106 differential protein spots, with 57 having an assigned function. The success in identification is possibly due to the increasing amount of genomic data available for model legume *Medicago*, pea and other important grain legume crops as a consequence of ambitious projects currently running in labs worldwide, and of European initiatives (*e.g.*, "New strategies to improve grain legume for food and feed", http://www.eugrainlegumes.org/pdfs/summary.pdf).

Out of the 77 spots that differentiated genotypes, 44 were successfully identified, and clustered according to their putative biological role (Table 2). Their functional significance is discussed below.

Several spots identified as proteins of the photosynthesis-carbohydrate metabolism and Krebs cycle occurred in larger amounts in JI2480 than in Messire plants. This could indi-

cate a greater efficiency of the former in transforming light into chemical energy, CO_2 assimilation, and obtaining intermediate metabolites from photoassimilates needed for biosynthetic pathways. There has long been evidence that a constitutive expression of resistance leads to a reduction in plant growth and fitness as a consequence of "metabolic competition" directed towards the synthesis of defense elements [29–31]. The increased intensity of spots corresponding to components of the primary metabolism and biosynthetic machinery in JI2480 plants could pay for the fitness cost of the constitutive resistance, hence resulting in more stress-resistant plants [32]. Thus, spots 16, 30 and 68 corresponded to the flavoenzyme ferredoxin-$NADP^+$ (oxido) reductase (FNR), to a chloroplastic FeS protein and to a plastoquinol-plastocyanin reductase, respectively, all of them components of the photosynthetic electronic chain responsible for converting light energy into chemical energy [33]. RubisCO (ribulose-1,5-biphosphate carboxylase oxygenase; spots 2 and 37, corresponding to the large and small subunit, respectively), is the key, first enzyme, of the CO_2 assimilation pathway. RubisCO activase (spot 1) is specifically involved in the activation of RubisCO through carbamylation. Carbonic anhydrase (spots 24 and 25) catalyzes the reversible hydration of CO_2 in C3 plants. In *Arabidopsis* and barley, resistance to *E. pisi* is dependent on salicylic acid (SA) accumulation [34], and, interestingly, it has been reported that carbonic anhydrase may function as a SA-binding protein. Moreover, silencing of the carbonic gene in tomato suppressed the gene-for-gene mediated hypersensitive response associated with resistance [35]. Triose-phosphate isomerase (spot 61) catalyses the interconversion of glyceraldehyde-3-phosphate and dihydroxyacetone phosphate, metabolites of the triose-phosphate pool that participate in several different pathways (glycolysis, pentose-phosphate) generating energy and carbon skeleton for biosynthetic reactions. Spot 3, identified as isocitrate dehydrogenase, and spots 12 and 14, corresponding to different forms of the enzyme malate dehydrogenase, belong to the citric acid cycle. This pathway has an amphibolic character providing energy, reducing equivalents and intermediates for biosynthetic pathways (*i.e.*, amino acids). It is important to consider that the changes in the protein profile observed could account for either gene induction/repression or for PTMs of proteins. Those modifications could render proteins more (or less) efficient for a specific function. Finally, the increased protein biosynthetic capacity of JI2480 compared to Messire correlates well with the presence in larger amounts in the former of spots 15 and 51, identified as a chloroplastic ribosomal protein L1 and a translation initiation factor, respectively.

Yet another major set of proteins differentiating genotypes, all of them unique or more abundant in the JI2480 resistant plants, corresponded to stress and defense related proteins. Spots 21, 22 and 29 were identified as proteins encoded by members of the highly duplicated family of nucleotide binding site-leucine-rich repeats (NBS-LRR) plant resistance genes that confer resistance to many plant pathogens [36]. Not surprisingly, a number of the proteins identified correspond to typical pathogenesis-related proteins (PRs) that display antimicrobial activity and accumulate to high levels in response to pathogen challenge. Some of these PRs are considered molecular markers for resistance against a broad range of pathogens including *E. pisi* [37]. Thus, spots 55 and 70 correspond to the thaumatin–like protein PR-5, and PR-1, respectively [38, 39] and spot 52 corresponds to a Kunitz-trypsin inhibitor [40]. Trypsin inhibitors inhibit extracellular fungal proteinases [41] and have been implicated in several physiological processes from symbiosis to plant defense [42–44]. Extensins (spot 57) belong to a family of extracellular proteins harboring (hydroxyl)proline-rich motifs that are also induced during pathogenesis and symbiosis [45, 46]. A possible role for extensins and exopolygalacturonase (spot 60) in resistance is proposed based on their involvement in cell wall modification and disassemblage [47–50]. The identification of two ripening-related proteins (spots 53 and 65) supports the view of a bi-functional role proposed for some of these proteins during plant defense responses and fruit ripening [51–53].

A possible role in resistance to *E. pisi* for the ABA-responsive protein (spot 45) identified in JI2480 is consistent with the proposed functional implications of these proteins during drought and general stress conditions [54, 55].

Spots 20, 72 and 42 were identified as phospholipid-hydroperoxide glutathione peroxidase, peroxidase and superoxide dismutase, respectively. These enzymes are part of the cellular antioxidant system involved in tolerance to oxidative stress, caused by reactive oxygen species (ROS) formed during normal metabolic processes or under biotic and abiotic stressing conditions. Peroxidases, induced by several stresses including pathogen infection, are involved in hydrogen peroxide detoxification and are associated with lignification and cell wall phenol deposition [56]. Phospholipid-hydroperoxide glutathione peroxidases (PHPGs) [57, 58] are implicated in protecting biomembranes from oxidative damage through removal of phospholipid hydroperoxides formed during abiotic stresses and pathogen infection [59, 60]. Superoxide dismutases, dramatically induced in response to treatments that trigger oxidative stress, catalyze the dismutation of superoxide into oxygen and hydrogen peroxide [61]. Data found in JI2480 shows a good correlation between a high level of photosynthetic enzymes, superoxide dismutase and peroxidase, consistent with a higher production of superoxide anions and hydrogen peroxide. In addition, resistance to a broad range of pathogens including *E. pisi* correlates with the occurrence of an oxidative burst [62], as part of the chemical defense or as part of the signal transduction that mediates defense gene activation [63].

Strictosidine synthase (spot 54), is a central enzyme of the biosynthetic pathway of monoterpene indole alkaloids, compounds associated with defense [64]. Consistent with our results, it has been shown that the expression of strictosidine synthase is induced by fungal elicitors through several signaling steps involving ROS [65–67].

From this set of data we can hypothesize that the constitutive presence of so many different stress- and defense-related proteins in JI2480 might render plants more resistant to pathogens. This will result in an extra energetic cost for the plant that must be paid for by increasing primary metabolism functions to maintain overall plant fitness and performance.

A number of spots differentiating genotypes were identified as proteins involved in more general functions. Thus, spots 31 and 69 corresponded to a proteasome iota subunit and spot 33 to an ubiquitin-conjugating enzyme component of the proteolytic pathway. These proteins take part in degradation processes of targeted proteins during a number of cellular processes [68, 69]. Spot 13 corresponds to a β-subunit of G-proteins involved in a wide variety of cellular processes in higher plants such as growth, development, hormone signaling and defense responses [70, 71]. On the other hand, spot 71 was identified as a small GTPase belonging to the Rab family that are regulators of vesicle trafficking [72].

When the pea leaf proteome was further analyzed in response to *E. pisi* infection at least 12 proteins were induced or modified in JI2480 leaves (Fig. 3B; Table 2). Most of them belong to the photosynthesis-carbohydrate metabolism and stress and defense category, and their biological role has been discussed above, with the exception of a chloroplast translation elongation factor (spot 106). The higher expression of the spot corresponding to this enzyme in infected JI2480 plants could reflect an increase in the protein biosynthetic capacity of plant cells needed upon pathogen challenge.

The analysis of the leaf proteome of infected Messire plants revealed an increase in spots corresponding to enzymes of the primary metabolism (Fig. 3C; Table 2), in a similar manner to that observed for JI2480 plants. These changes include ADP-glucose synthase (spot 87) that catalyzes the first committed step in the biosynthesis of starch [73]. These data support the hypothesis of energetic metabolism rearrangements taking place in the infected tissues to prime defense responses.

Two enzymes of the isoflavonoid pathway, 2'-hydroxyisoflavone reductase (spot 85) and isoflavone reductase (spot 91), have been identified in infected Messire plants. This is not surprising as the antimicrobial properties of these compounds and their involvement in legume symbiotic and pathogenic interactions are well documented [74]. A recent work in transgenic pea modifying the activity of this enzyme further supports its function in defense [75]. The changes observed in these enzymes in susceptible plants upon infection are in agreement with the idea that susceptible plants are not defenseless, but set up an inefficient defense, which is insufficient in terms of intensity, or extension, for stopping disease progression [76].

S-adenosylmethionine synthase (spot 81) and O-acetylserine (thiol)lyase (spot 89) are two enzymes involved in the synthesis of sulfur amino acids and sulfate assimilation pathways in plants [77, 78]. The involvement of these proteins in pea–*E. pisi* interaction remains unclear.

Other spots showing changes in Messire plants upon infection were identified as HSP70 (spots 78) and DegP protease (spot 84). HSP70 are components of the chloroplast import complex [79], and recent findings suggest a function for them in defense responses against pathogens [80]. DegP proteases are ATP-independent serine proteases that have been implicated in the degradation of luminal and thylakoid membrane proteins [81, 82]. The biological significance of this protein in our system remains unclear.

In summary, we have compared the leaf protein profile of two pea cultivars differing in their resistance phenotype to *E. pisi*. Using a combination of 2-DE and MALDI-TOF/TOF MS we have identified proteins differentially expressed between genotypes (JI2480 and Messire) and treatments (control and infected plants). Consistent with the larger number of spots differentially expressed between genotypes, we postulate that resistance to *E. pisi* in JI2480 plants is based on constitutive rather than inducible defense responses. The identified proteins mainly belong to three functional categories: photosynthesis, carbohydrate catabolism and stress and defense responses. The putative role of the identified proteins supports the hypothesis of an increased activity of the energetic metabolism in the resistant plants to pay for the cost of constitutive resistance. A much smaller number of proteins were modified after pathogen challenge. Those changes affected enzymes of the photosynthesis and carbohydrate catabolism along with some defense-related proteins. These results indicated that defense responses are activated in the susceptible genotype, supporting the idea that resistance is a very complex process depending not only on the activation of defenses, but more importantly, on the activation kinetics of these responses.

Up to date very little is known about the molecular aspects of the defense and resistance responses of legumes to powdery mildew disease. Our data provide an overview of the *P. sativum-E. pisi* interaction and shed light on the putative mechanisms involved in resistance. More significantly, the data obtained would help to study responses to disease as part of the biology of the whole plant and represent a starting platform for further studies including proteome subfractionation and the study of PTMs.

This work was supported by the EU "Grain Legume" Project.

5 References

[1] Smith, P. H., Foster, E. M., Boyd, L. A., Brown, J. K. M., *Plant Pathol.* 1996, *45*, 302–309.

[2] Nagaraju, V., Pal, A. B., *J. Agr. Sci.,* 1990, *24*, 68–71.

[3] Paulech, C., *Biologia (Bratislava)* 1968, *23*, 281–288.

[4] Viljanen-Rollinson, S. L. H., Gaunt, R. E., Frampton, C. M. A., Falloon R. E., McNeil, D. L., *Plant Pathol.* 1998, *47*, 137–147.

[5] Tiwari, K. R., Penner, G. A., Warkentin, T. D., Rashid, K. Y., *Can. J. Plant Pathol.* 1997, *19*, 267–271.

[6] Singh, U. P., Singh, H. B., *Trans. Br. Mycol. Soc.* 1983, *81*, 275–278.

[7] Falloon, R. E., Sutherland, P. W., Hallett, I. C., *Can. J. Bot.* 1989, *67*, 3410–3416.

[8] Sugawara, K., Singh, U. P., Kobayashi, K., Ogoshi, A., *J. Phytopathol.* 1998, *146*, 223–229.

[9] Stumpf, M. A., Gay, J. L., *Physiol. Mol. Plant Pathol.* 1989, *35*, 519–533.

[10] Canovas, F. M., Dumas-Gaudot, E., Recorbet, G., Jorrin, J. *et al.*, *Proteomics* 2004, *4*, 285–298.

[11] Jorrin, J. V., Rubiales, D., Dumas-Gaudot, E., Recorbet, G. *et al.*, *Euphytica* 2005, *in press*.

[12] Peltier, J. B., Friso, G., Kalume, D. E, Roepstorff, P. *et al.*, *Plant Cell* 2000, *12*, 319–341.

[13] Bardel, J., Louwagie, M., Jaquinod, M., Jourdain, A. *et al.*, *Proteomics* 2002, *2*, 880–898.

[14] Saalbach, G., Erik, P., Wienkoop, S., *Proteomics* 2002, *2*, 325–337.

[15] Repetto, O., Bestel-Corre, G., Dumas-Gaudot, E., Berta, G. *et al.*, *New Phytol.* 2003, *157*, 555–567.

[16] Castillejo, M. A., Amiour, N., Dumas-Gaudot, E., Rubiales, D., Jorrin, J. V., *Phytochemistry* 2004. *65*, 1817–1828.

[17] Fondevilla, S., Rubiales, D., Carver, T. L. W., *Eur. J. Plant Pathol.* 2005, in press.

[18] Rubiales, D., Brown, J. K. M., Martín, A., *Euphytica* 1993, *67*, 215–220.

[19] Rubiales, D., Carver, T. L. W., *Can. J. Bot.* 2000, *78*, 1561–1570.

[20] Carver, T. L. W., Roberts, P. C., Thomas, B. J., Lyngaer, M. F., *Physiol. Mol. Plant Pathol.* 2001, *58*, 209–228.

[21] Damerval, C., de Vienne, D., Zivy, M., Thiellement, H., *Electrophoresis* 1986, *7*, 52–54.

[22] Görg, A., Postel, W., Weser, J., Günther, S. *et al.*, *Electrophoresis* 1987, *8*, 45–51.

[23] Mathesius, U., Keijzers, G., Natera, S. H. A., Weinman, J. J. *et al.*, *Proteomics* 2001, *1*, 1424–1440.

[24] Jorge, I., Navarro, R. M., Lenz, C., Ariza, D. *et al.*, *Proteomics* 2005, *5*, 222–234.

[25] Schevchenko, A., Wilm, M., Vorm, O., Mann, M., *Anal. Chem.* 1996, *68*, 850–858.

[26] Perkins, D. N., Pappin, D. J. C., Creasy, D. M., Cottrell, J. S., *Electrophoresis* 1999, *20*, 3551–3567.

[27] Thiellement, H., Bahrman, N., Damerval, C., Plomion, C. *et al.*, *Electrophoresis* 1999, *20*, 2013–2026.

[28] Santoni, V., Delarue, M., Caboche, M., Bellini, C., *Planta* 1997, *202*, 62–69.

[29] Somssich, I. E., Hahlbrock, K., *Trends Plant Sci.* 1998, *3*, 86–90.

[30] Heil, M., Baldwin, I. T., *Trends Plant Sci.* 2002, *7*, 61–67.

[31] Brown, J. K. M., *Curr. Opin. Plant Biol.* 2002, *5*, 339–344.

[32] Burdon, J. J., Thrall, P. H., *Genome Biol.* 2003, *4*, 227.

[33] Deng, Z., Aliverti, A., Zanetti, G., Arakaki, A. K. *et al.*, *Nat. Struct. Biol.* 1999, *6*, 847–853.

[34] Delaney, T. P., Uknes, S., Vernooij, B., Friedrich, L. *et al.*, *Science* 1994, *266*, 1247–1250.

[35] Slaymaker, D. H., Navarre, D. A., Clark, D., del Pozo, O. *et al.*, *Proc. Natl. Acad. Sci. USA* 2002, *99*, 11640–11645.

[36] Schulze-Lefert, P., Vogel, J., *Trends Plant Sci.* 2000, *5*, 343–348.

[37] Van Loon, L. E., Van Strien., E. A., *Physiol. Mol. Plant Pathol.* 1999, *55*, 85–97.

[38] Ukness, S., Mauch-Mani, B., Moyer, M., Potter, S. *et al.*, *Plant Cell* 1992, *4*, 645–656.

[39] Kim, Y. J., Hwang, B. K., *Physiol. Plantarum* 2000, *108*, 51–60.

[40] Valueva, T. A., Mosolov, V. V., *Biochemistry (Moscow)* 2004, *69*, 1305–1309.

[41] Valueva, T. A., Revina, T. A., Gvozdeva, E. L., Gerasimova, N. G., Ozeretskovskaya, O. L., *Bioorg. Khim.* 2003, *29*, 499–504.

[42] Jofuku, K. D., Goldberg, R. B., *Plant Cell.* 1989, *1*, 1079–1093.

[43] Grunwald, U., Nyamsuren, O., Tamasloukht, M., Lapopin, L. *et al.*, *Plant Mol. Biol.* 2004, *55*, 553–566.

[44] Wulf, A., Manthey, K., Doll, J., Perlick, A. M. *et al.*, *Mol. Plant Microbe Interact.* 2003, *16*, 306–314.

[45] Colditz, F., Nyamsuren, O., Niehaus, K., Eubel, H. *et al.*, *Plant Mol. Biol.* 2004, *55*, 109–120.

[46] Rathbun, E. A., Naldrett, M. J., Brewin, N. J., *Mol. Plant-Microbe Interact.* 2002, *15*, 350–359.

[47] Bucher, M., Brunner, S., Zimmermann, P., Zardi, G. I. *et al.*, *Plant Physiol.* 2002, *128*, 911–923.

[48] Silva, N. F., Goring, D. R., *Plant Mol. Biol.* 2002, *50*, 667–685.

[49] Li, R., Rimmer, R., Buchwaldt, L., Sharpe, A. G. *et al.*, *Fungal Genet. Biol.* 2004, *41*, 735–753.

[50] Brummell, D. A., Dal Cin, V., Crisosto, C. H., Labavitch, J. M., *J. Exp. Bot.* 2004, *55*, 2029–2039.

[51] Real, M. D., Company, P., Garcia-Agustin, P., Bennett, A. B., Gonzalez-Bosch, C., *Planta* 2004, *220*, 80–86.

[52] Ohme-Takagi, M., Suzuki, K., Shinshi, H., *Plant Cell Physiol.* 2000, *41*, 1187–1192.

[53] Hadfield, K. A., Dang, T., Guis, M., Pech, J. C. *et al.*, *Plant Physiol.* 2000, *122*, 977–983.

[54] Iturriaga, E. A., Leech, M. J., Barratt, D. H., Wang, T. L., *Plant Mol. Biol.* 1994, *24*, 235–240.

[55] Oztur, Z. N., Talame, V., Deyholos, M., Michalowski, C. B. *et al.*, *Plant Mol. Biol.* 2002, *48*, 551–573.

[56] Passardi, F., Penel, C., Dunand, C., *Trends Plant Sci.* 2004, *9*, 534–540.

[57] Depege, N., Drevet, J., Boyer, N., *Eur. J. Biochem.* 1998, *253*, 445–451.

[58] Herbette, S., Lenne, C., Leblanc, N., Julien, J. L. *et al.*, *Eur. J. Biochem.* 2002, *269*, 2414–2420.

[59] Ursini, F., Maiorino, M., Gregolin, C., *Biochim. Biophys. Acta* 1985, *839*, 62–70.

[60] Chen, S., Vaghchhipawala, Z., Li, W., Asard, H., Dickman, M. B., *Plant Physiol.* 2004, *135*, 1630–1641.

[61] Bowler, C., Slooten, L., Vandenbranden, S., De Rycke, R. *et al.*, *EMBO. J.* 1991, *10*, 1723–1732.

[62] Xiao, S., Ellwood, S., Calis, O., Patrick, E. *et al.*, *Science* 2001, *291*, 118–120.

[63] Levine, A., Tenhaken, R., Dixon, R. A., Lamb., C. J., *Cell* 1994, *79*: 583–593.

[64] Kutchan, T. M., *Phytochemistry* 1993, *32*, 493–506.

[65] Pauw, B., van Duijn, B., Kijne, J. W., Memelink, J., *Plant Mol. Biol.* 2004, *55*, 797–805.

[66] Menke, F. L., Champion, A., Kijne, J. W., Memelink, J., *EMBO J.* 1999, *18*, 4455–4463.

[67] Fabbri, M., Delp, G., Schmidt, O., Theopold, U., *Biochem. Biophys. Res. Commun.* 2000, *271*, 191–196.

[68] Callis, J., Vierstra, R. D., *Curr. Opin. Plant Biol.* 2000, *3*, 381–386.

[69] Criqui, M. C., Engler, J. A., Camasses, A., Capron, A. *et al.*, *Plant Physiol.* 2002, *130*, 1230–1240.

[70] Assmann, S. M., *Plant Cell* 2002, *14 Suppl*, S355–357.

[71] Yang, Z., *Plant Cell* 2002, *14 Suppl*, S 375–378.

[72] Molendijk, A. J., Ruperti B., Palme, K., *Curr. Opin. Plant Biol.* 2004, *7*, 694–700.

[73] Preiss, J., *Annu. Rev. Microbiol.* 1984, *38*, 419–458.

[74] Dixon, R. A., in: Sankawa, U. (Ed.), *Comprehensive Natural Products Chemistry*, Vol. 1, Elsevier, Oxford 1999, pp. 773–823.

[75] Wu, Q., VanEtten, H. D., *Mol. Plant-Microbe. Interact.* 2004, *17*, 798–804.

[76] Glazebrook, J., Rogers, E. E., Ausubel, F. M., *Genetics* 1996, *143*, 973–982.

[77] Ravanel, S., Gakiere, B., Job, D., Douce, R., *Proc. Natl. Acad. Sci. USA* 1998, *95*, 7805–7812.

[78] Jost, R., Berkowitz, O., Wirtz, M., Hopkins, L. *et al.*, *Gene* 2000, *253*, 237–247.

[79] Jackson-Constan, D., Akita, M., Keegstra, K., *Biochim. Biophys. Acta* 2001, *1541*, 102–113.

[80] Galis, I., Smith, J. I., Jameson, P. E., *J. Plant Physiol.* 2004, *161*, 459–466.

[81] Adam, Z., Ostersetzer, O., *Biochem. Soc. Trans.* 2001, *29*, 427–430.

[82] Sinvany-Villalobo, G., Davydov, O., Ben-Ari, G., Zaltsman, A. *et al.*, *Plant Physiol.* 2004, *135*, 1336–1345.

PROTEOMICS

Supporting Information for Proteomics

DOI 10.1002/pmic.200500396

Miguel Curto, Luis E. Camafeita, Juan A. Lopez, Ana M. Maldonado, Diego Rubiales and Jesús V. Jorrín

A proteomic approach to study pea (*Pisum sativum*) responses to powdery mildew (*Erysiphe pisi*)

Supplemental Table 1. Spots that showed quantitative or qualitative changes among genotypes (Messire and JI2480) or treatments (inoculated and non-inoculated).

Spot[a] Number	Experimental[b]		Protein amount per gel[c] ($\bar{x}$ ± S.D) (C.V)[e]			
			Messire		JI2480	
	Mw	p*I*	Control	Inoculated	Control	Inoculated
1*	52.4	5.4	311 ± 75 (24)	320 ± 72 (22)	n.d[d]	n.d[d]
2*	51.3	5.5	n.d[d]	n.d[d]	78 ± 72 (91)	76 ± 69 (89)
3*	51.1	5.4	n.d[d]	n.d[d]	95 ± 26 (28)	92 ± 24 (25)
4	49.9	5.5	n.d[d]	n.d[d]	154 ± 113 (73)	150 ± 110 (71)
5*	41.3	5.5	n.d[d]	n.d[d]	542 ± 140 (26)	540 ± 130 (24)
6	40.1	5.9	n.d[d]	n.d[d]	130 ± 36 (28)	128 ± 32 (25)
7	36.9	5.8	n.d[d]	n.d[d]	108 ± 41 (38)	106 ± 37 (35)
8	39.1	6.0	n.d[d]	n.d[d]	76 ± 38 (51)	74 ± 37 (50)
9	41.6	6.3	n.d[d]	n.d[d]	109 ± 42 (38)	100 ± 39 (35)
10	43.1	7.3	n.d[d]	n.d[d]	227 ± 30 (13)	220 ± 28 (11)
11	40.4	7.4	n.d[d]	n.d[d]	42 ± 27 (8)	40 ± 23 (2)
12*	36.0	7.7	n.d[d]	n.d[d]	193 ± 50 (26)	190 ± 49 (25)
13*	33.0	7.5	n.d[d]	n.d[d]	90 ± 10 (11)	92 ± 9 (9)
14*	35.2	7.3	n.d[d]	n.d[d]	52 ± 4 (7)	50 ± 3 (6)
15*	24.0	5.8	n.d[d]	n.d[d]	66 ± 4 (7)	60 ± 2 (6)
16*	32.9	7.2	n.d[d]	n.d[d]	67 ± 5 (7)	65 ± 3 (4)
17	30.6	7.3	n.d[d]	n.d[d]	244 ± 110 (45)	242 ± 109 (44)
18	31.0	7.0	n.d[d]	n.d[d]	186 ± 85 (46)	186 ± 85 (43)
19	29.2	7.0	n.d[d]	n.d[d]	20 ± 3 (15)	20 ± 2 (15)
20*	20.5	6.0	n.d[d]	n.d[d]	202 ± 4 (2)	200 ± 4 (2)
21*	46.5	5.2	n.d[d]	n.d[d]	154 ± 22 (14)	159 ± 19 (13)
22*	14.7	7.0	n.d[d]	n.d[d]	156 ± 21 (13)	780± 117 (15)
23*	23.3	7.1	n.d[d]	n.d[d]	48 ± 6 (12)	46 ± 4 (12)
24*	35.2	7.1	n.d[d]	n.d[d]	141 ± 34 (24)	139 ± 30 (22)

Supplemental Table 1 continued

Spot[a] Number	Experimental[b]		Protein amount per gel[c] ($\bar{x}$ ± S.D) (C.V)[e]			
			Messire		JI2480	
	Mw	p*I*	Control	Inoculated	Control	Inoculated
25*	23.7	7.0	n.d[d]	n.d[d]	223 ± 28 (12)	220 ± 26 (12)
26	20.5	7.2	n.d[d]	n.d[d]	63 ± 17 (26)	60 ± 16 (26)
27*	17.8	7.3	n.d[d]	n.d[d]	103 ± 14 (13)	100 ± 12 (13)
28	19.2	6.8	n.d[d]	n.d[d]	66 ± 19 (29)	66 ± 18 (27)
29*	69.5	6.8	n.d[d]	n.d[d]	63 ± 9 (15)	61 ± 9 (12)
30*	23.0	8.0	n.d[d]	n.d[d]	140 ± 20 (14)	140 ± 19 (14)
31*	20.2	6.0	n.d[d]	n.d[d]	368 ± 64 (17)	366 ± 64 (17)
32	15.0	6.7	n.d[d]	n.d[d]	21 ± 2 (12)	20 ± 2 (10)
33*	14.6	6.9	n.d[d]	n.d[d]	10 ± 1 (14)	9 ± 1 (13)
34	11.2	6.9	n.d[d]	n.d[d]	21 ± 8 (37)	23 ± 7 (35)
35*	16.4	6.6	n.d[d]	n.d[d]	55 ± 10 (18)	58 ± 11 (19)
36	21.0	7.8	n.d[d]	n.d[d]	1784 ± 257 (14)	1789 ± 259 (15)
37*	19.0	7.5	n.d[d]	n.d[d]	48 ± 9 (20)	50 ± 9 (24)
38	7.8	6.5	n.d[d]	n.d[d]	15 ± 2 (12)	15 ± 4 (15)
39	15.1	6.4	n.d[d]	n.d[d]	51 ± 12 (24)	55 ± 12 (24)
40	15.6	6.3	n.d[d]	n.d[d]	79 ± 24 (30)	82 ± 26 (33)
41	15.7	6.1	n.d[d]	n.d[d]	161 ± 88 (55)	161 ± 88 (55)
42*	15.5	6.0	n.d[d]	n.d[d]	229 ± 33 (14)	231 ± 35 (16)
43	12.8	5.9	n.d[d]	n.d[d]	19 ± 7 (39)	21 ± 9 (40)
44	11.9	5.9	n.d[d]	n.d[d]	71 ± 26 (37)	77 ± 26 (40)
45*	16.5	5.8	n.d[d]	n.d[d]	190 ± 31 (17)	194 ± 34 (19)
46	10.2	5.7	n.d[d]	n.d[d]	19 ± 8 (39)	26 ± 4 (37)
47*	18.0	5.6	n.d[d]	n.d[d]	71 ± 11 (16)	79 ± 10 (16)
48*	17.6	5.4	n.d[d]	n.d[d]	12 ± 2 (12)	16 ± 1 (12)
49	10.6	5.5	103 ± 13 (11)	109 ± 12 (10)	894 ± 156 (17)	899 ± 150 (15)
50	14.6	5.7	n.d[d]	n.d[d]	25 ± 7 (29)	29 ± 7 (28)
51*	15.1	5.6	n.d[d]	n.d[d]	31 ± 6 (18)	37 ± 8 (18)

Supplemental Table 1 continued.

Spot[a] Number	Experimental[b]		Protein amount per gel[c] ($\bar{x}$ ± S.D) (C.V)[e]			
			Messire		JI2480	
	Mw	p*I*	Control	Inoculated	Control	Inoculated
52*	15.9	5.7	n.d[d]	n.d[d]	12 ± 4 (28)	18 ± 3 (25)
53*	17.5	5.2	n.d[d]	n.d[d]	38 ± 8 (20)	42 ± 9 (23)
54*	16.8	5.7	n.d[d]	n.d[d]	33 ± 11 (34)	36 ± 9 (32)
55*	24.1	5.0	n.d[d]	n.d[d]	69 ± 3 (4)	72 ± 2 (3)
56	20.1	6.0	n.d[d]	n.d[d]	49 ± 21 (42)	52 ± 25 (41)
57*	20.6	6.0	n.d[d]	n.d[d]	102 ± 42 (41)	100 ± 40 (39)
58*	27.4	5.8	n.d[d]	n.d[d]	302 ± 21 (7)	310 ± 15 (3)
59	20.1	5.5	275 ± 13 (11)	278 ± 14 (10)	n.d[d]	n.d[d]
60*	41.5	8.0	n.d[d]	n.d[d]	114 ± 8 (7)	448± 26 (6)
61*	23.0	6.0	n.d[d]	n.d[d]	282 ± 9 (3)	292 ± 10 (1)
62	24.1	5.8	73 ± 13 (11)	79 ± 15 (14)	108 ± 15 (14)	110 ± 14 (9)
63	23.2	6.1	n.d[d]	n.d[d]	433 ± 77 (18)	439 ± 76 (17)
64	24.0	6.1	n.d[d]	n.d[d]	179 ± 143 (80)	180 ± 150 (70)
65*	22.1	6.4	n.d[d]	n.d[d]	30 ± 2 (6)	39 ± 2 (4)
66	23.2	6.3	n.d[d]	n.d[d]	41 ± 13 (32)	49 ± 11 (30)
67	26.4	6.2	n.d[d]	n.d[d]	64 ± 10 (15)	66 ± 9 (13)
68*	25.1	8.0	n.d[d]	n.d[d]	30 ± 8 (27)	32 ± 9 (28)
69*	26.9	6.0	n.d[d]	n.d[d]	35 ± 6 (17)	39 ± 6 (19)
70*	26.7	7.9	n.d[d]	n.d[d]	7 ± 2 (28)	11 ± 3 (30)
71*	28.5	6.4	n.d[d]	n.d[d]	79 ± 15 (19)	83 ± 12 (20)
72*	35.9	6.6	n.d[d]	n.d[d]	77 ± 22 (29)	79 ± 20 (26)
73*	26.8	6.6	n.d[d]	n.d[d]	55 ± 6 (10)	59 ± 7 (9)
74*	34.4	6.8	n.d[d]	n.d[d]	100 ± 8 (8)	102 ± 8 (7)
75	27.0	5.2	406 ± 13 (11)	410 ± 15 (10)	n.d[d]	n.d[d]
76*	33.4	6.3	1578 ± 13 (11)	1580 ± 18 (12)	n.d[d]	n.d[d]

Supplemental Table 1 continued.

Spot[a]	Protein amount per gel[c]

Number	Experimental [b]		($\overline{x}$ ± S.D) (C.V) [e]			
			Messire		JI2480	
	Mw	p*I*	Control	Inoculated	Control	Inoculated
77	10.0	5.3	n.d [d]	n.d [d]	1884 ± 57 (3)	1884 ± 57 (3)
78*	73.1	5.8	n.d [d]	38± 5 (14)	n.d [d]	n.d [d]
79	57.6	6.2	n.d [d]	303± 36 (12)	n.d [d]	n.d [d]
80	57.0	6.0	n.d [d]	146± 37 (25)	n.d [d]	n.d [d]
81*	53.0	6.0	n.d [d]	133± 18 (14)	n.d [d]	n.d [d]
82*	50.8	5.5	n.d [d]	158± 24 (15)	n.d [d]	n.d [d]
83*	38.8	5.5	n.d [d]	52± 5 (10)	n.d [d]	n.d [d]
84*	45.9	5.7	n.d [d]	93± 8 (9)	n.d [d]	n.d [d]
85*	35.0	5.7	n.d [d]	78± 13 (17)	n.d [d]	n.d [d]
86*	41.7	5.8	n.d [d]	77± 9 (11)	n.d [d]	n.d [d]
87*	40.9	5.9	n.d [d]	136± 22 (16)	n.d [d]	n.d [d]
88*	40.8	6.4	102 ± 20 (19)	323± 46 (14)	112 ± 21 (14)	102 ± 15 (13)
89*	42.9	5.3	n.d [d]	107± 17 (16)	n.d [d]	n.d [d]
90*	40.9	7.2	n.d [d]	57± 4 (7)	n.d [d]	n.d [d]
91*	35.0	6.4	n.d [d]	136± 15 (11)	n.d [d]	n.d [d]
92*	41.6	5.6	169± 21 (13)	652± 67 (10)	180± 15 (10)	182± 13 (8)
93*	42.2	6.8	n.d [d]	313± 36 (12)	n.d [d]	n.d [d]
94	37.0	6.7	n.d [d]	569± 84 (15)	n.d [d]	n.d [d]
95*	32.8	5.4	n.d [d]	202± 21 (10)	n.d [d]	n.d [d]
96*	34.9	6.0	160± 20 (12)	502± 51 (10)	170± 18 (11)	178± 15 (9)
97	49.9	5.8	n.d [d]	n.d [d]	n.d [d]	22± 5 (21)
98	47.7	5.8	n.d [d]	n.d [d]	n.d [d]	36± 3 (8)
99	47.3	5.8	n.d [d]	n.d [d]	n.d [d]	27± 4 (16)
100	45.0	5.9	n.d [d]	n.d [d]	n.d [d]	20± 2 (8)
101*	44.1	5.9	n.d [d]	n.d [d]	n.d [d]	64± 4 (6)
102	44.8	6.0	n.d [d]	n.d [d]	n.d [d]	55± 8 (15)
103*	53.0	6.0	n.d [d]	n.d [d]	n.d [d]	226±8 (4)
104*	44.3	6.3	n.d [d]	n.d [d]	n.d [d]	23± 1 (3)
105*	40.8	6.0	n.d [d]	n.d [d]	n.d [d]	456± 79 (17)
106*	52.0	5.9	n.d [d]	n.d [d]	n.d [d]	193± 9 (5)

Supplemental Table 1 continued.

* Identified spots.

[a] Numbers correspond to the figures given in Figure 3.

[b] Experimental p*I* and *Mw*, calculated using the PD-Quest software.

[c] Protein amount values (ng/spot) are mean of three independent replicates ± standard deviation.

[d] Non-detected.

[e] Coefficient of variance.

Chapter 2: Two-dimensional electrophoresis based proteomic analysis of the pea (*Pisum sativum*) in response to *Mycosphaerella pinodes*

12822 *J. Agric. Food Chem.* **2010,** *58,* 12822–12832
DOI:10.1021/jf1036917

JOURNAL OF AGRICULTURAL AND FOOD CHEMISTRY
ARTICLE

Two-Dimensional Electrophoresis Based Proteomic Analysis of the Pea (*Pisum sativum*) in Response to *Mycosphaerella pinodes*

M. Ángeles Castillejo,*[,†,‡] Miguel Curto,[‡,§] Sara Fondevilla,[∥] Diego Rubiales,[†] and Jesús V. Jorrín[§]

[†]Institute for Sustainable Agriculture, CSIC, Apdo. 4084, 14080 Córdoba, Spain, [§]Department of Biochemistry and Molecular Biology, and [∥]Department of Genetics, University of Córdoba, 14071, Córdoba, Spain. [‡] Both authors contributed in the same way to the work

Responses to *Mycosphaerella pinodes* in pea were studied by using a proteomics approach. Two-dimensional electrophoresis (2-DE) was used in order to compare the leaf proteome of two pea cultivars displaying different phenotypes (susceptible and partial resistance to the fungus), as well as in response to the inoculation. Multivariate statistical analysis identified 84 differential protein spots under the experimental conditions (cultivars/treatments). All of these 84 protein spots were subjected to MALDI-TOF/TOF mass spectrometry to deduce their possible functions. A total of 31 proteins were identified using a combination of peptide mass fingerprinting (PMF) and MSMS fragmentation. Most of the identified proteins corresponded to enzymes belonging to photosynthesis, metabolism, transcription/translation and defense and stress categories. Results are discussed in terms of responses to pathogens.

KEYWORDS: Pea−*Mycosphaerella pinodes* interaction; pea proteome; plant responses to pathogens

INTRODUCTION

Aschochyta blight, caused by *Mycosphaerella pinodes* (Berk & Blox) Vesterg, the teleomorph of *Ascochyta pinodes* Jones, is the most important foliar disease of pea crop (*Pisum sativum* L.) worldwide. *M. pinodes* causes necrotic spots on all aerial parts of the pea plant and is responsible for important yield and seed quality losses (*1*). Genetic resistance appears to be the most practical method of control (*2*). However, although extensive searches have been carried out, only moderate resistance is available in pea cultivars, and this has been inadequate to control the disease (*3*−*6*). Higher levels of resistance have been identified in wild species of *Pisum* (*7*, *8*), but still have not been efficiently used in breeding programs.

Quantitative trait loci (QTL) analysis has identified numerous genomic regions involved in partial resistance to *M. pinodes* in pea (*9*−*13*). Physiological and biochemical studies of the pea−*M. pinodes* interaction reported that *M. pinodes* elicitor (*14*) induces some defense responses in pea, such as accumulation of the phytoalexin pisatin (*15*), activation of the genes encoding phenylalanine ammonia-lyase (PAL) and chalcone synthase (*16*), activation of PR proteins (β-1,3-glucanase, chitinases) (*17*), generation of superoxide anion (*18*), enhancement of ATPase activity (*18*), and activation of the polyphosphoinositide metabolism (*19*).

A large number of plant proteomic papers are collected in two recent reviews (*20*, *21*). To our knowledge most proteomic studies in legumes published to date have dealt with the model system *Medicago truncatula* while few proteomics studies have been reported with other legume species (*20*), a small number of them dealing with the responses to pathogens in pea (*22*−*27*). We will focus on those dealing with pathogenic fungi. Thus, Curto et al. (*25*) reported changes in the leaf proteome of two pea genotypes differing in their resistance to *Erysiphe pisi*. Using a 2-DE/mass spectrometry strategy, differentially regulated proteins between genotypes and treatments (control and infected leaves) were identified. The identified proteins mainly belong to three functional categories: photosynthesis, carbohydrate catabolism and stress/defense responses. Authors concluded that an increased activity of the energy metabolism in resistant plants occurred to compensate for the cost of constitutive resistance. Wen et al. (*26*) studied the reaction of pea to *Nectria hematococca* using a multidimensional protein identification technology, concluding that the root cap secretes a complex mixture of proteins that appear to function in protection of the root tip from infection. Finally, Amey et al. (*27*) used a 2-DE/mass spectrometry strategy to identify host proteins altering in abundance during *Peronospora viciae* infection of a susceptible pea cultivar. Among them they found proteins belonging to photosynthesis, carbohydrate metabolism and stress/defense-related category.

In the present study we aim to analyze the leaf pea proteome in response to *M. pinodes* inoculation. Based on previous investigation carried out to assess the partial resistance to *M. pinodes* in field pea (*28*), we have selected two cultivars displaying differential response to *M. pinodes*. Differences in the 2-DE map between the two cultivars, as well as in response to parasite infection, were analyzed, and some of the differential proteins were identified by MALDI-TOF/TOF mass spectrometry. Thirty-one proteins were identified, most of them belonging to the functional category of photosynthesis, metabolism, transcription/translation and defense and stress-related proteins.

*Corresponding author. E-mail: macastillejo@ias.csic.es. Tel: +34957499242. Fax: +34957499252.

 Published on Web 11/19/2010

MATERIALS AND METHODS

Plant Material and Inoculation. Two pea cultivars, 'Messire' and 'Radley', were used in the experiment. Messire cultivar is highly susceptible to *M. pinodes* while Radley has shown incomplete resistance that is still the highest level of resistance available so far in a pea cultivar (*5*, *28*, *29*).

Pea seeds were germinated in Petri dishes on wet fiber papers and kept in the dark at 20 °C for five days. When the root reached 4−5 cm length, plants were transferred to individual pots containing 250 cm^3 of a 1:1 sand−peat mixture and grown in a controlled environment (20 ± 2 °C with a 12 h dark/12 h light photoperiod, at 250 $\mu mol\ m^{-2}\ s^{-1}$). At 3−4 leaf stage (approximately 14 days after planting) half of the plants of each accession (8 of Messire and 12 of Radley) were inoculated with *M. pinodes*, whereas the remaining plants were inoculated with sterile water and used as controls. For inoculation the monoconidial *M. pinodes* isolate Co-99, derived from an isolate obtained from infected pea material collected in commercial fields at Córdoba (Spain), was used. A spore suspension was prepared by flooding the surface of 12−14 day old cultures with sterile water, scraping the colony with a needle and filtering the suspension through two layers of sterile cheesecloth. The concentration of spores in the solution obtained was further determined with a hemocytometer and adjusted to 5×10^5 spores per mL. Finally, Tween-20 (120 μL per 100 mL of suspension) was added as a wetting agent. The spore suspension was applied extending the suspension over the leaf surface using a small paintbrush. After inoculation high humidity was ensured during the first 24 h by ultrasonic humidifiers operating for 15 min every two hours. After that period the humidifiers were turned off. Controls, noninoculated plants, were maintained in the same environmental conditions as inoculated plants.

Leaves from inoculated and noninoculated plants were harvested 48 h after inoculation (hai), frozen in liquid nitrogen and stored at −80 °C until protein extraction.

Protein Extraction and Two-Dimensional Gel Electrophoresis. Proteins were extracted according to the TCA−acetone precipitation protocol (*30*) with some minor modifications. Leaf samples (ca. 2 g fresh weight) from three independent replicates per treatment and cultivar were ground with liquid nitrogen in the presence of glass powder by using a precooled mortar and pestle. The powder was suspended in −20 °C cold acetone containing 10% v/v TCA and 0.07% w/v DTT (4 mL per g of fresh tissue) and sonicated for 10 min on ice at 50 MHz by using an ultrasonic homogenizer 4710 series (Cole-Parmer). After standing for 1 h at −20 °C, the samples were centrifuged at 48400*g* for 30 min at 4 °C. The pellet was washed twice by resuspension in cold (−20 °C) acetone containing 0.07% w/v DTT, placing at −20 °C for 30 min and centrifuged at 27200*g* for 15 min at 4 °C. The resulting pellet was lyophilized for 10 min and resuspended in sample buffer, containing 8 M urea, 2% w/v CHAPS, 0.5% v/v Bio-Lyte 3-10 carrier ampholytes, 20 mM DTT and Bromophenol blue traces. Samples were sonicated for 5 min in an ultrasonic bath and incubated for 1 h at 35 °C. Samples were centrifuged at 27200*g* for 15 min at room temperature, and soluble proteins were determined by RCDC Protein Assay Kit (BioRad), according to the manufacturer's instructions.

IPG strips (BioRad) 7 cm wide pH gradients for analytical and 17 cm 5−8 pH gradient for preparative purposes were used. Strips were passively rehydrated for at least 12 h with 125 μL (7 cm) or 300 μL (17 cm) of sample buffer, containing 150 and 500 μg of protein, respectively. Strips were loaded onto a PROTEAN IEF System (BioRad, Hercules, CA, USA) and focused at 20 °C with increasing linear voltage according to the manufacturer's instructions: 250 V-4000 V until reaching 10000 V h for 7 cm IPG strips and 250 V-10000 V until reaching 40000 V h for 17 cm IPG strips. After IEF, strips were equilibrated by soaking first for 10 min in 375 mM Tris-HCl buffer pH 8.8, 6 M Urea, 2% SDS, 20% glycerol, solution and then for 10 min in the same solution containing 135 mM iodoacetamide.

Second dimension SDS−PAGE was performed using the Mini-Protean 3 System (7 cm strips), or the PROTEAN IIxi Cell System (BioRad) for the 17 cm strips. Electrophoresis was carried out at 20 °C in 12% house-made polyacrylamide gels until bromophenol blue reached the end of the gel, by using a constant voltage of 200 V (60 min) for small gels, and 30 mA (60 min) plus 50 mA (240−300 min) for preparative gels. Broad molecular range markers (BioRad) containing myosin (200 kDa), β-galactosidase (116.25 kDa), phosphorylase b (97.4 kDa), serum albumin (66.2 kDa), ovoalbumin (45 kDa), carbonic anhydrase (31 kDa), trypsin inhibitor (21.5 kDa), lysozyme (14.4 kDa) and aprotinin (6.5 kDa) were loaded beside the strip.

Small size gels were Coomassie stained according to Neuhoff et al. (*31*). Preparative gels were stained with CBB G-250 according to the procedure reported by Mathesius et al. (*32*). Gel images were captured with a GS800 imaging densitometer (BioRad), and initially analyzed with the PDQuest Advanced version 8.0.1 software (BioRad) using 10-fold over background as a minimum criterion for presence/absence. This software assigns unique standard spot numbers to each protein spot, termed SSP. Spot detection and matching errors were corrected manually based on the respective group consensus data. Normalized spot volumes (individual spot intensity/normalization factor) calculated for each gel based on total quantity in valid spots were determined, and these values used to designate the differential protein spots.

Mass Spectrometry Analysis and Database Searching. Mass spectrometry was performed at the Proteomics Facility, SCAI (University of Córdoba). Spots were excised manually from gels and digested with modified porcine trypsin (sequencing grade; Promega) by using a ProGest (Genomics Solution) digestion station. The digestion protocol used was that of Schevchenko et al. (*33*), with minor variations. Gel plugs were destained by incubation (twice for 30 min) with a solution containing 200 mM ammonium bicarbonate in 40% acetonitrile at 37 °C, then being subjected to three consecutive dehydration/rehydration cycles with pure acetonitrile and 25 mM ammonium bicarbonate in 40% acetonitrile, respectively, and finally dried at room temperature for 10 min. Then, 20 μL of trypsin, at a concentration of 12.5 ng/μL in 25 mM ammonium bicarbonate, was added to the dry gel pieces and the digestion proceeded at 37 °C for 12 h. Peptides were extracted from gel plugs by adding 10 μL of 1% (v/v) trifluoracetic acid (TFA) and incubating for 15 min. Peptide fragments from digested proteins were then crystallized with α-cyano-4-hydroxycinnamic acid as a matrix. The MS analysis was performed in a MALDI-TOF/TOF (4700 Proteomics Analyzer, Applied Biosystems, Foster City, CA, USA) mass spectrometer in the *m*/*z* range 800 to 4000, with an accelerating voltage of 25 kV. Spectra were internally calibrated with peptides from trypsin autolysis ($M + H^+ = 842.510$, $M + H^+ = 2211.105$). The three most abundant peptide ions were then subjected to fragmentation analysis, providing information that can be used to determine the peptide sequence.

A combined peptide mass fingerprinting (PMF) tandem MSMS search was performed using GPS Explorer software v. 3.5 (Applied Biosystems) over nonredundant NCBI database, using the MASCOTsearch engine (Matrix Science Ltd., London; http://www.matrixscience.com). The following parameters were allowed: taxonomy restrictions to *Viridiplantae*, a minimum of four peptides matches, a maximum of one miscleavage, 50 ppm mass tolerance, and peptide modifications by carbamidomethylcysteine and methionine oxidation were accepted. The confidence in the PMF matches was based on the score level (only scores greater than 67 are significant, $p < 0.05$) and confirmed by the accurate overlapping of the matched peptides with the major peaks of the mass spectrum.

Statistical Analysis of Protein Abundance Data. For statistical treatment and cluster analysis of protein abundance values, the web-based software NIA array analysis tool was utilized (*34*); available at http://lgsun.grc.nia.nih.gov/anova/index.html. This software tool selects statistically valid protein spots based on analysis of variance (ANOVA). After uploading the data table (spreadsheet in the Supporting Information) and indication of biological replications, the data were statistically analyzed using the following settings: error model "max (average, actual)", 0.01 proportion of highest variance values to be removed before variance averaging, 10 degrees of freedom for the Bayesian error model, 0.05 FDR threshold, zero permutations. First, hierarchical clustering was performed to check the entire data set, and the results were represented in dendrograms using the cluster function of the software. Second, the entire data set was analyzed by PCA using the following settings: covariance matrix type, three principal components, 1-fold change threshold for clusters, 0.6 correlation threshold for clusters. PCA results were represented as a biplot, with proteins more abundant in those experimental situations located in the same area of the graph. Protein spots data for this analysis were recorded (Supporting Information). Third, pairwise comparisons of protein spot mean abundance values were performed with the software tool using the following settings: 0.05 FDR, 1-fold change threshold. Fourth, histograms representing log average protein spot values were downloaded using the software.

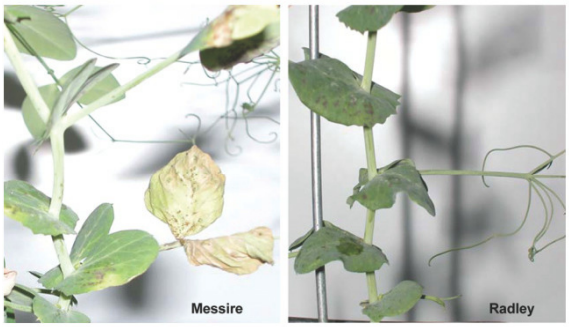

Figure 1. Symptoms observed about one week after *M. pinodes* inoculation on the lower leaves of susceptible Messire (left) and incomplete resistant Radley (right) pea cultivars.

RESULTS

Two-Dimensional Gel Electrophoresis and Mass Spectrometry Analysis. Symptoms observed about one week after *M. pinodes* inoculation are shown in **Figure 1**, although these were not yet visible at the time of leaf sampling for protein extraction (48 hai).

According to the results of small size 2-DE gels (Supporting Information), a deeper analysis was performed by using the narrowest pH gradient, 5 to 8 and 17 cm in length. For each of the conditions analyzed (cultivars and treatments), three replicates corresponding to independent protein extracts were made. As determined following the CBB staining of the gels and the use of the PDQuest software, an average of 315 ± 92 spots were resolved (**Figure 2a**,**b**). After normalization of protein spot images and manual verification, 84 differential protein spots were detected. The following criteria were used for considering a spot as being variable: (i) consistently present or absent in all three replicates; (ii) display cultivars- or treatment-ratios differing at least 1.5-fold; (iii) differences statistically significant ($p < 0.05$) between cultivars or treatments. To illustrate this, **Figure 2a** shows all of the differential protein spots on virtual gel and **Figure 2c** shows SSPs 1104 and 6408 on real gels. **Table 1** summarizes the features of the experiment.

Statistical Analysis of Protein Abundance and Expression Cluster Analysis. Abundance data of all of the 84 differential protein spots were analyzed using the web-based NIA array analysis software tool developed by Sharov et al. (*34*). This software uses analysis of variance (ANOVA) for statistical analysis of a large data set with multiple variables and subjects. Expression cluster analysis can be performed by a variety of methods including principal component analysis (PCA), obtaining a more accurate grouping of the samples and determining the most discriminant spots (*34*).

First, a hierarchical clustering of biological experiments and their repetitions were performed. We found that the experimental conditions could be divided into two large clusters in a dendrogram, namely, cluster 6 (Radley-inoculated and Radley-noninoculated) and cluster 5 (Messire-inoculated and Messire-noninoculated) (**Figure 3a**). This clustering indicated that Messire plants (clustering closest together) had protein abundance profiles similar and lightly different from those shown by Radley plants (clustering closest together) grown under the two experimental conditions (noninoculated and inoculated) across the experiments. The hierarchical clustering of biological repetitions confirmed that the data were reproducible for the experiments (Supporting Information).

Protein Spot Identification and Expression Pattern Analysis. The 84 differential protein spots were analyzed by MALDI-TOF/TOF after tryptic digestion, and the MS spectra were used to screen a *Viridiplantae* index of the nonredundant NCBI database (**Table 2**). Of the 84 protein spots analyzed, 31 were successfully identified with a high probability score and matched peptides for most of them, except spot 3103 with 2 matched peptides, which was accepted like valid identification due the high sequence coverage for a protein of low molecular weight. Photosynthetic, metabolic, transcriptional/translational and defense/stress-related proteins, with approximately 72% of identified proteins, dominated the 2-DE profile of leaf tissue. Only one protein (oxygen-evolving enhancer protein 1, gi|131384) was represented by more than one spot (3301 and 3305) with slightly different M_r and p*I* values (**Table 2**), hence corresponding to isoform or multiple forms/posttranslational modification variants of the same gene product.

Proteins identified were classified in the following functional categories: photosynthesis, glycolysis/glyconeogenesis, citrate cycle, glutamine biosynthetic process, metabolic process, protein binding, nucleic acid binding, transcription/translation, defense and stress related proteins, cellular processes and unknown. Considering the PCA analysis (**Figure 3b**), photosynthetic proteins were found in the categories of proteins correlated with PC1 (positive and negative direction) and PC2 (positive direction). Metabolic proteins were found in the categories of proteins correlated with PC1 (positive and negative direction) and PC3 (positive direction). Proteins belonging to transcription/translation category, as well as nucleic acid binding proteins, were found in PC1 and PC2 (positive direction). Defense and stress-related proteins were found in the categories of proteins correlated with PC1, PC2 (positive direction) and PC3 (negative direction). Proteins belonging to the cellular processes category were found in PC1 and PC3 (positive direction). The degree of protein abundance change within a specific PC was measured by the slope of regression of log-transformed protein abundance versus the corresponding eigenvector multiplied by the range of values within the eigenvector (*34*) (**Figure 3c**). **Figure 4** shows mean log abundance intensities for all 31 protein spots identified. We can appreciate associations with protein spot abundance patterns in the majority of the identified proteins.

A high proportion of photosynthetic (4/5), metabolic (4/6) and transcriptomic/translational, as well as nucleic acid binding (7/7) proteins, were found more abundant in Messire than Radley cultivar, when both inoculated and noninoculated plants were compared (**Figure 5**). Stress and defense-related proteins were found in all of the pairwise comparisons of protein abundance, with a clear trend to increase in inoculated plants. In general, a trend toward greater abundance of proteins is observed under inoculation in both cultivars.

DISCUSSION

In order to increase our current knowledge of the pea response mechanisms activated in response to *M. pinodes*, the leaf pea proteome was analyzed in noninoculated and inoculated plants of two cultivars displaying different phenotypes (susceptible and incomplete resistance). We used Radley as resistant, which was considered a good line to study the different mechanisms of resistance to *M. pinodes* as had previously shown the highest levels of incomplete resistance to *M. pinodes* available in pea germplasm (*5*, *28*, *29*).

Previous histological studies comparing *M. pinodes* development in Messire and Radley concluded that Radley possessed several mechanisms of resistance (*35*), some stopping the development of the pathogen at the epidermis and others restricting its growth in the mesophyll. Thus, resistance to *M. pinodes* in Radley was characterized by a lower success in colony establishment, associated with the rapid death of the epidermal cell being attacked by *M. pinodes* and by a smaller colony size (**Figure 1**).

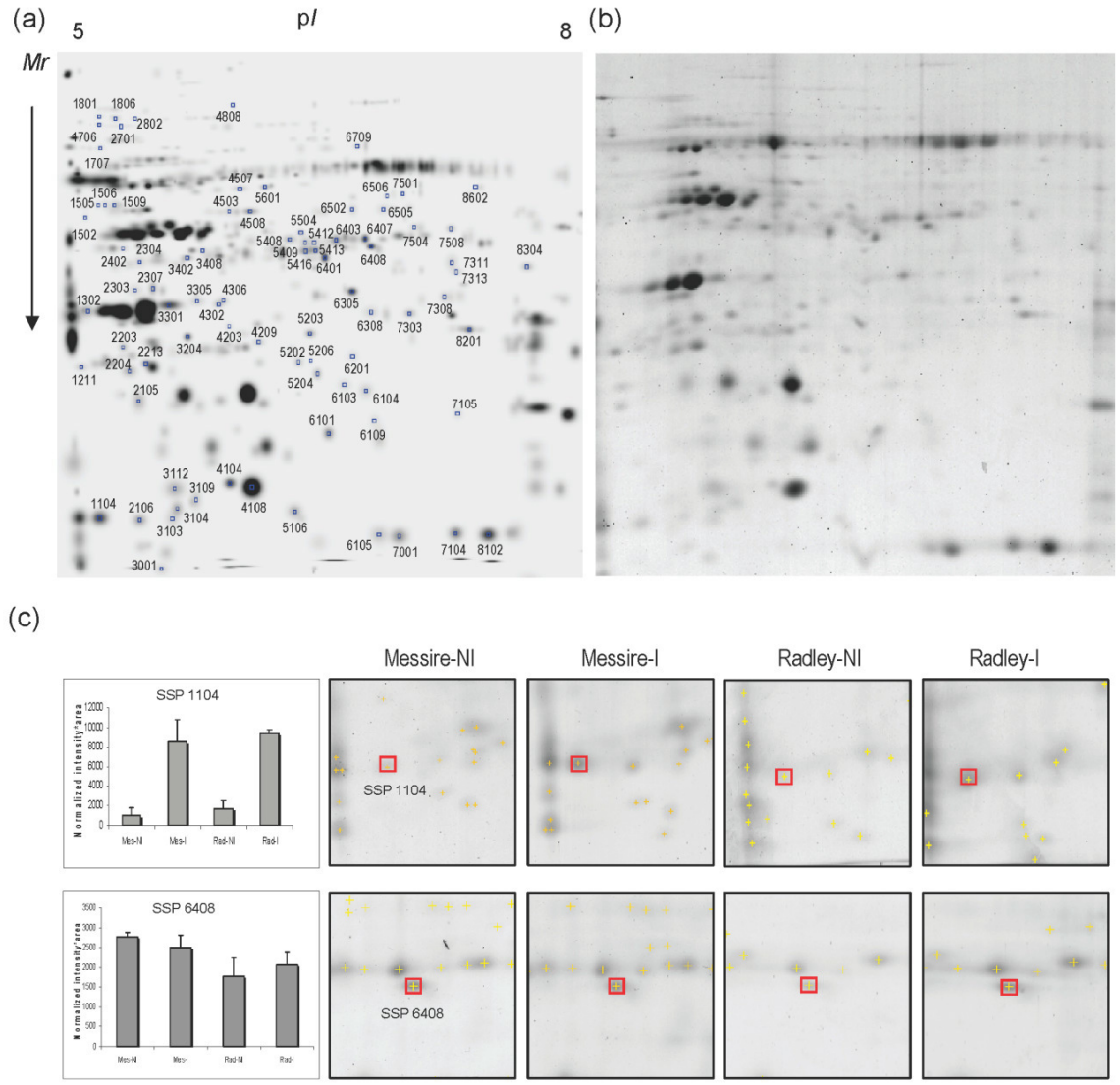

Figure 2. Location of 84 variable protein spots on a virtual two-dimensional gel (**a**). Representative Coomassie-stained 2-D protein gel of Messire cultivar (**b**). Representative protein spot images (**c**). Two protein spots were selected as examples to illustrate differential expression profiles: SSP1104 (up) and SSP6408 (down). On the left, graphs of mean abundance values for the respective protein spot are shown (standard deviations were calculated from the means of the three repetitions). Close-up regions of the Coomassie-stained 2-D gels are shown (from the left to right: Messire-NI, Messire-I, Radley-NI and Radley-I). The positions of the protein spots on the gels are marked by cross hairs. The respective differential protein spots, matched throughout all presented gels, are marked by boxed cross hairs.

The proteomic study was performed 48 hai, as at this time the pathogen had reached the pea leaf mesophyll and the different mechanisms of resistance could be acting. By using 2-DE and mass spectrometry we aim to identify key elements involved in the pea response to *M. pinodes*. Several proteins were identified differentiating cultivars, as well as in response to inoculation, although the results discussed here are limited to a small soluble fraction of the whole proteome, determined by the extraction protocol and the 2-DE separation technique utilized, with 5−8 p*I* and 10−100 kDa M_r as the best range to resolve most of the solubilized proteins, and above the detection limit for Coomassie staining. Under our experimental conditions, an average of 315 spots were resolved, this being the distribution pattern observed in leaf tissue from other plant species (*36*−*39*).

A multivariate analysis of data to detect outliers as well as clustering among the 2-DE gels was performed. Principal component analysis offers a strong approach to obtaining an overview of the main variation and of inter-relations between spots in the protein patterns (*40*). To perform this statistical cluster analysis, we employed a software tool designed for the analysis of biological gene chip data (*34*), but that has also been successfully used in the analysis of protein abundance data. This software identifies patterns in our data set and exploration of associations between protein spots and experimental conditions using PCA.

We found a similar protein abundance profile in the three replicates from each experimental condition, pointing out the reliability of our data. Multivariate analysis showed 84 differential protein spots, and all of them showed reproducible differential abundance behavior in pairwise comparisons of experimental conditions. All of the 84 protein spots were analyzed by mass spectrometry, and only 31 could be matched against the NCBI database. This low percentage of identified proteins is expected

Table 1. Summary of the Features of the Proteomic Experiment

features	number of protein spots
average of total spots detected in the Coomassie stained gels	315 ± 92
average of spots consistently present in all three replicates	154 ± 39
differential protein spots[a]	
total	84 (27% of spots detected)
between noninoculated cultivars	49
between inoculated cultivars	53
in Messire in response to inoculation	30
in Radley in response to inoculation	23
total identified spots	31
unique proteins[b]	30

[a] The 84 differential abundant proteins were selected using the PDQuest software. [b] Number of different proteins identified.

for those species which are absent or underrepresented in public databases as pea. About 52% of identified proteins belonged to legumes species, of which 39% corresponded to *Pisum sativum*. In all the pea-specific matches, theoretical and experimental p*I* and M_r were in good agreement, encouraging confidence in the identifications. Those cases in which differences between these values were observed could be interpreted in terms of protein degradation (lower experimental than theoretical M_r values), or may account for different post-translational protein modifications.

We discuss each functional group and the behavior pattern observed for the conditions studied (cultivars and response to *M. pinodes* inoculation). Among proteins differentiating cultivars were photosynthetic (spots 2105, 3301, 3305, 5202 and 7501), metabolic (spots 5408, 5413, 5504, 6408 and 7311), stress-related proteins (spots 5204 and 6403), and transcription/translation proteins (spots 2307, 3103, 4508, 6305, 6505, 6506 and 7313).

Photosynthetic proteins, as oxygen-evolving enhancer protein 2 (OEE2, spot 2105), OEE1 (spot 3305), light harvesting protein (spot 5202) and large subunit of RubisCo protein (spot 7501), were identified in larger amount in Messire when cultivars were compared. The OEE protein/complex has been implicated in photosynthetic oxygen evolution and is associated with the PSII complex, the site of the oxygen evolution in all higher plants and algae (*41*). We can associate the higher photosynthesis rate in Messire cultivar to a higher production of biomass (**Figure 1**).

Two enzymes belonging to energetic metabolism, such as malate dehydrogenase (MDH) (spots 6408 and 7311) and fructose-bisphosphate aldolase (spots 5413 and 7508), were identified displaying similar abundance patterns when cultivars and treatments were compared. These enzymes were more abundant in the susceptible noninoculated cultivar, and increased in the resistant cultivar in response to inoculation.

Spot 5504 was identified as an enzyme belonging to amino acid metabolism (glutamine-ammonia ligase or glutamine synthetase; GS). We found that this protein increased in Radley cultivar but decreased in Messire in response to inoculation. This enzyme has been found extensively related to abiotic stresses, such as salinity in potato (*42*), tomato (*43*), wheat (*44*), drought and high temperature in perennial grass (*Leymus chinensis*) (*45*), etc. GS can be associated with amino acid conversion, and amino acid composition might be altered due to several stresses, which could promote stress-resistance (*46*).

The biological interpretation of the differences observed when noninoculated cultivars were compared is a matter of speculation; however, taking into account physiological differences between both cultivars, we can postulate that it could be related to differences in the efficiency in energy utilization for growth and fitness purposes. As has been reported in other biological systems (*37*, *39*, *47*), a similar behavior for some of the photosynthetic and metabolic proteins identified in this work was observed in response to biotic and abiotic stress, with a clear trend to decrease in the susceptible and increase in the resistant genotype in response to the stress. This behavior suggests that differences observed could be related to efficiency in energy utilization as a consequence of the sink effect of the pathogen on the host plant.

Protein spot 5408 was identified as pyridoxal 5-phosphate (PLP)-dependent enzyme. PLP, the biologically active form of vitamin B6, has multiple roles as a versatile cofactor of enzymes that are mainly involved in the metabolism of amino acid compounds (*48*). We found the PLP dependent enzyme decreased in both cultivars after inoculation, but its relation with the response to *M. pinodes* is unclear.

Two nucleic acid binding proteins, namely, glycine-rich RNA binding protein (GRP, spot 3103) and far-red impaired response protein (spot 6505), displayed a similar behavior. Both proteins were found in different amounts when cultivars were compared, with a higher amount in the susceptible cultivar. Under inoculation a trend to increase in the susceptible cultivar was observed. Recent works provide evidence of the GRP role in the response of plants to pathogens. Thus, an increase of this protein in pea plants has been reported in response to *Peronospora viciae* inoculation (*27*). In a recent study we have found differential abundance of GRP in three *M. truncatula* genotypes in response to rust inoculation (*39*), supporting the hypothesis of its role in the response of plants to pathogens. Hudson et al. (*49*) found in *Arabidopsis* mutants in far-red impaired response (*far1*) a reduced responsiveness to continuous far-red light, which implies a specific requirement for FAR1 in phytochrome A signal transduction. In other work differences in the expression of this gene have been found in *Arabidopsis* plants infected with *Agrobacterium tumefaciens* (*50*). The relation of this protein in our work is uncertain.

Another binding protein, DNA-binding protein (spot 2307), as well as two transcriptional/translational proteins, reverse transcriptase (spot 6506) and elongation factor Tu (EF-Tu, spot 4508), were identified in higher amount in the susceptible noninoculated cultivar, with a trend to decrease in response to inoculation. Differential expression of this gene has been recorded in response to various abiotic stresses in pea plants, being downregulated in response to salinity and ABA treatment. This suggests that regulation of this gene may have an important role in plant adaptation to environmental stresses (*51*).

Proteins of defense response such as disease resistance response protein (PR10, spot 1104) and ABA-responsive protein (ABR17, spot 2106) were identified. Pathogenesis-related (PR) proteins are found in virtually all plants in response to pathogen infection and, in many cases, in response to abiotic stresses as well and include the PR10 family. PR10 proteins, having ribonuclease activity, were first described in *P. sativum* inoculated with *Fusarium solani* (*52*) and have been subsequently described to be induced in many species against abiotic and biotic extresses (*53*) including lentil against *Ascochyta lentis* (*54*). It has been reported that ABR17, a member of the group 10 family of pathogenesis-related proteins (PR 10), mediated stress tolerance to multiple abiotic stresses such as salinity, cold temperature, freezing (*55*). In a previous study ABR17 was identified in pea plants in response to the parasitic plant *Orobanche crenata* (*23*). Recently, several disease resistance genes were isolated and mapped in genomic regions of two pea genotypes containing QTLs for resistance to *M. pinodes* (*56*). In the present work, we found that ABR17 and PR10 proteins increased after inoculation in both cultivars, which suggests the involvement of these proteins in the defense response against *M. pinodes*.

Two stress response proteins were identified differentiating cultivars, with a higher amount in noninoculated Messire. These were

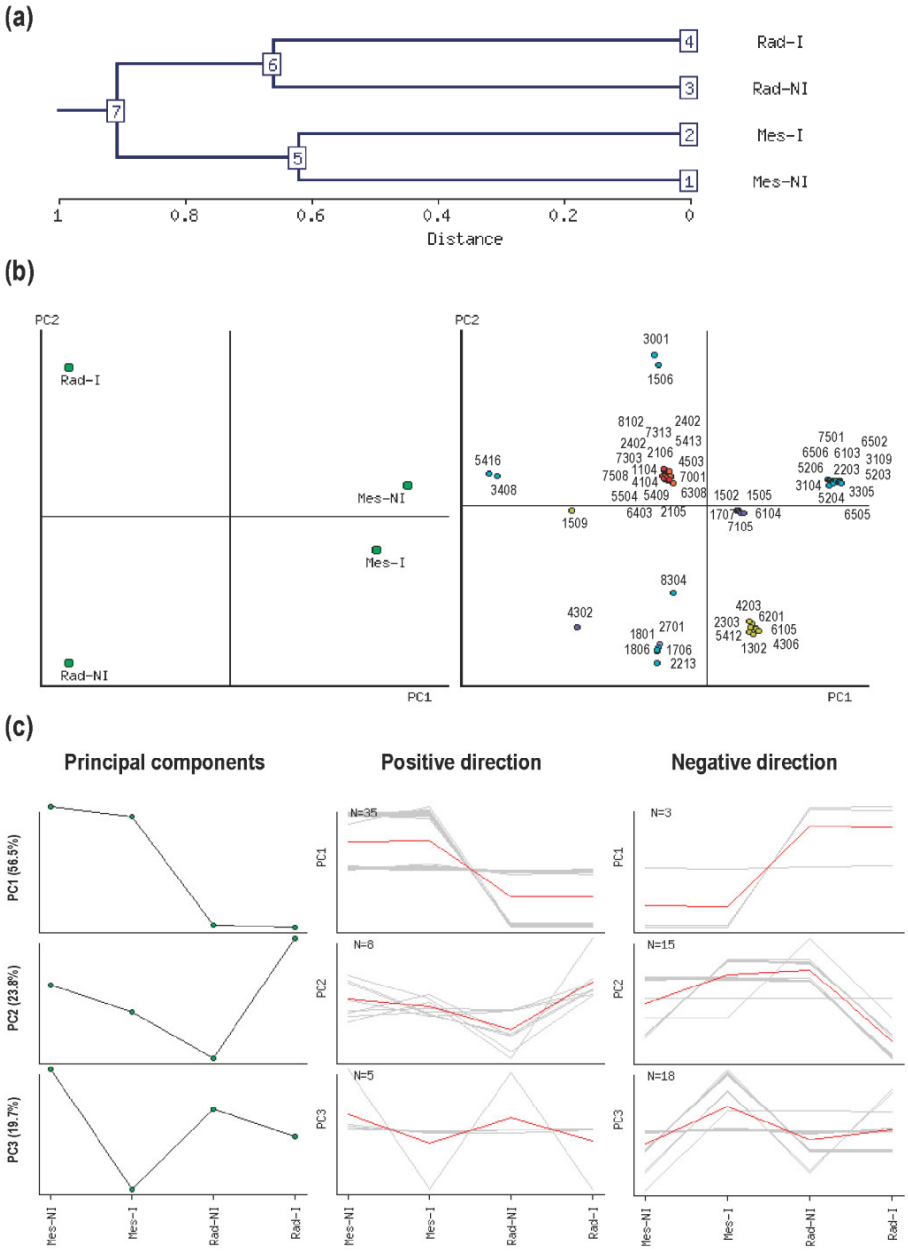

Figure 3. Statistical protein abundance cluster analysis of cultivars and response to *M. pinodes* inoculation using the ANOVA-based NIA array analysis tool (*34*). (**a**) Dendrogram showing hierarchical clustering of experimental conditions. The expression clusters are numbered from 1 to 7. (**b**) Two-dimensional biplots showing associations between experimental samples and protein spots generated by principal component analysis (PCA). Samples (left) and protein spots (right) were plotted in the first two component space. A short distance between samples and protein spots in the component space is indicative of similarity in expression profiles. (**c**) Protein spot abundance clustering based on PCA. For each PC, two clusters of proteins were identified that were positively and negatively correlated with the PC. Protein clustering was performed sequentially starting from the first PC. Proteins that were already clustered with a PC were not included in the clusters associated with subsequent PCs. Protein spots identified in this analysis are recorded in the Supporting Information.

annexin-like protein (spot 5204) and heat shock protein binding (Hsp, spot 6403). They also were found in different amounts in both cultivars in response to inoculation. Annexins constitute a ubiquitous family of more than 15 structurally related, membrane-binding proteins present in eukaryotic cells (*57*). Evidence has been reported for a potential role of the annexin-like protein in response to oxidative stress in bacteria and plants, suggesting that it may play a role in plant defense against various types of biotic as well as abiotic stresses (*58*). The generation of oxidative burst is one of the earliest responses to attempted pathogen attacks. Accumulation of reactive oxygen species (ROS) is associated with the occurrence of hypersensitive response, is effective against biotrophic fungi (*59*), can be toxic and inhibit fungal growth (*60*) and can act as signaling agents in plant defense (*61*). We found in our study that an annexin-like protein increased in both cultivars after inoculation, although it was more significant in the susceptible cultivar.

Table 2. Identification of Differential Spot Proteins by MALDI-TOF/TOF and Classification According to Their Functions

spot[a]	protein name	score	species (accession no.)	PM[b]/coverage %	*M*r/*p*I exptl (theor)[a]	functional category	more/less abundance change ratio (FDR)[c]
2105	oxygen-evolving enhancer protein 2, chloroplast precursor (OEE2)	116	*Pisum sativum* (gi131390)	12/46	27.5/5.5 (28.2/8.3)	photosynthesis	0.4 R_I/M_I (0.05)
3301	oxygen-evolving enhancer protein 1, chloroplast precursor (OEE1)	227	*Pisum sativum* (gi131384)	11/35	36.4/5.7 (35.1/6.3)	photosynthesis	4.8 R_I/R_{NI} (0)
3305	oxygen-evolving enhancer protein 1, chloroplast precursor (OEE1)	189	*Pisum sativum* (gi131384)	14/62	36.9/5.9 (35.1/6.3)	photosynthesis	3.4 M_I/M_{NI} (0.001), 0 R_{NI}/M_{NI} (0)
5202	light harvesting protein	68	*Pisum sativum* (gi|309673)	5/22	30.6/6.4 (29.6/8.8)	photosynthesis	0.5 R_{NI}/M_{NI} (0.0375)
7501	ribulose-1,5-bisphosphate carboxylase/oxygenase large subunit	79	*Polypodium furfuraceum* (gi|42541540)	12/32	56.6/7.0 (49.1/7.0)	photosynthesis	0 R_{NI}/M_{NI} (0)
5413	fructose-bisphosphate aldolase 2, chloroplast	223	*Pisum sativum* (gi|461501)	13/33	43.1/5.5 (38.0/5.5)	glycolysis/glyconeogenesis	2.1 R_{NI}/M_{NI} (0.0244), 0.4 R_I/R_{NI} (0.0007)
7508	fructose-bisphosphate aldolase, cytoplasmic isozyme 2	232	*Pisum sativum* (gi|1168410)	15/55	47.1/7.3 (38.6/6.8)	glycolysis/glyconeogenesis	2.2 R_I/R_{NI} (0.0219)
6408	malate dehydrogenase	165	*Glycine max* (gi|3193222)	8/29	43.7/6.8 (27.5/5.6)	citrate cycle	0.5 R_{NI}/M_{NI} (0.0302)
7311	malate dehydrogenase	223	*Pisum sativum* (gi|37725953)	14/40	41.5/7.3 (37.4/7.0)	citrate cycle	0.5 R_{NI}/M_{NI} (0.0382)
5504	glutamate-ammonia ligase (EC 6.3.1.2) 3A, cytosolic	102	*Pisum sativum* (gi|2129882)	6/15	46.1/6.4 (37.6/5.8)	glutamine biosynthetic process	1.9 R_I/M_I (0.0262)
5408	pyridoxal-5-phosphate-dependent enzyme, beta subunit	71	*Medicago truncatula* (gi|92876186)	9/28	44.7/6.4 (41.0/6.5)	metabolic process	0.5 R_I/M_I (0.0452)
2307	DNA-binding protein	89	*Arabidopsis thaliana* (gi|601843)	10/44	38.4/5.6 (21.1/7.7)	protein binding	0.5 R_{NI}/M_{NI} (0.049)
3103	glycine-rich RNA binding protein	75	*Medicago sativa* (gi|6273331)	2/20	19.8/5.7 (10.8/4.5)	nucleic acid binding	0 R_{NI}/M_{NI} (0)
6505	far-red impaired response protein	89	*Oryza sativa* (gi|42407459)	16/17	52.1/6.9 (82.0/8.9)	nucleic acid binding	0 R_{NI}/M_{NI} (0)
4508	elongation factor Tu, chloroplast precursor (EF-Tu)	223	*Pisum sativum* (gi|6015084)	13/31	51.5/6.1 (53.1/6.6)	transcription/translation	0.5 R_{NI}/M_{NI} (0.033)
6305	retrotransposon protein, putative, unclassified	95	*Oryza sativa* (gi|110288963)	24/16	38.0/6.7 (17.1/8.8)	transcription/translation	0.5 R_{NI}/M_{NI} (0.0375)
6506	reverse transcriptase	88	*Oryza sativa* (gi|20279456)	21/17	55.9/6.9 (171.6/8.8)	transcription/translation	0 R_{NI}/M_{NI} (0)
7313	50S ribosomal protein L1, chloroplast precursor (CL1)	188	*Pisum sativum* gi|1350625	10/57	40.4/7.3 (23.5/10.2)	transcription/translation	3.8 M_I/M_{NI} (0.0001), 0.34 R_I/M_I (0.0014)
1104	disease resistance response protein Pi49 (PR10)	359	*Pisum sativum* gi|118933	12/72	19.8/5.3 (16.8/4.9)	defense response	5.5 R_I/R_{NI} (0)
2106	ABA-responsive protein ABR17	91	*Pisum sativum* (gi|1703042)	8/57	19.7/5.5 (16.6/5.1)	defense response	7.1 R_I/R_{NI} (0)
5204	annexin-like protein	75	*Arabidopsis thaliana* (gi|51969286)	9/31	29.7/6.5 (36.6/7.7)	stress response	5.7 M_I/M_{NI} (0.0006), 0.1 R_I/M_I (0)
6403	heat shock protein binding	71	*Arabidopsis thaliana* (gi|15231204)	8/42	44.6/6.6 (17.5/10.0)	stress response	2.1 R_I/R_{NI} (0.0317), 0.4 R_{NI}/M_{NI} (0.0007)
2304	myosin class II heavy chain (ISS)	88	*Ostreococcus tauri* (gi|116057040)	20/17	41.7/5.5 (134.3/5.9)	cellular processes	2.2 M_I/M_{NI} (0.0059), 0.5 R_I/M_I (0.0215)
3104	myosin class II heavy chain (ISS)	76	*Ostreococcus tauri* (gi|116057804)	32/8	20.4/5.7 (468.5/6.2)	cellular processes	77.4 M_I/M_{NI} (0), 0 R_{NI}/M_{NI} (0)
1707	unknown protein	74	*Arabidopsis thaliana* gi|15223730	22/10	76.1/5.3 (217.2/4.8)	unknown	∞ M_I/M_{NI} (0), 0 R_I/M_I (0)
2701	unnamed protein product	94	*Ostreococcus tauri* (gi|116054844)	19/16	91.3/5.4 (108.8/5.4)	unknown	∞ M_I/M_{NI} (0), 0 R_I/R_{NI} (0)
3112	hypothetical protein	77	*Oryza sativa* (gi|50508931)	13/29	21.5/5.7 (29.6/5.8)	unknown	2.4 M_I/M_{NI} (0.01), 0.4 R_{NI}/M_{NI} (0.0044)
3408	hypothetical protein MtrDRAFT_AC140774g5v1	74	*Medicago truncatula* (gi|92870352)	6/48	43.1/5.9 (13.7/5.1)	unknown	∞ R_{NI}/M_{NI} (0)
4306	unknown protein	86	*Arabidopsis thaliana* (gi|15238179)	14/25	37.0/6.0 (63.0/7.6)	unknown	0 R_I/M_I (0)
5416	hypothetical protein	76	*Oryza sativa* (gi|53793527)	16/16	43.1/6.5 (100.5/10.7)	unknown	∞ R_{NI}/M_{NI} (0)
8201	hypothetical protein	96	*Arabidopsis thaliana* (gi|4467113)	23/24	33.8/7.4 (174.7/5.1)	unknown	0 R_{NI}/M_{NI} (0)

[a] Experimental mass (*M*r, kDa) and p*I* were calculated with PDQuest software (BioRad) and standard molecular mass markers. Theoretical values were retrieved from the protein database (NCBI). The software assigns a standard spot number to each spot (SSP). [b] PM: number of matched peptides with the homologous protein from database. Proteins with fragmented peptides sequences are given in boldface (see Supporting information containing data of peptide sequences). [c] The most drastic (more/less abundant) changes are given as normalized volume (calculated with PDQuest software) ratios: M_{NI} (Messire noninoculated), R_{NI} (Radley noninoculated), M_I (Messire inoculated), R_I (Radley inoculated). In brackets appears false discovery rate (FDR) values (0.05 threshold).

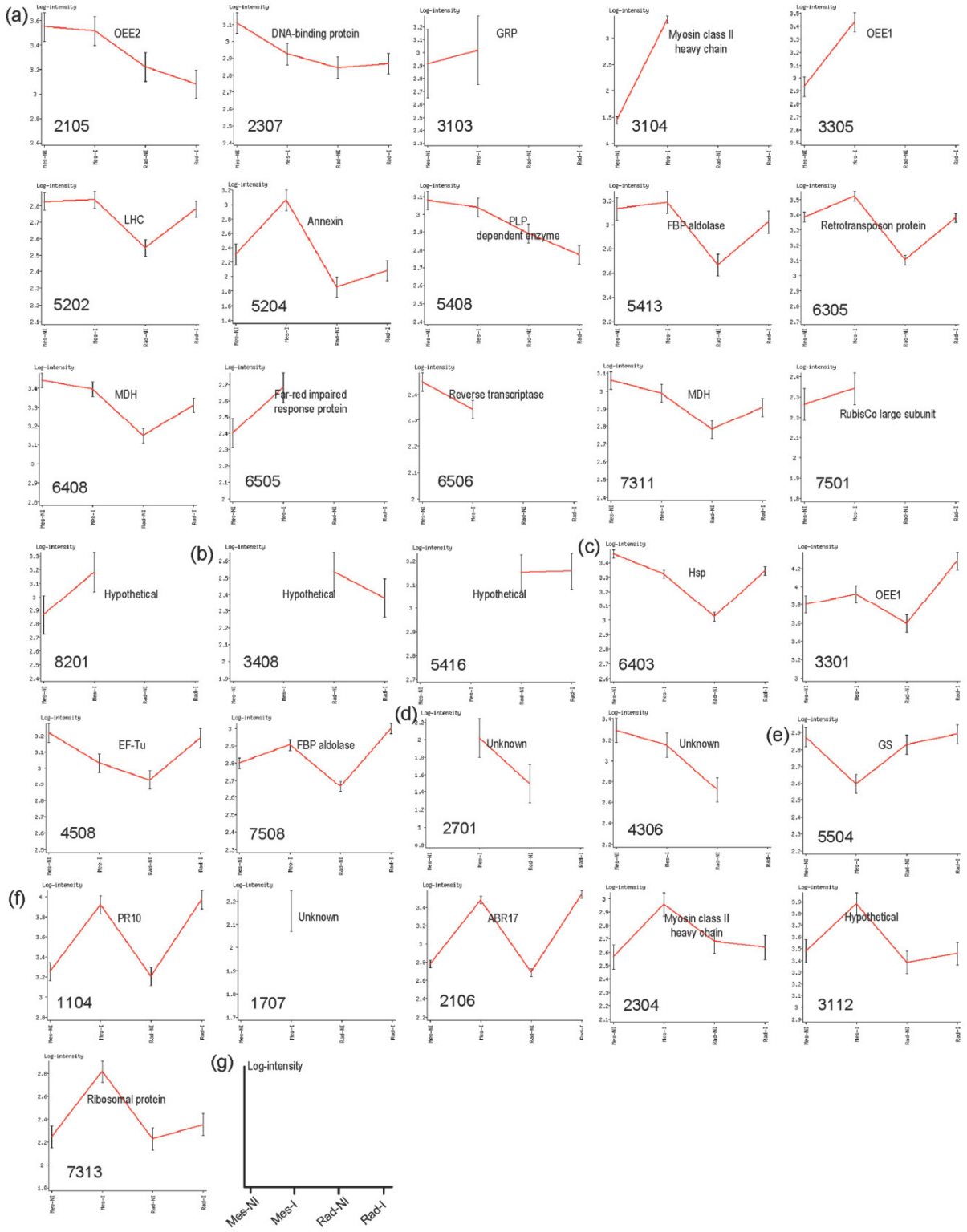

Figure 4. Mean log abundance intensities for protein spots identified by PCA and pairwise comparisons. (**a**) Protein spots positively correlated with PC1. (**b**) Protein spots negatively correlated with PC1. (**c**) Protein spots positively correlated with PC2. (**d**) Protein spots negatively correlated with PC2. (**e**) Protein spots positively correlated with PC3. (**f**) Protein spots negatively correlated with PC3. (**g**) Legend for graphs in panels a−f. The mean log intensity values were calculated from the sample replications.

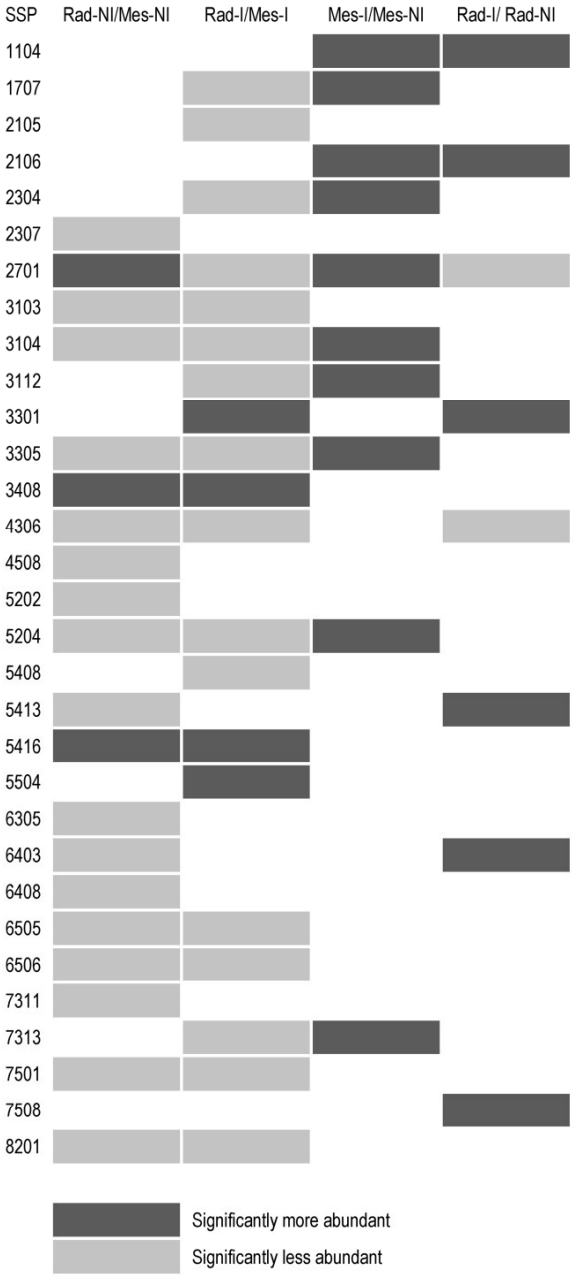

Figure 5. Expression patterns for 31 protein spots based on pairwise comparisons of their protein abundance values. Four pairwise comparisons were selected from hierarchical clustering results. The shading illustrates whether protein spots were more and less abundant. Two shades of gray were used to illustrate the significantly abundant (more or less abundant), or not significantly changed (white) in the respective pairwise comparison. The first column represents protein abundance changes when comparing both noninoculated cultivars, the second column comparing both inoculated cultivars, the third column inoculated versus noninoculated Messire cultivar, and the fourth column inoculated versus noninoculated Radley cultivar.

Molecular chaperones, also known as "heat-shock proteins" (Hsps), promote the correct folding and maturation of many other proteins in the cell. Small heat shock proteins (sHSPs) ranging from approximately 12 to 42 kDa, serve as a first line of defense against stress-induced cell damage by binding and maintaining denaturing proteins in a folding-competent state (*62*). We have identified an Hsp of 17.5 kDa that is more abundant in noninoculated Messire plants than in Radley, but that surprisingly increased in resistant plants after inoculation. The differential behavior of these stress-related proteins in both cultivars could contribute to different reaction mechanisms against *M. pinodes* inoculation.

Other proteins identified in this work correspond to different functional groups, and their relation to plant responses to parasitic plants is unclear. These are two myosin class II heavy chain (spots 2304 and 3104) belonging to the cellular processes category, which was found increased in inoculated susceptible plants. Myosins in plant cells are related to cell division, movement of mitochondria and chloroplast streaming, rearrangement of transvacuolar strands and statolith positioning (*63*). Recent proteomic studies have identified a myosin heavy chain-like protein accumulated in *in vitro* palms inoculated with the pathogen *Phoenix dactylifera* (*64*). Two other proteins belonging to the translation category, such as retrotransposon protein (spot 6305) and 50S ribosomal protein (spot 7313), were found more abundant in Messire cultivar. Finally, seven proteins were not able to be assigned to a known function (spots 1707, 2701, 3112, 3408, 4306, 5416 and 8201).

Based on the results obtained, we conclude that differences observed between noninoculated cultivars could be related to efficiency in energy utilization for growth and fitness purposes. With regard to the abundance pattern from differential identified proteins under inoculation we observed an increase of proteins involved in energetic and amino acid metabolism in the resistant cultivar, as well as a general increase in the amounts of proteins belonging to the defense and stress related category in both cultivars at the earliest stages of infection, coinciding with the moment the pathogen had reached the pea leaf mesophyll. A clear distinction between both cultivars cannot be made based on the defense and stress-related proteins identified in this study. However, most differences observed were related to efficiency in energy utilization, probably to compensate the cost of resistance, such as has been described in previous plant−pathogen interactions.

Data obtained in this work could help to study molecular aspects of the defense and resistance responses of legumes to Aschochyta blight, as well as being used in programs aimed at improving new crop varieties by means of plant breeding and biotechnology. Nevertheless, an integration of physiological and biochemical (genomics and high-throughput proteomics) approaches to study this plant−pathogen interaction, using a large collection of candidates, will be essential to elucidate target key elements of defense for *M. pinodes* infection.

ABBREVIATIONS USED

ABR, ABA-responsive protein; ANOVA, analysis of variance; CBB, Coomassie Brilliant Blue; CHAPS, 3-(3-cholamidopropyl)dimethylammonio-1-propane sulfonate; CHCA, α-cyano-4-hydroxycinnamic acid; DTT, dithiothreitol; EF-Tu, elongation factor Tu; FDR, false discovery rate; GRP, glycine-rich RNA binding protein; GS, glutamine synthetase; Hsp, heat shock protein; IEF, isoelectric focusing; IPG, immobilized pH gradient; MALDI-TOF, matrix assisted laser desorption/ionization time-of-flight; MDH, malate dehydrogenase; MS, mass spectrometry; OEE, oxygen-evolving enhancer protein; PCA, principal component analysis; PLP, pyridoxal 5-phosphate; PMF, peptide mass fingerprinting; PR, pathogenesis-related; ROS, reactive oxygen species; SDS, sodium dodecyl sulfate; SDS−PAGE, sodium dodecyl sulfate polyacrylamide gel electrophoresis; TCA, trichloroacetic acid; TFA, trifluoracetic acid; 2-DE, two-dimensional electrophoresis.

Supporting Information Available: A spreadsheet containing the data set of protein abundance intensity values for protein spots selected due to prospective differential expression behavior, a table containing the data of protein abundance cluster analysis based on PCA, a table containing the peptide sequences of identified proteins, and a representative 2-DE gel CBB stained from Messire plants in the 3−10 pH range. Most proteins were concentrated in the 5 to 8 pH range. This material is available free of charge via the Internet at http://pubs.acs.org.

LITERATURE CITED

(1) Béasse, C.; Ney, B.; Tivoli, B. Effects of pod infection by *Mycosphaerella pinodes* on yield components of pea. *Ann. Appl. Biol.* **1999**, *135*, 359−367.

(2) Zimmer, M. C.; Sabourin, D. Determining resistance reaction of field pea cultivars at the seedling stage to *Mycosphaerella pinodes*. *Phytopathology* **1986**, *76*, 878−881.

(3) Clulow, S. A.; Lewis, B. G.; Matthews, P. A pathotype clasification for *Mycosphaerella pinodes*. *J. Phytopathol.* **1991**, *131*, 322−332.

(4) Wroth, J. M. Host-pathogen relationship of the Ascochyta blight (*Mycosphaerella pinodes* (Berk & Blox) Vesterg) disease of field pea (*Pisum sativum* L.). University of Western Australia: Perth, 1996.

(5) Kraft, J. M. A search for resistance in peas to *Mycosphaerella pinodes*. *Plant Dis.* **1998**, *82*, 251−253.

(6) Fondevilla, S.; Cubero, J. I.; Rubiales, D. Inheritance of resistance to *Mycosphaerella pinodes* in two wild accessions of *Pisum*. *Eur. J. Plant Pathol.* **2007**, *119*, 53−58.

(7) Wroth, J. M. Evidence suggests that *Mycosphaerella pinodes* infection of *Pisum sativum* is inherited as a quantitative trait. *Euphytica* **1999**, *107*, 193−204.

(8) Fondevilla, S.; Avila, C. M.; Cubero, J. I.; Rubiales, D. Response to *Mycosphaerella pinodes* in a germplasm collection of *Pisum* spp. *Plant Breed.* **2005**, *124*, 313−315.

(9) Timmerman-Vaughan, G. M.; Frew, T. J.; Russel, A. C.; Khan, T.; Butler, R.; Gilpin, M.; Murray, S.; Falloon, K. QTL mapping of partial resistance to field epidemics of Ascochyta blight of pea. *Crop Sci.* **2002**, *42*, 2100−2111.

(10) Timmerman-Vaughan, G. M.; Frew, T. J.; Butler, R.; Murray, S.; Gilpin, M.; Falloon, K.; Johnston, P.; Lakeman, M. B.; Russell, A.; Khan, T. Validation of quantitative trait loci for Ascochyta blight resistance in pea (*Pisum sativum* L.), using populations from two crosses. *Theor. Appl. Genet.* **2004**, *109*, 1620−1631.

(11) Tar'an, B.; Warkentin, T.; Somers, D. J.; Miranda, D.; Vandenberg, A.; Blade, S.; Woods, S.; Bing, D.; DeKoeyer, D.; Penner, G. Quantitative trait loci for lodging resistance, plant height and partial resistance to Mycosphaerella blight in Weld pea (*Pisum sativum* L.). *Theor. Appl. Genet.* **2003**, *107*, 1482−1491.

(12) Prioul, S.; Frankewitz, A.; Deniot, G.; Morin, G.; Baranger, A. Mapping of quantitative trait loci for partial resistance to *Mycosphaerella pinodes* in pea (*Pisum sativum* L.), at the seedling and adult plant stages. *Theor. Appl. Genet.* **2004**, *108*, 1322−1334.

(13) Fondevilla, S.; Rubiales, D.; Zatovic, S.; Torres, A. M. Mapping of quantitative trait loci for resistance to *Mycosphaerella pinodes* in *Pisum sativum* subsp. *syriacum*. *Mol. Breeding* **2008**, *21*, 439−454.

(14) Shiraishi, T.; Saitoh, K.; Mo Kim, H.; Kato, T.; Tahara, M.; Oku, H.; Yamada, T.; Ichinose, Y. Two suppressors, supprescins A and B, secreted by a pea pathogen, *Mycosphaerella pinodes*. *Plant Cell Physiol.* **1992**, *33*, 663−667.

(15) Shiraishi, T.; Oku, H.; Tsuji, Y.; Ouchi, S. Inhibitory effect of pisatin on infection process of *Mycosphaerella pinodes* on pea. *Ann. Phytopathol. Soc. Jpn.* **1978**, *44*, 641−645.

(16) Yamada, T.; Shiraishi, T.; Ichinose, Y.; Kato, H.; Seki, H.; Murakami, Y., Regulation of genes for phenylpropanoid synthesis in pea elicitor and suppressor. In *Molecular aspects of phatogenicity and resistance: requirement for signal transduction*; Mills, D., Kunoh, H., Keen, N. T., Mayama, S., Eds.; American Phytopathological Society: St. Paul, 1996; pp 151−162.

(17) Yoshioka, H.; Shiraishi, T.; Nasu, K.; Yamada, T.; Ichinose, Y.; Oku, H. Suppression of activation of Chitinase and ss-1,3-glucanase in pea epicotyls by orthovanadate and suppressor from *Mycosphaerella pinodes*. *Ann. Phytopathol. Soc. Jpn.* **1992**, *58*, 405−410.

(18) Kiba, A.; Miyake, C.; Toyoda, K.; Ichinose, Y.; Yamada, T.; Shiraishi, T. Superoxide generation in extracts from isolated plant cell walls is regulated by fungal signal molecules. *Phytopathology* **1997**, *87*, 846−852.

(19) Toyoda, K.; Shiraishi, T.; Yoshioka, H.; Yamada, T.; Ichinose, Y.; Oku, H. Regulation of polyphosphoinositide metabolism in pea plasma membranes by elicitor and suppressor from a pea pathogen, *Mycosphaerella pinodes*. *Plant Cell Physiol.* **1992**, *33*, 445−452.

(20) Jorrín, J. V.; Rubiales, D.; Dumas-Gaudot, E.; Recorbet, G.; Maldonado, A.; Castillejo, M. A.; Curto, M. Proteomics: a promising approach to study biotic interaction in legumes. A review. *Euphytica* **2006**, *147*, 37−47.

(21) Jorrín-Novo, J. V.; Maldonado, A. M.; Echevarría-Zomeño, S.; Valledor, L.; Castillejo, M. A.; Curto, M.; Valero, J.; Sghaier, B.; Donoso, G.; Redondo, I. Plant Proteomics update (2007−2008). Second-generation proteomic techniques, an appropriate experimental design, and data analysis methods that meet MIAPE standards, increase plant proteome coverage and expand biological knowledge. *J. Proteomics* **2009**, *72*, 285−314.

(22) Repetto, O.; Bestel-Corre, G.; Dumas-Gaudot, E.; Berta, G.; Gianinazzi-Pearson, V.; Gianinazzi, S. Targeted proteomics to identify cadmium-induced protein modifications in *Glomus mosseae*-inoculated pea roots. *New Phytol.* **2003**, *157*, 555−567.

(23) Castillejo, M. A.; Amiour, N.; Dumas-Gaudot, E.; Rubiales, D.; Jorrín, J. V. A proteome approach to studying plant response to crenate broomrape (*Orobanche crenata*) in pea (*Pisum sativum*). *Phytochemistry* **2004**, *65*, 1817−1828.

(24) Schiltz, S.; Gallardo, K.; Huart, M.; Negroni, L.; Sommerer, N.; Burstin, J. Proteome reference maps of vegetative tissues in pea. An investigation of nitrogen mobilization from leaves during seed filling. *Plant Physiol.* **2004**, *135*, 2241−2260.

(25) Curto, M.; Camafeita, L. E.; López, J. A.; Maldonado, A. M.; Rubiales, D.; Jorrín, J. A proteomic approach to study pea (*Pisum sativum*) responses to powdery mildew (*Erysiphe pisi*). *Proteomics* **2006**, *6*, S163−S174.

(26) Wen, F.; VanEtten, H. D.; Tsaprailis, G.; Hawes, M. C. Extracellular proteins in pea root tip and border cell exudates. *Plant Physiol.* **2007**, *143*, 773−83.

(27) Amey, R. C.; Schleicher, T.; Slinn, J.; Lewis, M.; Macdonald, H.; Neill, S. J.; Spencer-Phillips, P. T. N. Proteomic analysis of a compatible interaction between *Pisum sativum* (pea) and the downy mildew pathogen *Peronospora viciae*. *Eur. J. Plant Pathol.* **2008**, *122*, 41−55.

(28) Xue, A. G.; Warkentin, T. D. Partial resistance to *Mycosphaerella pinodes* in filed pea. *Can. J. Plant Sci.* **2001**, *81*, 535−540.

(29) Xue, A. G.; Warkentin, T. D.; Gossen, B. D.; Burnett, P. A.; Vanderberg, A.; Rashid, K. Y. Pathogenic variation of western Canadian isolates of *Mycosphaerella pinodes* on selected *Pisum* genotypes. *Can. J. Bot.* **1998**, *20*, 189−193.

(30) Damerval, C.; de Vienne, D.; Zivy, M.; Thiellement, H. Technical improvements in two-dimensional electrophoresis increase the level of genetic variation detected in wheat-seedling proteins. *Electrophoresis* **1986**, *7*, 52−54.

(31) Neuhoff, V.; Stamm, R.; Eibl, H. Clear background and highly sensitive protein staining with Coomassie Blue dyes in polyacrylamide gels: A systematic analysis. *Electrophoresis* **1985**, *6*, 427−448.

(32) Mathesius, U.; Keijzers, G.; Natera, S. H. A.; Djordjevic, M. A.; Rolfe, B. G. Establishment of a root proteome referent map for the model legume *Medicago truncatula* using the expressed sequence tag database for peptide mass fingerprinting. *Proteomics* **2001**, *1*, 1424−1440.

(33) Schevchenko, A.; Wilm, M.; Vorm, O.; Mann, M. Mass spectrometric sequencing of proteins silver-stained polyacrylamide gels. *Anal. Chem.* **1996**, *68*, 850−858.

(34) Sharov, A. A.; Dudekula, D. B.; Ko, M. S. A web-based tool for PC and significance analysis of microarray data. *Bioinformatics* **2005**, *21*, 2548−2549.

(35) Fondevilla, S. Identification and characterization of sources of resistance to *Mycosphaerella pinodes* in *Pisum* spp. University of Córdoba, Spain, 2000.

(36) Jorge, I.; Navarro, R. M.; Lenz, C.; Ariza, D.; Porras, C.; Jorrín, J. Holm oak leaf proteome. Analytical and biological variability in the protein expression level assessed by 2-DE and protein identification by MS/MS de novo sequencing. *Proteomics* **2005**, *5*, 222−234.

(37) Castillejo, M. A.; Maldonado, A. M.; Ogueta, S.; Jorrín, J. V. Proteomic analysis of responses to drought stress in Sunflower (*Helianthus annuus*) leaves by 2DE gel electrophoresis and Mass Spectrometry. *Open Proteomics J.* **2008**, *1*, 59−71.

(38) Castillejo, M. A.; Kirchev, H.; Jorríın, J. V. Differences in the Triticale (X Triticosecale *Wittmack*) flag leaf 2-DE protein profile between varieties and nitrogen fertilization levels. *J. Agric. Food Chem.* **2010**, *58*, 5698−5707.

(39) Castillejo, M. A.; Susín, R.; Madrid, E.; Fernández-Aparicio, M.; Jorrín, J. V.; Rubiales, D. Two-dimensional gel electrophoresis-based proteomic analysis of the *Medicago truncatula*−rust (*Uromyces striatus*) interaction. *Ann. Appl. Biol.* **2010**, *157*, 243−257.

(40) Valledor, L.; Jorríın, J. V. Back to the basics: Maximizing the information obtained by quantitative two dimensional gel electrophoresis analyses by an appropriate experimental design and statistical analyses. *J. Proteomics* **2010**, July 23, Epub ahead of print.

(41) Mayfield, S. P.; Rahire, M.; Frank, G.; Zuber, H.; Rochaix, J. D. Expression of the nuclear gene encoding oxygen-evolving enhancer protein 2 is required for high levels of photosynthetic oxygen evolution in *Chlamydomonas reinhardtii*. *Proc. Natl. Acad. Sci. U.S.A.* **1987**, *84*, 749−753.

(42) Teixeira, J.; Fidalgo, F. Salt stress affects glutamine synthetase activity and mRNA accumulation on potato plants in an organ-dependent manner. *Plant Physiol. Biochem.* **2009**, *47*, 807−813.

(43) Debouba, M.; Gouiaa, H.; Valadierb, M.-H.; Ghorbela, M. H.; Suzukib, A. Salinity-induced tissue-specific diurnal changes in nitrogen assimilatory enzymes in tomato seedlings grown under high or low nitrate medium. *Plant Physiol. Biochem.* **2006**, *44*, 409−419.

(44) Wang, Z. Q.; Yuan, Y. Z.; Ou, J. Q.; Lin, Q. H.; Zhang, C. F. Glutamine synthetase and glutamate dehydrogenase contribute differentially to proline accumulation in leaves of wheat (*Triticum aestivum*) seedlings exposed to different salinity. *J. Plant Physiol.* **2007**, *164*, 695−701.

(45) Xu, Z. Z.; Zhou, G. S. Combined effects of water stress and high temperature on photosynthesis, nitrogen metabolism and lipid peroxidation of a perennial grass *Leymus chinensis*. *Planta* **2006**, *224*, 1080−1090.

(46) Rizhsky, L.; Liang, H. J.; Shuman, J.; Shulaev, V.; Davletova, S.; Mittler, R. When Defense pathways collide. The response of *Arabidopsis* to a combination of drought and heat stress. *Plant Physiol.* **2004**, *134*, 1683−1696.

(47) Castillejo, M. A.; Maldonado, A. M.; Dumas-Gaudot, E.; Fernández-Aparicio, M.; Susín, R.; Rubiales, D.; Jorrín, J. Differential expression proteomics to investigate responses and resistance to *Orobanche crenata* in *Medicago truncatula*. *BMC Genomics* **2009**, *10*, 294.

(48) Tanaka, T.; Tateno, Y.; Gojobori, T. Evolution of vitamin B6 (pyridoxine) metabolism by gain and loss of genes. *Mol. Biol. Evol.* **2005**, *22*, 243−250.

(49) Hudson, M.; Ringli, c.; Boylan, M. T.; Quail, P. H. The FAR1 locus encodes a novel nuclear protein specific to phytochrome A signaling. *Gene Dev.* **1999**, *13*, 2017−2027.

(50) Ditt, R. F.; Kerr, K. F.; Figueiredo, P.; Delrow, J.; Comai, L.; Nester, E. W. The *Arabidopsis thaliana* transcriptome in response to *Agrobacterium tumefaciens*. *Mol. Plant-Microbe Interact.* **2006**, *19*, 665−681.

(51) Singh, B. N.; Mishra, R. N.; Agarwal, P. K.; Goswami, M.; Nair, S.; Sopory, S. K.; Reddy, M. K. A pea chloroplast translation elongation factor that is regulated by abiotic factors. *Biochem. Biophys. Res. Commun.* **2004**, *320*, 523−530.

(52) Riggleman, R. C.; Fristensky, B.; Hadwiger, L. A. The disease resistance response in pea is associated with increased levels of specific mRNAs. *Plant Mol. Biol.* **1985**, *4*, 81−86.

(53) Liu, J.-J.; Ekramoddoullah, A. K. M. The family 10 of plant pathogenesis-related proteins: Their structure, regulation, and function in response to biotic and abiotic stresses. *Physiol. Mol. Plant Pathol.* **2006**, *68*, 3−13.

(54) Mustafa, B. M.; Coram, T. E.; Pang, E. C. K.; Taylor, P. W. J.; Ford, R. A cDNA microarray approach to decipher lentil (*Lens culinaris*) responses to *Ascochyta lentis*. *Australas. Plant Pathol.* **2009**, *38*, 617−631.

(55) Srivastava, S.; Rahman, M. H.; Shah, S.; Kav, N. N. V. Constitutive expression of the pea ABA-responsive 17 (ABR17) cDNA confers multiple stress tolerance in *Arabidopsis thaliana*. *Plant Biotechnol. J.* **2006**, *4*, 529−549.

(56) Prioul-Gervais, S.; Deniot, G.; Receveur, E.-M.; Frankewitz, A.; Fourmann, M.; Rameau, C.; Pilet-Nayel, M.-L.; Baranger, A. Candidate genes for quantitative resistance to *Mycosphaerella pinodes* in pea (*Pisum sativum* L.). *Theor. Appl. Genet.* **2007**, *114*, 971−984.

(57) Russo-Marie, F. Annexins, phospholipase A2 and the glucocorticoids. In *The Annexins*; Moss, S. E., Ed.; Portland Press: London and Chapel Hill, 1992; pp 35−46.

(58) Gidrol, X.; Sabelli, P. A.; Fern, Y. S.; Kush, A. K. Annexin-like protein from *Arabidopsis thaliana* rescues *AoxyR* mutant of *Escherichia coli* from H_2O_2 stress. *Proc. Natl. Acad. Sci. U.S.A.* **1996**, *93*, 11268−11273.

(59) Torres, M. A.; Jones, J. D.; Dangl, J. L. Pathogen-induced, NADPH oxidase-derived reactive oxygen intermediates suppress spread of cell death in *Arabidopsis thaliana*. *Nat. Genet.* **2005**, *37*, 1130−1134.

(60) Lu, H.; Higgins, V. J. The effect of hydrogen peroxide on the viability of tomato cells and of the pathogen *Cladosporium fulvum*. *Physiol. Mol. Plant Pathol.* **1999**, *54*, 131−143.

(61) Lamb, C.; Dixon, R. A. The oxidative burst in plant disease resistance. *Annu. Rev. Plant Physiol. Plant Mol. Biol.* **1997**, *48*, 251−275.

(62) Jaya, N.; Garcia, V.; Vierling, E. Substrate binding site flexibility of the small heat shock protein molecular chaperones. *Proc. Natl. Acad. Sci. U.S.A.* **2009**, *106*, 15604−15609.

(63) Ojangu, E.-L.; Jarve, K.; Paves, H.; Truve, E. *Arabidopsis thaliana* myosin XIK is involved in root hair as well as trichome morphogenesis on stems and leaves. *Protoplasma* **2007**, *230*, 193−202.

(64) Gómez-Vidal, S.; Salinas, J.; Tena, M.; Lopez-Llorca, L. V. Proteomic analysis of date palm (*Phoenix dactylifera* L.) responses to endophytic colonization by entomopathogenic fungi. *Electrophoresis* **2009**, *30*, 2996−3005.

Received for review September 23, 2010. Revised manuscript received November 5, 2010. Accepted November 8, 2010. Financial support by AGL2008-01239 is acknowledged. MAC acknowledges a postdoctoral contract funded by the Spanish programme 'Juan de la Cierva'.

Chapter 2, Supplementary material

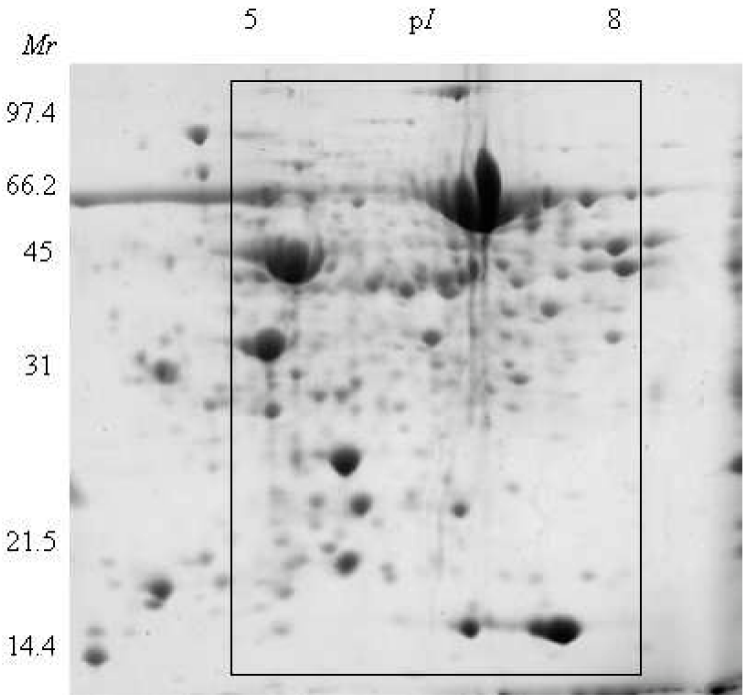

34x32mm (300 x 300 DPI)

Protein expression cluster analysis based on PCA			
	Log change	Correlation	FDR
PC1 positive direction			
5206	12.725	0.999	0
6709	12.811	0.998	0
8602	12.88	0.998	0
7501	12.856	0.997	0
6506	12.961	0.998	0
4808	13.032	0.998	0
6505	13.095	0.996	0
6502	13.175	0.997	0
3104	12.867	0.985	0
6103	13.37	0.997	0
7308	13.438	0.995	0
3103	13.547	0.997	0
2203	13.663	0.998	0
5203	13.598	0.996	0
8201	13.597	0.996	0
3109	13.702	0.9972	0
3305	13.756	0.995	0
7104	0.511	0.927	0.0406
8102	0.477	0.875	0.0398
6308	0.731	0.886	0.0034
2105	0.401	0.968	0.0518
5204	0.715	0.75	0.0018
7001	0.426	0.8	0.0018
7303	0.474	0.92	0.0004
2204	0.336	0.961	0.021
3402	0.319	0.998	0.0307
5413	0.327	0.769	0.0406
5408	0.238	0.939	0.1478
6109	0.293	0.82	0.3211
6408	0.2	0.849	0.2758
7311	0.19	0.878	0.316
6305	0.215	0.67	0.2193
3204	0.161	0.838	0.4404
2307	0.176	0.811	0.366
5202	0.175	0.701	0.366
PC1 negative direction			
3408	-13.018	-0.997	0
5416	-13.749	-0.998	0
5601	-0.194	-0.876	1
PC2 positive direction			
3301	0.627	0.915	0.0004
6407	0.289	0.844	0.3257
6403	0.33	0.745	0.2692
4508	0.283	0.877	0.3257
7508	0.296	0.859	0.3257
4108	0.1	0.785	1

4209	0.149	0.707	1
4507	0.11	0.814	1
PC2 negative direction			
4302	-12.245	-0.791	0
2802	-13.997	-0.847	0
1706	-14.011	-0.844	0
1801	-13.787	-0.838	0
1806	-14.124	-0.842	0
2701	-13.538	-0.834	0
2213	-15.029	-0.845	0
4203	-11.544	-0.784	0
6201	-11.765	-0.785	0
2303	-11.996	-0.796	0
5412	-12.409	-0.808	0
4306	-12.127	-0.777	0
1302	-12.59	-0.796	0
6105	-12.3	-0.775	0
6401	-0.068	-0.875	1
PC3 positive direction			
8304	14.972	0.85	0
2402	0.599	0.972	0.0053
4503	0.804	0.74	0
1211	0.238	0.896	1
5504	0.26	0.798	0.6659
PC3 negative direction			
6104	-12.816	-0.83	0
7105	-12.51	-0.83	0
1502	-12.198	-0.83	0
1707	-12.031	-0.83	0
1505	-11.893	-0.83	0
1506	-14.612	-0.85	0
3001	-15.176	-0.838	0
1509	-11.384	-0.756	0
1104	-0.8	-0.807	0
2106	-0.845	-0.788	0
4104	-0.498	-0.968	0.0002
7313	-0.589	-0.892	0.0001
3112	-0.42	-0.786	0.0153
5106	-0.374	-0.995	0.0903
2304	-0.371	-0.906	0.0211
5409	-0.401	-0.715	0.5502
6101	-0.149	-0.741	1
7504	-0.09	-0.989	1

PCA analysis was performed as described by Sharov et al. (*34*). This analysis allows for generation of associations between proteins and experimental conditions.

Peptides sequences of identified proteins by MALDI-TOF/TOF

Spot	Protein name	Species (number accession) [a]	Sequence of peptides matched (ion score) [b]
2105	Oxygen-evolving enhancer protein 2, chloroplast precursor (OEE2)	*Pisum sativum* (gil131390)	AKTNTDYLPYNGDGFK TNTDYLPYNGDGFK LLVPAKWNPSK WNPSKER EREFPGQVLR **EFPGQVLR (45)** YEDNFDATSNVSVLVQTTDKK SITDYGSPEEFLSK VDYLLGK QYYNISVLTR TADGDEGGKHQLITATVK KFVEDTASSFSVA
3301	Oxygen-evolving enhancer protein 1, chloroplast precursor (OEE1)	*Pisum sativum* (gil131384)	GSSFLDPK VPFLFTIK LTFDEIQSK **NTPLAFQNTK (55)** **RLTFDEIQSK (38)** LCLEPTSFTVK KLCLEPTSFTVK **GASTGYDNAVALPAGGR (49)** QLVASGKPDSFSGEFLVPSYR GASTGYDNAVALPAGGRGDEEELGK GTGTANQCPTIDGGVDSFSFKPGK
3305	Oxygen-evolving enhancer protein 1, chloroplast precursor (OEE1)	*Pisum sativum* (gil131384)	GSSFLDPK **VPFLFTIK (46)** GSSFLDPKGR LTFDEIQSK NTPLAFQNTK **RLTFDEIQSK (20)** LCLEPTSFTVK KLCLEPTSFTVK GASTGYDNAVALPAGGR DGIDYAAVTVQLPGGER QLVASGKPDSFSGEFLVPSYR FEEKDGIDYAAVTVQLPGGER GTGTANQCPTIDGGVDSFSFKPGK GTGTANQCPTIDGGVDSFSFKPGKYNAK
5202	Light harvesting protein	*Pisum sativum* (gil309673)	**QYFLGLEK (37)** WLAYGEVINGR FQDWAKPGSMGK QGGVDRPLWFASK FAMLGAVGAIAPEYLGK
7501	Ribulose-1,5-bisphosphate carboxylase/oxygenase large subunit	*Polypodium furfuraceum* (gil42541540)	EGNDIIR NHGMHFR AMHAVIDR SQAETGEIK DTDILAAFR DNGLLLHIHR

			EVTLGFVDLLR
			DRFLFVAEALFK
			MSGGDHIHAGTVVGK
			DDENVNSQPFMR
			IPPAYSKTFMGPPHGIQVER
			DTDILAAFRMTPQPGVPAEEAR
5413	Fructose-bisphosphate aldolase 2, chloroplast	*Pisum sativum* (gil461501)	TFEVAQK
			ALQNTALK
			SNSLAQLGK
			GSYADELVK
			AAQEALLFR (33)
			SAAYYQQGAR (32)
			YIGDGESEEAKK
			VAEYTLNLLHR (58)
			LDSIGLENTEANR
			TVVSIPNGPSALAVK
			VAEYTLNLLHRR
			SPNPWHVSFSYAR
			RLDSIGLENTEANR
7508	Fructose-bisphosphate aldolase, cytoplasmic isozyme 2	*Pisum sativum* (gil1168410)	CAAITER
			YYEAGAR (10)
			ALQQSTLK
			AAQDALLTR
			VAPEVIAEHTVR
			AKANSEATLGTYK
			GILAADESTGTIGKR
			GASNLGAGASESLHVK
			YHDELIANAAYIGTPGK
			SKYHDELIANAAYIGTPGK
			TAAGKPFVDVLNEAGVLPGIK
			IGANEPSEHSIHENAYGLAR (90)
			GTVELAGTDGETTTQGLDGLGAR
			VDKGTVELAGTDGETTTQGLDGLGAR
			ALSDHHVILEGTLLKPNMVTPGSDAPK
6408	Malate dehydrogenase	*Glycine max* (gil3193222)	TLCTAIAK
			AKTFYAGK
			AGTYDEKR
			LFGVTTLDVVR
			DDLFNINAGIVK (71)
			RLFGVTTLDVVR
			AIFDDDVIETLTK
			ALEGADVVIIPAGVPR (39)
7311	Malate dehydrogenase	*Pisum sativum* (gil37725953)	TLCEGVAK
			AGTYDPKR
			TELAGSIQK
			AKTELAGSIQK
			FANSCLHGLK
			LLGVTTLDVVR (11)
			IQNGGTEVVEAK
			KPGMTRDDLFK
			RLLGVTTLDVVR
			DDLFKINAGIVR

			AGAGSATLSMAYAAAK
			ANTFVAEVLGVDPR (47)
			VAILGAAGGIGQPLSLLLK
			GGAEEIYQLGPLNEYER (53)
5504	Glutamate-ammonia ligase (EC 6.3.1.2) 3A, cytosolic	*Pisum sativum* (gil2129882)	DIVDAHYK
			QGPYYCGIGADK (33)
			EHIAAYGEGNER
			TLPGPVSDPAKLPK
			HKEHIAAYGEGNER (31)
			QGPYYCGIGADKAYGR
5408	Pyridoxal-5-phosphate-dependent enzyme, beta subunit	*Medicago truncatula* (gil92876186)	YLSTVLFQK
			IQGIGAGFVPR
			FAISPRSISTR
			AFGAELVLTEAAK
			LIGVVFPSFGER
			IGYSMILDAEKK
			LILTMPASMSLER
			IREECENMQPEP (16)
			IHFETTGPEIWEDTR
2307	DNA-binding protein	*Arabidopsis thaliana* (gil601843)	AENRAQK
			AAVEAQLR
			AEEQKTSK
			KAAVEAQLR
			AAVEAQLRK
			IHNPPPVESK
			VAAIHKLAEEK
			DVILADLEKEK
			VDVESPAVLAPAK
			GEELLEAEEMGAKYR
3103	Glycine-rich RNA binding protein	*Medicago sativa* (gil6273331)	IINDRETGR
			AFSQYGEIVDSK (58)
6505	Far-red impaired response protein	*Oryza sativa* (gil42407459)	EKGFSVR
			MYNLRK
			SDIASVQK
			RISYAQK
			SCAIYLR
			YMQARQK
			DMYNFFVR
			DAMSKDVIQR
			SESLNSKLHR
			VAEDNQWLGR
			SNQRSESLNSK
			RLFWADPQSR
			SEEDGFIFYNR
			HTSVFIWICSIHK
			FKSEEDGFIFYNR
			MHTSVFIWICSIHKFK
4508	Elongation factor Tu, chloroplast precursor (EF-Tu)	*Pisum sativum* (gil6015084)	YIPIPQR
			FSAIVYVLK
			GTVATGRIER
			VGDVVDLVGLR (47)

			YDEIDAAPEER
			NTTVTGVEMFQK
			KYDEIDAAPEER (91)
			VTSIMNDKDEESK
			ILDDAMAGDNVGLLLR
			HYAHVDCPGHADYVK
			GITINTATVEYETETR
			KKPHLNIGTIGHVDHGK
			HSPFFAGYRPQFYMR
6305	Retrotransposon protein, putative, unclassified	*Oryza sativa* (gil110288963)	TKIFSYLK
			HRTWTTMR
			KIWEGGSSDK
			SMLEQQTSGK
			YWWSNQEK
			IDIRKPLMR
			TSGSRFQVQR
			GAVMAALNMQR
			SAGGGDEGEKPTK
			AMKLPLGLMTK
			CVSTVTYRIR
			INTDGAYSSNMK
			ALEDGPWMFNK
			INTDGAYSSNMK
			ALEDGPWMFNK
			MKAQSAMDEFR
			YNEDAGHLFFK
			DLVVMIDLDETK
			RALEDGPWMFNK
			SAVMFSPNTSSLEK
			AMFPAARVINGDPR
			ANLHHRGMDVDTR
			ASRNGCPGVSNWESGDDDFWK
			EVGEFMTMDLEEDGSAVGQFLRIK
6506	Reverse transcriptase	*Oryza sativa* (gil20279456)	EALDAIGDLK
			HRTWTTMR
			KIWEGGSSDK
			YWWSNQEK
			IDIRKPLMR
			GAVMAALNMQR
			SAGGGDEGEKPTK
			AMKLPLGLMTK
			CVSTVTYRIR
			ALEDGPWMFNK
			ANKSMSGIHQIK
			YNEDAGILFFK
			YLGLPVFVGRSR
			MANKSMSGIHQIK
			RALEDGPWMFNK
			GTQGEDEVTSPLKK
			SAVMFSPNTSSLEK
			ANLHHRGMDVDTR
			DKSAVMFSPNTSSLEK

			ASRNGCPGVSNWESGDDDFWK
			EVGEFMTMDLEEDGSAVGQFLRIK
7313	50S ribosomal protein L1, chloroplast precursor (CL1)	*Pisum sativum* gil1350625	RFLEIQK
			YNDQQLR (19)
			GGFMEFDK
			VAVLTQGER
			FVETVEAHFR
			TKFVETVEAHFR
			VAVLTQGERFDEAK (21)
			GTGKPIKVAVLTQGER
			NAGADLVGGEDLIEQIK (59)
			GGFMEFDKLIASPDMMPK
1104	Disease resistance response protein Pi49 (PR10)	*Pisum sativum* gil118933	AKGDGLFK
			LSAGPNGGSIAK
			LTFVEDGETK
			GDAAPSEEQLK
			ALVTDADNLTPK
			KLTFVEDGETK
			SIEIVEGNGGAGTIK (76)
			ALEGYCLAHPDYN (66)
			SIEIVEGNGGAGTIKK
			YFTKGDAAPSEEQLK (88)
			LTFVEDGETKHVLHK
			GVFNVEDEITSVVAPAILYK
2106	ABA-responsive protein ABR17	*Pisum sativum* (gil1703042)	AIEGYVLANPGY
			GDAALSDAVRDETK
			YHTKGDAALSDAVR
			LSILEDGKTNYVLHK
			EAQGVEIIEGNGGPGTIK
			VAFETIILAGSDGGSIVK
			GVFVFDDEYVSTVAPPK
			EAQGVEIIEGNGGPGTIKK
5204	Annexin -like protein	*Arabidopsis thaliana* (gil51969286)	NATQRSFIR
			FGSSINKFLK
			MGTDEWALTR
			DMLLALLGHDHA
			TAIKCLTYPEK
			ELDGELSGDFER
			VVMLWTLDPTER
			SFIRAVYAANYNK
			TSLEEDVAYHTSGNIR
6403	Heat shock protein binding	*Arabidopsis thaliana* (gil15231204)	VHAGAMGR
			DFMEIHK
			AIYDSTLR
			MAGTLVNSAGR
			VHAGAMGRSGR
			TARFYSGTAR
			RWETDQCW
			VYHPDASESDGRDFMEIHK
2304	Myosin class II heavy chain (ISS)	*Ostreococcus tauri* (gil116057040)	AGESATKR
			IADSDVAR
			STIEMRK

			AEFERVK
			TLELTQAK
			GGVAEITIR
			EAAGKSEAR
			NNRGILLK
			ERSAELEK
			ESEKEDLK
			TQLALAAAER
			DTIIETMRK
			EQRSLASPLR
			ELNVIIMAQIK
			EIANLRELNTR
			IEMEAGNSAAARR
			LRVMNSELLGSIK
			ELNAMLMKQLSAAR
			SMQANMALIVELESK
			IGIFGGACAMVSHIVR
3104	Myosin class II heavy chain (ISS)	*Ostreococcus tauri* (gil116057804)	ASRTQTR
			SLLAMQR
			WEYLVR
			ALRLQNR
			MILASRDK
			TAYSSSLEK
			LEHEIAALR
			VEEMIALEK
			LEDELGELR
			SADLLTAEHK
			LEMQVKELK
			LSQLSNDHSK
			DQLNATKGER
			DLSSKSESER
			FFSVSKGFSR
			ERLAQEDFR
			VFDSERSGLR
			IGFLNSQLSAK
			THETEVALER
			IIESQNAVIAR
			LLILSANMQAR
			AYTAEKLVDAR
			RWQATSDTTVR
			IRCMEDEAVER
			SKANSDAAFEHSR
			INELQALVASLEK
			AKVSDLESAFATAR
			SSEGANDDAVMQLK
			TKIDHLEAELATER
			VEEMIALEKQIGLLK
			DTDMLALREELASNGR
			IQALEDMVNDYQSSMHEAK
1707	Unknown protein	*Arabidopsis thaliana* gil15223730	ITEYHR
			SMVQAKR
			VVEKETK

			WMAWRK
			NENGSSRK
			TSTSGAMEK
			NEHEEKK
			QTKDGSLGK
			GVKEDEVVGK
			LDKEDTCGK
			KIHEHEER
			DLGVSGRYIK
			HSEDRNLIK
			EFGSDDDIAR
			SYEDWTHEK
			NETEGQESTGLR
			IEEEKGLADSNK
			GKQGMTAENMLR
			AELNTEEDSFKK
			QGMTAENMLRQR
			LESADEVDKMVEK
			NAEEEMQDKIDR
2701	Unnamed protein product	*Ostreococcus tauri* (gi|116054844)	SDLMQLK
			YQSAESR
			ESLEKIK
			EKINSTR
			KMEVADR
			LHSTLTAK
			ESLERTR
			DVSMLQGK
			QLDMESDR
			VEISTLRTR
			VNHLTADLAK
			EFEEMNER
			QKYQSAESR
			RVQDETNSR
			QTWQNERVR
			DLLQQSITSID
			DVECIMCTEAER
			EAFAARLAAASEK
			RAFEMEMADLK
3112	Hypothetical protein	*Oryza sativa* (gi|50508931)	VFDHFR
			MSPLGRR
			EERVQMK
			KEIGSSSSR
			TAASASGRNR
			EEMEEERR
			VLHNGFSPSR
			SLENALEKAR
			ELEGANGKLVK
			RTVDMLAASVR
			TTRPSLLGVGGRK
			MLQMAEVWREER
			SRPGPSPPAYGGCAKR
3408	Hypothetical protein	*Medicago truncatula*	DEYAWK

	MtrDRAFT_AC140774g5v1	(gi|92870352)	VRYSAFK
			MSEVVQIER
			TASYMPLLIR
			MSEVVQIERR
			VMITPMDSLDDLK
4306	Unknown protein	*Arabidopsis thaliana* (gi|15238179)	HEVETLEAK
			MKMEDHIR
			TSICHVALQA
			LEESGELGNR
			DNTQTEENR
			LSMEIKDQK
			ELEMELVKK
			EFNEEMKSK
			MEEAKTEVEK
			GNRAVSETQFK
			TNQVSETQMRLK
			LECREAQESLLK
			EKEFELLSLGEGK
			DNNMKHEVETLEAK
5416	Hypothetical protein	*Oryza sativa* (gi|53793527)	KVLAEIAK
			KWDDWK
			AAETEAASR
			AAELEARAK
			AELDAAWAR
			DFKILVQR
			LGPLPQATLR
			SVEAMVEVGR
			QLAMRPRAR
			EDALTERER
			RSVEAMVEVGR
			QLPGQLATRPR
			DLADREAAVTIR
			AERAELDAAWAR
			LAGEVGPGMLWDAVSR
			TIADLQGALDSSAGEVEALR
8201	Hypothetical protein	*Arabidopsis thaliana* (gi|4467113)	QEATKSR
			NCSANLR
			EIAELKR
			HSDAERR
			AEIMTVGGR
			AELEQNQNLR
			HEEDVVTEDR
			TSEAEKTELVK
			ENNNGETIGSPR
			ANEELQRCLR
			AELETKQTELK
			FGPVLLEDFEK
			NAALAKAQMEIK
			NMMSGLDEASEK
			VISHARSSDSEK
			LRINSQFATLR
			QTLSMKDAYFK

	EERESVACLLK
	DDVVVKMEEEK
	NMMSGLDEASEK
	EGNCYSLLMEQLDQK
	EMLEESTKTQLLLQEK
	KMMIIELEGEISSLSQK

[a] Number accession from NCBI database.
[b] Sequences of the peptides matched. Fragmented peptides and ion score are given in boldface.

Chapter 3: Plant defense responses in *Medicago truncatula* unveiled by microarray analysis

Plant Mol Biol Rep
DOI 10.1007/s11105-014-0770-9

ORIGINAL PAPER

Plant Defense Responses in *Medicago truncatula* Unveiled by Microarray Analysis

Miguel Curto · Franziska Krajinski · Helge Küster · Diego Rubiales

Abstract Plant defense responses are made up of broad plant defense mechanisms that involve an integrated signaling pathway. Powdery mildew caused by *Erysiphe pisi* is one of the most important diseases of pea. However, the mechanisms and pathways involved in the resistance against *E. pisi* are yet undiscovered. We studied the transcriptome of two *Medicago truncatula* genotypes, the powdery mildew susceptible commercial variety Parabinga and the resistant accession SA1306, at 4 and 12 h after *E. pisi* infection, using Mt16kOLI1 microarrays. Four hundred and forty six probes were differentially expressed between the two *M. truncatula* genotypes along the time points studied. RNA accumulation patterns suggest that the most prominent responses to pathogen infection occur at early infection stages. Most of the regulated genes are related to cell wall reinforcement, flavonoid, and phenylpropanoid biosynthesis. In addition, pathogenesis-related proteins and signaling pathways controlled by jasmonic acid and salicylic acid were found to be regulated during pathogen infection. This study provides the first comprehensive view of the genes and pathways activated in the *E. pisi*/*M. truncatula* pathosystem, allowing the identification of targets against this important disease.

Keywords *Erysiphe pisi* · Pea · Legume · *Medicago truncatula* · Microarray

Electronic supplementary material The online version of this article (doi:10.1007/s11105-014-0770-9) contains supplementary material, which is available to authorized users.

M. Curto (✉) · D. Rubiales
CSIC, Institute for Sustainable Agriculture, Apdo.4084, 14080 Córdoba, Spain
e-mail: b72curum@uco.es

D. Rubiales
e-mail: diego.rubiales@ias.csic.es

F. Krajinski
Max Planck Institute of Molecular Plant Physiology, Wissenschaftspark Golm, Am Muehlenberg 1, 14476 Potsdam, Germany
e-mail: krajinski@mpimp-golm.mpg.de

H. Küster
Institute for Plant Genetics, Unit IV—Plant Genomics, Leibniz Universität Hannover, Herrenhäuser Str. 2, 30419 Hannover, Germany
e-mail: helge.kuester@genetik.uni-hannover.de

Published online: 12 August 2014

Introduction

Legumes play a critical role in crop rotation thanks to their ability to fix atmospheric nitrogen. They are major protein source suppliers for human food and animal feed. Among them, *Medicago truncatula* has become a model as it presents the biologic key attributes; self-fertile, rapid generation time, and small diploid genome (Cook 1999; Singh et al. 2007). These key attributes have allowed applying the molecular and genetic tools developed in this legume species (Rose 2008). To facilitate the study of the plant–microbe interaction in legume crops, different tools for classical, molecular, and reverse genetics, along with functional genomics, have been developed in *M. truncatula* model species (Ameline-Torregrosa et al. 2006; Rispail et al. 2010; Young and Udvardi 2009). Plant breeding projects have been successfully carried out in *M. truncatula* developing resistant lines to a wide range of plant pathogens (Fernández-Aparicio et al. 2008; Rubiales et al. 2011; Tivoli et al. 2006). In addition, the results obtained from these studies have been further compared with the most agronomical crop legumes and found to present a high degree of synteny between them (Hougaard et al. 2008; Rose 2008).

Powdery mildews are biotrophic plant pathogens that seriously constraint crop production worldwide (Bélanger et al. 2002). Especially, *Erysiphe* spp. causes considerable losses in various important legume crops (Sillero et al. 2006). Powdery

mildew of pea is caused by *E. pisi* DC, in the past often reported as *E. polygoni* DC. This fungus has been classified into three physiologically specialized forms, f.sp. *pisi* specialized on *Pisum*, f.sp. *medicaginis* specialized on *Medicago*, and f.sp. *vicia sativa*, specialized on *Vicia* (Falloon and Viljanen-Rollinson 2001). The most desirable strategy to control this disease is the use of resistant cultivars (Fondevilla and Rubiales 2012). Several genes involved in resistance to powdery mildew have been reported in several plant species including barley, *Arabidopsis*, and pea (Barilli et al. 2014; Fondevilla et al. 2007, 2008; Schulze-Lefert and Panstruga 2003; Yang et al. 2013). Resistance in *M. truncatula* has been reported and resistance mechanisms histologically (Prats et al. 2007) and genetically (Ameline-Torregrosa et al. 2008) characterized; however, molecular mechanisms involved in the plant defense are poorly understood (Foster-Hartnett et al. 2007; Panstruga and Spanu 2014; Spanu and Panstruga 2012; Yaege and Stuteville 2002).

High-throughput techniques have enabled the analysis of the expression profile of multiple genes and protein in a large number of studies (Wan et al. 2002). Among them, DNA microarray technology provides a valuable tool for gene expression analysis (Uttamchandani et al. 2009; Wan et al. 2002) giving full and detailed information of metabolic pathways involved in the analyzed system. DNA microarray platforms (Küster et al. 2004) have been successfully developed and applied to study some *M. truncatula* pathosystems (Dita et al. 2009; Fondevilla et al. 2011; Nyamsuren et al. 2007). Previous studies have analyzed the *E. pisi*/*M. truncatula* pathosystem using different genotypes and microarray platforms containing 4481(Samac et al. 2011) and 6000 (Foster-Hartnett et al. 2007) probes, respectively. In spite of the results gathered from these studies, the *M. truncatula*/*E. pisi* pathosystem is still insufficiently understood (Spanu and Panstruga 2012; Yaege and Stuteville 2002). A more comprehensive platform representing more genes is required to identify pathways implicated in this phytopathogenic interaction. *M. truncatula* Mt16kOLI1 microarrays composed of 16086 70-mer oligonucleotides (Küster et al. 2007) have been used. This study provides comprehensive information on molecular responses in particular in the early infection process allowing to increase the knowledge of mechanisms involved in the resistance to *E. pisi*. The results obtained in this work thus provide targets to develop breeding programs that increase host resistance to *E. pisi* infection.

Experimental Procedures

Plant Material, Growth Conditions and Inoculation

The study was accomplished through an analysis of two genotypes of *M. truncatula*, the susceptible cultivar (cv.) Parabinga and the resistant SA1306 accession (Prats et al. 2007). Histological assessments allowed to study and confirm the resistance and susceptibility to *E. pisi* in SA1306 and Parabinga genotypes (Fig. S1).

Seeds of both *M. truncatula* genotypes were presoaked in filter paper at 4 °C for 24 h and germinated during 48 h in darkness conditions in a growth chamber at 65 % relative humidity and 20 °C. Seedlings of *M. truncatula* were placed on pots into a 1:2 mixture of expanded clay and vermiculite, fertilized with half-strength Hoagland's solution (Hoagland and Arnon 1950) three times a week, and grown (25 °C, 12-h photoperiod, 250 μmol/m^2 light intensity, 80 % relative humidity) during 4 weeks until the plant inoculation.

The pathogen used was the isolate CO05 of *E. pisi* f.sp. *medicaginis*, derived from a population collected on *M. truncatula* plants at Córdoba, Spain (Prats et al. 2007). It was maintained and propagated, by infecting Parabinga plants, until the inoculation. One day before inoculation, the highly infected plants were shacked to remove old conidia so as to produce a vigorous inoculum with young spores. For plant inoculation, we used a setting tower to give an inoculum density of 5 conidia mm^{-2} (Prats et al. 2007). Six plants of each genotype were inoculated at the same time keeping six non-infected plants as a control. Four replicates were performed with leaflets of control and *E. pisi* infected plants at 4 and 12 h for each *M. truncatula* genotype analyzed. The samples were immediately washed with water, blot dried with filter paper, frozen in liquid nitrogen, and stored at −80 °C until RNA extraction.

Microscopy

Second-formed leaves of inoculated and control (non-inoculated) plants of both genotypes were excised at 48 and 72 h after inoculation (hai) and processed for microscopy to perform the assays per triplicate. Leaves were fixed with acetic acid/ethanol (1:3) and washed with lactoglycerol and water as described by Rubiales et al. (Rubiales and Carver 2000). Each genotype was represented by three leaves in three replicates each. To avoid displacing spores, fungal structures were previously stained by spraying leaves gently with 95 % ethanol containing methyl blue (0.2 %). For each replicate, the percentage of germination was calculated by microscopic observation of 100 conidia for the presence of a germ tube. Further developmental stages were evaluated by scoring 100 germlings with mature appressoria. The colony size was also assessed by scoring the number of hyphal tips produced by each one of 20 colonies evaluated. The host cell death was examined on leaflets fixed at 48 hai to analyze the cell content under bright field and differential interface contrast in 20 colonies with secondary hyphae. Analysis of variance, accompanied of Levene's homoscedasticity and Kolmogorov–Smirnov normality tests, allowed analyzing the developmental stages in both genotypes studied (Table S1).

RNA Isolation and cDNA Synthesis

Total RNA was isolated from collected samples following the LiCl method (Franken and Gnädinger 1994). The resulting RNA samples were purified and concentrated to 1.20 μg μl^{-1} using Microcon-30 YM columns (Millipore, Schwalbach, Germany). RNA was quantified using a spectrophotometer ND-100 (NanoDrop Technologies, Wilmington, DE). Sixty micrograms of total RNA was treated using RNase-free DNaseI (Turbo DNA free, Ambion), according to the manufacter's protocol, to avoid any possible DNA contaminations. The purity and integrity of RNA samples after DNase treatment were checked by spectrophotometry and by electrophoresis on a 3 % (*v*/*w*) agarose gel. To confirm the absence of genomic DNA, a control PCR experiment was carried out using specific primers designed to amplify a genomic fragment of *M. truncatula* ubiquitin gene (Fw, 5′-GTCCTCTAAG GTTTAATGAACCGG-3′; Rv, 5′-GAAAGACACAGCCA AGTTGCAC-3′) which amplify a non-coding sequence on the *ubiquitin* gene (Kakar et al. 2008).

First-strand complementary DNA (cDNA) synthesis of total RNA was carried out by quantitative polymerase chain reaction (qPCR) with oligo-dT12–18 (Qiagen, Hilden, Germany), using SuperScript III reverse transcriptase (Invitrogen GmbH, Karlsruhe, Germany) following the instructions of the supplier. The efficiency of cDNA synthesis was assessed by qPCR, using specific primers to amplify segments in the 5′ (Fw 5′-3′:TTGGAGACGGATTCCATT GCT/Rv 5′-3′: GCCAATTCCTTCCCTTCGAA) and 3′ (Fw 5′-3′:GGCCCTAGAACATTTCCTGTGG/Rv 5′-3′:TTGG CAACCAAAATGTTCCC) regions of *M. truncatula Ubiquitin* gene. The qPCR reactions were performed per triplicate in an ABI PRISM 7900 HT Sequence Detection System (Applied Biosystem, Foster City, CA, USA). Each PCR contained 20 ng cDNA (≈2 μl), 0.3 μM of each primer and 10 μl of 2× SYBR® Green Power Maxter Mix reagent (Applied Biosystem, Warringen, UK) in a final volume of 20 μl. The thermal profile used was as follows: 1 cycle to activate the polymerase (95 °C for 10 min), followed of 40 amplification cycles (95 °C for 15 s, 60 °C for 1 min) and a final cycle corresponding to the dissociation curve (95 °C for 15 s, 60 °C for 1 min, 95 °C for 30 s).

Microarray Hybridization and Statistical Analysis of Microarray Data

Microarray experiments were performed using Mt16kOLI1 microarrays (Küster et al. 2007). An array definition file can be downloaded from the European Bioinformatics Institute (EBI) website under accession number A-MEXP-85. Previously to microarray hybridization, the absence of contaminating genomic DNA was verified by PCR analysis in all cDNA samples using primer pairs designed to amplify a genomic fragment of the control gene ubiquitin (Kakar et al. 2008). The microarray hybridizations were carried out using four independent replicates per experimental treatment, according to instructions detailed by Küster et al. (Küster et al. 2004). The images of microarray hybridizations were analyzed using the imagine 5.5 software (BioDiscovery, Los Angeles) as described by Hohnjec et al. (Hohnjec et al. 2005).

Hybridization intensity values obtained were imported into the EMMA 2.8.2 array analysis software (Dondrup et al. 2003) and normalized via the Lowess method using a floor value of 20. The genes differentially expressed in response to *E. pisi* infection were identified in both genotypes at the analyzed time point by applying student's *t* test and linear models for microarray data (LIMMA) tests (Smyth 2004), both followed by false discovery rate (FDR) correction at level 0.05. Genes were regarded as regulated with a minimum $\log_2$ expression ratio of 0.8 and $p \leq 0.05$ for both statistical tests.

qPCR Experiments

Ten differently expressed genes in the microarray experiments were analyzed in all cDNA samples by qPCR in order to validate the microarray expression profiles (Table S2). PCR reactions were carried out in an ABI PRISM 7900 HT Sequence Detection System (Applied Biosystem, Foster City, CA, USA). SYBR® Green was used to quantify dsDNA synthesis. Reactions contained 20 ng cDNA (≈2 μl), 0.3 μM of each primer, and 10 μl of 2× SYBR® Green Power Maxter Mix reagent (Applied Biosystem, Warringen, UK) in a final volume of 20 μl. The thermal profile used was as described for the cDNA synthesis.

In addition, the reference *M. truncatula MtUbi*, *MtGapdh*, and *MtPdf2* genes [UBIQUITIN, glyceraldehyde 3 phosphate dehydrogenase (GADPH), and protein phosphatase 2A subunit A3 (PDF2), respectively] were amplified for all cDNA samples obtained using specific primer pairs (Kakar et al. 2008) to carry out the transcript normalization process.

SDS software ver. 2.3 (Applied Biosystems) was used to analyze fluorescent signals and calculate the quantification cycle (Cq) (Bustin et al. 2009). The baseline data were collected from the fluorescence signal between 3 and 15 cycles and used to correct the fluorescence signal of the samples. The qPCR efficiencies and correlation coefficients (R^2), from linear regression analysis, were calculated for each performed PCR reaction by the software LinRegPCR ver. 7.5 as described by Kakar et al. (Kakar et al. 2008).

The expression levels of the three reference genes were analyzed by the geNorm software (Hellemans et al. 2007). The pairwise comparison and geometric averaging of the reference genes allowed calculating their gene expression stability as well as to select the most stable reference genes (Vandesompele et al. 2002). The selected reference genes

were used for transcript normalization of the ten genes evaluated in the microarray validation assay. The expression values of each assayed gene were calculated from the formula $E^{-\Delta Cq}$, where ΔCq (Cq of target gene−Cq of average selected reference genes, using the average values of PCR efficiencies (E) and fluorescent signals. The relative expression of each gene, in response to *E. pisi* infection, was calculated as $E^{-\Delta\Delta Cq}$, where ΔΔCq (Cq of the target gene−Cq of average selected reference genes) infected condition (Cq of the target gene−Cq of average selected reference genes) untreated condition (Livak and Schmittgen 2001), using the average values of PCR efficiencies (E) and fluorescent signals. In addition, pairwise Pearson correlation coefficients were calculated to study the degree of correlation between microarray and qPCR experiments (Table S3).

Results

M. truncatula/*E. pisi* Pathosystem

The study was accomplished through an analysis of two genotypes of *M. truncatula*, the susceptible cultivar (cv.) Parabinga and the resistant SA1306 accession. Differences in the response to *E. pisi* between the two genotypes were macroscopically clearly visible 2 weeks after inoculation, with profuse sporulation in the susceptible Parabinga genotype and absence of symptoms in the resistant SA1306 genotype (Fig. S1c, d). Histological studies showed a lower ability of *E. pisi* to develop fungal structures in the SA1306 genotype. Colony formation was much higher in Parabinga than in SA1306 (Fig. S1e, f; Table S1). The hypersensitive response associated with epidermal cell death observed as host cell cytoplasm disorganization (Fig. S1f) was negligible in Parabinga but marked in SA1306.

Four hundred and forty six probes out of 16,086 probes on the microarray were significantly regulated ($p<0.05$; $0.8\leq M\leq -0.8$) in the two *M. truncatula* genotypes in response to *E. pisi* infection at the studied time points (Table S4). Two hundred and ninety five of them showed sequence similarities to genes of known functional categories described by Journet et al. (Journet et al. 2002) (Fig. 1). Most of these probes found to be differentially expressed belong to categories related to stress and defense responses. Among them, the most represented category was "Secondary metabolism and hormone metabolism" (15.25 %), followed by "Abiotic stimuli and development," "Cell Wall," "Defense and cell rescue," "Protein synthesis and processing," and "Primary metabolism" (around 10 % each). Genes included in the categories "Gene expression and RNA metabolism" (7.79 %) and "Miscellaneous" (7.11 %) as well as "Membrane transport" (5.76 %) were well represented. The categories "Signal transduction and post-translational regulation," "Chromatin and DNA metabolism," and "Cytoskeleton" were weekly represented (around 2 % each). The two remaining categories, "Vesicular trafficking, secretion and protein sorting" and "Cell division cycle," were only represented by three (TC89776, TC78263, TC76333) and one (TC80244) regulated probes, respectively (Table S4).

Seventy six from 295 genes, that showed sequence similarities to genes of know functional categories described by Journet et al. (Journet et al. 2002), were differentially regulated in SA1306 compared to Parabinga ($0.8\leq F\leq -0.8$, $p\leq 0.05$). These genes were analyzed in this study to obtain a global view of genes induced during the resistance to *E. pisi*. Genes that were induced ($F\geq 0.8$) or repressed ($F\leq -0.8$) in SA1306 compared to Parabinga were considered upregulated and repressed, respectively (Fig. 1, Table 1). Most of them (48/76) were regulated at 4 hai, meanwhile around 30 % of sequences (24/76) were regulated at 12 hai. The four remaining sequences were regulated at both time points. These genes belonged to Cell Wall and Defense and cell rescue categories encoding proteins involved in nodulation (TC92730, TC77131) and defense processes (BG45222, TC77149), respectively. All of these sequences were induced at 4 hai and repressed at 12 hai, except the sequence TC77131 that was upregulated at both time points (Table 1).

The vast proportions of regulated genes at 4 hai were induced at this time point (38/48). These sequences mainly belong to categories related to defense and stress responses (Table 1). Among them, the categories Defense and cell rescue, Cell Wall, Secondary metabolism and hormone metabolism, and Gene expression and RNA metabolism are the most represented (Table 1). The 12th A category Defense and cell rescue, as expected, was the most induced in the resistant genotype including sequences involved in cell death and defense processes. Among them are some genes encoding pathogenesis-related proteins as "pathogenesis-related protein 4A (PRP4A)," "pathogenesis-related protein (pprg2)," and "endochitinase precursor" (PR-3). In addition, some sequences involved in defense responses were also upregulated in SA1306, which were the cases of "glutathione S-transferase" and some sequences related to reactive oxygen species (ROS) metabolism, such as peroxidases. The Cell Wall category was also one of the most represented categories at 4 hai, including some induced sequences involved in cell wall reinforcement, such as "glucan endo-1,3-beta-D-glucosidase," "expansin," "1,3-beta-glucanase," and "pectinase (*AT3g62110*)". An important number of sequences belonged to Secondary metabolism and hormone metabolism were also significantly regulated in response to infection at 4 hai in SA1306 compared to susceptible genotype. The induced sequences encode proteins that are involved in diverse stress and defense mechanisms, such as xenobiotic, triterpenoids, and flavonoid metabolisms. Among them, three sequences

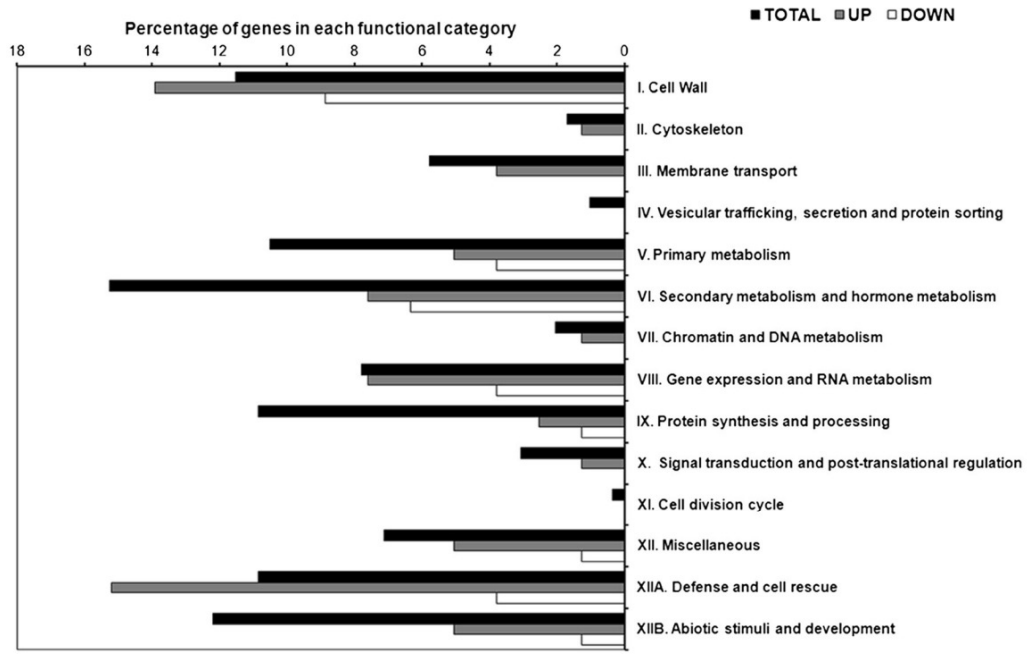

Fig. 1 Functional classification of regulated genes in *M. truncatula* genotypes in response to *E. pisi* infection. All proteins encoded by *E. pisi*-induced genes were grouped into the known functional categories according to Journet et al. (Journet et al. 2002). The genes differentially expressed in SA1306 compared to Parabinga after inoculation with *E. pisi* were also represented. Only genes that met the prerequisites $0.8 \leq F$ value ≤ -0.8 and $P \leq 0.05$ were considered as upregulated and downregulated in this representation, respectively. Additional information of genes is given in Table S4

involved in deoxychalcone biosynthesis are noteworthy, two of them encoding chalcone reductases and one a chalcone synthase, respectively. The eighth category Gene expression and RNA metabolism included several upregulated genes belonging to broad transcription factor families including zinc finger and MYB transcription factor families. Nevertheless, a low proportion of regulated genes were repressed at 4 hai (10/48). These sequences encoded proteins that are involved in different processes including cell wall extension (AW69363, TC89013), amino acid metabolism (TC92381), chlorophyll biosynthesis (TC85935), transcription (TC87794, TC88380), protein synthesis (TC85227), symbiotic interactions (TC91876), ROS metabolism (TC86399), and environmental stresses (TC85566).

Moreover, a minor proportion of regulated genes were differentially expressed in SA1306 compared to Parabinga at 12 hai (24/76). The most represented categories at this time point are Cell Wall, Secondary metabolism and hormone metabolism, Primary metabolism, and Gene expression and RNA metabolism, respectively. The remaining categories Cytoskeleton, Membrane transport, Chromatin and DNA metabolism, Miscellaneous, and Abiotic stimuli and development included only one regulated sequence in each one of them (Table 1). The half of regulated genes at 12 hai (13/24) were induced, including sequences encoding proteins involved in cell wall metabolism (TC76880, BF51916, TC86491), energy metabolism (TC88949, TC86005), transcription (TC88569, TC89017), and gibberellin signaling pathway (TC78048). Moreover, a similar number of sequences (11/24) were repressed at this time point, which belonged mainly to metabolism of inositol phosphates (TC85537, TC85538), amino acid biosynthesis (TC85436, TC89059), and secondary metabolism (TC77029, TC82902, TC85609, and TC87678).

E. pisi Infection Induces in SA1306 a Set of Genes Involved in Broad Defense Mechanisms

Microarray experiments identified a set of regulated genes involved in a wide range of defense mechanisms in the resistant genotype SA1306 in response to *E. pisi* infection (Table 1, Fig. 2). Among them, an important number of genes belong to cell wall metabolism, as "early nodulin 12A," "nodulin MtN3," "nodulin MtN19," and expansin, involved in cell wall strengthening and elongation processes (Table 1). These enzymes contribute to pathogen resistance playing an important role in the guard against the spore penetration by means of physical barriers as cell wall appositions (CWAs) (Fig. 2). In addition, several cell wall hydrolases as glucan endo-1,3-beta-D-glucosidase, 1,3-beta-glucanase, endoxyloglucan transferase, and pectinase (*At3g62110*) were also upregulated in SA1306 (Table 1). These enzymes are involved in the

Table 1 Most differentially expressed genes in SA1306 compared to Parabinga in response to *Erysiphe pisi* infection

MtGI[a]	Description	Fold change (F)[b]		FC[c]	Time[d]
		F4	F12		
TC78899	Glucan endo-1,3-beta-D-glucosidase	3,217*	−0,612	I	4 hai
TC84433	1,3-beta-glucanase	2,664*	−0,403	I	4 hai
TC77134	Early nodulin 12A	1,847*	−0,048	I	4 hai
TC76965**	Nodulin MtN19	1,464*	−1,677	I	4 hai
TC82045	Expansin	1,722*	−0,14	I	4 hai
TC91378	Pectinase (*AT3g62110*)	1,185*	−0,236	I	4 hai
AW69363	Beta-glucosidase	−1,092*	0,213	I	4 hai
TC89013	Expansin	−1,035*	0,112	I	4 hai
TC89099	Lipid transfer protein SDi-9 drought-induced	1.410*	−0.312	III	4 hai
TC93816	ABC transporter	1.275*	0.104	III	4 hai
TC82383	Light-harvesting chlorophyll-a/b binding protein LhcII-1.3	1.409*	0.195	V	4 hai
TC84044	Glutamine synthetase I	1.143*	−0.119	V	4 hai
TC92381	Cysteine synthase	−0.987*	0.427	V	4 hai
TC77840	Cytochrome P450	2.531*	0.289	VI	4 hai
TC82770	Chalcone reductase	1.472*	−0.263	VI	4 hai
AW77474	Chalcone reductase	1.390*	0.518	VI	4 hai
TC85138	Chalcone synthase 8	1.350*	−0.212	VI	4 hai
TC77268	Dihydroflavonol 4-reductase-like	1.179*	−0.582	VI	4 hai
TC85935	Protochlorophyllide reductase	−0.895*	0.403	VI	4 hai
TC84988	Zinc finger protein	1.740*	−0.068	VIII	4 hai
TC78266	MYB-related transcription factor VlMYBB1-1	1.135*	−0.076	VIII	4 hai
TC81518	BZR1 protein	1.101*	−0.237	VIII	4 hai
TC84865	Pinin protein	1.080*	0.205	VIII	4 hai
TC87794	bZIP transcription factor 2	−2.675*	0.712	VIII	4 hai
TC88380	Glutamyl-tRNA reductase precursor	−1,104*	n.v.	VIII	4 hai
TC89991	Putative ubiquitin fusion-degradation protein	1.571*	−0.155	IX	4 hai
TC80669	DnaK-type molecular chaperone HSP71.2	0.828*	−1.142	IX	4 hai
TC85227	AT4g29060	−1.123*	0.659	IX	4 hai
TC85793	Fiber annexin	0.822*	−0.162	X	4 hai
TC86157	Albumin 1 precursor (PA1)	4.843*	−2.04	XII	4 hai
TC85729	Lectin-related polypeptide	3.477*	−0.17	XII	4 hai
TC93496	Chloroplast nucleoid DNA-binding protein	1.554*	0.106	XII	4 hai
TC91876	Lectin 4	−0.837*	0.064	XII	4 hai
TC87236	Pathogenesis-related protein 4A (PRP4A)	1.843*	−1.094	XIIA	4 hai
TC76641	Pathogenesis related-protein (pprg2)	1.175*	−0.337	XIIA	4 hai
TC76642	Pathogenesis related-protein (pprg2)	0.943*	−0.399	XIIA	4 hai
TC77110	Putative steroid membrane binding protein	1.048*	0.543	XIIA	4 hai
TC80969	Glutathione S-transferase	3.105*	−0.377	XIIA	4 hai
TC85453	Glutathione S-transferase	1.162*	−0.367	XIIA	4 hai
TC82258	Endochitinase precursor	1.836*	−0.456	XIIA	4 hai
TC85170	Peroxidase	1.786*	−0.973	XIIA	4 hai
TC85974	Peroxidase	0.805*	0.01	XIIA	4 hai
TC87547	Probable glucosyl transferase	0.983*	0.672	XIIA	4 hai
TC86399	Thioredoxin homolog F22O13.5	−0.837*	0.477	XIIA	4 hai
TC79353	Dehydration-responsive protein (RD22)	2.533*	0.264	XIIB	4 hai
TC87759	UVB-resistance protein-like	0.880*	−0.174	XIIB	4 hai
TC80479	Heat shock protein 17.7	0.801*	−1.538	XIIB	4 hai

Table 1 (continued)

MtGI[a]	Description	Fold change (F)[b]		FC[c]	Time[d]
		F4	F12		
TC85566	18.2 kDa class I heat shock protein	−0.904*	−0.758	XIIB	4 hai
TC76880	Endoxyloglucan transferase	−0,008	1,883*	I	12 hai
BF51916	Nodulin~geneid K10D20.11	0,622	1,095*	I	12 hai
TC86491	Expansin	−0,541	0,876*	I	12 hai
TC76965(2)**	Nodulin MtN19	−0,071	−1,966*	I	12 hai
TC89193	Nodulin MtN3	0,260	−1,064*	I	12 hai
TC85537	Myo-inositol-1-phosphate synthase	0,274	−1,066*	I	12 hai
TC85538	Myo-inositol-1-phosphate synthase	0,535	−0,966*	I	12 hai
TC76675	Tubulin alpha-1 chain.	−0.525	0.891*	II	12 hai
TC79734	Putative oligopeptide transporter protein	−0.617	1.433*	III	12 hai
TC88949	NADH dehydrogenase subunit 2	−0.662	1.257*	V	12 hai
TC86005	Probable cytochrome oxidase subunit (cbb3-type)	−0.222	0.830*	V	12 hai
TC85436	Asparagine synthetase	0.090	−1.359*	V	12 hai
TC89059	Cysteine methyltransferase	0.784	−0.883*	V	12 hai
TC78048	Gibberellin-regulated protein GASA4	0.185	0.960*	VI	12 hai
TC77029	Putative ripening-related protein	n.v.***	−1,302*	VI	12 hai
TC82902	Short chain alcohol dehydrogenase-like	0.429	−1.251*	VI	12 hai
TC85609	Cytochrome P450	−0.415	−2.122*	VI	12 hai
TC87678	Mucin-like protein	0.385	−1.070*	VI	12 hai
TC88255	DNA-damage-repair/toleration protein DRT100 precursor	0.661	1.588*	VII	12 hai
TC88569	WRKY transcription factor 6	0.018	0.926*	VIII	12 hai
TC89017	Probable B-box zinc finger protein	−0.115	0.835*	VIII	12 hai
TC88609	NAC domain protein NAC2	0.454	−0.852*	VIII	12 hai
TC91372	Legumin A precursor	−1.923	3.907*	XII	12 hai
TC76542	Cold acclimation responsive protein BudCAR5	−0.707	1.519*	XIIB	12 hai
TC77131	Early nodulin 12A	2,589*	0,861*	I	Common
TC92730	Nodulin MtN3	1,717*	−2,524*	I	Common
BG45222	Pathogenesis-related protein 4A (PRP4A)	2.311*	−0.839*	XIIA	Common
TC77149	Thaumatin (MDTL1)	1.979*	−1.670*	XIIA	Common

Regulated genes ($0.8 \leq F \leq -0.8$, $p \leq 0.05$) at 4 and 12 h after inoculation (hai), as well as both time points (common), are listed and sorted by functional categories (FC)

[a] MtGI, identifier in the TIGR *M. truncatula* Gene index (MtGI 7)

[b] Fold change (F), $\log_2$ expression ratio SA1306/Parabinga, at 4 (F4) and 12 (F12) h after inoculation

[c] Functional categories (FC) as defined Journet et al. (Journet et al. 2002)

[d] Time point when gene were regulated ($0.8 \leq F \leq -0.8$, $p \leq 0.05$)

*Genes that showed at least 0.8 *F* value at significance level of 0.05 for LIMMA and Student's *t* tests, respectively (both included FDR correction). Additional information is given in Table S3

**The sequences TC76965 and TC76965(2) correspond to the *M. truncatula* 70-mer oligonucleotides probe identifiers (ID) MT015318 and MT015656, respectively. Additional information of sequences is given in Table S4

n.v. no values were compiled

hydrolysis of polysaccharides of cell wall releasing oligogalacturonides which play a critical function as elicitor molecules in the pathogen-associated molecular pattern (PAMP) perception (Fig. 2). Thus, several sequences that encode transmembrane pattern recognition receptors (PRRs) that are capable to perceive PAMPs, such as PRP4A, pathogenesis-related protein (pprg2), and endochitinase precursor, were also detected as upregulated in SA1306 (Table 1).

In addition, a sequence encoding a "receptor-protein kinase (FERONIA)" was upregulated in SA1306 as well as in Parabinga (around 1.5-fold) in response to *E. pisi* infection (Table 2, Fig. 2). This receptor is activated by cell wall

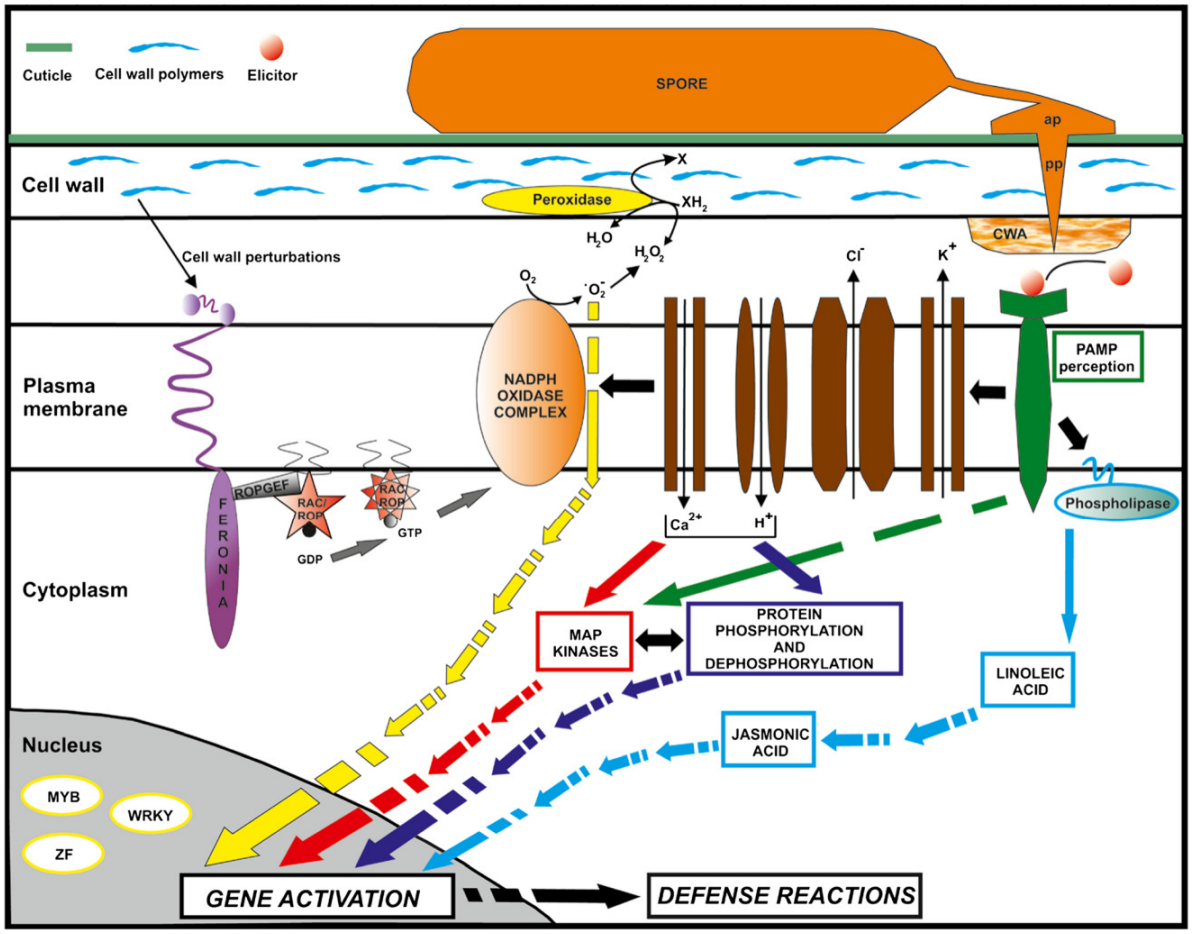

Fig. 2 Diagram of resistance mechanisms. *E. pisi* spore try to penetrate the cuticle and the cell wall, by means of appressorium (ap) and penetration peg (pp) formation. The signal-transduction chain from PAMP perception to gene activation starts by the recognition of the elicitor by its receptor (*green arrows*). The elicitor binding stimulates transient ion fluxes, K^+, Cl^-, H^+ and Ca^{2+}, as well as the activation of MAP kinases. Influxes of H^+ and Ca^{2+} are a prerequisite for the activation of MAP kinases (*red arrows*) and the NADPH oxidase, which together with peroxidase catalyze the ROIs that act as second messengers in gene activation (*yellow arrows*). Protein phosphorylation/dephosphorylation processes (*violet arrows*) are regulated by MAP kinases and H^+ and Ca^{2+} influxes. The elicitor recognition stimulates also the generation of jasmonic acid by phospholipase (*blue arrows*). In addition, the FERONIA receptor activates RAC/ROPs (*gray arrows*) which activate the NADPH oxidase to stimulate ROIs production (*yellow arrows*). *CWA*, cell wall appositions; *GDP*, guanidine diphosphate; *GTP*, guanidine triphosphate; *MAP*, mitogen-activated protein; *RAC/ROP*, RAC- and Rho-related GTPases; *ROIs*, reactive oxygen intermediates. Modified from (Odjakova and Hadjiivanova 2001)

perturbations stimulating the RAC/ROPs complex that acts on NADPH oxidase playing an important role in the production of reactive oxygen intermediates (ROIs) (Fig. 2). In fact, several enzymes involved in oxidative burst, such as "peroxidase," were also detected as upregulated (Table 1, Fig. 2). These produced ROIs play a critical role as second messengers for gene activation (Fig. 2). Moreover, two sequences encoding "lectin-related polypeptide" and "lipid transfer protein SDi-9 drought-induced," involved in plant defense, were also expressed more in the resistant SA1306 genotype than in Parabinga (Table 1).

Furthermore, some sequences encoding transcription factor (TF) families involved in the transcriptional reprogramming associated with the plant immune response, such as "WRKY transcription factor 6," "probable B-box zinc finger protein," and "MYB-related transcription factor VlMYBB1-1" were also upregulated in SA1306 (Table 1, Fig. 2). Moreover, some sequences encoding proteins involved in detoxification mechanisms, such as glutathione S-transferase, "putative oligopeptide transporter protein," and "ATP binding cassette (ABC) transporter," were also expressed more in SA1306 than in Parabinga (Table 1). Furthermore, other genes encoding

Table 2 Expression ratios of ten genes used in the verification experiments

Gene name	Expression ratios					
	4 hai			12 hai		
	M^a		F^b (Mic/qPCR)[c]	M^a		F^b (Mic/qPCR)[c]
	PB (Mic/qPCR)[c]	SA (Mic/qPCR)[c]		PB (Mic/qPCR)[c]	SA (Mic/qPCR)[c]	
Lectin-related polypeptide	−1.95/−2.63	1.53/3.90	3.48/6.53	−0.14/−1.63	−0.31/−0.48	−0.17/1.15
UL26.5 gene	−1.21/−2.34	2.09/3.78	3.30/6.12	1.18/2.16	1.14/3.26	−0.03/1.10
Thaumatin (MDTL1)	0.23/1.06	2.21/5.60	1.98/4.54	0.69/0.31	−0.98/−1.82	−1.67/−2.13
Pathogenesis-related protein 4 (PRP4A)	0.38/0.64	2.22/4.28	1.84/3.64	0.04/0.51	−1.05/−1.98	−1.09/−2.49
Dehydration-responsive protein (RD22)	−0.59/−1.03	1.94/3.06	2.53/4.09	−0.08/0.63	0.19/0.20	0.26/−0.43
Disease resistance response protein 39	1.44/3.13	−4.18/−8.11	−5.63/−11.24	−0.66/−0.5	1.58/5.47	2.23/5.97
Endoxyloglucan transferase	−0.22/−0.43	−0.23/−0.12	−0.01/0.31	0.24/0.74	2.12/3.33	1.88/2.59
Ripening regulated protein (DDTFR18)	1.49/3.22	0.54/0.16	−0.95/−3.06	−0.38/−0.85	n.c./ −0.31	n.c./0.54
Receptor-protein kinase (FERONIA)	1.63/3.49	1.36/1.57	−0.27/−1.92	1.64/2.93	1.18/1.67	−0.45/−1.26
Pathogenesis related-protein (pprg2)	1.45/2.92	1.08/1.91	−0.37/−1.01	0.60/1.83	0.10/0.72	−0.51/−1.11

Relative gene expression ratios (*M*) and their fold change expression ratios (*F*), SA1306 (SA) compared to Parabinga (PB), at 4 and 12 h after *E. pisi* inoculation obtained by microarray (Mic), and qPCR experiments are showed

hai hour after *E. Pisi* inoculation

[a] Relative gene expression ratio (*M*), $\log_2$ expression ratios inoculated/control, at 4 and 12 h after *E. Pisi* inoculation

[b] Fold change expression ratio (*F*), $\log_2$ expression ratio SA1306/Parabinga, at 4 and 12 h after *E. Pisi* inoculation

[c] Date obtained by Mt16kOLI1 microarray experiments (Mic) and real-time quantitative polymerase chain reaction experiments (qPCR)

nc non-calculated values

"cytochrome P450," "chalcone reductase," "chalcone synthase," and "dihydroflavonol 4-reductase-like," and "probable glucosyl transferase" involved in medicarpin biosynthesis and phenylpropanoid metabolism were also upregulated in SA1306. In addition, some genes involved in abiotic stresses such as "dehydration-responsive protein RD22," "UVB-resistance protein-like," "cold acclimation responsive protein BudCAR5," and "heat shock protein 17.7" were also upregulated in SA1306 (Table 1).

These results prompt that a higher expression of genes involved in defense mechanism, mainly belonging to PAMP perception and oxidative burst processes, trigger downstream responses mediated by MAP kinase signaling and protein phosphorylation and dephosphorylation processes that mediate gene activation and defense responses (Fig. 2).

Selection of Reference Genes and qPCR Validation of Microarray Results

Three reference genes were tested by real-time qPCR as reference genes in order to determine which of them were best suited, among the genotypes and time points assayed, for transcript normalization. All reference genes showed a high average expression stability ($M<0.35$); among them, the *MtPdf2* and *MtUbi* genes showed the lowest average expression stability (*M*) indicating a greatest transcript stability (Fig. 3). In addition, the pairwise variation (*V*) was 0.1049 when comparing a normalization factor based on the two or three stable targets, which indicates that the optimal number of reference genes in this experiment situation is two. Therefore, the two reference genes that showed most transcript stability, *MtUbi* and *MtPdf2*, were used for transcript normalization of the ten genes evaluated by qPCR in the microarray validation assay.

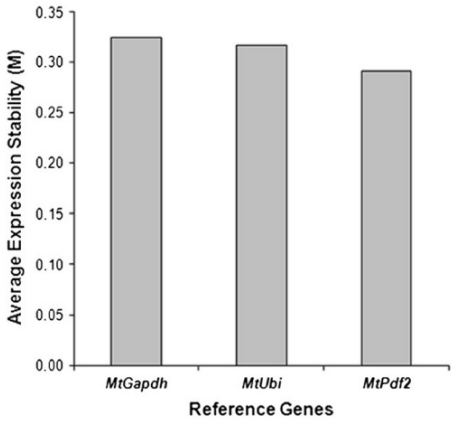

Fig. 3 Selection of reference genes used for transcript normalization. Transcript levels of three reference genes were analyzed by qPCR among the genotypes and time points assayed. The average expression stability (*M*) was calculated by geNorm software

Ten genes were selected to confirm the microarray experiments carried out among the genotypes and assayed time points. The normalized expression values obtained by qPCR showed the same trend as those obtained by microarray studies (Table 2, Table S2). The sequence encoding a lectin-related polypeptide (TC85729) was around 4-fold more expressed in SA1306 than in Parabinga, at 4 h after *E. pisi* inoculation. However, the sequence showed almost no regulation in SA1306 at 12 h after *E. pisi* infection. Therefore, SA1306 shows a higher level of expression of this gene than Parabinga after inoculation. A similar case was detected in the gene *UL26.5* (TC77132), which was also expressed more in SA1306 than in Parabinga at 4 h after infection, mainly due to a constitutive higher expression in SA1306.

The "thaumatin (MDTL1)" protein encoded by the sequence (TC77149) was also induced greater in SA1306 than in Parabinga in response to *E. pisi* infection at 4 h after *E. pisi* inoculation, which was due to the higher expression level in SA1306. However, this gene was downregulated in SA1306 at 12 h. Consequently, this sequence was upregulated and repressed in SA1306 compared to Parabinga at 4 and 12 h after pathogen inoculation, respectively. In contrast, in Parabinga, this sequence showed almost no regulation at both assayed time points. A similar expression profile was detected in the PRP4A sequence (TC87236), which showed a higher expression level in SA1306 than in Parabinga at 4 h after *E. pisi* infection. Meanwhile, the sequence was downregulated in SA1306 at 12 h. The expression of this sequence was also almost not regulated in Parabinga at both evaluated time points.

The sequence encoding the dehydration-responsive protein (RD22) (TC79353) was expressed more in SA1306 than in Parabinga at 4 h after infection; meanwhile, it was almost not regulated in Parabinga. Hence, SA1306 showed a higher level of expression of this gene than that of Parabinga after inoculation. Moreover, the gene *DRR230-b* encoding the "disease resistance response protein 39 (DRR230-b)" (TC82368) was expressed more in SA1306 than in Parabinga at 12 h after *E. pisi* inoculation but less expressed at 4 h.

The protein endoxyloglucan transferase, encoded by the sequence (TC76880), was detected around two times more in SA1306 than in Parabinga at 12 h after *E. pisi* inoculation and almost not regulated at 4 h after inoculation. Therefore, SA1306 showed a higher level of expression of this gene than Parabinga after inoculation. On the other hand, the "ripening-regulated protein (DDTFR18)" (TC92066) was almost not regulated in SA1306; in contrast, Parabinga showed a high expression of this sequence at 4 h after inoculation. Consequently, this sequence was expressed less in SA1306 than in Parabinga after *E. pisi* inoculation.

The sequence encoding the receptor-protein kinase (FERONIA) (TC91527) was upregulated (around 1.5-fold) in both genotypes in response to *E. pisi* infection at both assayed time points. Hence, this gene had a higher expression level in both genotypes in response to *E. pisi* inoculation. A similar case was the sequence encoding the pathogenesis-related protein (pprg2) (TC76638), with similar expression levels in both genotypes, although slightly less in SA1306 than in Parabinga.

Pairwise Pearson correlation coefficients calculated indicated a highly degree of concordance between qPCR and microarray techniques (Table S3). Therefore, the results obtained from qPCR support those from the microarray-based expression profiles. However, as we expected from previous publications (Demidenko et al. 2011; Morey et al. 2006), the values observed in qPCR in general were slightly higher than those obtained from microarray results.

Discussion

Resistance to powdery mildew in *M. truncatula* is carried out at different fungal developmental stages (Prats et al. 2007). Some approaches have found that the powdery mildew resistance is a complex trait, which is performed by a wide variety of genes that act additively providing resistance (Eichmann and Hückelhoven 2008; Foster-Hartnett et al. 2007; Hückelhoven 2005; Yang et al. 2013). These approaches have given some insight into defense responses induced after *E. pisi* infection, which showed a strong upregulation of pathogenesis-related genes (PR10, PR4A) and other defense genes belonging to phenylpropanoid pathway, signal transduction, senescence, cell wall metabolism, and abiotic stress as well as to hypersensitive response. In spite of these studies carried out with this pathogen, the molecular mechanisms involved in the plant defense remain undiscovered (Hückelhoven 2005; Panstruga and Spanu 2014; Spanu and Panstruga 2012; Yaege and Stuteville 2002). Our study provides deep and comprehensive information of the metabolic pathways involved in a new *E. pisi*/*M. truncatula* pathosystem, which will help to develop new genetic tools in the breeding program of this legume.

The histological assessments confirmed the resistance and susceptibility to *E. pisi* in Parabinga and SA1306, respectively. Several mechanisms capable of monitoring changes in the cell wall are carried out by cellular signaling responses (Cheung and Wu 2011; Ringli 2010). Hence, it is generally accepted that the plant cell wall functions as a continuum whereby encounters at the exoskeleton are transmitted to the cytoplasm whose responses affect cellular activities as well as their extracellular properties (Ringli 2010). Several genes involved in cell wall metabolism were expressed more in SA1306 than in Parabinga, such as endoxyloglucan transferase and expansin, which are involved in cell wall elongation. Also, some sequences encoding early nodulin 12A, a putative

proline-rich cell wall protein (Govers et al. 1991) involved in cell wall strengthening, were upregulated. This cell wall reinforcement may play an important role in the development of physical barriers hampering the expansion of *E. pisi* in SA1306. In addition, enzymes related to cell wall remodeling such as cell wall hydrolases glucan endo-1,3-beta-D-glucosidase, 1,3-beta-glucanase, and pectinase (*At3g62110*) were also upregulated. These proteins take part in the hydrolysis of polysaccharides of plant cell walls releasing oligogalacturonides that act as elicitor molecules in the defense reaction (Etzler 1998).

Additionally to cell wall hydrolases, a sequence (TC91527) encoding a receptor-protein kinase (FERONIA) was detected as upregulated in both genotypes in response to *E. pisi* infection. Some studies have evidenced that FERONIA is involved in the resistance to the fungal pathogen powdery mildew, suppressing hyphal growth (Cheung and Wu 2011; Kessler et al. 2010). Hence, cell wall integrity sensing has been suggested to be one of the mechanisms to detect pathogen attack (Hématy et al. 2009). In relation to the ROIs, some enzymes involved in the production of hydrogen peroxide (H_2O_2), such as "peroxidases" were also expressed more in SA1306 than in Parabinga. H_2O_2 plays an important role in the ROI stress (Passardi et al. 2005), which is required for the cross-linking of hydroxyproline and lignification processes in the cell wall (Brady and Fry 1997; Brisson et al. 1994) as well as for signaling (Lamb and Dixon 1997). This accumulation of ROIs is associated with the hypersensitive response that could play a role in SA1306 resistance to *E. pisi* (Torres et al. 2005).

The pathogen recognition is a critical defensive responsive of plants against infection by invading pathogens. Several sequences involved in this recognition process, such as pathogenesis-related (PR) proteins, PRP4A, pathogenesis-related protein (pprg2), and endochitinase precursor, were upregulated in SA1306 in response to *E. pisi* infection. Two sequences encoding a PRP4A, which have been described to contain a hevein domain that is capable of binding chitin (Bravo et al. 2003), were upregulated in SA1306. Also, pathogenesis-related protein (pprg2) which has been clearly involved in *M. truncatula* response to *E. pisi* infection (Samac et al. 2011) was detected as more expressed in SA1306 compared to Parabinga. The endochitinase precursor also named as PR-3, which is an antifungal protein that catalyzes chitin degradation by cleaving the internal bonds of the β-1,4-glycoside present in chitin, were also upregulated in SA1306 (Ferreira et al. 2007). In relation to pathogen recognition process, phytohormones regulate PAMP-triggered immunity (Koornneef and Pieterse 2008). In our study, two sequences encoding proteins involved in plant steroid metabolism, "putative steroid membrane binding protein" and "BZR1 protein," were found to be upregulated after *E. pisi* infection. Several genetic studies have suggested that steroid hormones may act as ligand for plant leucine-rich repeat receptor kinases (LRR-RLKs) (Yin et al. 2002), which have been characterized to mediate extracellular signals for disease resistance in plants (He et al. 2000; Song et al. 1995). Additionally, BZR1 protein is a nuclear component of the brassinosteroid signal transduction pathway. In the plant, brassinosteroids are perceived by a plasma membrane-localized receptor kinase. Thus, BZR1 is a positive regulator of the brassinosteroid signaling pathway (Wang et al. 2002). Thus, our data revealed that the plant steroids can play an important role in the defense mechanism of *M. truncatula* against *E. pisi* infection.

Transcription factors are integral to the signaling of the plant defense responses (Grant and Mansfield 1999; Libault et al. 2009). Our results reveal several regulated genes involved in signal transduction pathways, such as some transcription factor (TF) families including WRKY, zinc finger (ZF) and MYB TFs, which are involved in phytohormone metabolism such as that of jasmonic acid (JA) mediating the transcriptional reprogramming associated with the plant immune response. One sequence encoding a WRKY transcription factor 6 was expressed more in SA1306 than in Parabinga. Several studies have reported that WRKY TFs play a role in the transcriptional reprogramming associated with the plant immune response (Eulgem and Somssich 2007). In addition, the WRKY3 and WRKY6 TFs have been reported to increase the levels of jasmonic acid (JA) and JA-isoleucine (Rushton et al. 2010) as well as being a common component in salicylic acid (SA) and JA-mediated signaling pathways (Li et al. 2004). Also, two sequences encoding zinc finger TFs, "zinc finger protein" and probable B-box zinc finger protein, and one encoding a MYB-related transcription factor VlMYBB1-1 were upregulated in SA1306. Zinc finger and MYB TFs have been described to mediate defense responses in plants (Epple et al. 2003; Jin and Martin 1999; Takatsuji 1998). Thus, our results reinforce the previous studies suggesting the important role of these proteins in resistance to *E. pisi* in *M. truncatula*.

In addition, several sequences encoding enzymes involved in phenylpropanoid metabolism, such as cytochrome P450, chalcone reductase, chalcone synthase and dihydroflavonol 4-reductase-like, were expressed more in the resistant genotype SA1306 than in the susceptible Parabinga. Cytochrome P450 protein has been described to be involved in medicarpin biosynthesis, one of the major antimicrobial phytoalexin in the forage legume alfalfa (*Medicago sativa L.*) (Kessmann et al. 1990). Chalcone reductase co-acts with chalcone synthase enzyme and uses the same substrates, p-coumaroyl-CoA and malonyl-CoA (Joung et al. 2003), which may link this chalcone reductase to flavonoid biosynthesis. Moreover, dihydroflavonol-4-reductase is the key enzyme for the conversion of dihydroflavonols to flavan-3,3-diols (leucoanthocyanidins), as well as for their stereospecific reduction (the precursors of anthocyanins and

proanthocyanidins) in the flavonoid biosynthetic pathway (Holton and Cornish 1995). Also, a sequence encoding a probable glucosyl transferase, which acts conjugating glucose to other plant compounds, was also upregulated in SA1306. In addition, UDP-glucuronosyltransferases (UGTs) play an important role by regulating the levels of signaling compounds such as SA by converting active molecules into inactive conjugated forms (Hennig et al. 1993). Hence, these proteins may play an important task in developing *M. truncatula* defense mechanisms against *E. pisi*.

Detoxification processes also play an important role against pathogen. Thus, several enzymes involved in these detoxification processes, such as glutathione S-transferase, putative oligopeptide transporter protein and ABC transporter, were induced in SA1306 after *E. pisi* infection. Thus, two sequences encoding a glutathione S-transferase were expressed more in SA1306 than in Parabinga. This enzyme plays a role in several metabolic processes involved in the detoxification of a wide variety of toxic compounds in plants (Dixon et al. 2002). In addition, one sequence encoding a putative oligopeptide transporter protein (OPT) was also upregulated in SA1306 genotype. The OPT transporter has been described to be able to transport glutathione or conjugates in higher plants (Stacey et al. 2002; Tsay et al. 2007), which could co-acts with the glutathione S-transferase. Also, one gene encoding an ABC transporter was found to be more expressed in SA1306 than in Parabinga. ABC transporters are found in a wide range of organisms from all kingdoms of life, which transport a diverse array of molecules, including ions, nutrients, secondary metabolites, and lipids across various cellular membranes. Some of them have been described to play roles in defense against plant pathogens, such as the PDR subfamily, and in transport of xenobiotics (Zhang et al. 2010).

In addition to genes previously reported, other genes involved in defense responses were also regulated in *M. truncatula* genotypes analyzed after *E. pisi* infection. Thus, one sequence encoding a lectin-related polypeptide was also upregulated in the resistant genotype SA1306. Several lectins have been characterized in *M. truncatula*; among them, LecRKs have been considered to play a role in defense as part of an innate immunity response, i.e. agglutinating receptor molecules to enhance the response to external stimuli and to amplify the signal from the receptor (De Hoff et al. 2009). Another gene encoding a lipid transfer protein SDi-9 drought-induced was also upregulated in SA1306. Lipid transfer protein have been identified in several defense responses including cutin biosynthesis, surface wax formation, and plant defense and adaptation of the plant to environmental changes (Kader 1996). Also, some genes involved in abiotic stresses were also upregulated higher in SA1306 than in Parabinga, such as heat shock protein 17.7. Noteworthy, previous studies have described that the heat stress-induced resistance against powdery mildew infection, due to the production of both superoxide anions and hydrogen peroxide, triggered wide defense reactions including increased activities of peroxidase phenoloxidase, polyphenoloxidase, β-1,3-glucanase, chitinase as well as the accumulation of phenolic compounds, insoluble extension, and ethylene production (Schweizer et al. 1995). In addition, ROS provide a crucial link in the cross talk of different responses suggesting that plant cells sense ROS via heat shock transcription factors which, in turn, activate heat shock proteins (HSPs) expression (Timperio et al. 2008).

On the other hand, some sequences encoding proteins that are involved in primary metabolism, such as photosynthesis "light-harvesting chlorophyll-a/b binding protein LhcII-1.3" and energy metabolism "NADH dehydrogenase subunit 2" and "probable cytochrome oxidase subunit (cbb3-type)," were also differently regulated in SA1306 and Parabinga. The overexpression of these energetic pathways may help to recover the energetic drain involved in the widespread defense mechanism performed earlier. Some plant research studies have concluded that resistance can be costly and that the energetic metabolism is the key to the plant fitness (Purrington 2000).

The microarray results suggest that resistance to *E. pisi* in SA1306 is due to a higher expression of genes involved in several defense pathways. Thus, this study reveals that several pathogenesis-related proteins, such as PRP4A, pathogenesis-related protein (pprg2), peroxidases and enzymes belonging to phenylpropanoid metabolism as well as several proteins involved in signaling pathways controlled by JA and SA acids play an important role in the development of defense responses of *Medicago* to *E. pisi*.

Conclusions

Our study provides a global picture of the genes regulated during resistance to *E. pisi*, on the grounds of statistical significance of differential gene expression profiles. These results provide new comprehensive data concerning the mechanisms involved in *E. pisi* resistance in *M. truncatula*. A wide variety of mechanisms and pathways were detected to be regulated in *M. truncatula* in response to *E. pisi* infection, which mainly included cell wall reinforcement, phenylpropanoids and phytoalexins biosynthesis, pathogenesis-related proteins, burst oxidative-related proteins, and signaling pathways controlled by jasmonic and salicylic acids. The genes identified in this work are a usefully tool to perform reverse genetic studies. Mechanisms and pathways identified in this study will aid in developing new breeding programs in legumes.

Acknowledgments This work was supported by the Grain Legumes Integrated Project (FP6-2002-FOOD-1-506223) and Spanish project AGL2011-22524. M. Curto was funded by Spanish Research Training programme (FPI). Drs. E. Prats and S. Fondevilla are thanked for

providing help with microscopy assessments. We are grateful to Carolina Johnstone for grammatical review. Special thanks to Bielefeld University Center for Biotechnology for providing microarray platform, hybridization facilities, and bioinformatics support.

References

Ameline-Torregrosa C, Dumas B, Krajinski F, Esquerre-Tugaye M-T, Jacquet C (2006) Transcriptomic approaches to unravel plant–pathogen interactions in legumes. Euphytica 147:25–36

Ameline-Torregrosa C, Cazaux M, Danesh D, Chardon F, Cannon SB, Esquerré-Tugayé M-T, Dumas B, Young ND, Samac DA, Huguet T, Jacquet C (2008) Genetic dissection of resistance to anthracnose and powdery mildew in *Medicago truncatula*. Mol Plant-Microbe Interact 21:61–69

Barilli E, Rubiales D, Gjetting T, Lyngkjaer MF (2014) Differential gene transcript accumulation in peas in response to powdery mildew (*Erysiphe pisi*) attack. Euphytica 195:1–16

Bélanger RR, Bushnell WR, Aleid JD, Carver TLW (2002) The powdery mildews: a comprehensive treatise. APS Press, St Paul

Brady JD, Fry SC (1997) Formation of di-isodityrosine and loss of isodityrosine in the cell walls of tomato cell-suspension cultures treated with fungal elicitors or H_2O_2. Plant Physiol 115:87–92

Bravo JM, Campo S, Murillo I, Coca M, San Segundo B (2003) Fungus- and wound-induced accumulation of mRNA containing a class II chitinase of the pathogenesis-related protein 4 (PR-4) family of maize. Plant Mol Biol 52:745–759

Brisson LF, Tenhaken R, Lamb C (1994) Function of oxidative cross-linking of cell wall structural proteins in plant disease resistance. Plant Cell 6:1703–1712

Bustin SA, Benes V, Garson JA, Hellemans J, Huggett J, Kubista M, Mueller R, Nolan T, Pfaffl MW, Shipley GL, Vandesompele J, Wittwer CT (2009) The MIQE guidelines: minimum information for publication of quantitative real-time PCR experiments. Clin Chem 55:611–622

Cheung AY, Wu H-M (2011) THESEUS 1, FERONIA and relatives: a family of cell wall-sensing receptor kinases? Curr Opin Plant Biol 14:632–641

Cook DR (1999) *Medicago truncatula*—a model in the making! Curr Opin Plant Biol 2:301–304

De Hoff P, Brill L, Hirsch A (2009) Plant lectins: the ties that bind in root symbiosis and plant defense. Mol Genet Genomics 282:1–15

Demidenko NV, Logacheva MD, Penin AA (2011) Selection and validation of reference genes for quantitative real-time PCR in buckwheat (*Fagopyrum esculentum*) based on transcriptome sequence data. PLoS One 6:e19434

Dita MA, Die JV, Román B, Krajinski F, Küster H, Moreno MT, Cubero JI, Rubiales D (2009) Gene expression profiling of *Medicago truncatula* roots in response to the parasitic plant *Orobanche crenata*. Weed Res 49:66–80

Dixon D, Lapthorn A, Edwards R (2002) Plant glutathione transferases. Genome Biol 3:3004.1–3004.10

Dondrup M, Goesmann A, Bartels D, Kalinowski J, Krause L, Linke B, Rupp O, Sczyrba A, Puhler A, Meyer F (2003) EMMA: a platform for consistent storage and efficient analysis of microarray data. J Biotechnol 106:135–146

Eichmann R, Hückelhoven R (2008) Accommodation of powdery mildew fungi in intact plant cells. J Plant Physiol 165:5–18

Epple P, Mack AA, Morris VRF, Dangl JL (2003) Antagonistic control of oxidative stress-induced cell death in *Arabidopsis* by two related, plant-specific zinc finger proteins. Proc Natl Acad Sci U S A 100:6831–6836

Etzler ME (1998) Oligosaccharide signaling of plant cells. J Cell Biochem Suppl 72:123–128

Eulgem T, Somssich IE (2007) Networks of WRKY transcription factors in defense signaling. Curr Opin Plant Biol 10:366–371

Falloon RE, Viljanen-Rollinson SLH (2001) Powdery mildew. Compendium of pea diseases and pests. APS Press, St. Paul

Fernández-Aparicio M, Pérez-de-Luque A, Prats E, Rubiales D (2008) Variability of interactions between barrel medic (*Medicago truncatula*) genotypes and *Orobanche* species. Ann Appl Biol 153:117–126

Ferreira RB, Monteiro S, Freitas R, Santos CN, Chen Z, Batista LM, Duarte J, Borges A, Teixeira AR (2007) The role of plant defence proteins in fungal pathogenesis. Mol Plant Pathol 8:677–700

Fondevilla S, Rubiales D (2012) Powdery mildew control in pea. A review. Agron Sustain Dev 32:401–409

Fondevilla S, Torres AM, Moreno MT, Rubiales D (2007) Identification of a new gene for resistance to powdery mildew in *Pisum fulvum*, a wild relative of pea. Breed Sci 57:181–184

Fondevilla S, Rubiales D, Moreno M, Torres A (2008) Identification and validation of RAPD and SCAR markers linked to the gene *Er3* conferring resistance to *Erysiphe pisi* DC in pea. Mol Breed 22:193–200

Fondevilla S, Küster H, Krajinski F, Cubero J, Rubiales D (2011) Identification of genes differentially expressed in a resistant reaction to *Mycosphaerella pinodes* in pea using microarray technology. BMC Genomics 12:28

Foster-Hartnett D, Danesh D, Peñuela S, Sharopova N, Endre G, Vandenbosch KA, Young ND, Samac DA (2007) Molecular and cytological responses of *Medicago truncatula* to *Erysiphe pisi*. Mol Plant Pathol 8:307–319

Franken P, Gnädinger F (1994) Analysis of parsley arbuscular endomycorrhiza: infection development and mRNA levels of defense related genes. Mol Plant-Microbe Interact 7:612–620

Govers F, Harmsen H, Heidstra R, Michielsen P, Prins M, Kammen A, Bisseling T (1991) Characterization of the pea ENOD12B gene and expression analyses of the two ENOD12 genes in nodule, stem and flower tissue. Mol Gen Genet 228:160–166

Grant M, Mansfield J (1999) Early events in host-pathogen interactions. Curr Opin Plant Biol 2:312–319

He Z, Wang Z-Y, Li J, Zhu Q, Lamb C, Ronald P, Chory J (2000) Perception of brassinosteroids by the extracellular domain of the receptor kinase BRI1. Science 288:2360–2363

Hellemans J, Mortier G, De Paepe A, Speleman F, Vandesompele J (2007) qBase relative quantification framework and software for management and automated analysis of real-time quantitative PCR data. Genome Biol 8:R19

Hématy K, Cherk C, Somerville S (2009) Host–pathogen warfare at the plant cell wall. Curr Opin Plant Biol 12:406–413

Hennig J, Malamy J, Grynkiewicz G, Indulski J, Klessig DF (1993) Interconversion of the salicylic acid signal and its glucoside in tobacco. Plant J 4:593–600

Hoagland DR, Arnon DI (1950) The water-culture method of growing plants without soil. Calif Agric Exp Station Circ 347:1–32

Hohnjec N, Vieweg MF, Puhler A, Becker A, Küster H (2005) Overlaps in the transcriptional profiles of *Medicago truncatula* roots inoculated with two different *Glomus* fungi provide insights into the genetic program activated during arbuscular mycorrhiza. Plant Physiol 137:1283–1301

Holton TA, Cornish EC (1995) Genetics and biochemistry of anthocyanin biosynthesis. Plant Cell 7:1071–1083

Hougaard BK, Madsen LH, Sandal N, de Carvalho Moretzsohn M, Fredslund J, Schauser L, Nielsen AM, Rohde T, Sato S, Tabata S, Bertioli DJ, Stougaard J (2008) Legume anchor markers link syntenic regions between *Phaseolus vulgaris*, *Lotus japonicus*, *Medicago truncatula* and *Arachis*. Genetics 179:2299–2312

Hückelhoven R (2005) Powdery mildew susceptibility and biotrophic infection strategies. FEMS Microbiol Lett 245:9–17

Jin H, Martin C (1999) Multifunctionality and diversity within the plant *MYB*-gene family. Plant Mol Biol 41:577–585

Joung J-Y, Mangai Kasthuri G, Park J-Y, Kang W-J, Kim H-S, Yoon B-S, Joung H, Jeon J-H (2003) An overexpression of chalcone reductase of *Pueraria montana* var. *lobata* alters biosynthesis of anthocyanin and 5′-deoxyflavonoids in transgenic tobacco. Biochem Biophys Res Commun 303:326–331

Journet EP, van Tuinen D, Gouzy J, Crespeau H, Carreau V, Farmer MJ, Niebel A, Schiex T, Jaillon O, Chatagnier O, Godiard L, Micheli F, Kahn D, Gianinazzi-Pearson V, Gamas P (2002) Exploring root symbiotic programs in the model legume *Medicago truncatula* using EST analysis. Nucleic Acids Res 30:5579–5592

Kader J-C (1996) Lipid-transfer proteins in plants. Annu Rev Plant Physiol Plant Mol Biol 47:627–654

Kakar K, Wandrey M, Czechowski T, Gaertner T, Scheible WR, Stitt M, Torres-Jerez I, Xiao YL, Redman JC, Wu HC, Cheung F, Town CD, Udvardi MK (2008) A community resource for high-throughput quantitative RT-PCR analysis of transcription factor gene expression in *Medicago truncatula*. Plant Methods 4:18

Kessler SA, Shimosato-Asano H, Keinath NF, Wuest SE, Ingram G, Panstruga R, Grossniklaus U (2010) Conserved molecular components for pollen tube reception and fungal invasion. Science 330: 968–971

Kessmann H, Choudhary AD, Dixon RA (1990) Stress responses in alfalfa (*Medicago sativa* L.) III. Induction of medicarpin and cytochrome P450 enzyme activities in elicitor-treated cell suspension cultures and protoplasts. Plant Cell Rep 9:38–41

Koornneef A, Pieterse CMJ (2008) Cross talk in defense signaling. Plant Physiol 146:839–844

Küster H, Hohnjec N, Krajinski F, El Yahyaoui F, Manthey K, Gouzy J, Dondrup M, Meyer F, Kalinowski J, Brechenmacher L, van Tuinen D, Gianinazzi-Pearson V, Pühler A, Gamas P, Becker A (2004) Construction and validation of cDNA-based Mt6k-RIT macro- and microarrays to explore root endosymbioses in the model legume *Medicago truncatula*. J Biotechnol 108:95–113

Küster H, Becker A, Firnhaber C, Hohnjec N, Manthey K, Perlick AM, Bekel T, Dondrup M, Henckel K, Goesmann A, Meyer F, Wipf D, Requena N, Hildebrandt U, Hampp R, Nehls U, Krajinski F, Franken P, Pühler A (2007) Development of bioinformatic tools to support EST-sequencing, in silico- and microarray-based transcriptome profiling in mycorrhizal symbioses. Phytochemistry 68:19–32

Lamb C, Dixon RA (1997) The oxidative burst in plant disease resistance. Annu Rev Plant Physiol Plant Mol Biol 48:251–275

Li J, Brader G, Palva ET (2004) The WRKY70 transcription factor: a node of convergence for jasmonate-mediated and salicylate-mediated signals in plant defense. Plant Cell 16:319–331

Libault M, Joshi T, Benedito VA, Xu D, Udvardi MK, Stacey G (2009) Legume transcription factor genes: what makes legumes so special? Plant Physiol 151:991–1001

Livak KJ, Schmittgen TD (2001) Analysis of relative gene expression data using real-time quantitative PCR and the $2^{-\Delta\Delta CT}$ Method. Methods 25:402–408

Morey J, Ryan J, Van Dolah F (2006) Microarray validation: factors influencing correlation between oligonucleotide microarrays and real-time PCR. Biol Proced Online 8:175–193

Nyamsuren O, Firnhaber C, Hohnjec N, Becker A, Küster H, Krajinski F (2007) Suppression of the pathogen-inducible *Medicago truncatula* putative protease-inhibitor *MtTi2* does not influence root infection by *Aphanomyces euteiches* but results in transcriptional changes from wildtype roots. Plant Sci 173:84–95

Odjakova M, Hadjiivanova C (2001) The complexity of pathogen defense in plants. Bulg J Plant Physiol 27:101–109

Panstruga R, Spanu PD (2014) Powdery mildew genomes reloaded. New Phytol 202:13–14

Passardi F, Cosio C, Penel C, Dunand C (2005) Peroxidases have more functions than a swiss army knife. Plant Cell Rep 24:255–265

Prats E, Llamas MJ, Rubiales D (2007) Characterization of resistance mechanisms to *Erysiphe pisi* in *Medicago truncatula*. Phytopathology 97:1049–1053

Purrington CB (2000) Costs of resistance. Curr Opin Plant Biol 3:305–308

Ringli C (2010) Monitoring the outside: cell wall-sensing mechanisms. Plant Physiol 153:1445–1452

Rispail N, Kaló P, Kiss GB, Ellis THN, Gallardo K, Thompson RD, Prats E, Larrainzar E, Ladrera R, González EM, Arrese-Igor C, Ferguson BJ, Gresshoff PM, Rubiales D (2010) Model legumes contribute to faba bean breeding. Field Crops Res 115:253–269

Rose RJ (2008) *Medicago truncatula* as a model for understanding plant interactions with other organisms, plant development and stress biology: past, present and future. Funct Plant Biol 35:253–264

Rubiales D, Carver TL (2000) Defence reactions of *Hordeum chilense* accessions to three formae speciales of cereal powdery mildew fungi. Can J Bot 78:1561–1570

Rubiales D, Castillejo MA, Madrid E, Barilli E, Rispail N (2011) Legume breeding for rust resistance: lessons to learn from the model *Medicago truncatula*. Euphytica 180:89–98

Rushton PJ, Somssich IE, Ringler P, Shen QJ (2010) WRKY transcription factors. Trends Plant Sci 15:247–258

Samac DA, Peñuela S, Schnurr JA, Hunt EN, Foster-Hartnett D, Vandenbosch KA, Gantt JS (2011) Expression of coordinately regulated defence response genes and analysis of their role in disease resistance in *Medicago truncatula*. Mol Plant Pathol 12:786–798

Schulze-Lefert P, Panstruga R (2003) Establishment of biotrophy by parasitic fungi and reprogramming of host cells for disease resistance. Annu Rev Phytopathol 41:641–667

Schweizer P, Vallélian-Bindschedler L, Mösinger E (1995) Heat-induced resistance in barley to the powdery mildew fungus *Erysiphe graminis* f.sp. *hordei*. Physiol Mol Plant Pathol 47:51–66

Sillero JC, Fondevilla S, Davidson J, Patto MCV, Warkentin TD, Thomas J, Rubiales D (2006) Screening techniques and sources of resistance to rusts and mildews in grain legumes. Euphytica 147:255–272

Singh RJ, Chung GH, Nelson RL (2007) Landmark research in legumes. Genome 50:525–537

Smyth GK (2004) Linear models and empirical Bayes methods for assessing differential expression in microarray experiments. Stat Appl Genet Mol Biol 3:1

Song W-Y, Wang G-L, Chen L-L, Kim H-S, Pi L-Y, Holsten T, Gardner J, Wang B, Zhai W-X, Zhu L-H, Fauquet C, Ronald P (1995) A receptor kinase-like protein encoded by the rice disease resistance gene, *Xa21*. Science 270:1804–1806

Spanu PD, Panstruga R (2012) Powdery mildew genomes in the cross-hairs. New Phytol 195:20–22

Stacey G, Koh S, Granger C, Becker JM (2002) Peptide transport in plants. Trends Plant Sci 7:257–263

Takatsuji H (1998) Zinc-finger transcription factors in plants. Cell Mol Life Sci 54:582–596

Timperio AM, Egidi MG, Zolla L (2008) Proteomics applied on plant abiotic stresses: role of heat shock proteins (HSP). J Proteome 71: 391–411

Tivoli B, Baranger A, Sivasithamparam K, Barbetti MJ (2006) Annual *Medicago*: from a model crop challenged by a spectrum of necrotrophic pathogens to a model plant to explore the nature of disease resistance. Ann Bot 98:1117–1128

Torres MA, Jones JDG, Dangl JL (2005) Pathogen-induced, NADPH oxidase-derived reactive oxygen intermediates suppress spread of cell death in *Arabidopsis thaliana*. Nat Genet 37:1130–1134

Tsay Y-F, Chiu C-C, Tsai C-B, Ho C-H, Hsu P-K (2007) Nitrate transporters and peptide transporters. FEBS Lett 581:2290–2300

Uttamchandani M, Neo JL, Ong BNZ, Moochhala S (2009) Applications of microarrays in pathogen detection and biodefence. Trends Biotechnol 27:53–61

Vandesompele J, De Preter K, Pattyn F, Poppe B, Van Roy N, De Paepe A, Speleman F (2002) Accurate normalization of real-time quantitative RT-PCR data by geometric averaging of multiple internal control genes. Genome Biol 3:research0034.1–research0034.11

Wan J, Dunning M, Bent A (2002) Probing plant-pathogen interactions and downstream defense signaling using DNA microarrays. Funct Integr Genom 2:259–273

Wang Z-Y, Nakano T, Gendron J, He J, Chen M, Vafeados D, Yang Y, Fujioka S, Yoshida S, Asami T, Chory J (2002) Nuclear-localized BZR1 mediates brassinosteroid-induced growth and feedback suppression of brassinosteroid biosynthesis. Dev Cell 2:505–513

Yaege JR, Stuteville DL (2002) Reactions of accessions in the annual *Medicago* core germ plasm collection to *Erysiphe pisi*. Plant Dis 86: 312–315

Yang S, Tang F, Caixetab ET, Zhu H (2013) Epigenetic regulation of a powdery mildew resistance gene in *Medicago truncatula*. Mol Plant 6:2000–2003

Yin Y, Wu D, Chory J (2002) Plant receptor kinases: systemin receptor identified. Proc Natl Acad Sci U S A 99:9090–9092

Young ND, Udvardi M (2009) Translating *Medicago truncatula* genomics to crop legumes. Curr Opin Plant Biol 12:193–201

Zhang Q, Blaylock LA, Harrison MJ (2010) Two *Medicago truncatula* half-ABC transporters are essential for arbuscule development in arbuscular mycorrhizal symbiosis. Plant Cell 22:1483–1497

Plant Molecular Biology Reporter
Supplementary File

Plant defense responses in *Medicago truncatula* unveiled by microarray analysis

Miguel Curto[1*], Franziska Krajinski[2], Helge Küster[3] and Diego Rubiales[1]

[1]CSIC, Institute for Sustainable Agriculture, Apdo.4084, E-14080, Córdoba, Spain.
[2]Max Planck Institute of Molecular Plant Physiology, Wissenschaftspark Golm, Am Muehlenberg 1, 14476, Potsdam, Germany.
[3]Institute for Plant Genetics, Unit IV - Plant Genomics, Leibniz Universität Hannover, Herrenhäuser Str. 2, D-30419 Hannover, Germany

*To whom correspondence should be addressed:
Miguel Curto
CSIC, Institute for Sustainable Agriculture, Apdo. 4084, E-14080 Córdoba, Spain.
E-mail: b72curum@uco.es
Tel: +34 957199215
Fax: +34 957499252

Table S1 Histological studies of *E. pisi* development of *M. truncatula* genotypes. Studies were carried out in both genotypes using three leaves for each biologic replicate. Data correspond to mean values (expressed in percentage) of germinated spores, germlings forming an appressorium, colonies established, number of hyphal tips per established colony and colonies associated with epidermal cell death, respectively.

Genotype	*E. pisi* developmental stages				
	% Germination[a]	% Appressoria[b]	% Colonies[c]	% Colony size[d]	% Death cells[e]
Parabinga	57.7	21.6	58.0*	9.5*	0.5
SA1306	23.0	12.3	18.3	2.8	8.0*

[a]Germlings with a germtube longer than the conidium, 100 spores were visualized.
[b]Germlings reached an epidermal cell forming an appressorium, 100 germlings were visualized.
[c]Colonies established out of the appressoria, 20 established colonies were visualized.
[d]Number of hyphal tips per colony established as measurement of the colony size, 20 established colonies were visualized.
[e]Colonies associated with epidermal cell death, 20 established colonies were visualized.
*Statistically significant differences ($p<0.01$)

Table S2 Genes and primer sequences used in the real-time quantitative polymerase chain reaction (qPCR) experiments.

ID[a]	MtGI[b]	Gene name	Forward primer (5'-3')	Reverse primer (5'-3')
MT000245	TC85729	Lectin-related polypeptide	CTGATTATGCTCATATTGGAA	CCATGCGTATATGTTTTGTAT
MT007367	TC77132	UL26.5 gene	CTTCTTAAAATGGCTAAATCC	AAAAACCTTAACCAAATCAAG
MT000412	TC77149	Thaumatin (MDTL1)	AATTAAAAGGTTCTGATGGAA	AGGTAGTAGTCCAATCAAGGA
MT014548	TC87236	Pathogenesis-related protein 4 (PRP4A)	GATTAATTGATTCATTCAGCA	AAGTGCAATCATGTTATGTGT
MT014090	TC79353	Dehydration-responsive protein (RD22)	AGAATTACCCTTATGCAGTGT	ACCAATAGGATTTGTTTGTTT
MT006316	TC82368	Disease resistance response protein 39 (DRR230-b)	TAAACTGCATAAGTGATCGTC	TTAATCCATCATCCACACTTA
MT014301	TC76880	Endoxyloglucan transferase	TTACAACAGTTTATGGAATGC	CGTTTTCTATCAGTGCAATAG
MT013687	TC92066	Ripening regulated protein (DDTFR18)	AGGAACTAGCTTCACCATTAG	TCCACATAAAGTTTGTTATGC
MT004404	TC91527	Receptor-protein kinase (FERONIA)	CTTAGGAACCAATGCTACTCT	TGTGTATCGACTATCACCATT
MT014167	TC76638	Pathogenesis related-protein (pprg2)	ATGGGTGTTTTTACTTTCAAT	TCTAGACTTTCATCCAATCCT

[a] Identifiers of *M. truncatula* 70-mer oligonucleotide
[b] TIGR *M. truncatula* Gene Index 7.0 release (MtGI 7.0).

Table S3 Correlation tables of microarray values to qPCR measurements for ten genes validated. Pearson correlations coefficients for evaluated genes are given as log_2 expression ratio between microarray and qPCR experiments.

	TC87236[a]		**TC79353**[a]		**TC85729**[a]		**TC76880**[a]		**TC82368**[a]	
	Micro[b]	qPCR[c]	Micro[b]	qPCR[c]	Micro[b]	qPCR[c]	Micro[b]	qPCR[c]	Micro[b]	qPCR[c]
TC87236[a] Micro[b]	1	0,9955								
TC87236[a] PCR[c]	0,9955	1								
TC79353[a] Micro[b]			1	0,9715						
TC79353[a] PCR[c]			0,9715	1						
TC85729[a] Micro[b]					1	0,9791				
TC85729[a] PCR[c]					0,9791	1				
TC76880[a] Micro[b]							1	0,9959		
TC76880[a] PCR[c]							0,9959	1		
TC82368[a] Micro[b]									1	0,9952
TC82368[a] PCR[c]									0,9952	1

	TC92066[a]		**TC76638**[a]		**TC91527**[a]		**TC77132**[a]		**TC77149**[a]	
	Micro[b]	qPCR[c]	Micro[b]	qPCR[c]	Micro[b]	qPCR[c]	Micro[b]	qPCR[c]	Micro[b]	qPCR[c]
TC92066[a] Micro[b]	1	0,9641								
TC92066[a] PCR[c]	0,9641	1								
TC76638[a] Micro[b]			1	0,9229						
TC76638[a] PCR[c]			0,9229	1						
TC91527[a] Micro[b]					1	0,9182				
TC91527[a] PCR[c]					0,9182	1				
TC77132[a] Micro[b]							1	0,9810		
TC77132[a] PCR[c]							0,98101	1		
TC77149[a] Micro[b]									1	0,9768
TC77149[a] PCR[c]									0,97686	1

[a] TIGR M. truncatula Gene Index 7.0 release (MtGI 7.0).
[b] Date obtained from Mt16kOLI1 microarray platform.
[c] Date obtained from real-time quantitative PCR experiments.

Table S4 Regulated genes in *Medicago truncatula* genotypes analyzed, SA1306 (SA) and Parabinga (PB), in response to *Erysiphe pisi* infection at 4 and 12 hours after inoculation (hai). Relative gene expression ratios (M) are listed and sorted by functional categories (FC). Genes were considered differentially expressed in response to *E. pisi* infection if to meet the prerequisites $p \leq 0.05$ and $M \leq -0.8$ or $M \geq 0.8$. ID = *M. truncatula* 70mer oligonucleotides probe identifiers. MtGI = Accesion number according to TIGR *M. truncatula* Gene Index (Mt GI 7.0). FC = functional categories as defined by Journet et al. (Journet et al. 2002). M= Average log2 differential expression ratios (inoculated/control). F= Fold change expression ratios of differentially expressed genes in SA1306 compared to Parabinga, log2 expression ratio SA1306/Parabinga, at 4 (F_4hai) and 12 (F_12hai) hours after *E. pisi* inoculation. Cells filled in red and green means that the sequence was up- ($0.8 \leq M$) and down-regulated ($M \leq -0.8$), at significance level $p \leq 0.05$, respectively. * n.v: no values were compiled. (See the excel file attached "Table S4.xlsx").

Supplementary Table S4

ID	MtGI	FC	M_PB_4hai	M_SA_4hai	M_PB_12hai	M_SA_12hai	F_4hai	F_12hai
MT000072	TC76375	I	1,519606833	-0,110016747	-0,176863893	-0,228876592	-1,62962358	-0,0520127
MT011069	TC80494	I	1,345595151	-0,117597757	-0,146758908	-0,38466264	-1,46319291	-0,23790373
MT000773	TC86295	I	1,304237786	0,16878539	0,213910895	-0,001598968	-1,1354524	-0,21550986
MT007014	TC85301	I	0,983559496	-0,447952186	0,249252644	-0,120417457	-1,43151168	-0,3696701
MT015153	TC85603	I	0,911972639	-0,124087557	-0,108999005	0,095684712	-1,0360602	0,204683717
MT015278	TC76902	I	0,886588848	-0,424286645	-0,237582328	-0,339759746	-1,31087549	-0,10217742
MT015141	TC76686	I	0,885863151	-0,121821863	0,018025171	0,266874699	-1,00768501	0,248849528
MT013135	TC93728	I	0,845623021	-0,450967602	0,391247143	0,46655509	-1,29659062	0,075307947
MT009791	TC86798	I	0,835450319	-0,355235666	0,104440239	-0,086185357	-1,19068599	-0,1906256
MT008450	TC78751	I	0,833566371	-0,381186488	0,339075706	-0,08925237	-1,21475286	-0,42832808
MT015175	TC85240	I	-0,835415132	0,424665208	-0,096170671	-0,263554858	1,26008034	-0,16738419
MT015318	TC76965	I	0,421959719	1,886170446	-0,264643567	-1,94181129	1,464210727	-1,67716772
MT005786	TC84433	I	-1,325865362	1,338389416	0,561440754	0,157505098	2,664254777	-0,40393566
MT001907	TC78899	I	-1,947088619	1,270283333	0,96555058	0,353441745	3,217371953	-0,61210884
MT011114	TC82045	I	-0,54702592	1,175555301	0,055962267	-0,084425199	1,72258122	-0,14038747
MT006064	TC91378	I	-0,263318608	0,921969479	-0,057162496	-0,293867968	1,185288087	-0,23670547
MT014283	TC85611	I	0,595749128	0,858805273	-0,009815489	0,375071303	0,263056146	0,384886792
MT015415	AW69363	I	0,286503738	-0,80589593	0,030096699	0,243119568	-1,09239967	0,21302287
MT010321	TC89013	I	0,201177675	-0,834304812	0,056925201	0,169319057	-1,03548249	0,112393855
MT013510	TC91374	I	0,419506233	0,232265611	-0,818578612	-0,262615901	-0,18724062	0,55596271
MT014301	TC76880	I	-0,223772706	-0,232183059	0,238491262	2,122093538	-0,00841035	1,883602275
MT006446	TC83652	I	0,370974964	0,419678422	0,341889329	0,841487235	0,048703459	0,499597906
MT003498	TC89193	I	0,012481388	0,273250725	0,188976102	-0,875775959	0,260769337	-1,06475206
MT007772	TC77702	I	-0,723036852	0,227856498	-0,628759506	-0,896307455	0,95089335	-0,26754795
MT015656	TC76965	I	0,673310775	0,601367529	-0,21556952	-2,181585372	-0,07194325	-1,96601585
MT013435	TC93811	I	-1,73014855	0,354164341	1,350692753	-0,053670643	2,084312891	-1,4043634
MT007152	TC85538	I	0,362548118	0,897994573	-0,429573849	-1,395660801	0,535446455	-0,96608695
MT013453	TC92730	I	-0,391615381	1,325490809	0,041153407	-2,48311061	1,71710619	-2,52426402
MT015434	TC86491	I	-0,386897446	-0,928163045	0,13855958	1,015078921	-0,5412656	0,876519341
MT004767	BF51916	I	-0,886409077	-0,263992161	0,079180106	1,174606585	0,622416916	1,095426479
MT000539	TC86161	I	0,938727509	1,393629593	0,833162144	0,490146258	0,454902084	-0,34301589
MT014058	TC85537	I	0,853751193	1,128430317	0,242075651	-0,824370049	0,274679123	-1,0664457
MT007366	TC77131	I	-0,860107802	1,72979254	0,977582071	1,839380754	2,589900342	0,861798683
MT015329	TC77134	I	-0,649076073	1,198019768	1,056928832	1,008322043	1,847095841	-0,04860679
MT013202	TC92727	II	0,91759058	n.v.*	0,210849359	n.v.*	n.v.*	n.v.*
MT013001	TC77912	II	-0,350534584	-0,944607298	-0,027136831	0,08036163	-0,59407271	0,107498461
MT007750	TC77577	II	0,168845531	-0,125149581	-0,328874772	-0,814924181	-0,29399511	-0,48604941
MT004723	TC81283	II	0,776527664	-0,06579449	-0,252269332	-0,835478896	-0,84232215	-0,58320956
MT015217	TC76675	II	-0,407429517	-0,932968446	0,073043143	0,964643341	-0,52553893	0,891600199
MT001467	TC78619	III	1,132539253	-0,309356892	0,009497005	-0,296924387	-1,44189614	-0,30642139
MT004151	TC90269	III	0,817015143	-0,206254134	0,33403375	-0,062395864	-1,02326928	-0,39642961
MT009485	TC88928	III	0,804346873	1,068374773	0,953236644	-0,019482389	0,2640279	-0,97271903
MT007017	TC85263	III	-0,814878921	-0,616113927	-0,401479134	0,409338326	0,198764994	0,81081746
MT007278	TC76540	III	-0,897935074	-0,178672263	0,097108024	0,267302958	0,719262811	0,170194934
MT009641	TC89494	III	-0,898200109	-0,777247292	-0,176841313	0,07819774	0,120952818	0,255039053
MT000463	TC77299	III	-0,907791872	-0,373266804	-0,099424289	-0,357387441	0,534525068	-0,25796315

Supplementary Table S4 continued

ID	MtGI	FC	M_PB_4hai	M_SA_4hai	M_PB_12hai	M_SA_12hai	F_4hai	F_12hai
MT007063	TC76533	III	-1,137354327	0,173068162	0,120648095	0,172255107	1,310422489	0,051607012
MT009747	TC80175	III	-1,264067253	0,306660213	-0,113187243	-0,39657215	1,570727466	-0,28338491
MT002075	TC79087	III	-1,345061428	-0,547415537	0,584116024	-0,449299279	0,797645891	-1,0334153
MT012181	TC89099	III	-0,337524502	1,073426298	0,13847864	-0,174071368	1,4109508	-0,31255001
MT006497	TC93816	III	-0,305420879	0,9698803	0,060132024	0,16467624	1,275301178	0,104544216
MT000554	TC77007	III	-0,643475474	-0,964413381	-0,26709513	-0,326672621	-0,32093791	-0,05957749
MT009717	TC79773	III	-1,128970562	-0,546190275	-0,336393133	n.v.*	0,582780287	n.v.*
MT007306	TC77185	III	0,575680831	0,51215754	-0,93085151	0,042793432	-0,06352329	0,973644941
MT014170	TC85486	III	0,280187096	0,198695066	0,226853449	0,957995364	-0,08149203	0,731141915
MT009405	TC79734	III	0,045408852	-0,572410687	-0,62861934	0,80470066	-0,61781954	1,43332
MT011141	TC89776	IV	0,952137173	0,275675207	0,405655766	0,527295998	-0,67646197	0,121640232
MT001368	TC78263	IV	-0,881720841	-0,666524434	-0,029195523	-0,00810672	0,215196407	0,021088803
MT000231	TC76333	IV	0,025968126	0,422456718	-0,866845701	-0,467774388	0,396488592	0,399071313
MT005945	TC82519	V	1,497621475	-0,750744767	0,068303102	-0,689374511	-2,24836624	-0,75767761
MT007660	TC86252	V	1,046542606	0,342628166	-0,015009187	-0,65976076	-0,70391444	-0,64475157
MT002800	TC89253	V	0,963191512	0,180917638	0,166083519	-0,211099682	-0,78227387	-0,3771832
MT007577	TC77406	V	0,918139002	-0,031599307	-0,078409327	-0,179962477	-0,94973831	-0,10155315
MT014000	TC85476	V	-0,812848393	-0,783364499	-0,150751181	0,484497404	0,029483894	0,635248585
MT007374	TC77126	V	-0,815136473	-0,741707215	-0,144697418	0,38650186	0,073429259	0,531199278
MT015265	TC85634	V	-0,821643985	-0,629273363	-0,19477641	0,09998457	0,192370622	0,294760979
MT000780	TC77724	V	-0,831765127	-0,583325056	-0,375801656	0,068664934	0,24844007	0,44446659
MT000779	TC77723	V	-0,832135861	-0,468060305	-0,43597663	-0,122289291	0,364075556	0,313687339
MT014342	BQ15008	V	-0,941277447	-0,372077393	-0,143246521	-0,08272943	0,569200053	0,060517092
MT007195	TC85638	V	-1,002298712	-0,565265927	-0,264076038	0,242692461	0,437032784	0,5067685
MT014285	TC85612	V	-1,012029209	-0,61319389	-0,197706725	0,189197733	0,398835319	0,386904459
MT015099	TC76505	V	-1,036564609	-0,750474514	0,317048627	0,721749552	0,286090095	0,404700925
MT015098	TC76509	V	-1,20177875	-0,705091569	0,470236153	0,719211937	0,49668718	0,248975784
MT013315	TC92246	V	-1,376847264	-0,455011579	-0,089468399	n.v.*	0,921835685	n.v.*
MT004422	TC82383	V	-0,427712338	0,981438827	-0,268374831	-0,073087704	1,409151165	0,195287126
MT006366	TC84044	V	-0,262822237	0,880869327	-0,080229529	-0,200035661	1,143691563	-0,11980613
MT014052	TC85534	V	0,294720703	0,822504223	-0,039387309	-0,271368987	0,527783521	-0,23198168
MT000840	TC86629	V	-0,776716252	-0,868855739	-0,080693014	-0,230098082	-0,09213949	-0,14940507
MT012740	TC92381	V	-0,063892663	-1,051080027	0,061686223	0,489152292	-0,98718736	0,427466068
MT000004	TC76692	V	-1,533796984	-1,532704829	-0,163500168	0,111549047	0,001092155	0,275049216
MT015383	TC86005	V	0,78587642	0,563875411	0,344714677	1,174933759	-0,22200101	0,830219082
MT009361	TC88949	V	0,349555012	-0,312904465	-0,207203202	1,050271128	-0,66245948	1,25747433
MT005302	TC93774	V	-0,357932113	-0,610774535	0,236958149	0,964159107	-0,25284242	0,727200958
MT015094	TC76507	V	-0,071686333	-0,535013403	0,358764415	0,881242135	-0,46332707	0,522477721
MT011588	TC88596	V	-0,021474159	-0,410263607	0,648642745	0,862608392	-0,38878945	0,213965647
MT014051	AA66057	V	-0,221656111	-0,253509637	0,450997555	0,85432856	-0,03185353	0,403331005
MT015096	BG45649	V	0,039161485	-0,278383406	0,161700645	0,826160966	-0,31754489	0,664460321
MT015375	BQ14499	V	0,221173797	-0,105214717	0,410915916	0,807352173	-0,32638851	0,396436257
MT010922	TC89059	V	0,186349337	0,971179467	0,078025938	-0,805250475	0,78483013	-0,88327641
MT013999	TC85436	V	0,664927484	0,755209641	0,185496645	-1,173996641	0,090282157	-1,35949329
MT013687	TC92066	VI	1,492237046	0,539160856	-0,377978244	n.v.*	-0,95307619	n.v.*
MT007633	TC86326	VI	1,413598788	-0,252574312	0,365918119	n.v.*	-1,6661731	n.v.*

Supplementary Table S4 continued

ID	MtGI	FC	M_PB_4hai	M_SA_4hai	M_PB_12hai	M_SA_12hai	F_4hai	F_12hai
MT011855	TC90968	VI	1,373060079	-0,1342951	-0,170756542	-0,468838618	-1,50735518	-0,29808208
MT009102	TC87521	VI	1,253330313	-0,249147232	-0,393647014	-0,72188951	-1,50247754	-0,3282425
MT000247	TC85700	VI	1,184887439	-0,865672382	-0,258171818	0,202254133	-2,05055982	0,46042595
MT008188	TC87122	VI	1,171449516	-0,56556643	-0,296315754	0,111654653	-1,73701595	0,407970407
MT014938	TC83315	VI	1,160185416	0,574697709	n.v.*	n.v.*	-0,58548771	n.v.*
MT007505	TC77223	VI	1,075150533	0,79998625	-0,708659445	-0,081317153	-0,27516428	0,627342292
MT007426	TC86070	VI	0,99147299	-0,393119577	-0,312045644	-0,314086864	-1,38459257	-0,00204122
MT000244	TC76883	VI	0,905160883	-0,194925723	0,445423015	-0,246410227	-1,10008661	-0,69183324
MT014034	TC78280	VI	0,856434983	n.v.*	0,758267942	n.v.*	n.v.*	n.v.*
MT001070	TC78077	VI	0,849705154	-0,241614255	-0,245281117	-0,518535077	-1,09131941	-0,27325396
MT014220	TC85388	VI	0,823863451	0,116405236	0,612022504	0,529231326	-0,70745821	-0,08279118
MT015234	TC85257	VI	-0,803409392	-0,184728027	-0,510912623	-0,253656825	0,618681365	0,257255798
MT005924	TC93694	VI	-0,859987918	-0,163944037	-0,231204621	0,018227353	0,696043881	0,249431973
MT006643	TC84653	VI	-1,177461058	0,507768169	-0,278235851	0,512738367	1,685229227	0,790974218
MT014616	TC79096	VI	-1,430407518	-0,469183622	0,160907774	-0,359283402	0,961223896	-0,52019118
MT002445	TC80289	VI	-1,57655707	0,842089413	-0,002402763	-0,21332065	2,418646484	-0,21091789
MT015146	TC85138	VI	-0,045192546	1,305463282	0,34338074	0,131231635	1,350655828	-0,2121491
MT014588	AW77474	VI	-0,406741358	0,983893546	-0,3715442	0,147115726	1,390634903	0,518659926
MT000507	TC77268	VI	-0,239535183	0,939572243	-0,049976596	-0,63279711	1,179107426	-0,58282051
MT007937	TC77840	VI	-1,614296651	0,91679315	-0,34495771	-0,055950768	2,531089801	0,289006942
MT002126	TC88134	VI	0,58612489	0,908478267	-0,019782903	-0,149709175	0,322353377	-0,12992627
MT007391	TC77145	VI	0,207743171	0,812321311	0,162662685	-0,120340335	0,60457814	-0,28300302
MT008290	TC78288	VI	-0,230834255	-0,816568041	0,082533913	0,052113884	-0,58573379	-0,03042003
MT014009	TC76992	VI	-0,479753231	-1,091555392	-0,377941883	-0,583454302	-0,61180216	-0,20551242
MT007362	TC85935	VI	-0,269524572	-1,164854676	-0,208907194	0,195027613	-0,8953301	0,403934807
MT002406	TC88485	VI	0,923910298	0,88743269	0,111983506	-0,084622526	-0,03647761	-0,19660603
MT002917	TC80626	VI	-1,248288209	-0,858568552	0,227287098	0,07046786	0,389719657	-0,15681924
MT003137	TC78559	VI	0,372238664	0,161540849	1,203905342	0,37194882	-0,21069782	-0,83195652
MT014270	TC85521	VI	0,218940114	0,53447058	1,029241123	0,601926719	0,315530466	-0,4273144
MT014269	TC85521	VI	0,008173324	0,385155955	1,002028481	0,364927143	0,376982631	-0,63710134
MT016054	TC85246	VI	-0,405661689	-0,729269748	-0,838292781	0,274718564	-0,32360806	1,113011344
MT011894	TC80804	VI	0,14409748	-3,989867922	-1,025636017	0,093888789	-4,1339654	1,119524806
MT015525	TC78048	VI	-0,51254389	-0,326555819	-0,022527685	0,937611598	0,185988071	0,960139284
MT014241	TC85478	VI	1,557109496	-0,200606493	1,425021432	0,929481768	-1,75771599	-0,49553966
MT010962	TC81425	VI	0,229030755	-0,678733715	0,3288908	0,907444616	-0,90776447	0,578553816
MT007483	TC76928	VI	0,193240883	-0,295584779	0,412268014	0,895443608	-0,48882566	0,483175594
MT007961	TC86135	VI	-0,278920364	0,254029634	-0,310560118	-0,931279317	0,532949997	-0,6207192
MT000302	TC77029	VI	n.v.*	0,384360003	0,32778828	-0,975000206	n.v.*	-1,30278849
MT014280	TC85609	VI	0,821296426	0,405936455	1,02461108	-1,098353258	-0,41535997	-2,12296434
MT004722	TC82902	VI	-0,204198176	0,224864365	0,12012971	-1,131078689	0,429062541	-1,2512084
MT001841	TC87678	VI	0,123578346	0,5085947	-0,177509291	-1,248074986	0,385016354	-1,07056569
MT000305	TC85779	VI	-0,070477735	0,178578556	-0,670286861	-1,328203773	0,249056291	-0,65791691
MT004582	TC82770	VI	-0,285976413	1,186848275	-0,81909163	-1,082501719	1,472824688	-0,26341009
MT015374	TC86097	VII	0,915701268	-0,331575061	0,302754592	-0,203468061	-1,24727633	-0,50622265
MT000745	TC77625	VII	0,815102223	0,087299463	-0,151447467	0,158150537	-0,72780276	0,309598004
MT007293	TC85722	VII	0,397036817	0,859944035	-0,211987129	-0,000202145	0,462907218	0,211784985

Supplementary Table S4 continued

ID	MtGI	FC	M_PB_4hai	M_SA_4hai	M_PB_12hai	M_SA_12hai	F_4hai	F_12hai
MT015247	TC85799	VII	-0,340482995	-0,979869366	-0,214233985	0,078013311	-0,63938637	0,292247296
MT009256	TC88255	VII	-0,607997391	0,053462402	-0,58183613	1,006691835	0,661459793	1,588527965
MT001978	TC79387	VII	-0,26367129	-0,284670414	0,208162311	0,990760983	-0,02099912	0,782598672
MT006200	TC91850	VIII	1,462856249	-0,033835778	-0,097020085	-0,571079458	-1,49669203	-0,47405937
MT001094	TC78189	VIII	1,39729897	0,171586818	-0,160740811	-0,062218005	-1,22571215	0,098522806
MT006176	TC88846	VIII	1,172607196	0,076144867	2,704291226	-1,115724228	-1,09646233	-3,82001545
MT006399	TC83706	VIII	1,060377216	-0,100248422	0,019697598	-0,286403039	-1,16062564	-0,30610064
MT000920	TC86494	VIII	1,023745628	0,038769208	0,465235903	-0,578821694	-0,98497642	-1,0440576
MT003228	TC89837	VIII	-0,802893874	0,316721657	-0,665739584	-0,128533295	1,119615531	0,537206289
MT001073	TC86729	VIII	-0,850616974	-0,075242556	-0,379450167	0,045683286	0,775374418	0,425133453
MT011401	TC79757	VIII	-1,027130304	0,310890632	-0,279807543	-0,150055254	1,338020936	0,129752289
MT008455	TC88292	VIII	-1,043366492	-0,333353824	-0,168456522	0,760166963	0,710012669	0,928623485
MT013898	TC84988	VIII	-0,707624006	1,032886121	-0,338965839	-0,40722888	1,740510127	-0,06826304
MT010689	TC81518	VIII	0,027049151	1,128762862	0,03241485	-0,205414719	1,101713711	-0,23782957
MT015124	AL37119	VIII	0,784602489	0,956533912	0,330646347	0,74152566	0,171931423	0,410879313
MT006777	TC84865	VIII	-0,22509759	0,855512053	-0,31743446	-0,111704087	1,080609643	0,205730373
MT001884	TC78266	VIII	-0,287368221	0,848001601	-0,405804488	-0,482527452	1,135369822	-0,07672296
MT009253	TC88380	VIII	0,220099939	-0,884476821	-0,088532864	n.v.*	-1,10457676	n.v.*
MT000984	TC77695	VIII	-0,999330679	-0,81698385	-0,131531405	0,211214686	0,182346829	0,342746091
MT003433	TC81534	VIII	0,330667667	0,15216919	1,28251638	0,067708052	-0,17849848	-1,21480833
MT002345	TC89017	VIII	-0,152798985	-0,267955323	0,151148174	0,98652707	-0,11515634	0,835378896
MT005424	TC92499	VIII	-0,186417038	-0,329576351	0,073631332	0,858906093	-0,14315931	0,785274761
MT009262	TC88569	VIII	-0,621755582	-0,603377144	-0,103214663	0,822809295	0,018378438	0,926023959
MT009487	TC88609	VIII	-0,000991484	0,453457178	-0,214817673	-1,067431603	0,454448662	-0,85261393
MT009598	TC79845	VIII	-0,103662006	-0,205134172	1,092822039	1,383079263	-0,10147217	0,290257225
MT008663	TC87794	VIII	1,145631881	-1,52981117	0,101167884	0,813907426	-2,67544305	0,712739542
MT009486	TC80140	IX	1,238606401	-0,082853483	-0,227602992	-0,004163923	-1,32145988	0,223439069
MT015100	BG44893	IX	1,025859066	0,146030078	0,687413343	0,577197306	-0,87982899	-0,11021604
MT014309	TC85761	IX	-0,814308254	0,68827797	-0,196346467	-0,046198916	1,502586224	0,150147551
MT007418	TC86029	IX	-0,846756413	-0,266259782	-0,157247066	-0,213675172	0,58049663	-0,05642811
MT001258	TC87268	IX	-0,884547476	-0,529915396	0,074814276	-0,065136901	0,35463208	-0,13995118
MT000320	TC85840	IX	-0,977052234	-0,220828274	0,450290132	0,533053616	0,75622396	0,082763483
MT000211	TC85600	IX	-0,997749792	0,133552123	0,210997801	-0,018208873	1,131301915	-0,22920667
MT001720	TC78335	IX	-1,098506934	-0,936311752	-0,243580992	-0,020560948	0,162195182	0,223020044
MT007202	TC85394	IX	-1,115858764	-0,235815453	0,187067865	0,187349348	0,880043311	0,000281483
MT001110	TC78139	IX	-1,129246696	0,386644623	-1,336346693	-1,056699411	1,515891318	0,279647282
MT014509	TC78239	IX	-1,169230935	-0,451730914	0,375279508	-0,193260042	0,717500021	-0,56853955
MT007200	TC85391	IX	-1,175772549	-0,210742013	-0,072292022	0,107343863	0,965030535	0,179635885
MT014555	TC78712	IX	-1,304674735	-0,429571161	-0,219122739	-0,373272287	0,875103574	-0,15414955
MT014263	TC85392	IX	-1,400451531	-0,744212242	0,294662053	0,213399898	0,656239289	-0,08126216
MT014556	TC78711	IX	-1,457085705	-0,805425078	-0,172929943	n.v.*	0,651660627	n.v.*
MT012599	TC92317	IX	-1,51217925	-0,061582791	0,163476116	-0,413087942	1,450596459	-0,57656406
MT003740	TC89991	IX	-0,456162872	1,115341048	0,04102895	-0,114061505	1,57150392	-0,15509046
MT002869	TC85227	IX	0,297673074	-0,825861876	0,015073057	0,674841241	-1,12353495	0,659768185
MT007960	TC86755	IX	-0,661909102	-0,894203581	0,252102217	-0,026257838	-0,23229448	-0,27836005
MT000772	TC77582	IX	-1,077340521	-1,217598468	0,335042346	0,037407587	-0,14025795	-0,29763476

Supplementary Table S4 continued

ID	MtGI	FC	M_PB_4hai	M_SA_4hai	M_PB_12hai	M_SA_12hai	F_4hai	F_12hai
MT000874	TC77828	IX	-1,011954996	-0,875000366	0,544663991	0,223554638	0,13695463	-0,32110935
MT002505	TC78598	IX	-1,490380922	-1,142825107	0,463426445	0,159704392	0,347555814	-0,30372205
MT003764	TC80669	IX	-2,074445338	-1,245821343	0,704647343	-0,438054817	0,828623995	-1,14270216
MT007519	TC77302	IX	-1,705157542	-0,929679628	0,194120484	-0,352429975	0,775477914	-0,54655046
MT014261	TC85392	IX	-1,510271986	-0,977068859	0,201872573	-0,075872057	0,533203127	-0,27774463
MT015495	TC77626	IX	-1,506333787	-1,247859167	0,318788988	-0,750381073	0,25847462	-1,06917006
MT003691	TC80374	IX	0,256728749	0,064420674	0,901923021	0,39633906	-0,19230807	-0,50558396
MT015105	TC76514	IX	0,687307873	0,107780246	0,803208776	0,745222161	-0,57952763	-0,05798662
MT000177	TC76751	IX	-0,03456009	0,186722428	0,381531332	0,857839731	0,221282517	0,476308399
MT014284	TC76813	IX	-0,019117596	0,363162698	-0,636284278	-0,828285323	0,382280294	-0,19200105
MT007027	TC76560	IX	-0,372052073	0,72191484	-0,60356591	-1,001029337	1,093966913	-0,39746343
MT005323	TC92446	IX	0,901231954	-0,560742428	1,191418692	1,102252483	-1,46197438	-0,08916621
MT014357	TC77108	X	1,229882577	0,102582192	0,389983402	0,375150746	-1,12730038	-0,01483266
MT012454	TC90937	X	1,037986889	0,774039575	0,513773131	0,249943361	-0,26394731	-0,26382977
MT000364	TC77108	X	0,935589363	-0,027504059	0,432095405	0,406712675	-0,96309342	-0,02538273
MT013130	TC83662	X	0,848242329	0,017319028	0,476774177	-0,321705131	-0,8309233	-0,79847931
MT015384	TC85993	X	-1,089220991	-0,045395871	-0,360604064	-0,129599342	1,04382512	0,231004721
MT007340	TC85793	X	0,013946994	0,835963392	-0,090298409	-0,252757852	0,822016398	-0,16245944
MT008936	TC87997	X	0,521016039	-0,257691315	1,493701583	0,245853321	-0,77870735	-1,24784826
MT010780	TC90444	X	1,446814157	1,693670238	1,079351547	1,377836031	0,246856081	0,298484484
MT004404	TC91527	X	1,630221152	1,363539042	1,635555534	1,183821643	-0,26668211	-0,45173389
MT002918	TC80244	XI	0,88349786	-0,243233361	-0,405486539	-0,078253117	-1,12673122	0,327233422
MT007486	TC86157	XII	-2,908886091	1,934226856	1,800824554	-0,245197518	4,843112947	-2,04602207
MT015301	TC76953	XII	1,886220247	-0,219549371	-0,668093264	n.v.*	-2,10576962	n.v.*
MT015873	TC78824	XII	1,362784972	0,425437769	-0,294772755	-0,979011182	-0,9373472	-0,68423843
MT013884	TC92267	XII	1,228684621	0,084824054	0,007230653	1,293986153	-1,14386057	1,2867555
MT014141	TC76474	XII	1,217558311	0,771890729	-0,067384854	0,327686649	-0,44566758	0,395071503
MT001052	TC86813	XII	1,180733071	0,407910503	-0,268198866	-1,218061518	-0,77282257	-0,94986265
MT014789	TC91228	XII	1,05480857	-0,292699079	-0,234106336	-0,540564708	-1,34750765	-0,30645837
MT005457	TC92173	XII	0,840585358	-0,391965398	-0,225416007	-0,384409244	-1,23255076	-0,15899324
MT002464	TC88477	XII	-0,856037136	-0,637939046	-0,201139253	1,038370061	0,21809809	1,239509315
MT000245	TC85729	XII	-1,945632875	1,531764594	-0,136210352	-0,306698494	3,477397469	-0,17048814
MT011957	TC93496	XII	-0,691862809	0,862742173	-0,180820102	-0,073904887	1,554604982	0,106915215
MT012187	TC91876	XII	-0,041213083	-0,87838651	-0,169885243	-0,105678258	-0,83717343	0,064206984
MT014200	TC76579	XII	-0,35970488	-0,884091292	-0,274365262	0,610829446	-0,52438641	0,885194708
MT011574	TC86954	XII	-0,970243225	-0,88795846	-0,060701232	-1,310184453	0,082284764	-1,24948322
MT001639	TC86955	XII	-0,938672547	-0,947073846	-0,257814029	-0,270052784	-0,0084013	-0,01223875
MT009315	TC88787	XII	-0,279298425	-1,012839684	-0,472318229	-0,169685217	-0,73354126	0,302633012
MT002369	TC78796	XII	-0,868610365	-0,949089375	0,009909715	n.v.*	-0,08047901	n.v.*
MT010010	TC79553	XII	0,0987456	0,29602894	0,82961086	n.v.*	0,19728334	n.v.*
MT014204	BQ14378	XII	-0,112054083	0,132986622	-0,445315217	-1,160948949	0,245040704	-0,71563373
MT004376	TC91372	XII	0,531852297	-1,392147331	-1,25271354	2,654893181	-1,92399963	3,90760672
MT000940	TC78074	XII	0,804577543	-0,593873219	0,574592464	1,004592175	-1,39845076	0,429999711
MT007132	TC85453	XIIA	-0,00277083	1,160118414	0,140603697	-0,227117161	1,162889244	-0,36772086
MT004689	TC80969	XIIA	-1,389098954	1,71616279	-0,010701892	-0,387823726	3,105261744	-0,37712183
MT014167	TC76638	XIIA	1,450746891	1,077260972	0,603589832	0,098470954	-0,37348592	-0,50511888

Supplementary Table S4 continued

ID	MtGI	FC	M_PB_4hai	M_SA_4hai	M_PB_12hai	M_SA_12hai	F_4hai	F_12hai
MT006316	TC82368	XIIA	1,444022725	-4,181289733	-0,656026873	1,578133406	-5,62531246	2,234160279
MT000310	TC85789	XIIA	1,127678623	0,623982522	0,404660992	-0,18372355	-0,5036961	-0,58838454
MT011971	TC77729	XIIA	1,08614779	n.v.*	-0,072897699	-0,750632919	n.v.*	-0,67773522
MT007967	TC86659	XIIA	1,044274159	0,366036266	0,415333319	-0,079495016	-0,67823789	-0,49482834
MT015363	TC77138	XIIA	0,883780152	-0,367422566	0,68527334	-1,260270321	-1,25120272	-1,94554366
MT008094	TC78159	XIIA	-1,080314844	-0,517422575	-1,215464674	-0,384774151	0,562892269	0,830690523
MT000937	TC86595	XIIA	-1,088431398	-0,555336588	0,040176554	0,138203658	0,53309481	0,098027105
MT005620	TC91689	XIIA	-1,392656385	-0,719891247	-0,189458685	0,054243451	0,672765138	0,243702136
MT001870	TC87275	XIIA	-1,596384309	-0,477727878	-0,51837841	0,501773964	1,118656431	1,020152374
MT014548	TC87236	XIIA	0,381449763	2,224748603	0,039213439	-1,054899533	1,84329884	-1,09411297
MT000433	TC85974	XIIA	0,77219543	1,577390813	0,480104818	0,490478328	0,805195382	0,01037351
MT006759	TC82258	XIIA	-0,588885601	1,247989701	0,29472222	-0,161692786	1,836875302	-0,45641501
MT015067	TC85170	XIIA	-0,544912575	1,241786529	0,640788751	-0,332817594	1,786699104	-0,97360634
MT000362	TC77110	XIIA	-0,093549929	0,95516857	-0,178468234	0,364659172	1,048718499	0,543127406
MT000082	TC76640	XIIA	0,547727264	0,823026521	0,063572302	-0,256648648	0,275299257	-0,32022095
MT008427	TC87547	XIIA	-0,172855267	0,810431298	0,04840348	0,721314866	0,983286565	0,672911386
MT014747	TC81568	XIIA	-0,572838515	-0,839316013	-0,47651551	0,567855915	-0,2664775	1,044371425
MT007702	TC86399	XIIA	-0,244492634	-1,082308214	-0,192602439	0,284789287	-0,83781558	0,477391726
MT014169	TC76642	XIIA	1,265200573	2,20836399	0,37320872	-0,026440527	0,943163417	-0,39964925
MT014166	TC76643	XIIA	1,117088869	1,601124169	0,464634671	0,116514508	0,4840353	-0,34812016
MT014168	TC76641	XIIA	1,009874234	2,18561888	0,481841724	0,144488451	1,175744646	-0,33735327
MT001232	TC87208	XIIA	-0,829972239	-0,825642852	-0,16273832	0,039109674	0,004329387	0,201847994
MT015106	TC76511	XIIA	1,076726714	0,159268236	1,124403865	0,457463938	-0,91745848	-0,66693993
MT015058	TC85182	XIIA	-0,366414873	-0,034430009	0,908177053	0,795656463	0,331984864	-0,11252059
MT010749	TC89651	XIIA	-0,255114634	-0,009576232	-0,997525533	-0,751412996	0,245538402	0,246112537
MT015062	TC85180	XIIA	0,045663452	0,052179889	0,415757892	0,977659337	0,006516437	0,561901445
MT007933	TC77910	XIIA	0,52516433	-0,269644788	0,212880413	0,896499902	-0,79480912	0,683619489
MT000412	TC77149	XIIA	0,233991033	2,213252256	0,686278608	-0,984254845	1,979261223	-1,67053345
MT014136	BG45222	XIIA	-0,069902512	2,241231129	-0,418893112	-1,258759771	2,311133642	-0,83986666
MT004877	TC80109	XIIB	-0,801515713	-0,54178449	0,508699738	-0,355695356	0,259731223	-0,86439509
MT014260	TC85396	XIIB	-0,809065229	-0,535860958	0,137666035	0,070814366	0,273204271	-0,06685167
MT015163	BQ14418	XIIB	-0,861740503	-0,360407711	-0,249642934	0,166454084	0,501332792	0,416097019
MT000733	TC77585	XIIB	-0,954323093	-0,503611646	-0,068688262	-0,346946757	0,450711447	-0,2782585
MT015200	TC85438	XIIB	-1,001996272	-0,732064394	0,161731698	0,278247778	0,269931878	0,11651608
MT013942	TC85119	XIIB	-1,073183119	-0,682967385	1,123899087	n.v.*	0,390215734	n.v.*
MT015366	TC86017	XIIB	-1,11015738	-0,503767313	0,93102959	n.v.*	0,606390068	n.v.*
MT009324	TC79123	XIIB	-1,29215935	-0,498627595	-0,0671156	-0,27331368	0,793531755	-0,20619808
MT014262	TC85390	XIIB	-1,482305526	-0,762945378	0,289085723	-0,344822188	0,719360148	-0,63390791
MT014090	TC79353	XIIB	-0,590751741	1,942558331	-0,078834292	0,18578904	2,533310072	0,264623332
MT014258	TC76698	XIIB	0,308288433	0,992077279	-0,335420181	-0,576873563	0,683788847	-0,24145338
MT008741	TC87759	XIIB	0,016928165	0,897817323	0,034118893	-0,140267997	0,880889159	-0,17438689
MT000401	TC77174	XIIB	-0,704237822	-0,813285285	0,234957002	0,476895012	-0,10904746	0,24193801
MT014319	TC85785	XIIB	-0,779853321	-0,823999514	0,269930268	0,234882221	-0,04414619	-0,03504805
MT016071	TC80479	XIIB	-1,803624351	-1,001754806	1,20008305	-0,338215414	0,801869544	-1,53829846
MT003866	CB89462	XIIB	-1,368339613	-1,010214621	1,398930572	-0,432235237	0,358124992	-1,83116581
MT014320	TC85788	XIIB	-0,707320903	-1,05424629	0,733240001	0,103080437	-0,34692539	-0,63015956

Supplementary Table S4 continued

ID	MtGI	FC	M_PB_4hai	M_SA_4hai	M_PB_12hai	M_SA_12hai	F_4hai	F_12hai
MT009933	TC80686	XIIB	-0,643082288	-1,218438821	0,524445339	-0,758047383	-0,57535653	-1,28249272
MT015438	TC85567	XIIB	-1,024248644	-1,275267955	0,707045051	-0,31941224	-0,25101931	-1,02645729
MT010741	TC88992	XIIB	-2,155169343	-1,469193222	1,305169072	-0,911205437	0,685976121	-2,21637451
MT015439	TC85565	XIIB	-1,387046918	-1,495769203	0,793501735	-0,81213079	-0,10872228	-1,60563253
MT013719	TC82472	XIIB	-1,402223739	-1,59442243	1,709912283	n.v.*	-0,19219869	n.v.*
MT008969	TC85494	XIIB	-1,729622047	-1,70571045	0,33582926	1,108218873	0,023911597	0,772389613
MT014499	TC85568	XIIB	-1,861296478	-1,803273769	0,53538009	-0,222012943	0,058022709	-0,75739303
MT015437	TC85564	XIIB	-2,140454168	-1,822215312	0,843975958	-0,242470233	0,318238856	-1,08644619
MT001799	TC85566	XIIB	-0,924620166	-1,829352618	0,608039341	-0,150838724	-0,90473245	-0,75887807
MT006276	TC88091	XIIB	-1,564504697	-1,452311375	0,50915047	0,75121254	0,112193322	0,242062069
MT008665	TC86930	XIIB	-1,407950556	-1,159070127	0,073340494	-0,798529774	0,248880429	-0,87187027
MT009116	TC86873	XIIB	-1,494961242	-0,95360535	0,633740574	n.v.*	0,541355892	n.v.*
MT009612	TC78900	XIIB	-0,979418822	-1,112067506	0,149513237	-0,443025453	-0,13264868	-0,59253869
MT012016	TC81087	XIIB	-1,655799781	-1,291300729	0,516316327	-1,11295153	0,364499052	-1,62926786
MT014756	TC81367	XIIB	-1,72000749	-1,164755353	1,856961028	0,001845321	0,555252137	-1,85511571
MT015199	TC85439	XIIB	-1,149475061	-0,989851473	0,317291541	0,121331336	0,159623588	-0,19596021
MT015365	TC86015	XIIB	-0,892470957	-1,302280139	0,008229294	-0,560432196	-0,40980918	-0,56866149
MT007029	TC76542	XIIB	0,634497169	-0,073340235	-0,000858544	1,518960537	-0,7078374	1,519819081
MT015173	TC85252	XIIB	-1,0960021	-0,656672547	-0,406171752	-0,9658934	0,439329553	-0,55972165
MT010934	TC81117	XIIC	1,658787843	-0,750280428	-0,193286057	-0,063967521	-2,40906827	0,129318536
MT012696	TC83260	XIIC	1,579625857	n.v.*	0,350565143	n.v.*	n.v.*	n.v.*
MT014494	TC86674	XIIC	1,403207745	-0,024929334	-0,259366405	-0,62093268	-1,42813708	-0,36156628
MT009827	TC80744	XIIC	1,390108687	-0,687330221	-0,115931585	0,154488231	-2,07743891	0,270419816
MT013959	TC82213	XIIC	1,377706856	-0,486482629	0,647484624	0,297366416	-1,86418948	-0,35011821
MT002288	BF63310	XIIC	1,346605478	0,809553095	0,096033667	-0,516378553	-0,53705238	-0,61241222
MT008248	TC78185	XIIC	1,335485257	0,160266078	-0,26257734	-0,56634992	-1,17521918	-0,30377258
MT011865	TC91326	XIIC	1,262221347	-0,034073698	-0,139651625	-0,357180946	-1,29629504	-0,21752932
MT008343	TC87362	XIIC	1,235992273	-0,051610756	-0,247500627	-0,640264326	-1,28760303	-0,3927637
MT013294	TC92691	XIIC	1,193056746	-4,316259191	3,701636436	n.v.*	-5,50931594	n.v.*
MT003986	TC81902	XIIC	1,130421557	-0,051305463	-0,505322067	-0,348820107	-1,18172702	0,15650196
MT005507	TC83259	XIIC	1,12103359	-0,12140424	-0,129697314	-0,359658952	-1,24243783	-0,22996164
MT012999	TC81381	XIIC	1,088407426	-0,711942275	0,073521431	-0,76041485	-1,8003497	-0,83393628
MT009542	TC88150	XIIC	1,042330949	-1,021317112	0,160181934	0,458989745	-2,06364806	0,298807811
MT007737	TC86325	XIIC	0,957112446	-0,011655245	-0,098425432	-0,062590127	-0,96876769	0,035835306
MT007936	TC86677	XIIC	0,956115624	-0,237154252	-0,129367948	0,597285843	-1,19326988	0,726653791
MT002683	TC89218	XIIC	0,950576193	-0,117417022	-0,460773504	-0,505666844	-1,06799321	-0,04489334
MT013992	TC76325	XIIC	0,93678325	-0,967084881	-0,064899213	0,423266517	-1,90386813	0,48816573
MT010691	TC81641	XIIC	0,882596956	-0,038001544	-0,315396458	-0,181375069	-0,9205985	0,134021389
MT007663	TC77654	XIIC	0,881397395	-0,107936897	-0,246612662	0,464765575	-0,98933429	0,711378237
MT014121	TC76469	XIIC	0,852347331	0,370168346	0,112418276	0,130433054	-0,48217898	0,018014778
MT005328	TC93323	XIIC	0,851301854	-0,209792159	0,367579802	0,093808943	-1,06109401	-0,27377086
MT007562	TC86179	XIIC	0,817109036	0,393957242	-0,240905231	0,470232474	-0,42315179	0,711137705
MT009823	TC80287	XIIC	-0,80103014	-0,019388295	-0,164532809	-0,502402942	0,781641845	-0,33787013
MT001050	TC78039	XIIC	-0,807933464	-0,73704003	-0,368170507	-0,054938376	0,070893434	0,31323213
MT001412	TC87358	XIIC	-0,808860375	0,214239019	-0,097769807	-0,482220284	1,023099393	-0,38445048
MT014961	AW56104	XIIC	-0,816652289	-0,50446701	-0,22031519	0,544170812	0,312185279	0,764486002

Supplementary Table S4 continued

ID	MtGI	FC	M_PB_4hai	M_SA_4hai	M_PB_12hai	M_SA_12hai	F_4hai	F_12hai
MT001214	TC87128	XIIC	-0,861108921	-0,286795562	0,029849578	0,2631427	0,574313359	0,233293121
MT000771	TC86489	XIIC	-0,869042746	-0,635974761	-0,668313151	-0,024858959	0,233067985	0,643454191
MT000025	TC76399	XIIC	-0,876102846	-0,149249079	-0,150083761	0,414445747	0,726853767	0,564529507
MT000273	TC85752	XIIC	-0,912348341	-0,088763515	-0,40663321	-0,291927064	0,823584825	0,114706146
MT015025	BG58134	XIIC	-0,912552548	-0,341907084	0,015304813	0,361169187	0,570645464	0,345864373
MT008086	TC78078	XIIC	-0,926810153	-0,351294184	-0,069186362	-0,146990085	0,575515968	-0,07780372
MT008664	TC79056	XIIC	-0,951859497	-0,224126539	-0,04104988	-0,446352543	0,727732959	-0,40530266
MT009089	TC88519	XIIC	-0,954827211	-0,59768699	-0,115352883	0,093963873	0,357140221	0,209316757
MT006018	TC93488	XIIC	-0,991985466	-0,012269707	-0,198527661	-0,341423937	0,979715759	-0,14289628
MT008340	TC87239	XIIC	-1,004982367	-0,704352213	0,002058503	0,091317041	0,300630155	0,089258538
MT010666	TC81511	XIIC	-1,029654046	-0,308967091	-0,064547248	0,062625582	0,720686955	0,12717283
MT010678	TC89906	XIIC	-1,030622694	0,033472355	0,085361279	-0,125587032	1,064095048	-0,21094831
MT002843	TC80476	XIIC	-1,04307602	-0,372731399	-0,045750697	-0,578213393	0,670344621	-0,5324627
MT009065	TC88353	XIIC	-1,052230455	-0,597602593	-0,024389484	-0,347870589	0,454627862	-0,32348111
MT013576	TC81041	XIIC	-1,077650091	-0,10119847	0,07137465	-0,516292981	0,976451621	-0,58766763
MT015698	BG64851	XIIC	-1,078047075	-0,480946906	0,154263407	0,352021939	0,597100169	0,197758531
MT002415	TC79940	XIIC	-1,083412602	-0,297284218	-0,006518927	0,140376386	0,786128384	0,146895313
MT001674	TC87334	XIIC	-1,0910873	-0,505194859	-0,265093599	-0,313882806	0,585892441	-0,04878921
MT013511	TC80005	XIIC	-1,092318796	-0,174361334	0,355080323	n.v.*	0,917957461	n.v.*
MT001529	TC87000	XIIC	-1,197819219	0,472392943	0,120244217	0,248042829	1,670212162	0,127798612
MT003303	TC90424	XIIC	-1,212624614	-0,565751679	0,048851811	-0,690566846	0,646872935	-0,73941866
MT004763	TC88407	XIIC	-1,271281128	-0,127843848	0,214020347	-0,693975498	1,14343728	-0,90799585
MT010945	TC90487	XIIC	-1,339527923	-0,407224216	-0,591120951	-0,69712504	0,932303707	-0,10600409
MT004643	TC82677	XIIC	-1,361008455	0,313222319	-0,045026927	0,152962619	1,674230774	0,197989546
MT004876	TC82801	XIIC	-0,734651393	1,179221751	0,521399319	0,091847893	1,913873144	-0,42955143
MT006278	TC84165	XIIC	-0,456424663	1,216125208	-0,178846618	0,038658685	1,672549871	0,217505303
MT001602	TC87631	XIIC	-0,489907825	1,134440832	-0,030781145	-0,095964884	1,624348657	-0,06518374
MT001188	TC78456	XIIC	0,693941479	0,9942767	0,019856733	-0,411395786	0,30033522	-0,43125252
MT012110	TC91966	XIIC	0,672029673	0,92140563	0,031747893	-0,266130839	0,249375958	-0,29787873
MT011416	TC81177	XIIC	-0,14028875	0,883810076	0,150883624	-0,6431254	1,024098826	-0,79400902
MT006587	TC92688	XIIC	-0,179425579	0,848686145	0,232169353	-0,067591232	1,028111724	-0,29976059
MT014692	BF64714	XIIC	-0,429145646	0,837351322	-0,666957829	0,096331985	1,266496968	0,763289814
MT009071	TC88334	XIIC	-0,053086422	0,82875807	-0,083381617	-0,542429302	0,881844492	-0,45904769
MT015536	TC78577	XIIC	-0,667454784	0,820549075	-0,184418864	0,060614036	1,488003859	0,2450329
MT006918	TC84349	XIIC	-0,399609491	0,820543727	-0,355793811	-0,488675321	1,220153219	-0,13288151
MT002195	TC88019	XIIC	0,14523872	0,814631801	0,279299615	-0,365910099	0,669393081	-0,64520971
MT014587	TC86784	XIIC	-0,508910535	0,812367006	-0,402990505	0,075534784	1,321277541	0,478525289
MT003767	TC81542	XIIC	0,161231393	0,802111017	-0,016629797	0,157059812	0,640879624	0,173689609
MT015878	TC82587	XIIC	0,513078625	-0,818579373	0,081554819	-1,069347987	-1,331658	-1,15090281
MT007517	TC77378	XIIC	0,104801827	-0,86415902	-0,325129971	-0,205394836	-0,96896085	0,119735135
MT007608	TC76532	XIIC	-0,203721594	-0,87514991	-0,633063632	-0,215945201	-0,67142832	0,417118432
MT000976	TC86722	XIIC	-0,404755641	-0,981822371	-0,248192168	-0,103365647	-0,57706673	0,14482652
MT007688	TC77428	XIIC	-0,805567012	-0,988940565	0,151514941	-0,23770946	-0,18337355	-0,3892244
MT008323	TC87140	XIIC	-0,508197378	-1,034369582	-0,421892027	0,350014848	-0,5261722	0,771906875
MT010267	TC89661	XIIC	-0,188671913	-1,076949744	-0,071037945	0,341964776	-0,88827783	0,413002721
MT015426	TC77537	XIIC	-1,070948233	-1,132607591	0,633992452	-0,210619498	-0,06165936	-0,84461195

Supplementary Table S4 continued

ID	MtGI	FC	M_PB_4hai	M_SA_4hai	M_PB_12hai	M_SA_12hai	F_4hai	F_12hai
MT014739	AW69721	XIIC	-0,699984697	-1,203171567	-0,243476312	0,440479986	-0,50318687	0,683956298
MT012546	TC87092	XIIC	-0,032845855	-1,296036757	-0,476905083	0,075901954	-1,2631909	0,552807037
MT000081	TC76639	XIIC	0,870837236	0,812259059	0,418962415	0,456139397	-0,05857818	0,037176982
MT000408	TC77146	XIIC	-0,880763047	-0,941100605	0,393680791	-0,117509457	-0,06033756	-0,51119025
MT003596	TC88633	XIIC	-1,311470711	1,637726379	-0,110606492	-0,027421257	2,949197089	0,083185235
MT007631	TC86172	XIIC	-1,809579033	-0,952819036	0,561925673	-0,048704096	0,856759997	-0,61062977
MT010669	TC79382	XIIC	-1,421425515	-1,787815871	0,697675014	-0,712814938	-0,36639036	-1,41048995
MT014439	TC86482	XIIC	-0,906136088	-0,920525588	0,457111921	-0,618682781	-0,0143895	-1,0757947
MT015852	TC91302	XIIC	-0,914062519	0,806724028	-0,270225168	-0,118522626	1,720786547	0,151702541
MT009654	TC78871	XIIC	0,682725235	-0,152509345	0,922401937	0,356659048	-0,83523458	-0,56574289
MT013395	TC84308	XIIC	0,18562007	-0,299919536	0,900643935	0,500549512	-0,48553961	-0,40009442
MT001641	TC87051	XIIC	0,561646023	0,261750674	0,885053079	0,380164501	-0,29989535	-0,50488858
MT014404	TC85985	XIIC	-0,529232841	-0,657791691	-0,810874135	0,147370449	-0,12855885	0,958244584
MT002460	TC89035	XIIC	0,051227548	-1,157784039	-1,304602804	0,585191613	-1,20901159	1,889794417
MT004938	TC84340	XIIC	-0,059356807	-0,122260508	0,125982601	1,007132938	-0,0629037	0,881150337
MT005377	TC84485	XIIC	-0,010708412	0,146591669	-0,443595509	0,977989884	0,157300082	1,421585393
MT002086	TC79688	XIIC	-0,040650625	-0,849861512	-0,425855629	0,977087345	-0,80921089	1,402942974
MT002224	TC87920	XIIC	-0,263477176	-0,920406833	-0,204118178	0,962065516	-0,65692966	1,166183694
MT001031	TC77980	XIIC	-0,027601758	-0,458456894	0,449160838	0,961389522	-0,43085514	0,512228684
MT001039	TC86864	XIIC	0,082274091	0,143014247	0,285783045	0,898194742	0,060740156	0,612411697
MT008207	TC77959	XIIC	-0,291430246	-0,118769645	0,360885571	0,885859477	0,172660601	0,524973906
MT015454	BI30951	XIIC	0,021819807	-0,53151329	0,149397388	0,835046592	-0,5533331	0,685649204
MT015628	TC78426	XIIC	0,050428347	-0,193162752	-0,157687357	-0,8088599	-0,2435911	-0,65117254
MT012595	TC92329	XIIC	0,211466377	-0,08694406	-0,082720347	-0,82703037	-0,29841044	-0,74431002
MT015627	TC79321	XIIC	-0,047139683	-0,025031376	0,529744871	-0,999657988	0,022108307	-1,52940286
MT015165	TC85296	XIIC	0,095559945	0,571793903	-0,6244707	-1,2260959	0,476233958	-0,6016252
MT001805	TC79328	XIIC	0,727271965	-0,412442058	-1,363563083	-1,865857741	-1,13971402	-0,50229466
MT000258	TC76869	XIIC	0,902975001	-0,652757911	-1,00062561	0,145819496	-1,55573291	1,146445106
MT015302	TC76952	XIIC	1,462782782	0,585953087	-0,98425365	-0,994301823	-0,8768297	-0,01004817
MT006284	TC83627	XIIC	-1,087335653	0,429928344	0,250051524	0,887806422	1,517263997	0,637754898
MT007297	TC76955	XIIC	0,82139406	0,204129951	-0,793059025	-1,057818124	-0,61726411	-0,2647591
MT003593	TC88705	XIIC	1,404562479	0,791424271	0,758731705	1,157793868	-0,61313821	0,399062163
MT003446	TC87092	XIIC	-0,714784804	-2,067426232	-1,852534517	-0,154418886	-1,35264143	1,698115631
MT009271	TC79339	XIIC	1,005583478	0,913343232	-1,253350791	-0,297564569	-0,09224025	0,955786222
MT007367	TC77132	XIIC	-1,209825297	2,089955001	1,177019332	1,144232182	3,299780298	-0,03278715
MT003758	TC81593	XIIC	1,548428621	1,182839085	1,244519582	1,501394462	-0,36558954	0,25687488
MT010824	TC90049	XIIC	-0,482605823	1,016548463	-0,155180387	-0,203117047	1,499154286	-0,04793666
MT000892	TC86599	XIV	2,374437885	0,273946171	-0,437407652	n.v.*	-2,10049171	n.v.*
MT000653	TC86446	XIV	1,085390521	0,28511558	0,631818306	0,571590837	-0,80027494	-0,06022747
MT010495	TC89769	XIV	1,045517681	0,27817879	0,354803471	-0,112084645	-0,76733889	-0,46688812
MT014812	TC91446	XIV	0,932561728	0,166813879	0,41944509	-0,318533264	-0,76574785	-0,73797835
MT014923	TC92139	XIV	0,923001498	0,182892609	0,395971234	0,379952748	-0,74010889	-0,01601849
MT013829	TC91771	XIV	0,884026619	0,004152001	0,780951069	0,158943076	-0,87987462	-0,62200799
MT015611	TC87738	XIV	0,875045431	-0,507404907	0,404658568	0,142049639	-1,38245034	-0,26260893
MT015958	TC92603	XIV	0,861015754	-0,106788685	0,127334716	-0,16935619	-0,96780444	-0,29669091
MT014774	TC81492	XIV	0,858459227	0,532148517	0,03508607	-0,36953508	-0,32631071	-0,40462115

Supplementary Table S4 continued

ID	MtGI	FC	M_PB_4hai	M_SA_4hai	M_PB_12hai	M_SA_12hai	F_4hai	F_12hai
MT000158	TC76697	XIV	-0,801601879	-0,359134549	-0,234058735	-0,584453723	0,44246733	-0,35039499
MT006062	TC84829	XIV	-0,806108436	0,729235315	-0,006998039	0,046783469	1,535343751	0,053781508
MT013126	TC84850	XIV	-0,842717739	-0,343336389	0,162050346	0,199538863	0,499381351	0,037488517
MT011916	TC81165	XIV	-0,870114011	-0,604878772	0,205253115	0,553868594	0,265235239	0,348615479
MT014669	TC80141	XIV	-0,920203863	-0,400763311	-0,479156651	0,358005549	0,519440553	0,8371622
MT014823	TC90780	XIV	-0,9487841	-0,507412049	-0,328475213	n.v.*	0,441372051	n.v.*
MT005922	TC82086	XIV	-0,991177824	-0,17473061	-0,098971801	-0,440764411	0,816447214	-0,34179261
MT014411	TC86379	XIV	-1,021385492	0,370101602	-0,172774717	-0,455335931	1,391487095	-0,28256121
MT004125	BE94108	XIV	-1,074372056	-0,680053691	-0,321380798	n.v.*	0,394318365	n.v.*
MT015596	BE20409	XIV	-1,779858633	1,115810417	-0,063247343	-0,547213766	2,89566905	-0,48396642
MT003320	TC89154	XIV	0,484226077	0,979336288	0,245620796	0,571458835	0,49511021	0,325838039
MT008604	TC87488	XIV	-0,223807704	0,917418636	-0,122430525	0,012736352	1,14122634	0,135166877
MT006231	TC83613	XIV	-0,401993977	0,819063818	-0,307338701	-0,18140349	1,221057795	0,125935211
MT015347	AW68680	XIV	0,620001919	0,813973351	-0,010439571	0,432261723	0,193971433	0,442701295
MT005099	TC83594	XIV	-0,733814083	-0,835921515	-0,229221127	0,490356041	-0,10210743	0,719577168
MT014529	TC78304	XIV	-0,56629637	-1,34815706	-0,569169765	-0,214729389	-0,78186069	0,354440376
MT006841	TC83641	XIV	-0,500991224	-1,645377594	0,033744589	-0,037177763	-1,14438637	-0,07092235
MT015703	TC88700	XIV	1,345142542	1,473384216	1,014238228	1,8155235	0,128241674	0,801285272
MT012877	BQ15051	XIV	0,386325104	-0,219548985	1,000976762	0,508168573	-0,60587409	-0,49280819
MT003782	TC89951	XIV	-0,22672127	-0,537672865	0,896183627	0,745715814	-0,31095159	-0,15046781
MT007409	No homolo	XIV	-0,401821712	-0,74002909	0,832908432	-0,250781853	-0,33820738	-1,08369028
MT008940	TC79463	XIV	-0,363662338	-0,120754494	-0,802459319	-0,230770966	0,242907844	0,571688353
MT012205	TC80302	XIV	0,444448083	-3,77795307	-1,048480545	0,733355138	-4,22240115	1,781835684
MT015036	TC93762	XIV	0,085846983	-0,476601721	-1,059958169	-0,54929171	-0,5624487	0,510666459
MT015913	TC91945	XIV	0,294881296	0,57470668	0,725215222	1,299016347	0,279825384	0,573801125
MT011400	TC91514	XIV	-0,649192091	-0,297370873	-0,432096399	0,969789231	0,351821218	1,40188563
MT004065	TC82608	XIV	0,189646392	-1,995284538	-0,246559887	0,882649773	-2,18493093	1,129209659
MT003404	TC81242	XIV	-0,234219253	0,449691038	-0,21704507	-0,813636102	0,683910291	-0,59659103
MT005448	TC93242	XIV	0,627181872	0,565650326	0,961763588	0,825036592	-0,06153155	-0,136727
MT000936	TC78069	XIV	2,025455392	0,371944387	1,505813858	1,031724746	-1,65351101	-0,47408911
MT009367	TC79510	XIV	0,346255881	0,190556093	-1,162146808	-1,047678843	-0,15569979	0,114467965
MT009425	TC89030	XIV	0,085062152	0,127416003	-0,347190641	1,16739418	0,042353851	1,514584821

Fig. S1 *Erysiphe pisi* (*E. pisi*) development on *Medicago truncatula* leaves genotypes analyzed in this assay. **a** Macroscopic disease symptoms in Parabinga before *E. pisi* inoculation. **b** Macroscopic disease symptoms in SA1306 before *E. pisi* inoculation. **c** Macroscopic disease symptoms in Parabinga fourteen days after *E. pisi* inoculation. **d** Macroscopic disease symptoms in SA1306 fourteen days after *E. pisi* inoculation. **e** Microscope pictures of *E. pisi* development on Parabinga leaf epidermal cells. C= conidium; PH= Primary hyphae; SH= Secondary hyphae. **f** Microscope pictures of *E. pisi* development on SA1306 leaf epidermal cells. EDC= Epidermal death cell.

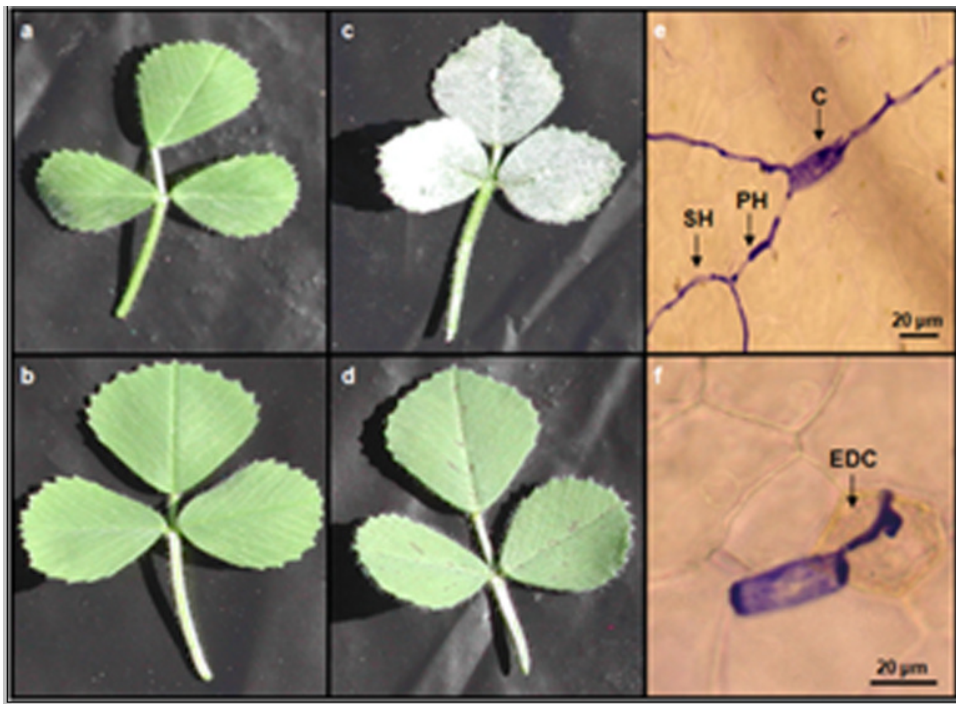

Chapter 4: Transcriptional regulation network of *Medicago truncatula* during *Erysiphe pisi* infection

Transcriptional regulation network of *Medicago truncatula* during *Erysiphe pisi* infection

Miguel Curto[1*], Franziska Krajinski[2], Armin Schlereth[2], Diego Rubiales[1]

[1]Institute for Sustainable Agriculture, CSIC, Apdo.4084, E-14080, Córdoba, Spain.
[2]Max Planck Institute of Molecular Plant Physiology, Science Park, 14476 Potsdam-Golm, Germany.

*To whom correspondence should be addressed:

Miguel Curto

Institute for Sustainable Agriculture, CSIC, Apdo. 4084, E-14080 Córdoba, Spain.

E-mail: b72curum@uco.es

Tel: +34 957199215

Fax: +34 957499252

Email addresses:

MC: b72curum@uco.es
FK: krajinski@mpimp-golm.mpg.de
AS: schlereth@mpimp-golm.mpg.de
DR: diego.rubiales@ias.csic.es

Paper submitted on 31 July 2014; current status: under review

Abstract

Resistance to powdery mildew has been studied in a number of plant species, yet the molecular mechanisms remain largely unknown. Transcription factors (TFs) play a critical role in the plant defense response by regulating the transcriptional machinery which coordinates the expression of a large group of genes involved in plant defense. Using high-throughput quantitative real-time PCR (qPCR) technology more than 1,000 *Medicago truncatula* TFs were screened in a pair of susceptible and resistant genotypes of *M. truncatula* after 4 h of *Erysiphe pisi* infection. Seventy nine TF genes, belonging to 33 families showed a significant transcriptional change in response to *E. pisi* infection. Forty eight TF genes were differentially expressed in the resistant genotypes compared to the susceptible one in response to *E. pisi* infection, including pathogenesis-related transcriptional factor/ethylene response factor (AP2/EREBP), WRKY, MYB and homeodomain (HD) gene families involved in known defense responses. Our results suggest that these TF genes are among the *E. pisi* responsive genes in resistant *M. truncatula* that may constitute a regulatory network which controls the transcriptional changes in defense genes involved in resistance to *E. pisi*.

Keywords: *Erysiphe pisi*, Legumes, *Medicago truncatula*, Transcriptomics.

Introduction

Plants grown in the natural environment are confronted by a variety of pathogens. Remaining healthy depends on their ability to recognize pathogens and to activate defense mechanisms against them. The plant defense responses are regulated by a broad number of signaling pathways. Transcription factors (TFs) control the transfer of genetic information from DNA to RNA by activation or repression of transcription, playing important roles in plant development and defense by regulating different signaling pathways (Singh et al. 2002; Udvardi et al. 2007). Data from several plant genome projects suggest that more than five percent of the plant genome encodes TF sequences (around 2,000 TFs) (Riechmann and Ratcliffe 2000). Therefore, many biologic processes, including responses to pathogens, are controlled by multiple genes managed by TFs (Singh et al. 2002). Several analyses have shown their differential expression in plants as responses to interactions with biotic and abiotic effectors (Udvardi et al. 2007). It is contradictory that in spite of the importance of legumes as source of protein and oil, and taking part in the symbiotic nitrogen fixation, only less than one percent of the transcript-specific regulation roles of TFs have been characterized (Udvardi et al. 2007). Among legumes, *Medicago truncatula* is a model presenting several biologic key attributes such as self-fertility, rapid generation time and small diploid genome (Singh et al. 2007) that have facilitated the use of molecular and genetic tools (Rose 2008).

Powdery mildews are biotrophic plant pathogens that seriously constraint crop production worldwide (Bélanger et al. 2002). Especially *Erysiphe* spp. causes considerable losses in various important legume crops (Sillero et al. 2006). This fungus has been classified into three physiologically specialized forms, f.sp. *pisi* specialized on *Pisum*, f.sp. *medicaginis* specialized on *Medicago*, and f.sp. *vicia sativa*, specialized on

Vicia (Falloon and Viljanen-Rollinson 2001). Breeding for powdery mildew resistance is the most desirable strategy to control this disease by means of resistant cultivars (Fondevilla and Rubiales 2012). Consequently, several genes involved in resistance to powdery mildew have been reported in different plant species (Barilli et al. 2014; Curto et al. 2014; Fondevilla et al. 2007, 2008; Yang et al. 2013). Resistance to *E. pisi* in *M. truncatula* has been reported and resistance mechanisms histologically (Prats et al. 2007) and genetically (Ameline-Torregrosa et al. 2008) characterized, however molecular mechanisms involved in the plant defense are poorly understood (Panstruga and Spanu 2014). Because TFs are transcribed at low levels, a sensitive and efficient method is required for their study. qPCR satisfies this requirements and several platforms have been established for different plant models, such as *Arabidopsis thaliana* and *Medicago truncatula* (Czechowski et al. 2004; Kakar et al. 2008). The aim of the present study was to identify the transcription factor-encoding genes involved in the *E. pisi*/*M. truncatula* pathosystem, and to provide a model for the regulatory network controlling the expression of TF genes in this pathosystem.

Materials and methods

Plant material, growth conditions and inoculation

The study was performed through an analysis of two genotypes of *M. truncatula*, the commercial cultivar (cv.) Parabinga and the accession SA1306, shown to be susceptible and resistant, respectively to *E. pisi* f. sp. *medicaginis* (Curto et al. 2014).

The seeds of *M. truncatula* were pre-soaked in filter paper, kept in darkness conditions at 4ºC for 24 h, and germinated in dark for 48 h in a growth chamber at 65% relative humidity and 20°C. The seedlings were placed on pots (125 ml) containing a 1:1 mixture of perlite and sand substrate, fertilized with half-strength Hoagland's solution (Hoagland and Arnon 1950) three times a week, and grown (25ºC, 12 h photoperiod, 250 µmol/m^2 light intensity, 80% relative humidity) during four weeks until the plant inoculation.

As pathogen, we used the isolated CO05 of *E. pisi* f. sp. *medicaginis* derived from a mildew population collected on *M. truncatula* plants at Córdoba (Prats et al. 2007). It was maintained and propagated by infecting Parabinga plants, until the inoculation. One day before inoculation the highly infected plants were shacked to remove old conidia in order to produce an inoculum with vigorous young spores. The plant inoculation was carried out equally in both lines using a setting tower to give an inoculum density of 5 conidia mm^{-2} (Prats et al. 2007). Three independent biological replicates were performed in both *M. truncatula* genotypes studied.

RNA extraction, cDNA synthesis and qPCR assays

Leaflets of both *M. truncatula* genotypes were harvested four hours after *E. pisi* inoculation, as resistance responses begin at early infection stages (Prats et al. 2007). The samples were immediately washed with water, blot dried with filter paper, frozen in

liquid nitrogen and stored at -80ºC until RNA extraction. RNA was purified from collected samples using the Nucleospin RNA II kit (MACHEREY-NAGEL, Bethlehem, USA) following the manufacturer's procedure (Vogelstein and Gillespie 1979). The integrity of total RNA was assessed on 1% agarose gels (samples were denatured in formaldehyde/formamide buffer), as well as its quantity and purity by using a Nanodrop Spectrophotometer ND-100 (NanoDrop Technologies, Wilington, DE) to measure the optical density. RNA samples were digested with RNase-free DNase1 (Ambion Inc., Houston, TX), according to the manufacturer's protocol. The absence of genomic DNA was checked by PCR analysis using primers designed on the *M. truncatula* ubiquitin gene intron sequence (Kakar et al. 2008).

The synthesis of the first-strand cDNA was carried out with oligo-dT12–18 (Qiagen, Hilden, Germany), using SuperScript III reverse transcriptase (Invitrogen GmbH, Karlsruhe, Germany). The efficiency of cDNA synthesis was performed by qPCR amplification of 5` and 3` regions of two reference genes, GAPDH (*Glyceraldehyde 3 phosphate dehydrogenase*) and Ubiquitin (Kakar et al. 2008). A single peak in the dissociation curve at the end of the PCR reaction confirmed the specificity of the amplification.

A *M. truncatula* transcription factor platform composed of more than 1,000 *Medicago truncatula* TFs gene-specific primers was used to carry out the real-time quantitative PCR (qPCR) experiments (Kakar et al. 2008). The qPCR reactions were carried out per triplicate in an optical 384-well plate with an ABI PRISM® 7900 HT Sequence Detection System (Applied Biosystem, Foster City, CA, USA) as described (Kakar et al. 2008).

Normalization and data analysis

SDS software ver. 2.3 (Applied Biosystems) was used to analyze fluorescent signals and calculate the quantification cycle (Cq) (Bustin et al. 2009). The baseline data were collected from the fluorescence signal between cycles 3 to 15, and used to correct the fluorescence signal of the samples. The PCR efficiencies (E) and correlation coefficients (R^2) from linear regression analysis were calculated for each performed PCR reaction by the software LinRegPCR ver. 7.5 as described (Kakar et al. 2008) (Table S1). The amplification reactions with $R^2 < 0.99$ that showed efficiencies lower than 1.8 were excluded for further analysis (24.4 % of reactions). TF genes were considered detected if they were expressed in at least two biological replicates with a Cq<40.

Eight reference genes encoding *Pentatricopeptide repeat protein* (PPRrep; TC96273), *Protein phosphatase 2A subunit A3* (PDF 2; TC107161), *Polypyrimidine tract-binding protein homolog* (PTB; TC111751), *Helicase* (CB892427), *Ubiquitin* (TC102473), *Ubiquitin-protein ligase 7* (UPL7; TC111218), *Ubiquitin-conjugating enzyme E2* (UBC; AW686873) and *Ubiquitin-conjugating enzyme E2 9* (UBC9; TC106312) (Kakar et al. 2008) were studied in order to determine the best suited reference genes for transcript normalization. The expression stability of the eight reference genes was analyzed by the geNorm software (Hellemans et al. 2007; Vandesompele et al. 2002) for each cDNA sample under study. In addition, pair-wise comparison analysis allowed determining the optimal number of reference genes in this assay (Vandesompele et al. 2002).

Expression values were calculated from E^{Cq} of each individual plot. To normalize the gene expression of each PCR reaction, ratios of the geometric mean of the selected reference genes to the different biological conditions were used using the formula:

($E_{ref}^{(Cq\ ref)}/E_{gene}^{(Cq\ gene)}$). The relative induction/repression of TFs from *E. pisi* infected samples compared to untreated samples was calculated using the formula: $((E_{ref}^{(Cq\ ref)}/E_{gene}^{(Cq\ gene)})_{infected\ condition} /(E_{ref}^{(Cq\ ref)}/E_{gene}^{(Cq\ gene)})_{untreated\ condition}$).

Non-parametric Levene´s test and Spearman´s correlation coefficient were used to verify the equality of variances in the samples and to study the similarity between TF gene expression profiles, respectively. In addition, a factorial analysis of variance (Kruskal-Wallis ANOVA) was also performed to measure the similarity between gene expression profiles as well as between samples. TF genes showing statistically significant differences ($P<0.05$) were clustered using a hierarchical cluster analysis by complete linkage. A model for the regulatory network controlling the expression of regulated genes induced by *E. pisi* in both *M. truncatula* genotypes studied was built using NodeXL (http://nodexl.codeplex.com).

Results

Evaluation of resistance in *Medicago truncatula* genotypes

Leaflets for qPCR profiling were harvested four hours after *E. pisi* inoculation. Differences in the response to *E. pisi* between the two genotypes were not yet visible at the time the leaves were sampled for RNA extraction. Powdery mildew infection was macroscopically clearly visible on remaining leaflets two weeks after inoculation, with profuse sporulation in the susceptible Parabinga genotype and absence of symptoms in the resistant SA1306 genotype (Fig. 1). Thus, previous studies revealed a lower ability of *E. pisi* to develop fungal structures in SA1306 genotype (Curto et al. 2014). Hence, colony formation was much higher in Parabinga than in SA1306. In addition, the hypersensitive response associated with epidermal cell death was negligible in Parabinga, but marked in SA1306 (Curto et al. 2014).

Selection of reference genes

Eight reference genes were studied to determine the best suited ones for transcript normalization. All reference genes showed high average expression stability (M <0.66), among them the *UBC9*, *Helicase*, *PTB* and *UPL7* reference genes showed the lower average expression stability (M) indicating a greater transcript stability (Fig. 2a). The pair-wise variation (V) was also calculated allowing to determine the effect of adding a gene ($V_{n/n+1}$), indicating that the inclusion of a third gene ($V_{3/4}$) or more genes ($V_{4/5}$, $V_{5/6}$, $V_{6/7}$ and $V_{7/8}$) has no significant effect. Thus, the $V_{2/3}$ was the highest V value (Fig. 2b) indicating that the optimal number reference targets in this experimental situation is two. Therefore, the two reference genes that showed the higher transcript stability, *UBC9* and *Helicase*, were selected as the best reference genes for this experiment and used for transcript normalization of the analyzed TF genes.

Expression patterns of TF genes in *M. truncatula* following *E. pisi* infection

We analyzed and compared the expression patterns of TF genes in the susceptible cv. Parabinga and the resistant SA1306 genotypes (Fig. 1). Previous histological assessments, confirmed the resistance and susceptibility to *E. pisi* of SA1306 and Parabinga genotypes (Curto et al. 2014). The qPCR TF platform allowed identifying the TF genes differentially expressed in the resistant SA1306 and the susceptible Parabinga *M. truncatula* genotypes in response to *E. pisi* infection. A total of 623 genes of the qPCR TF platform (59.6%) were considered detected (Cq<40; n≥2) and 95 from them showed statistically significant differences (P<0.05). We studied the expression pattern of these genes that showed statistically significant differences through a hierarchical clustering analysis based on gene expression profiles (Fig. 3, Table S2). Genes were considered differentially up- or down-regulated if they met the prerequisites p≤0.05 and

M≥0.7 or M≤-0.7, respectively. The genes were clustered into ten groups with different expression patterns (Fig. 3a).

The first group (GI) includes 15 genes that were down-regulated in SA1306. Moreover, in Parabinga seven of these genes were not expressed differentially and eight were regulated, one of which (TF233) was up-regulated and seven were repressed, respectively (Fig. 3b). These genes belong to twelve TF families, three Zn-Finger members (C_2H_2 (Zn), TTF-type (Zn) and LIM), AP2/EREBP, AUX/IAA, bHLH, BTB/POZ, E2F, HMG, MYB/HD-like, NAC and SBP TF families (Table S2). The second group (GII) includes thirteen genes which were down-regulated in Parabinga, except for one gene (TF631) that was not expressed differentially. Moreover, in the resistant SA1306 genotypes six of these genes were regulated, three were up-regulated (TF626, TF913 and TF962) and the other three repressed (TF265, TF393 and TF716). Of the thirteen genes included in the second group, four belong to Zn-finger families, three are C_2C_2 (Zn) genes and one gene (TF767) belongs to the C_3H-type I (Zn) family. The remaining genes belong to AP2/EREBP, DDT, HD, HD-like, HSF, NAC, RR and WRKY TF families.

Groups III, IV and V include genes that were induced in both genotypes. Group III contains six genes which showed lower transcription levels in SA1306 than in Parabinga. These genes belong to AP2/EREBP, HD, HD-like, MYB and MYB/HD-like TF families. Moreover, group IV includes nine genes that showed a stronger transcription activation in the resistant SA1306 genotype. These genes belong to bHLH, C_2H_2 (Zn), HD, HD-like, MADS, MYB and PHD TF families. Group V contains ten genes that showed similar up-regulation expression patterns in both susceptible and resistant genotypes, except for four genes (TF136, TF386, TF473 and TF497) which were expressed more in Parabinga. Genes of this fifth group encode proteins belonging

to AP2/EREBP, ARF, bHLH, GRAS, HD, HTH, NAC, RR and DHHC (Zn) TF families.

Genes clustered in groups VI and VII were mainly not expressed differentially in both genotypes. None of the genes included in group VI were regulated whereas seven of the eleven genes of group VII were regulated. The TF97, TF140 and TF537 genes were induced in both genotypes and they are members of HD-like, PHD and bZIP TF families, respectively. The remaining four regulated genes of group VII were specifically up-regulated in Parabinga (TF429, TF588) and SA1306 (TF372, TF464), respectively. These genes are included in HD (TF372, TF588), bZIP (TF464) and MYB/HD-like (TF429) TF families.

Group VIII includes six genes which were induced in Parabinga and not differentially expressed in SA1306. These genes belong to bHLH, FHA, MYB/HD-like and three Zn-finger TF families (C_2C_2, CCHC and U1-type). The eight genes included in group IX were induced in SA1306, whereas in Parabinga half of them were up-regulated (TF200, TF552, TF797 and TF814) and the remaining genes were not expressed differentially. Genes of group IX are members of ARID, C_2H_2 (Zn), HD, HD-like, NAC and SBP TF families. Finally group X includes eight genes which were mostly up-regulated in SA1306 and not differentially expressed in Parabinga. All genes belonging to this group were induced in the resistant genotype, except for two genes (TF295 and TF562) that were not expressed differentially. Meanwhile, only one repressed gene (TF660) was detected in Parabinga. The genes of this last cluster belong to Zn finger families C_2C_2, CCHC, HD, HD-like, JUMONJI, MYB/HD-like and SBP TF families.

Transcription factor regulatory network induced by *E. pisi* infection in *M. truncatula*

The qPCR platform allowed the identification of TF genes expressed differentially in the two *M. truncatula* genotypes in response to *E. pisi* infection. These genotypes show phenotypic differences in response to *E. pisi* infection (Fig. 1), such as profuse sporulation, colony formation and hypersensitive response associated with epidermal cell death (Curto et al. 2014). We analyzed and compared the gene expression profiles of these genes in order to determine if and how their gene expression was affected by *E. pisi* infection among both genotypes. Around eighty percent of TF genes (79/95 genes) that showed statistically significant differences ($P<0.05$) were regulated at least 1.6-fold changes ($0.7 \geq M \geq 0.7$) (Table S3). To study the regulatory network controlling the expression and interactions of these seventy nine genes during *E. pisi* infection, we further analyzed their expression in the susceptible Parabinga and the resistant SA1306 genotypes.

Our analysis revealed that 16 and 18 of the 79 TF genes were specifically regulated in Parabinga and in SA1306, respectively. The remaining 45 genes were regulated in both genotypes (Fig. 4, Table S3). In the susceptible Parabinga genotype 10 of the 16 specifically regulated genes were induced and the remaining 6 genes were repressed. Most of the ten genes specifically induced in Parabinga are members of MYB/HD-like (TF143, TF429 and TF934), HD (TF588) and C_2C_2 (TF389), CCHC (TF349) and U1-type (TF179) Zn finger families. The rest of the up-regulated genes belong to RR (TF276), FHA (TF481) and bHLH (TF1007) TF families. Moreover, the six genes specifically down-regulated in Parabinga are included in RR (TF448), AP2/EREBP (TF546), NAC (TF598), HD-family (TF618), C_3H- type 1 (Zn) (TF767) and DDT (TF822) TF families. Meanwhile the resistant SA1306 genotype showed 11 and 7 genes specifically up- and down-regulated, respectively. Four of the 11 genes specifically

induced in SA1306 are members of HD/HD-like (TF158, TF372, and TF666) and MYB/HD-like (TF726) TF families. The remaining seven up-regulated genes belong to SBP (TF540, TF901), C_2C_2 (Zn) (TF308), C_2H_2 (Zn) (TF982), bZIP (TF464), ARID (TF27) and JUMONJI (TF1009) TF families. Moreover, the genes down-regulated in SA1306 are included in LIM (TF8), C_2H_2 (Zn) (TF101), TTF-type (Zn) (TF388), MYB/HD-like (TF244), bHLH (TF425), E2F (TF691) and AUX/IAA (TF780) TF families.

The genes regulated in both genotypes were mainly up-regulated, displaying 30 induced and 10 repressed genes, respectively. Most of these thirty induced genes are included in HD-like, HD and MYB TF families (Fig. 4, Table S3). In addition, a subset of these induced genes belong to bHLH (TF333, TF600, TF639), Zn finger families (TF87, TF270, TF428), AP2/EREBP (TF3, TF473), NAC (TF136, TF200), PHD (TF140, TF879), MADS (TF322, TF563), GRAS (TF296), ARF (TF386), bZIP (TF537) and HTH (TF565) families. In addition, the ten repressed genes are included mainly in Zn finger families, C_2C_2 (TF265, TF393, TF716) and C_2H_2 (TF823). The remaining down-regulated genes are included in AP2/EREBP (TF303, TF855), SBP (TF436), NAC (TF479), bHLH (TF485), and BTB/POZ (TF700) families. Interestingly, four of five common regulated genes were induced in SA1306 and repressed in Parabinga, and belong to HD- like (TF626), CCHC (Zn) (TF660), WRKY (TF913) and AP2/EREBP (TF962) TF families. The fifth remaining gene TF233 (HMG) was up-regulated in Parabinga and repressed in SA1306.

A total of 48 out of the 79 regulated genes ($P<0.05$; $-0.7 \geq M \geq 0.7$) in SA1306, were specially assessed in this study for showing a differential expression in SA1306 compared to Parabinga ($-0.7 \geq F \geq 0.7$) in response to *E. pisi* infection, and they belong to 25 TF families (Table 1, Table S3). Among them, the most represented TF families are

HD-like, C_2H_2 (Zn), AP2/EREBP, MYB/HD-like and HD/HD, which include around half of the genes. The bHLH, C_2C_2/DOF (Zn), HD/HD-ZIP, MYB, NAC and SBP TF families are also represented (4% each). The rest of TF families include only one gene (Table 1). Eleven of 25 families include genes expressed more ($F \geq 0.7$) in SA1306 than in Parabinga. Among them, the genes belonging to ARID, WRKY family/WRKY, C_2C_2 (Zn)/DOF, SBP, HD-like, MADS and CCHC (Zn) families were expressed around two fold in SA1306 compared to Parabinga. Meanwhile only three families, TTF-type (Zn), bHLH and HMG, include genes that were expressed less ($F \leq -2$) in SA1306 than in Parabinga. Moreover, families HD/HD-ZIP and NAC include genes that were, in general, induced in both genotypes. However, the AP2/ERBP family was expressed more in SA1306 and almost not regulated in Parabinga (Table 1).

Discussion

High-throughput methods have allowed identifying genes potentially associated with specific processes and characterizing the regulatory networks that control their expression (Caldana et al. 2007; Czechowski et al. 2004). Among them, DNA microarray has been successfully used to characterize global gene expression patterns in *M. truncatula* (Curto et al. 2014; Dita et al. 2009; Foster-Hartnett et al. 2007; Samac et al. 2011; Zhang et al. 2014) providing detailed information of metabolic pathways involved in the analyzed systems. Previous studies have analyzed the *E. pisi/M. truncatula* pathosystem (Curto et al. 2014; Foster-Hartnett et al. 2007; Samac et al. 2011) using different genotypes and microarray platforms, such as Mt16kOLI1, Mt16kOLI1plus (Küster et al. 2004, 2007) and Affymetrix GeneChip® (http://www.affymetrix.com). These studies have increased the knowledge of mechanisms involved in *E. pisi* resistance in *M. truncatula*, which are agreement that a wide variety of mechanisms and pathways are involved in *E. pisi* resistance including pathogenesis-related genes (i.e. *PR10*, *Pprg2*), as well as other genes involved in signal transduction, cell wall metabolism and abiotic stress. In spite of DNA microarray has been shown to be five times less sensitive than real-time quantitative PCR (qPCR) (Czechowski et al. 2004), qPCR remains a technique used for low- to middle-scale studies due to its high cost. Several large-scale TF profiling approaches have employed the *M. truncatula* qPCR-based platform available (Kakar et al. 2008) in various studies (Gao et al. 2010; Madrid et al. 2010; Verdier et al. 2008; Villegas-Fernández et al. 2014). In this study, we screened the TF transcriptome of *M. truncatula* for altered expression during *E. pisi* infection using qPCR, and many novel TF genes as candidates for further functional studies have been unveiled. Previous histological assessments showed that the resistance mechanisms carried out by the resistant genotype SA1306 is

mainly related to hampering the spore germination and further colony establishment by epidermal cell death as a hypersensitive response to *E. pisi* germlings that reach to develop appressoria (Curto et al. 2014). Several mechanisms capable of monitoring changes in the cell wall are carried out by cellular signaling responses (Cheung and Wu 2011; Ringli 2010). We studied the expression patterns of more than 1,000 *M. truncatula* TFs genes (Kakar et al. 2008) in both *M. truncatula* genotypes in response to *E. pisi* infection, and found that 95 of the TF genes analyzed (15%) were expressed differentially. Similar proportion of regulated TF genes was found in response to infection by *Uromyces striatus* (≈13%) (Madrid et al. 2010) and *Botrytis* spp. (≈20%) (Villegas-Fernández et al. 2014). Forty eight out of the 95 TFs showed significant differences in the resistant SA1306 genotype compared to the susceptible Parabinga ($-0.7 \geq F \geq 0.7$) in response to *E. pisi* infection, suggesting that they play a critical role in the resistance mechanism against pathogen infection. Based on the results shown in Figure 4, we suggest a model for the regulatory network controlling the expression of the TF genes involved in *M. truncatula* resistance to *E. pisi*. A subset of these genes were specifically regulated in the resistant SA1306 genotype suggesting that they act as major regulators of transcription throughout *E. pisi* defense responses. These TF genes belong to ten TF families, AUX/IAA, bHLH, E2F, HD, JUMONJI, MYB and zinc finger families (C_2C_2, C_2H_2, LIM and SBP), which are involved in known defense pathways (Table 1).

Zinc finger families represent half of these genes specifically regulated in the resistant SA1306 genotype, and are members of C_2H_2 (Zn), SBP, C_2C_2/DOF and LIM TF families. The C_2H_2 (Zn) family constitutes one of the largest TF families in plants (Ciftci-Yilmaz and Mittler 2008), which playing a critical role as key transcriptional repressors involved in the defense response of plants to stress (Brayer and Segal 2008;

Ciftci-Yilmaz and Mittler 2008; Kiełbowicz-Matuk 2012). This results support those from the recent study reported that have used the same qPCR TF platform (Villegas-Fernández et al. 2014). Thus, C_2H_2 (Zn) TF genes should play an important role of the defensive reaction of *M. truncatula* to biotrophic and necrotrophic pathogens. Moreover, the SBP zinc transcription factor family has been characterized in many plant species showing diverse functions in the regulation of diverse biological processes (Hou et al. 2013). Thus, studies have reported the relationship between SBP genes and plant disease resistance, such as programmed cell death in *Arabidopsis* (Stone et al. 2005). Hence, previous studies are in agreement that programmed cell death, frequently associated to host cell death, is a common plant defence mechanisms against *E. pisi* (Barilli et al. 2014; Curto et al. 2006). In addition, a member of the SPB TF family (*VpSBP5*) has been reported to be induced by powdery mildew (*E. necator*) (Hou et al. 2013), suggesting that this TF is involved in the resistance to powdery mildew by inducing salicylic acid and methyl jasmonate molecular signals. Moreover, the family C_2C_2 (Zn)/ DOF is one the main one in plants that has divergent physiological roles (Yanagisawa 2002) including defense gene expression in response to salicylic acid and oxidative stress signals (Chen et al. 1996; Yanagisawa 2002) and phytohormone-regulated expression (De Paolis et al. 1996; Yanagisawa 2002). Recent studies have shown that *E. pisi* infection induce several enzymes, such as *psCHS1* and *PEAPAL2*, involved in phenylpropanoid biosynthesis leading to biosynthesis of phytoalexin production (Barilli et al. 2014), reinforcing the role of phenylpropanoid pathway in the elicited defence. Our findings are in agreement with these previous studies, suggesting the important role of these TF families in resistance to *E. pisi* in *M. truncatula*.

The LIM zinc TF family has also been characterized to be involved in the resistance mechanism against pathogens. Thus, several studies have revealed that this family has

the capacity to regulate the expression of some lignin biosynthetic genes (Rogers and Campbell 2004). Lignification has been shown to be an important mechanism in host defense against pathogen invasion. Thus, previous studies have reported the role of lignification processes into the *M. truncatula* defence responses against to *E. pisi* infection (Prats et al. 2007). Further studies have unveiled that lignification processes in the cell wall are linked to ROIs stress (Brady and Fry 1997; Brisson et al. 1994), as well as for signaling (Lamb and Dixon 1997). These results are in agreement with the experience of recent study (Barilli et al. 2014), in which enzymes involved in ROIs stress, such as peroxidase *Prx7*, are regulated in *M. truncatula* after *E. pisi* inoculation. In addition, further studies have found that monolignol biosynthesis plays a critical role in cell wall apposition mediated defense against powdery mildew fungus penetration (Bhuiyan et al. 2009). ROIs is associated with the hypersensitive response (Torres et al. 2005) which has been related to programmed cell death (hypersensitive response) that playing a critical role in resistance to *E. pisi* (Barilli et al. 2014).

Our results reveal also a subset of TF genes that encode TFs with a HD (homeodomain) protein domain, which showed a different expression pattern in the resistant SA1306 compared to the susceptible Parabinga genotype in response to *E. pisi* infection. These genes belong to HD-like and HD family/HD, respectively. The homeodomain protein domain is ubiquitous, and functions as a transcriptional regulator. Research studies have unveiled that this family may play a role in the defense response against fungal necrotroph pathogens regulated by jasmonic acid (Coego et al. 2005; Korfhage et al. 1994; Villegas-Fernández et al. 2014). One of these TF families, MYB/HD-like, encode HD and MYB domains which has highly diversified biological functions (Coego et al. 2005; Jin and Martin 1999; McGrath et al. 2005). In addition, a recent study has revealed that several homeodomain-like TF families are involved in the defence

responses in *M. truncatula* when confronted with necrotrophic pathogens, *B. fabae* and *B. cinerea* (Villegas-Fernández et al. 2014), supporting that this TF families may play an important role in the defensive mechanism of *M. truncatula* to fungal pathogens. Moreover, our results show that the Auxin/Indole-3-acetic acid (AUX/IAA) family was repressed in the resistant SA1306 genotype in response to *E. pisi* infection. This result suggests that this family may play a role in the resistance mechanism against *E. pisi*. Furthermore, previous studies have shown that pathogen infection results in imbalances in auxin levels as well as in changes in the expression of genes involved in auxin signaling. Hence, down regulation of auxin signaling has been shown to contribute to plant induced immune responses in *Arabidopsis* (Navarro et al. 2006). The bHLH transcription factors were also induced in the resistant genotype in response to *E. pisi* infection. Our findings are in agreement with the results obtained by Villegas-Fernández et al. (2014). In addition, the bHLH transcription factors shown to be include key TF regulating the expressions of jasmonic acid responsive genes (Fernández-Calvo et al. 2011), mediating the transcriptional reprogramming associated with the plant immune response.

Our results also indicate that E2F and JUMONJI TF families are involved in the defense response against *E. pisi*. The E2F transcription factor family has been described to induce the transcription of genes required for cell cycle progression and DNA replication (Vandepoele et al. 2005). In addition, more than one hundred E2F target genes have been identified, including genes involved in several processes as defense responses and signaling (Ramirez-Parra et al. 2003). On the other hand, JUMONJI is a TF family that plays a role in the histone methylation process (Li et al. 2013). Dimethylated or trimethylated histone H3 lysine 27 (H3K27me2/3) marks silent or repressed genes involved in stress responses in plants. Li et al. (2013) studied the

jumonji C protein gene *JMJ705* that is induced by stress signals during pathogen infection, and is involved in methyl jasmonate–induced dynamic removal of H3K27me3 and in gene activation increasing their basal and induced expression during pathogen infection (Balciunas and Ronne 2000; Li et al. 2013). It is noteworthy that recent studies have reported that JUMONJI TF family may be involved in the defence response to fungal pathogen, reinforcing the role of this TF family in the defence responses against fungal pathogens (Villegas-Fernández et al. 2014).

An important number of TF genes were equally regulated in Parabinga and SA1306 genotypes. Most of them were induced in both genotypes in response to *E. pisi* infection, including genes involved in plant disease resistance belonging to AP2/EREBP (Dietz et al. 2010; Gutterson and Reuber 2004; Singh et al. 2002; Villegas-Fernández et al. 2014), C_2H_2 (Zn) (Ciftci-Yilmaz and Mittler 2008; Villegas-Fernández et al. 2014), MYB (Singh et al. 2002; Villegas-Fernández et al. 2014), HD (Coego et al. 2005; Villegas-Fernández et al. 2014), MYB/HD-like (Coego et al. 2005; Singh et al. 2002), NAC (Dangl and Jones 2001; Villegas-Fernández et al. 2014) and PHD (Libault et al. 2007; Villegas-Fernández et al. 2014) TF families. Interestingly, the susceptible and resistant genotypes showed different expression patterns in five of these TF genes in response to *E. pisi* infection (Fig. 4). Four of these five genes (TF626, TF660, TF913 and TF962), encode TFs belonging to known defense system pathways, which were induced in SA1306 and repressed in Parabinga, respectively. TF962 encodes a member of AP2/EREBP (pathogenesis-related transcriptional factor and ethylene response factor) is known to be linked to the response to abiotic and biotic stresses (Dietz et al. 2010), as well as to be involved in the response to a chitin fungal elicitor and in the metabolism of the plant hormone methyl jasmonate (Libault et al. 2007; McGrath et al. 2005). Results obtained were similar to those generated in *M. truncatula* in response to

Botrytis infection, in which AP2/EREBP was shown to be a key in regulating defence response (Villegas-Fernández et al. 2014). TF913 encodes a WRKY protein, whose family has been shown to be a key component in the regulation of plant disease resistance (Eulgem and Somssich 2007). Previous studies have shown that WRKY TF family are involved in the regulation of *R* gene-mediated disease resistance as well as in the regulation of transcriptional reprogramming associated with plant immune responses (Eulgem and Somssich 2007). Thus, recent studies have provided conclusive genetic proof that WRKY factors are key regulators of the defense transcriptome and disease resistance (Buscaill and Rivas 2014; Eulgem and Somssich 2007).Hence, several genes encoding WRKY proteins (*AtWRKY18, AtWRKY40*) have been identified to confer resistance against to powdery mildew fungus (Shen et al. 2007). In addition, *AtWRKY18* have been characterized to act as a positive regulator required for full SAR (Wang et al. 2006), whose transcriptional expression may be is linked to *AtWRKY70* which modulate the cross-talk between signaling parthways regulating salicylic acid (SA)-dependent and jasmonic acid-dependent responses (Eulgem and Somssich 2007). These results are according with finding by recent studies in *M. truncatula*, which have described that WRKY TFs constitute the core of the defensive reaction of *M. truncatula* to *Uromyces* and *Botrytis* (Madrid et al. 2010; Villegas-Fernández et al. 2014), supporting the critical role of this TF family in the plant defence responses against to fungal pathogens.

The Zn finger family CCHC (TF660) was also detected as induced in SA1306 and repressed in Parabinga. This family plays important roles in plants (Ciftci-Yilmaz and Mittler 2008; Villegas-Fernández et al. 2014), due to the domain CCHC found in plant glycine-rich proteins (GRPs) class IVb. These proteins have been found to be involved in wide plant defense responses, such as the GRP protein *NtCIG1* from *Nicotiana tabacum* which plays a critical role in the callose deposition process reinforcing the cell

wall during plant defense responses against pathogens (Mangeon et al. 2010). In addition, several TF genes encoding CCHC TF proteins has shown to be involved in the defence response of *M. truncatula* against *Botrytis* spp. (Villegas-Fernández et al. 2014), which indicate that this family should play an important role in defence regulation responses. Moreover, a member of HD-like (TF626) was also induced in the resistant genotype and highly repressed in Parabinga. This family has been found to be involved in the defense response against fungal necrotroph pathogens regulated by jasmonic acid (Coego et al. 2005; Korfhage et al. 1994; Villegas-Fernández et al. 2014). Concerning the ten sequences that were commonly repressed in both genotypes, we suggest that they could play a role suppressing genes involved in photosynthetic metabolism reducing the photosynthetic rate, such as previously suggested (Bolton 2009; Swarbrick et al. 2006).

In spite of the progress in characterizing TFs, those involved in the expression of stress-related genes in plants remain undiscovered (Singh et al. 2002). Particularly, the TFs involved in the defense mechanisms against *E. pisi* need to be clarified in order to completely understand the mechanisms involved in the plant´s defense against this pathogen. We have identified a collection of TFs and suggest a regulatory network that controls the expression in *M. truncatula* of genes involved in resistance to *E. pisi*. These results will help to systematically decipher the functional roles of TF genes and to develop new strategies against powdery mildew.

Acknowledgments

This work was supported by the European Commission FP6 Framework Programme Grain Legume Integrated Project (FOOD-CT-2004-506223) and by Spanish project AGL2011-22524 co-financed by FEDER. We are grateful to Udvardi research Group (Max Planck Institute of Molecular Plant Physiology, Potsdam – Golm Germany) for advice and support and to Carolina Johnstone for grammatical review.

References

Ameline-Torregrosa C, Cazaux M, Danesh D, Chardon F, Cannon SB, Esquerré-Tugayé M-T, Dumas B, Young ND, Samac DA, Huguet T, Jacquet C (2008) Genetic dissection of resistance to anthracnose and powdery mildew in *Medicago truncatula*. Mol Plant-Microbe Interact 21:61-69

Balciunas D, Ronne H (2000) Evidence of domain swapping within the jumonji family of transcription factors. Trends Biochem Sci 25:274-276

Barilli E, Rubiales D, Gjetting T, Lyngkjaer MF (2014) Differential gene transcript accumulation in peas in response to powdery mildew (*Erysiphe pisi*) attack. Euphytica 195:1-16

Bélanger RR, Bushnell WR, Dik AJ, Carver TLW (2002) The powdery mildews: a comprehensive treatise. St Paul, MN, USA: APS Press.

Bhuiyan NH, Selvaraj G, Wei Y, King J (2009) Role of lignification in plant defense. Plant Signal Behav 4:158-159

Bolton MD (2009) Primary metabolism and plant defense-fuel for the fire. Mol Plant-Microbe Interact 22:487-497

Brady JD, Fry SC (1997) Formation of di-isodityrosine and loss of isodityrosine in the cell walls of tomato cell-suspension cultures treated with fungal elicitors or H_2O_2. Plant Physiol 115:87-92

Brayer KJ, Segal DJ (2008) Keep your fingers off my DNA: protein-protein interactions mediated by C2H2 zinc finger domains. Cell Biochem Biophys 50:111-131

Brisson LF, Tenhaken R, Lamb C (1994) Function of oxidative cross-linking of cell wall structural proteins in plant disease resistance. Plant Cell 6:1703-1712

Buscaill P, Rivas S (2014) Transcriptional control of plant defence responses. Curr Opin Plant Biol 20:35-46

Bustin SA, Benes V, Garson JA, Hellemans J, Huggett J, Kubista M, Mueller R, Nolan T, Pfaffl MW, Shipley GL, Vandesompele J, Wittwer CT (2009) The MIQE guidelines: minimum information for publication of quantitative real-time PCR experiments. Clin Chem 55:611-622

Caldana C, Scheible W-R, Mueller-Roeber B, Ruzicic S (2007) A quantitative RT-PCR platform for high-throughput expression profiling of 2500 rice transcription factors. Plant Methods 3:7

Ciftci-Yilmaz S, Mittler R (2008) The zinc finger network of plants. Cell Mol Life Sci 65:1150-1160

Coego A, Ramirez V, Gil MJ, Flors V, Mauch-Mani B, Vera P (2005) An *Arabidopsis* homeodomain transcription factor, *OVEREXPRESSOR OF CATIONIC PEROXIDASE 3*, mediates resistance to infection by necrotrophic pathogens. Plant Cell 17:2123-2137

Curto M, Camafeita E, Lopez JA, Maldonado AM, Rubiales D, Jorrín JV (2006) A proteomic approach to study pea (*Pisum sativum*) responses to powdery mildew (*Erysiphe pisi*). Proteomics 6:S163-S174

Curto M, Krajinski F, Schlereth A, Rubiales D (2014) Plant defense responses in *Medicago truncatula* unveiled by microarray analysis. Plant Mol Biol Rep, in press

Czechowski T, Bari RP, Stitt M, Scheible W-R, Udvardi MK (2004) Real-time RT-PCR profiling of over 1400 *Arabidopsis* transcription factors: unprecedented sensitivity reveals novel root- and shoot-specific genes. Plant J 38:366-379

Chen W, Chao G, Singh KB (1996) The promoter of a H_2O_2-inducible, *Arabidopsis* glutathione S-transferase gene contains closely linked OBF- and OBP1-binding sites. Plant J 10:955-966

Cheung AY, Wu H-M (2011) THESEUS 1, FERONIA and relatives: a family of cell wall-sensing receptor kinases? Curr Opin Plant Biol 14:632-641

Dangl JL, Jones JDG (2001) Plant pathogens and integrated defence responses to infection. Nature 411:826-833

De Paolis A, Sabatini S, De Pascalis L, Costantino P, Capone I (1996) A *rolB* regulatory factor belongs to a new class of single zinc finger plant proteins. Plant J 10:215-223

Dietz K-J, Vogel M, Viehhauser A (2010) AP2/EREBP transcription factors are part of gene regulatory networks and integrate metabolic, hormonal and environmental signals in stress acclimation and retrograde signalling. Protoplasma 245:3-14

Dita MA, Die JV, Román B, Krajinski F, Küster H, Moreno MT, Cubero JI, Rubiales D (2009) Gene expression profiling of *Medicago truncatula* roots in response to the parasitic plant *Orobanche crenata*. Weed Res 49:66-80

Eulgem T, Somssich IE (2007) Networks of WRKY transcription factors in defense signaling. Curr Opin Plant Biol 10:366-371

Falloon RE, Viljanen-Rollinson SLH (2001) Powdery mildew. Compendium of pea diseases and pests. APS Press, St. Paul, USA.

Fernández-Calvo P, Chini A, Fernández-Barbero G, Chico J-M, Gimenez-Ibanez S, Geerinck J, Eeckhout D, Schweizer F, Godoy M, Franco-Zorrilla JM, Pauwels L, Witters E, Puga MI, Paz-Ares J, Goossens A, Reymond P, De Jaeger G, Solano R (2011) The *Arabidopsis* bHLH transcription factors MYC3 and MYC4 are targets of JAZ repressors and act additively with MYC2 in the activation of jasmonate responses. Plant Cell 23:701-715

Fondevilla S, Torres AM, Moreno MT, Rubiales D (2007) Identification of a new gene for resistance to powdery mildew in *Pisum fulvum*, a wild relative of pea. Breed Sci 57:181-184

Fondevilla S, Rubiales D, Moreno M, Torres A (2008) Identification and validation of RAPD and SCAR markers linked to the gene *Er3* conferring resistance to *Erysiphe pisi* DC in pea. Mol Breed 22:193-200

Fondevilla S, Rubiales D (2012) Powdery mildew control in pea. A review. Agron Sustain Dev 32:401-409

Foster-Hartnett D, Danesh D, Peñuela S, Sharopova N, Endre G, Vandenbosch KA, Young ND, Samac DA (2007) Molecular and cytological responses of *Medicago truncatula* to *Erysiphe pisi*. Mol Plant Pathol 8:307-319

Gao L-L, Kamphuis LG, Kakar K, Edwards OR, Udvardi MK, Singh KB (2010) Identification of potential early regulators of aphid resistance in *Medicago truncatula* via transcription factor expression profiling. New Phytol 186:980-994

Gutterson N, Reuber TL (2004) Regulation of disease resistance pathways by AP2/ERF transcription factors. Curr Opin Plant Biol 7:465-471

Hellemans J, Mortier G, De Paepe A, Speleman F, Vandesompele J (2007) qBase relative quantification framework and software for management and automated analysis of real-time quantitative PCR data. Genome Biol 8:R19

Hoagland DR, Arnon DI (1950) The water-culture method of growing plants without soil. Calif Agric Exp Stn Circ 347:1-32

Hou H, Yan Q, Wang X, Xu H (2013) A SBP-Box gene *VpSBP5* from chinese wild *Vitis* Species Responds to *Erysiphe necator* and defense signaling molecules. Plant Mol Biol Rep 31:1261-1270

Jin H, Martin C (1999) Multifunctionality and diversity within the plant *MYB*-gene family. Plant Mol Biol 41:577-585

Kakar K, Wandrey M, Czechowski T, Gaertner T, Scheible W-R, Stitt M, Torres-Jerez I, Xiao Y, Redman J, Wu H, Cheung F, Town C, Udvardi M (2008) A community resource for high-throughput quantitative RT-PCR analysis of transcription factor gene expression in *Medicago truncatula*. Plant Methods 4:18

Kiełbowicz-Matuk A (2012) Involvement of plant C2H2-type zinc finger transcription factors in stress responses. Plant Sci 185–186:78-85

Korfhage U, Trezzini GF, Meier I, Hahlbrock K, Somssich IE (1994) Plant homeodomain protein involved in transcriptional regulation of a pathogen defense-related gene. Plant Cell 6:695-708

Küster H, Hohnjec N, Krajinski F, El Yahyaoui F, Manthey K, Gouzy J, Dondrup M, Meyer F, Kalinowski J, Brechenmacher L, van Tuinen D, Gianinazzi-Pearson V, Pühler A, Gamas P, Becker A (2004) Construction and validation of cDNA-based Mt6k-RIT macro- and microarrays to explore root endosymbioses in the model legume *Medicago truncatula*. J Biotech 108:95-113

Küster H, Becker A, Firnhaber C, Hohnjec N, Manthey K, Perlick AM, Bekel T, Dondrup M, Henckel K, Goesmann A, Meyer F, Wipf D, Requena N, Hildebrandt U, Hampp R, Nehls U, Krajinski F, Franken P, Pühler A (2007) Development of bioinformatic tools to support EST-sequencing, *in silico*- and microarray-based transcriptome profiling in mycorrhizal symbioses. Phytochemistry 68:19-32

Lamb C, Dixon RA (1997) The oxidative burst in plant disease resistance. Annu Rev Plant Physiol Plant Mol Biol 48:251-275

Li T, Chen X, Zhong X, Zhao Y, Liu X, Zhou S, Cheng S, Zhou D-X (2013) Jumonji C domain protein *JMJ705*-mediated removal of histone H3 lysine 27 trimethylation is involved in defense-related gene activation in rice. Plant Cell 25:4725-4736

Libault M, Wan J, Czechowski T, Udvardi M, Stacey G (2007) Identification of 118 *Arabidopsis* transcription factor and 30 ubiquitin-ligase genes responding to chitin, a plant-defense elicitor. Mol Plant-Microbe Interact 20:900-911

Madrid E, Gil J, Rubiales D, Krajinski F, Schlereth A, Millán T (2010) Transcription factor profiling leading to the identification of putative transcription factors involved in the *Medicago truncatula–Uromyces striatus* interaction. Theor Appl Genet 121:1311-1321

Mangeon A, Junqueira RM, Sachetto-Martins G (2010) Functional diversity of the plant glycine-rich proteins superfamily. Plant signal behav 5:99-104

McGrath KC, Dombrecht B, Manners JM, Schenk PM, Edgar CI, Maclean DJ, Scheible W-R, Udvardi MK, Kazan K (2005) Repressor- and activator-type ethylene response factors functioning in jasmonate signaling and disease resistance identified via a genome-wide screen of *Arabidopsis* transcription factor gene expression. Plant Physiol 139:949-959

Navarro L, Dunoyer P, Jay F, Arnold B, Dharmasiri N, Estelle M, Voinnet O, Jones JDG (2006) A plant miRNA contributes to antibacterial resistance by repressing auxin signaling. Science 312:436-439

Panstruga R, Spanu PD (2014) Powdery mildew genomes reloaded. New Phytol 202:13-14

Prats E, Llamas MJ, Rubiales D (2007) Characterization of resistance mechanisms to *Erysiphe pisi* in *Medicago truncatula*. Phytopathology 97:1049-1053

Ramirez-Parra E, Fründt C, Gutierrez C (2003) A genome-wide identification of E2F-regulated genes in *Arabidopsis*. Plant J 33:801-811

Riechmann JL, Ratcliffe OJ (2000) A genomic perspective on plant transcription factors. Curr Opin Plant Biol 3:423-434

Ringli C (2010) Monitoring the outside: cell wall-sensing mechanisms. Plant Physiol 153:1445-1452

Rogers LA, Campbell MM (2004) The genetic control of lignin deposition during plant growth and development. New Phytol 164:17-30

Rose RJ (2008) *Medicago truncatula* as a model for understanding plant interactions with other organisms, plant development and stress biology: past, present and future. Funct Plant Biol 35:253-264

Samac DA, Peñuela S, Schnurr JA, Hunt EN, Foster-Hartnett D, Vandenbosch KA, Gantt JS (2011) Expression of coordinately regulated defence response genes and analysis of their role in disease resistance in *Medicago truncatula*. Mol Plant Pathol 12:786-798

Shen Q-H, Saijo Y, Mauch S, Biskup C, Bieri S, Keller B, Seki H, Ülker B, Somssich IE, Schulze-Lefert P (2007) Nuclear activity of MLA immune receptors links isolate-specific and basal disease-resistance responses. Science 315:1098-1103

Sillero J, Fondevilla S, Davidson J, Patto M, Warkentin T, Thomas J, Rubiales D (2006) Screening techniques and sources of resistance to rusts and mildews in grain legumes. Euphytica 147:255-272

Singh KB, Foley RC, Oñate-Sánchez L (2002) Transcription factors in plant defense and stress responses. Curr Opin Plant Biol 5:430-436

Singh RJ, Chung GH, Nelson RL (2007) Landmark research in legumes. Genome 50:525-537

Stone JM, Liang X, Nekl ER, Stiers JJ (2005) *Arabidopsis AtSPL14*, a plant-specific SBP-domain transcription factor, participates in plant development and sensitivity to fumonisin B1. Plant J 41:744-754

Swarbrick PJ, Schulze-Lefert P, Scholes JD (2006) Metabolic consequences of susceptibility and resistance (race-specific and broad-spectrum) in barley leaves challenged with powdery mildew. Plant Cell Environ 29:1061-1076

Torres MA, Jones JDG, Dangl JL (2005) Pathogen-induced, NADPH oxidase–derived reactive oxygen intermediates suppress spread of cell death in *Arabidopsis thaliana*. Nat Genet 37:1130-1134

Udvardi MK, Kakar K, Wandrey M, Montanari O, Murray J, Andriankaja A, Zhang J-Y, Benedito V, Hofer JMI, Chueng F, Town CD (2007) Legume transcription factors: global regulators of plant development and response to the environment. Plant Physiol 144:538-549

Vandepoele K, Vlieghe K, Florquin K, Hennig L, Beemster GTS, Gruissem W, Van de Peer Y, Inzé D, De Veylder L (2005) Genome-wide identification of potential plant E2F target genes. Plant Physiol 139:316-328

Vandesompele J, De Preter K, Pattyn F, Poppe B, Van Roy N, De Paepe A, Speleman F (2002) Accurate normalization of real-time quantitative RT-PCR data by geometric averaging of multiple internal control genes. Genome Biol 3:research0034.0031 - research0034.0011

Verdier J, Kakar K, Gallardo K, Le Signor C, Aubert G, Schlereth A, Town C, Udvardi M, Thompson R (2008) Gene expression profiling of *M. truncatula* transcription factors identifies putative regulators of grain legume seed filling. Plant Mol Biol 67:567-580

Villegas-Fernández AM, Krajinski F, Schlereth A, Madrid E, Rubiales D (2014) Characterisation by transcription factor expression profiling of the interaction *Medicago truncatula – Botrytis spp*. Plant Mol Biol Rep, in press

Vogelstein B, Gillespie D (1979) Preparative and analytical purification of DNA from agarose. Proc Natl Acad Sci USA 76:615-619

Wang D, Amornsiripanitch N, Dong X (2006) A genomic approach to identify regulatory nodes in the transcriptional network of systemic acquired resistance in plants. PLoS Pathog 2:e123

Yanagisawa S (2002) The Dof family of plant transcription factors. Trends Plant Sci 7:555-560

Yang S, Tang F, Caixetab ET, Zhu H (2013) Epigenetic regulation of a powdery mildew resistance gene in *Medicago truncatula*. Mol Plant 6:2000-2003

Zhang J-Y, Cruz De Carvalho MH, Torres-Jerez I, Kang YUN, Allen SN, Huhman DV, Tang Y, Murray J, Sumner LW, Udvardi MK (2014) Global reprogramming of transcription and metabolism in *Medicago truncatula* during progressive drought and after rewatering. Plant Cell Env, in press

Figures

Fig. 1 Macroscopic disease symptoms in the susceptible cultivar Parabinga (a) and in the resistant SA1306 accession (b).

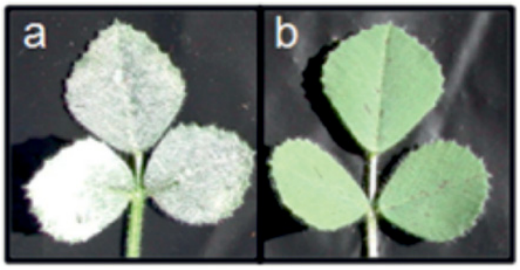

Fig. 2 Evaluation of candidate reference genes analyzed using geNorm software. Expression stability (a) and pair-wise variation (b) plots for the eight reference genes studied. A lower M value indicates a more stable expression. The pair-wise variation (V) values indicate the optimal number of reference genes.

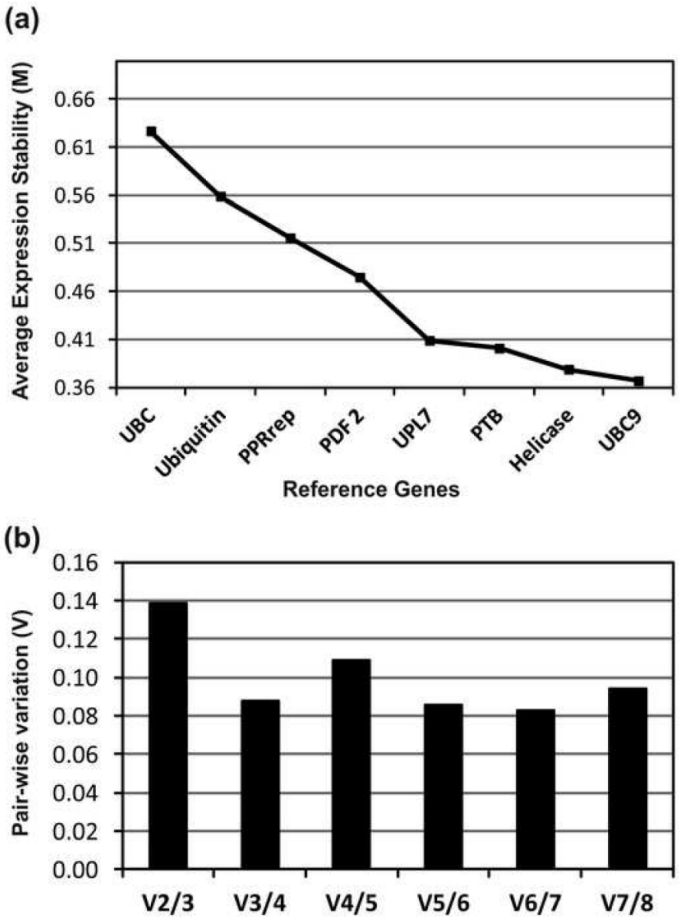

Fig. 3 Expression profiles of TF genes. (A) Heat map showing expression profiles of 95 genes that were differentially expressed in Parabinga (PB) and SA1306 (SA) *M. truncatula* genotypes in response to *E. Pisi* infection. Genes were considered differentially expressed if they met the prerequisites p≤0.05 and M ≤-0.7 or M≥0.7. Up-regulation (M≥0.7) is indicated in red; down-regulation (M≤-0.7) in green; black indicates no differential expression. The heat map expression profiles are grouped by yellow rectangles (I to X). (B) Percentages of regulated genes detected in Parabinga (PB) and in SA1306 (SA) are shown for each of the ten clusters (groups GI to GX). Additional information is available in table S2.

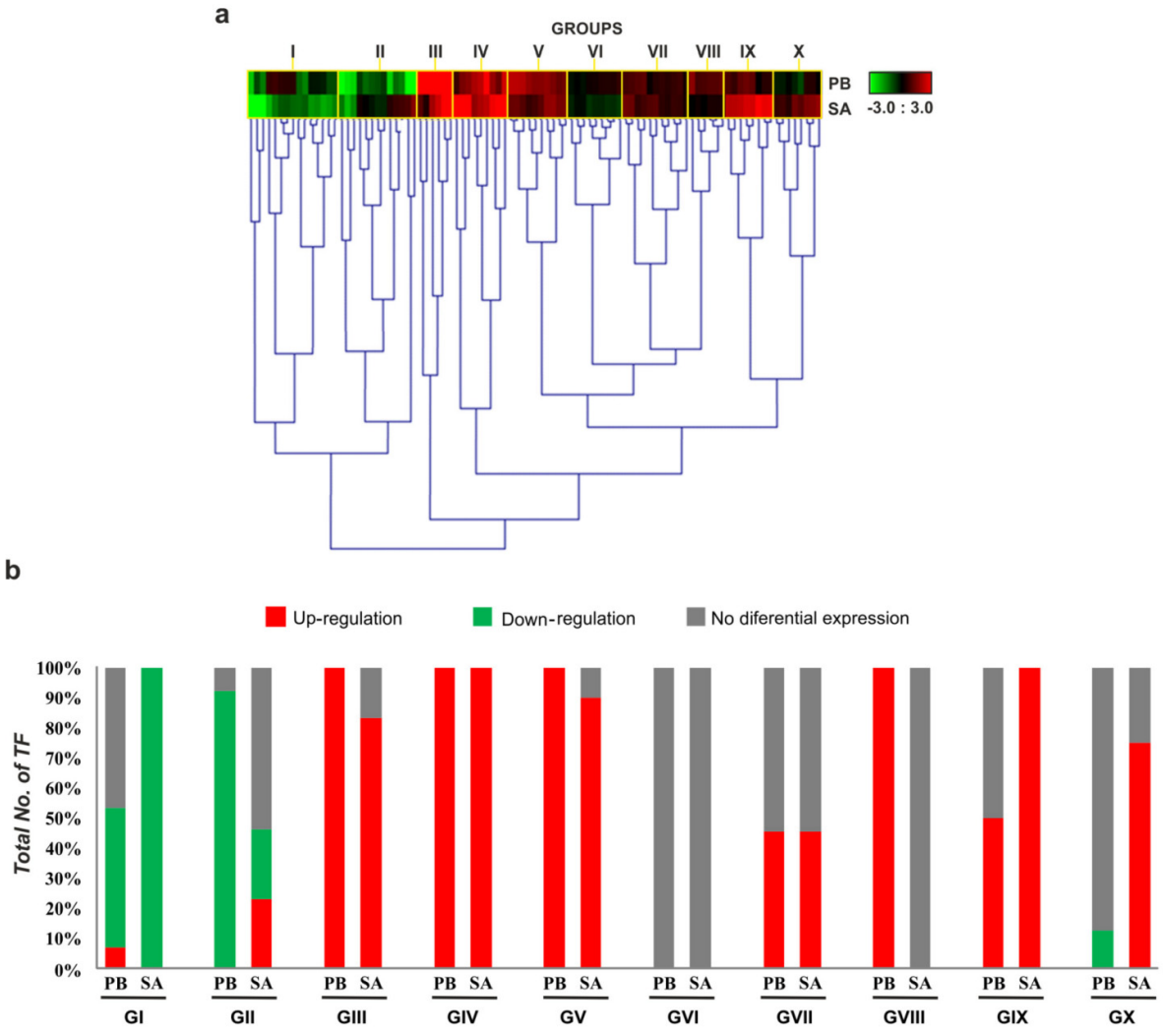

Fig. 4 A model for the regulatory network that controls the expression of *E. Pisi*-induced TF genes ($p \leq 0.05$; $-0.7 \geq M \geq 0.7$) in Parabinga (PB; diamond) and SA1306 (SA; square) *M. truncatula* genotypes. Solid diamonds and solid squares indicate the TF genes regulated in Parabinga and SA1306, respectively. The TF genes that were regulated in both genotypes are indicated by solid spheres. Up- and down-regulation are indicated by red and green lines, respectively. The colours of the solid diamonds, solid squares and solid spheres indicate TF families: Green (bHLH); black (HD family; HD-Like; MYB; MYB/HD-like); orange (ARF; GRAS); red (AP2/ERBP; WRKY); blue (Zn-fingers TF families; bZIP); olive green (FHA; NAC); violet (RR); pink (SBP; BTB/POZ); grey (HMG; HTH); brown (E2F; DDT); sky-blue (LIM; PHD); pea green (JUMONJI; ARID); dark pink (AUX/IAA; MADS). A detailed description of these genes is shown in table S3.

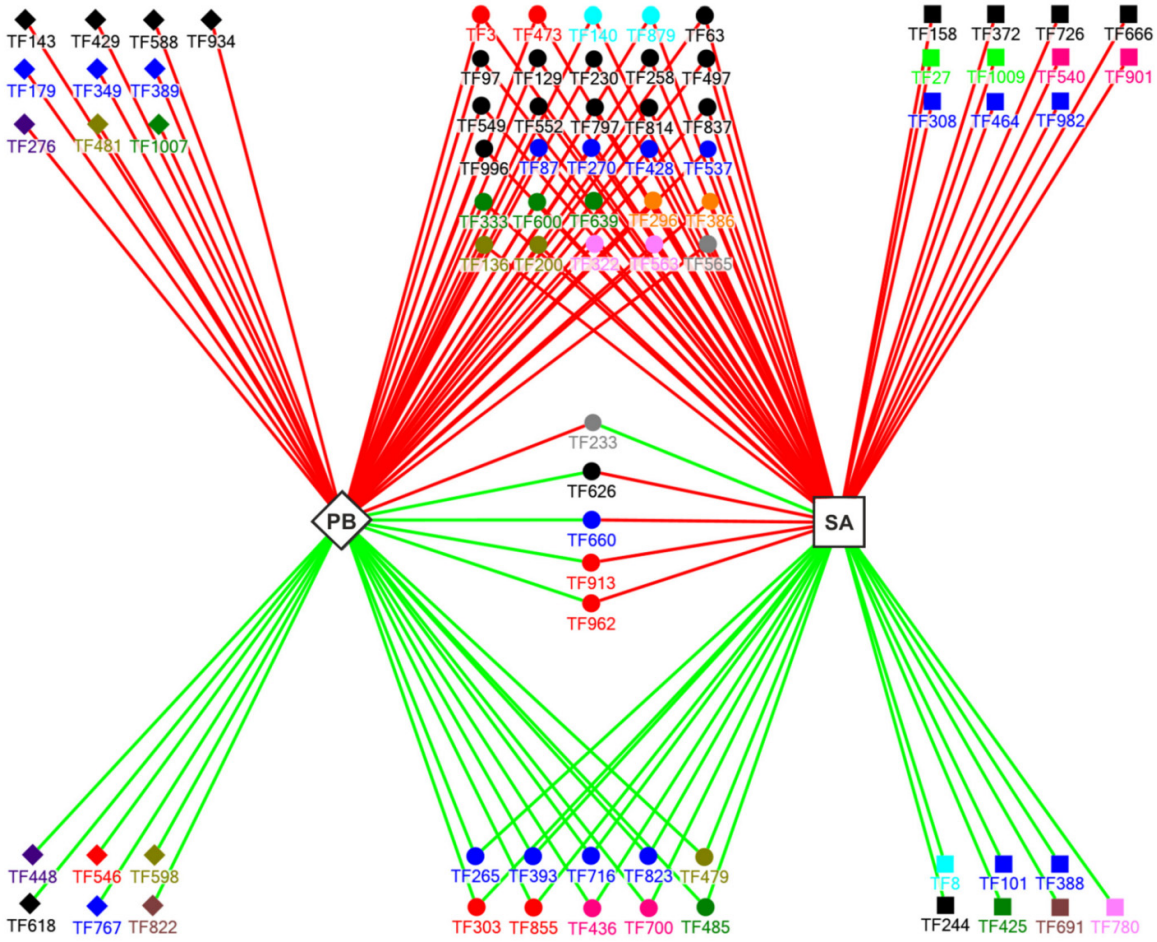

Table 1 Most differentially expressed genes in SA1306 compared to Parabinga in response to *Erysiphe pisi* infection.

TF family; subfamily[a]	**ID**[b]	**InterPro No.**[c]	**Domain Function**[d]	**Expression pattern**[e]
AP2/EREBP	TF3 TF303 TF473 TF962	**IPR001471**	**D**	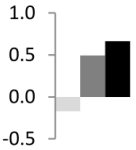
ARF	TF386	**IPR003340 IPR010525 IPR011525**	**D**	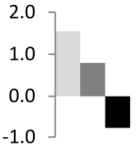
ARID	TF27	IPR001606	D	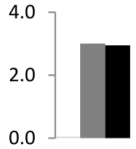
AUX/IAA	TF780	**IPR003311**	**D**	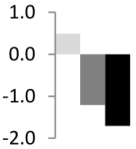
bHLH	TF425 TF485	IPR001092	D	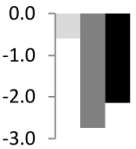
BTB/POZ	TF700	IPR000210	P	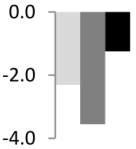
C_2C_2 (Zn); DOF	TF265 TF308	***IPR003851***	***D***	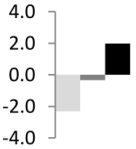

Table 1, continued

C_2C_2 (Zn); GATA	TF716	*IPR000679*	*D*	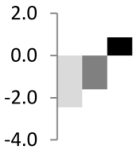
C_2H_2 (Zn)	TF101 TF270 TF428 TF823 TF982	*IPR007087*	*NA*	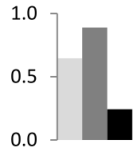
CCHC (Zn)	TF660	*IPR001878*	*NA*	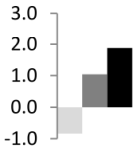
E2F	TF691	IPR003316	D	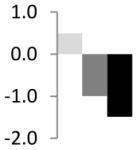
HD family; HD	TF258 TF372 TF497	IPR001356	D	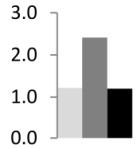
HD family; HD-ZIP	TF549 TF552	IPR006712	P	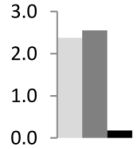
HD-like	TF158 TF230 TF626 TF666 TF797 TF814 TF996	IPR009057	D	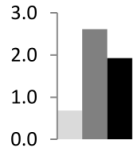

Table 1, continued

HMG	TF233	IPR000637	D	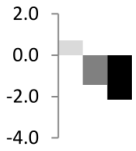
JUMONJI	TF1009	IPR003347	D	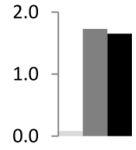
LIM	TF8	*IPR001781*	*P*	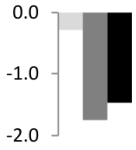
MADS	TF563	IPR002100	D	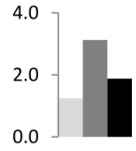
MYB	TF63 TF837	IPR001005	D	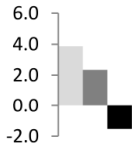
MYB/HD-like	TF129 TF244 TF726	IPR001005 IPR009057	D	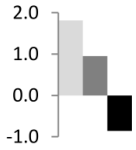
NAC	TF136 TF200	**IPR003441**	**D**	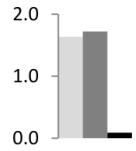

Table 1, continued

PHD	TF879	*IPR001965*	*P*	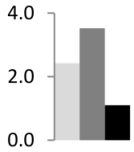
SBP	TF540 TF901	**IPR004333**	**D**	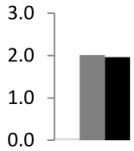
TTF-type (Zn)	TF388	IPR006580	D	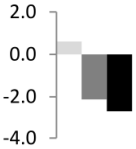
WRKY family; WRKY	TF913	**IPR003657**	**D**	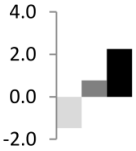

[a] TF families; sub-families are showed as described (Kakar et al. 2008). Plant-specific families are indicated in **bold**. Zn fingers TF families are marked in *cursive*.
[b] TF gene identification number. Additional information is given in Table S1.
[c] Accession numbers of InterPro database (http://www.ebi.ac.uk/interpro/).
[d] D = DNA binding domain; P = protein-protein interaction domain; NA = nucleic acid (DNA and RNA) binding domain; RD = receiver domain
[e] Histograms represent the average $\log_2$ differential expression ratios (inoculated/control) for Parabinga (light grey column) and SA1306 (grey column) genotypes. The fold change expression ratios of genes in SA1306 compared to Parabinga (black column), was calculated as $\log_2$ expression ratio SA1306/Parabinga. Additional information is given in Tables S2 and S3.

Plant Molecular Biology Reporter
Supplementary File

Transcriptional regulation network of *Medicago truncatula* during *Erysiphe pisi* infection

Miguel Curto[1*], Franziska Krajinski[2], Armin Schlereth[2], Diego Rubiales[1]

[1]Institute for Sustainable Agriculture, CSIC, Apdo.4084, E-14080, Córdoba, Spain.
[2]Max Planck Institute of Molecular Plant Physiology, Science Park, 14476 Potsdam-Golm, Germany.

*To whom correspondence should be addressed:

Miguel Curto

Institute for Sustainable Agriculture, CSIC, Apdo. 4084, E-14080 Córdoba, Spain.

E-mail: b72curum@uco.es

Tel: +34 957199215

Fax: +34 957499252

Paper submitted on 31 July 2014; current status: under review

Table S1 Complete list of TF genes. The accession numbers (AC), the TIGR *Medicago* gene accession numbers (TC) if available, as well as the transcription factor family and the subfamily names are shown as described Kakar et al. (Kakar et al. 2008). The quantification cycle (Cq), PCR efficiencies (PCReff) and correlation coefficients for the qPCR reactions performed on both *Medicago truncatula* genotypes, Parabinga and SA1306, in three biological replicates are indicated.

ID	TF Family	TF Subfamily	PB control rep 1			PB control rep 2			PB control rep 3			PB infected rep 1			PB infected rep 2			PB infected rep 3		
			Cq	PCReff	R^2	Cq	PCReff	R^2	Cq	PCReff	R^2	Cq	PCReff	R^2	Cq	PCReff	R^2	Cq	PCReff	R^2
TF1	HSF		22,97	1,89	1,00	23,61	1,87	1,00	22,69	1,96	1,00	21,98	1,72	1,00	22,35	1,89	1,00	22,59	1,86	1,00
TF2	HSF		22,33	1,97	1,00	21,94	1,90	1,00	22,36	1,89	1,00	21,48	1,99	1,00	23,81	1,75	1,00	25,75	1,93	1,00
TF3	AP2/EREBP		25,98	1,87	1,00	24,27	2,02	1,00	22,96	1,98	1,00	25,76	1,83	1,00	20,82	1,86	1,00	22,98	1,89	1,00
TF4	MYB		27,67	1,92	1,00	26,25	1,87	1,00	26,06	1,99	1,00	27,26	1,93	1,00	23,60	1,75	1,00	24,51	1,94	1,00
TF5	AP2/EREBP		26,92	1,99	1,00	26,39	2,01	1,00	24,47	1,92	1,00	26,70	1,88	1,00	24,03	1,89	1,00	25,46	1,98	1,00
TF6	MYB/HD-like		29,91	1,65	1,00	29,24	1,98	1,00	24,97	1,82	1,00	28,43	1,68	1,00	28,83	1,66	1,00	30,04	1,62	1,00
TF7	HD-like		23,91	1,88	1,00	24,64	1,95	1,00	23,87	1,98	1,00	23,53	1,78	1,00	24,00	1,93	1,00	24,29	2,08	1,00
TF8	LIM		24,20	1,72	1,00	24,17	1,84	1,00	24,45	1,91	1,00	23,65	1,97	1,00	23,94	1,89	1,00	23,86	1,96	1,00
TF9	CCHC (Zn)		26,22	1,78	1,00	25,88	1,84	1,00	26,23	1,91	1,00	24,72	1,90	1,00	26,91	1,81	1,00	27,05	1,90	1,00
TF10	RR		25,23	1,80	1,00	25,05	1,76	1,00	25,02	1,85	1,00	23,63	1,81	1,00	23,82	1,90	1,00	23,99	1,87	1,00
TF11	CCHC (Zn)		22,17	1,80	1,00	22,11	1,99	1,00	22,28	1,86	1,00	21,89	1,88	1,00	22,12	2,00	1,00	22,09	1,88	1,00
TF12	MYB/HD-like		22,53	2,07	1,00	23,25	1,88	1,00	22,59	1,88	1,00	22,06	1,94	1,00	22,28	1,93	1,00	22,72	1,86	1,00
TF13	KRAB box		24,68	1,83	1,00	24,51	1,89	1,00	25,73	1,92	1,00	25,46	1,92	1,00	28,31	1,82	1,00	28,57	1,84	1,00
TF14	GRAS		23,50	1,94	1,00	24,04	1,90	1,00	23,03	1,83	1,00	22,75	1,84	1,00	23,27	1,90	1,00	23,12	1,83	1,00
TF15	CCHC (Zn)		26,74	1,83	1,00	27,35	1,83	0,99	21,09	1,84	1,00	25,05	1,78	1,00	25,94	1,85	1,00	26,01	1,89	1,00
TF16	bZIP		22,26	2,03	1,00	22,89	1,79	1,00	21,80	1,81	1,00	21,86	1,77	1,00	22,68	1,71	1,00	22,40	1,81	1,00
TF17	MADS		29,03	1,83	1,00	30,01	1,78	1,00	29,03	1,85	1,00	28,28	1,87	1,00	29,88	2,15	1,00	31,05	1,83	1,00
TF18	NAC		27,74	1,74	1,00	27,78	1,83	1,00	28,27	1,77	1,00	27,66	1,75	1,00	28,02	1,68	1,00	27,86	1,75	1,00
TF19	NAC		28,54	1,79	1,00	27,92	1,79	1,00	28,39	1,76	1,00	27,87	1,82	1,00	27,69	1,84	1,00	27,80	1,90	1,00
TF20	CCAAT	CCAAT-HAP3	20,42	2,02	1,00	20,83	2,03	1,00	21,01	1,98	1,00	20,54	1,95	1,00	20,75	2,01	1,00	20,80	2,03	1,00
TF21	AP2/EREBP		28,35	1,88	1,00	26,08	1,85	1,00	24,81	1,88	1,00	28,06	1,91	1,00	24,49	1,86	1,00	25,85	1,81	1,00
TF22	bZIP		21,68	1,84	1,00	22,19	1,87	0,99	22,49	1,98	1,00	21,51	2,09	1,00	21,68	1,76	1,00	21,66	1,74	1,00
TF23	bZIP		21,94	1,87	1,00	22,57	1,94	1,00	21,74	2,11	1,00	20,95	2,00	1,00	21,28	1,88	1,00	21,47	1,98	1,00
TF24	MYB		29,47	1,80	1,00	29,62	1,79	1,00	27,54	1,86	1,00	29,51	1,77	1,00	25,88	1,81	1,00	28,22	1,82	1,00
TF25	MYB		21,69	1,94	1,00	21,43	1,83	1,00	22,29	2,14	1,00	21,51	1,89	1,00	21,35	1,84	1,00	21,11	1,89	1,00
TF26	ARID		31,61	1,72	1,00	30,31	1,74	1,00	28,38	1,81	1,00	31,33	1,70	1,00	27,80	1,80	1,00	29,61	1,68	1,00
TF27	ARID		25,83	1,86	1,00	25,95	1,84	1,00	24,91	1,92	1,00	24,38	1,91	1,00	27,10	1,82	1,00	28,83	1,78	1,00
TF28	C_2H_2 (Zn)		28,46	1,79	1,00	28,19	1,93	1,00	22,07	1,90	1,00	26,67	1,86	1,00	27,56	1,79	1,00	27,70	1,89	1,00
TF29	C_2H_2 (Zn)		26,02	1,73	1,00	25,25	1,83	1,00	27,01	1,89	1,00	25,42	1,79	1,00	22,02	1,97	1,00	29,00	2,28	0,78
TF30	WRKY family	WRKY	24,56	1,97	1,00	24,92	2,03	1,00	22,13	1,97	1,00	22,89	1,98	1,00	24,96	1,95	1,00	25,16	1,92	1,00
TF31	CCHC (Zn)		28,59	1,91	1,00	28,15	1,86	1,00	27,81	1,86	1,00	26,12	1,76	1,00	30,79	1,77	1,00	31,73	1,62	1,00
TF32	AP2/EREBP		23,87	1,85	1,00	24,49	2,01	1,00	23,55	1,82	1,00	22,47	1,91	1,00	22,68	1,90	1,00	22,82	1,96	1,00
TF33	HD family	HD-PHD finger	25,16	1,85	1,00	24,84	1,91	1,00	25,07	1,76	1,00	24,64	1,89	1,00	24,70	1,89	1,00	25,01	1,88	1,00
TF34	CCHC (Zn)		23,78	1,86	1,00	23,36	1,89	1,00	18,58	2,01	1,00	22,19	1,96	1,00	23,38	1,91	1,00	23,54	2,07	1,00
TF35	bHLH		26,80	1,85	1,00	27,14	2,11	1,00	25,89	1,90	1,00	26,33	1,86	1,00	26,18	1,89	1,00	26,63	1,85	1,00
TF36	HD family	HD-PHD finger	23,63	1,96	1,00	23,12	1,91	1,00	23,33	1,91	1,00	22,22	1,93	1,00	23,89	1,91	1,00	24,97	1,93	1,00
TF37	CCHC (Zn)		27,94	1,82	1,00	27,71	1,81	1,00	23,98	1,81	1,00	27,11	1,74	1,00	28,14	1,75	1,00	29,14	1,68	1,00
TF38	bZIP		27,71	1,65	1,00	27,59	1,68	1,00	26,51	1,48	1,00	25,59	1,77	1,00	28,99	1,52	1,00	31,46	1,64	1,00
TF39	bZIP		29,48	1,78	1,00	27,80	1,79	1,00	21,54	1,89	1,00	26,71	1,76	1,00	28,38	1,72	1,00	28,07	1,71	1,00
TF40	MYB/HD-like		25,10	1,94	1,00	25,67	1,97	1,00	25,35	1,79	1,00	24,44	1,87	1,00	24,94	1,91	1,00	24,93	1,87	1,00
TF41	ARF		29,68	1,86	1,00	30,78	1,73	1,00	24,84	1,70	1,00	28,51	1,58	1,00	30,06	1,82	1,00	31,01	1,59	1,00
TF42	JUMONJI		23,76	1,95	1,00	23,97	2,33	0,99	19,38	2,00	1,00	21,87	1,77	1,00	22,68	1,91	1,00	22,90	1,79	1,00
TF43	CCHC (Zn)		33,73	1,27	1,00	32,17	1,74	1,00	34,11	1,70	1,00	30,72	1,78	1,00	32,97	1,85	1,00	36,85	1,43	1,00
TF44	MADS		33,19	1,50	1,00	30,80	1,47	1,00	32,46	1,43	1,00	29,09	1,56	1,00	30,49	1,47	1,00	30,15	1,58	1,00

Table S1, continued

TF45	MADS		31,50	1,89	1,00	31,60	1,71	1,00	32,78	1,63	1,00	29,90	1,81	1,00	30,44	1,96	1,00	32,68	1,82	1,00
TF46	MYB/HD-like		28,83	1,96	1,00	29,29	1,87	1,00	28,22	1,90	1,00	27,78	1,84	1,00	28,57	1,82	1,00	29,43	1,81	1,00
TF47	LIM		29,45	1,68	1,00	29,56	1,59	1,00	29,95	1,69	1,00	29,83	1,58	1,00	31,09	1,65	1,00	31,81	1,59	1,00
TF48	bHLH		25,93	1,94	1,00	25,06	1,37	1,00	24,12	1,90	1,00	26,65	1,23	1,00	23,57	1,90	1,00	25,45	2,05	1,00
TF49	MYB/HD-like		25,38	1,87	1,00	24,96	1,86	1,00	25,68	1,86	1,00	25,08	1,84	1,00	26,56	1,76	1,00	28,43	1,78	1,00
TF50	HD family	HD	27,91	1,84	1,00	27,83	1,83	1,00	27,86	1,84	1,00	28,40	1,83	1,00	28,94	1,79	1,00	29,19	1,76	1,00
TF51	bHLH		27,98	1,92	1,00	27,60	1,91	1,00	28,25	1,85	1,00	29,80	1,76	1,00	29,56	1,90	1,00	31,34	2,04	1,00
TF52	bHLH		29,16	1,87	1,00	28,85	2,00	1,00	23,55	1,94	1,00	27,77	1,88	1,00	28,51	1,95	1,00	29,58	1,88	1,00
TF53	HTH	AraC	21,19	1,61	1,00	21,37	1,63	1,00	17,52	2,09	1,00	20,75	1,75	1,00	21,11	1,91	1,00	21,32	1,97	1,00
TF54	ZF DHHC		22,93	1,85	1,00	22,82	1,84	1,00	23,29	1,94	1,00	21,43	1,90	1,00	21,68	1,87	1,00	21,79	1,90	1,00
TF55	HTH	FIS	24,18	1,89	1,00	23,89	1,77	1,00	24,24	1,92	1,00	23,43	2,04	0,99	23,47	1,92	1,00	23,79	1,85	1,00
TF56	AS2		26,59	1,90	1,00	25,71	2,44	1,00	23,98	1,93	1,00	26,47	1,89	1,00	22,51	2,06	1,00	24,03	1,99	1,00
TF57	HMG		23,63	1,84	1,00	23,62	2,04	1,00	23,33	1,96	1,00	23,80	1,91	0,99	22,60	2,12	1,00	23,50	1,88	1,00
TF58	C_2H_2 (Zn)		33,20	1,48	1,00	30,72	1,78	1,00	28,97	1,82	1,00	31,63	1,79	1,00	28,38	1,80	1,00	29,72	1,90	1,00
TF59	C_2H_2 (Zn)		29,76	1,84	1,00	31,55	1,77	1,00	25,86	1,88	1,00	29,88	1,80	1,00	29,10	1,73	1,00	30,40	1,83	1,00
TF60	NGN		22,12	1,86	1,00	22,74	1,88	1,00	21,94	1,97	1,00	22,31	1,92	1,00	22,95	1,74	0,99	22,78	1,77	1,00
TF61	HD-like		27,98	1,80	1,00	28,26	1,93	1,00	23,41	1,74	1,00	26,69	1,80	1,00	27,73	1,74	1,00	27,90	1,89	1,00
TF62	KRAB box		31,43	1,51	1,00	33,01	1,52	1,00	31,19	1,56	1,00	31,48	1,48	1,00	30,94	1,60	1,00	32,90	1,57	1,00
TF63	MYB		31,98	1,98	1,00	31,32	1,93	1,00	32,45	1,89	1,00	30,23	1,88	1,00	30,16	2,01	1,00	30,18	1,92	1,00
TF64	MYB/HD-like		28,87	1,69	1,00	27,24	1,63	1,00	22,75	1,71	1,00	25,64	1,69	1,00	27,64	1,74	0,99	28,06	1,76	1,00
TF65	MYB/HD-like		27,20	1,91	1,00	26,84	1,90	1,00	27,87	1,92	1,00	26,63	1,88	1,00	28,94	1,86	1,00	32,34	1,91	1,00
TF66	S1Fa-like		21,45	1,96	1,00	21,84	1,87	1,00	21,97	1,91	1,00	21,82	1,92	1,00	22,10	1,94	1,00	22,10	1,93	1,00
TF67	S1Fa-like		20,38	1,87	1,00	20,76	2,00	1,00	20,99	1,91	1,00	20,68	1,90	1,00	20,74	1,98	1,00	20,64	1,90	1,00
TF68	CCHC (Zn)		35,89	1,78	1,00	33,63	2,47	1,00	28,65	1,87	1,00	32,19	1,91	1,00	33,52	1,89	1,00	36,65	1,75	1,00
TF69	MYB		33,87	1,54	1,00	32,76	1,64	1,00	31,21	1,59	1,00	32,23	1,67	1,00	31,70	1,59	1,00	32,59	1,20	1,00
TF70	MYB		27,35	1,92	1,00	25,94	1,93	1,00	23,75	1,88	1,00	26,39	1,89	1,00	23,09	1,98	1,00	24,58	1,98	1,00
TF71	EIL		19,86	2,02	1,00	20,29	2,05	1,00	20,44	1,90	1,00	19,75	1,98	1,00	19,77	1,89	1,00	19,91	1,91	1,00
TF72	MYB/HD-like		31,16	1,72	1,00	32,51	1,69	1,00	29,01	1,81	1,00	n.d.	1,38	1,00	31,05	1,63	1,00	34,10	1,56	1,00
TF73	MYB/HD-like		31,30	1,80	1,00	31,24	1,79	1,00	31,35	1,66	1,00	29,27	1,83	1,00	29,82	1,76	1,00	30,33	1,78	1,00
TF74	MYB/HD-like		31,31	1,73	1,00	30,98	1,65	1,00	26,66	1,72	1,00	32,75	1,66	1,00	31,65	1,81	1,00	33,89	1,38	1,00
TF75	MYB/HD-like		22,23	2,00	1,00	21,46	1,97	1,00	17,13	2,10	1,00	21,03	1,91	1,00	21,65	1,94	1,00	21,52	1,97	1,00
TF76	MYB		34,12	1,78	1,00	30,34	1,77	1,00	30,11	1,76	1,00	33,07	1,79	1,00	28,46	1,87	1,00	29,98	1,83	1,00
TF77	MYB		23,15	1,91	1,00	21,47	1,92	1,00	19,26	1,67	1,00	23,28	1,94	1,00	17,85	1,95	1,00	19,95	1,97	1,00
TF78	C_2H_2 (Zn)		31,21	1,77	1,00	29,64	1,72	1,00	27,94	2,05	1,00	31,56	1,71	1,00	28,21	1,81	1,00	28,42	1,79	1,00
TF79	C_2H_2 (Zn)		25,30	1,90	1,00	24,24	1,94	1,00	23,44	1,85	1,00	24,37	2,07	1,00	20,71	2,21	1,00	22,35	2,00	1,00
TF80	HTH	FIS	26,94	1,92	1,00	25,43	1,84	1,00	23,25	1,91	1,00	26,33	1,90	1,00	22,02	1,91	1,00	25,99	1,91	1,00
TF81	C_2H_2 (Zn)		25,98	1,90	1,00	25,32	1,82	1,00	21,45	1,90	1,00	24,26	1,93	1,00	25,10	1,66	1,00	25,47	1,64	1,00
TF82	EIL		32,31	1,52	1,00	39,38	1,31	0,99	31,79	1,55	1,00	31,52	1,57	1,00	31,59	1,63	1,00	32,03	1,64	1,00
TF83	EIL		27,05	1,85	1,00	27,41	1,84	1,00	26,69	1,88	1,00	27,19	1,88	1,00	31,01	1,72	1,00	31,28	1,82	1,00
TF84	bZIP		25,53	1,74	1,00	25,90	1,83	1,00	21,61	1,91	1,00	24,96	1,87	1,00	24,85	1,77	1,00	24,75	1,99	1,00
TF85	HD-like		27,63	1,83	1,00	26,62	1,83	1,00	20,55	1,93	1,00	25,30	1,94	1,00	25,67	1,90	1,00	26,63	1,96	1,00
TF86	HD-like		26,16	1,80	1,00	27,33	1,87	1,00	23,51	1,97	1,00	26,70	1,90	1,00	26,20	1,84	1,00	25,74	1,94	1,00
TF87	ZF DHHC		25,32	1,86	1,00	25,92	1,89	1,00	25,22	1,91	1,00	23,60	2,00	1,00	23,92	1,84	1,00	24,34	1,90	1,00
TF88	HD-like		24,15	1,93	1,00	23,19	1,89	1,00	19,29	2,00	1,00	26,00	1,70	1,00	24,08	1,92	1,00	23,67	1,87	1,00
TF89	TPR		23,88	1,90	1,00	24,60	1,96	1,00	23,08	1,86	1,00	23,35	1,93	1,00	23,67	1,85	1,00	23,73	1,91	1,00

Table S1, continued

TF90	bHLH		32,47	1,86	1,00	30,90	1,85	1,00	28,27	1,89	1,00	30,24	1,86	1,00	31,14	1,85	1,00	31,37	2,00	1,00
TF91	bHLH		33,66	1,61	1,00	31,80	1,75	1,00	35,58	1,69	1,00	32,98	1,68	1,00	33,54	1,61	1,00	36,60	1,35	1,00
TF92	CCHC (Zn)		24,10	2,00	1,00	24,75	1,90	1,00	23,71	1,90	1,00	23,55	1,90	1,00	23,92	1,84	1,00	24,81	1,89	1,00
TF93	bZIP		35,56	1,70	1,00	32,86	1,79	1,00	32,46	1,75	1,00	37,13	1,75	1,00	29,75	1,80	1,00	31,35	1,92	1,00
TF94	bZIP		32,65	1,66	1,00	35,33	1,68	1,00	31,83	1,68	1,00	31,84	1,64	1,00	36,18	1,72	1,00	n.d.	1,34	0,98
TF95	HD-like		24,50	1,92	1,00	24,62	1,87	1,00	24,24	1,89	1,00	23,49	1,85	1,00	23,27	1,96	1,00	23,54	2,04	1,00
TF96	LIM		19,67	1,90	1,00	19,97	1,93	1,00	20,13	2,08	1,00	20,25	1,98	1,00	20,28	1,97	1,00	20,46	2,03	1,00
TF97	HD-like		24,63	1,87	1,00	24,69	1,86	1,00	24,76	1,86	1,00	23,39	1,88	1,00	23,37	1,90	1,00	23,38	1,91	1,00
TF98	LIM		19,69	1,97	1,00	20,20	1,99	1,00	19,53	1,97	1,00	19,72	1,93	1,00	19,92	2,03	1,00	20,23	2,06	1,00
TF99	C_2H_2 (Zn)		22,35	1,89	1,00	22,51	1,92	1,00	19,01	1,93	1,00	21,99	1,86	1,00	22,40	1,93	1,00	22,30	1,76	1,00
TF100	MYB/HD-like		24,56	2,00	1,00	25,08	1,98	1,00	24,24	2,03	1,00	22,92	1,99	1,00	23,30	1,80	1,00	23,53	1,86	0,99
TF101	C_2H_2 (Zn)		23,89	1,83	1,00	24,37	1,93	1,00	23,55	1,92	1,00	23,47	1,96	1,00	24,01	1,91	1,00	24,30	1,90	1,00
TF102	MYB		23,95	1,92	1,00	23,58	1,93	1,00	21,95	2,01	1,00	23,58	1,86	1,00	20,38	1,95	1,00	21,91	1,99	1,00
TF103	C_2H_2 (Zn)		32,75	1,71	1,00	33,09	1,59	1,00	36,67	1,58	1,00	n.d.	1,38	0,96	30,93	1,64	1,00	33,29	1,61	1,00
TF104	bHLH		32,49	1,94	0,99	31,98	1,79	1,00	26,72	1,84	1,00	30,44	1,77	1,00	30,81	1,76	1,00	31,67	1,77	1,00
TF105	PHD		29,12	1,89	1,00	27,65	1,88	1,00	28,09	1,86	1,00	26,58	2,03	1,00	33,07	1,80	1,00	30,87	1,74	1,00
TF106	RR		28,09	1,59	1,00	27,41	1,68	1,00	25,03	1,75	1,00	26,62	1,83	1,00	28,03	1,66	0,99	28,53	1,17	1,00
TF107	MADS		30,91	1,85	1,00	32,48	1,74	1,00	27,51	1,26	0,98	30,94	1,81	1,00	29,91	1,77	1,00	30,80	1,63	1,00
TF108	MADS		29,85	1,96	1,00	30,25	1,77	1,00	23,56	1,88	1,00	28,61	2,05	1,00	28,97	1,85	1,00	29,88	1,81	1,00
TF109	CCHC (Zn)		20,73	1,97	1,00	20,38	1,91	1,00	20,33	1,88	1,00	19,60	1,84	1,00	22,21	1,90	1,00	22,56	1,84	1,00
TF110	PHD		25,90	1,87	1,00	25,85	1,24	1,00	25,78	1,92	1,00	25,96	2,03	1,00	25,58	2,04	1,00	25,45	1,80	1,00
TF111	bZIP		24,96	1,90	1,00	25,12	1,85	1,00	20,99	1,95	1,00	23,56	1,78	1,00	24,08	1,77	1,00	24,32	1,85	1,00
TF112	C_2C_2 (Zn)	DOF	25,46	1,61	1,00	25,14	1,35	1,00	24,94	1,63	1,00	24,55	1,69	1,00	26,21	1,68	1,00	26,65	1,70	1,00
TF113	C_2C_2 (Zn)	DOF	25,93	1,80	1,00	26,62	1,75	1,00	26,13	1,86	1,00	26,09	1,75	1,00	23,85	1,96	1,00	25,19	1,96	1,00
TF114	CCHC (Zn)		28,89	1,85	1,00	30,18	1,77	1,00	27,54	1,84	1,00	29,07	1,82	1,00	28,57	1,77	1,00	30,40	1,83	1,00
TF115	CAMTA		22,47	1,95	1,00	22,37	1,87	1,00	22,65	1,90	1,00	n.d.	1,58	0,94	21,83	2,04	1,00	21,89	1,92	1,00
TF116	LIM		29,20	1,92	1,00	29,89	1,79	1,00	29,65	1,80	1,00	30,42	1,82	1,00	28,76	1,88	1,00	29,69	1,83	1,00
TF117	LIM		23,99	1,94	1,00	23,88	1,84	1,00	23,29	1,91	1,00	24,81	1,84	1,00	22,91	1,80	1,00	23,99	1,64	1,00
TF118	CCHC (Zn)		22,65	1,91	1,00	23,17	1,96	1,00	21,92	1,93	1,00	22,37	1,93	1,00	22,51	1,99	1,00	22,98	1,90	1,00
TF119	CAMTA		26,22	1,75	1,00	25,93	1,86	1,00	26,62	1,77	1,00	25,28	1,93	1,00	25,39	1,83	1,00	25,51	1,81	1,00
TF120	MYB		21,37	1,96	1,00	21,74	1,91	1,00	21,62	1,97	1,00	22,09	1,87	1,00	22,04	1,99	1,00	22,27	1,95	1,00
TF121	FHA		23,24	1,83	1,00	23,32	1,80	1,00	23,07	1,72	1,00	22,39	1,91	1,00	23,08	1,87	1,00	23,12	1,91	1,00
TF122	MYB/HD-like		22,49	1,83	1,00	26,14	1,64	0,99	22,12	1,76	1,00	25,72	1,46	0,98	22,86	2,01	1,00	22,93	1,88	1,00
TF123	FHA		22,71	1,93	1,00	23,11	1,90	1,00	24,52	1,79	1,00	22,70	1,83	1,00	22,99	2,32	1,00	22,91	1,84	1,00
TF124	AP2/EREBP		25,36	1,87	1,00	24,75	1,84	1,00	24,32	1,66	1,00	24,23	1,85	1,00	25,57	1,85	1,00	25,97	1,85	1,00
TF125	AP2/EREBP		22,61	1,80	1,00	22,15	1,72	1,00	23,49	1,64	1,00	22,38	1,71	1,00	24,11	1,71	1,00	25,66	1,68	1,00
TF126	AP2/EREBP		24,91	1,77	1,00	25,61	1,83	1,00	24,96	1,84	1,00	26,15	1,75	1,00	23,48	1,92	1,00	25,34	1,93	1,00
TF127	CCHC (Zn)		32,43	1,28	1,00	32,72	1,57	1,00	28,59	1,81	1,00	30,69	1,75	1,00	31,61	1,67	1,00	32,76	1,67	1,00
TF128	ZF DHHC		24,43	1,86	1,00	24,41	1,87	1,00	24,26	1,73	1,00	23,84	1,94	1,00	24,33	1,91	1,00	24,45	1,81	1,00
TF129	MYB/HD-like		25,41	1,90	1,00	25,41	1,89	1,00	24,59	1,42	1,00	21,34	1,87	1,00	21,73	1,80	1,00	21,84	1,84	1,00
TF130	CCHC (Zn)		27,46	1,94	1,00	26,43	2,02	1,00	21,60	1,90	1,00	25,49	1,93	1,00	26,23	1,83	1,00	26,87	1,88	1,00
TF131	HD-like		26,28	2,00	1,00	25,99	1,99	1,00	25,17	1,86	1,00	26,06	1,91	1,00	24,21	1,97	1,00	25,47	1,76	1,00
TF132	HD-like		28,00	2,08	1,00	27,92	1,91	1,00	25,26	1,77	1,00	28,08	1,81	1,00	27,89	1,84	1,00	28,01	1,78	1,00
TF133	NAC		27,55	1,78	1,00	27,58	1,74	1,00	27,63	1,96	1,00	25,60	1,60	1,00	27,07	1,94	1,00	26,81	1,84	1,00
TF134	HD-like		26,69	1,82	1,00	27,66	1,81	1,00	27,42	1,74	1,00	26,40	1,79	1,00	26,58	1,82	1,00	26,95	1,85	1,00

Table S1, continued

TF135	NAC		26,91	1,87	1,00	26,87	1,85	1,00	26,67	1,80	1,00	26,55	2,11	1,00	26,30	1,90	1,00	26,96	1,62	1,00
TF136	NAC		22,58	1,95	1,00	23,44	2,15	1,00	22,26	1,93	1,00	21,69	1,89	1,00	22,19	1,93	1,00	22,15	1,98	1,00
TF137	NAC		25,29	1,86	1,00	25,26	1,95	1,00	24,79	1,89	1,00	25,13	1,89	1,00	23,91	1,94	1,00	24,77	1,75	1,00
TF138	HD-like		27,02	1,96	1,00	28,06	1,86	1,00	27,91	1,88	1,00	27,69	1,96	1,00	27,09	1,90	1,00	27,95	1,86	1,00
TF139	NAC		22,85	1,87	1,00	23,23	1,82	1,00	23,79	1,93	1,00	22,48	1,93	1,00	22,57	1,84	1,00	22,44	1,92	1,00
TF140	PHD		23,35	1,85	1,00	23,20	1,88	1,00	23,63	1,92	1,00	22,63	1,85	1,00	22,92	1,94	1,00	22,77	1,84	1,00
TF141	MYB/HD-like		26,98	1,93	1,00	26,82	1,81	1,00	25,75	1,68	1,00	25,71	1,97	1,00	27,37	1,84	1,00	28,33	1,90	1,00
TF142	C_2C_2 (Zn)	CO-like	26,33	1,87	1,00	27,01	1,78	1,00	26,04	1,88	1,00	26,44	1,89	1,00	26,38	1,88	1,00	26,80	1,78	1,00
TF143	MYB/HD-like		29,48	1,84	1,00	29,24	1,85	1,00	27,94	1,80	1,00	29,16	1,83	1,00	26,27	1,94	1,00	27,93	1,75	1,00
TF144	C_2C_2 (Zn)	CO-like	25,83	1,94	1,00	25,55	1,92	1,00	24,00	1,90	1,00	25,95	1,91	1,00	22,66	1,89	1,00	24,59	2,05	1,00
TF145	MYB		22,36	1,85	1,00	20,74	1,70	1,00	23,50	2,00	1,00	22,84	1,96	1,00	18,99	1,84	1,00	19,99	1,54	0,99
TF146	MYB		27,56	1,81	1,00	26,91	1,90	1,00	22,10	1,90	1,00	26,20	1,79	1,00	26,23	1,83	1,00	27,42	1,88	1,00
TF147	ARF		19,88	1,97	1,00	20,20	1,86	1,00	20,38	1,88	1,00	20,10	2,01	1,00	20,05	1,96	1,00	20,98	2,43	1,00
TF148	ARF		20,06	1,90	1,00	20,77	2,05	1,00	19,81	1,93	1,00	19,63	1,98	1,00	19,85	1,98	1,00	20,01	1,94	1,00
TF149	MYB/HD-like		24,35	1,89	1,00	24,33	1,95	1,00	23,65	1,91	1,00	25,67	1,81	1,00	23,31	1,96	1,00	23,85	1,83	1,00
TF150	MYB		24,39	1,87	1,00	23,81	1,84	1,00	22,41	1,72	1,00	22,39	1,88	1,00	23,91	1,98	1,00	24,90	1,88	1,00
TF151	PHD		29,65	1,83	1,00	30,08	2,02	1,00	27,55	1,80	1,00	29,87	1,78	1,00	29,74	1,77	1,00	30,35	1,80	1,00
TF152	CCHC (Zn)		27,04	1,75	1,00	26,56	1,75	1,00	27,15	1,59	1,00	26,16	1,78	1,00	29,00	1,71	1,00	21,49	1,21	1,00
TF153	CCHC (Zn)		29,89	1,84	1,00	30,80	1,93	1,00	25,74	1,90	1,00	29,83	1,55	1,00	31,32	1,78	1,00	32,10	1,79	1,00
TF154	AP2/EREBP		29,43	1,87	1,00	29,17	1,81	1,00	23,83	2,05	1,00	28,12	1,66	1,00	28,93	1,88	1,00	29,59	1,71	1,00
TF155	AP2/EREBP		28,80	1,80	1,00	28,51	1,78	1,00	23,40	1,72	1,00	27,85	1,81	1,00	28,25	1,77	1,00	29,27	1,73	1,00
TF156	HMG		23,33	1,86	1,00	22,66	1,91	1,00	23,23	1,87	1,00	23,86	1,96	1,00	21,79	1,90	1,00	22,78	1,95	1,00
TF157	C_2C_2 (Zn)	CO-like	20,26	1,90	1,00	21,00	1,98	1,00	19,97	1,91	1,00	21,92	1,96	1,00	22,14	1,88	1,00	22,33	1,97	1,00
TF158	HD-like		35,16	1,81	1,00	32,51	1,84	1,00	31,57	1,73	1,00	31,18	1,86	1,00	32,65	1,90	1,00	32,87	1,93	1,00
TF159	CCHC (Zn)		26,18	1,92	1,00	25,69	1,93	1,00	26,21	1,67	1,00	25,29	1,98	1,00	27,58	1,89	1,00	28,14	1,84	1,00
TF160	HD-like		30,24	1,74	1,00	30,94	1,86	1,00	27,81	1,86	1,00	31,29	1,61	1,00	26,67	1,90	1,00	28,74	2,19	1,00
TF161	C_2H_2 (Zn)		23,89	1,90	1,00	23,78	1,88	1,00	23,94	1,58	1,00	23,59	2,02	1,00	24,00	1,92	1,00	23,99	1,94	1,00
TF162	NAC		28,43	1,84	1,00	27,69	1,76	1,00	28,01	1,62	1,00	27,50	1,84	1,00	30,10	1,84	1,00	30,11	1,83	1,00
TF163	WRKY family	WRKY	27,91	1,86	1,00	28,02	1,84	1,00	28,86	1,79	1,00	27,79	1,81	1,00	27,63	1,81	1,00	28,32	1,83	1,00
TF164	AS2		24,05	1,74	1,00	23,79	1,21	1,00	23,55	1,93	1,00	26,66	1,56	1,00	22,57	1,29	0,99	22,63	1,17	1,00
TF165	HD-like		20,19	1,98	1,00	20,15	1,91	1,00	20,38	1,92	1,00	20,35	2,06	1,00	19,93	1,87	1,00	19,89	1,83	1,00
TF166	Lambda-DB		28,75	1,86	1,00	27,62	1,84	1,00	23,10	1,87	1,00	26,52	1,97	1,00	27,06	2,01	1,00	28,01	1,99	1,00
TF167	Lambda-DB		27,39	1,88	1,00	26,26	1,93	1,00	24,60	1,93	1,00	27,04	1,90	1,00	23,47	2,00	1,00	24,89	1,76	1,00
TF168	HMG		24,17	1,98	1,00	24,33	1,99	1,00	24,38	1,98	1,00	24,70	1,86	1,00	24,20	1,81	1,00	24,68	1,89	1,00
TF169	MYB/HD-like		31,47	1,86	1,00	32,73	1,67	1,00	26,19	1,83	1,00	32,83	1,65	1,00	32,84	1,63	1,00	32,46	1,58	1,00
TF170	MYB/HD-like		21,88	2,04	1,00	21,60	1,92	1,00	18,40	1,84	1,00	21,31	2,06	1,00	22,25	1,85	1,00	21,60	1,86	1,00
TF171	MYB		24,41	1,92	1,00	24,84	1,89	1,00	22,16	1,93	1,00	23,49	1,84	1,00	24,24	1,85	1,00	23,98	1,81	1,00
TF172	MYB		26,64	1,85	1,00	25,68	1,94	1,00	26,70	1,86	1,00	26,65	1,90	1,00	28,95	1,93	1,00	31,22	1,89	1,00
TF173	C_2H_2 (Zn)		21,30	2,00	1,00	21,41	1,96	1,00	20,43	1,87	1,00	21,50	1,94	1,00	19,52	1,89	1,00	20,76	1,94	1,00
TF174	C_2H_2 (Zn)		33,91	1,79	1,00	n.d.	1,39	1,00	30,61	1,90	1,00	36,76	1,31	1,00	33,18	2,31	0,99	32,59	1,72	1,00
TF175	HMG		31,74	1,54	1,00	31,40	1,75	1,00	n.d.	1,47	0,99	33,81	1,55	1,00	29,29	1,72	1,00	31,74	1,61	1,00
TF176	bHLH		31,04	1,67	1,00	28,46	1,84	1,00	23,09	1,73	1,00	26,69	1,77	1,00	27,73	1,75	1,00	28,32	1,76	1,00
TF177	HD-like		25,89	1,90	1,00	26,91	1,79	1,00	23,94	1,86	1,00	24,99	1,89	1,00	25,78	1,97	1,00	26,21	1,79	1,00
TF178	bHLH		28,18	1,96	1,00	26,72	1,94	1,00	26,65	1,93	1,00	26,97	1,85	1,00	25,38	1,86	1,00	25,54	1,82	1,00
TF179	U1-type (Zn)		24,42	1,93	1,00	24,10	1,93	1,00	24,52	1,86	1,00	24,12	1,85	1,00	24,45	1,87	1,00	24,67	1,87	1,00

Table S1, continued

TF180	CCHC (Zn)		24,58	1,94	1,00	24,05	2,01	1,00	22,76	1,89	1,00	23,21	1,86	1,00	24,56	1,75	1,00	24,95	1,85	1,00
TF181	CCHC (Zn)		27,97	1,84	1,00	27,66	1,82	1,00	26,01	1,77	1,00	27,07	1,88	1,00	27,65	1,86	1,00	28,06	1,81	1,00
TF182	CCHC (Zn)		30,45	1,91	1,00	31,29	1,55	1,00	25,41	2,58	1,00	30,86	1,67	1,00	30,37	1,77	1,00	32,62	1,65	1,00
TF183	CCHC (Zn)		27,01	1,97	1,00	27,24	1,73	0,99	23,40	1,80	1,00	25,52	1,82	1,00	25,92	1,90	1,00	26,55	1,89	1,00
TF184	JUMONJI		21,83	2,01	1,00	20,24	1,83	1,00	19,48	2,14	1,00	21,36	1,99	1,00	18,87	1,95	1,00	19,27	1,86	1,00
TF185	JUMONJI		27,86	1,88	1,00	27,40	1,94	1,00	28,21	1,88	1,00	28,27	1,87	1,00	30,21	2,02	1,00	30,02	1,86	1,00
TF186	JUMONJI		26,85	1,91	1,00	26,32	1,96	1,00	26,47	1,92	1,00	29,87	1,92	1,00	27,84	1,90	1,00	29,47	1,95	1,00
TF187	JUMONJI		30,70	1,96	1,00	29,72	1,80	1,00	30,45	1,82	1,00	31,59	1,90	1,00	31,47	1,93	1,00	31,48	1,84	1,00
TF188	JUMONJI		25,37	1,89	1,00	26,49	1,87	1,00	27,33	1,87	1,00	26,96	1,86	1,00	26,93	1,81	1,00	27,47	1,91	1,00
TF189	JUMONJI		39,58	1,41	0,99	35,31	1,47	1,00	31,96	1,71	1,00	33,56	1,66	1,00	30,75	1,67	1,00	33,15	1,68	1,00
TF190	bHLH		26,14	1,91	1,00	24,15	1,90	1,00	18,78	1,90	1,00	23,54	1,84	1,00	24,73	1,77	1,00	25,31	1,85	1,00
TF191	bHLH		32,33	1,76	1,00	35,04	1,77	1,00	33,48	1,68	1,00	37,92	1,51	0,99	29,09	1,78	1,00	31,48	1,77	1,00
TF192	NAC		27,56	1,87	1,00	27,98	1,86	1,00	25,07	1,89	1,00	27,90	1,82	1,00	27,68	1,86	1,00	27,98	1,88	1,00
TF193	ARID		24,12	1,92	1,00	24,24	1,93	1,00	24,20	1,88	1,00	24,08	1,90	1,00	24,27	1,92	1,00	24,32	1,93	1,00
TF194	MYB/HD-like		22,43	1,74	1,00	22,21	2,01	1,00	18,21	1,99	1,00	22,38	1,90	1,00	22,23	1,82	1,00	22,60	2,09	1,00
TF195	MYB/HD-like		26,25	1,88	1,00	25,71	1,91	1,00	26,21	1,72	1,00	26,61	1,79	1,00	26,61	1,79	1,00	29,38	2,17	1,00
TF196	EIL		20,01	1,94	1,00	20,70	1,95	1,00	19,83	1,95	1,00	19,52	1,95	1,00	19,81	2,08	1,00	19,94	1,95	1,00
TF197	EIL		20,26	1,97	1,00	20,59	1,91	0,99	20,52	1,98	1,00	20,40	2,17	1,00	20,11	1,75	1,00	20,28	2,09	1,00
TF198	MYB		26,92	1,91	1,00	26,17	1,92	1,00	24,52	1,95	1,00	26,68	1,93	1,00	23,35	1,85	1,00	24,98	1,90	1,00
TF199	NAC		23,72	1,98	1,00	24,09	1,93	1,00	23,92	1,98	1,00	23,49	1,95	1,00	23,34	1,97	1,00	23,67	1,79	1,00
TF200	NAC		21,97	1,91	1,00	21,28	1,94	1,00	21,52	1,90	1,00	20,35	1,93	1,00	21,92	1,83	1,00	22,52	1,84	1,00
TF201	WRKY family	WRKY	28,56	1,92	1,00	29,37	1,95	1,00	28,54	1,91	1,00	28,13	2,12	1,00	28,81	2,17	1,00	28,61	1,88	1,00
TF202	MYB		32,27	1,82	1,00	31,71	1,86	1,00	30,35	1,62	1,00	31,91	1,88	1,00	28,37	1,86	1,00	30,68	1,86	1,00
TF203	ZF DHHC		24,20	1,94	1,00	25,11	2,11	1,00	22,49	1,93	1,00	23,82	1,92	1,00	24,24	1,95	1,00	24,24	1,90	1,00
TF204	JUMONJI		24,67	2,03	1,00	24,85	1,87	1,00	24,75	1,89	1,00	24,17	1,91	1,00	24,56	1,86	1,00	24,70	1,92	1,00
TF205	JUMONJI		31,95	1,80	1,00	32,18	1,75	1,00	29,88	1,80	1,00	31,93	1,81	1,00	28,76	1,82	1,00	30,02	1,76	1,00
TF206	C_2C_2 (Zn)	YABBY	21,58	1,94	1,00	21,98	2,06	1,00	23,03	1,97	1,00	22,45	1,99	1,00	22,17	1,96	1,00	22,17	1,90	1,00
TF207	C_2C_2 (Zn)	YABBY	21,84	1,91	1,00	22,42	1,91	1,00	22,35	1,96	1,00	22,11	1,91	1,00	22,26	1,88	1,00	22,49	1,97	1,00
TF208	CCHC (Zn)		30,48	1,81	1,00	29,59	1,77	1,00	30,47	1,52	1,00	30,95	1,81	1,00	31,01	1,84	1,00	34,75	1,72	1,00
TF209	CCHC (Zn)		26,37	1,83	1,00	25,81	1,72	1,00	22,39	2,05	1,00	25,00	2,11	1,00	25,37	1,99	1,00	26,05	2,11	1,00
TF210	p53-like		27,94	1,89	1,00	27,19	1,75	0,98	21,66	1,83	1,00	31,49	1,58	1,00	26,14	1,78	1,00	26,21	1,74	1,00
TF211	CCHC (Zn)		29,10	1,87	1,00	28,87	1,80	1,00	28,35	1,86	1,00	31,68	1,16	0,93	23,92	1,72	1,00	24,86	1,99	0,99
TF212	HTH	FIS	29,24	1,73	1,00	27,76	1,76	1,00	25,11	1,78	1,00	28,99	1,64	1,00	25,12	1,60	1,00	31,66	1,61	1,00
TF213	ARF		30,72	1,86	1,00	29,43	1,93	1,00	29,00	1,67	1,00	28,92	1,81	1,00	29,80	1,73	1,00	29,49	1,33	0,99
TF214	bZIP		23,86	1,88	1,00	24,36	1,93	1,00	22,52	1,86	1,00	23,23	2,17	1,00	23,38	1,77	1,00	23,26	1,84	1,00
TF215	TCP		22,77	1,99	1,00	23,26	1,94	1,00	20,96	1,90	1,00	21,70	1,95	1,00	22,03	1,98	1,00	22,26	1,92	1,00
TF216	ARF		26,89	1,85	1,00	26,86	1,94	1,00	21,55	1,90	1,00	25,96	1,94	1,00	26,97	2,07	1,00	27,66	1,82	1,00
TF217	PHD		23,72	1,89	1,00	23,66	2,03	1,00	23,86	1,89	1,00	23,46	1,91	1,00	24,04	1,87	1,00	24,02	1,25	1,00
TF218	ABI3-VP1		27,96	1,86	1,00	28,10	1,88	1,00	27,34	1,88	1,00	26,74	1,90	1,00	29,92	1,82	1,00	31,26	1,83	1,00
TF219	WRKY family	WRKY	26,99	1,92	1,00	26,83	1,91	1,00	26,58	1,93	1,00	25,48	1,92	1,00	27,09	1,89	1,00	28,19	1,94	1,00
TF220	MADS		30,95	1,76	1,00	30,60	1,78	1,00	33,00	1,77	1,00	30,65	1,82	1,00	30,47	1,69	1,00	30,50	1,75	1,00
TF221	MADS		27,83	1,83	1,00	26,87	1,81	1,00	26,27	1,98	1,00	27,22	2,13	1,00	24,71	1,88	1,00	25,02	1,82	1,00
TF222	C_2C_2 (Zn)	YABBY	28,32	1,91	1,00	27,81	1,93	1,00	25,95	1,89	1,00	27,39	1,87	1,00	24,73	1,89	1,00	26,16	1,87	1,00
TF223	TTF-type (Zn)		28,40	1,77	1,00	27,88	1,90	0,98	23,82	1,96	1,00	28,23	1,61	1,00	26,50	1,85	1,00	27,44	1,82	1,00
TF224	CCHC (Zn)		31,44	1,84	1,00	32,91	1,78	1,00	26,53	1,77	1,00	30,56	1,84	1,00	30,98	1,79	1,00	31,83	1,76	1,00
TF225	CCHC (Zn)		28,55	1,79	1,00	29,02	1,95	1,00	22,97	1,91	1,00	27,10	1,83	1,00	28,07	1,81	1,00	28,75	1,84	1,00

Table S1, continued

TF226	WRKY family	WRKY	30,47	1,84	1,00	29,21	2,05	1,00	24,57	1,84	1,00	28,56	1,85	1,00	28,97	1,85	1,00	29,74	1,91	1,00
TF227	BD		24,14	1,90	1,00	24,91	1,89	1,00	23,81	1,85	1,00	23,39	1,94	1,00	23,52	1,87	1,00	23,94	1,97	1,00
TF228	bHLH		29,50	1,84	1,00	30,18	1,74	1,00	27,70	1,82	1,00	29,10	1,74	1,00	29,35	1,80	1,00	30,13	1,80	1,00
TF229	PHD		20,99	1,88	1,00	21,59	1,89	1,00	20,10	1,99	1,00	20,70	1,97	1,00	21,57	2,05	1,00	21,75	1,92	1,00
TF230	HD-like		21,01	1,96	1,00	20,77	1,85	1,00	21,08	1,90	1,00	20,47	1,91	1,00	20,85	1,90	1,00	20,77	1,85	1,00
TF231	C_2H_2 (Zn)		29,90	1,88	1,00	30,07	1,90	1,00	28,87	1,89	1,00	28,79	1,97	1,00	30,26	1,97	1,00	31,49	1,84	1,00
TF232	ABI3-VP1		30,12	1,85	1,00	30,25	1,83	1,00	36,46	1,33	1,00	31,49	1,72	1,00	33,16	1,66	1,00	32,55	1,76	1,00
TF233	HMG		21,76	1,90	1,00	21,96	1,82	1,00	22,19	1,94	1,00	22,05	1,87	1,00	21,88	1,86	1,00	21,95	1,83	1,00
TF234	MADS		28,95	1,98	1,00	28,86	1,85	1,00	29,00	1,95	1,00	29,39	1,76	1,00	30,73	1,74	1,00	31,07	1,86	1,00
TF235	NAC		28,85	1,87	1,00	27,52	1,95	1,00	27,00	1,87	1,00	28,16	1,84	1,00	26,15	1,89	1,00	26,31	1,90	1,00
TF236	bZIP		23,88	1,93	1,00	23,34	1,92	1,00	23,23	1,93	1,00	23,22	1,99	1,00	22,33	1,92	1,00	23,12	1,92	1,00
TF237	CCHC (Zn)		25,71	1,88	1,00	24,68	1,95	1,00	19,39	1,93	1,00	24,37	2,08	1,00	25,14	2,08	1,00	25,25	1,78	1,00
TF238	CCHC (Zn)		26,48	1,84	1,00	26,55	1,89	1,00	22,54	1,84	1,00	25,70	1,87	1,00	25,81	1,91	1,00	26,48	1,90	1,00
TF239	CCHC (Zn)		30,89	1,84	1,00	31,50	1,89	0,99	26,49	1,91	1,00	n.d.	1,84	0,98	29,90	1,95	1,00	30,55	1,93	1,00
TF240	CCHC (Zn)		28,02	1,88	1,00	28,29	1,78	1,00	23,74	1,88	1,00	27,23	1,89	1,00	27,66	1,88	1,00	28,41	1,78	1,00
TF241	CCHC (Zn)		24,45	1,91	1,00	23,95	1,96	1,00	25,89	1,90	1,00	23,67	1,98	1,00	24,60	1,95	1,00	25,23	1,87	1,00
TF242	SNF2		23,41	1,95	1,00	23,25	1,90	1,00	23,45	1,90	1,00	23,00	1,97	1,00	23,25	1,85	1,00	23,43	1,86	1,00
TF243	CCHC (Zn)		27,34	1,87	1,00	27,24	1,82	1,00	29,85	1,88	1,00	27,58	1,81	1,00	29,40	1,82	1,00	32,11	1,21	1,00
TF244	MYB/HD-like		23,24	1,95	1,00	23,17	1,93	1,00	23,44	1,88	1,00	23,11	1,95	1,00	23,42	1,87	1,00	23,43	1,88	1,00
TF245	WRKY family	WRKY	25,75	1,60	1,00	27,26	2,14	0,99	25,40	1,57	1,00	24,69	1,58	1,00	24,92	1,60	1,00	25,23	1,68	1,00
TF246	WRKY family	WRKY	24,60	1,87	1,00	24,60	1,84	1,00	24,96	1,93	1,00	23,91	1,83	1,00	24,02	1,78	1,00	24,22	1,88	1,00
TF247	C_2H_2 (Zn)		30,00	1,74	1,00	29,71	1,85	1,00	30,58	1,76	1,00	32,38	1,30	1,00	30,61	1,80	1,00	32,22	1,70	1,00
TF248	MYB/HD-like		23,11	1,92	1,00	23,00	1,89	1,00	23,51	1,97	1,00	22,68	1,98	1,00	23,07	1,93	1,00	33,91	1,19	1,00
TF249	C_2H_2 (Zn)		29,21	1,82	1,00	29,20	1,87	1,00	28,71	1,85	1,00	30,39	1,33	0,88	23,77	1,91	1,00	25,08	1,74	1,00
TF250	CCHC (Zn)		30,39	1,85	1,00	31,14	1,85	1,00	27,76	1,83	1,00	28,46	1,84	1,00	29,23	1,84	1,00	30,19	1,82	1,00
TF251	C_2H_2 (Zn)		27,64	2,23	1,00	26,83	1,84	1,00	22,96	1,85	1,00	25,89	1,93	1,00	26,49	1,99	1,00	26,46	1,73	1,00
TF252	C_2H_2 (Zn)		26,09	1,80	1,00	25,75	1,88	0,99	21,71	1,84	1,00	23,77	1,80	1,00	24,34	1,77	1,00	24,94	1,67	1,00
TF253	HTH	FIS	28,32	1,80	1,00	28,61	1,81	1,00	28,49	1,77	1,00	27,85	1,93	1,00	29,95	1,80	1,00	30,37	1,92	1,00
TF254	C_2H_2 (Zn)		29,00	1,79	1,00	28,83	1,81	1,00	27,55	1,88	1,00	26,53	1,80	1,00	26,23	1,79	1,00	25,89	2,05	1,00
TF255	HTH	FIS	25,61	1,88	1,00	24,65	2,01	1,00	23,17	1,90	1,00	25,81	1,82	1,00	22,27	1,89	1,00	28,30	1,27	0,97
TF256	CCHC (Zn)		29,79	1,85	1,00	29,28	1,96	1,00	24,59	1,75	1,00	28,44	1,83	1,00	29,18	1,95	1,00	29,92	1,89	1,00
TF257	AP2/EREBP		26,56	2,00	1,00	27,10	1,86	1,00	25,79	1,89	1,00	27,15	1,88	1,00	27,07	1,98	1,00	27,00	1,90	1,00
TF258	HD family	HD	18,93	2,02	1,00	17,57	2,37	1,00	17,82	2,28	1,00	21,42	1,98	1,00	16,04	2,25	0,99	19,63	1,95	1,00
TF259	CCAAT	CCAAT-HAP3	28,71	1,80	1,00	28,21	1,83	1,00	23,67	1,86	1,00	27,34	1,77	1,00	27,88	1,82	1,00	28,04	1,77	1,00
TF260	CCAAT	CCAAT-HAP3	26,79	1,77	1,00	26,22	2,03	1,00	24,97	1,79	1,00	25,62	1,65	1,00	26,67	1,73	1,00	27,05	1,90	1,00
TF261	MYB		28,76	1,69	1,00	29,31	1,82	1,00	29,91	1,79	1,00	28,33	1,82	1,00	29,71	1,86	1,00	32,18	1,72	1,00
TF262	CCHC (Zn)		23,78	2,05	1,00	23,87	2,04	1,00	23,97	1,89	1,00	25,11	1,93	1,00	25,30	1,95	1,00	25,15	1,93	1,00
TF263	CCHC (Zn)		29,08	1,80	1,00	28,62	1,74	1,00	30,98	1,66	1,00	30,53	1,71	1,00	31,93	1,73	1,00	34,89	1,49	1,00
TF264	PHD		22,01	1,91	1,00	22,35	2,05	1,00	22,49	1,98	1,00	21,98	2,01	1,00	22,13	1,81	1,00	22,20	1,90	1,00
TF265	C_2C_2 (Zn)	DOF	23,83	1,92	1,00	23,76	1,82	1,00	23,93	1,91	1,00	26,50	1,93	1,00	28,56	1,86	1,00	28,91	1,96	1,00
TF266	CCAAT	CCAAT-HAP3	21,75	1,82	1,00	22,84	1,33	0,99	24,92	1,34	0,99	25,12	1,71	1,00	22,15	1,91	1,00	22,95	1,25	1,00
TF267	BTB/POZ		28,96	1,88	1,00	30,50	1,96	1,00	29,24	1,85	1,00	29,01	1,85	1,00	28,66	1,81	1,00	30,47	1,88	1,00
TF268	bZIP		24,79	1,99	1,00	23,97	2,05	1,00	24,17	1,94	1,00	24,51	1,91	1,00	25,51	1,96	1,00	26,08	1,85	1,00
TF269	BD		31,15	1,95	1,00	32,53	1,96	1,00	34,07	1,63	1,00	31,71	2,05	1,00	39,28	1,23	0,99	33,81	1,66	1,00
TF270	C_2H_2 (Zn)		25,43	2,06	1,00	25,20	1,91	1,00	26,13	1,87	1,00	24,96	1,84	1,00	26,04	1,87	1,00	27,16	1,85	1,00

Table S1, continued

TF271	C_2H_2 (Zn)		26,32	1,85	1,00	25,56	1,98	1,00	20,51	1,90	1,00	24,91	1,86	1,00	25,32	1,82	1,00	26,01	1,82	1,00
TF272	C_2H_2 (Zn)		31,05	1,80	1,00	29,82	1,74	1,00	30,86	1,60	1,00	30,74	1,74	1,00	30,78	1,67	1,00	34,46	1,69	1,00
TF273	PHD		22,97	1,96	1,00	23,00	2,08	1,00	22,91	1,87	1,00	22,43	1,92	1,00	23,19	2,09	1,00	22,77	1,88	1,00
TF274	C_2H_2 (Zn)		28,66	2,06	1,00	28,11	1,68	1,00	23,73	3,08	1,00	27,05	1,87	1,00	27,95	2,64	1,00	28,46	2,09	0,99
TF275	HSF		26,56	1,22	1,00	27,08	1,87	1,00	22,92	1,85	1,00	25,43	1,89	1,00	26,44	1,82	1,00	27,06	1,97	1,00
TF276	RR		22,37	1,93	1,00	22,60	1,96	1,00	21,54	1,93	1,00	21,14	1,87	1,00	21,70	1,89	1,00	21,81	1,87	1,00
TF277	E2F		22,49	1,94	1,00	22,20	2,07	1,00	21,98	1,87	1,00	20,73	1,90	1,00	21,48	1,84	1,00	21,45	1,52	1,00
TF278	MYB		22,66	1,92	1,00	22,55	1,77	1,00	22,90	2,39	1,00	23,51	1,83	1,00	22,98	1,90	1,00	24,05	1,60	0,99
TF279	MYB/HD-like		22,55	1,94	1,00	23,11	2,04	1,00	21,84	1,98	1,00	22,83	1,96	1,00	23,35	1,92	1,00	23,59	1,92	1,00
TF280	WRKY family	WRKY	23,19	1,93	1,00	23,15	2,09	1,00	23,22	2,00	1,00	22,53	1,91	1,00	22,92	1,91	1,00	22,88	1,93	1,00
TF281	WRKY family	WRKY	23,34	1,96	1,00	23,51	1,88	1,00	24,84	1,89	1,00	23,81	1,90	1,00	23,93	1,96	1,00	23,87	2,05	1,00
TF282	WRKY family	WRKY	26,64	1,81	1,00	26,86	1,83	1,00	25,57	1,91	1,00	26,65	1,90	1,00	24,73	1,86	1,00	25,98	1,77	1,00
TF283	CCHC (Zn)		28,52	1,85	1,00	30,10	1,90	1,00	26,92	1,78	1,00	29,28	1,87	1,00	28,42	1,77	1,00	30,93	1,76	1,00
TF284	MYB/HD-like		29,71	1,80	1,00	30,76	1,84	1,00	29,54	1,78	1,00	29,90	1,71	1,00	29,61	1,83	1,00	30,21	1,74	1,00
TF285	MYB/HD-like		28,29	1,86	1,00	27,89	1,89	1,00	30,69	1,77	1,00	30,78	1,85	1,00	30,23	1,86	1,00	30,99	1,82	1,00
TF286	PHD		24,46	1,94	1,00	24,36	1,90	1,00	24,40	1,90	1,00	24,36	1,90	1,00	24,55	1,88	1,00	24,64	1,92	1,00
TF287	PHD		24,31	1,92	1,00	24,17	1,91	1,00	24,18	1,95	1,00	24,20	2,02	1,00	24,35	1,87	1,00	25,01	1,95	1,00
TF288	HD family	HD-ZIP	26,61	1,84	1,00	27,32	1,88	1,00	26,51	1,77	1,00	26,33	1,89	1,00	26,36	1,85	1,00	26,53	1,82	1,00
TF289	E2F		25,31	1,89	1,00	24,77	1,74	1,00	25,52	2,02	1,00	24,83	2,02	1,00	26,28	1,88	1,00	26,91	2,06	0,99
TF290	E2F		26,62	1,88	1,00	27,53	1,97	1,00	26,78	1,89	1,00	26,64	1,93	1,00	26,98	1,85	1,00	27,15	2,04	1,00
TF291	C_2H_2 (Zn)		32,42	1,72	1,00	30,62	1,72	1,00	27,46	1,79	1,00	30,12	1,71	1,00	30,81	1,71	1,00	31,58	1,61	1,00
TF292	ZIM		28,22	1,87	1,00	26,36	1,87	1,00	24,54	1,87	1,00	27,65	1,96	1,00	23,14	1,90	1,00	24,73	1,96	1,00
TF293	HMG		31,81	1,94	1,00	32,48	1,83	1,00	28,86	1,95	1,00	32,11	1,89	1,00	27,20	1,89	1,00	30,94	1,94	1,00
TF294	CCHC (Zn)		21,41	1,86	1,00	22,04	1,96	1,00	21,10	1,90	1,00	21,21	1,97	1,00	21,20	1,91	1,00	21,40	1,81	1,00
TF295	HD family	HD	26,63	1,95	1,00	26,37	1,94	1,00	26,64	1,91	1,00	26,34	1,96	1,00	27,63	1,94	1,00	27,82	1,89	1,00
TF296	GRAS		24,81	1,93	1,00	24,72	1,91	1,00	24,98	1,90	1,00	23,16	1,87	1,00	23,96	1,93	1,00	23,99	1,71	1,00
TF297	GRAS		24,27	1,87	1,00	24,60	1,93	1,00	20,73	1,98	1,00	22,92	1,87	1,00	23,19	1,86	1,00	23,48	1,85	1,00
TF298	WRKY family	WRKY	22,36	1,86	1,00	22,40	1,83	1,00	22,59	1,88	1,00	21,51	1,88	1,00	21,68	1,92	1,00	21,58	1,84	1,00
TF299	CCHC (Zn)		24,09	1,91	1,00	24,10	1,88	1,00	26,54	1,89	1,00	22,67	1,92	1,00	25,68	1,86	1,00	27,25	1,78	1,00
TF300	AP2/EREBP		33,82	1,27	1,00	30,32	1,70	1,00	28,72	1,78	1,00	30,54	1,74	1,00	27,61	1,73	1,00	28,98	1,70	1,00
TF301	PHD		21,12	1,90	1,00	21,84	1,95	1,00	20,42	1,93	1,00	20,73	1,88	1,00	21,68	1,90	1,00	21,85	1,90	1,00
TF302	AP2/EREBP		26,36	1,92	1,00	25,32	1,96	1,00	20,32	1,97	1,00	25,33	1,93	1,00	25,88	1,89	1,00	26,28	1,71	1,00
TF303	AP2/EREBP		24,95	1,82	1,00	24,93	1,83	1,00	24,75	1,89	1,00	25,04	1,88	1,00	24,25	1,96	1,00	25,32	1,89	1,00
TF304	CCHC (Zn)		29,74	1,78	1,00	29,02	1,82	1,00	34,64	1,61	1,00	35,55	12,54	0,69	37,27	1,58	1,00	37,73	1,70	1,00
TF305	MYB/HD-like		22,98	1,72	1,00	23,66	1,79	1,00	21,96	1,84	1,00	22,50	1,78	1,00	23,15	1,77	0,99	23,50	1,80	1,00
TF306	MYB		22,21	1,88	1,00	22,61	1,85	1,00	22,81	1,90	1,00	22,28	1,48	1,00	22,61	2,00	1,00	22,78	1,76	1,00
TF307	C3H	C3H-type 1 (Zn)	23,40	1,85	1,00	24,18	2,09	1,00	22,79	1,90	1,00	23,40	1,87	1,00	23,43	1,97	1,00	23,45	1,78	1,00
TF308	C_2C_2 (Zn)	DOF	24,05	1,90	1,00	23,67	1,90	1,00	20,25	2,00	1,00	22,67	1,91	1,00	23,68	1,95	1,00	23,43	1,92	1,00
TF309	GRF		30,48	1,85	1,00	29,88	1,79	1,00	24,61	1,96	1,00	28,97	1,87	1,00	29,91	1,83	1,00	30,74	1,88	1,00
TF310	RR		39,51	1,30	1,00	n.d.	1,27	0,46	39,86	1,32	1,00	34,40	1,19	0,96	n.d.	1,11	0,99	32,33	1,64	1,00
TF311	MYB		22,93	1,99	1,00	22,88	1,84	1,00	23,29	2,47	1,00	22,89	1,99	1,00	22,98	1,88	1,00	23,00	1,84	1,00
TF312	SNF2		23,33	1,92	1,00	23,16	1,89	1,00	23,37	1,91	1,00	23,11	1,93	1,00	23,15	1,93	1,00	23,32	1,87	1,00
TF313	MYB		22,98	1,94	1,00	23,61	2,11	1,00	22,68	1,93	1,00	22,42	1,92	1,00	22,77	1,89	1,00	22,88	1,90	1,00
TF314	GRAS		27,29	1,94	1,00	26,09	1,92	1,00	25,12	1,90	1,00	27,53	2,01	0,99	23,09	1,90	1,00	24,97	2,06	1,00
TF315	AS2		20,72	1,97	1,00	20,91	2,04	1,00	20,98	1,86	1,00	20,68	1,93	1,00	21,00	1,99	1,00	20,69	1,94	1,00

Table S1, continued

TF316	AP2/EREBP		31,09	1,76	1,00	32,34	1,69	1,00	28,19	1,75	1,00	30,08	1,71	1,00	29,51	1,59	1,00	31,45	1,77	1,00
TF317	CCAAT	CCAAT-HAP3	24,00	1,74	1,00	24,68	2,01	1,00	23,66	1,84	1,00	24,01	1,89	1,00	24,09	2,03	1,00	24,32	1,23	1,00
TF318	CCHC (Zn)		30,25	1,73	1,00	29,27	1,51	1,00	25,09	1,67	1,00	27,78	1,82	1,00	29,75	1,80	1,00	30,74	1,81	1,00
TF319	CCHC (Zn)		24,81	1,87	1,00	25,79	1,92	1,00	24,42	1,84	1,00	24,41	1,91	1,00	24,01	1,92	1,00	25,49	1,94	1,00
TF320	MADS		24,94	1,98	1,00	23,13	1,96	1,00	20,68	2,06	1,00	23,79	1,93	1,00	20,30	2,05	1,00	21,98	1,99	1,00
TF321	MADS		29,90	1,78	1,00	30,33	1,71	1,00	25,16	1,84	1,00	27,40	1,81	1,00	27,86	1,95	1,00	28,20	1,81	1,00
TF322	MADS		25,81	2,13	1,00	26,77	1,92	1,00	24,70	1,94	1,00	24,96	1,96	1,00	25,63	1,86	1,00	26,51	1,90	1,00
TF323	MADS		30,62	1,86	1,00	29,80	1,87	1,00	28,41	1,79	1,00	27,81	1,91	1,00	28,41	1,44	1,00	28,78	1,79	1,00
TF324	AP2/EREBP		23,21	1,83	1,00	23,82	2,11	1,00	23,03	2,11	1,00	21,51	1,91	1,00	21,58	1,79	1,00	21,76	2,16	1,00
TF325	C3H	C3H-type 1 (Zn)	23,27	1,95	1,00	22,96	2,07	1,00	20,94	1,92	1,00	22,54	1,89	1,00	23,12	1,91	1,00	23,00	1,86	1,00
TF326	C_2H_2 (Zn)		25,74	1,75	1,00	25,84	1,82	1,00	26,09	1,73	1,00	25,88	1,79	1,00	26,72	2,25	1,00	28,08	1,65	1,00
TF327	ABI3-VP1		24,61	1,88	1,00	24,78	1,88	1,00	25,42	1,94	1,00	24,99	1,96	1,00	24,60	1,91	1,00	24,99	1,83	1,00
TF328	ABI3-VP1		27,02	2,03	1,00	25,73	1,90	0,99	24,95	1,91	1,00	25,83	2,06	1,00	24,33	1,67	1,00	24,73	1,65	1,00
TF329	ABI3-VP1		24,57	1,93	1,00	24,96	2,13	1,00	24,99	1,90	1,00	24,10	2,02	1,00	24,28	1,83	1,00	24,27	1,81	1,00
TF330	WRKY family	WRKY	24,32	1,79	1,00	24,68	1,86	1,00	21,63	1,64	1,00	23,94	1,83	1,00	24,11	1,71	1,00	24,40	1,70	1,00
TF331	WRKY family	WRKY	24,83	1,91	1,00	24,74	1,98	1,00	20,93	2,01	1,00	23,51	1,93	1,00	23,77	1,89	1,00	24,24	1,95	1,00
TF332	MYB		25,56	1,86	1,00	25,54	1,89	1,00	24,67	1,86	1,00	24,36	1,84	1,00	23,68	1,83	1,00	24,57	1,90	1,00
TF333	bHLH		26,24	1,78	1,00	26,21	1,83	1,00	26,47	1,86	1,00	23,98	1,83	1,00	24,15	1,86	1,00	24,24	1,81	1,00
TF334	CCHC (Zn)		28,86	1,80	1,00	28,04	1,82	1,00	29,04	1,67	1,00	26,95	1,79	1,00	28,10	1,82	1,00	28,28	1,72	1,00
TF335	MADS		24,72	1,79	1,00	25,26	1,87	1,00	21,54	1,91	1,00	24,63	1,89	1,00	25,65	1,74	1,00	25,88	1,92	1,00
TF336	MYB/HD-like		25,10	1,88	1,00	24,89	1,76	1,00	24,97	1,84	1,00	24,91	1,91	1,00	24,17	1,92	1,00	24,24	1,89	1,00
TF337	TTF-type (Zn)		30,58	1,83	1,00	31,46	1,76	1,00	28,85	1,80	1,00	31,72	1,82	1,00	32,10	1,77	1,00	32,72	1,76	1,00
TF338	C_2C_2 (Zn)	DOF	23,59	2,17	1,00	22,39	1,92	1,00	24,26	1,88	1,00	23,52	2,00	1,00	21,30	1,97	1,00	22,54	2,03	1,00
TF339	AP2/EREBP		32,05	1,75	1,00	31,92	1,76	1,00	27,83	1,86	1,00	32,12	1,71	1,00	30,34	1,89	1,00	30,60	1,71	1,00
TF340	AS2		29,80	1,66	1,00	29,21	1,76	1,00	27,11	1,81	1,00	28,58	1,59	1,00	26,60	1,77	1,00	27,82	1,61	1,00
TF341	C_2H_2 (Zn)		26,86	1,85	1,00	27,13	1,61	1,00	24,96	1,92	1,00	23,99	2,03	1,00	24,81	1,87	1,00	24,72	1,96	1,00
TF342	CCHC (Zn)		30,17	1,58	1,00	36,00	1,66	1,00	30,76	1,74	1,00	31,38	1,80	1,00	30,58	1,81	1,00	34,14	1,83	1,00
TF343	bZIP		26,74	1,80	1,00	27,49	1,81	1,00	26,93	1,81	1,00	27,41	1,91	1,00	25,16	1,85	1,00	26,93	1,84	1,00
TF344	WRKY family	WRKY	22,95	1,91	1,00	23,25	2,03	1,00	20,69	1,88	1,00	22,33	1,83	1,00	22,42	1,97	1,00	22,35	1,85	1,00
TF345	PHD		23,64	2,18	1,00	23,57	1,86	1,00	23,53	1,89	1,00	23,34	1,87	1,00	23,11	1,95	1,00	22,83	1,80	1,00
TF346	CCHC (Zn)		21,39	1,98	1,00	21,10	1,85	1,00	21,80	1,91	1,00	20,93	2,11	1,00	22,62	1,82	1,00	23,23	1,88	1,00
TF347	C_2H_2 (Zn)		18,62	2,50	1,00	18,01	2,21	1,00	18,74	1,74	1,00	18,24	2,24	1,00	18,95	1,66	0,99	19,33	1,62	0,99
TF348	TTF-type (Zn)		26,08	1,90	1,00	25,41	1,91	1,00	20,07	1,92	1,00	24,77	1,90	1,00	25,63	1,91	1,00	26,50	1,84	1,00
TF349	CCHC (Zn)		24,74	1,86	1,00	25,57	1,85	1,00	24,41	1,93	1,00	23,82	1,91	1,00	24,13	1,91	1,00	24,28	1,82	1,00
TF350	AP2/EREBP		23,53	1,84	1,00	23,57	1,92	1,00	23,71	1,87	1,00	22,95	2,14	1,00	22,93	1,83	1,00	23,06	1,85	1,00
TF351	bHLH		23,21	1,81	1,00	23,71	1,79	1,00	22,82	1,87	1,00	22,97	1,86	1,00	22,94	1,83	1,00	23,11	1,86	1,00
TF352	AP2/EREBP		28,06	1,87	1,00	27,82	1,86	1,00	27,65	1,85	1,00	28,12	1,79	1,00	27,39	1,94	1,00	27,79	1,93	1,00
TF353	AUX/IAA		21,57	1,93	1,00	21,81	1,95	1,00	21,38	1,89	1,00	20,38	1,86	1,00	20,61	1,96	1,00	20,67	1,94	1,00
TF354	HD family	HD	24,03	1,86	1,00	23,98	1,81	1,00	24,36	1,90	1,00	23,84	2,39	1,00	23,72	1,90	1,00	23,73	1,95	1,00
TF355	HD-like		30,45	1,87	1,00	29,41	1,98	1,00	30,02	1,85	1,00	28,64	1,44	0,99	26,33	1,93	1,00	27,02	2,02	1,00
TF356	HD-like		27,57	1,84	1,00	27,14	1,83	1,00	21,64	2,12	1,00	28,29	1,77	1,00	27,19	1,82	1,00	26,81	1,84	1,00
TF357	CCAAT	CCAAT-HAP3	21,49	1,87	1,00	22,17	1,95	1,00	20,38	1,99	1,00	21,12	1,89	1,00	21,15	1,88	1,00	21,40	1,85	1,00
TF358	C3H	C3H-type 1 (Zn)	30,07	1,60	1,00	30,21	1,64	1,00	26,63	1,45	1,00	28,32	1,62	1,00	30,05	1,57	1,00	30,72	1,50	1,00
TF359	HTH	FIS	23,44	1,86	1,00	23,43	1,85	1,00	23,31	1,90	1,00	25,05	1,41	0,98	24,00	1,94	1,00	23,85	1,84	1,00
TF360	bZIP		25,21	1,83	1,00	25,40	1,94	1,00	25,43	1,88	1,00	24,50	1,88	1,00	25,06	1,91	1,00	24,82	1,92	1,00
TF361	bZIP		n.d.	1,22	1,00	33,58	1,51	1,00	32,45	1,57	1,00	n.d.	1,87	0,92	31,64	1,54	1,00	33,01	1,61	1,00

Table S1, continued

TF362	bZIP		39,02	1,56	0,94	31,66	1,74	1,00	31,59	1,77	1,00	32,69	1,70	1,00	30,14	1,53	1,00	31,32	1,81	1,00
TF363	CCHC (Zn)		27,56	1,88	1,00	29,25	1,83	1,00	22,11	2,06	1,00	26,01	1,91	1,00	27,77	1,88	1,00	27,72	1,92	1,00
TF364	CCAAT	CCAAT-HAP3	24,01	1,85	1,00	24,90	1,90	1,00	23,75	1,91	1,00	23,98	1,85	1,00	24,59	1,94	1,00	25,64	1,86	1,00
TF365	C_2H_2 (Zn)		23,20	1,91	1,00	23,12	1,90	1,00	23,23	1,92	1,00	23,16	1,92	1,00	23,37	1,88	1,00	23,48	1,88	1,00
TF366	HMG		26,31	1,93	1,00	26,30	1,88	1,00	26,02	1,90	1,00	26,47	1,99	1,00	25,99	1,93	1,00	26,92	1,87	1,00
TF367	HD family	HD	28,14	1,91	1,00	28,62	1,88	1,00	24,35	1,87	1,00	27,35	1,86	1,00	27,71	1,78	1,00	28,47	1,80	1,00
TF368	HD-like		25,70	1,82	1,00	25,56	1,83	1,00	25,71	1,89	1,00	25,95	1,74	1,00	26,30	1,65	1,00	26,84	1,95	0,97
TF369	MYB/HD-like		23,97	1,95	1,00	23,87	1,92	1,00	23,97	1,86	1,00	22,89	1,98	1,00	22,79	1,94	1,00	22,87	1,98	1,00
TF370	HD family	HD	22,20	1,83	1,00	22,15	1,90	1,00	22,01	1,94	1,00	21,73	1,91	1,00	21,20	2,12	1,00	21,16	1,92	1,00
TF371	MYB/HD-like		24,69	1,82	1,00	25,00	1,90	1,00	24,67	1,89	1,00	24,22	1,78	1,00	23,72	1,74	1,00	24,48	1,99	1,00
TF372	HD family	HD	24,03	1,86	1,00	24,51	1,92	1,00	23,32	1,80	1,00	23,25	1,84	1,00	23,91	1,92	1,00	24,43	1,85	1,00
TF373	MYB		25,69	1,86	1,00	26,01	1,83	1,00	23,87	1,74	1,00	24,91	1,91	1,00	24,83	1,85	1,00	25,08	1,92	1,00
TF374	SNF2		24,68	1,92	1,00	24,44	1,87	1,00	24,39	1,88	1,00	24,19	1,93	1,00	24,62	1,87	1,00	24,63	1,94	1,00
TF375	SNF2		31,55	1,81	1,00	32,12	1,75	1,00	29,44	1,83	1,00	30,52	1,84	1,00	31,78	1,79	1,00	32,99	1,78	1,00
TF376	PHD		25,58	2,01	1,00	25,59	2,03	1,00	24,79	1,93	1,00	24,87	2,04	1,00	23,90	1,85	1,00	24,46	2,01	1,00
TF377	MYB/HD-like		21,69	2,04	1,00	22,28	1,92	1,00	21,70	1,89	1,00	22,10	1,91	1,00	22,20	1,94	1,00	22,72	1,68	1,00
TF378	TrpR		24,80	1,88	1,00	24,97	2,03	1,00	25,18	1,91	1,00	24,79	1,94	1,00	24,83	1,96	1,00	24,85	1,88	1,00
TF379	TrpR		29,29	2,01	1,00	29,67	1,97	1,00	30,73	1,91	1,00	29,92	1,83	1,00	29,94	1,83	1,00	29,84	1,85	1,00
TF380	AP2/EREBP		29,69	1,95	1,00	30,69	1,78	1,00	25,45	1,85	1,00	27,45	1,85	1,00	27,01	1,69	1,00	27,29	1,77	1,00
TF381	LFY		27,66	1,93	1,00	26,46	1,79	1,00	27,49	2,04	1,00	26,92	1,80	1,00	23,36	1,90	1,00	25,08	1,96	1,00
TF382	MADS		30,38	1,73	1,00	29,61	2,12	0,99	25,05	1,87	1,00	27,62	1,79	1,00	28,66	1,71	1,00	29,43	1,66	1,00
TF383	MYB/HD-like		27,42	1,85	1,00	27,45	1,87	1,00	27,34	1,91	1,00	26,94	1,78	1,00	29,69	1,80	1,00	30,79	1,83	1,00
TF384	HD-like		27,77	1,67	1,00	28,49	1,76	1,00	27,97	1,73	1,00	27,73	1,90	1,00	27,92	1,81	1,00	29,86	1,66	1,00
TF385	DDT		23,67	1,92	1,00	23,48	1,90	1,00	23,73	1,96	1,00	23,66	1,95	1,00	23,84	1,88	1,00	23,94	1,91	1,00
TF386	ARF		23,46	1,85	1,00	23,46	1,92	1,00	23,52	1,92	1,00	23,02	1,85	1,00	23,06	1,81	1,00	22,98	1,87	1,00
TF387	C_2C_2 (Zn)	DOF	25,85	1,90	1,00	26,02	1,76	1,00	25,06	1,81	1,00	24,42	1,95	1,00	24,70	1,96	1,00	25,47	1,83	1,00
TF388	TTF-type (Zn)		24,61	1,90	1,00	25,16	1,94	1,00	23,83	1,91	1,00	23,95	1,95	1,00	24,34	1,88	1,00	24,73	1,90	1,00
TF389	C_2C_2 (Zn)	DOF	29,57	1,81	1,00	30,17	1,82	1,00	28,18	1,77	1,00	27,94	1,82	1,00	27,97	1,83	1,00	28,14	1,77	1,00
TF390	R3H		23,66	1,94	1,00	23,62	2,08	1,00	22,24	1,94	1,00	23,34	1,87	1,00	21,47	2,07	1,00	22,45	1,92	1,00
TF391	R3H		22,24	1,99	1,00	22,51	1,92	1,00	22,43	1,92	1,00	22,83	1,95	1,00	22,96	1,81	1,00	22,65	2,05	1,00
TF392	MYB/HD-like		26,33	1,83	1,00	26,42	1,92	1,00	26,88	1,87	1,00	25,73	1,91	1,00	26,23	1,86	1,00	27,08	1,86	1,00
TF393	C_2C_2 (Zn)	DOF	24,34	1,81	1,00	24,85	1,92	1,00	24,40	1,95	1,00	26,14	2,04	1,00	26,67	1,84	1,00	26,84	1,95	1,00
TF394	NAC		20,57	1,97	1,00	19,75	2,02	1,00	16,83	1,89	1,00	20,61	1,88	1,00	20,11	1,95	1,00	20,71	1,96	1,00
TF395	MYB/HD-like		26,77	1,77	1,00	27,04	1,93	1,00	23,64	1,77	1,00	25,91	1,97	1,00	26,16	1,81	1,00	26,56	1,28	1,00
TF396	bHLH		29,59	1,89	1,00	28,60	1,87	1,00	24,06	1,90	1,00	27,37	1,92	1,00	27,91	1,88	1,00	28,23	1,77	1,00
TF397	bHLH		30,05	1,64	1,00	29,27	1,22	1,00	29,58	1,50	1,00	28,65	1,61	1,00	31,49	1,58	1,00	35,58	1,48	1,00
TF398	MADS		30,08	1,83	1,00	28,34	1,75	1,00	26,86	1,93	1,00	28,48	1,84	1,00	26,66	1,77	1,00	27,23	1,82	1,00
TF399	MADS		27,32	1,99	1,00	25,28	1,92	1,00	22,89	1,91	1,00	27,49	1,91	1,00	21,81	1,91	1,00	23,94	1,90	1,00
TF400	bZIP		22,05	1,97	1,00	21,76	2,00	1,00	21,99	1,94	1,00	22,50	1,91	1,00	22,69	1,94	1,00	22,83	1,77	1,00
TF401	TPR		25,51	1,87	1,00	25,93	2,09	1,00	23,73	1,91	1,00	25,07	1,93	1,00	25,09	1,91	1,00	25,67	1,96	1,00
TF402	bZIP		22,01	2,13	1,00	21,82	1,88	1,00	22,17	1,80	1,00	21,18	1,88	1,00	21,67	1,87	1,00	21,62	2,24	1,00
TF403	TPR		25,95	1,86	1,00	26,91	2,17	1,00	25,89	2,03	1,00	25,29	1,86	1,00	25,92	1,75	1,00	26,28	1,98	1,00
TF404	MYB		24,23	1,87	1,00	23,94	1,84	1,00	24,05	1,64	1,00	23,29	1,85	1,00	24,13	1,84	1,00	23,93	2,00	1,00
TF405	NAC		30,88	1,94	1,00	29,77	1,94	1,00	27,93	1,90	1,00	29,53	1,91	1,00	26,93	1,81	1,00	27,45	1,87	1,00
TF406	NAC		36,89	1,67	1,00	36,12	1,70	1,00	34,42	1,68	1,00	34,02	1,78	1,00	32,91	1,98	1,00	32,86	1,66	1,00
TF407	NAC		24,76	1,89	1,00	24,45	1,88	1,00	24,28	1,83	1,00	23,75	1,91	1,00	25,30	1,91	1,00	26,04	1,82	1,00

Table S1, continued

TF408	MYB/HD-like		24,96	1,76	1,00	24,75	1,78	1,00	24,89	1,75	1,00	24,09	1,71	1,00	26,06	1,84	1,00	27,56	1,73	1,00
TF409	NAC		25,10	1,88	1,00	24,86	1,98	1,00	25,32	1,69	1,00	24,90	1,94	1,00	25,61	1,90	1,00	25,78	1,90	1,00
TF410	MYB		24,62	2,01	1,00	23,55	1,93	1,00	22,21	1,87	1,00	24,00	1,90	1,00	20,55	1,86	1,00	21,69	1,80	1,00
TF411	MYB/HD-like		32,43	1,62	1,00	32,68	1,74	1,00	32,72	1,66	1,00	30,72	1,75	1,00	32,26	1,56	1,00	36,36	1,67	1,00
TF412	CCHC (Zn)		33,14	1,76	1,00	31,97	1,76	1,00	28,76	1,68	1,00	30,47	1,78	1,00	32,63	1,65	1,00	31,94	1,73	1,00
TF413	bZIP		24,68	1,76	1,00	24,06	2,06	1,00	24,70	1,56	1,00	25,92	1,33	1,00	26,12	1,94	1,00	26,24	2,45	1,00
TF414	PHD		20,29	2,02	1,00	20,15	1,89	1,00	20,18	1,90	1,00	20,51	2,04	1,00	20,53	1,90	1,00	20,58	1,85	1,00
TF415	GRF		27,74	1,95	1,00	27,51	1,85	1,00	27,57	2,12	1,00	27,94	1,82	0,97	21,97	1,99	1,00	23,45	1,94	1,00
TF416	C_2H_2 (Zn)		31,42	1,77	1,00	30,01	1,83	1,00	30,79	1,90	1,00	29,77	1,82	1,00	31,06	1,78	1,00	30,81	1,80	1,00
TF417	CCHC (Zn)		36,46	1,68	1,00	31,84	1,72	1,00	32,41	1,60	1,00	33,70	1,76	1,00	33,49	1,70	1,00	36,60	1,50	1,00
TF418	C3H	C3H-type 1 (Zn)	28,55	1,87	1,00	29,04	1,65	1,00	26,45	1,67	1,00	28,21	1,74	1,00	27,83	1,77	1,00	28,49	1,65	1,00
TF419	BD		32,76	1,78	1,00	32,03	1,78	1,00	33,89	1,64	1,00	30,93	1,79	1,00	31,59	1,75	1,00	33,78	1,77	1,00
TF420	ARF		26,31	2,02	1,00	26,24	1,91	1,00	26,36	1,87	1,00	25,97	1,92	1,00	25,30	1,81	1,00	25,99	1,81	1,00
TF421	ARF		26,67	1,84	1,00	25,21	1,91	1,00	23,55	1,91	1,00	26,01	1,90	1,00	22,56	1,85	1,00	24,07	2,00	1,00
TF422	ARF		32,06	1,75	1,00	32,45	1,78	1,00	32,33	1,60	1,00	32,50	1,81	1,00	35,27	1,72	1,00	38,63	1,53	1,00
TF423	ARF		25,18	1,88	1,00	24,71	1,91	1,00	25,37	1,88	1,00	24,38	1,86	1,00	25,61	1,90	1,00	26,22	1,91	1,00
TF424	CCHC (Zn)		29,06	1,88	1,00	30,99	1,52	1,00	28,25	1,61	1,00	28,39	1,75	1,00	28,80	1,79	1,00	29,95	1,61	1,00
TF425	bHLH		29,69	1,86	1,00	29,54	1,90	1,00	29,41	1,73	1,00	29,56	1,89	1,00	28,38	1,98	1,00	30,38	1,91	1,00
TF426	C_2H_2 (Zn)		24,19	2,20	1,00	24,83	2,05	1,00	21,34	1,98	1,00	22,56	1,95	1,00	23,06	1,90	1,00	23,16	1,92	1,00
TF427	bHLH		38,03	1,30	1,00	33,19	1,61	1,00	32,47	1,98	1,00	35,20	1,46	1,00	28,51	1,81	1,00	30,83	1,69	1,00
TF428	C_2H_2 (Zn)		24,00	1,91	1,00	24,50	2,03	1,00	24,82	2,08	1,00	23,37	1,90	1,00	23,14	2,00	1,00	22,98	1,89	1,00
TF429	MYB/HD-like		24,51	1,92	1,00	24,84	1,90	1,00	24,05	1,92	1,00	24,04	1,88	1,00	24,18	1,92	1,00	24,17	1,87	1,00
TF430	MYB		23,46	1,85	1,00	23,49	1,99	1,00	23,29	2,01	1,00	23,45	1,94	1,00	24,45	1,61	1,00	23,23	2,03	1,00
TF431	MADS		27,64	1,96	1,00	26,49	1,87	1,00	25,40	1,92	1,00	27,40	1,92	1,00	24,68	1,94	1,00	25,77	1,87	1,00
TF432	MADS		30,85	1,95	1,00	29,38	1,92	1,00	28,61	1,87	1,00	32,19	2,40	1,00	28,65	1,75	1,00	29,44	1,80	1,00
TF433	MADS		24,40	1,98	1,00	22,97	2,07	1,00	21,85	2,01	1,00	24,92	2,00	1,00	22,02	1,74	1,00	22,70	1,92	1,00
TF434	bZIP		21,21	1,99	1,00	21,74	1,99	1,00	19,12	1,80	1,00	20,65	1,86	1,00	21,00	2,08	1,00	21,34	1,94	1,00
TF435	CCHC (Zn)		29,92	1,88	1,00	31,26	1,88	1,00	27,39	1,88	1,00	28,48	1,91	1,00	30,55	1,88	1,00	30,98	1,88	1,00
TF436	SBP		28,68	1,80	1,00	28,52	1,84	1,00	23,96	1,88	1,00	27,41	1,84	1,00	27,62	1,86	1,00	27,70	1,86	1,00
TF437	CCHC (Zn)		22,16	1,98	1,00	22,16	1,85	1,00	18,72	2,03	1,00	20,52	1,98	1,00	21,36	1,88	1,00	21,78	1,90	1,00
TF438	PHD		23,14	1,87	1,00	23,49	1,84	1,00	22,25	1,96	1,00	22,07	1,95	1,00	22,77	1,85	1,00	22,86	1,91	1,00
TF439	C3H	C3H-type 1 (Zn)	22,65	1,94	1,00	23,18	1,98	1,00	21,71	1,85	1,00	22,20	1,93	1,00	22,54	1,87	1,00	22,65	1,93	0,99
TF440	AS2		22,94	1,99	1,00	21,83	1,93	1,00	21,31	1,98	1,00	23,66	1,99	1,00	20,85	1,96	1,00	21,13	1,98	1,00
TF441	JUMONJI		25,97	1,90	1,00	24,74	1,93	1,00	22,47	1,92	1,00	23,74	1,84	1,00	25,08	1,96	1,00	25,10	1,88	1,00
TF442	CCHC (Zn)		23,54	1,87	1,00	23,90	1,94	1,00	23,20	1,95	1,00	22,36	1,90	1,00	22,97	1,95	1,00	22,96	1,91	1,00
TF443	CCHC (Zn)		27,44	1,85	1,00	27,31	1,87	1,00	27,31	1,80	1,00	27,04	1,90	1,00	29,76	1,74	1,00	30,94	1,69	1,00
TF444	AS2		29,34	2,45	1,00	27,98	1,92	1,00	26,32	1,96	1,00	29,25	1,98	1,00	25,92	1,77	1,00	26,72	2,16	1,00
TF445	C_2H_2 (Zn)		23,98	2,01	1,00	23,68	1,89	1,00	23,94	1,92	1,00	23,29	2,00	1,00	24,03	1,88	1,00	23,71	1,90	1,00
TF446	HD-like		26,32	1,67	1,00	27,13	1,68	1,00	24,77	1,79	1,00	26,97	1,80	1,00	26,60	1,72	1,00	27,43	1,76	1,00
TF447	C_2H_2 (Zn)		24,10	2,19	1,00	24,32	1,87	1,00	23,50	1,83	1,00	23,42	2,02	1,00	23,66	1,95	1,00	24,39	1,90	1,00
TF448	RR		21,33	1,91	1,00	21,50	1,90	1,00	21,77	1,94	1,00	21,67	1,91	1,00	22,36	2,02	1,00	22,10	1,99	1,00
TF449	CCHC (Zn)		23,98	1,91	1,00	24,28	1,90	1,00	23,25	1,86	1,00	22,97	1,96	1,00	23,61	1,88	1,00	23,48	1,90	1,00
TF450	MYB/HD-like		26,16	1,86	1,00	26,57	1,77	1,00	24,68	1,83	1,00	25,90	1,84	1,00	26,30	1,86	1,00	26,31	1,84	1,00
TF451	ZF DHHC		25,23	1,24	1,00	23,91	1,81	1,00	24,60	1,91	1,00	24,38	1,78	1,00	24,40	1,88	1,00	24,92	1,86	1,00
TF452	ZF DHHC		30,91	1,81	1,00	30,33	1,83	1,00	30,08	1,74	1,00	29,85	1,85	1,00	28,91	1,81	1,00	31,68	1,43	1,00

Table S1, continued

TF453	ZF DHHC		24,02	1,87	1,00	23,87	1,91	1,00	24,12	1,94	1,00	23,84	1,88	1,00	24,17	1,90	1,00	24,30	1,98	1,00
TF454	ZF DHHC		23,83	1,85	1,00	23,51	1,80	1,00	26,11	1,90	1,00	24,96	1,91	1,00	25,47	1,98	1,00	26,51	2,05	1,00
TF455	C_2H_2 (Zn)		23,98	1,77	1,00	23,93	1,72	1,00	19,11	2,54	1,00	22,52	1,84	1,00	23,57	1,98	1,00	23,89	1,65	1,00
TF456	C_2H_2 (Zn)		22,86	2,01	1,00	22,84	1,90	1,00	23,38	1,89	1,00	24,83	1,69	1,00	23,07	1,87	1,00	23,48	1,89	1,00
TF457	RR		35,38	1,75	1,00	32,16	1,80	1,00	30,54	1,87	1,00	33,35	1,78	1,00	30,75	1,69	1,00	32,29	1,75	1,00
TF458	C_2H_2 (Zn)		24,26	2,04	1,00	24,96	1,96	1,00	24,23	1,94	1,00	23,76	1,92	1,00	23,94	1,86	1,00	24,07	1,81	1,00
TF459	NAC		23,22	1,82	1,00	23,92	1,90	1,00	23,07	1,86	1,00	21,30	1,97	1,00	21,71	1,97	1,00	22,03	1,74	1,00
TF460	GRF		28,21	1,84	1,00	28,31	1,94	1,00	28,05	1,78	1,00	28,23	1,92	1,00	27,46	2,00	1,00	28,67	1,95	1,00
TF461	WRKY family	WRKY	19,36	2,24	1,00	20,26	2,00	1,00	17,77	2,12	1,00	19,89	1,95	1,00	19,87	1,89	1,00	20,14	2,01	1,00
TF462	bHLH		23,25	1,91	1,00	22,89	1,89	1,00	23,27	1,99	1,00	21,87	1,88	1,00	22,34	1,90	1,00	22,23	1,96	1,00
TF463	bHLH		22,90	1,92	1,00	22,94	1,89	1,00	23,15	1,90	1,00	23,06	2,32	1,00	22,69	1,69	1,00	22,91	1,70	1,00
TF464	bZIP		23,60	1,91	1,00	23,51	1,87	1,00	23,68	1,91	1,00	22,94	1,91	1,00	23,21	1,90	1,00	23,26	1,90	1,00
TF465	MYB/HD-like		26,82	1,86	1,00	27,00	1,81	1,00	22,71	1,93	1,00	25,66	1,81	1,00	26,25	1,84	1,00	26,76	1,78	1,00
TF466	JUMONJI		29,93	1,76	1,00	30,22	1,73	1,00	31,51	1,75	1,00	30,09	2,10	1,00	34,72	1,58	1,00	32,44	2,00	1,00
TF467	PHD		28,72	2,04	1,00	28,05	1,85	1,00	24,25	1,88	1,00	26,62	1,85	1,00	27,28	1,85	1,00	27,84	1,87	1,00
TF468	PHD		30,76	1,79	1,00	31,86	1,82	1,00	31,90	1,84	1,00	30,37	1,84	1,00	30,59	1,83	1,00	34,27	1,83	1,00
TF469	HD family	HD	27,53	1,89	1,00	27,34	1,99	1,00	27,31	1,90	1,00	26,76	1,89	1,00	28,54	1,90	1,00	28,65	2,00	1,00
TF470	HD family	HD	27,28	1,90	1,00	26,91	1,90	1,00	25,88	1,91	1,00	27,63	1,91	1,00	25,29	1,90	1,00	26,44	2,00	1,00
TF471	C_2H_2 (Zn)		22,76	1,98	1,00	22,48	1,99	1,00	22,66	1,79	1,00	21,56	1,95	1,00	21,74	1,82	1,00	21,90	1,87	1,00
TF472	RR		22,52	1,79	1,00	23,30	1,87	1,00	22,14	1,72	1,00	22,03	1,86	1,00	22,09	1,81	1,00	22,40	1,79	1,00
TF473	AP2/EREBP		23,19	1,96	1,00	23,80	1,94	1,00	23,01	1,91	1,00	21,97	1,94	1,00	22,10	1,90	1,00	22,15	1,85	1,00
TF474	MADS		26,24	1,89	1,00	25,66	1,96	1,00	20,27	1,91	1,00	25,53	1,86	1,00	25,55	1,90	1,00	26,93	1,78	1,00
TF475	bZIP		23,75	1,88	1,00	24,22	1,91	1,00	23,31	1,90	1,00	23,97	1,90	1,00	24,34	1,86	1,00	24,89	1,91	1,00
TF476	ABI3-VP1		24,39	2,00	1,00	24,54	1,93	1,00	24,83	1,86	1,00	24,00	1,87	1,00	24,55	1,83	1,00	25,11	1,76	0,99
TF477	NAC		27,36	1,92	1,00	26,22	1,91	1,00	24,53	1,99	1,00	26,91	1,96	1,00	23,55	2,02	1,00	24,79	1,86	1,00
TF478	HD-like		21,71	1,94	1,00	21,63	1,92	1,00	21,97	1,92	1,00	22,69	1,96	1,00	22,47	2,10	1,00	22,49	1,94	1,00
TF479	NAC		21,42	2,01	1,00	19,81	2,30	1,00	21,28	1,95	1,00	22,07	1,93	1,00	22,37	2,01	1,00	22,99	2,29	1,00
TF480	ZF-HD		29,35	1,92	1,00	28,16	2,06	1,00	26,01	1,90	1,00	29,97	1,93	1,00	24,46	1,91	1,00	26,93	1,98	1,00
TF481	FHA		22,86	1,96	1,00	23,24	1,90	1,00	23,03	1,91	1,00	22,75	1,90	1,00	23,08	1,89	1,00	23,25	1,86	1,00
TF482	HD family	HD	25,93	1,90	1,00	25,84	1,87	1,00	25,64	1,84	1,00	26,05	1,91	1,00	26,04	1,87	1,00	26,30	1,81	1,00
TF483	HD family	HD	23,86	1,84	1,00	23,37	1,97	1,00	22,29	1,92	1,00	24,77	1,91	1,00	20,91	1,93	1,00	22,68	1,96	1,00
TF484	HD-like		32,25	1,79	1,00	31,92	1,78	1,00	30,31	1,82	1,00	31,91	1,85	1,00	29,98	1,88	1,00	32,28	1,78	1,00
TF485	bHLH		22,95	1,81	1,00	23,80	1,80	0,99	22,55	1,76	1,00	22,05	1,92	1,00	22,63	1,92	1,00	23,21	1,77	0,99
TF486	PHD		22,85	1,92	1,00	22,83	1,94	1,00	22,89	1,95	1,00	22,25	1,84	1,00	22,41	1,87	1,00	22,48	1,90	1,00
TF487	ABI3-VP1		30,84	1,81	1,00	29,99	1,65	1,00	24,90	1,78	1,00	27,94	1,87	1,00	28,40	1,77	1,00	30,41	1,61	1,00
TF488	BTB/POZ		20,40	1,92	1,00	21,72	2,09	1,00	20,35	1,93	1,00	19,65	1,95	1,00	22,44	1,84	1,00	23,37	1,86	1,00
TF489	PHD		27,41	1,85	1,00	27,50	1,87	1,00	28,31	1,63	1,00	25,72	1,85	1,00	28,24	1,86	1,00	28,79	1,86	1,00
TF490	PHD		27,17	1,92	1,00	27,34	1,78	1,00	25,94	1,86	1,00	26,89	1,86	1,00	27,37	2,07	1,00	27,16	1,81	1,00
TF491	PHD		28,45	1,94	1,00	27,87	1,82	1,00	22,48	1,92	1,00	26,80	1,97	1,00	27,32	1,96	1,00	28,62	1,93	1,00
TF492	HD-like		27,56	1,98	1,00	27,52	1,81	1,00	26,26	1,96	1,00	27,58	1,87	1,00	24,97	1,85	1,00	26,37	1,90	1,00
TF493	AP2/EREBP		27,43	1,87	1,00	26,70	1,75	1,00	27,41	1,73	1,00	27,93	1,80	1,00	27,86	1,64	1,00	28,28	1,85	1,00
TF494	C_2H_2 (Zn)		22,88	2,00	1,00	22,17	2,26	1,00	22,37	1,90	1,00	21,45	1,88	1,00	23,18	1,89	1,00	22,97	2,01	1,00
TF495	C_2H_2 (Zn)		25,06	1,84	1,00	25,13	1,88	1,00	25,21	1,80	1,00	24,70	1,82	1,00	25,53	1,87	1,00	25,34	1,79	1,00
TF496	JUMONJI		23,50	1,92	1,00	23,29	1,89	1,00	23,60	1,98	1,00	22,91	1,88	1,00	24,02	1,94	1,00	23,60	1,95	1,00
TF497	HD family	HD	24,18	2,01	1,00	24,22	1,93	1,00	24,21	1,98	1,00	23,59	1,88	1,00	23,96	1,89	1,00	23,89	1,89	1,00

Table S1, continued

TF498	HMG		31,83	1,89	1,00	n.d.	1,50	0,94	34,37	1,76	1,00	28,02	1,11	0,96	28,73	1,91	1,00	29,23	1,86	1,00
TF499	U1-type (Zn)		23,43	1,85	1,00	23,29	1,91	1,00	23,56	1,82	1,00	22,80	1,80	1,00	23,73	1,79	1,00	23,51	1,87	1,00
TF500	ZF DHHC		24,52	1,97	1,00	24,31	1,89	1,00	24,59	1,98	1,00	24,00	2,08	1,00	24,32	1,88	1,00	24,07	2,25	1,00
TF501	ZF DHHC		28,28	1,92	1,00	28,83	1,91	1,00	28,69	1,93	1,00	28,81	2,05	1,00	29,14	1,25	1,00	28,49	1,90	1,00
TF502	bHLH		28,04	1,78	1,00	27,62	1,73	1,00	27,84	1,81	1,00	27,48	1,71	1,00	26,99	1,68	1,00	28,16	1,69	1,00
TF503	TCoA		25,53	1,94	1,00	26,90	1,84	1,00	25,22	1,97	1,00	24,99	1,99	1,00	25,22	1,88	1,00	26,38	1,19	1,00
TF504	bHLH		23,64	1,92	1,00	23,63	1,89	1,00	23,76	2,00	1,00	22,91	1,91	1,00	26,38	1,88	1,00	26,87	1,92	1,00
TF505	bHLH		24,74	1,93	1,00	24,23	1,88	1,00	24,55	1,88	1,00	23,48	2,03	1,00	24,15	1,97	1,00	24,68	1,91	1,00
TF506	bHLH		23,06	1,95	1,00	23,10	1,94	1,00	24,73	1,93	1,00	23,49	1,88	1,00	25,89	1,76	1,00	26,94	1,76	1,00
TF507	ABI3-VP1		26,34	1,89	1,00	25,49	1,84	1,00	21,49	1,94	1,00	24,24	1,86	1,00	25,37	1,86	1,00	26,11	1,79	1,00
TF508	ZF DHHC		21,69	1,91	1,00	21,99	1,98	1,00	22,09	2,02	1,00	20,93	1,93	1,00	21,34	1,92	1,00	21,39	1,96	1,00
TF509	BTB/POZ		28,90	1,63	1,00	28,80	1,72	1,00	28,43	1,67	1,00	28,21	1,81	1,00	29,42	1,64	1,00	28,96	1,73	1,00
TF510	ARF		30,23	1,72	1,00	31,61	1,71	1,00	31,24	1,73	1,00	30,35	1,74	1,00	29,84	1,85	1,00	31,24	1,81	1,00
TF511	MADS		n.d.	1,44	0,96	n.d.	1,30	0,99	n.d.	1,32	1,00	n.d.	1,25	1,00	n.d.	1,21	0,99	n.d.	1,28	0,99
TF512	MADS		32,97	1,57	1,00	35,29	1,56	1,00	n.d.	1,21	0,99	n.d.	1,37	0,99	31,72	1,63	1,00	n.d.	1,19	0,91
TF513	ARF		21,99	1,96	1,00	21,82	1,85	1,00	22,09	1,95	1,00	20,94	1,99	1,00	21,26	1,91	1,00	21,35	1,98	1,00
TF514	ZIM		30,62	1,84	1,00	31,82	1,84	1,00	30,38	1,87	1,00	31,89	1,73	1,00	29,60	1,91	1,00	31,93	1,81	1,00
TF515	ZIM		25,60	1,91	1,00	24,50	1,83	1,00	19,62	2,21	1,00	24,86	1,82	1,00	18,76	1,92	1,00	15,80	1,99	0,98
TF516	ARF		21,62	1,96	1,00	21,51	1,95	1,00	21,78	2,04	1,00	20,58	2,19	0,99	20,78	2,03	1,00	20,92	1,95	1,00
TF517	bHLH		20,97	1,92	1,00	21,77	1,96	1,00	20,83	1,94	1,00	21,05	1,93	1,00	21,24	1,87	1,00	21,59	1,83	1,00
TF518	C_2H_2 (Zn)		21,91	1,92	1,00	23,20	1,84	1,00	24,27	1,87	1,00	24,03	1,93	1,00	25,65	1,88	1,00	26,93	1,97	1,00
TF519	WRKY family	LLR-WRKY	23,06	1,85	1,00	22,73	1,83	1,00	23,03	1,94	1,00	22,06	1,84	1,00	25,43	1,82	1,00	26,79	1,90	1,00
TF520	C_2H_2 (Zn)		22,35	1,94	1,00	22,31	1,92	1,00	22,67	1,94	1,00	22,36	1,88	1,00	22,77	1,97	1,00	22,65	2,04	1,00
TF521	A20-like		22,12	1,90	1,00	22,72	1,90	1,00	21,31	2,03	1,00	21,31	1,94	1,00	21,76	1,97	1,00	21,97	1,92	1,00
TF522	C_2H_2 (Zn)		28,48	1,86	1,00	28,90	1,90	1,00	28,99	1,83	1,00	28,39	1,82	1,00	28,06	1,93	1,00	27,98	1,86	1,00
TF523	MYB/HD-like		29,34	1,88	1,00	28,27	1,85	1,00	29,50	1,89	1,00	27,72	1,88	1,00	28,31	1,88	1,00	28,63	1,79	1,00
TF524	MADS		24,85	1,90	1,00	24,81	1,93	1,00	24,78	1,92	1,00	23,82	1,90	1,00	25,50	1,94	1,00	26,13	1,93	1,00
TF525	MADS		36,99	1,59	1,00	33,95	1,77	1,00	31,84	1,91	1,00	32,35	1,78	1,00	33,36	1,73	1,00	n.d.	1,28	0,92
TF526	MADS		24,33	1,89	1,00	24,07	1,94	1,00	24,42	1,88	1,00	23,85	1,89	1,00	24,28	1,85	1,00	24,28	2,06	1,00
TF527	BTB/POZ		22,42	1,90	1,00	22,23	1,89	1,00	22,62	2,08	1,00	22,83	1,88	1,00	23,42	1,90	1,00	23,49	1,92	1,00
TF528	CCHC (Zn)		27,94	1,81	0,99	28,71	1,72	1,00	25,58	1,86	1,00	27,83	1,92	1,00	27,74	1,79	1,00	28,80	1,71	1,00
TF529	CCHC (Zn)		24,63	2,01	1,00	25,07	1,93	1,00	22,77	1,95	1,00	24,43	1,76	0,99	24,58	1,86	1,00	24,74	1,99	1,00
TF530	CCHC (Zn)		30,70	1,90	1,00	29,84	1,87	1,00	25,58	1,86	1,00	29,55	1,85	1,00	29,71	1,79	1,00	30,39	1,96	1,00
TF531	CCHC (Zn)		21,80	1,93	1,00	21,65	1,88	1,00	21,96	2,12	1,00	20,41	1,94	1,00	23,68	1,86	1,00	25,08	1,89	1,00
TF532	PHD		30,20	1,77	1,00	30,62	1,77	1,00	26,07	1,85	1,00	29,29	1,82	1,00	29,64	1,81	1,00	31,72	1,82	1,00
TF533	CCHC (Zn)		21,30	1,87	1,00	21,60	1,90	1,00	21,92	1,96	1,00	20,71	2,11	1,00	21,75	1,98	1,00	21,97	1,91	1,00
TF534	CCHC (Zn)		24,42	1,88	1,00	25,11	1,34	0,99	23,90	1,71	1,00	24,05	1,78	1,00	24,59	1,73	1,00	24,83	1,86	1,00
TF535	CCHC (Zn)		25,62	1,89	1,00	22,42	2,02	1,00	20,77	1,96	1,00	20,59	1,94	1,00	22,69	1,93	1,00	21,70	1,88	1,00
TF536	TAZ		21,65	1,83	1,00	20,85	1,85	1,00	20,04	2,20	1,00	21,61	1,97	1,00	18,84	1,86	1,00	20,02	1,76	1,00
TF537	bZIP		21,93	1,92	1,00	22,42	1,98	1,00	21,74	1,96	1,00	21,39	1,92	1,00	21,81	1,91	1,00	21,85	1,93	1,00
TF538	GRAS		27,88	1,82	1,00	27,57	1,90	1,00	21,64	1,94	1,00	26,33	1,89	1,00	26,81	1,85	1,00	27,75	1,85	1,00
TF539	PHD		25,49	1,67	1,00	25,47	1,84	1,00	26,14	1,90	1,00	25,92	2,16	1,00	26,24	1,18	1,00	26,52	1,67	1,00
TF540	SBP		21,41	1,88	1,00	21,69	1,82	1,00	21,83	1,90	1,00	21,10	1,91	1,00	21,53	1,96	1,00	21,49	1,87	1,00
TF541	MADS		29,41	1,78	1,00	29,50	1,68	1,00	26,43	1,73	1,00	28,61	1,69	1,00	28,50	1,74	1,00	28,96	1,68	1,00
TF542	MADS		29,27	1,64	1,00	28,96	1,69	1,00	29,86	1,80	1,00	28,34	1,79	1,00	28,58	1,75	1,00	28,48	1,76	1,00
TF543	BD		21,74	1,99	1,00	21,66	1,84	1,00	21,67	1,91	1,00	21,58	1,90	1,00	21,97	1,92	1,00	21,97	1,89	1,00

Table S1, continued

TF544	BD		24,95	1,80	1,00	24,75	1,89	1,00	24,96	1,72	1,00	24,67	1,96	1,00	24,80	2,17	1,00	25,04	1,97	1,00
TF545	CCHC (Zn)		24,16	1,84	1,00	23,83	1,86	1,00	19,86	1,92	1,00	23,34	1,86	1,00	23,49	1,93	1,00	24,61	1,89	1,00
TF546	AP2/EREBP		26,36	1,86	1,00	26,91	1,90	1,00	24,60	1,71	1,00	26,64	1,99	1,00	27,17	1,85	1,00	27,04	1,91	1,00
TF547	Lambda-DB		29,38	1,89	1,00	27,03	1,91	1,00	22,07	1,94	1,00	25,74	1,83	1,00	26,62	2,01	1,00	27,19	1,85	1,00
TF548	HD-like		28,10	1,75	1,00	28,50	1,65	1,00	28,60	1,66	1,00	28,29	1,75	1,00	27,46	1,72	1,00	28,94	1,96	0,99
TF549	HD family	HD-ZIP	23,64	1,96	1,00	24,27	1,88	1,00	23,34	2,31	1,00	22,43	1,89	1,00	22,81	1,94	1,00	22,88	1,82	1,00
TF550	HD-like		23,10	2,03	1,00	24,07	2,13	1,00	22,68	1,90	1,00	21,83	1,90	1,00	22,67	1,84	1,00	22,57	2,01	1,00
TF551	CCHC (Zn)		24,02	1,99	1,00	25,13	1,90	1,00	24,14	1,94	1,00	23,98	2,00	1,00	23,93	1,97	1,00	25,05	1,81	1,00
TF552	HD family	HD-ZIP	23,77	1,90	1,00	24,18	1,86	1,00	23,55	1,89	1,00	22,59	1,93	1,00	22,62	1,91	1,00	22,68	1,89	1,00
TF553	NRs		28,85	1,84	1,00	29,55	1,88	1,00	28,40	1,77	1,00	32,28	1,25	1,00	28,38	1,75	1,00	27,53	2,05	1,00
TF554	NRs		30,44	1,73	1,00	27,84	1,75	1,00	33,39	1,62	1,00	28,85	1,80	1,00	22,99	1,83	1,00	24,72	1,86	1,00
TF555	EIL		29,38	1,81	1,00	28,91	2,03	1,00	22,89	2,00	1,00	28,00	1,85	1,00	28,57	1,75	1,00	28,47	1,76	1,00
TF556	MADS		28,63	1,88	1,00	28,21	1,89	1,00	28,69	1,83	1,00	27,26	1,91	1,00	27,48	1,90	1,00	27,58	1,97	1,00
TF557	AP2/EREBP		25,88	1,97	1,00	25,54	1,96	1,00	26,56	1,92	1,00	25,15	1,93	1,00	26,85	1,92	1,00	26,64	1,95	1,00
TF558	MYB/HD-like		26,65	1,95	1,00	25,65	1,97	1,00	26,29	1,92	1,00	25,94	1,91	1,00	28,43	1,95	1,00	28,92	1,93	1,00
TF559	ZF DHHC		23,89	1,91	1,00	24,45	1,90	1,00	21,15	1,94	1,00	23,56	1,90	1,00	23,97	1,88	1,00	24,20	1,93	1,00
TF560	JUMONJI		24,75	2,06	1,00	24,71	1,91	1,00	24,85	1,97	1,00	26,62	2,13	1,00	23,37	1,91	1,00	24,06	1,92	1,00
TF561	CCHC (Zn)		30,38	1,90	1,00	30,91	1,74	1,00	27,63	1,86	1,00	30,16	1,82	1,00	29,65	1,85	1,00	31,00	1,67	1,00
TF562	HD family	HD	24,05	1,95	1,00	24,05	1,91	1,00	24,28	1,84	1,00	23,78	1,91	1,00	24,22	1,92	1,00	24,18	1,93	1,00
TF563	MADS		27,75	1,89	1,00	26,72	1,87	1,00	27,92	1,91	1,00	25,51	1,88	1,00	26,17	1,91	1,00	26,00	1,94	1,00
TF564	GRF		26,34	1,94	1,00	25,71	1,92	1,00	21,14	1,82	1,00	24,75	1,83	1,00	25,29	1,81	1,00	25,81	1,88	1,00
TF565	HTH	FIS	22,96	1,90	1,00	23,25	1,98	1,00	23,45	1,90	1,00	24,03	1,28	0,91	23,03	1,88	1,00	22,98	1,89	1,00
TF566	SBP		21,57	2,10	1,00	21,55	2,02	1,00	21,65	1,89	1,00	21,28	1,94	1,00	21,50	1,83	1,00	21,17	1,80	1,00
TF567	AS2		22,20	1,89	1,00	21,51	1,45	1,00	26,26	1,75	0,99	21,94	1,85	1,00	22,26	1,80	1,00	22,33	1,73	1,00
TF568	MYB/HD-like		24,89	1,89	1,00	24,75	1,83	1,00	24,52	1,91	1,00	23,57	1,93	1,00	25,27	2,05	1,00	25,51	1,87	1,00
TF569	AP2/EREBP		26,61	1,89	1,00	25,97	1,94	1,00	21,46	1,73	1,00	24,22	1,80	1,00	25,99	1,75	1,00	26,34	1,78	1,00
TF570	HTH	FIS	23,18	1,88	1,00	22,99	1,83	1,00	23,71	1,85	1,00	22,66	2,03	1,00	22,93	1,88	1,00	22,93	1,87	1,00
TF571	MADS		23,18	1,85	1,00	23,16	2,01	1,00	23,29	1,86	1,00	22,13	2,01	1,00	23,21	1,91	1,00	22,95	1,94	1,00
TF572	MADS		22,99	1,96	1,00	23,83	1,92	1,00	23,76	1,89	1,00	23,56	1,95	1,00	26,90	1,84	1,00	29,33	1,87	1,00
TF573	MADS		26,01	1,87	1,00	26,39	1,88	1,00	20,66	1,98	1,00	25,11	1,90	1,00	25,46	1,91	1,00	26,31	1,83	1,00
TF574	JUMONJI		25,16	1,88	1,00	25,24	2,03	1,00	25,25	1,87	1,00	24,61	1,95	1,00	25,06	2,19	1,00	24,82	1,85	1,00
TF575	HD-like		24,69	2,15	1,00	24,30	1,79	1,00	24,87	1,95	1,00	23,80	2,05	1,00	27,26	1,90	1,00	28,54	1,66	1,00
TF576	C3H	C3H-type 1 (Zn)	18,49	1,89	1,00	18,30	2,15	1,00	19,34	2,04	1,00	18,06	1,91	1,00	20,99	1,92	1,00	21,34	1,83	1,00
TF577	bZIP		26,87	1,92	1,00	28,84	1,79	1,00	28,46	1,71	1,00	29,62	1,72	1,00	29,47	1,80	1,00	32,44	1,80	1,00
TF578	MYB/HD-like		29,23	1,71	1,00	28,19	1,76	1,00	28,95	1,68	1,00	28,89	1,83	1,00	30,18	1,78	1,00	32,00	1,50	1,00
TF579	CCHC (Zn)		29,52	1,87	1,00	29,09	1,89	1,00	28,90	1,79	1,00	28,43	1,92	1,00	30,80	1,84	1,00	32,47	1,90	1,00
TF580	MYB/HD-like		28,87	1,84	1,00	28,06	1,83	1,00	28,69	1,83	1,00	29,58	1,79	1,00	30,67	1,81	1,00	31,13	1,75	1,00
TF581	TCP		31,88	1,37	1,00	30,40	1,86	1,00	30,97	1,78	1,00	32,18	1,83	1,00	30,57	1,90	1,00	n.d.	1,67	0,99
TF582	BD		22,30	1,78	1,00	22,25	1,89	1,00	22,57	1,84	1,00	22,91	1,87	1,00	22,16	2,07	1,00	22,18	1,92	1,00
TF583	GRF		31,69	1,78	1,00	31,74	1,89	1,00	32,33	1,70	1,00	31,22	1,77	1,00	31,02	1,78	1,00	32,77	1,68	1,00
TF584	JUMONJI		24,55	1,98	1,00	24,65	1,90	1,00	24,41	1,85	1,00	23,79	1,98	1,00	24,48	1,94	1,00	24,51	1,91	1,00
TF585	C_2H_2 (Zn)		31,01	1,83	1,00	28,26	1,84	1,00	27,40	1,75	1,00	30,66	1,84	1,00	27,04	1,78	1,00	28,35	1,74	1,00
TF586	RR		23,83	1,97	1,00	23,96	1,93	1,00	24,67	1,93	1,00	24,19	1,87	1,00	24,55	1,86	1,00	24,65	1,71	1,00
TF587	AP2/EREBP		25,31	1,22	1,00	25,75	1,65	1,00	26,06	1,21	1,00	25,37	1,73	1,00	25,61	1,76	1,00	26,14	1,62	1,00
TF588	HD family	HD	19,49	1,97	1,00	20,02	1,96	1,00	19,26	1,97	1,00	18,85	2,05	1,00	19,18	1,84	1,00	19,11	2,03	1,00
TF589	MBF		20,99	1,91	1,00	21,26	1,94	1,00	21,65	1,96	1,00	21,30	1,94	1,00	21,04	1,90	1,00	21,53	1,96	1,00

Table S1, continued

TF590	AS2		25,92	1,77	1,00	24,55	1,89	1,00	22,98	1,89	1,00	25,44	1,83	1,00	21,95	1,91	1,00	23,72	1,80	1,00
TF591	AP2/EREBP		29,19	1,76	1,00	30,86	1,71	1,00	28,76	1,72	1,00	27,93	1,80	1,00	28,97	1,81	1,00	28,95	1,72	1,00
TF592	MADS		24,47	1,82	1,00	24,31	1,90	1,00	27,41	1,86	1,00	27,89	1,82	1,00	27,96	1,83	1,00	29,28	1,80	1,00
TF593	HD-like		25,36	1,75	1,00	26,58	1,83	0,99	24,45	1,78	1,00	24,72	1,76	1,00	24,98	1,77	1,00	25,22	1,74	1,00
TF594	bZIP		31,20	1,86	1,00	29,15	1,89	1,00	24,44	1,88	1,00	28,81	1,84	1,00	29,47	1,81	1,00	30,35	1,85	1,00
TF595	ABI3-VP1		36,57	1,55	1,00	32,27	1,76	1,00	32,66	1,67	1,00	32,15	1,75	1,00	32,85	1,80	1,00	39,52	1,41	0,99
TF596	ABI3-VP1		33,73	1,65	1,00	39,08	1,38	0,99	38,87	1,24	1,00	n.d.	2,94	0,85	n.d.	1,14	0,99	37,81	1,60	1,00
TF597	NAC		21,48	1,91	1,00	21,43	1,93	1,00	21,76	2,27	1,00	21,34	2,11	1,00	21,84	1,88	1,00	22,16	1,72	1,00
TF598	NAC		22,78	1,84	1,00	22,63	1,87	1,00	23,07	1,86	1,00	22,69	1,92	1,00	22,84	1,93	1,00	22,94	1,91	1,00
TF599	AP2/EREBP		25,55	1,81	1,00	25,33	1,87	1,00	25,76	1,80	1,00	25,27	1,61	1,00	25,89	1,78	1,00	25,94	1,81	1,00
TF600	bHLH		24,05	1,88	1,00	23,98	1,92	1,00	24,41	1,94	1,00	23,54	1,84	1,00	23,72	1,89	1,00	23,84	1,87	1,00
TF601	AP2/EREBP		25,24	1,80	1,00	25,10	1,91	1,00	24,26	1,89	1,00	24,82	1,87	1,00	23,14	2,01	1,00	24,09	1,86	1,00
TF602	bHLH		22,33	2,02	1,00	22,40	1,89	1,00	22,27	2,03	1,00	23,31	1,73	1,00	21,44	2,08	1,00	22,18	1,84	1,00
TF603	BED-type (Zn)		23,08	1,93	1,00	22,65	1,98	1,00	23,11	1,70	1,00	21,85	1,93	1,00	24,49	1,79	1,00	26,11	1,77	1,00
TF604	CCAAT	CCAAT-HAP3	24,02	1,84	1,00	24,62	1,89	1,00	23,75	1,89	1,00	22,93	2,16	1,00	23,04	1,85	1,00	23,56	2,02	1,00
TF605	PHD		23,39	1,84	1,00	23,54	2,07	1,00	21,48	1,92	1,00	22,64	1,84	1,00	22,72	1,81	1,00	22,82	1,92	1,00
TF606	ARID		27,20	1,86	1,00	27,15	1,82	1,00	27,10	1,83	1,00	25,53	1,89	1,00	27,41	1,84	1,00	26,98	1,83	1,00
TF607	C_2C_2 (Zn)	GATA	30,01	1,90	1,00	30,87	1,84	1,00	29,37	1,85	1,00	29,88	1,88	1,00	29,83	1,84	1,00	31,22	1,89	1,00
TF608	C_2C_2 (Zn)	GATA	29,62	1,84	1,00	28,39	1,59	1,00	28,65	1,77	1,00	27,61	1,95	1,00	29,70	1,57	1,00	30,68	1,20	1,00
TF609	MYB		26,72	2,08	1,00	26,05	1,98	1,00	25,96	1,88	1,00	26,69	1,83	1,00	25,32	1,49	1,00	26,32	1,98	1,00
TF610	TCP		22,07	1,93	1,00	22,23	1,94	1,00	22,10	1,89	1,00	21,54	1,97	1,00	21,95	1,83	1,00	21,87	1,93	1,00
TF611	bHLH		23,38	1,91	1,00	23,29	1,95	1,00	23,75	1,79	1,00	23,08	1,89	1,00	23,42	1,76	1,00	23,63	1,84	1,00
TF612	MYB/HD-like		23,46	1,94	1,00	24,10	1,89	1,00	22,40	1,77	1,00	22,76	1,89	1,00	23,04	1,99	1,00	23,34	2,03	1,00
TF613	GRAS		25,40	1,87	1,00	25,20	1,88	1,00	24,68	1,91	1,00	24,06	1,91	1,00	26,54	1,90	1,00	28,70	1,76	1,00
TF614	MYB/HD-like		26,53	1,81	1,00	26,08	1,90	1,00	26,72	1,72	1,00	25,33	1,83	1,00	25,90	1,83	1,00	26,50	2,06	1,00
TF615	C_2H_2 (Zn)		21,17	1,86	1,00	18,84	1,94	1,00	15,35	2,11	0,99	17,87	1,91	1,00	19,09	1,87	1,00	19,12	1,97	1,00
TF616	C_2H_2 (Zn)		27,46	1,95	1,00	27,11	1,96	1,00	20,91	1,93	1,00	25,85	1,88	1,00	27,14	1,82	1,00	27,92	2,01	1,00
TF617	MYB/HD-like		26,19	1,83	1,00	26,11	1,79	1,00	26,19	1,83	1,00	25,17	2,04	1,00	25,84	1,97	0,99	25,81	1,86	0,99
TF618	HD family	HD	28,30	1,98	1,00	28,20	1,90	1,00	28,28	1,98	1,00	28,12	1,93	1,00	30,98	1,85	1,00	33,51	1,91	1,00
TF619	MADS		30,45	1,81	1,00	30,18	1,78	1,00	30,31	1,74	1,00	30,66	1,78	1,00	26,66	1,94	1,00	28,55	1,97	1,00
TF620	MADS		31,68	1,79	1,00	28,65	1,86	1,00	27,20	1,95	1,00	30,05	1,82	1,00	25,32	1,73	1,00	28,15	2,01	1,00
TF621	C3H	C3H-type 1 (Zn)	23,91	2,01	1,00	23,78	1,96	1,00	23,90	1,88	1,00	23,20	1,88	1,00	23,49	1,86	1,00	23,50	2,00	1,00
TF622	CCHC (Zn)		30,44	1,75	1,00	30,47	1,73	1,00	29,37	1,82	1,00	29,49	1,80	1,00	31,94	1,80	1,00	35,94	1,76	1,00
TF623	bHLH		23,59	2,06	1,00	24,21	1,92	1,00	23,34	2,06	1,00	23,60	1,91	1,00	23,85	1,97	1,00	24,07	1,98	1,00
TF624	HD-like		28,20	1,93	1,00	27,58	1,90	1,00	28,45	1,87	1,00	27,77	1,94	1,00	28,63	1,92	1,00	28,43	1,90	1,00
TF625	HD-like		25,88	1,91	1,00	25,66	1,81	1,00	25,98	1,84	1,00	25,12	1,84	1,00	25,44	2,01	1,00	25,58	1,86	1,00
TF626	HD-like		29,33	1,87	1,00	28,27	1,78	1,00	29,13	1,81	1,00	28,25	2,00	1,00	29,05	1,93	1,00	30,76	2,00	1,00
TF627	AP2/EREBP		29,21	1,58	1,00	29,30	1,66	1,00	29,92	1,72	1,00	28,04	1,80	1,00	28,48	1,69	1,00	28,14	1,85	1,00
TF628	AP2/EREBP		23,05	1,90	1,00	22,90	1,91	1,00	23,12	1,90	1,00	22,89	1,97	1,00	23,18	1,90	1,00	22,96	1,97	1,00
TF629	AP2/EREBP		31,34	1,74	1,00	30,51	1,85	1,00	33,62	1,74	1,00	28,24	1,83	1,00	28,28	1,85	1,00	28,56	1,89	1,00
TF630	CCHC (Zn)		30,31	1,82	1,00	29,53	1,91	1,00	23,98	1,81	1,00	29,22	1,75	1,00	29,84	1,97	1,00	31,10	1,87	0,99
TF631	HSF		24,10	1,91	1,00	24,71	1,82	1,00	23,87	1,88	1,00	23,65	1,90	1,00	24,06	1,93	1,00	24,10	1,97	1,00
TF632	CCHC (Zn)		29,93	1,94	1,00	29,59	1,94	1,00	25,84	1,99	1,00	27,93	1,82	1,00	29,05	1,79	1,00	29,33	2,05	1,00
TF633	CCHC (Zn)		25,84	1,91	1,00	24,94	1,90	1,00	20,12	1,89	1,00	23,47	1,90	1,00	24,97	1,91	1,00	25,56	1,79	1,00
TF634	CCHC (Zn)		35,47	1,66	1,00	34,99	1,53	1,00	29,45	1,50	1,00	33,08	1,68	1,00	32,21	1,37	1,00	33,47	1,58	1,00
TF635	MADS		29,89	1,83	1,00	30,38	1,57	1,00	25,27	1,85	1,00	27,45	1,88	1,00	27,32	1,96	1,00	28,14	1,86	1,00

Table S1, continued

TF636	MADS		27,22	1,98	1,00	27,97	1,78	1,00	23,38	1,83	1,00	26,77	1,81	1,00	26,70	1,86	1,00	27,74	1,84	1,00
TF637	MADS		26,99	1,89	1,00	26,75	2,05	1,00	28,34	1,81	1,00	32,20	1,53	1,00	23,20	1,95	1,00	23,84	2,14	1,00
TF638	CCHC (Zn)		30,74	1,74	1,00	29,95	1,81	1,00	25,58	1,82	1,00	30,21	1,70	1,00	29,77	1,81	1,00	31,69	1,53	1,00
TF639	bHLH		22,78	1,95	1,00	22,79	1,93	1,00	23,06	1,90	1,00	21,97	1,92	1,00	22,31	1,96	1,00	22,36	1,82	1,00
TF640	RR		26,88	1,84	1,00	25,99	1,90	1,00	24,61	1,96	1,00	27,65	1,94	1,00	23,20	1,91	1,00	24,81	1,89	1,00
TF641	MYB		26,16	1,85	1,00	26,20	1,84	1,00	26,01	1,78	1,00	25,69	1,82	1,00	26,00	1,83	1,00	25,90	2,00	1,00
TF642	CCHC (Zn)		27,03	1,85	1,00	26,45	1,86	1,00	22,59	1,91	1,00	25,51	1,91	1,00	25,60	2,07	1,00	26,61	1,74	1,00
TF643	HD family	HD	22,12	1,85	1,00	22,22	1,91	1,00	22,55	1,84	1,00	21,40	1,96	1,00	21,53	1,79	1,00	21,47	1,90	1,00
TF644	CCHC (Zn)		27,65	1,91	1,00	27,69	1,87	1,00	28,14	1,85	1,00	26,79	1,92	1,00	26,56	1,83	1,00	26,88	1,89	1,00
TF645	FHA		24,16	2,11	1,00	24,07	1,85	1,00	24,23	1,87	1,00	23,63	1,74	1,00	23,86	1,84	1,00	23,90	1,79	1,00
TF646	C_2C_2 (Zn)	GATA	28,81	1,81	1,00	28,48	1,80	1,00	28,98	1,83	1,00	26,85	1,83	1,00	27,22	1,89	1,00	27,57	1,87	1,00
TF647	bZIP		24,47	1,89	1,00	25,06	1,82	1,00	24,15	1,89	1,00	24,88	1,82	1,00	25,20	1,22	1,00	25,45	1,96	1,00
TF648	HTH	AraC	23,09	1,93	1,00	22,47	1,90	1,00	23,49	1,88	1,00	23,04	2,01	1,00	23,94	1,87	1,00	23,85	1,96	1,00
TF649	C3H	C3H-type 1 (Zn)	21,80	1,96	1,00	21,45	1,91	1,00	21,82	1,96	1,00	22,55	1,89	1,00	21,88	1,95	1,00	21,96	1,96	1,00
TF650	C_2C_2 (Zn)	CO-like	27,26	1,93	1,00	27,14	1,95	1,00	27,50	1,85	1,00	28,14	1,82	1,00	26,95	1,93	1,00	27,31	1,84	1,00
TF651	SRS		24,74	1,91	1,00	24,52	1,87	1,00	25,16	1,84	1,00	24,41	1,95	1,00	25,83	1,85	1,00	26,90	1,87	1,00
TF652	ZF DHHC		23,00	1,88	1,00	22,42	1,91	1,00	23,04	1,98	1,00	22,23	1,73	1,00	22,85	1,98	1,00	23,09	2,03	1,00
TF653	ZF DHHC		22,82	1,80	1,00	22,22	1,72	1,00	23,42	2,11	1,00	22,30	1,96	1,00	22,57	2,04	1,00	22,86	1,95	0,99
TF654	NAC		26,36	2,09	1,00	25,84	1,92	1,00	25,50	1,88	1,00	25,94	1,90	1,00	26,36	1,88	1,00	27,01	1,98	1,00
TF655	ABI3-VP1		28,61	1,87	1,00	28,23	1,87	1,00	28,59	1,87	1,00	27,76	1,90	1,00	31,74	1,77	1,00	31,72	1,76	1,00
TF656	CCHC (Zn)		24,45	1,88	1,00	25,51	1,83	1,00	24,50	1,63	1,00	24,38	1,92	1,00	24,31	1,85	1,00	25,31	1,95	1,00
TF657	CCHC (Zn)		24,34	1,81	1,00	25,13	1,98	1,00	20,26	1,91	1,00	24,50	1,88	1,00	24,49	1,79	1,00	24,80	1,98	1,00
TF658	CCHC (Zn)		29,95	1,67	1,00	29,31	1,76	1,00	29,76	1,72	1,00	29,27	1,79	1,00	30,49	1,75	1,00	30,28	1,74	1,00
TF659	MYB/HD-like		28,61	1,96	1,00	28,07	1,84	1,00	28,48	1,93	1,00	28,61	1,86	1,00	28,85	1,94	1,00	29,61	1,92	1,00
TF660	CCHC (Zn)		24,34	1,97	1,00	23,95	1,94	1,00	24,03	1,99	1,00	23,66	1,94	1,00	25,86	1,91	1,00	26,96	1,99	1,00
TF661	C_2H_2 (Zn)		28,27	1,70	1,00	27,89	1,69	1,00	21,60	2,06	0,99	25,91	1,85	1,00	27,09	1,95	1,00	27,23	1,79	1,00
TF662	WRKY family	WRKY	24,90	1,92	1,00	24,85	1,86	1,00	24,20	1,90	1,00	23,42	1,95	1,00	24,41	1,91	1,00	24,83	1,84	1,00
TF663	WRKY family	WRKY	26,84	1,90	1,00	26,50	1,75	1,00	26,64	2,10	1,00	25,87	1,85	1,00	26,11	1,85	1,00	26,86	2,14	1,00
TF664	RR		31,52	1,43	1,00	29,98	1,63	1,00	25,48	1,92	1,00	31,22	1,45	0,98	27,30	2,07	0,99	26,02	1,87	1,00
TF665	MYB/HD-like		24,04	1,91	1,00	23,88	1,92	1,00	23,86	1,82	1,00	23,10	1,88	1,00	23,31	1,99	1,00	23,43	1,93	1,00
TF666	HD-like		21,65	1,97	1,00	21,75	1,93	1,00	21,99	1,97	1,00	21,34	2,00	1,00	21,67	1,97	1,00	21,46	1,88	1,00
TF667	HD family	HD-ZIP	28,27	1,75	1,00	27,29	1,83	1,00	28,43	1,85	1,00	29,47	1,82	1,00	28,95	1,73	1,00	29,84	1,71	1,00
TF668	HMG		25,87	1,85	1,00	26,46	1,89	1,00	27,10	1,90	1,00	26,82	1,98	1,00	26,62	1,88	1,00	26,53	1,82	1,00
TF669	bZIP		26,27	1,82	1,00	26,05	1,74	1,00	25,90	1,95	1,00	26,25	1,88	1,00	27,03	1,83	1,00	28,50	1,83	1,00
TF670	bZIP		23,36	1,76	1,00	23,64	1,76	1,00	23,43	1,87	1,00	22,31	1,81	1,00	21,81	1,81	1,00	21,88	1,82	1,00
TF671	GRAS		28,20	1,79	1,00	28,27	1,80	1,00	29,31	1,75	1,00	29,24	1,83	1,00	30,20	1,76	1,00	33,41	1,78	1,00
TF672	GRAS		36,64	1,67	1,00	n.d.	1,20	0,98	36,52	1,55	1,00	n.d.	2,90	0,88	n.d.	1,38	0,99	n.d.	1,27	0,88
TF673	CCHC (Zn)		24,28	1,89	1,00	23,57	1,93	1,00	21,10	2,02	1,00	23,90	1,90	0,99	23,86	2,04	1,00	24,24	1,98	1,00
TF674	MYB		21,56	2,02	1,00	21,95	1,95	1,00	21,47	1,99	1,00	20,16	1,95	1,00	22,09	1,91	1,00	23,67	1,99	1,00
TF675	TTF-type (Zn)		27,74	1,99	1,00	27,41	1,85	1,00	27,79	1,86	1,00	27,95	1,98	1,00	27,35	1,77	1,00	27,89	1,89	1,00
TF676	MYB		23,76	2,01	1,00	23,68	1,86	1,00	24,06	1,98	1,00	23,37	1,95	1,00	23,58	1,89	1,00	23,66	1,77	1,00
TF677	GRF		30,47	1,66	1,00	30,09	1,74	1,00	24,87	1,75	1,00	30,27	1,59	1,00	28,92	1,71	1,00	30,33	1,64	1,00
TF678	RR		29,34	1,84	1,00	27,72	1,85	1,00	27,67	1,90	1,00	30,30	1,84	1,00	24,83	1,89	1,00	26,98	1,80	1,00
TF679	RR		24,98	1,92	1,00	24,06	1,88	1,00	28,71	1,93	1,00	26,84	1,21	0,98	20,43	1,95	1,00	21,74	1,92	1,00
TF680	MYB/HD-like		24,74	1,94	1,00	24,27	1,88	1,00	20,40	1,96	1,00	22,37	1,91	1,00	23,31	1,80	1,00	23,58	1,91	1,00
TF681	MYB/HD-like		28,50	1,85	1,00	28,18	1,84	1,00	21,95	1,86	1,00	26,81	1,85	1,00	27,41	1,86	1,00	27,66	1,87	1,00

Table S1, continued

TF682	ssDB TR		23,10	1,94	1,00	23,58	1,89	1,00	21,97	1,88	1,00	22,46	1,85	1,00	22,81	1,90	1,00	23,11	1,90	1,00
TF683	SBP		25,58	1,89	1,00	25,28	1,77	1,00	20,69	1,97	1,00	24,12	1,86	1,00	24,72	1,80	1,00	25,34	1,85	1,00
TF684	C_2C_2 (Zn)	DOF	26,03	1,87	1,00	26,88	2,05	1,00	25,66	1,80	1,00	24,73	1,70	1,00	24,99	1,98	1,00	25,52	1,20	1,00
TF685	C_2C_2 (Zn)	DOF	28,54	1,87	1,00	28,56	1,92	1,00	28,97	1,84	1,00	27,35	1,83	1,00	29,65	1,76	1,00	31,99	1,78	1,00
TF686	C3H	C3H-type 1 (Zn)	23,61	1,89	1,00	24,04	1,93	1,00	22,31	1,89	1,00	22,56	1,90	1,00	23,42	1,95	1,00	23,23	1,86	1,00
TF687	BTB/POZ		22,54	1,97	1,00	22,26	1,95	1,00	22,57	1,93	1,00	23,26	1,91	1,00	23,82	1,90	1,00	23,18	1,90	1,00
TF688	bHLH		27,16	1,85	1,00	27,01	1,89	1,00	27,34	1,71	0,99	26,85	1,79	1,00	27,13	1,76	1,00	26,70	1,87	1,00
TF689	AUX/IAA		22,87	1,70	1,00	23,30	1,70	1,00	22,20	1,92	1,00	22,27	1,87	1,00	23,00	1,82	0,99	24,68	1,70	1,00
TF690	bZIP		24,55	1,84	1,00	24,98	1,77	1,00	24,05	1,79	1,00	23,58	1,88	1,00	23,95	1,89	1,00	24,53	1,72	1,00
TF691	E2F		21,57	1,88	1,00	22,20	1,95	1,00	19,82	1,89	1,00	19,99	1,92	1,00	20,94	1,91	1,00	21,04	1,94	1,00
TF692	E2F		23,90	1,89	1,00	24,46	1,93	1,00	23,67	1,90	1,00	24,10	1,86	1,00	24,43	1,79	1,00	24,77	1,85	1,00
TF693	CCHC (Zn)		28,62	1,76	1,00	28,17	1,68	1,00	29,05	1,75	1,00	30,49	1,62	1,00	31,31	1,67	1,00	31,06	1,61	1,00
TF694	ARF		28,94	1,79	1,00	28,19	1,68	1,00	29,01	1,75	1,00	30,49	1,70	1,00	30,88	1,67	1,00	34,86	1,68	1,00
TF695	ARF		32,89	1,78	1,00	34,78	1,73	1,00	30,96	1,71	1,00	35,65	1,75	1,00	37,57	1,42	1,00	n.d.	4,83	0,84
TF696	ARF		19,27	2,02	1,00	18,71	2,01	1,00	17,57	2,19	1,00	19,97	1,97	1,00	16,99	2,21	0,99	18,10	2,29	0,99
TF697	ARF		29,96	1,80	1,00	29,13	1,84	1,00	27,90	1,81	1,00	30,31	1,82	1,00	27,07	1,93	1,00	28,49	1,83	1,00
TF698	MYB		23,89	1,93	1,00	24,26	1,92	1,00	24,34	1,91	1,00	23,94	1,91	1,00	24,15	1,85	1,00	24,12	1,89	1,00
TF699	GRAS		24,89	2,01	1,00	24,72	1,80	1,00	23,01	1,78	1,00	24,97	1,84	1,00	22,66	1,92	1,00	23,68	1,83	1,00
TF700	BTB/POZ		21,18	1,93	1,00	21,26	1,85	1,00	21,41	1,83	1,00	24,37	1,83	1,00	24,58	1,84	1,00	24,39	1,90	1,00
TF701	bZIP		28,26	1,99	1,00	29,22	2,13	0,99	23,56	2,00	1,00	27,16	1,91	1,00	27,66	2,19	1,00	28,02	1,92	1,00
TF702	bZIP		29,18	1,91	1,00	28,48	1,83	1,00	29,56	1,90	1,00	26,80	1,55	1,00	29,91	1,92	1,00	30,76	1,75	1,00
TF703	HD-like		28,54	1,88	1,00	28,88	1,76	1,00	27,53	1,84	1,00	30,53	1,67	1,00	26,18	1,84	1,00	27,42	1,68	1,00
TF704	HD-like		28,52	1,81	1,00	28,52	1,90	1,00	24,15	1,77	1,00	27,12	1,73	1,00	27,63	1,88	1,00	28,29	1,85	1,00
TF705	Tc/PD		23,64	1,88	1,00	23,42	1,91	1,00	23,72	1,97	1,00	23,22	1,92	1,00	23,80	1,91	1,00	23,23	1,81	1,00
TF706	GRAS		28,40	1,74	1,00	28,21	1,79	1,00	28,81	1,87	1,00	28,06	1,81	1,00	29,53	1,73	1,00	31,13	1,74	1,00
TF707	AP2/EREBP		30,56	1,91	1,00	31,97	1,84	1,00	26,17	1,94	1,00	30,70	1,91	1,00	29,92	1,86	1,00	30,23	1,87	1,00
TF708	SNF2		26,22	1,91	1,00	26,96	1,90	1,00	26,33	1,90	1,00	25,92	2,04	1,00	28,21	1,87	1,00	29,69	1,89	1,00
TF709	bHLH		27,25	1,91	1,00	27,11	1,90	1,00	27,53	1,84	1,00	26,86	1,94	1,00	28,18	1,98	1,00	29,37	1,90	1,00
TF710	SNF2		22,37	1,93	1,00	22,47	1,90	1,00	22,44	1,95	1,00	21,72	2,00	1,00	22,02	1,84	1,00	22,33	1,87	1,00
TF711	C_2C_2 (Zn)	YABBY	22,49	1,84	1,00	22,94	1,88	1,00	22,27	1,92	1,00	21,94	1,92	1,00	22,39	1,89	1,00	22,54	2,05	1,00
TF712	CCHC (Zn)		29,46	1,96	1,00	29,81	1,94	1,00	25,45	1,91	1,00	28,41	1,94	1,00	29,33	1,85	1,00	30,18	1,95	1,00
TF713	CCHC (Zn)		32,56	1,79	1,00	34,07	1,60	1,00	26,67	1,84	1,00	31,40	1,62	1,00	33,00	1,71	1,00	32,60	1,62	1,00
TF714	HD family	HD	24,00	1,88	1,00	24,01	1,92	1,00	24,14	1,86	1,00	23,31	1,90	1,00	24,06	1,99	1,00	23,58	1,90	1,00
TF715	C_2C_2 (Zn)	GATA	25,49	1,91	1,00	25,34	1,98	1,00	25,01	1,93	1,00	24,77	1,95	1,00	26,54	1,86	1,00	27,01	1,95	1,00
TF716	C_2C_2 (Zn)	GATA	26,34	1,96	1,00	26,11	1,82	1,00	26,32	1,86	1,00	27,16	1,83	1,00	26,89	2,00	1,00	27,27	2,10	1,00
TF717	FHA		25,78	1,86	1,00	25,97	1,84	1,00	26,15	1,82	1,00	25,64	1,82	1,00	25,36	1,76	1,00	27,26	1,79	1,00
TF718	CCHC (Zn)		29,95	1,82	1,00	28,43	1,72	1,00	31,15	1,51	1,00	29,68	1,66	1,00	30,65	1,64	1,00	33,52	1,49	1,00
TF719	GRF		31,17	1,68	1,00	31,25	2,10	1,00	26,52	1,70	1,00	30,32	1,47	1,00	29,67	1,27	1,00	31,61	1,36	1,00
TF720	CCHC (Zn)		25,06	1,90	1,00	25,41	1,88	1,00	25,40	1,99	1,00	24,19	1,87	1,00	27,17	1,82	1,00	28,76	1,85	1,00
TF721	MYB/HD-like		29,89	1,83	1,00	29,27	1,93	1,00	24,66	2,03	1,00	28,78	1,87	1,00	29,18	1,74	1,00	28,70	1,82	1,00
TF722	MYB/HD-like		30,09	1,84	1,00	29,24	1,79	1,00	23,38	1,92	1,00	28,36	1,92	1,00	28,99	1,77	1,00	30,68	1,76	1,00
TF723	MYB		29,94	2,03	1,00	28,36	1,92	1,00	25,85	1,89	1,00	28,93	1,92	1,00	24,67	1,88	1,00	26,24	1,90	1,00
TF724	MYB		31,21	1,88	1,00	29,18	1,81	1,00	29,64	1,74	1,00	31,67	1,79	1,00	27,78	1,85	1,00	27,86	1,80	1,00
TF725	AP2/EREBP		26,30	1,89	1,00	24,84	1,93	1,00	23,50	1,96	1,00	25,70	1,84	1,00	22,99	1,90	1,00	23,91	1,96	1,00
TF726	MYB/HD-like		23,61	1,89	1,00	23,28	1,88	1,00	23,68	1,89	1,00	22,39	1,95	1,00	23,02	1,84	1,00	22,98	1,95	1,00

Table S1, continued

TF727	C_2H_2 (Zn)		23,55	2,02	1,00	23,80	1,86	1,00	23,95	1,85	1,00	23,51	2,01	1,00	23,34	1,93	1,00	23,61	1,89	1,00
TF728	C_2H_2 (Zn)		29,30	1,78	1,00	28,66	1,78	1,00	26,84	1,79	1,00	28,70	1,72	1,00	25,49	1,85	1,00	27,12	1,46	1,00
TF729	C_2H_2 (Zn)		31,86	1,55	1,00	30,83	1,66	1,00	29,38	1,74	1,00	32,42	1,57	1,00	28,86	1,67	1,00	29,86	1,76	1,00
TF730	MYB/HD-like		23,77	1,92	1,00	23,11	1,96	1,00	19,01	1,99	1,00	22,42	1,93	1,00	23,21	1,92	1,00	23,64	1,87	1,00
TF731	MYB/HD-like		26,40	1,88	1,00	25,71	1,88	1,00	25,80	1,70	1,00	24,13	1,82	1,00	26,27	1,82	1,00	29,07	1,80	1,00
TF732	MYB		28,70	1,80	1,00	28,97	1,79	1,00	29,00	1,73	1,00	27,50	1,79	1,00	30,26	1,76	1,00	31,54	1,78	1,00
TF733	MYB		29,52	1,78	1,00	28,94	1,78	1,00	28,05	1,83	1,00	29,57	1,84	1,00	31,65	1,73	1,00	32,90	1,49	1,00
TF734	MYB		27,83	1,87	1,00	28,46	1,83	1,00	24,99	1,93	1,00	27,31	1,84	1,00	28,06	1,88	1,00	28,43	1,90	1,00
TF735	CCHC (Zn)		30,55	1,76	1,00	29,93	1,73	1,00	25,42	1,79	1,00	30,48	1,84	1,00	29,84	1,79	1,00	32,55	1,74	1,00
TF736	MYB		29,67	1,83	1,00	29,14	1,79	1,00	26,55	1,87	1,00	27,97	1,82	1,00	28,02	1,84	1,00	29,93	1,82	1,00
TF737	AS2		24,28	1,85	1,00	23,39	2,00	1,00	21,75	1,85	1,00	24,03	2,01	1,00	20,76	1,90	1,00	25,06	1,75	1,00
TF738	MBF		22,32	1,98	0,99	22,26	1,86	1,00	23,79	2,77	1,00	28,45	1,58	0,99	24,25	1,91	1,00	23,45	1,87	1,00
TF739	CCHC (Zn)		23,33	1,92	1,00	23,76	1,95	1,00	20,42	1,84	1,00	22,85	2,00	1,00	22,86	1,93	1,00	23,44	2,14	1,00
TF740	CCHC (Zn)		23,53	1,94	1,00	23,03	1,88	1,00	19,85	1,96	1,00	22,77	1,85	1,00	23,00	2,42	1,00	22,50	1,86	1,00
TF741	MYB/HD-like		27,02	1,94	1,00	26,95	1,81	1,00	26,24	1,84	1,00	27,60	1,90	1,00	27,79	1,87	1,00	27,84	2,12	1,00
TF742	AS2		37,84	1,59	0,99	38,15	1,19	1,00	36,79	1,27	1,00	n.d.	1,44	1,00	34,63	1,60	1,00	36,94	1,48	1,00
TF743	MYB/HD-like		32,06	1,80	1,00	31,39	1,80	1,00	32,38	1,55	1,00	31,86	1,76	1,00	36,78	1,36	1,00	33,08	1,73	1,00
TF744	MYB/HD-like		26,77	1,89	1,00	26,52	1,93	1,00	27,39	1,89	1,00	26,57	1,84	1,00	28,93	1,99	1,00	29,68	1,63	1,00
TF745	SSB protein		30,81	1,82	1,00	29,40	1,80	1,00	30,58	1,79	1,00	31,35	1,84	1,00	27,39	1,75	0,99	26,80	1,87	1,00
TF746	TUB		24,60	1,91	1,00	23,71	1,99	1,00	18,98	1,97	1,00	22,93	1,90	1,00	23,73	1,85	1,00	25,09	1,88	1,00
TF747	HD family	HD	30,22	1,64	1,00	29,24	1,23	0,94	32,92	1,59	1,00	24,74	2,36	0,98	31,73	1,52	1,00	32,88	1,43	1,00
TF748	ARF		22,10	1,93	1,00	22,03	1,93	1,00	22,24	1,91	1,00	21,24	1,87	1,00	21,43	1,93	1,00	21,35	2,06	1,00
TF749	ARF		23,40	1,93	1,00	22,99	1,97	1,00	23,50	1,80	1,00	22,70	1,88	1,00	25,72	1,90	1,00	27,66	1,88	1,00
TF750	WRKY family	WRKY	31,84	2,04	1,00	30,01	1,89	1,00	28,62	1,91	1,00	31,54	1,95	1,00	27,91	2,01	1,00	28,20	1,85	1,00
TF751	TTF-type (Zn)		27,35	1,78	1,00	27,06	1,80	1,00	28,70	1,73	1,00	26,93	1,83	1,00	28,41	1,70	1,00	29,90	1,63	1,00
TF752	MADS		30,85	1,63	1,00	30,49	1,84	1,00	27,34	1,73	1,00	27,75	1,69	1,00	28,93	1,71	1,00	29,69	1,21	1,00
TF753	CCHC (Zn)		24,37	2,33	1,00	23,36	1,90	1,00	24,74	1,92	1,00	24,05	1,87	1,00	26,25	1,82	1,00	26,30	1,83	1,00
TF754	C_2C_2 (Zn)	CO-like	21,11	1,94	1,00	21,71	1,98	1,00	20,77	2,12	1,00	19,84	2,16	1,00	19,90	2,03	1,00	19,98	1,98	1,00
TF755	C3H	C3H-type 1 (Zn)	22,77	1,89	1,00	22,91	1,93	1,00	18,61	1,90	1,00	22,73	1,87	1,00	22,35	1,99	1,00	22,50	1,88	1,00
TF756	bHLH		24,53	2,00	1,00	25,41	1,46	0,99	22,84	2,00	1,00	24,62	1,29	1,00	24,57	1,84	1,00	24,88	1,32	1,00
TF757	LIM		19,32	1,48	1,00	n.d.	1,36	0,98	21,66	1,27	1,00	24,27	1,33	1,00	20,86	1,29	1,00	21,48	1,29	1,00
TF758	Euk_TF		21,65	1,92	1,00	22,01	1,91	1,00	18,39	1,89	1,00	21,13	1,93	1,00	21,50	1,99	1,00	21,88	1,95	1,00
TF759	YEATS		23,43	2,09	1,00	23,62	2,19	1,00	23,86	1,89	1,00	23,27	1,84	1,00	20,91	1,89	1,00	21,14	2,01	1,00
TF760	C3H	C3H-type 1 (Zn)	21,47	2,04	1,00	21,18	1,89	1,00	21,56	1,92	1,00	20,48	1,98	1,00	20,90	2,00	1,00	20,81	2,19	1,00
TF761	C3H	C3H-type 1 (Zn)	21,27	1,91	1,00	21,33	2,07	1,00	21,47	1,88	1,00	20,81	1,89	1,00	20,75	1,83	1,00	20,85	1,81	1,00
TF762	bHLH		23,77	1,89	1,00	23,69	1,87	1,00	24,00	1,93	1,00	22,59	1,87	1,00	23,27	1,85	1,00	23,27	2,05	1,00
TF763	CCHC (Zn)		26,90	1,84	1,00	28,07	1,90	1,00	25,83	1,76	1,00	26,75	1,84	1,00	26,78	1,84	1,00	28,12	1,90	1,00
TF764	YEATS		23,42	2,06	1,00	23,81	1,91	1,00	23,95	1,91	1,00	24,02	1,86	1,00	23,71	1,91	1,00	23,75	1,85	1,00
TF765	bZIP		22,99	1,87	1,00	23,60	2,02	1,00	21,80	1,95	1,00	22,33	1,86	1,00	22,81	1,90	1,00	22,81	1,81	1,00
TF766	C3H	C3H-type 1 (Zn)	35,41	1,66	1,00	36,28	1,67	1,00	28,45	1,80	1,00	31,19	1,72	1,00	34,16	1,71	1,00	33,20	1,82	1,00
TF767	C3H	C3H-type 1 (Zn)	25,90	1,86	1,00	25,62	1,84	1,00	25,98	1,92	1,00	25,57	1,92	1,00	26,74	2,00	1,00	27,43	1,80	1,00
TF768	AP2/EREBP		29,70	1,80	1,00	29,67	1,86	1,00	24,11	2,02	1,00	37,85	1,89	0,99	27,66	2,01	1,00	28,01	1,72	1,00
TF769	AP2/EREBP		29,28	1,88	1,00	28,88	1,95	1,00	23,74	1,92	1,00	25,95	1,89	1,00	26,48	1,88	1,00	26,80	1,93	1,00
TF770	AP2/EREBP		29,24	1,80	1,00	29,05	1,88	1,00	23,39	1,87	1,00	27,07	1,91	1,00	27,77	1,89	1,00	27,95	1,87	1,00
TF771	AP2/EREBP		29,70	1,90	1,00	29,76	1,91	1,00	23,93	1,93	1,00	28,23	1,91	1,00	28,87	1,82	1,00	30,08	1,82	1,00
TF772	CCHC (Zn)		27,75	1,69	1,00	26,87	1,83	1,00	26,50	1,86	1,00	25,41	1,90	1,00	26,36	1,88	1,00	26,93	2,05	1,00

Table S1, continued

TF773	ABI3-VP1		35,88	1,63	1,00	34,22	1,66	1,00	39,50	1,55	1,00	n.d.	1,28	0,99	n.d.	1,13	0,98	36,24	1,68	1,00
TF774	ABI3-VP1		28,67	1,82	1,00	29,27	1,89	1,00	24,01	1,98	1,00	27,78	2,03	1,00	28,15	1,95	1,00	28,05	1,80	1,00
TF775	MYB/HD-like		27,77	1,92	1,00	27,20	1,93	1,00	27,39	1,79	1,00	27,32	1,90	1,00	28,26	1,92	1,00	27,92	1,93	1,00
TF776	ABI3-VP1		28,81	1,73	1,00	27,96	1,74	1,00	28,01	1,84	1,00	27,53	1,83	1,00	28,06	1,76	1,00	28,98	1,83	1,00
TF777	ABI3-VP1		25,13	1,88	1,00	24,96	1,97	1,00	24,98	1,93	1,00	24,61	1,91	1,00	24,67	1,79	1,00	24,87	1,96	1,00
TF778	ABI3-VP1		27,64	1,80	1,00	27,32	1,90	1,00	27,41	1,81	1,00	27,79	1,77	1,00	28,86	1,77	1,00	27,88	1,84	1,00
TF779	ABI3-VP1		24,20	1,90	1,00	24,11	1,91	1,00	24,25	1,95	1,00	23,32	1,91	1,00	23,73	1,91	1,00	23,80	1,87	1,00
TF780	AUX/IAA		24,76	1,90	1,00	25,08	1,83	1,00	22,25	1,81	1,00	24,02	1,92	1,00	24,27	1,85	1,00	24,60	1,75	1,00
TF781	MYB/HD-like		24,48	1,90	1,00	22,92	1,98	1,00	18,50	2,00	1,00	23,94	1,72	1,00	22,75	1,92	1,00	22,98	2,04	1,00
TF782	HTH	FIS	31,55	1,69	1,00	32,16	1,69	1,00	32,23	1,68	1,00	26,46	1,24	0,98	n.d.	1,23	0,99	29,57	1,58	1,00
TF783	CCHC (Zn)		27,34	1,80	1,00	26,25	1,77	1,00	29,01	1,76	1,00	28,00	1,68	1,00	29,87	1,69	1,00	30,87	1,76	1,00
TF784	NAC		29,54	1,87	1,00	28,97	1,80	1,00	26,12	1,93	1,00	28,38	1,90	1,00	29,34	1,87	1,00	29,93	1,91	1,00
TF785	CCHC (Zn)		30,00	1,74	1,00	29,64	1,80	1,00	29,99	1,76	1,00	29,11	1,73	1,00	30,19	1,76	1,00	31,59	1,74	1,00
TF786	MADS		24,78	1,90	1,00	25,15	1,92	1,00	24,41	1,86	1,00	23,68	1,92	1,00	24,41	1,95	1,00	24,75	1,89	1,00
TF787	MADS		24,81	1,86	1,00	24,61	1,25	1,00	24,87	1,89	1,00	24,31	1,84	1,00	24,12	1,89	1,00	24,37	1,91	1,00
TF788	bHLH		26,67	1,92	1,00	26,15	1,92	1,00	20,63	1,95	1,00	25,89	1,80	1,00	26,07	1,89	1,00	27,38	1,81	1,00
TF789	bHLH		33,48	1,71	1,00	32,12	1,75	1,00	30,97	1,83	1,00	30,64	1,77	1,00	31,76	1,70	1,00	33,93	1,77	1,00
TF790	WRKY family	WRKY	26,48	1,83	1,00	25,60	1,75	1,00	22,13	1,77	1,00	25,69	1,70	1,00	25,39	1,85	1,00	26,24	1,57	1,00
TF791	DDT		24,66	1,96	1,00	24,83	1,91	1,00	24,97	1,89	1,00	24,79	2,00	1,00	24,87	1,90	1,00	25,07	1,92	1,00
TF792	TrpR		24,15	2,02	1,00	23,06	1,94	1,00	23,98	1,92	1,00	24,78	1,91	1,00	21,65	1,93	1,00	22,41	1,97	1,00
TF793	MYB/HD-like		24,08	1,90	1,00	23,84	1,90	1,00	24,24	2,02	1,00	24,04	1,83	1,00	23,91	2,04	1,00	23,92	2,06	1,00
TF794	MYB/HD-like		24,06	1,84	1,00	25,15	1,81	1,00	24,96	2,00	1,00	24,21	2,01	1,00	24,28	1,83	1,00	25,81	1,71	1,00
TF795	bHLH		27,38	1,81	1,00	26,88	1,81	1,00	27,07	1,84	1,00	25,98	1,81	1,00	28,68	1,81	1,00	29,40	1,82	1,00
TF796	GRF		30,64	1,88	1,00	30,52	1,81	1,00	27,98	1,78	1,00	28,62	1,88	1,00	30,01	1,70	1,00	29,22	1,84	1,00
TF797	HD-like		27,71	1,81	1,00	28,50	1,84	1,00	26,65	1,79	1,00	27,35	1,75	1,00	27,61	1,82	1,00	28,58	1,82	1,00
TF798	C_2H_2 (Zn)		22,11	2,11	1,00	22,09	2,07	1,00	21,87	1,98	1,00	21,72	1,86	1,00	23,71	1,92	1,00	24,50	1,88	1,00
TF799	C_2H_2 (Zn)		24,97	1,47	1,00	24,52	2,06	1,00	24,78	1,88	1,00	26,07	1,24	0,98	24,07	1,78	1,00	24,58	1,82	1,00
TF800	CCHC (Zn)		28,41	2,18	1,00	28,49	1,76	1,00	23,74	1,92	1,00	28,05	1,94	1,00	27,76	1,86	1,00	30,67	2,12	1,00
TF801	HD-like		24,66	1,91	1,00	24,23	1,87	1,00	24,47	1,86	1,00	23,98	1,89	1,00	24,32	1,88	1,00	24,43	1,89	1,00
TF802	CCHC (Zn)		24,08	1,91	1,00	24,37	2,11	1,00	20,66	1,90	1,00	23,28	1,93	1,00	24,09	1,96	1,00	24,39	2,00	1,00
TF803	ARF		29,38	1,72	1,00	29,52	1,84	1,00	29,98	1,81	1,00	29,07	1,74	1,00	30,53	1,84	1,00	35,37	1,71	1,00
TF804	ARF		27,92	1,84	1,00	26,44	1,93	1,00	25,80	1,83	1,00	26,10	1,90	1,00	28,91	1,79	1,00	30,06	1,86	1,00
TF805	CCHC (Zn)		25,56	1,86	1,00	26,04	1,84	1,00	24,97	1,89	1,00	24,73	1,88	1,00	25,03	1,81	1,00	25,31	1,79	1,00
TF806	bZIP		24,04	1,92	1,00	24,54	1,92	1,00	20,50	2,08	1,00	22,50	1,79	1,00	23,54	1,85	1,00	24,07	1,85	1,00
TF807	bZIP		25,73	1,81	1,00	26,07	1,87	1,00	25,07	1,87	1,00	25,43	1,93	1,00	24,21	1,78	1,00	24,91	1,75	1,00
TF808	MYB/HD-like		20,67	1,87	1,00	21,27	2,03	1,00	19,67	1,96	1,00	19,42	2,05	1,00	19,68	1,91	1,00	19,72	2,04	1,00
TF809	AP2/EREBP		26,88	1,79	1,00	26,57	1,86	1,00	26,67	2,02	1,00	26,25	1,83	1,00	27,30	1,82	1,00	27,45	1,70	1,00
TF810	HD family	HD-ZIP	23,63	1,90	1,00	24,29	1,89	1,00	23,48	1,83	1,00	22,68	1,86	1,00	23,10	1,95	1,00	23,18	1,95	1,00
TF811	MYB/HD-like		22,25	1,86	1,00	22,06	1,81	1,00	22,36	2,02	1,00	21,58	1,92	1,00	22,14	1,77	1,00	22,26	1,85	1,00
TF812	bHLH		21,87	1,90	1,00	21,76	1,99	1,00	19,80	1,96	1,00	21,42	1,96	1,00	21,35	1,82	1,00	21,71	1,94	1,00
TF813	ABI3-VP1		31,43	1,74	1,00	30,31	1,71	1,00	31,25	1,72	1,00	31,22	1,72	1,00	33,22	1,68	1,00	38,59	1,31	1,00
TF814	HD-like		23,20	1,86	1,00	24,40	1,70	1,00	23,06	2,01	1,00	21,92	1,86	1,00	24,17	1,83	1,00	25,02	1,87	1,00
TF815	bZIP		23,52	1,92	1,00	23,37	1,91	1,00	23,52	2,25	1,00	23,12	1,89	1,00	23,53	1,90	1,00	23,59	1,82	1,00
TF816	MYB/HD-like		23,60	1,85	1,00	24,17	1,82	1,00	23,30	1,93	1,00	22,48	1,92	1,00	22,72	1,89	1,00	22,68	1,94	1,00
TF817	C_2C_2 (Zn)	DOF	23,88	1,91	1,00	24,60	2,00	1,00	23,78	1,78	1,00	25,18	1,85	1,00	25,51	1,90	1,00	25,78	1,87	1,00
TF818	HD-like		23,88	1,94	1,00	23,70	1,88	1,00	24,15	1,82	1,00	23,60	1,88	1,00	23,93	1,91	1,00	23,95	1,96	1,00

Table S1, continued

TF819	MYB/HD-like		22,29	1,95	1,00	22,98	1,94	1,00	22,36	1,94	1,00	23,41	2,10	1,00	23,25	1,94	1,00	23,69	1,83	1,00
TF820	AP2/EREBP		28,67	1,80	1,00	29,75	1,87	1,00	28,74	1,82	1,00	28,97	2,03	1,00	29,07	1,82	1,00	28,83	1,98	1,00
TF821	AP2/EREBP		29,95	1,73	1,00	28,62	1,96	1,00	23,10	1,77	1,00	29,23	1,78	1,00	28,47	1,79	1,00	29,37	1,77	1,00
TF822	DDT		25,37	2,14	1,00	25,42	1,99	1,00	25,27	1,95	1,00	26,02	2,09	1,00	25,57	2,00	1,00	26,30	2,12	1,00
TF823	C_2H_2 (Zn)		26,15	1,84	1,00	27,12	1,96	1,00	25,44	1,89	1,00	26,01	2,02	1,00	26,44	1,93	1,00	26,60	1,97	1,00
TF824	C_2H_2 (Zn)		26,09	2,02	1,00	26,09	1,70	1,00	26,77	1,89	1,00	26,41	1,86	1,00	26,55	1,91	1,00	26,45	1,72	1,00
TF825	CCHC (Zn)		28,65	1,86	1,00	28,43	1,85	1,00	29,52	1,97	1,00	27,67	1,86	1,00	28,92	1,85	1,00	29,00	1,82	1,00
TF826	AS2		23,58	1,94	1,00	22,65	1,89	1,00	21,62	1,92	1,00	22,63	2,01	1,00	22,02	1,63	1,00	21,55	1,98	1,00
TF827	C_2C_2 (Zn)	DOF	24,06	1,87	1,00	24,34	1,98	1,00	24,30	1,85	1,00	24,37	1,89	1,00	24,37	1,77	1,00	24,31	1,81	1,00
TF828	bHLH		33,85	1,81	1,00	36,31	1,82	1,00	27,96	1,89	1,00	31,70	1,88	1,00	31,95	1,81	1,00	31,86	1,73	1,00
TF829	bHLH		24,76	1,84	1,00	24,55	1,82	1,00	24,61	1,88	1,00	25,25	1,83	1,00	25,27	1,86	1,00	25,92	1,90	1,00
TF830	PHD		24,03	1,84	1,00	23,98	1,92	1,00	23,78	1,80	1,00	22,64	1,71	1,00	23,80	1,91	1,00	24,02	1,88	1,00
TF831	RR		20,36	1,99	1,00	20,23	2,03	1,00	20,54	2,34	1,00	23,18	1,95	1,00	23,52	1,93	1,00	23,91	1,95	1,00
TF832	bZIP		22,96	1,86	1,00	22,41	1,83	1,00	22,25	2,10	1,00	21,17	1,91	1,00	21,47	1,96	1,00	21,93	1,81	1,00
TF833	HD-like		27,31	1,88	1,00	27,63	1,91	1,00	25,29	1,86	1,00	26,78	1,89	1,00	27,31	1,94	1,00	27,68	1,92	1,00
TF834	HD family	HD	26,03	1,83	1,00	25,56	1,79	1,00	25,66	1,83	1,00	26,00	1,92	1,00	24,46	1,91	1,00	25,49	1,86	1,00
TF835	bHLH		23,20	1,84	1,00	23,98	1,84	1,00	22,82	1,93	1,00	23,18	1,91	1,00	23,19	1,82	1,00	23,25	2,12	1,00
TF836	MYB		24,36	1,99	1,00	23,13	2,05	1,00	22,01	2,13	1,00	23,97	1,84	1,00	20,73	1,83	1,00	22,01	1,84	1,00
TF837	MYB		23,44	1,93	1,00	23,82	1,99	1,00	23,99	2,96	1,00	23,56	1,89	1,00	23,55	1,94	1,00	24,10	1,88	1,00
TF838	MYB/HD-like		24,27	1,98	1,00	23,81	1,99	1,00	19,55	2,36	1,00	22,74	1,87	1,00	23,76	1,87	1,00	24,35	1,88	1,00
TF839	MYB/HD-like		22,78	2,00	1,00	23,33	2,14	1,00	18,87	1,94	1,00	21,85	1,99	1,00	22,32	1,94	1,00	22,68	1,86	1,00
TF840	HD family	HD	23,96	1,95	1,00	23,88	1,76	1,00	24,70	2,64	1,00	23,22	1,84	1,00	23,80	1,85	1,00	23,85	2,08	1,00
TF841	NAC		26,51	1,26	0,99	25,91	1,72	1,00	26,06	1,96	1,00	25,90	1,75	1,00	25,04	2,04	1,00	25,53	1,20	1,00
TF842	PHD		20,48	2,01	1,00	20,41	1,89	1,00	20,58	1,94	1,00	20,16	1,92	1,00	20,50	1,98	1,00	20,36	1,85	1,00
TF843	HD-like		25,39	1,97	1,00	24,97	1,92	1,00	26,06	1,92	1,00	25,63	1,92	1,00	24,66	1,96	1,00	25,42	1,89	1,00
TF844	MYB		22,70	1,94	1,00	23,19	1,95	1,00	23,26	1,92	1,00	22,68	1,91	1,00	23,20	1,89	1,00	23,18	1,93	1,00
TF845	bHLH		19,48	2,00	1,00	19,69	1,97	1,00	19,85	1,99	1,00	20,21	1,90	1,00	20,03	1,87	1,00	20,41	1,92	1,00
TF846	SRS		25,68	1,93	1,00	31,63	1,52	1,00	23,31	1,89	1,00	25,01	2,09	1,00	21,84	1,92	1,00	23,49	1,91	1,00
TF847	JUMONJI		27,83	1,73	1,00	27,73	1,69	1,00	27,38	1,71	1,00	27,10	1,75	1,00	27,42	1,72	1,00	28,17	1,75	1,00
TF848	MYB/HD-like		23,48	1,94	1,00	22,80	1,87	1,00	24,67	1,93	1,00	23,99	1,89	1,00	24,18	1,81	1,00	24,06	1,79	1,00
TF849	MYB		26,58	1,96	1,00	25,93	1,88	1,00	25,33	2,00	1,00	25,64	1,95	1,00	23,41	1,92	1,00	24,83	1,90	1,00
TF850	WRKY family	WRKY	21,61	1,90	1,00	22,06	1,92	1,00	21,40	1,98	1,00	21,17	1,93	1,00	21,70	1,94	1,00	21,60	1,95	1,00
TF851	HD-like		28,32	1,81	0,99	28,93	1,77	1,00	27,88	1,69	1,00	27,81	1,77	1,00	27,89	1,87	1,00	28,79	1,71	1,00
TF852	MYB/HD-like		23,54	2,52	1,00	23,93	1,88	1,00	20,86	2,04	1,00	22,57	1,89	1,00	22,73	1,86	1,00	23,06	1,96	1,00
TF853	AP2/EREBP		26,59	1,93	1,00	27,58	1,84	1,00	26,60	1,85	1,00	25,56	1,89	1,00	27,81	1,88	1,00	28,77	1,84	1,00
TF854	AP2/EREBP		26,61	1,86	1,00	26,51	1,89	1,00	25,97	1,91	1,00	28,41	1,82	1,00	27,79	1,97	1,00	28,76	2,07	1,00
TF855	AP2/EREBP		23,01	1,99	1,00	23,28	1,95	1,00	23,35	1,90	1,00	23,52	1,96	1,00	23,19	2,09	1,00	23,82	1,72	1,00
TF856	bZIP		24,92	1,76	1,00	24,76	1,84	1,00	20,35	1,94	1,00	23,91	2,18	1,00	24,57	1,77	0,99	24,90	1,76	1,00
TF857	CCAAT	CCAAT-HAP3	21,60	1,86	1,00	22,29	2,05	1,00	21,24	1,95	1,00	20,60	1,96	1,00	20,98	2,04	1,00	21,09	1,88	1,00
TF858	bHLH		27,27	1,93	1,00	27,81	1,90	1,00	26,67	1,86	1,00	26,72	1,84	1,00	26,93	1,88	1,00	27,26	1,87	1,00
TF859	HD-like		26,35	1,89	1,00	27,68	1,89	1,00	26,12	1,84	1,00	26,55	1,92	1,00	25,83	1,84	1,00	27,65	1,74	1,00
TF860	WRKY family	WRKY	30,33	1,84	1,00	n.d.	1,16	1,00	32,16	1,81	1,00	38,93	1,40	1,00	31,43	1,85	1,00	32,69	1,85	1,00
TF861	WRKY family	WRKY	31,72	1,79	1,00	31,10	1,82	1,00	31,18	1,79	1,00	31,30	1,80	1,00	33,09	1,75	1,00	31,44	1,81	1,00
TF862	HD-like		30,45	1,88	1,00	29,43	1,87	1,00	26,20	1,81	1,00	28,84	1,74	1,00	29,35	1,76	1,00	29,90	1,67	1,00
TF863	CCHC (Zn)		32,52	1,78	1,00	30,86	1,64	1,00	31,10	1,79	1,00	32,37	1,83	1,00	33,45	1,74	1,00	38,32	1,22	1,00
TF864	RR		23,50	1,92	1,00	23,26	1,81	1,00	23,57	1,95	1,00	28,77	1,70	1,00	26,62	1,86	1,00	27,56	1,91	1,00

Table S1, continued

TF865	MYB/HD-like		30,19	1,89	1,00	30,48	1,81	1,00	29,95	1,78	1,00	31,19	1,85	1,00	32,76	1,77	1,00	31,20	1,80	1,00
TF866	JUMONJI		24,26	1,97	1,00	24,16	1,90	1,00	20,57	1,73	1,00	23,19	1,83	1,00	23,66	1,83	1,00	24,23	1,82	1,00
TF867	C_2H_2 (Zn)		21,25	2,00	1,00	21,14	1,89	1,00	20,72	1,95	1,00	19,98	1,93	1,00	22,29	1,96	1,00	23,99	1,89	1,00
TF868	MYB		25,42	1,95	1,00	25,60	1,85	1,00	25,97	1,81	1,00	24,91	1,79	1,00	25,42	1,76	0,99	25,64	1,84	0,99
TF869	MADS		27,91	1,83	1,00	27,37	1,96	1,00	25,75	1,54	1,00	26,57	1,90	1,00	n.d.	1,51	0,99	27,48	1,71	1,00
TF870	HD family	HD	32,26	1,78	1,00	31,24	1,81	1,00	28,94	1,76	1,00	34,96	1,73	1,00	30,85	1,84	1,00	32,31	1,71	0,99
TF871	HTH	FIS	26,37	1,89	1,00	25,01	1,89	1,00	23,29	1,93	1,00	26,31	2,31	1,00	21,39	1,85	1,00	22,84	1,89	0,99
TF872	CCHC (Zn)		29,91	1,87	1,00	31,78	1,88	1,00	26,32	1,97	1,00	30,61	1,93	1,00	31,12	1,84	1,00	30,99	1,88	1,00
TF873	HMG		22,52	1,92	1,00	22,81	1,93	1,00	22,84	1,92	1,00	23,33	1,90	1,00	23,44	1,95	1,00	23,55	1,96	1,00
TF874	HD family	HD	22,00	1,87	1,00	22,19	1,90	1,00	21,66	1,96	1,00	22,11	2,00	1,00	21,25	1,99	1,00	21,72	1,91	1,00
TF875	WRKY family	WRKY	15,51	1,84	0,99	14,99	1,76	0,98	15,39	1,80	0,99	15,64	1,94	0,99	16,35	2,06	1,00	17,05	2,11	1,00
TF876	CCHC (Zn)		27,95	1,85	1,00	27,53	1,84	1,00	24,78	1,79	1,00	25,95	1,82	1,00	27,63	1,82	1,00	28,44	1,99	1,00
TF877	CCHC (Zn)		25,65	1,90	1,00	24,84	1,91	1,00	20,28	1,90	1,00	24,03	1,91	1,00	25,52	1,86	1,00	25,73	2,16	1,00
TF878	ARF		24,83	1,90	1,00	25,31	1,93	1,00	25,10	1,87	1,00	24,01	1,98	1,00	23,81	1,88	1,00	24,91	1,88	1,00
TF879	PHD		23,13	2,05	1,00	24,62	1,73	1,00	23,60	1,91	1,00	22,80	1,93	1,00	23,14	1,92	1,00	23,15	1,81	1,00
TF880	NAC		25,00	1,99	1,00	23,32	1,94	1,00	21,10	1,94	1,00	25,65	1,90	1,00	20,19	1,99	1,00	22,65	1,92	1,00
TF881	AP2/EREBP		25,24	1,76	1,00	23,38	1,98	1,00	25,49	1,84	1,00	24,44	1,60	1,00	24,13	1,81	1,00	24,26	2,11	1,00
TF882	WRKY family	WRKY	29,21	1,86	1,00	28,74	1,76	1,00	26,85	1,73	1,00	28,81	1,76	1,00	28,48	1,86	1,00	29,43	1,71	1,00
TF883	CCHC (Zn)		29,43	1,89	1,00	27,91	1,88	1,00	22,27	1,86	1,00	27,43	1,91	1,00	28,59	1,89	1,00	30,00	1,91	1,00
TF884	ABI3-VP1		23,19	1,95	1,00	22,68	1,89	1,00	22,46	2,00	1,00	21,99	1,93	1,00	23,27	2,00	1,00	25,39	1,90	1,00
TF885	ABI3-VP1		32,90	1,73	1,00	31,32	1,74	1,00	26,89	1,76	1,00	32,71	1,75	1,00	32,12	1,71	1,00	32,01	1,74	1,00
TF886	HMG		23,21	1,76	1,00	23,63	1,84	1,00	23,78	1,81	1,00	23,66	1,87	1,00	23,71	1,91	1,00	24,08	1,77	1,00
TF887	AP2/EREBP		24,81	1,85	1,00	25,80	1,97	1,00	23,38	1,86	1,00	22,70	1,90	1,00	22,87	1,92	1,00	23,22	1,87	1,00
TF888	MYB/HD-like		25,92	1,93	1,00	25,34	1,93	1,00	25,58	1,87	1,00	28,71	1,90	1,00	29,69	1,83	1,00	29,81	2,01	1,00
TF889	C3H	C3H-type 1 (Zn)	30,59	1,83	1,00	29,20	1,86	1,00	23,74	1,96	1,00	28,48	1,86	1,00	28,50	1,82	1,00	29,35	1,79	1,00
TF890	C_2H_2 (Zn)		26,39	1,83	1,00	25,80	1,86	1,00	21,11	1,86	1,00	24,55	1,81	1,00	25,21	1,85	1,00	25,68	1,79	1,00
TF891	TUB		24,02	1,91	1,00	23,88	1,91	1,00	23,97	1,99	1,00	23,71	1,90	1,00	23,76	1,89	1,00	23,86	2,04	1,00
TF892	TUB		33,33	1,78	1,00	32,06	1,78	1,00	34,88	1,81	1,00	36,89	1,86	1,00	32,19	1,89	1,00	36,96	1,78	1,00
TF893	HMG		n.d.	2,02	0,92	39,37	1,24	1,00	34,42	1,64	1,00	38,57	1,45	1,00	32,48	1,73	1,00	n.d.	1,14	0,99
TF894	HMG		30,36	1,76	1,00	28,47	1,85	1,00	28,71	1,77	1,00	30,08	1,77	1,00	25,59	1,84	1,00	27,75	1,81	1,00
TF895	CCAAT	CCAAT-HAP3	32,24	1,83	1,00	35,56	1,76	1,00	30,41	1,82	1,00	33,66	1,77	1,00	31,93	1,83	1,00	31,97	1,87	1,00
TF896	CCHC (Zn)		27,82	1,84	1,00	29,11	1,79	1,00	27,48	1,80	1,00	27,52	1,79	1,00	28,00	1,79	1,00	29,02	1,78	1,00
TF897	SBP		23,75	1,86	1,00	22,75	2,01	1,00	21,03	1,95	1,00	23,80	1,88	1,00	19,95	1,93	1,00	21,89	1,76	1,00
TF898	JUMONJI		31,27	1,91	1,00	29,68	1,89	1,00	30,69	1,77	1,00	32,73	1,80	1,00	32,88	1,72	1,00	32,51	2,02	1,00
TF899	TCP		21,58	2,00	1,00	22,26	1,88	1,00	21,44	1,90	1,00	21,52	1,88	1,00	21,86	1,92	1,00	21,95	1,94	1,00
TF900	CCHC (Zn)		26,28	1,82	1,00	27,41	1,98	1,00	23,90	1,88	1,00	24,76	1,91	1,00	24,91	1,80	1,00	25,65	1,97	1,00
TF901	SBP		22,81	1,90	1,00	22,96	1,96	1,00	23,25	1,91	1,00	22,78	1,93	1,00	22,68	1,95	1,00	22,87	1,88	1,00
TF902	CCHC (Zn)		24,02	1,95	1,00	24,04	2,29	1,00	19,82	1,95	1,00	22,52	2,00	1,00	23,24	1,91	1,00	23,97	2,06	1,00
TF903	SBP		24,93	1,97	1,00	25,51	1,85	1,00	24,22	1,97	1,00	24,42	1,89	1,00	24,48	1,77	1,00	25,05	1,91	1,00
TF904	bZIP		20,31	1,95	1,00	20,42	1,86	1,00	20,52	1,95	1,00	20,23	1,94	1,00	19,73	1,97	1,00	20,27	1,98	1,00
TF905	RR		30,75	1,81	1,00	28,48	1,88	1,00	27,76	1,90	1,00	29,70	2,01	1,00	26,93	1,89	1,00	27,47	1,79	1,00
TF906	GRAS		29,65	1,94	1,00	28,67	1,95	1,00	27,00	1,90	1,00	30,59	1,94	1,00	26,07	1,93	1,00	27,92	1,84	1,00
TF907	MYB		23,40	1,89	1,00	23,55	1,97	1,00	23,64	1,85	1,00	22,69	1,91	1,00	22,96	1,88	1,00	23,08	1,90	1,00
TF908	C3H	C3H-type 1 (Zn)	27,51	1,81	1,00	27,05	1,74	1,00	26,29	1,88	1,00	27,95	1,73	1,00	25,48	1,86	1,00	27,07	1,74	1,00
TF909	C3H	C3H-type 1 (Zn)	31,42	1,33	1,00	32,96	1,73	1,00	30,31	1,80	1,00	32,56	1,72	1,00	29,33	1,71	1,00	30,41	1,88	1,00
TF910	C3H	C3H-type 1 (Zn)	26,99	1,87	1,00	25,32	1,73	1,00	23,78	1,90	1,00	27,10	1,80	1,00	22,30	1,89	1,00	24,23	1,77	1,00

Table S1, continued

TF911	C3H	C3H-type 1 (Zn)	32,77	1,80	1,00	32,24	1,91	1,00	29,31	1,90	1,00	33,87	1,93	1,00	28,08	1,87	1,00	29,94	1,87	1,00
TF912	C3H	C3H-type 1 (Zn)	31,96	1,80	1,00	n.d.	1,40	0,99	38,52	1,39	1,00	n.d.	1,42	1,00	31,84	1,71	1,00	32,97	1,62	1,00
TF913	WRKY family	WRKY	23,06	1,85	1,00	22,97	2,01	1,00	23,10	1,92	1,00	22,66	1,97	1,00	22,70	2,18	1,00	22,89	1,99	1,00
TF914	ARF		22,75	1,96	1,00	22,50	1,94	1,00	22,88	1,97	1,00	21,80	1,94	1,00	21,72	2,53	1,00	21,80	1,91	1,00
TF915	PHD		21,83	1,90	1,00	21,83	2,29	1,00	17,45	1,99	1,00	20,37	1,96	1,00	20,51	2,14	1,00	20,87	1,96	1,00
TF916	CCHC (Zn)		28,70	1,78	1,00	28,30	2,05	1,00	28,05	1,96	1,00	27,09	1,82	1,00	27,72	1,87	1,00	28,26	2,04	1,00
TF917	MYB/HD-like		27,27	1,99	1,00	26,92	1,90	1,00	22,41	1,94	1,00	26,08	1,92	1,00	26,81	1,90	1,00	26,71	1,88	1,00
TF918	GRAS		27,72	1,82	1,00	27,53	1,90	1,00	27,82	2,00	1,00	28,20	1,94	1,00	29,51	1,79	1,00	29,15	1,84	1,00
TF919	GRAS		29,54	1,87	1,00	28,67	1,91	1,00	30,63	2,07	0,99	28,95	2,04	1,00	30,03	1,79	1,00	31,42	1,82	1,00
TF920	GRAS		27,56	1,92	1,00	27,08	1,89	1,00	25,42	1,88	1,00	27,29	1,76	1,00	25,33	1,88	1,00	26,32	1,83	1,00
TF921	GRAS		28,63	1,80	1,00	27,03	1,90	1,00	26,54	1,86	1,00	26,95	1,89	1,00	24,88	2,06	1,00	24,76	1,85	1,00
TF922	GRAS		31,75	1,93	1,00	32,00	1,85	1,00	32,66	1,84	1,00	32,88	1,89	1,00	34,09	1,89	1,00	32,96	1,88	1,00
TF923	HD-like		29,70	1,73	1,00	30,17	1,81	1,00	29,31	1,80	1,00	30,11	1,79	1,00	30,07	1,86	1,00	33,25	1,83	1,00
TF924	C_2H_2 (Zn)		33,62	1,78	1,00	32,11	1,78	1,00	26,74	1,87	1,00	32,45	1,61	1,00	32,51	1,81	1,00	32,23	1,76	1,00
TF925	C_2H_2 (Zn)		24,86	1,84	1,00	23,65	1,97	1,00	27,35	1,78	1,00	26,67	1,85	1,00	29,47	1,80	1,00	30,76	1,65	1,00
TF926	CCHC (Zn)		28,10	1,80	1,00	28,09	1,87	1,00	27,68	2,05	1,00	25,94	1,87	1,00	27,97	1,91	1,00	28,94	1,80	1,00
TF927	ABI3-VP1		30,95	1,59	1,00	28,37	1,66	1,00	27,44	1,74	1,00	30,08	1,66	1,00	25,54	1,67	1,00	27,49	1,59	1,00
TF928	HMG		31,11	1,92	1,00	28,93	1,94	1,00	29,07	1,94	1,00	29,95	1,86	1,00	27,13	2,08	1,00	27,96	1,90	1,00
TF929	C_2H_2 (Zn)		20,55	1,96	1,00	20,35	2,04	1,00	19,15	1,99	1,00	20,56	1,94	1,00	19,28	2,09	1,00	20,33	2,01	1,00
TF930	AP2/EREBP		24,02	1,86	1,00	23,76	1,89	1,00	22,97	1,97	1,00	23,27	1,84	1,00	21,97	1,83	1,00	22,61	2,19	1,00
TF931	bZIP		22,77	1,89	1,00	23,43	1,91	1,00	22,59	1,84	1,00	22,51	1,83	1,00	22,70	1,78	1,00	22,91	2,06	1,00
TF932	MYB		29,29	1,74	1,00	27,36	1,74	1,00	27,75	1,81	1,00	28,75	1,70	1,00	25,06	1,88	1,00	26,81	1,70	1,00
TF933	MYB/HD-like		n.d.	1,21	0,85	32,68	1,74	1,00	31,40	1,84	1,00	n.d.	1,46	0,97	33,58	1,84	1,00	32,87	1,79	1,00
TF934	MYB/HD-like		28,70	1,98	1,00	30,07	1,93	1,00	27,76	1,80	1,00	27,96	1,84	1,00	28,00	1,82	1,00	29,72	1,84	1,00
TF935	RR		25,48	1,88	1,00	25,84	2,01	1,00	25,72	1,97	1,00	26,15	1,85	1,00	25,27	1,83	1,00	26,00	1,99	1,00
TF936	MYB		25,76	1,98	1,00	25,67	1,86	1,00	26,29	1,87	1,00	26,40	1,92	1,00	26,50	2,03	1,00	26,65	1,79	1,00
TF937	HD-like		26,66	2,00	1,00	25,69	1,90	1,00	23,38	1,94	1,00	25,94	2,04	1,00	22,86	1,97	1,00	23,97	2,09	1,00
TF938	WRKY family	WRKY	24,50	1,97	1,00	24,84	1,89	1,00	23,23	1,92	1,00	23,73	1,90	1,00	22,33	2,02	1,00	23,52	1,71	1,00
TF939	MADS		24,65	1,90	1,00	24,61	1,92	1,00	24,67	1,93	1,00	24,62	1,94	1,00	25,63	2,02	1,00	25,77	1,87	1,00
TF940	AP2/EREBP		20,87	1,86	1,00	21,25	1,91	1,00	21,14	1,99	1,00	19,94	1,92	1,00	19,95	1,92	1,00	20,36	1,99	1,00
TF941	HD family	HD	23,63	1,91	1,00	23,89	1,92	1,00	23,93	1,94	1,00	23,03	1,99	1,00	22,93	1,95	1,00	23,20	1,91	1,00
TF942	AP2/EREBP		20,99	1,91	1,00	21,36	1,94	1,00	21,62	2,09	1,00	20,37	1,92	1,00	20,65	1,94	1,00	20,80	2,07	1,00
TF943	AP2/EREBP		24,66	1,80	0,99	24,87	1,80	1,00	24,80	1,84	1,00	24,62	1,75	1,00	24,86	1,81	1,00	24,87	1,64	1,00
TF944	A20-like		20,10	1,42	1,00	20,20	1,53	1,00	17,80	1,67	0,99	19,34	1,32	1,00	19,92	1,35	1,00	19,90	1,30	1,00
TF945	ABI3-VP1		25,52	1,88	1,00	24,55	2,01	1,00	21,13	1,88	1,00	24,21	1,95	1,00	25,25	1,97	1,00	25,53	1,89	1,00
TF946	bZIP		30,14	1,80	1,00	29,50	1,73	1,00	27,83	1,74	1,00	28,29	1,79	1,00	28,62	1,81	1,00	28,74	1,75	1,00
TF947	HD-like		25,65	1,90	1,00	25,95	1,97	1,00	22,32	1,94	1,00	24,78	1,96	1,00	25,42	1,91	1,00	25,72	1,86	1,00
TF948	ABI3-VP1		31,96	1,73	1,00	30,70	1,91	0,99	24,88	1,77	1,00	29,13	1,68	1,00	30,95	1,69	1,00	32,33	1,64	1,00
TF949	HD-like		25,42	1,88	1,00	24,57	1,91	1,00	24,60	1,78	1,00	27,15	1,86	1,00	22,96	2,03	1,00	24,77	1,90	1,00
TF950	BTB/POZ		23,46	1,78	1,00	23,42	1,93	1,00	23,46	1,87	1,00	23,06	1,88	1,00	23,44	1,93	1,00	23,32	2,03	1,00
TF951	CCHC (Zn)		27,91	1,81	1,00	27,96	1,70	1,00	23,56	1,76	1,00	27,63	1,77	1,00	27,29	1,77	1,00	28,92	1,76	1,00
TF952	CCHC (Zn)		23,31	1,91	1,00	23,65	1,93	1,00	22,61	2,05	1,00	23,33	1,90	1,00	23,14	1,88	1,00	23,12	1,82	1,00
TF953	PHD		30,71	1,74	1,00	30,17	1,51	1,00	29,54	1,78	1,00	32,58	1,75	1,00	29,88	1,77	1,00	31,01	1,74	1,00
TF954	AP2/EREBP		25,41	1,84	1,00	26,59	2,00	1,00	24,08	1,92	1,00	23,95	1,84	1,00	24,17	1,90	1,00	24,11	2,11	1,00
TF955	AP2/EREBP		23,81	1,82	1,00	24,44	1,98	1,00	23,51	2,08	1,00	23,55	1,89	1,00	23,85	1,93	1,00	23,93	1,90	1,00
TF956	C_2C_2 (Zn)	YABBY	24,42	1,92	1,00	24,63	1,97	1,00	24,99	1,95	1,00	24,77	1,88	1,00	25,59	1,78	1,00	25,27	2,03	1,00

Table S1, continued

TF957	HMG		20,78	1,95	1,00	21,17	2,08	1,00	21,30	1,94	1,00	20,49	1,93	1,00	20,73	1,95	1,00	20,66	1,81	1,00
TF958	ABI3-VP1		30,63	1,50	0,99	37,86	1,76	1,00	29,15	1,76	1,00	27,85	1,49	0,99	34,25	1,63	1,00	25,91	1,75	1,00
TF959	C_2H_2 (Zn)		23,25	1,91	1,00	23,50	1,92	1,00	23,60	1,89	1,00	23,33	1,89	1,00	23,20	1,85	1,00	23,42	1,94	1,00
TF960	C3H	C3H-type 1 (Zn)	23,44	1,88	1,00	23,55	1,89	1,00	23,96	1,87	1,00	23,80	1,89	1,00	23,31	1,91	1,00	23,19	1,86	1,00
TF961	CCHC (Zn)		36,96	1,23	1,00	39,01	1,54	0,96	n.d.	1,44	0,98	38,13	1,33	0,99	n.d.	1,22	1,00	n.d.	1,30	0,96
TF962	AP2/EREBP		34,23	1,99	1,00	32,92	2,04	1,00	n.d.	1,54	0,77	38,91	2,01	1,00	n.d.	1,22	0,94	36,50	1,85	1,00
TF963	GRAS		23,53	1,95	1,00	24,10	1,90	1,00	23,99	1,91	1,00	23,87	1,91	1,00	23,99	1,89	1,00	24,10	1,76	1,00
TF964	AS2		27,98	1,86	1,00	26,32	1,83	1,00	24,17	1,88	1,00	28,10	1,96	1,00	23,89	1,88	1,00	25,21	1,98	1,00
TF965	WRKY family	WRKY	27,11	1,93	1,00	27,58	1,84	1,00	27,08	1,86	1,00	27,52	1,91	1,00	27,26	1,85	1,00	27,44	1,82	1,00
TF966	AP2/EREBP		33,96	1,64	1,00	31,55	1,65	1,00	30,19	1,78	1,00	32,16	1,79	1,00	28,63	1,70	1,00	30,68	1,69	1,00
TF967	MYB		27,25	1,92	1,00	34,76	1,38	1,00	25,23	1,99	1,00	27,04	2,09	1,00	23,96	1,77	1,00	25,46	1,63	1,00
TF968	C_2C_2 (Zn)	DOF	26,88	1,95	1,00	26,45	1,86	1,00	25,21	1,97	1,00	27,78	1,90	1,00	23,20	1,92	1,00	25,02	1,87	1,00
TF969	HD family	HD	30,68	1,87	1,00	29,52	1,82	1,00	27,43	1,86	1,00	32,38	1,81	1,00	26,09	1,59	1,00	28,33	1,76	1,00
TF970	C_2H_2 (Zn)		30,54	1,63	1,00	28,91	1,64	1,00	27,45	1,69	1,00	29,72	1,65	1,00	27,18	1,71	1,00	28,65	1,69	1,00
TF971	MYB		29,72	1,76	1,00	n.d.	1,58	0,88	31,89	1,64	1,00	23,94	1,41	1,00	24,08	1,89	1,00	25,62	1,91	1,00
TF972	WRKY family	WRKY	26,38	1,87	1,00	25,58	1,79	1,00	23,68	1,96	1,00	27,70	1,78	1,00	22,95	1,82	1,00	24,81	1,83	1,00
TF973	MYB		n.d.	1,41	0,86	32,94	1,85	1,00	33,35	1,72	1,00	32,78	1,92	1,00	30,74	2,10	0,99	32,70	2,27	1,00
TF974	MYB		27,61	1,83	1,00	27,65	1,90	1,00	26,95	1,83	1,00	30,07	1,84	1,00	27,42	1,77	1,00	29,41	1,74	1,00
TF975	MYB		32,97	1,76	1,00	31,25	1,97	1,00	29,13	1,84	1,00	32,72	1,74	1,00	27,68	1,74	1,00	30,07	1,85	1,00
TF976	MYB		31,32	1,71	1,00	28,51	1,87	1,00	26,57	1,97	1,00	29,77	1,84	1,00	26,13	2,07	1,00	27,26	1,78	1,00
TF977	SRS		24,42	1,84	1,00	24,64	1,85	1,00	24,73	1,90	1,00	23,90	2,18	1,00	24,36	1,75	1,00	24,14	1,75	1,00
TF978	C_2C_2 (Zn)	CO-like	31,24	1,25	1,00	n.d.	1,58	1,00	31,44	1,77	1,00	24,02	1,18	0,97	31,78	1,72	1,00	33,71	1,58	1,00
TF979	CCHC (Zn)		24,93	1,91	1,00	25,31	2,04	1,00	22,76	1,91	1,00	24,47	1,97	1,00	21,87	1,90	1,00	22,69	1,89	1,00
TF980	SBP		26,43	1,76	1,00	26,57	1,75	1,00	26,42	1,80	1,00	26,05	1,87	1,00	25,82	1,87	1,00	26,05	1,82	1,00
TF981	bZIP		28,58	1,95	1,00	28,27	2,04	1,00	26,84	1,93	1,00	27,60	1,95	1,00	25,94	1,91	1,00	26,97	1,89	1,00
TF982	C_2H_2 (Zn)		23,95	1,86	1,00	23,97	1,73	1,00	23,09	1,93	1,00	23,31	1,91	1,00	22,30	1,89	1,00	22,97	1,88	1,00
TF983	MYB		23,97	1,86	1,00	24,19	1,89	1,00	24,59	1,89	1,00	24,48	1,91	1,00	24,66	1,80	1,00	24,54	1,64	1,00
TF984	bHLH		26,79	1,82	1,00	26,02	2,05	1,00	26,57	1,82	1,00	27,28	1,80	1,00	25,70	1,86	1,00	26,80	1,18	1,00
TF985	C3H	C3H-type 1 (Zn)	33,55	1,58	1,00	31,89	1,77	1,00	29,65	1,79	1,00	30,66	1,73	1,00	28,31	1,78	1,00	30,06	1,83	1,00
TF986	C3H	C3H-type 1 (Zn)	31,15	1,72	1,00	30,81	1,71	1,00	28,97	1,82	1,00	33,60	1,67	1,00	28,45	1,75	1,00	28,52	1,81	1,00
TF987	C3H	C3H-type 1 (Zn)	33,33	1,40	1,00	31,90	1,71	1,00	29,52	1,81	1,00	38,64	1,57	1,00	28,35	1,81	1,00	30,82	1,71	1,00
TF988	HD-like		27,26	1,89	1,00	27,33	1,78	1,00	25,50	1,92	1,00	27,58	1,81	1,00	24,65	1,65	1,00	27,44	1,67	1,00
TF989	C3H	C3H-type 1 (Zn)	26,78	1,90	1,00	27,10	1,89	1,00	27,95	1,98	1,00	27,33	1,91	1,00	26,00	1,86	1,00	27,20	2,17	1,00
TF990	NAC		23,08	1,89	1,00	23,08	1,95	1,00	23,28	1,96	1,00	23,03	1,97	1,00	22,66	1,94	1,00	23,01	1,93	1,00
TF991	MADS		30,70	1,83	1,00	28,60	1,90	1,00	27,34	1,96	1,00	29,59	1,87	1,00	26,24	1,89	1,00	28,06	1,85	1,00
TF992	MADS		32,77	1,62	1,00	31,83	1,75	1,00	31,98	1,69	1,00	19,14	1,22	0,96	27,79	1,88	1,00	29,46	1,76	1,00
TF993	NAC		25,66	1,95	1,00	26,23	1,88	1,00	26,16	1,94	1,00	26,36	1,91	1,00	26,47	1,77	1,00	26,42	1,80	1,00
TF994	TCP		20,96	1,95	1,00	21,12	1,93	1,00	21,46	1,99	1,00	22,41	1,87	1,00	22,29	1,92	1,00	22,36	2,01	1,00
TF995	bHLH		25,94	1,85	1,00	25,36	1,90	1,00	21,08	1,93	1,00	25,22	1,89	1,00	25,86	1,80	1,00	25,76	1,90	1,00
TF996	HD-like		23,38	2,03	1,00	22,32	2,32	1,00	23,47	1,99	1,00	22,50	1,87	1,00	19,24	1,98	1,00	20,67	2,17	1,00
TF997	HD-like		30,49	1,68	1,00	29,70	1,86	1,00	28,33	1,65	1,00	30,79	1,80	1,00	27,90	1,85	1,00	29,90	1,78	1,00
TF998	CCHC (Zn)		22,68	1,87	1,00	22,59	1,98	1,00	22,75	1,85	1,00	22,36	1,89	1,00	22,79	1,93	1,00	22,80	2,02	1,00
TF999	MADS		28,73	1,69	1,00	28,37	1,66	1,00	28,86	1,65	1,00	29,02	1,70	1,00	29,21	1,67	1,00	30,38	1,85	1,00
TF1000	MADS		28,71	1,79	1,00	28,62	1,91	1,00	29,16	1,21	1,00	28,47	1,86	1,00	29,30	1,81	1,00	30,76	1,67	1,00
TF1001	C_2H_2 (Zn)		21,41	2,07	1,00	21,72	1,97	1,00	21,77	1,95	1,00	21,83	1,84	1,00	22,34	1,74	1,00	21,98	1,30	1,00

Table S1, continued

TF1002	CCAAT	CCAAT-HAP3	29,90	1,86	1,00	29,98	1,94	1,00	30,05	1,80	1,00	31,61	1,85	1,00	27,32	1,89	1,00	28,75	1,83	1,00
TF1003	MYB		29,15	1,75	1,00	28,65	1,81	1,00	26,26	1,77	1,00	27,91	1,69	1,00	25,87	1,71	1,00	26,75	1,62	1,00
TF1004	JUMONJI		22,46	1,91	1,00	22,57	1,89	1,00	22,81	2,05	1,00	22,53	1,95	1,00	28,12	1,45	0,99	22,91	1,83	1,00
TF1005	MYB		22,36	1,94	1,00	22,45	1,93	1,00	22,11	1,94	1,00	22,57	1,89	1,00	22,23	1,93	1,00	22,55	1,90	1,00
TF1006	bHLH		27,97	1,96	1,00	27,81	1,90	1,00	28,16	1,86	1,00	27,50	1,96	1,00	29,43	1,89	1,00	30,36	1,89	1,00
TF1007	bHLH		23,54	1,84	1,00	23,88	1,85	1,00	26,98	1,79	1,00	22,65	1,83	1,00	23,14	1,84	1,00	23,56	1,85	1,00
TF1008	AP2/EREBP		28,91	1,81	1,00	28,93	1,77	1,00	28,76	1,76	1,00	29,45	1,70	1,00	27,88	1,70	1,00	29,69	1,94	1,00
TF1009	JUMONJI		26,94	1,90	1,00	26,92	1,87	1,00	26,83	1,80	1,00	27,78	1,89	1,00	28,22	1,81	1,00	28,26	1,86	1,00
TF1010	PHD		26,99	1,92	1,00	27,03	1,88	1,00	27,34	1,92	1,00	26,61	1,95	1,00	26,59	1,84	1,00	27,05	1,82	1,00
TF1011	ZF-HD		22,92	1,88	1,00	23,19	1,82	1,00	24,08	1,85	1,00	23,53	1,85	1,00	23,37	2,01	1,00	23,40	1,89	1,00
TF1012	MYB		23,79	1,87	1,00	24,01	1,95	1,00	24,23	1,87	1,00	23,99	2,02	1,00	23,90	1,71	1,00	24,01	1,79	1,00
TF1013	bHLH		25,76	1,87	1,00	26,02	1,81	1,00	26,43	1,89	1,00	26,68	1,76	1,00	26,00	1,79	1,00	26,99	1,87	1,00
TF1014	C_2C_2 (Zn)	GATA	22,47	1,99	1,00	22,81	1,85	1,00	22,97	1,98	1,00	23,06	2,91	1,00	23,19	1,94	1,00	23,14	1,76	1,00
TF1015	PHD		22,28	1,93	1,00	22,45	1,91	1,00	22,24	1,98	1,00	22,28	1,95	1,00	21,32	1,86	1,00	21,95	1,86	1,00
TF1016	CCHC (Zn)		27,84	1,87	1,00	27,83	2,01	1,00	28,06	1,86	1,00	27,23	1,73	1,00	28,86	1,85	1,00	31,40	1,77	1,00
TF1017	C3H	C3H-type 1 (Zn)	23,99	1,93	1,00	23,72	1,90	1,00	24,08	2,03	1,00	23,33	1,90	1,00	23,88	2,01	1,00	23,58	1,87	1,00
TF1018	AS2		32,88	1,66	1,00	31,36	1,67	1,00	30,81	1,67	1,00	30,77	1,72	1,00	29,57	1,74	1,00	28,93	1,65	1,00
TF1019	PHD		25,03	1,96	1,00	25,30	1,83	1,00	25,65	1,87	1,00	24,76	1,82	1,00	25,07	1,85	1,00	24,78	1,24	1,00
TF1020	GRAS		25,17	1,99	1,00	23,11	1,91	1,00	22,12	1,94	1,00	24,95	1,89	1,00	21,53	1,94	1,00	22,95	2,22	1,00
TF1021	AP2/EREBP		26,74	1,88	1,00	27,10	1,91	1,00	27,03	1,93	1,00	26,29	1,90	1,00	25,60	1,92	1,00	26,40	1,87	1,00
TF1022	PHD		21,62	1,99	1,00	21,53	1,95	1,00	21,31	1,91	1,00	20,22	2,34	1,00	22,82	1,80	1,00	23,12	1,95	1,00
TF1023	PHD		30,63	1,75	1,00	30,42	1,68	1,00	30,97	1,70	1,00	n.d.	1,13	0,96	30,20	1,78	1,00	31,79	1,79	1,00
TF1024	TCoAp15		22,31	1,94	1,00	22,63	2,01	1,00	22,61	1,90	1,00	22,63	1,95	1,00	22,44	1,91	1,00	22,77	1,89	1,00
TF1025	WRKY family	WRKY	30,43	1,80	1,00	29,61	1,77	1,00	28,20	1,68	1,00	30,24	1,39	1,00	26,95	1,84	1,00	27,43	1,80	1,00
TF1026	AS2		22,66	1,98	1,00	22,29	1,93	1,00	21,09	1,98	1,00	22,02	1,89	1,00	19,81	1,96	1,00	21,00	1,81	1,00
TF1027	C_2H_2 (Zn)		24,34	1,86	1,00	24,53	1,87	1,00	24,47	1,89	1,00	23,30	1,92	1,00	23,03	1,87	1,00	23,30	1,57	1,00
TF1028	MYB		24,40	1,85	1,00	24,61	1,76	1,00	26,20	1,86	1,00	24,93	1,84	1,00	22,89	1,79	1,00	24,13	1,86	1,00
TF1029	EIL		30,97	1,71	1,00	31,68	1,88	1,00	28,02	1,65	1,00	30,34	1,96	1,00	27,58	1,77	1,00	29,36	1,85	1,00
TF1030	C_2C_2 (Zn)	GATA	23,37	1,98	1,00	22,26	1,97	1,00	22,67	1,93	1,00	23,62	1,93	1,00	19,51	1,98	1,00	21,38	1,77	1,00
TF1031	MYB		24,34	1,88	1,00	23,67	1,92	1,00	24,43	1,90	1,00	23,64	1,91	1,00	21,38	2,01	1,00	22,48	1,93	1,00
TF1032	NIN-like		25,65	1,94	1,00	24,53	1,84	1,00	23,95	1,86	1,00	26,00	1,91	1,00	23,54	1,87	1,00	23,81	1,83	1,00
TF1033	HTH	FIS	21,00	2,02	1,00	19,76	2,00	1,00	20,02	2,00	1,00	21,46	1,99	1,00	18,04	2,49	1,00	19,62	2,14	1,00
TF1034	NAC		23,34	1,96	1,00	23,53	1,91	1,00	23,73	1,96	1,00	21,67	1,91	1,00	21,53	1,87	1,00	21,77	1,96	1,00
TF1035	ABI3-VP1		27,45	1,88	1,00	26,77	1,90	1,00	25,86	1,89	1,00	27,97	1,97	1,00	23,38	1,86	1,00	25,16	1,78	1,00
TF1036	ABI3-VP1		31,45	1,88	1,00	28,94	1,91	1,00	30,92	1,87	1,00	30,16	1,87	1,00	25,92	1,92	1,00	27,55	1,87	1,00
TF1037	ABI3-VP1		24,71	1,87	1,00	22,86	1,84	1,00	20,73	1,94	1,00	24,94	1,80	1,00	19,82	1,88	1,00	21,53	1,82	1,00
TF1038	ABI3-VP1		29,91	1,84	1,00	29,49	1,86	1,00	27,88	1,92	1,00	30,70	1,77	1,00	27,02	1,82	1,00	28,01	1,79	1,00
TF1039	ABI3-VP1		30,26	1,89	1,00	29,10	1,74	1,00	27,02	1,84	1,00	31,52	1,79	1,00	26,13	1,98	1,00	27,18	1,92	1,00
TF1040	MADS		22,95	1,85	1,00	21,80	1,87	1,00	19,74	1,89	1,00	22,40	1,87	1,00	18,50	1,92	1,00	20,21	1,98	1,00
TF1041	HD family	HD	21,50	1,97	1,00	21,82	2,11	1,00	22,04	1,90	1,00	21,69	1,91	1,00	21,70	1,92	1,00	21,70	1,85	1,00
TF1042	C3H	C3H-type 1 (Zn)	22,25	1,90	1,00	22,58	1,91	1,00	22,16	1,97	1,00	22,49	1,90	1,00	21,57	1,96	1,00	22,19	1,86	1,00
TF1043	GRAS		35,04	1,65	1,00	31,68	1,62	1,00	31,83	1,72	1,00	34,17	1,66	1,00	32,28	1,69	1,00	33,65	1,62	1,00
TF1044	CCAAT	CCAAT-HAP3	20,55	1,89	1,00	20,97	1,99	1,00	21,22	1,91	1,00	21,27	1,94	1,00	21,09	1,92	1,00	21,25	2,00	1,00
TF1045	C_2H_2 (Zn)		23,50	1,95	1,00	23,90	1,84	1,00	22,35	1,95	1,00	22,98	2,03	1,00	23,37	1,86	1,00	23,47	1,92	1,00

Table S1, continued

ID	TF Family	TF Subfamily	SA control rep 1			SA control rep 2			SA control rep 3			SA infected rep 1			SA infected rep 2			SA infected rep 3		
			Cq	PCReff	R^2	Cq	PCReff	R^2	Cq	PCReff	R^2	Cq	PCReff	R^2	Cq	PCReff	R^2	Cq	PCReff	R^2
TF1	HSF		26,68	1,73	1,00	26,65	1,77	1,00	26,75	1,77	1,00	27,17	1,76	1,00	26,37	1,83	1,00	25,47	1,94	1,00
TF2	HSF		22,74	1,92	1,00	22,13	1,97	1,00	19,46	1,82	1,00	19,92	2,02	1,00	20,15	1,88	1,00	19,67	1,99	1,00
TF3	AP2/EREBP		26,18	1,83	1,00	24,44	1,91	1,00	18,72	2,36	1,00	24,16	1,86	1,00	21,89	2,00	1,00	23,22	2,00	1,00
TF4	MYB		28,14	1,82	1,00	24,77	1,90	1,00	20,68	2,12	1,00	22,94	1,99	1,00	22,82	1,98	1,00	24,88	1,95	1,00
TF5	AP2/EREBP		28,19	1,89	1,00	24,79	1,97	1,00	21,58	1,96	1,00	24,30	1,91	1,00	22,43	1,94	1,00	24,45	1,88	1,00
TF6	MYB/HD-like		28,50	2,01	1,00	27,93	1,74	1,00	26,25	1,98	1,00	30,23	1,64	1,00	29,74	1,61	1,00	27,76	1,79	1,00
TF7	HD-like		24,08	1,88	1,00	24,15	1,91	1,00	24,67	1,82	1,00	25,34	1,77	1,00	24,46	1,92	1,00	23,98	1,95	1,00
TF8	LIM		24,50	1,92	1,00	25,16	1,90	1,00	25,77	1,82	1,00	26,24	1,85	1,00	25,15	2,27	1,00	24,24	1,87	1,00
TF9	CCHC (Zn)		26,58	1,77	1,00	26,74	1,99	1,00	21,84	1,72	1,00	23,13	1,78	1,00	24,78	1,88	1,00	24,20	1,82	1,00
TF10	RR		26,97	1,95	1,00	27,32	1,97	1,00	26,57	1,73	1,00	27,88	1,71	1,00	27,59	1,77	1,00	27,65	1,74	1,00
TF11	CCHC (Zn)		21,78	1,96	1,00	21,93	1,97	1,00	22,10	1,92	1,00	22,50	2,04	1,00	21,95	1,94	1,00	21,77	1,97	1,00
TF12	MYB/HD-like		22,45	1,87	1,00	22,48	1,86	1,00	22,94	1,81	1,00	22,67	1,85	1,00	22,45	1,94	1,00	21,79	1,87	1,00
TF13	KRAB box		25,56	1,92	1,00	25,52	1,89	1,00	21,82	2,09	1,00	23,08	1,93	1,00	22,98	1,86	1,00	22,66	1,92	1,00
TF14	GRAS		23,56	1,87	1,00	23,72	1,88	1,00	24,05	1,81	1,00	23,47	1,93	1,00	23,43	1,89	1,00	22,63	1,86	1,00
TF15	CCHC (Zn)		27,29	1,99	1,00	24,08	2,13	1,00	22,15	1,92	1,00	27,04	1,86	1,00	27,92	1,88	1,00	23,15	1,78	1,00
TF16	bZIP		21,89	1,84	1,00	22,12	1,86	1,00	21,51	1,91	1,00	21,64	1,82	1,00	21,53	1,88	1,00	20,86	1,85	1,00
TF17	MADS		29,33	1,82	1,00	30,11	1,86	1,00	23,67	1,86	1,00	26,05	1,93	1,00	28,37	1,86	1,00	28,57	1,81	1,00
TF18	NAC		27,43	1,78	1,00	27,84	1,79	1,00	27,38	1,81	1,00	26,34	1,86	1,00	25,43	1,81	1,00	25,02	1,85	1,00
TF19	NAC		26,85	1,80	1,00	30,43	1,46	1,00	27,55	1,75	1,00	25,91	1,81	1,00	25,51	1,88	1,00	25,16	1,88	1,00
TF20	CCAAT	CCAAT-HAP3	20,37	1,93	1,00	21,08	1,93	1,00	20,67	1,96	1,00	21,86	1,88	1,00	20,89	2,10	1,00	20,56	1,89	1,00
TF21	AP2/EREBP		29,77	1,79	1,00	27,93	1,75	1,00	21,31	1,82	1,00	25,14	1,88	1,00	23,62	1,87	1,00	25,52	1,90	1,00
TF22	bZIP		21,57	2,02	1,00	23,19	2,28	1,00	22,34	1,88	1,00	22,20	2,18	1,00	21,19	1,84	1,00	20,55	2,02	1,00
TF23	bZIP		22,22	1,90	1,00	22,13	1,90	1,00	23,17	2,13	1,00	21,49	1,93	1,00	21,36	2,07	1,00	20,76	1,85	1,00
TF24	MYB		32,07	1,70	1,00	29,41	1,79	1,00	23,80	2,25	1,00	27,88	1,91	1,00	25,73	1,82	1,00	27,65	1,87	1,00
TF25	MYB		22,21	1,86	1,00	22,53	1,81	1,00	20,06	2,13	1,00	21,69	1,79	1,00	20,60	1,79	1,00	20,42	2,04	1,00
TF26	ARID		34,78	1,55	1,00	29,44	1,67	1,00	23,84	1,86	1,00	28,04	1,94	1,00	27,48	1,97	1,00	29,72	1,75	1,00
TF27	ARID		25,83	1,86	1,00	27,28	1,88	1,00	21,16	2,04	1,00	21,50	1,91	1,00	24,25	1,82	1,00	23,46	1,84	1,00
TF28	C_2H_2 (Zn)		29,47	1,67	1,00	26,16	1,64	1,00	23,07	1,70	1,00	30,56	1,76	1,00	34,24	1,75	1,00	25,29	2,07	1,00
TF29	C_2H_2 (Zn)		29,60	1,74	1,00	23,38	1,91	1,00	19,35	1,90	1,00	22,12	1,88	1,00	21,40	2,01	1,00	21,75	2,00	1,00
TF30	WRKY family	WRKY	23,21	2,02	1,00	22,81	2,03	1,00	21,35	1,97	1,00	24,38	1,89	1,00	24,18	1,95	1,00	21,98	1,90	1,00
TF31	CCHC (Zn)		28,81	1,78	1,00	28,05	1,84	1,00	23,91	1,77	1,00	26,07	1,95	1,00	27,04	1,72	1,00	26,01	1,69	1,00
TF32	AP2/EREBP		24,18	1,78	1,00	24,30	1,83	1,00	24,71	2,02	1,00	22,81	1,91	1,00	22,82	1,96	1,00	22,28	1,89	1,00
TF33	HD family	HD-PHD finger	24,66	1,79	1,00	24,84	1,92	1,00	25,09	1,68	1,00	25,51	1,78	1,00	24,86	1,83	1,00	24,63	1,79	1,00
TF34	CCHC (Zn)		25,21	1,95	1,00	22,31	1,89	1,00	18,90	1,87	0,99	26,60	1,94	1,00	25,79	1,94	1,00	20,14	1,96	1,00
TF35	bHLH		26,00	1,74	1,00	25,77	1,75	1,00	25,94	1,82	1,00	26,33	1,93	1,00	26,04	1,83	1,00	25,52	1,96	1,00
TF36	HD family	HD-PHD finger	23,34	1,91	1,00	23,32	1,93	1,00	19,32	1,96	1,00	20,35	2,06	1,00	21,67	1,93	1,00	21,11	1,96	1,00
TF37	CCHC (Zn)		29,69	1,80	1,00	26,97	1,84	1,00	25,76	1,92	1,00	31,23	1,56	1,00	30,15	1,76	1,00	26,05	2,05	1,00
TF38	bZIP		27,73	1,75	1,00	27,59	1,72	1,00	22,94	1,75	1,00	24,30	1,50	1,00	26,07	1,72	1,00	24,84	1,75	1,00
TF39	bZIP		30,80	1,62	1,00	26,90	1,76	1,00	21,74	1,91	1,00	34,12	1,55	1,00	30,86	1,67	1,00	24,69	1,85	1,00
TF40	MYB/HD-like		25,65	1,93	1,00	25,14	1,97	1,00	24,46	1,83	1,00	25,22	1,93	1,00	24,93	1,90	1,00	23,88	1,91	1,00
TF41	ARF		29,94	1,25	1,00	27,95	3,33	1,00	25,51	1,70	1,00	28,76	1,94	1,00	29,46	1,72	1,00	27,89	1,76	1,00

Table S1, continued

TF42	JUMONJI		24,10	1,88	1,00	21,57	1,81	1,00	19,17	1,98	1,00	24,57	1,84	1,00	24,87	1,99	1,00	21,05	1,86	1,00
TF43	CCHC (Zn)		31,84	1,75	1,00	34,13	1,76	1,00	27,18	1,79	1,00	29,17	1,72	1,00	29,95	1,76	1,00	30,26	1,79	1,00
TF44	MADS		30,78	1,51	1,00	30,17	1,46	1,00	28,40	1,58	1,00	30,00	1,55	1,00	28,36	1,62	1,00	28,05	1,56	1,00
TF45	MADS		34,06	1,76	1,00	33,05	1,78	1,00	30,38	1,84	1,00	35,72	1,77	1,00	33,16	1,71	1,00	30,37	1,85	1,00
TF46	MYB/HD-like		29,11	1,91	1,00	29,57	1,89	1,00	24,34	1,83	1,00	26,35	1,87	1,00	27,70	1,90	1,00	27,41	1,99	1,00
TF47	LIM		30,84	1,61	1,00	33,41	1,71	1,00	28,34	1,96	1,00	29,22	1,65	1,00	28,70	1,72	1,00	28,44	1,65	1,00
TF48	bHLH		24,36	1,82	1,00	24,51	1,35	1,00	21,22	1,96	1,00	24,36	1,88	1,00	23,16	1,85	1,00	24,22	1,51	1,00
TF49	MYB/HD-like		25,58	1,85	1,00	25,65	1,86	1,00	21,05	1,95	1,00	22,68	1,89	1,00	23,85	1,86	1,00	23,38	1,85	1,00
TF50	HD family	HD	27,15	1,82	1,00	27,02	1,82	1,00	25,32	2,04	1,00	28,82	1,84	1,00	28,90	1,78	1,00	27,87	1,76	1,00
TF51	bHLH		28,70	2,05	1,00	28,40	1,98	1,00	23,97	1,98	1,00	26,13	1,95	1,00	26,43	1,87	1,00	27,13	1,92	1,00
TF52	bHLH		28,99	1,88	1,00	26,76	1,69	1,00	24,95	1,94	1,00	31,00	1,82	1,00	29,68	1,91	1,00	26,57	1,99	1,00
TF53	HTH	AraC	21,45	1,47	1,00	19,82	1,79	1,00	17,99	1,95	1,00	22,32	1,98	1,00	23,17	1,97	1,00	18,88	2,21	1,00
TF54	ZF DHHC		22,89	1,84	1,00	22,99	1,85	1,00	22,79	1,93	1,00	22,13	1,90	1,00	21,58	1,86	1,00	21,36	1,96	1,00
TF55	HTH	FIS	23,59	1,72	1,00	24,09	2,03	1,00	23,25	1,80	1,00	24,21	1,72	0,99	23,77	1,87	1,00	23,16	1,78	1,00
TF56	AS2		25,95	1,86	1,00	25,05	1,96	1,00	20,58	1,97	1,00	23,09	2,01	1,00	22,48	1,88	1,00	24,48	1,86	1,00
TF57	HMG		24,30	1,85	1,00	23,78	2,06	1,00	20,68	1,69	1,00	25,30	1,87	1,00	21,98	1,82	1,00	23,30	1,93	1,00
TF58	C_2H_2 (Zn)		32,62	1,82	1,00	29,89	1,86	1,00	25,01	1,87	1,00	27,93	1,82	1,00	27,17	1,77	1,00	29,66	1,74	1,00
TF59	C_2H_2 (Zn)		30,02	1,76	1,00	26,93	1,89	1,00	24,56	1,82	1,00	30,45	1,86	1,00	30,92	1,76	1,00	26,78	1,80	1,00
TF60	NGN		22,07	1,82	1,00	22,18	1,84	1,00	22,80	1,79	1,00	23,55	1,89	1,00	23,36	1,95	1,00	22,70	1,91	1,00
TF61	HD-like		28,49	1,79	1,00	26,61	2,00	1,00	24,50	1,70	1,00	29,05	1,67	1,00	29,24	1,90	1,00	27,14	1,86	1,00
TF62	KRAB box		29,65	1,61	1,00	30,82	1,61	1,00	28,14	1,56	1,00	30,34	1,34	1,00	32,94	1,46	1,00	29,86	1,58	1,00
TF63	MYB		32,03	1,91	1,00	32,19	1,89	1,00	28,71	1,97	1,00	29,25	1,89	1,00	27,42	2,01	1,00	27,08	1,93	1,00
TF64	MYB/HD-like		27,81	1,79	0,99	25,77	1,67	1,00	24,86	1,62	0,99	30,73	1,41	0,99	29,34	1,78	1,00	24,45	1,80	1,00
TF65	MYB/HD-like		28,34	2,03	1,00	27,44	1,90	1,00	23,35	1,93	1,00	24,43	2,06	1,00	25,45	2,08	1,00	25,15	1,94	1,00
TF66	S1Fa-like		21,01	1,97	1,00	21,73	1,95	1,00	21,50	1,82	1,00	22,52	2,01	1,00	21,56	1,87	1,00	21,43	2,06	1,00
TF67	S1Fa-like		20,29	1,98	1,00	20,62	1,92	1,00	18,86	1,90	1,00	21,37	1,95	1,00	19,70	1,91	1,00	20,33	2,00	1,00
TF68	CCHC (Zn)		38,28	1,65	1,00	n.d.	1,53	1,00	27,99	2,01	1,00	34,87	2,00	1,00	36,45	1,71	1,00	31,10	1,89	1,00
TF69	MYB		32,77	1,58	1,00	32,33	1,67	1,00	29,21	1,62	1,00	31,77	1,81	1,00	30,11	1,57	1,00	33,20	1,63	1,00
TF70	MYB		28,16	1,86	1,00	23,96	1,86	1,00	20,40	2,02	1,00	24,74	2,01	1,00	21,70	1,94	1,00	24,01	1,88	1,00
TF71	EIL		20,24	1,88	1,00	20,70	1,93	1,00	18,94	1,92	1,00	21,45	2,08	1,00	19,85	1,93	1,00	19,66	1,95	1,00
TF72	MYB/HD-like		32,02	1,78	1,00	31,89	1,71	1,00	29,49	1,74	1,00	31,65	2,08	1,00	30,65	1,90	1,00	29,63	1,85	1,00
TF73	MYB/HD-like		28,29	1,84	1,00	28,12	1,90	1,00	26,10	1,84	1,00	28,20	1,72	1,00	28,27	1,82	1,00	27,73	1,84	1,00
TF74	MYB/HD-like		31,53	1,65	1,00	30,86	1,47	0,99	27,58	1,77	1,00	35,69	1,53	1,00	34,59	1,66	1,00	29,24	1,82	1,00
TF75	MYB/HD-like		24,09	1,96	1,00	20,07	1,90	1,00	19,54	1,92	1,00	24,73	1,84	1,00	25,35	1,87	1,00	19,47	2,03	1,00
TF76	MYB		35,85	1,71	1,00	29,85	1,82	1,00	25,45	1,90	1,00	28,96	2,31	1,00	27,58	1,80	1,00	30,13	1,87	1,00
TF77	MYB		26,53	1,93	1,00	20,57	1,79	1,00	16,31	1,93	0,99	19,71	2,25	0,99	18,25	2,00	1,00	20,46	1,89	1,00
TF78	C_2H_2 (Zn)		33,23	1,66	1,00	29,10	1,82	1,00	23,95	1,83	1,00	28,01	1,82	1,00	26,44	1,77	1,00	27,33	1,79	1,00
TF79	C_2H_2 (Zn)		26,29	1,90	1,00	22,12	1,79	1,00	19,01	1,86	1,00	22,18	1,85	1,00	20,16	1,96	1,00	22,70	1,84	1,00
TF80	HTH	FIS	31,97	1,82	1,00	23,34	1,94	1,00	18,33	2,18	1,00	21,98	1,94	1,00	19,86	1,93	1,00	23,37	1,81	1,00
TF81	C_2H_2 (Zn)		26,06	1,73	1,00	23,38	1,82	1,00	22,12	1,77	1,00	25,92	1,69	1,00	26,74	1,81	1,00	25,56	1,86	1,00
TF82	EIL		38,67	1,29	1,00	33,46	1,48	1,00	27,18	1,72	1,00	30,53	1,67	1,00	29,66	1,57	1,00	30,42	1,64	1,00
TF83	EIL		27,35	1,87	1,00	27,44	1,87	1,00	22,80	1,86	1,00	23,97	1,88	1,00	25,79	1,89	1,00	25,23	1,90	1,00
TF84	bZIP		26,12	1,85	1,00	24,26	1,88	1,00	21,92	1,80	1,00	25,59	1,76	1,00	26,59	1,77	1,00	23,33	1,86	1,00

Table S1, continued

TF85	HD-like		32,16	1,75	1,00	24,28	1,88	1,00	21,47	1,85	1,00	33,08	1,84	1,00	30,00	1,77	1,00	23,65	1,92	1,00
TF86	HD-like		26,17	1,95	1,00	25,31	1,93	1,00	22,18	1,84	1,00	27,82	1,95	1,00	27,35	1,86	1,00	24,10	1,83	1,00
TF87	ZF DHHC		25,31	1,90	1,00	25,36	1,88	1,00	25,60	1,88	1,00	24,47	1,86	1,00	24,41	1,90	1,00	23,63	1,91	1,00
TF88	HD-like		24,65	1,92	1,00	22,47	1,91	1,00	19,49	1,98	1,00	25,86	1,92	1,00	25,31	1,94	1,00	20,67	1,98	1,00
TF89	TPR		24,04	1,90	1,00	23,97	1,87	1,00	23,80	1,89	1,00	23,78	1,87	1,00	24,05	1,92	1,00	23,46	1,97	1,00
TF90	bHLH		31,31	1,80	1,00	31,46	2,01	0,99	29,69	2,16	1,00	31,33	1,94	1,00	32,30	1,62	1,00	30,27	1,85	1,00
TF91	bHLH		30,70	1,77	1,00	32,89	1,67	1,00	28,61	1,66	1,00	32,17	1,60	1,00	29,68	1,73	1,00	30,30	1,64	1,00
TF92	CCHC (Zn)		23,70	1,91	1,00	23,68	1,94	1,00	23,92	1,77	1,00	23,97	1,90	1,00	23,47	1,92	1,00	22,67	2,01	1,00
TF93	bZIP		33,38	1,78	1,00	34,08	1,71	1,00	29,71	1,75	1,00	30,56	1,95	1,00	29,32	1,77	1,00	29,22	1,88	1,00
TF94	bZIP		32,58	1,70	1,00	37,29	1,44	1,00	26,47	1,78	1,00	28,36	1,76	1,00	29,57	1,76	1,00	28,54	1,75	1,00
TF95	HD-like		24,75	1,89	1,00	24,62	1,87	1,00	23,05	1,90	1,00	24,45	1,87	1,00	23,42	1,92	1,00	23,62	1,91	1,00
TF96	LIM		19,22	1,96	1,00	19,79	1,90	1,00	19,62	1,95	1,00	21,05	2,54	1,00	20,01	2,11	1,00	19,67	1,94	1,00
TF97	HD-like		24,59	1,89	1,00	24,61	1,92	1,00	23,39	1,94	1,00	23,60	1,85	1,00	23,85	1,89	1,00	23,46	1,93	1,00
TF98	LIM		19,55	1,92	1,00	19,82	2,12	1,00	20,21	2,03	1,00	20,53	2,86	1,00	20,23	2,29	1,00	19,68	1,97	1,00
TF99	C_2H_2 (Zn)		23,01	1,90	1,00	21,82	2,04	1,00	19,86	1,89	1,00	23,17	1,76	1,00	22,61	1,86	1,00	20,93	1,92	1,00
TF100	MYB/HD-like		25,23	1,93	1,00	25,50	1,86	1,00	25,98	1,83	1,00	25,05	1,96	1,00	24,72	2,00	1,00	24,15	2,03	1,00
TF101	C_2H_2 (Zn)		24,80	1,85	1,00	24,48	1,86	1,00	24,72	1,87	1,00	25,05	1,90	1,00	24,86	1,96	1,00	24,11	2,04	1,00
TF102	MYB		24,93	2,11	1,00	21,53	1,92	1,00	18,47	1,86	1,00	22,11	2,17	1,00	19,98	1,85	1,00	21,91	1,93	1,00
TF103	C_2H_2 (Zn)		n.d.	2,17	0,96	33,21	1,33	1,00	28,85	1,66	1,00	32,41	1,61	1,00	29,74	1,65	1,00	31,60	1,58	1,00
TF104	bHLH		32,85	1,79	1,00	29,54	1,74	1,00	29,05	2,02	1,00	32,04	1,75	1,00	31,42	1,83	1,00	29,44	1,89	1,00
TF105	PHD		28,74	1,86	1,00	29,22	1,89	1,00	22,65	1,97	1,00	24,27	1,54	1,00	26,00	1,98	1,00	25,51	1,95	1,00
TF106	RR		28,54	1,60	1,00	26,82	1,78	1,00	24,13	1,71	1,00	28,64	1,45	1,00	29,04	1,32	1,00	26,09	1,83	1,00
TF107	MADS		31,51	1,67	1,00	29,71	1,74	1,00	27,87	1,81	1,00	31,53	1,78	1,00	33,24	1,81	1,00	29,18	1,86	1,00
TF108	MADS		30,65	1,98	1,00	27,86	2,13	1,00	25,29	1,86	1,00	30,57	1,94	1,00	30,92	1,94	1,00	27,01	1,98	1,00
TF109	CCHC (Zn)		21,49	1,89	1,00	20,81	2,15	1,00	16,40	2,10	0,99	18,44	1,89	1,00	19,92	2,01	1,00	18,96	2,15	1,00
TF110	PHD		24,54	1,85	1,00	24,63	1,84	1,00	24,77	1,44	1,00	25,76	1,64	1,00	25,44	1,23	1,00	24,93	1,22	1,00
TF111	bZIP		25,45	1,88	1,00	23,68	2,04	1,00	21,15	1,91	1,00	25,34	1,83	1,00	26,04	1,72	1,00	22,68	1,96	1,00
TF112	C_2C_2 (Zn)	DOF	25,40	1,71	1,00	25,49	1,70	1,00	21,32	1,81	1,00	23,21	1,73	1,00	23,63	1,68	1,00	23,64	1,73	1,00
TF113	C_2C_2 (Zn)	DOF	26,78	1,88	1,00	25,26	1,88	1,00	21,17	1,86	1,00	24,75	1,86	1,00	22,87	1,85	1,00	25,10	1,88	1,00
TF114	CCHC (Zn)		29,17	1,88	1,00	28,48	1,84	1,00	27,96	1,84	1,00	30,43	1,94	1,00	30,07	1,81	1,00	27,87	1,88	1,00
TF115	CAMTA		21,72	1,99	1,00	21,78	1,95	1,00	18,44	1,97	1,00	20,38	1,94	1,00	20,84	1,92	1,00	20,53	1,82	1,00
TF116	LIM		28,64	1,84	1,00	28,49	1,84	1,00	25,72	1,80	1,00	27,97	1,84	1,00	26,44	1,82	1,00	27,14	1,90	1,00
TF117	LIM		23,36	1,87	1,00	23,46	1,92	1,00	20,47	1,74	1,00	26,23	1,84	1,00	21,42	1,92	1,00	22,88	1,85	1,00
TF118	CCHC (Zn)		22,72	1,93	1,00	22,85	1,93	1,00	22,99	1,91	1,00	23,32	1,83	1,00	22,93	1,91	1,00	22,52	2,00	1,00
TF119	CAMTA		26,64	2,05	1,00	26,40	1,79	1,00	23,62	1,77	1,00	24,89	1,91	1,00	25,33	1,87	1,00	24,84	2,10	1,00
TF120	MYB		20,94	1,88	1,00	21,37	1,99	1,00	19,93	1,96	1,00	22,38	1,95	1,00	21,45	1,86	1,00	21,40	1,92	1,00
TF121	FHA		23,60	2,02	1,00	23,63	1,93	1,00	23,50	1,86	1,00	23,52	1,99	1,00	23,07	1,87	1,00	22,82	1,97	1,00
TF122	MYB/HD-like		24,44	1,20	1,00	25,13	2,04	0,97	32,00	1,82	0,86	28,64	2,54	0,99	25,28	1,27	1,00	25,32	4,38	0,99
TF123	FHA		23,13	1,89	1,00	23,93	1,95	1,00	23,02	1,81	1,00	23,82	1,91	1,00	23,20	1,81	1,00	22,73	2,00	1,00
TF124	AP2/EREBP		25,19	1,90	1,00	24,97	1,94	1,00	20,23	2,03	1,00	23,07	1,87	1,00	24,65	1,87	1,00	23,77	1,89	1,00
TF125	AP2/EREBP		23,45	1,68	1,00	23,69	1,72	1,00	21,28	1,64	0,99	22,30	2,10	1,00	20,96	1,69	1,00	20,18	1,84	1,00
TF126	AP2/EREBP		25,55	1,81	1,00	24,51	1,87	1,00	21,42	1,94	1,00	24,62	1,93	1,00	22,77	1,84	1,00	25,21	1,88	1,00
TF127	CCHC (Zn)		31,97	1,70	1,00	30,86	1,74	1,00	28,27	1,38	1,00	33,48	1,93	1,00	32,23	1,70	1,00	29,54	1,74	1,00

Table S1, continued

TF128	ZF DHHC		24,01	1,89	1,00	23,94	1,96	1,00	24,72	1,76	1,00	25,20	1,82	1,00	24,54	1,98	1,00	23,95	1,82	1,00
TF129	MYB/HD-like		25,02	1,90	1,00	25,19	1,94	1,00	21,58	1,82	1,00	21,47	1,89	1,00	21,29	1,87	1,00	21,24	1,97	1,00
TF130	CCHC (Zn)		27,71	1,90	1,00	24,86	1,84	1,00	21,66	1,89	1,00	30,29	1,72	1,00	28,54	1,83	1,00	24,45	1,98	1,00
TF131	HD-like		26,46	1,87	1,00	25,78	1,89	1,00	21,46	1,99	1,00	25,17	1,85	1,00	23,75	1,91	1,00	25,17	1,88	1,00
TF132	HD-like		27,67	1,84	1,00	27,47	1,96	0,99	25,49	1,85	1,00	28,36	2,00	1,00	28,92	1,75	1,00	26,94	1,88	1,00
TF133	NAC		26,80	1,92	1,00	26,78	1,88	1,00	27,27	2,02	1,00	27,31	1,82	1,00	27,19	1,92	1,00	26,69	1,87	1,00
TF134	HD-like		28,26	1,77	1,00	28,11	2,01	0,99	26,05	1,89	1,00	28,98	1,71	1,00	27,74	1,76	1,00	27,12	1,79	1,00
TF135	NAC		26,25	1,94	1,00	26,21	1,99	1,00	26,76	1,90	1,00	27,00	1,85	1,00	26,93	1,84	1,00	26,17	1,84	1,00
TF136	NAC		23,08	1,87	1,00	23,15	1,92	1,00	23,59	1,91	1,00	22,74	1,89	1,00	22,75	1,89	1,00	21,92	1,89	1,00
TF137	NAC		25,09	1,92	1,00	24,44	1,91	1,00	21,35	1,92	1,00	24,25	1,83	1,00	22,98	1,94	1,00	24,27	1,93	1,00
TF138	HD-like		29,25	1,88	1,00	30,26	1,91	1,00	23,97	2,12	1,00	28,30	1,96	1,00	26,56	1,83	1,00	28,78	1,82	1,00
TF139	NAC		23,15	1,96	1,00	23,81	1,85	1,00	23,28	1,89	1,00	23,52	1,84	1,00	22,84	1,87	1,00	22,48	1,99	1,00
TF140	PHD		23,12	1,89	1,00	23,17	1,89	1,00	23,64	1,84	1,00	23,46	1,83	1,00	22,92	1,84	1,00	22,62	1,84	1,00
TF141	MYB/HD-like		26,48	1,98	1,00	25,94	2,00	1,00	22,28	1,80	1,00	24,75	1,83	1,00	26,30	1,89	1,00	25,42	1,88	1,00
TF142	C_2C_2 (Zn)	CO-like	27,56	1,78	1,00	27,62	1,78	1,00	27,64	1,84	1,00	27,20	1,87	1,00	26,96	1,84	1,00	26,50	1,84	1,00
TF143	MYB/HD-like		29,79	1,76	1,00	26,72	1,83	1,00	24,11	1,85	1,00	26,95	1,80	1,00	25,07	1,82	1,00	27,18	1,81	1,00
TF144	C_2C_2 (Zn)	CO-like	26,86	1,91	1,00	23,73	1,92	1,00	19,97	1,87	1,00	23,19	1,90	1,00	22,01	1,86	1,00	24,38	1,96	1,00
TF145	MYB		24,95	1,90	1,00	20,13	1,85	1,00	16,82	2,23	0,99	18,88	2,40	1,00	18,37	2,05	1,00	19,44	2,07	1,00
TF146	MYB		28,33	1,81	1,00	25,54	1,83	1,00	23,11	1,78	1,00	27,89	1,73	1,00	29,21	1,73	1,00	24,47	1,88	1,00
TF147	ARF		20,00	1,88	1,00	20,88	1,95	1,00	20,38	1,87	1,00	21,07	1,89	1,00	20,15	1,94	1,00	19,87	1,96	1,00
TF148	ARF		20,57	2,06	1,00	20,39	1,86	1,00	20,55	1,87	1,00	20,58	1,91	1,00	20,56	1,99	1,00	19,81	1,85	1,00
TF149	MYB/HD-like		25,58	1,87	1,00	23,37	1,90	1,00	20,80	1,88	1,00	23,89	1,94	1,00	21,99	1,82	1,00	22,37	1,94	1,00
TF150	MYB		23,81	1,99	1,00	23,33	1,97	1,00	20,90	1,90	1,00	21,74	1,93	1,00	22,49	1,87	1,00	22,01	1,94	1,00
TF151	PHD		29,79	1,75	1,00	29,67	1,76	1,00	27,19	1,86	1,00	31,81	1,79	1,00	30,30	1,77	1,00	28,47	1,80	1,00
TF152	CCHC (Zn)		31,93	1,74	1,00	27,77	1,72	1,00	22,83	1,91	1,00	25,86	1,94	1,00	25,53	1,76	1,00	24,50	2,07	1,00
TF153	CCHC (Zn)		26,86	1,90	1,00	27,19	1,76	1,00	26,83	1,89	1,00	28,05	1,81	1,00	27,56	1,81	1,00	27,34	1,88	1,00
TF154	AP2/EREBP		31,42	1,65	1,00	27,86	1,71	1,00	25,64	1,60	1,00	30,08	1,61	1,00	30,08	2,67	0,99	27,10	1,34	1,00
TF155	AP2/EREBP		30,74	1,88	1,00	27,08	1,80	1,00	25,06	1,76	1,00	31,64	1,78	1,00	31,27	1,78	1,00	26,32	1,85	1,00
TF156	HMG		24,14	1,90	1,00	21,73	1,95	1,00	19,10	1,98	1,00	21,98	1,88	1,00	20,61	1,90	1,00	21,44	1,88	1,00
TF157	C_2C_2 (Zn)	CO-like	20,30	1,96	1,00	20,52	1,98	1,00	20,95	2,05	1,00	22,73	1,80	1,00	22,71	2,18	1,00	22,01	1,91	1,00
TF158	HD-like		31,42	1,83	1,00	31,10	1,87	1,00	28,07	1,88	1,00	30,45	1,83	1,00	30,99	1,82	1,00	30,72	1,80	1,00
TF159	CCHC (Zn)		26,97	2,03	1,00	26,69	1,92	1,00	21,45	1,99	1,00	23,37	1,84	1,00	24,38	1,80	1,00	23,75	1,85	1,00
TF160	HD-like		29,81	1,72	1,00	27,74	1,83	1,00	24,15	1,84	1,00	27,50	1,96	1,00	26,12	1,78	1,00	28,39	1,87	1,00
TF161	C_2H_2 (Zn)		23,31	1,99	1,00	23,34	1,86	1,00	23,67	1,84	1,00	24,08	2,07	1,00	23,46	1,85	1,00	23,25	1,91	1,00
TF162	NAC		28,94	1,76	1,00	28,54	1,87	1,00	24,32	1,78	1,00	26,36	1,86	1,00	27,55	1,95	1,00	26,99	1,87	1,00
TF163	WRKY family	WRKY	28,99	1,78	1,00	28,96	1,79	1,00	29,79	1,79	1,00	29,66	1,76	1,00	28,48	1,80	1,00	27,82	1,83	1,00
TF164	AS2		27,88	1,20	1,00	25,17	1,78	1,00	19,94	1,25	1,00	24,08	1,93	1,00	21,20	1,79	1,00	22,17	1,78	1,00
TF165	HD-like		18,97	1,97	1,00	19,17	2,08	1,00	19,26	2,02	1,00	20,08	1,92	1,00	19,55	2,16	1,00	19,27	1,87	1,00
TF166	Lambda-DB		28,58	1,89	1,00	25,64	1,89	1,00	23,81	1,82	1,00	29,18	1,90	1,00	29,37	1,88	1,00	25,18	1,93	1,00
TF167	Lambda-DB		29,20	1,81	1,00	24,70	1,96	1,00	20,97	1,92	1,00	23,67	2,04	1,00	22,26	2,01	1,00	24,68	1,90	1,00
TF168	HMG		24,61	1,96	1,00	25,08	1,93	1,00	24,83	1,86	1,00	26,03	2,05	1,00	24,96	1,99	1,00	24,17	1,82	1,00
TF169	MYB/HD-like		31,39	1,71	1,00	29,92	1,71	1,00	27,27	1,80	1,00	32,31	1,69	1,00	34,19	1,72	1,00	30,15	1,93	1,00
TF170	MYB/HD-like		21,99	1,96	1,00	21,60	2,00	1,00	19,83	1,88	1,00	21,37	2,03	1,00	23,29	2,06	1,00	20,25	1,89	1,00

Table S1, continued

TF171	MYB		24,79	2,02	1,00	24,47	2,00	1,00	22,87	2,03	1,00	24,79	1,84	1,00	24,72	1,90	1,00	23,35	1,92	1,00
TF172	MYB		28,61	1,88	1,00	29,14	1,85	1,00	23,03	1,87	1,00	24,93	1,87	1,00	25,56	1,91	1,00	24,54	1,91	1,00
TF173	C_2H_2 (Zn)		21,13	1,82	1,00	20,05	2,11	1,00	18,73	2,31	1,00	20,14	2,35	1,00	18,90	1,90	1,00	20,29	1,85	1,00
TF174	C_2H_2 (Zn)		n.d.	1,37	0,94	34,13	1,71	1,00	29,93	1,76	1,00	n.d.	1,26	0,81	n.d.	1,84	1,00	32,35	1,81	1,00
TF175	HMG		32,40	1,64	1,00	30,55	1,81	1,00	26,59	1,68	1,00	32,40	1,58	1,00	27,71	1,76	1,00	29,14	1,75	1,00
TF176	bHLH		30,37	1,67	1,00	26,96	1,93	0,99	27,79	1,60	1,00	30,46	1,59	1,00	28,86	1,44	1,00	26,06	1,77	1,00
TF177	HD-like		25,54	1,88	1,00	25,29	1,89	1,00	24,32	1,92	1,00	27,00	1,79	1,00	26,08	1,90	1,00	24,90	1,97	1,00
TF178	bHLH		31,02	1,84	1,00	26,52	1,88	1,00	22,42	1,85	1,00	24,91	1,87	1,00	23,95	1,85	1,00	25,65	1,93	1,00
TF179	U1-type (Zn)		24,35	1,93	1,00	24,52	1,94	1,00	24,64	1,92	1,00	24,95	1,90	1,00	24,62	1,93	1,00	24,47	1,93	1,00
TF180	CCHC (Zn)		26,91	1,86	1,00	22,68	1,91	1,00	20,68	1,90	1,00	26,16	1,76	1,00	27,07	1,76	1,00	21,98	1,92	1,00
TF181	CCHC (Zn)		28,38	1,73	1,00	27,75	1,73	1,00	29,00	1,68	1,00	29,37	1,79	1,00	28,56	1,77	1,00	27,60	1,89	1,00
TF182	CCHC (Zn)		29,73	1,86	1,00	27,73	1,70	1,00	27,60	1,82	1,00	30,80	1,72	1,00	29,83	1,89	1,00	28,92	1,76	1,00
TF183	CCHC (Zn)		27,00	1,90	1,00	25,28	2,09	1,00	23,32	1,88	1,00	27,41	1,93	1,00	27,34	1,89	1,00	24,34	2,13	0,91
TF184	JUMONJI		23,06	1,93	1,00	19,00	2,04	1,00	15,95	1,71	0,99	18,08	2,31	1,00	17,17	2,29	1,00	19,15	1,95	1,00
TF185	JUMONJI		28,95	1,84	1,00	28,92	1,74	1,00	23,92	1,91	1,00	26,27	1,82	1,00	26,97	2,05	1,00	25,43	1,98	1,00
TF186	JUMONJI		26,74	1,91	1,00	26,77	1,94	1,00	22,64	1,93	1,00	23,71	1,85	1,00	23,96	1,92	1,00	24,28	1,95	1,00
TF187	JUMONJI		30,60	1,86	1,00	30,67	1,91	1,00	27,92	1,85	1,00	29,17	1,77	1,00	29,77	1,90	1,00	28,94	1,86	1,00
TF188	JUMONJI		25,70	1,89	1,00	26,66	1,85	1,00	27,27	1,88	1,00	27,98	1,83	1,00	26,24	1,88	1,00	25,81	1,91	1,00
TF189	JUMONJI		32,01	1,70	1,00	32,85	1,68	1,00	28,85	1,77	1,00	33,86	1,65	1,00	31,96	1,66	1,00	31,06	1,58	1,00
TF190	bHLH		27,00	1,86	1,00	22,57	1,97	1,00	19,98	2,08	1,00	26,85	1,75	1,00	27,93	1,83	1,00	21,52	1,89	1,00
TF191	bHLH		35,69	1,67	1,00	30,52	1,81	1,00	26,35	1,86	1,00	29,97	1,80	1,00	27,96	1,80	1,00	30,62	1,81	1,00
TF192	NAC		27,23	1,87	1,00	26,89	1,86	1,00	25,82	1,91	1,00	28,86	1,84	1,00	29,02	1,82	1,00	27,05	1,90	1,00
TF193	ARID		23,87	1,93	1,00	23,88	1,88	1,00	24,01	1,81	1,00	24,88	2,03	1,00	24,60	1,86	1,00	24,40	1,86	1,00
TF194	MYB/HD-like		25,28	1,32	1,00	21,93	1,94	1,00	18,37	2,36	1,00	24,07	1,79	1,00	24,18	1,98	1,00	19,98	2,09	1,00
TF195	MYB/HD-like		25,46	1,79	1,00	26,10	1,96	1,00	23,48	1,88	1,00	23,00	2,00	1,00	23,81	1,93	1,00	24,47	1,97	1,00
TF196	EIL		20,57	1,88	1,00	20,44	1,98	1,00	21,24	2,04	1,00	20,83	2,16	1,00	20,30	1,99	1,00	19,58	1,95	1,00
TF197	EIL		20,28	1,87	1,00	20,90	1,90	1,00	18,98	1,59	1,00	20,89	1,83	1,00	19,55	2,83	1,00	19,94	1,88	1,00
TF198	MYB		24,60	1,96	1,00	23,58	1,91	1,00	22,18	1,93	1,00	23,26	1,95	1,00	21,98	1,97	1,00	23,39	1,99	1,00
TF199	NAC		23,71	1,92	1,00	23,95	1,98	1,00	22,94	1,75	1,00	24,29	1,92	1,00	23,11	1,97	1,00	23,09	1,86	1,00
TF200	NAC		21,43	1,88	1,00	21,44	1,87	1,00	17,34	2,30	0,99	19,00	1,99	1,00	20,20	1,80	1,00	19,11	1,92	1,00
TF201	WRKY family	WRKY	31,16	1,88	1,00	30,84	1,91	1,00	27,15	1,82	1,00	28,99	1,80	1,00	27,70	1,89	1,00	27,83	1,93	1,00
TF202	MYB		35,01	1,78	1,00	29,67	1,92	1,00	25,56	1,89	1,00	29,63	1,84	1,00	27,76	1,88	1,00	31,67	1,85	1,00
TF203	ZF DHHC		24,26	1,89	1,00	23,97	2,02	1,00	22,55	1,88	1,00	24,88	1,87	1,00	24,85	1,88	1,00	23,92	1,95	1,00
TF204	JUMONJI		24,49	1,90	1,00	24,58	1,95	1,00	23,27	1,83	1,00	24,75	1,95	1,00	24,61	2,06	1,00	24,17	1,92	1,00
TF205	JUMONJI		36,83	1,53	1,00	30,78	1,74	1,00	26,25	1,88	1,00	30,60	1,81	1,00	28,47	1,83	1,00	31,16	1,78	1,00
TF206	C_2C_2 (Zn)	YABBY	21,17	1,95	1,00	21,73	1,97	1,00	21,66	2,03	1,00	23,55	1,91	1,00	22,07	1,95	1,00	22,06	2,06	1,00
TF207	C_2C_2 (Zn)	YABBY	21,80	1,95	1,00	21,77	1,90	1,00	22,30	1,80	1,00	23,36	1,26	1,00	22,92	1,88	1,00	22,27	1,84	1,00
TF208	CCHC (Zn)		31,68	1,90	1,00	30,94	1,75	1,00	26,82	2,10	1,00	28,17	1,88	1,00	28,42	1,85	1,00	27,91	1,81	1,00
TF209	CCHC (Zn)		26,61	1,91	1,00	24,38	1,87	1,00	21,37	1,92	1,00	27,10	1,89	1,00	27,02	1,87	1,00	n.d.	2,51	0,92
TF210	p53-like		27,79	2,02	1,00	24,37	1,92	1,00	21,95	2,03	1,00	28,00	1,87	1,00	27,60	1,93	1,00	23,40	1,93	1,00
TF211	CCHC (Zn)		36,67	1,67	1,00	32,26	1,81	1,00	31,00	1,74	1,00	32,76	1,80	1,00	23,06	1,88	1,00	n.d.	1,24	0,95
TF212	HTH	FIS	30,46	1,72	1,00	29,44	1,68	0,99	23,25	1,45	1,00	26,90	1,74	1,00	24,48	1,65	1,00	26,85	1,82	1,00
TF213	ARF		30,99	1,74	1,00	29,64	1,80	1,00	24,92	1,51	1,00	30,34	1,33	1,00	31,79	1,77	1,00	26,86	1,89	1,00

Table S1, continued

TF214	bZIP		23,99	1,89	1,00	23,87	2,23	1,00	23,34	1,95	1,00	23,85	1,86	1,00	24,02	1,94	1,00	23,33	1,90	1,00
TF215	TCP		22,45	1,93	1,00	22,35	1,99	1,00	21,68	1,91	1,00	22,16	2,02	1,00	22,26	2,07	1,00	21,29	1,99	1,00
TF216	ARF		27,86	1,83	1,00	24,94	1,95	1,00	22,48	1,98	1,00	28,43	1,80	1,00	29,96	1,79	1,00	25,43	1,92	1,00
TF217	PHD		23,52	1,90	1,00	23,73	1,90	1,00	23,95	1,93	1,00	24,35	1,94	1,00	23,85	1,24	1,00	23,47	1,92	1,00
TF218	ABI3-VP1		29,81	1,82	1,00	28,68	1,91	1,00	22,40	2,17	1,00	24,77	1,83	1,00	26,30	1,82	1,00	24,80	1,83	1,00
TF219	WRKY family	WRKY	27,63	1,90	1,00	27,92	1,92	1,00	21,65	1,91	1,00	23,39	1,93	1,00	25,03	1,90	1,00	24,65	1,90	1,00
TF220	MADS		33,75	1,64	1,00	32,73	1,50	1,00	27,75	1,67	1,00	30,73	1,76	1,00	29,86	1,80	1,00	30,34	1,77	1,00
TF221	MADS		28,46	1,84	1,00	26,38	1,88	1,00	20,79	1,91	1,00	28,91	1,85	1,00	22,79	1,96	1,00	24,62	2,07	1,00
TF222	C_2C_2 (Zn)	YABBY	29,38	1,87	1,00	27,01	1,88	1,00	22,00	1,99	1,00	24,96	1,92	1,00	23,58	1,84	1,00	25,68	1,93	1,00
TF223	TTF-type (Zn)		27,18	1,78	1,00	25,19	1,83	1,00	24,01	1,93	1,00	27,43	2,01	1,00	27,12	2,02	1,00	25,06	2,14	1,00
TF224	CCHC (Zn)		31,33	1,77	1,00	30,98	1,79	1,00	29,56	1,79	1,00	32,30	1,67	1,00	n.d.	1,75	0,99	30,07	1,96	1,00
TF225	CCHC (Zn)		29,45	1,74	1,00	26,15	1,77	1,00	23,99	1,82	1,00	30,96	1,77	1,00	30,79	1,73	1,00	25,60	1,88	1,00
TF226	WRKY family	WRKY	30,68	1,85	1,00	28,01	1,87	1,00	25,02	1,92	1,00	30,57	1,89	1,00	29,83	1,85	1,00	26,40	2,08	1,00
TF227	BD		24,62	1,77	1,00	24,82	1,90	1,00	25,08	1,86	1,00	23,84	1,87	1,00	23,71	1,90	1,00	23,21	1,86	1,00
TF228	bHLH		29,87	1,72	1,00	29,39	1,96	1,00	27,60	1,75	1,00	30,32	1,84	1,00	29,98	1,80	1,00	28,94	1,82	1,00
TF229	PHD		19,90	2,07	1,00	19,99	1,98	1,00	19,92	1,87	1,00	20,97	1,95	1,00	20,93	1,94	1,00	20,40	1,94	1,00
TF230	HD-like		20,25	2,09	1,00	20,27	1,87	1,00	20,87	3,69	1,00	21,70	2,08	1,00	21,37	1,88	1,00	21,24	1,97	1,00
TF231	C_2H_2 (Zn)		31,47	1,88	1,00	31,13	1,87	1,00	24,08	1,87	1,00	26,40	1,78	1,00	28,19	1,86	1,00	27,02	2,13	1,00
TF232	ABI3-VP1		29,85	1,87	1,00	32,81	1,78	1,00	27,22	1,95	1,00	29,96	1,93	1,00	30,10	1,86	1,00	29,45	1,94	1,00
TF233	HMG		21,34	1,95	1,00	21,79	1,92	1,00	21,13	1,91	1,00	22,66	1,89	1,00	21,95	2,01	1,00	21,58	2,09	1,00
TF234	MADS		31,43	1,72	1,00	32,10	1,72	1,00	32,16	1,55	1,00	34,57	1,82	0,99	32,32	1,76	1,00	29,95	1,87	1,00
TF235	NAC		31,57	1,81	1,00	27,77	1,95	1,00	21,68	1,86	1,00	25,23	1,89	1,00	24,19	1,93	1,00	26,20	1,88	1,00
TF236	bZIP		23,98	1,92	1,00	23,10	1,94	1,00	20,15	2,00	1,00	23,78	1,86	1,00	21,46	1,88	1,00	21,41	1,91	1,00
TF237	CCHC (Zn)		27,45	1,81	1,00	23,02	1,76	1,00	20,48	1,92	1,00	29,23	1,87	1,00	29,85	1,83	1,00	21,96	1,84	1,00
TF238	CCHC (Zn)		26,33	1,94	1,00	25,74	1,78	1,00	22,72	2,01	1,00	26,70	1,92	1,00	26,42	1,91	1,00	24,18	1,89	1,00
TF239	CCHC (Zn)		30,23	1,93	1,00	31,50	1,92	1,00	26,45	1,98	1,00	32,02	1,85	1,00	31,16	1,93	1,00	28,35	1,97	1,00
TF240	CCHC (Zn)		27,90	1,86	1,00	27,08	1,81	1,00	22,91	1,85	1,00	28,38	1,97	1,00	28,70	1,86	1,00	25,35	1,98	1,00
TF241	CCHC (Zn)		24,46	1,92	1,00	23,39	1,92	1,00	21,96	2,03	1,00	25,17	1,90	1,00	25,76	1,93	1,00	22,81	1,89	1,00
TF242	SNF2		22,85	1,99	1,00	23,17	1,93	1,00	23,04	1,95	1,00	23,89	1,99	1,00	22,99	1,89	1,00	22,86	1,92	1,00
TF243	CCHC (Zn)		30,50	1,97	1,00	29,91	1,87	1,00	25,57	1,94	1,00	26,27	1,91	1,00	25,95	1,94	1,00	25,01	1,84	1,00
TF244	MYB/HD-like		23,03	1,87	1,00	23,11	1,90	1,00	23,63	1,90	1,00	24,07	1,88	1,00	23,57	1,92	1,00	23,25	2,05	1,00
TF245	WRKY family	WRKY	25,99	1,61	1,00	26,01	1,60	1,00	26,17	1,63	1,00	25,44	1,66	1,00	25,59	1,58	1,00	24,79	1,57	1,00
TF246	WRKY family	WRKY	24,22	1,85	1,00	24,74	1,77	1,00	23,94	1,64	1,00	24,99	1,72	1,00	24,55	1,76	1,00	23,65	1,87	1,00
TF247	C_2H_2 (Zn)		29,70	1,81	1,00	29,79	1,82	1,00	25,02	1,84	1,00	30,99	1,68	1,00	27,36	1,89	1,00	27,79	1,85	1,00
TF248	MYB/HD-like		22,49	2,00	1,00	22,64	2,14	1,00	21,64	1,91	1,00	23,54	1,94	1,00	23,09	1,96	1,00	22,41	1,89	1,00
TF249	C_2H_2 (Zn)		30,41	1,77	1,00	30,39	1,81	1,00	30,17	1,72	1,00	32,35	1,71	1,00	23,00	1,98	1,00	31,51	1,81	1,00
TF250	CCHC (Zn)		28,95	1,99	1,00	29,54	1,87	1,00	27,96	1,85	1,00	29,99	1,84	1,00	29,97	1,87	1,00	28,89	2,02	1,00
TF251	C_2H_2 (Zn)		27,72	1,85	1,00	25,72	1,89	1,00	23,51	1,35	0,99	27,53	1,79	1,00	28,00	1,89	1,00	24,56	2,07	1,00
TF252	C_2H_2 (Zn)		25,84	1,78	1,00	25,86	1,76	1,00	21,79	1,92	1,00	26,02	1,44	1,00	26,17	1,78	1,00	22,89	1,86	1,00
TF253	HTH	FIS	29,40	1,85	1,00	29,31	1,88	1,00	23,38	1,86	1,00	25,40	1,86	1,00	27,30	1,85	1,00	26,35	1,84	1,00
TF254	C_2H_2 (Zn)		27,62	1,86	1,00	27,50	1,97	1,00	21,43	1,87	1,00	26,12	1,77	1,00	24,49	2,06	1,00	26,01	1,95	1,00
TF255	HTH	FIS	29,51	1,80	1,00	24,17	1,90	1,00	19,98	1,73	1,00	22,61	1,95	1,00	21,51	1,90	1,00	23,30	1,78	1,00
TF256	CCHC (Zn)		30,44	1,88	1,00	28,95	1,89	1,00	24,23	1,87	1,00	29,86	1,81	1,00	30,92	1,94	1,00	27,00	1,94	1,00

Table S1, continued

TF257	AP2/EREBP		26,69	1,87	1,00	26,84	1,89	1,00	25,97	1,87	1,00	26,89	1,84	1,00	27,20	1,86	1,00	26,51	1,97	1,00
TF258	HD family	HD	24,20	2,04	1,00	17,29	2,09	1,00	14,79	1,33	0,97	16,55	1,88	0,99	15,85	2,23	0,99	16,46	2,03	1,00
TF259	CCAAT	CCAAT-HAP3	29,76	1,80	1,00	27,29	1,84	1,00	23,93	1,82	1,00	28,80	1,78	1,00	29,96	1,82	1,00	25,77	1,98	1,00
TF260	CCAAT	CCAAT-HAP3	28,32	1,77	1,00	24,58	1,92	1,00	22,31	1,91	1,00	28,43	1,73	1,00	28,84	1,75	1,00	23,67	1,86	1,00
TF261	MYB		30,07	1,85	1,00	29,26	1,80	1,00	23,05	1,81	1,00	25,69	1,80	1,00	26,52	1,84	1,00	25,89	1,88	1,00
TF262	CCHC (Zn)		22,92	2,00	1,00	23,02	2,00	1,00	23,63	1,87	1,00	25,57	1,89	1,00	24,87	1,88	1,00	24,83	1,99	1,00
TF263	CCHC (Zn)		31,43	1,72	1,00	30,62	1,77	1,00	25,60	1,77	1,00	27,69	1,80	1,00	27,23	1,98	1,00	26,76	1,90	1,00
TF264	PHD		22,07	1,89	1,00	22,43	1,80	1,00	22,62	2,07	1,00	22,96	1,85	1,00	21,96	1,86	1,00	21,66	1,99	1,00
TF265	C_2C_2 (Zn)	DOF	23,34	1,81	1,00	23,22	1,92	1,00	21,43	2,06	1,00	24,37	1,89	1,00	26,39	1,88	1,00	25,97	1,85	1,00
TF266	CCAAT	CCAAT-HAP3	21,99	2,01	1,00	22,02	1,97	1,00	22,24	1,99	1,00	26,37	2,02	1,00	22,00	2,06	1,00	21,35	1,87	1,00
TF267	BTB/POZ		28,88	1,88	1,00	30,28	1,88	1,00	26,18	1,86	1,00	28,55	1,83	1,00	32,31	1,71	1,00	30,50	1,82	1,00
TF268	bZIP		24,45	1,90	1,00	24,85	1,89	1,00	19,73	1,89	1,00	22,17	1,91	1,00	23,07	1,89	1,00	22,33	1,94	1,00
TF269	BD		31,82	1,86	1,00	32,59	1,72	1,00	30,67	1,74	1,00	31,24	1,88	1,00	30,50	1,90	1,00	30,39	2,06	1,00
TF270	C_2H_2 (Zn)		27,53	2,25	1,00	26,61	1,95	1,00	23,43	1,99	1,00	27,33	1,82	1,00	24,24	1,87	1,00	24,09	1,94	1,00
TF271	C_2H_2 (Zn)		27,74	1,81	1,00	24,40	1,89	1,00	22,06	2,12	1,00	28,17	1,80	1,00	28,85	1,78	1,00	23,20	1,81	1,00
TF272	C_2H_2 (Zn)		30,48	1,70	1,00	29,70	1,60	1,00	27,84	1,81	1,00	29,47	1,73	1,00	29,59	1,73	1,00	29,13	1,71	1,00
TF273	PHD		22,72	1,85	1,00	23,02	1,86	1,00	23,12	1,87	1,00	22,80	1,76	1,00	22,20	1,83	1,00	22,46	1,87	1,00
TF274	C_2H_2 (Zn)		29,80	1,70	1,00	27,08	1,77	1,00	24,47	1,87	1,00	30,08	2,52	1,00	30,81	1,75	1,00	26,13	1,78	1,00
TF275	HSF		27,27	1,82	1,00	25,73	1,92	1,00	24,44	1,81	1,00	27,73	2,00	1,00	27,93	1,70	1,00	24,77	1,69	1,00
TF276	RR		22,84	1,93	1,00	22,97	1,93	1,00	23,46	1,89	1,00	22,26	1,88	1,00	21,81	2,12	1,00	21,25	1,92	1,00
TF277	E2F		24,53	1,89	1,00	20,43	1,91	1,00	18,17	1,92	0,99	23,22	1,82	1,00	25,07	1,85	1,00	20,11	2,17	1,00
TF278	MYB		21,96	1,92	1,00	22,25	1,85	1,00	21,51	2,06	1,00	24,51	1,86	1,00	22,25	1,90	1,00	22,91	1,77	1,00
TF279	MYB/HD-like		22,39	1,94	1,00	22,30	1,88	1,00	21,78	1,94	1,00	23,84	1,91	1,00	23,84	1,94	1,00	22,71	1,98	1,00
TF280	WRKY family	WRKY	22,74	1,87	1,00	22,88	1,97	1,00	22,69	1,83	1,00	22,85	1,86	1,00	22,68	1,98	1,00	22,40	2,51	1,00
TF281	WRKY family	WRKY	24,77	1,93	1,00	24,16	1,91	1,00	24,03	1,79	1,00	24,07	1,90	1,00	23,01	1,94	1,00	22,83	1,93	1,00
TF282	WRKY family	WRKY	26,94	1,98	1,00	26,15	1,94	1,00	21,90	2,01	1,00	25,66	1,99	1,00	24,22	1,96	1,00	25,94	1,89	1,00
TF283	CCHC (Zn)		28,58	1,93	1,00	28,94	1,86	1,00	29,51	1,92	1,00	29,98	1,85	1,00	29,02	1,90	1,00	28,01	1,94	0,99
TF284	MYB/HD-like		30,94	1,71	1,00	29,90	1,77	1,00	26,59	1,67	1,00	27,72	1,72	1,00	28,34	1,86	1,00	27,61	1,86	1,00
TF285	MYB/HD-like		30,19	1,88	1,00	31,15	1,80	1,00	25,42	1,94	1,00	27,47	1,85	1,00	27,23	1,92	1,00	25,98	1,88	1,00
TF286	PHD		23,97	1,86	1,00	24,21	1,91	1,00	23,24	1,73	1,00	23,96	1,82	1,00	24,25	1,84	1,00	24,02	1,96	1,00
TF287	PHD		23,86	1,98	1,00	23,96	1,87	1,00	21,51	1,97	1,00	23,49	1,88	1,00	23,30	1,89	1,00	22,95	1,96	1,00
TF288	HD family	HD-ZIP	26,89	1,88	1,00	27,06	1,90	1,00	27,07	1,83	1,00	28,28	1,77	1,00	27,68	1,79	1,00	27,00	1,97	1,00
TF289	E2F		25,12	1,82	1,00	25,46	1,62	1,00	21,65	1,78	1,00	23,43	1,81	1,00	23,58	1,73	1,00	23,65	1,89	1,00
TF290	E2F		27,24	1,95	1,00	27,00	1,92	1,00	27,23	2,12	1,00	27,35	1,91	1,00	27,42	1,88	1,00	26,78	1,86	1,00
TF291	C_2H_2 (Zn)		31,42	1,74	1,00	29,94	1,70	1,00	27,34	1,90	1,00	30,43	1,70	1,00	32,59	1,72	1,00	29,04	1,80	1,00
TF292	ZIM		31,62	1,89	1,00	24,88	1,89	1,00	20,28	1,90	1,00	23,80	1,83	1,00	22,49	1,87	1,00	24,86	1,87	1,00
TF293	HMG		30,73	1,88	1,00	28,95	1,87	1,00	23,97	1,95	1,00	27,70	2,00	0,99	26,01	1,84	1,00	27,69	1,87	1,00
TF294	CCHC (Zn)		21,65	1,92	1,00	21,41	1,76	1,00	21,78	1,76	1,00	21,72	2,03	1,00	21,73	2,05	1,00	21,25	1,92	1,00
TF295	HD family	HD	26,77	1,86	1,00	26,73	1,90	1,00	21,38	1,96	1,00	23,23	1,92	1,00	25,25	1,90	1,00	24,78	1,91	1,00
TF296	GRAS		24,51	1,95	1,00	24,58	1,91	1,00	25,31	1,85	1,00	23,57	1,79	1,00	22,86	1,87	1,00	22,66	1,97	1,00
TF297	GRAS		24,98	1,94	1,00	23,60	1,95	1,00	21,54	1,92	1,00	23,49	2,17	1,00	23,19	1,93	1,00	22,00	1,86	1,00
TF298	WRKY family	WRKY	n.d.	1,17	0,99	22,06	1,85	1,00	22,49	1,95	1,00	22,13	1,97	1,00	21,67	1,83	1,00	21,41	1,85	1,00
TF299	CCHC (Zn)		24,68	1,87	1,00	24,32	1,86	1,00	18,89	1,96	1,00	20,33	1,79	1,00	22,29	1,98	1,00	21,69	1,97	1,00

Table S1, continued

TF300	AP2/EREBP		30,87	1,72	1,00	28,83	1,77	1,00	24,60	1,99	1,00	27,74	1,73	1,00	25,63	1,80	1,00	28,39	1,77	1,00
TF301	PHD		19,95	1,97	1,00	19,99	1,93	1,00	20,13	1,93	1,00	20,98	1,96	1,00	21,02	1,94	1,00	20,48	1,90	1,00
TF302	AP2/EREBP		27,76	1,95	1,00	24,70	1,71	1,00	20,93	1,91	1,00	28,01	1,98	1,00	28,21	1,79	1,00	23,41	2,00	1,00
TF303	AP2/EREBP		24,47	1,92	1,00	24,09	1,92	1,00	22,46	1,96	1,00	25,24	1,89	1,00	23,41	2,15	1,00	24,67	2,01	1,00
TF304	CCHC (Zn)		30,18	1,80	1,00	30,00	1,89	1,00	26,79	1,72	1,00	29,32	1,76	1,00	28,00	1,82	1,00	26,96	1,90	1,00
TF305	MYB/HD-like		23,26	1,56	1,00	23,35	1,72	1,00	25,36	1,70	0,99	24,67	1,66	1,00	23,99	1,82	1,00	22,91	2,04	1,00
TF306	MYB		22,44	1,87	1,00	22,86	1,91	1,00	22,29	1,99	1,00	24,01	2,25	1,00	22,81	1,91	1,00	22,51	1,95	1,00
TF307	C3H	C3H-type 1 (Zn)	23,63	2,03	1,00	23,77	1,88	1,00	23,99	2,08	1,00	23,96	1,89	1,00	23,92	1,96	1,00	23,34	1,86	1,00
TF308	C_2C_2 (Zn)	DOF	24,10	1,89	1,00	22,87	1,92	1,00	19,57	2,46	1,00	24,31	1,87	1,00	24,10	1,93	1,00	21,40	2,10	1,00
TF309	GRF		31,93	1,62	1,00	29,89	1,80	1,00	25,98	1,77	1,00	31,81	1,84	1,00	33,20	1,76	1,00	27,62	2,00	1,00
TF310	RR		34,90	1,83	1,00	36,06	1,70	1,00	35,06	1,71	1,00	37,90	1,75	1,00	30,59	1,82	1,00	34,85	1,73	1,00
TF311	MYB		23,15	1,96	1,00	23,20	1,91	1,00	21,82	1,95	1,00	23,64	1,83	1,00	22,96	1,94	1,00	22,85	1,98	1,00
TF312	SNF2		22,96	1,91	1,00	22,96	1,95	1,00	22,68	1,86	1,00	23,36	1,93	1,00	23,08	1,93	1,00	22,80	1,90	1,00
TF313	MYB		22,97	1,86	1,00	23,04	1,91	1,00	23,06	1,74	1,00	23,61	1,91	1,00	23,63	1,91	1,00	22,98	1,97	1,00
TF314	GRAS		29,21	1,82	1,00	23,83	2,13	1,00	20,59	2,02	1,00	23,60	1,89	1,00	21,89	1,90	1,00	24,84	2,01	1,00
TF315	AS2		21,33	2,75	1,00	21,61	1,94	1,00	17,69	2,11	1,00	20,55	1,98	1,00	20,28	1,80	1,00	20,53	1,98	1,00
TF316	AP2/EREBP		30,58	1,65	1,00	30,59	1,80	1,00	28,44	2,05	1,00	32,49	1,57	1,00	34,54	1,73	1,00	30,70	1,73	1,00
TF317	CCAAT	CCAAT-HAP3	24,32	1,86	1,00	24,57	1,88	1,00	24,88	1,90	1,00	24,74	1,81	1,00	24,50	1,91	1,00	23,78	1,90	1,00
TF318	CCHC (Zn)		29,57	1,80	1,00	28,19	1,70	1,00	25,77	1,80	1,00	30,12	1,80	1,00	30,20	1,76	1,00	29,29	1,79	1,00
TF319	CCHC (Zn)		24,10	1,87	1,00	24,19	1,92	1,00	24,52	1,89	1,00	24,24	1,71	1,00	24,14	1,88	1,00	23,39	1,94	1,00
TF320	MADS		28,28	1,94	1,00	21,51	1,98	1,00	16,86	2,07	1,00	20,19	1,95	1,00	19,81	1,95	1,00	21,47	2,05	1,00
TF321	MADS		29,31	1,80	1,00	28,94	1,77	1,00	24,81	1,93	1,00	26,62	1,85	1,00	26,65	1,89	1,00	25,71	1,92	1,00
TF322	MADS		25,98	1,88	1,00	25,80	1,91	1,00	25,09	1,93	1,00	25,11	1,84	1,00	24,80	1,93	1,00	23,96	1,87	1,00
TF323	MADS		29,39	1,89	1,00	28,97	2,02	1,00	24,57	1,85	1,00	27,01	1,86	1,00	26,82	1,96	1,00	25,74	1,86	1,00
TF324	AP2/EREBP		23,56	1,94	1,00	23,69	2,11	1,00	23,69	1,90	1,00	21,95	1,86	1,00	21,47	2,16	1,00	20,59	1,89	1,00
TF325	C3H	C3H-type 1 (Zn)	24,00	1,93	1,00	22,45	1,93	1,00	20,73	1,93	1,00	24,10	1,85	1,00	25,23	1,87	1,00	21,31	1,94	1,00
TF326	C_2H_2 (Zn)		25,97	1,81	1,00	26,20	2,35	1,00	27,52	1,37	1,00	28,61	1,58	1,00	26,35	1,75	1,00	26,03	1,85	1,00
TF327	ABI3-VP1		25,26	1,88	1,00	26,25	1,88	1,00	23,70	2,13	1,00	26,57	1,86	1,00	25,44	1,89	1,00	25,70	1,90	1,00
TF328	ABI3-VP1		28,10	1,67	1,00	25,80	1,93	1,00	20,68	1,92	1,00	23,48	1,94	1,00	23,44	1,70	1,00	24,28	2,13	1,00
TF329	ABI3-VP1		24,25	1,83	1,00	24,92	2,04	1,00	24,15	1,86	1,00	24,77	1,95	1,00	23,99	1,96	1,00	23,98	2,01	1,00
TF330	WRKY family	WRKY	24,94	1,83	1,00	24,07	2,06	1,00	21,45	1,65	1,00	24,56	1,93	1,00	24,48	1,95	1,00	22,39	1,78	1,00
TF331	WRKY family	WRKY	25,04	1,94	1,00	23,98	1,89	1,00	20,03	2,13	1,00	25,48	1,94	1,00	25,42	1,94	1,00	22,46	1,96	1,00
TF332	MYB		25,33	1,88	1,00	24,64	1,92	1,00	21,98	1,87	1,00	24,18	1,89	1,00	23,04	2,08	1,00	23,72	2,08	1,00
TF333	bHLH		25,20	2,05	1,00	25,70	1,82	1,00	25,48	1,89	1,00	24,85	1,89	1,00	23,88	1,85	1,00	23,51	1,96	1,00
TF334	CCHC (Zn)		29,21	1,76	1,00	26,85	1,73	1,00	23,64	1,92	1,00	29,37	1,69	1,00	29,31	1,88	1,00	28,00	1,79	1,00
TF335	MADS		27,00	2,17	0,99	24,34	1,86	1,00	23,40	1,79	1,00	27,35	2,08	1,00	27,11	1,83	1,00	23,57	1,95	1,00
TF336	MYB/HD-like		24,58	1,89	1,00	24,60	1,85	1,00	24,84	1,87	1,00	24,74	1,89	1,00	24,51	1,83	1,00	24,13	1,94	1,00
TF337	TTF-type (Zn)		38,19	1,31	1,00	31,29	1,76	1,00	29,62	1,80	1,00	32,16	1,74	1,00	36,62	1,75	1,00	30,27	1,85	1,00
TF338	C_2C_2 (Zn)	DOF	25,52	1,87	1,00	22,09	1,91	1,00	20,31	1,97	1,00	22,03	2,04	1,00	19,97	1,98	1,00	20,98	1,25	1,00
TF339	AP2/EREBP		35,98	1,80	1,00	30,98	1,85	1,00	27,87	1,46	1,00	31,28	1,28	1,00	32,17	1,74	1,00	31,11	1,85	1,00
TF340	AS2		32,92	1,70	1,00	28,72	1,75	1,00	22,89	1,78	1,00	26,81	1,77	1,00	26,04	1,59	1,00	27,33	1,77	1,00
TF341	C_2H_2 (Zn)		24,52	1,98	1,00	24,36	1,96	1,00	20,34	1,86	1,00	22,78	1,96	1,00	24,91	1,83	1,00	24,46	1,54	1,00
TF342	CCHC (Zn)		32,97	1,77	1,00	30,64	1,89	1,00	30,03	1,74	1,00	32,15	1,78	1,00	31,81	1,81	1,00	30,30	1,88	1,00

Table S1, continued

TF343	bZIP		29,12	1,76	1,00	26,76	1,71	1,00	23,11	1,88	1,00	27,93	1,75	1,00	24,97	1,80	1,00	26,63	1,81	1,00
TF344	WRKY family	WRKY	23,48	1,93	1,00	23,14	2,12	1,00	21,60	1,99	1,00	22,67	1,79	1,00	22,76	1,83	1,00	21,72	1,99	1,00
TF345	PHD		23,04	1,91	1,00	23,07	1,87	1,00	23,42	1,84	1,00	23,18	1,98	1,00	23,28	1,86	1,00	23,08	1,93	1,00
TF346	CCHC (Zn)		21,17	2,01	1,00	21,33	1,93	1,00	18,72	1,82	1,00	20,71	1,75	1,00	19,68	2,36	1,00	18,85	1,90	1,00
TF347	C_2H_2 (Zn)		19,17	1,90	1,00	19,04	1,82	1,00	15,66	1,22	0,98	16,36	1,37	0,98	17,30	1,87	1,00	17,34	1,83	1,00
TF348	TTF-type (Zn)		27,06	1,88	1,00	23,85	1,84	1,00	20,97	2,13	1,00	27,73	1,93	1,00	27,73	1,87	1,00	22,76	1,86	1,00
TF349	CCHC (Zn)		25,32	2,00	1,00	25,13	1,80	1,00	25,67	1,87	1,00	24,85	1,94	1,00	24,83	1,91	1,00	24,22	1,92	1,00
TF350	AP2/EREBP		23,64	1,87	1,00	23,63	1,86	1,00	22,21	1,83	1,00	23,40	1,93	1,00	23,29	1,94	1,00	22,98	1,90	1,00
TF351	bHLH		23,03	1,85	1,00	23,16	1,87	1,00	23,70	1,83	1,00	22,99	2,04	1,00	22,88	1,90	1,00	22,27	1,83	1,00
TF352	AP2/EREBP		27,48	1,89	1,00	27,19	1,84	1,00	22,87	1,82	1,00	24,62	1,77	1,00	26,49	1,94	1,00	25,80	1,82	1,00
TF353	AUX/IAA		21,71	1,83	1,00	21,93	1,90	1,00	22,61	2,00	1,00	21,08	1,86	1,00	20,89	2,00	1,00	20,40	1,91	1,00
TF354	HD family	HD	24,65	1,74	1,00	24,75	1,98	1,00	24,54	1,86	1,00	25,40	1,83	1,00	24,28	1,85	1,00	24,15	1,86	1,00
TF355	HD-like		31,17	1,84	1,00	32,08	1,84	1,00	30,98	1,83	1,00	32,38	1,82	1,00	25,82	1,87	1,00	32,14	1,87	1,00
TF356	HD-like		28,48	1,75	1,00	25,76	1,86	1,00	22,56	1,86	1,00	30,34	1,78	1,00	30,55	1,77	1,00	24,81	1,96	1,00
TF357	CCAAT	CCAAT-HAP3	21,67	1,90	1,00	21,37	1,89	1,00	21,03	1,91	1,00	21,57	2,05	1,00	21,55	1,93	1,00	20,96	1,91	1,00
TF358	C3H	C3H-type 1 (Zn)	31,06	1,56	1,00	29,15	1,64	1,00	29,56	1,71	1,00	31,17	1,50	1,00	30,13	1,58	1,00	28,94	1,69	1,00
TF359	HTH	FIS	22,75	1,87	1,00	22,82	1,90	1,00	20,46	1,88	1,00	22,98	1,86	1,00	24,20	1,92	1,00	23,68	1,99	1,00
TF360	bZIP		25,35	1,96	1,00	25,66	1,95	1,00	23,06	1,94	1,00	24,88	2,00	1,00	25,17	1,94	1,00	24,31	1,88	1,00
TF361	bZIP		n.d.	1,66	0,99	33,73	1,42	1,00	28,70	1,67	1,00	33,98	1,49	1,00	30,32	1,50	1,00	31,49	1,55	1,00
TF362	bZIP		36,42	1,65	1,00	30,96	1,66	1,00	27,42	1,75	1,00	30,79	1,77	1,00	29,59	1,75	1,00	30,55	1,74	1,00
TF363	CCHC (Zn)		28,89	1,88	1,00	25,07	1,96	1,00	23,45	1,96	1,00	30,32	1,75	1,00	30,99	1,85	1,00	24,31	1,92	1,00
TF364	CCAAT	CCAAT-HAP3	23,81	1,92	1,00	23,88	1,92	1,00	24,23	1,94	1,00	24,06	1,92	1,00	23,89	1,92	1,00	23,37	2,05	1,00
TF365	C_2H_2 (Zn)		22,47	1,87	1,00	22,72	2,08	1,00	22,96	1,86	1,00	24,61	1,57	1,00	24,09	1,94	1,00	23,80	1,97	1,00
TF366	HMG		25,57	1,91	1,00	26,04	1,94	1,00	23,03	1,90	1,00	27,26	1,89	1,00	24,73	1,82	1,00	25,95	1,87	1,00
TF367	HD family	HD	27,98	1,82	1,00	27,41	1,84	1,00	24,79	1,85	1,00	28,97	1,86	1,00	29,46	1,90	1,00	26,97	1,88	1,00
TF368	HD-like		25,58	1,83	1,00	25,59	1,92	1,00	27,33	1,60	1,00	27,32	1,53	1,00	26,25	1,73	1,00	25,81	1,75	1,00
TF369	MYB/HD-like		23,50	1,97	1,00	23,31	1,85	1,00	23,56	1,97	1,00	23,05	1,95	1,00	23,15	1,86	1,00	22,92	2,03	1,00
TF370	HD family	HD	22,85	1,93	1,00	22,59	1,91	1,00	19,85	1,89	1,00	21,73	1,67	1,00	20,90	1,93	1,00	21,47	1,92	1,00
TF371	MYB/HD-like		28,28	1,75	1,00	26,40	1,77	1,00	22,12	1,89	1,00	25,12	1,91	1,00	24,40	1,83	1,00	25,47	1,77	1,00
TF372	HD family	HD	29,61	1,86	1,00	30,43	1,96	1,00	29,68	1,86	1,00	29,70	1,86	1,00	29,22	1,94	1,00	28,64	1,88	1,00
TF373	MYB		29,30	1,70	1,00	28,53	1,92	1,00	25,06	1,73	1,00	28,42	1,77	1,00	28,70	1,72	1,00	26,31	1,79	1,00
TF374	SNF2		24,11	1,91	1,00	23,98	1,93	1,00	24,15	1,84	1,00	24,55	1,93	1,00	24,54	1,86	1,00	24,31	1,85	1,00
TF375	SNF2		35,54	1,72	1,00	31,23	1,77	1,00	29,45	1,78	1,00	29,88	1,83	1,00	29,91	1,88	1,00	29,78	1,84	1,00
TF376	PHD		26,57	1,91	1,00	25,83	1,89	1,00	22,11	1,89	1,00	24,22	1,91	1,00	22,70	1,90	1,00	23,77	1,96	1,00
TF377	MYB/HD-like		21,88	2,02	1,00	21,79	1,98	1,00	22,31	1,95	1,00	22,29	1,86	1,00	22,10	1,96	1,00	21,47	1,87	1,00
TF378	TrpR		24,62	1,89	1,00	24,85	1,95	1,00	22,30	1,90	1,00	24,73	1,85	1,00	23,61	1,95	1,00	24,34	1,89	1,00
TF379	TrpR		29,92	1,88	1,00	30,99	1,77	1,00	28,54	1,96	1,00	31,11	1,77	1,00	30,04	1,79	1,00	29,15	1,89	1,00
TF380	AP2/EREBP		32,07	1,78	1,00	29,64	1,87	1,00	25,62	1,79	1,00	29,98	1,93	1,00	29,89	1,67	1,00	26,76	1,90	1,00
TF381	LFY		27,91	1,82	1,00	24,40	1,87	1,00	20,96	1,36	1,00	24,05	1,66	1,00	22,14	1,85	1,00	25,11	1,97	1,00
TF382	MADS		33,74	1,86	1,00	30,75	1,77	1,00	23,41	1,65	1,00	31,50	1,76	1,00	31,62	1,67	1,00	26,97	1,87	1,00
TF383	MYB/HD-like		28,09	1,98	1,00	28,23	1,83	1,00	25,70	1,82	1,00	25,53	2,02	1,00	25,48	1,85	1,00	25,56	1,88	1,00
TF384	HD-like		28,60	1,79	1,00	28,58	1,74	1,00	30,69	2,09	1,00	29,96	1,81	1,00	29,52	1,77	1,00	28,32	1,94	1,00
TF385	DDT		23,41	1,89	1,00	23,63	1,88	1,00	22,96	1,94	1,00	23,98	1,89	1,00	24,20	1,93	1,00	23,64	1,84	1,00

Table S1, continued

TF386	ARF		23,30	1,94	1,00	23,37	1,95	1,00	23,35	1,83	1,00	23,66	1,88	1,00	23,44	1,73	1,00	23,03	1,82	1,00
TF387	C_2C_2 (Zn)	DOF	24,75	1,81	1,00	24,27	1,79	1,00	21,84	1,80	1,00	22,58	1,77	1,00	23,94	1,79	1,00	23,46	1,86	1,00
TF388	TTF-type (Zn)		32,29	1,85	1,00	29,36	1,85	1,00	26,95	1,97	1,00	33,61	1,88	1,00	35,53	1,85	1,00	28,27	1,91	1,00
TF389	C_2C_2 (Zn)	DOF	30,11	1,82	1,00	30,30	1,76	1,00	29,58	1,81	1,00	28,96	1,88	1,00	28,90	1,94	1,00	28,33	1,80	1,00
TF390	R3H		23,83	1,94	1,00	21,92	2,50	1,00	19,21	1,93	1,00	21,45	1,90	1,00	20,62	1,91	1,00	22,19	1,95	1,00
TF391	R3H		22,27	1,94	1,00	22,62	2,00	1,00	19,66	2,81	1,00	22,48	1,67	1,00	21,95	1,95	1,00	22,50	1,94	1,00
TF392	MYB/HD-like		26,48	1,88	1,00	26,31	1,89	1,00	23,83	1,85	1,00	25,38	1,89	1,00	26,10	1,94	1,00	25,62	1,88	1,00
TF393	C_2C_2 (Zn)	DOF	23,64	1,87	1,00	23,65	1,97	1,00	24,25	1,89	1,00	26,62	1,91	1,00	26,19	1,90	1,00	25,70	1,96	1,00
TF394	NAC		21,58	1,94	1,00	19,87	1,94	1,00	16,60	1,92	0,99	21,13	1,92	1,00	21,68	1,92	1,00	17,85	2,08	1,00
TF395	MYB/HD-like		27,26	1,92	1,00	26,67	1,91	1,00	24,31	1,95	1,00	28,33	1,76	1,00	28,15	1,87	1,00	25,26	1,85	1,00
TF396	bHLH		29,61	1,88	1,00	26,71	2,07	1,00	24,42	1,95	1,00	29,64	1,81	1,00	30,65	1,86	1,00	25,14	1,94	1,00
TF397	bHLH		30,66	1,55	1,00	30,09	1,55	1,00	28,10	1,57	1,00	28,51	1,42	1,00	28,11	1,63	1,00	27,74	1,61	1,00
TF398	MADS		33,46	1,84	1,00	30,45	1,72	0,99	23,13	1,82	1,00	25,20	1,99	1,00	23,89	1,84	1,00	25,93	2,03	1,00
TF399	MADS		30,51	1,88	1,00	22,68	1,88	1,00	19,91	1,91	1,00	23,09	1,92	1,00	21,65	2,03	1,00	24,42	1,92	1,00
TF400	bZIP		21,00	1,95	1,00	21,30	2,02	1,00	21,32	1,97	1,00	23,95	1,81	1,00	23,65	1,91	1,00	23,25	1,92	1,00
TF401	TPR		24,79	1,87	1,00	25,08	1,92	1,00	24,31	1,96	1,00	25,20	1,92	1,00	24,68	1,87	1,00	24,02	1,92	1,00
TF402	bZIP		21,78	1,89	1,00	21,87	1,89	1,00	22,30	1,86	1,00	22,07	1,86	1,00	21,64	1,91	1,00	21,36	1,90	1,00
TF403	TPR		25,79	1,85	1,00	25,82	1,88	1,00	25,97	1,91	1,00	25,80	1,95	1,00	25,68	1,89	1,00	25,18	1,91	1,00
TF404	MYB		24,00	2,27	1,00	24,07	1,87	1,00	22,46	1,92	1,00	23,11	1,87	1,00	23,31	1,88	1,00	23,13	1,87	1,00
TF405	NAC		37,69	1,76	1,00	29,93	1,90	1,00	23,77	1,90	1,00	25,98	2,07	1,00	27,08	1,93	1,00	28,11	2,00	1,00
TF406	NAC		35,13	1,74	1,00	32,99	1,74	1,00	28,94	1,78	1,00	32,04	1,74	1,00	30,49	1,83	1,00	32,79	1,80	1,00
TF407	NAC		25,20	1,88	1,00	25,64	1,86	1,00	20,16	1,88	1,00	23,62	1,84	1,00	23,82	1,91	1,00	22,63	1,95	1,00
TF408	MYB/HD-like		24,65	1,85	1,00	24,72	1,76	1,00	23,60	1,65	1,00	22,29	1,54	1,00	23,08	1,76	1,00	22,77	1,71	1,00
TF409	NAC		25,30	1,91	1,00	25,43	1,78	1,00	22,67	1,88	1,00	24,51	1,82	1,00	24,09	1,96	1,00	23,14	2,00	1,00
TF410	MYB		24,42	1,92	1,00	23,03	1,87	1,00	17,98	1,93	1,00	20,88	1,86	1,00	20,30	1,90	1,00	21,78	1,84	1,00
TF411	MYB/HD-like		38,27	1,18	1,00	33,30	1,64	1,00	29,86	1,74	1,00	33,11	1,61	1,00	34,88	1,68	1,00	33,54	1,58	1,00
TF412	CCHC (Zn)		32,02	1,74	1,00	30,52	1,73	1,00	29,02	1,68	1,00	31,13	1,75	1,00	31,61	1,55	1,00	30,79	1,73	1,00
TF413	bZIP		25,05	1,89	1,00	25,02	1,37	1,00	22,36	1,93	1,00	23,72	1,94	1,00	23,49	1,88	1,00	22,45	1,96	1,00
TF414	PHD		19,93	1,96	1,00	20,05	2,05	1,00	20,32	1,90	1,00	20,83	1,90	1,00	20,33	1,89	1,00	20,18	2,12	1,00
TF415	GRF		34,26	1,77	1,00	30,31	1,93	1,00	29,50	1,82	1,00	32,38	1,51	1,00	22,38	2,01	1,00	31,11	1,72	1,00
TF416	C_2H_2 (Zn)		32,30	1,46	1,00	32,14	1,59	1,00	28,74	1,82	1,00	30,17	1,83	1,00	32,57	1,40	1,00	28,96	1,87	1,00
TF417	CCHC (Zn)		32,35	1,70	1,00	32,99	1,71	1,00	30,76	1,79	1,00	36,92	1,33	0,99	34,33	1,76	1,00	31,75	1,78	1,00
TF418	C3H	C3H-type 1 (Zn)	28,12	1,82	1,00	28,25	1,60	1,00	28,29	1,62	1,00	28,65	1,82	1,00	27,76	1,90	1,00	27,71	1,77	1,00
TF419	BD		32,49	1,78	1,00	35,51	1,77	1,00	28,49	1,85	1,00	31,96	1,79	1,00	30,46	1,84	1,00	30,34	1,79	1,00
TF420	ARF		25,86	1,87	1,00	26,16	1,86	1,00	23,58	1,87	1,00	26,65	1,93	1,00	25,20	1,88	1,00	25,70	1,87	1,00
TF421	ARF		30,34	1,73	1,00	23,37	1,96	1,00	19,57	1,94	1,00	22,63	2,45	1,00	21,37	1,89	1,00	24,04	1,92	1,00
TF422	ARF		32,79	1,80	1,00	31,71	1,74	1,00	28,90	1,88	1,00	30,71	1,87	1,00	30,60	1,87	1,00	31,82	1,86	1,00
TF423	ARF		25,31	1,89	1,00	25,62	1,95	1,00	20,56	1,89	1,00	23,39	1,93	1,00	24,31	1,88	1,00	23,33	1,99	1,00
TF424	CCHC (Zn)		28,98	1,79	1,00	28,07	1,83	1,00	29,45	2,01	1,00	28,67	1,72	1,00	28,95	1,77	1,00	28,22	1,82	1,00
TF425	bHLH		30,00	1,88	1,00	29,62	1,88	1,00	27,58	1,86	1,00	29,51	2,03	1,00	30,92	1,88	1,00	29,29	1,93	1,00
TF426	C_2H_2 (Zn)		24,83	1,83	1,00	23,97	1,90	1,00	23,88	1,87	1,00	22,81	1,91	1,00	22,77	2,32	1,00	21,97	1,91	1,00
TF427	bHLH		n.d.	1,40	0,93	32,71	1,71	1,00	27,59	1,81	1,00	30,16	1,69	1,00	28,90	1,74	1,00	30,04	1,62	1,00
TF428	C_2H_2 (Zn)		24,18	1,91	1,00	24,67	1,96	1,00	22,91	1,96	1,00	23,10	1,87	1,00	22,24	1,87	1,00	21,83	2,03	1,00

Table S1, continued

TF429	MYB/HD-like		24,67	1,93	1,00	24,67	2,03	1,00	23,62	1,98	1,00	24,96	1,96	1,00	24,91	1,91	1,00	24,05	1,97	1,00
TF430	MYB		23,75	1,93	1,00	23,47	2,02	1,00	21,00	1,89	1,00	22,99	1,96	1,00	22,27	1,86	1,00	22,83	1,95	1,00
TF431	MADS		29,06	1,90	1,00	26,37	1,91	1,00	21,95	2,03	1,00	25,66	2,01	1,00	23,39	1,90	1,00	25,25	1,89	1,00
TF432	MADS		31,54	1,87	1,00	31,36	1,55	1,00	24,34	1,96	1,00	27,95	1,91	1,00	26,85	1,86	1,00	27,33	1,97	1,00
TF433	MADS		28,08	1,84	1,00	23,03	1,90	1,00	19,59	2,02	1,00	22,31	2,01	1,00	20,66	1,95	1,00	21,91	1,94	1,00
TF434	bZIP		21,37	2,03	1,00	21,05	1,94	1,00	20,36	1,92	1,00	20,88	1,89	1,00	20,87	1,92	1,00	20,05	2,22	1,00
TF435	CCHC (Zn)		30,29	1,88	1,00	29,22	2,15	1,00	27,46	1,90	1,00	30,61	1,80	1,00	31,45	1,90	1,00	29,22	1,99	1,00
TF436	SBP		28,78	1,83	1,00	28,10	1,88	1,00	26,04	1,92	1,00	28,18	1,94	1,00	28,10	1,88	1,00	26,92	2,03	1,00
TF437	CCHC (Zn)		22,30	1,90	1,00	20,40	1,96	1,00	19,00	2,28	1,00	22,78	1,84	1,00	22,96	1,97	1,00	19,54	2,03	1,00
TF438	PHD		26,61	1,86	1,00	26,05	1,89	1,00	24,63	1,84	1,00	26,28	1,88	1,00	25,86	1,88	1,00	25,22	1,93	1,00
TF439	C3H	C3H-type 1 (Zn)	22,85	1,91	1,00	22,79	1,94	1,00	22,01	2,04	1,00	22,95	1,80	1,00	23,08	1,94	1,00	22,36	1,90	1,00
TF440	AS2		24,85	1,95	1,00	22,01	2,01	1,00	17,82	1,97	1,00	20,54	1,98	1,00	19,15	2,10	1,00	20,72	2,02	1,00
TF441	JUMONJI		26,85	1,92	1,00	25,25	1,99	1,00	21,67	2,07	1,00	27,32	1,93	1,00	28,30	1,94	1,00	22,95	1,97	1,00
TF442	CCHC (Zn)		24,00	1,96	1,00	23,94	1,97	1,00	24,50	1,88	1,00	23,93	1,86	1,00	23,45	1,96	1,00	22,85	1,95	1,00
TF443	CCHC (Zn)		28,21	1,76	1,00	27,94	1,72	1,00	23,64	1,92	1,00	24,76	1,77	0,99	25,82	1,87	1,00	24,88	1,96	1,00
TF444	AS2		30,39	1,82	1,00	26,22	1,90	1,00	22,25	1,72	1,00	25,30	2,06	1,00	23,77	1,92	1,00	26,47	1,97	1,00
TF445	C_2H_2 (Zn)		23,34	1,88	1,00	23,44	1,95	1,00	23,98	1,87	1,00	24,35	1,78	1,00	23,49	1,93	1,00	23,35	2,16	1,00
TF446	HD-like		29,34	1,62	0,99	26,91	1,81	1,00	26,87	1,61	1,00	28,60	1,59	1,00	27,39	1,66	1,00	25,60	1,90	1,00
TF447	C_2H_2 (Zn)		23,87	1,93	1,00	23,97	1,88	1,00	25,09	1,99	1,00	24,51	2,05	1,00	24,31	2,04	0,99	23,80	1,93	1,00
TF448	RR		22,08	1,94	1,00	22,58	1,92	1,00	22,59	1,96	1,00	23,30	1,92	1,00	22,10	2,00	1,00	21,77	1,95	1,00
TF449	CCHC (Zn)		23,86	1,91	1,00	23,99	1,89	1,00	23,93	1,85	1,00	23,78	1,93	1,00	23,64	2,02	1,00	23,06	1,92	1,00
TF450	MYB/HD-like		26,31	1,86	1,00	26,09	1,79	1,00	25,38	1,79	1,00	26,90	1,86	1,00	26,92	1,90	1,00	25,99	1,88	1,00
TF451	ZF DHHC		23,68	1,99	1,00	24,45	1,82	1,00	23,69	1,76	1,00	25,95	2,11	1,00	24,83	1,96	1,00	24,42	2,05	1,00
TF452	ZF DHHC		31,41	1,89	1,00	30,10	1,78	1,00	28,13	1,78	1,00	30,55	2,05	1,00	29,94	1,87	1,00	30,31	1,81	1,00
TF453	ZF DHHC		23,34	1,95	1,00	23,60	2,04	1,00	23,93	1,86	1,00	24,84	2,02	1,00	24,19	1,92	1,00	23,82	1,92	1,00
TF454	ZF DHHC		24,91	1,86	1,00	24,89	1,88	1,00	20,13	1,81	1,00	21,90	1,66	1,00	22,46	1,95	1,00	21,39	2,05	1,00
TF455	C_2H_2 (Zn)		24,25	1,79	1,00	22,16	1,78	1,00	19,57	1,74	1,00	24,60	1,39	1,00	24,92	1,92	1,00	20,86	1,90	1,00
TF456	C_2H_2 (Zn)		22,92	1,95	1,00	23,08	1,80	1,00	24,01	1,71	1,00	24,43	1,79	1,00	22,88	1,88	1,00	22,66	1,85	1,00
TF457	RR		36,07	1,79	1,00	33,00	1,87	1,00	27,11	1,88	1,00	30,04	1,77	1,00	28,80	1,86	1,00	30,87	1,85	1,00
TF458	C_2H_2 (Zn)		24,98	1,83	1,00	24,80	1,86	1,00	25,73	1,84	1,00	25,90	1,82	1,00	24,52	1,86	1,00	24,28	2,00	1,00
TF459	NAC		23,03	1,94	1,00	23,00	1,85	1,00	23,74	1,82	1,00	22,16	2,00	1,00	21,74	1,92	1,00	21,10	2,04	1,00
TF460	GRF		27,35	1,93	1,00	26,85	1,87	1,00	24,49	1,78	1,00	27,63	1,91	1,00	26,75	1,82	1,00	26,00	1,91	1,00
TF461	WRKY family	WRKY	21,48	2,05	1,00	19,81	2,28	1,00	17,69	1,91	0,99	21,18	2,04	1,00	22,06	2,09	1,00	18,76	2,07	1,00
TF462	bHLH		23,17	1,84	1,00	23,12	1,98	1,00	22,51	2,06	1,00	21,89	1,94	1,00	21,79	1,91	1,00	21,42	2,02	1,00
TF463	bHLH		22,68	1,91	1,00	22,50	1,83	1,00	20,79	1,90	1,00	22,88	1,80	1,00	22,30	1,76	1,00	21,93	1,88	1,00
TF464	bZIP		24,40	1,93	1,00	23,92	1,88	1,00	24,96	1,97	1,00	24,71	1,90	1,00	23,77	1,87	1,00	23,68	1,95	1,00
TF465	MYB/HD-like		27,22	1,81	1,00	25,74	1,82	1,00	21,99	1,90	1,00	28,07	1,82	1,00	27,06	1,86	1,00	24,54	1,94	1,00
TF466	JUMONJI		30,36	1,70	1,00	29,93	1,86	1,00	27,14	2,20	1,00	29,18	1,76	1,00	28,37	1,91	1,00	27,59	1,99	1,00
TF467	PHD		26,90	1,86	1,00	26,57	1,93	1,00	24,06	1,86	1,00	26,95	1,96	1,00	27,15	1,90	1,00	25,97	1,92	1,00
TF468	PHD		30,39	1,88	1,00	31,14	1,90	1,00	25,60	1,93	1,00	29,43	1,86	1,00	29,97	1,93	1,00	28,98	1,88	1,00
TF469	HD family	HD	26,83	1,89	1,00	27,53	1,67	1,00	23,51	2,00	1,00	26,01	1,97	1,00	26,45	1,94	1,00	26,80	1,93	1,00
TF470	HD family	HD	27,93	1,90	1,00	26,04	1,95	1,00	21,65	1,97	1,00	24,58	1,92	1,00	24,39	1,98	1,00	26,09	1,96	1,00
TF471	C_2H_2 (Zn)		22,00	1,83	1,00	22,30	1,86	1,00	22,60	1,84	1,00	22,14	1,87	1,00	21,73	1,89	1,00	21,45	2,02	1,00

Table S1, continued

TF472	RR		23,20	1,80	1,00	23,36	1,78	1,00	23,73	1,74	1,00	22,69	1,75	1,00	22,60	1,85	1,00	21,91	1,79	1,00
TF473	AP2/EREBP		23,61	1,89	1,00	23,57	1,83	1,00	24,11	1,89	1,00	22,24	1,94	1,00	22,03	1,87	1,00	21,55	1,92	1,00
TF474	MADS		30,46	1,84	1,00	23,48	1,92	1,00	21,89	2,13	1,00	28,68	1,92	1,00	29,10	1,94	1,00	22,78	1,95	1,00
TF475	bZIP		23,94	1,84	1,00	21,20	1,48	0,99	24,29	1,87	1,00	25,44	1,93	1,00	25,35	1,89	1,00	24,80	1,87	1,00
TF476	ABI3-VP1		24,97	1,98	1,00	25,15	1,92	1,00	21,60	1,79	1,00	23,67	1,74	1,00	23,96	1,98	1,00	23,29	1,99	1,00
TF477	NAC		26,78	1,93	1,00	24,71	1,94	1,00	20,71	2,00	1,00	24,03	1,94	1,00	22,50	1,90	1,00	24,77	1,98	1,00
TF478	HD-like		21,44	1,92	1,00	21,64	1,91	1,00	19,31	2,02	1,00	21,30	1,98	1,00	22,40	1,28	0,99	20,70	2,04	1,00
TF479	NAC		22,11	1,83	1,00	22,18	1,84	1,00	17,12	2,05	0,99	18,45	2,19	1,00	20,80	1,89	1,00	19,49	2,09	1,00
TF480	ZF-HD		30,52	1,90	1,00	26,53	1,91	1,00	21,92	1,98	1,00	27,30	1,95	1,00	23,88	1,96	1,00	27,26	1,97	1,00
TF481	FHA		25,28	1,87	1,00	25,22	1,90	1,00	22,42	1,88	1,00	25,48	1,87	1,00	24,97	1,86	1,00	25,43	1,83	1,00
TF482	HD family	HD	25,31	1,86	1,00	25,34	1,90	1,00	24,32	1,87	1,00	25,91	2,04	1,00	25,46	1,92	1,00	25,20	1,93	1,00
TF483	HD family	HD	25,21	1,87	1,00	23,35	1,94	1,00	19,34	1,96	1,00	22,71	1,95	1,00	20,74	1,94	1,00	22,27	1,97	1,00
TF484	HD-like		30,40	1,88	1,00	30,37	1,96	1,00	27,80	1,88	1,00	28,34	1,98	1,00	30,56	1,85	1,00	29,53	1,90	1,00
TF485	bHLH		23,51	1,48	1,00	23,92	1,80	1,00	24,99	2,03	1,00	22,70	2,19	1,00	22,03	2,14	1,00	21,61	1,71	1,00
TF486	PHD		22,34	1,83	1,00	22,78	1,80	1,00	22,45	1,78	1,00	22,52	1,81	1,00	22,41	1,95	1,00	22,32	1,87	1,00
TF487	ABI3-VP1		30,46	1,74	1,00	28,95	2,03	0,99	25,78	1,80	1,00	31,58	1,74	1,00	31,75	1,79	1,00	27,32	1,84	1,00
TF488	BTB/POZ		20,83	1,98	1,00	20,71	1,93	1,00	17,52	1,90	1,00	20,76	2,08	1,00	19,15	1,98	1,00	18,48	2,15	1,00
TF489	PHD		26,85	1,84	1,00	27,04	1,95	1,00	21,88	1,87	1,00	23,71	1,83	1,00	24,80	1,86	1,00	24,54	1,93	1,00
TF490	PHD		27,05	2,30	1,00	27,01	2,02	1,00	26,49	1,76	1,00	27,85	1,99	1,00	28,04	1,85	1,00	27,22	1,94	1,00
TF491	PHD		29,31	2,03	1,00	26,58	1,93	1,00	25,17	1,93	1,00	30,18	1,87	1,00	30,93	1,94	1,00	25,53	1,94	1,00
TF492	HD-like		28,21	1,79	1,00	26,70	1,85	1,00	24,23	1,93	1,00	26,09	1,84	1,00	24,20	1,86	1,00	26,38	1,84	1,00
TF493	AP2/EREBP		27,03	1,72	1,00	27,00	1,79	1,00	23,75	1,76	1,00	25,97	1,85	1,00	26,23	1,74	1,00	25,81	1,68	1,00
TF494	C_2H_2 (Zn)		22,88	1,76	1,00	22,78	1,86	1,00	19,15	2,07	1,00	20,43	1,82	1,00	21,54	1,92	1,00	20,80	1,88	1,00
TF495	C_2H_2 (Zn)		24,72	1,87	1,00	25,07	1,98	1,00	23,78	1,80	1,00	24,57	1,76	1,00	24,32	1,86	1,00	24,25	1,73	1,00
TF496	JUMONJI		23,30	1,90	1,00	23,40	1,86	1,00	23,18	1,92	1,00	23,74	1,98	1,00	23,30	1,92	1,00	22,94	1,92	1,00
TF497	HD family	HD	23,76	1,93	1,00	23,92	1,97	1,00	21,84	1,75	1,00	22,95	1,93	1,00	23,26	1,97	1,00	23,03	1,98	1,00
TF498	HMG		n.d.	2,21	0,90	n.d.	1,17	0,96	32,84	1,79	1,00	n.d.	1,26	0,99	28,31	1,85	1,00	n.d.	1,26	1,00
TF499	U1-type (Zn)		23,30	1,84	1,00	23,26	1,82	1,00	21,13	1,82	1,00	22,30	2,01	1,00	22,51	2,04	1,00	21,87	2,01	1,00
TF500	ZF DHHC		24,26	1,92	1,00	24,34	1,90	1,00	24,15	1,89	1,00	24,38	1,86	1,00	24,21	1,83	1,00	24,00	1,82	1,00
TF501	ZF DHHC		28,19	2,06	1,00	28,19	1,91	1,00	24,77	1,83	1,00	26,95	1,75	1,00	27,30	1,82	1,00	27,28	1,90	1,00
TF502	bHLH		27,30	1,71	1,00	27,19	1,66	1,00	29,30	1,60	1,00	30,36	1,67	1,00	27,60	1,75	1,00	26,93	1,63	1,00
TF503	TCoA		27,00	1,94	1,00	26,84	1,74	1,00	27,87	1,77	1,00	28,05	1,91	1,00	27,05	1,80	1,00	26,24	1,72	1,00
TF504	bHLH		24,46	1,96	1,00	24,23	1,92	1,00	19,33	1,94	1,00	20,99	1,88	1,00	21,91	2,04	1,00	21,27	1,97	1,00
TF505	bHLH		24,57	1,95	1,00	24,63	1,89	1,00	20,54	1,98	1,00	22,95	1,91	1,00	23,20	1,94	1,00	22,95	1,97	1,00
TF506	bHLH		24,98	1,90	1,00	24,74	1,82	1,00	21,75	2,01	1,00	22,13	1,87	1,00	21,80	1,91	1,00	21,04	1,95	1,00
TF507	ABI3-VP1		26,24	1,86	1,00	24,42	1,85	1,00	23,58	1,86	1,00	28,55	1,83	1,00	28,76	1,88	1,00	23,73	1,99	1,00
TF508	ZF DHHC		21,99	2,03	1,00	21,25	1,98	1,00	19,09	1,89	1,00	21,67	1,97	1,00	21,69	1,97	1,00	20,78	2,01	1,00
TF509	BTB/POZ		29,38	1,63	1,00	29,27	1,71	1,00	27,37	1,77	1,00	30,73	1,69	1,00	30,11	1,69	1,00	28,45	1,73	1,00
TF510	ARF		34,11	1,62	1,00	32,70	1,66	1,00	27,62	1,79	1,00	30,97	1,85	1,00	31,59	1,70	1,00	30,98	1,74	1,00
TF511	MADS		n.d.	1,17	1,00	n.d.	1,19	0,99	n.d.	1,23	0,99	n.d.	1,17	0,95	n.d.	1,18	1,00	n.d.	1,34	0,95
TF512	MADS		n.d.	1,44	0,98	32,89	1,68	1,00	33,37	1,60	1,00	39,56	1,38	0,96	33,22	1,34	1,00	32,21	1,56	1,00
TF513	ARF		22,40	1,88	1,00	22,51	1,90	1,00	22,62	1,87	1,00	21,91	1,83	1,00	21,56	1,92	1,00	21,45	1,92	1,00
TF514	ZIM		31,76	1,82	1,00	34,18	1,79	1,00	27,69	1,83	1,00	30,44	1,83	1,00	29,81	1,79	1,00	31,38	1,81	1,00

Table S1, continued

TF515	ZIM		20,51	1,94	1,00	22,69	2,17	1,00	19,94	1,90	1,00	22,08	1,85	1,00	21,72	1,83	1,00	23,06	1,91	1,00
TF516	ARF		21,83	1,89	1,00	22,24	1,88	1,00	22,22	1,88	1,00	21,52	1,88	1,00	21,13	1,90	1,00	20,83	1,87	1,00
TF517	bHLH		20,75	1,94	1,00	21,06	1,79	1,00	21,65	1,91	1,00	22,08	1,87	1,00	21,71	1,86	1,00	21,35	2,12	1,00
TF518	C_2H_2 (Zn)		24,49	1,88	1,00	24,57	1,90	1,00	19,68	1,99	1,00	21,73	2,15	1,00	21,01	1,93	1,00	20,47	1,88	1,00
TF519	WRKY family	LLR-WRKY	24,71	1,90	1,00	26,28	1,97	1,00	16,83	2,09	1,00	19,88	1,94	1,00	21,89	1,84	1,00	20,17	1,88	1,00
TF520	C_2H_2 (Zn)		22,07	1,98	1,00	22,08	1,92	1,00	21,47	1,92	1,00	23,32	1,95	1,00	22,39	1,89	1,00	22,29	1,98	1,00
TF521	A20-like		21,63	1,97	1,00	21,46	1,92	1,00	20,33	1,97	1,00	21,86	1,87	1,00	21,82	1,99	1,00	21,05	1,91	1,00
TF522	C_2H_2 (Zn)		28,54	1,90	1,00	28,05	1,81	1,00	26,86	1,98	1,00	27,60	1,92	1,00	26,46	2,08	1,00	26,26	2,03	1,00
TF523	MYB/HD-like		28,77	1,83	1,00	28,35	1,86	1,00	29,07	1,75	1,00	28,19	1,83	1,00	26,52	1,78	1,00	26,13	1,86	1,00
TF524	MADS		24,57	1,93	1,00	24,46	1,91	1,00	21,53	1,87	1,00	22,22	1,92	1,00	23,41	1,97	1,00	22,91	1,92	1,00
TF525	MADS		39,77	1,39	0,99	32,81	1,75	1,00	31,40	1,72	1,00	30,87	1,89	1,00	31,88	1,78	1,00	31,24	1,81	1,00
TF526	MADS		23,59	1,90	1,00	23,61	1,98	1,00	22,54	1,95	1,00	24,25	1,89	1,00	24,39	1,83	1,00	24,04	1,90	1,00
TF527	BTB/POZ		21,94	1,90	1,00	22,18	1,98	1,00	22,27	1,98	1,00	22,57	2,65	1,00	22,10	1,86	1,00	21,90	1,97	1,00
TF528	CCHC (Zn)		28,48	1,88	1,00	28,09	1,82	1,00	25,83	1,78	1,00	29,74	1,84	1,00	28,80	1,85	1,00	26,96	1,86	1,00
TF529	CCHC (Zn)		24,93	1,82	1,00	24,40	1,93	1,00	23,85	1,66	1,00	25,53	1,83	1,00	25,43	1,69	1,00	24,10	1,98	1,00
TF530	CCHC (Zn)		30,31	1,82	1,00	28,31	1,67	1,00	26,67	1,82	1,00	31,92	1,68	1,00	32,03	1,83	1,00	28,29	1,84	1,00
TF531	CCHC (Zn)		22,40	1,93	1,00	22,42	1,95	1,00	17,95	2,21	1,00	19,28	2,13	1,00	20,36	1,99	1,00	19,50	1,84	1,00
TF532	PHD		29,59	1,22	1,00	29,35	1,77	1,00	27,67	1,99	1,00	30,95	1,22	1,00	30,88	1,94	1,00	28,35	1,93	1,00
TF533	CCHC (Zn)		21,53	1,86	1,00	21,65	1,99	1,00	19,44	2,04	1,00	21,46	1,88	1,00	20,87	1,95	1,00	20,00	1,91	1,00
TF534	CCHC (Zn)		24,16	1,25	1,00	24,03	1,72	1,00	24,57	1,68	1,00	25,13	1,90	1,00	24,63	1,63	1,00	24,12	1,88	1,00
TF535	CCHC (Zn)		21,63	1,82	1,00	21,99	1,93	1,00	19,79	2,05	1,00	21,26	2,13	1,00	20,78	2,07	1,00	24,07	2,09	1,00
TF536	TAZ		22,40	1,97	1,00	20,75	1,89	1,00	17,65	2,17	1,00	19,75	1,86	1,00	18,06	1,98	1,00	19,83	1,92	1,00
TF537	bZIP		21,46	1,94	1,00	21,63	1,90	1,00	22,03	1,98	1,00	21,65	1,95	1,00	21,45	1,93	1,00	20,85	1,91	1,00
TF538	GRAS		28,43	1,65	1,00	25,18	1,69	1,00	23,31	1,94	1,00	29,01	1,94	1,00	30,79	1,80	1,00	24,51	1,90	1,00
TF539	PHD		24,35	1,72	1,00	24,39	1,86	1,00	25,20	1,65	1,00	25,66	2,05	1,00	24,20	1,88	1,00	23,86	1,86	1,00
TF540	SBP		21,75	1,92	1,00	22,25	1,97	1,00	21,22	1,90	1,00	22,67	1,83	1,00	21,57	1,86	1,00	21,26	1,91	1,00
TF541	MADS		30,40	1,77	1,00	29,44	1,74	1,00	25,91	1,80	1,00	30,51	1,72	1,00	31,57	1,72	1,00	28,81	2,01	1,00
TF542	MADS		29,85	1,72	1,00	29,69	1,68	1,00	25,70	1,76	1,00	28,35	1,75	1,00	28,97	1,67	1,00	28,14	1,69	1,00
TF543	BD		21,07	1,96	1,00	21,23	2,04	1,00	21,76	1,87	1,00	22,33	1,94	1,00	21,63	2,05	1,00	21,56	1,93	1,00
TF544	BD		24,13	1,93	1,00	24,48	1,91	1,00	24,76	2,08	1,00	25,74	1,81	1,00	24,61	1,89	1,00	24,61	1,90	1,00
TF545	CCHC (Zn)		24,56	1,88	1,00	21,78	1,99	1,00	21,59	1,89	1,00	25,45	1,81	1,00	25,98	1,88	1,00	20,94	1,89	1,00
TF546	AP2/EREBP		26,17	1,95	1,00	26,50	1,98	1,00	25,96	2,06	1,00	27,87	1,91	1,00	27,34	2,01	1,00	26,88	1,91	1,00
TF547	Lambda-DB		28,52	1,80	1,00	25,32	1,89	1,00	22,45	1,90	1,00	28,91	1,80	1,00	31,28	1,78	1,00	24,34	1,94	1,00
TF548	HD-like		27,00	1,73	1,00	27,57	1,71	1,00	25,16	1,99	1,00	27,77	1,73	1,00	26,87	1,64	1,00	26,90	1,70	1,00
TF549	HD family	HD-ZIP	23,75	1,93	1,00	23,73	1,99	1,00	23,81	1,92	1,00	22,36	1,81	1,00	22,06	1,95	1,00	21,42	1,91	1,00
TF550	HD-like		22,98	1,89	1,00	21,80	2,02	1,00	19,13	1,94	1,00	23,20	1,98	1,00	23,37	1,84	1,00	20,66	1,87	1,00
TF551	CCHC (Zn)		23,81	1,87	1,00	24,73	1,82	1,00	24,69	1,76	1,00	24,69	1,79	1,00	23,83	1,97	1,00	23,25	1,82	1,00
TF552	HD family	HD-ZIP	23,79	1,93	1,00	23,92	1,88	1,00	23,76	1,91	1,00	22,54	1,89	1,00	22,30	1,91	1,00	21,83	1,87	1,00
TF553	NRs		30,00	1,84	1,00	31,42	1,70	1,00	30,55	1,72	1,00	30,93	1,64	1,00	27,24	1,79	1,00	29,55	1,75	1,00
TF554	NRs		32,00	1,79	1,00	31,17	1,72	1,00	30,07	1,84	1,00	31,02	1,68	1,00	23,67	1,76	1,00	31,77	1,69	1,00
TF555	EIL		33,59	1,69	1,00	27,02	1,75	1,00	24,45	1,45	0,98	31,20	1,99	1,00	32,96	1,67	1,00	25,97	2,04	1,00
TF556	MADS		29,50	1,88	1,00	31,72	1,84	1,00	29,04	1,85	1,00	25,78	1,95	1,00	25,86	2,00	1,00	25,23	1,80	1,00
TF557	AP2/EREBP		25,47	2,02	1,00	25,70	1,92	1,00	19,80	1,94	1,00	22,12	2,50	1,00	24,40	1,98	1,00	23,58	1,93	1,00

Table S1, continued

TF558	MYB/HD-like		27,58	1,97	1,00	28,22	1,86	1,00	22,10	1,92	1,00	24,47	2,06	1,00	25,98	1,90	1,00	24,67	1,93	1,00
TF559	ZF DHHC		24,21	1,88	1,00	23,74	1,88	1,00	21,98	1,76	1,00	24,73	1,86	1,00	24,86	1,90	1,00	23,02	1,83	1,00
TF560	JUMONJI		24,11	1,94	1,00	24,95	1,92	1,00	24,91	1,96	1,00	26,37	1,86	1,00	23,86	1,92	1,00	24,53	1,94	1,00
TF561	CCHC (Zn)		29,17	1,91	1,00	29,24	1,82	1,00	29,39	1,76	1,00	29,94	1,85	1,00	30,94	1,83	1,00	28,28	2,07	1,00
TF562	HD family	HD	23,80	1,95	1,00	23,95	1,93	1,00	24,23	1,91	1,00	24,38	1,89	1,00	23,85	1,92	1,00	23,72	1,94	1,00
TF563	MADS		27,12	1,88	1,00	27,10	1,94	1,00	20,92	2,29	1,00	22,65	1,93	1,00	23,55	1,95	1,00	23,25	1,97	1,00
TF564	GRF		26,82	1,87	1,00	23,84	1,88	1,00	21,78	1,90	1,00	27,04	1,93	1,00	27,21	1,85	1,00	23,02	1,83	1,00
TF565	HTH	FIS	22,76	1,91	1,00	23,26	1,92	1,00	23,56	1,92	1,00	23,56	1,83	1,00	22,55	1,89	1,00	22,49	1,95	1,00
TF566	SBP		21,01	1,86	1,00	21,27	1,98	1,00	20,88	1,89	1,00	21,30	2,10	1,00	21,02	1,95	1,00	20,76	1,93	1,00
TF567	AS2		22,17	1,72	1,00	22,67	1,98	1,00	21,17	1,79	1,00	23,27	1,84	1,00	22,02	1,78	1,00	21,77	1,88	1,00
TF568	MYB/HD-like		24,35	2,15	1,00	24,48	2,01	1,00	19,84	1,90	1,00	21,61	2,06	1,00	22,11	1,85	1,00	22,06	1,85	1,00
TF569	AP2/EREBP		27,31	1,94	1,00	24,24	2,03	1,00	22,19	1,86	1,00	27,93	1,82	1,00	28,15	1,96	1,00	23,14	1,87	1,00
TF570	HTH	FIS	23,33	1,93	1,00	23,32	1,84	1,00	22,73	1,98	1,00	23,16	1,81	1,00	22,51	1,72	1,00	22,09	1,90	1,00
TF571	MADS		23,26	1,91	1,00	23,43	1,82	1,00	23,90	1,85	1,00	22,14	1,88	1,00	21,79	2,15	1,00	21,39	1,86	1,00
TF572	MADS		24,84	1,94	1,00	24,68	1,87	1,00	20,20	1,96	1,00	22,46	2,01	1,00	22,52	1,89	1,00	21,62	2,03	1,00
TF573	MADS		27,43	1,95	1,00	23,70	1,92	1,00	22,19	2,18	1,00	28,68	1,93	1,00	31,53	1,87	1,00	23,43	1,96	1,00
TF574	JUMONJI		24,44	1,92	1,00	24,81	2,01	1,00	25,23	1,99	1,00	25,28	1,89	1,00	24,53	1,83	1,00	24,46	1,98	1,00
TF575	HD-like		26,32	1,93	1,00	26,78	1,79	1,00	20,00	1,85	1,00	23,99	1,78	1,00	23,03	1,92	1,00	21,85	2,00	1,00
TF576	C3H	C3H-type 1 (Zn)	19,98	2,02	1,00	19,83	1,90	1,00	15,93	1,31	0,98	17,43	1,98	1,00	17,86	2,58	1,00	16,87	1,96	1,00
TF577	bZIP		28,59	1,84	1,00	28,69	1,85	1,00	25,42	1,83	1,00	27,47	1,76	1,00	27,57	1,86	1,00	27,18	1,82	1,00
TF578	MYB/HD-like		29,42	1,86	1,00	29,05	1,60	1,00	24,91	2,04	1,00	26,27	1,92	1,00	27,93	1,82	1,00	27,50	1,77	1,00
TF579	CCHC (Zn)		29,68	1,91	1,00	30,43	2,06	1,00	24,41	1,89	1,00	26,00	1,89	1,00	27,63	1,99	1,00	27,44	1,89	1,00
TF580	MYB/HD-like		28,73	1,82	1,00	28,92	1,77	1,00	24,47	1,86	1,00	26,40	1,89	1,00	27,39	1,79	1,00	26,64	1,84	1,00
TF581	TCP		31,63	1,92	1,00	31,61	1,88	1,00	31,98	1,73	1,00	32,32	1,76	1,00	31,19	1,58	1,00	30,23	1,79	1,00
TF582	BD		22,08	1,95	1,00	22,23	2,01	1,00	22,62	1,98	1,00	22,73	1,92	1,00	22,22	1,97	1,00	21,92	1,97	1,00
TF583	GRF		32,07	1,78	1,00	30,88	1,79	1,00	26,08	1,87	1,00	31,83	1,91	1,00	33,96	1,70	1,00	29,86	1,82	1,00
TF584	JUMONJI		24,43	1,94	1,00	24,36	1,90	1,00	21,74	2,08	1,00	23,72	1,83	1,00	24,31	2,00	1,00	23,74	1,86	1,00
TF585	C_2H_2 (Zn)		32,71	2,06	0,99	27,89	1,75	1,00	22,79	1,90	1,00	27,43	1,86	1,00	25,36	1,85	1,00	27,30	1,78	1,00
TF586	RR		23,43	1,80	1,00	25,09	2,06	1,00	23,41	2,00	0,99	24,51	1,79	1,00	23,63	1,76	1,00	23,29	2,06	1,00
TF587	AP2/EREBP		25,57	2,02	1,00	25,90	1,64	1,00	25,79	1,28	1,00	27,17	1,66	1,00	24,92	1,62	1,00	24,94	1,77	1,00
TF588	HD family	HD	19,83	1,99	1,00	19,92	1,99	1,00	20,50	1,91	1,00	19,70	1,86	1,00	19,58	2,02	1,00	18,85	2,09	1,00
TF589	MBF		21,08	1,96	1,00	21,45	1,91	1,00	20,52	1,88	1,00	22,58	1,93	1,00	21,21	1,99	1,00	20,87	1,93	1,00
TF590	AS2		29,49	1,84	1,00	23,23	1,99	1,00	19,81	1,88	0,99	22,93	2,01	1,00	21,09	2,10	1,00	23,39	2,00	1,00
TF591	AP2/EREBP		29,50	1,79	1,00	28,92	1,74	1,00	29,86	1,79	1,00	29,32	1,68	1,00	27,91	1,96	1,00	27,69	1,94	1,00
TF592	MADS		27,29	1,76	1,00	27,46	1,79	1,00	21,72	1,94	1,00	24,40	1,91	1,00	23,16	1,98	1,00	22,30	2,04	1,00
TF593	HD-like		27,06	1,89	1,00	26,28	1,63	1,00	26,40	1,74	1,00	27,41	1,67	1,00	26,53	1,70	1,00	25,91	1,76	1,00
TF594	bZIP		31,02	1,35	1,00	28,05	1,85	1,00	25,26	2,01	1,00	30,21	1,80	1,00	30,55	1,82	1,00	27,58	1,99	1,00
TF595	ABI3-VP1		39,18	1,33	1,00	35,10	1,74	1,00	26,77	1,78	1,00	30,06	1,73	1,00	29,88	1,89	1,00	28,86	1,97	1,00
TF596	ABI3-VP1		34,97	1,71	1,00	34,62	1,67	1,00	27,32	1,94	1,00	31,00	1,70	1,00	30,74	1,76	1,00	30,96	1,72	1,00
TF597	NAC		21,00	1,87	1,00	21,09	1,22	1,00	21,84	1,78	1,00	22,59	2,08	1,00	21,69	1,80	1,00	21,45	2,01	1,00
TF598	NAC		22,50	1,89	1,00	22,72	1,97	1,00	21,95	1,88	1,00	22,97	1,90	1,00	22,79	1,99	1,00	22,16	1,95	1,00
TF599	AP2/EREBP		26,24	1,82	1,00	25,81	1,77	1,00	21,98	1,94	1,00	26,21	1,90	1,00	24,83	1,99	1,00	24,15	1,86	1,00
TF600	bHLH		24,21	1,89	1,00	24,17	2,03	1,00	24,25	1,88	1,00	23,69	1,98	1,00	23,11	1,83	1,00	22,94	1,90	1,00

Table S1, continued

TF601	AP2/EREBP		25,71	1,78	1,00	24,01	1,94	1,00	20,73	1,89	1,00	23,70	1,89	1,00	22,68	1,84	1,00	24,45	1,83	1,00
TF602	bHLH		22,31	1,99	1,00	22,04	1,88	1,00	19,46	1,92	1,00	22,34	1,83	1,00	20,95	1,91	1,00	21,92	1,91	1,00
TF603	BED-type (Zn)		23,23	1,80	1,00	23,24	1,79	1,00	19,57	1,94	1,00	20,95	1,85	1,00	21,48	1,89	1,00	20,87	1,95	1,00
TF604	CCAAT	CCAAT-HAP3	23,95	1,64	1,00	24,27	2,20	1,00	25,19	1,92	1,00	23,92	1,88	1,00	23,50	2,09	1,00	22,83	1,84	1,00
TF605	PHD		22,80	1,96	1,00	22,52	1,78	1,00	21,98	1,89	1,00	22,79	1,87	1,00	22,92	1,78	1,00	22,20	1,95	1,00
TF606	ARID		26,85	1,87	1,00	27,05	1,89	1,00	22,63	1,87	1,00	24,33	1,81	1,00	25,84	1,84	1,00	24,73	1,90	1,00
TF607	C_2C_2 (Zn)	GATA	29,14	1,94	1,00	28,56	1,86	1,00	26,09	1,88	1,00	27,47	1,89	1,00	28,14	1,90	1,00	27,76	1,90	1,00
TF608	C_2C_2 (Zn)	GATA	27,72	1,90	1,00	27,67	1,98	1,00	24,43	1,72	1,00	27,95	1,69	1,00	26,90	1,75	1,00	26,41	1,76	1,00
TF609	MYB		25,84	1,93	1,00	25,59	1,92	1,00	22,66	2,12	1,00	n.d.	1,31	0,95	24,41	1,97	1,00	25,60	1,85	1,00
TF610	TCP		21,42	1,89	1,00	21,32	1,92	1,00	21,63	1,96	1,00	22,79	1,90	1,00	22,64	1,91	1,00	22,49	1,93	1,00
TF611	bHLH		23,39	1,95	1,00	23,10	1,79	1,00	23,09	1,86	0,99	23,81	1,85	1,00	23,07	1,88	1,00	22,74	1,83	1,00
TF612	MYB/HD-like		23,96	1,96	1,00	23,98	1,79	1,00	23,22	1,88	1,00	23,70	1,88	1,00	23,85	1,85	1,00	23,19	1,92	1,00
TF613	GRAS		25,03	1,92	1,00	24,81	1,90	1,00	21,88	1,85	1,00	22,63	1,79	1,00	23,36	1,94	1,00	22,92	1,86	1,00
TF614	MYB/HD-like		26,11	1,73	1,00	26,31	1,83	1,00	24,75	1,71	1,00	27,23	1,82	1,00	25,58	1,22	1,00	25,29	1,85	1,00
TF615	C_2H_2 (Zn)		22,13	1,77	1,00	18,98	1,95	1,00	15,68	1,40	0,98	23,24	1,86	1,00	22,79	1,87	1,00	16,79	1,97	1,00
TF616	C_2H_2 (Zn)		29,34	1,79	1,00	26,11	1,74	1,00	21,91	1,67	1,00	30,55	2,00	1,00	29,32	1,82	1,00	24,23	1,93	1,00
TF617	MYB/HD-like		25,98	1,96	1,00	26,26	1,86	1,00	25,01	1,72	1,00	26,58	1,29	1,00	25,87	1,87	1,00	25,56	1,88	1,00
TF618	HD family	HD	29,33	1,84	1,00	29,44	1,85	1,00	23,24	1,87	1,00	25,42	1,94	1,00	26,38	1,97	1,00	26,00	1,91	1,00
TF619	MADS		31,55	1,79	1,00	30,05	2,00	0,99	23,40	1,91	1,00	27,94	1,85	1,00	24,96	1,85	1,00	28,49	1,82	1,00
TF620	MADS		34,41	1,63	1,00	27,37	2,24	1,00	23,40	1,76	1,00	27,23	1,85	1,00	24,97	1,83	1,00	28,06	1,72	1,00
TF621	C3H	C3H-type 1 (Zn)	23,46	1,93	1,00	23,56	1,93	1,00	23,82	1,96	1,00	23,67	1,87	1,00	23,30	2,15	1,00	22,95	1,84	1,00
TF622	CCHC (Zn)		29,68	1,81	1,00	30,20	1,78	1,00	25,52	1,90	1,00	26,64	1,90	1,00	28,05	1,79	1,00	27,57	1,85	1,00
TF623	bHLH		24,08	1,93	1,00	24,02	1,84	1,00	24,26	1,92	1,00	24,62	1,88	1,00	24,57	1,93	1,00	24,10	2,07	1,00
TF624	HD-like		27,47	1,89	1,00	27,57	1,94	1,00	23,88	1,95	1,00	25,57	1,94	1,00	27,14	1,95	1,00	26,62	1,93	1,00
TF625	HD-like		26,20	1,85	1,00	26,13	1,85	1,00	23,39	2,00	1,00	24,47	1,81	1,00	24,32	1,84	1,00	24,15	1,90	1,00
TF626	HD-like		29,21	1,83	1,00	29,21	1,84	1,00	23,40	1,94	1,00	25,33	1,89	1,00	27,30	1,85	1,00	26,27	1,90	1,00
TF627	AP2/EREBP		27,58	1,71	1,00	27,83	1,76	1,00	27,26	1,74	1,00	29,14	1,78	1,00	28,88	1,76	1,00	28,29	1,74	1,00
TF628	AP2/EREBP		22,35	1,93	1,00	22,41	1,22	1,00	22,40	1,92	1,00	23,22	1,87	1,00	22,92	1,90	1,00	22,72	1,99	1,00
TF629	AP2/EREBP		27,89	1,81	1,00	28,46	1,82	1,00	27,57	1,76	1,00	30,55	1,75	1,00	27,95	1,75	1,00	28,87	1,77	1,00
TF630	CCHC (Zn)		25,94	1,95	1,00	25,84	1,91	1,00	24,68	1,83	1,00	25,91	1,85	1,00	25,36	1,99	1,00	24,98	2,07	1,00
TF631	HSF		24,57	1,91	1,00	24,73	1,86	1,00	25,27	1,86	1,00	24,80	1,98	1,00	24,36	1,90	1,00	24,17	1,94	1,00
TF632	CCHC (Zn)		30,52	1,82	1,00	29,21	1,85	1,00	23,99	1,98	1,00	30,49	1,81	1,00	31,57	1,79	1,00	26,85	2,01	1,00
TF633	CCHC (Zn)		26,83	1,97	1,00	23,37	1,87	1,00	21,13	1,91	1,00	26,60	1,82	1,00	25,96	1,97	1,00	22,57	1,88	1,00
TF634	CCHC (Zn)		33,54	1,57	1,00	31,88	1,57	1,00	31,18	1,49	1,00	36,43	1,51	1,00	36,09	1,88	1,00	33,66	1,64	1,00
TF635	MADS		30,01	1,88	1,00	28,85	1,59	1,00	24,97	1,83	1,00	26,82	1,78	1,00	26,72	1,94	1,00	25,88	2,11	1,00
TF636	MADS		29,59	1,76	1,00	27,06	1,78	1,00	24,80	1,49	1,00	27,36	1,76	1,00	27,45	1,87	1,00	25,90	1,83	1,00
TF637	MADS		27,77	2,00	1,00	27,18	1,89	1,00	27,95	1,88	1,00	27,02	1,86	1,00	22,99	2,01	1,00	26,33	1,98	1,00
TF638	CCHC (Zn)		30,45	1,85	1,00	29,66	1,80	1,00	27,58	1,50	1,00	32,09	1,74	1,00	30,86	1,82	1,00	28,55	1,89	1,00
TF639	bHLH		22,31	1,93	1,00	22,35	1,88	1,00	23,08	1,93	1,00	22,72	1,86	1,00	21,94	1,84	1,00	21,75	1,92	1,00
TF640	RR		30,46	1,79	1,00	25,61	1,89	1,00	20,24	2,06	1,00	23,42	1,94	1,00	22,84	1,96	1,00	24,91	1,91	1,00
TF641	MYB		25,53	1,79	1,00	25,35	1,83	1,00	25,95	1,81	1,00	26,49	1,90	1,00	25,70	1,86	1,00	25,30	1,81	1,00
TF642	CCHC (Zn)		25,93	1,88	1,00	25,93	1,93	1,00	22,93	1,89	1,00	27,98	1,77	1,00	26,12	1,95	1,00	23,65	2,03	1,00
TF643	HD family	HD	24,15	1,65	1,00	24,32	1,76	1,00	23,42	1,90	1,00	23,61	1,96	1,00	23,14	1,82	1,00	22,87	1,84	1,00

Table S1, continued

TF644	CCHC (Zn)		30,80	1,81	1,00	31,58	1,87	1,00	24,98	1,91	1,00	27,68	1,88	1,00	28,63	1,84	1,00	27,51	1,93	1,00
TF645	FHA		23,67	1,91	1,00	23,78	1,89	1,00	23,99	1,85	1,00	24,12	1,96	1,00	23,57	1,92	1,00	23,26	1,89	1,00
TF646	C_2C_2 (Zn)	GATA	28,49	1,78	1,00	28,38	1,78	1,00	28,39	1,79	1,00	27,02	1,76	1,00	26,39	1,86	1,00	25,88	1,84	1,00
TF647	bZIP		25,69	1,81	1,00	25,96	1,84	1,00	26,32	1,82	1,00	25,33	1,87	1,00	24,91	1,91	1,00	24,25	1,78	1,00
TF648	HTH	AraC	23,27	1,91	1,00	23,13	1,93	1,00	20,81	2,04	1,00	23,25	1,87	1,00	21,91	1,99	1,00	21,69	2,09	1,00
TF649	C3H	C3H-type 1 (Zn)	21,90	1,99	1,00	21,60	2,00	1,00	18,77	2,09	1,00	20,05	2,00	1,00	20,86	1,96	1,00	20,75	1,93	1,00
TF650	C_2C_2 (Zn)	CO-like	25,96	1,85	1,00	26,29	1,82	1,00	26,18	1,84	1,00	25,93	2,00	1,00	25,27	1,96	1,00	24,98	1,90	1,00
TF651	SRS		25,13	1,85	1,00	25,40	1,88	1,00	19,86	1,90	1,00	21,92	1,88	1,00	23,30	1,97	1,00	22,38	2,03	1,00
TF652	ZF DHHC		22,95	1,80	1,00	22,89	1,25	1,00	20,43	2,02	1,00	21,41	1,84	1,00	21,55	1,99	1,00	21,07	2,09	1,00
TF653	ZF DHHC		22,88	1,91	1,00	22,96	1,88	1,00	21,26	1,68	1,00	22,18	2,10	1,00	21,38	1,87	1,00	20,97	1,58	1,00
TF654	NAC		26,36	1,94	1,00	26,82	1,76	1,00	21,93	1,87	1,00	24,24	1,89	1,00	24,97	1,93	1,00	24,29	1,98	1,00
TF655	ABI3-VP1		29,30	1,82	1,00	29,55	1,83	1,00	24,56	1,91	1,00	25,88	1,87	1,00	27,43	1,96	1,00	26,98	1,91	1,00
TF656	CCHC (Zn)		23,79	1,95	1,00	23,88	1,88	1,00	24,11	1,90	1,00	23,83	1,95	1,00	23,56	1,89	1,00	23,18	1,88	1,00
TF657	CCHC (Zn)		24,30	1,96	1,00	23,46	1,94	1,00	21,51	1,88	1,00	24,56	1,89	1,00	24,37	1,95	1,00	22,53	1,93	1,00
TF658	CCHC (Zn)		29,33	1,80	1,00	30,77	1,75	1,00	26,78	1,87	1,00	28,28	1,83	1,00	28,32	1,80	1,00	28,24	1,81	1,00
TF659	MYB/HD-like		28,53	1,92	1,00	29,39	2,01	1,00	24,82	1,91	1,00	28,15	1,94	1,00	27,86	1,86	1,00	27,41	1,81	1,00
TF660	CCHC (Zn)		23,78	1,93	1,00	23,71	1,93	1,00	20,75	1,96	1,00	21,55	1,94	1,00	22,39	1,89	1,00	22,07	1,98	1,00
TF661	C_2H_2 (Zn)		27,53	1,80	1,00	25,32	1,79	1,00	23,67	1,60	0,99	28,30	1,86	1,00	28,08	1,86	1,00	24,43	2,22	1,00
TF662	WRKY family	WRKY	24,59	1,93	1,00	24,71	1,88	1,00	20,46	1,81	1,00	22,09	1,95	1,00	23,61	1,86	1,00	23,14	1,92	1,00
TF663	WRKY family	WRKY	26,63	1,84	1,00	26,56	1,75	1,00	23,48	1,72	1,00	25,17	1,78	1,00	25,07	1,79	1,00	24,52	1,79	1,00
TF664	RR		34,78	1,66	0,99	25,70	1,79	1,00	25,35	1,80	1,00	24,79	1,88	1,00	26,24	1,59	0,99	28,61	1,71	1,00
TF665	MYB/HD-like		23,53	1,96	1,00	23,77	1,95	1,00	23,09	1,82	1,00	23,37	1,91	1,00	23,08	1,91	1,00	22,88	1,91	1,00
TF666	HD-like		21,41	1,93	1,00	21,46	2,14	1,00	21,61	1,95	1,00	21,80	1,85	1,00	21,47	1,92	1,00	21,12	1,92	1,00
TF667	HD family	HD-ZIP	27,92	1,88	1,00	27,93	1,87	1,00	25,74	1,79	1,00	27,60	1,87	1,00	28,27	1,79	1,00	27,18	1,81	1,00
TF668	HMG		25,95	1,87	1,00	25,83	1,96	1,00	23,47	1,91	1,00	25,80	1,93	1,00	25,62	1,93	1,00	25,63	1,93	1,00
TF669	bZIP		25,69	1,92	1,00	25,91	1,88	1,00	21,52	1,92	1,00	23,97	2,01	1,00	26,21	1,77	1,00	24,59	1,94	1,00
TF670	bZIP		24,23	1,81	1,00	23,82	1,80	1,00	23,55	1,75	1,00	22,85	1,85	1,00	22,96	1,83	1,00	22,53	1,81	1,00
TF671	GRAS		31,95	1,85	1,00	30,50	1,86	1,00	24,94	1,93	1,00	27,21	2,05	1,00	26,64	1,84	1,00	25,85	1,88	1,00
TF672	GRAS		35,16	1,70	1,00	35,21	1,67	1,00	34,14	1,79	1,00	n.d.	1,19	0,98	35,73	1,63	1,00	33,72	1,71	1,00
TF673	CCHC (Zn)		25,37	1,98	1,00	24,58	2,02	1,00	21,47	1,93	1,00	24,88	1,90	1,00	25,65	2,00	1,00	23,00	2,05	1,00
TF674	MYB		21,63	1,94	1,00	21,80	1,93	1,00	16,70	2,01	1,00	19,35	1,94	1,00	19,89	2,09	1,00	19,56	1,94	1,00
TF675	TTF-type (Zn)		32,96	1,90	1,00	32,89	1,85	1,00	25,82	1,97	1,00	29,40	1,85	1,00	30,35	1,86	1,00	29,64	1,86	1,00
TF676	MYB		23,46	1,88	1,00	23,49	1,87	1,00	22,82	1,92	1,00	23,81	1,74	1,00	23,56	1,93	1,00	23,19	1,81	1,00
TF677	GRF		33,69	1,50	1,00	32,78	1,61	1,00	25,19	1,75	1,00	30,47	1,53	1,00	32,95	1,26	1,00	27,99	1,86	1,00
TF678	RR		33,16	1,72	1,00	25,27	1,91	1,00	21,92	1,99	1,00	25,06	1,88	1,00	24,61	1,81	1,00	26,38	1,84	1,00
TF679	RR		26,65	1,98	1,00	26,67	1,84	1,00	27,92	2,38	1,00	27,91	1,92	1,00	20,29	1,98	1,00	27,18	1,91	1,00
TF680	MYB/HD-like		25,81	1,91	1,00	23,09	1,93	1,00	19,00	2,03	1,00	26,07	1,81	1,00	26,33	1,90	1,00	21,40	1,93	1,00
TF681	MYB/HD-like		29,17	1,72	1,00	26,04	2,47	1,00	22,90	1,86	1,00	30,48	1,81	1,00	29,88	1,74	1,00	25,99	1,99	1,00
TF682	ssDB TR		23,49	1,93	1,00	23,40	1,91	1,00	22,95	1,83	1,00	23,90	2,14	1,00	23,93	2,06	1,00	23,09	1,88	1,00
TF683	SBP		25,54	1,94	1,00	24,61	1,83	1,00	21,57	1,86	1,00	25,89	1,84	1,00	25,85	1,87	1,00	23,20	2,08	1,00
TF684	C_2C_2 (Zn)	DOF	26,05	1,74	1,00	26,44	1,78	1,00	27,54	2,19	1,00	25,28	1,73	1,00	24,99	1,92	1,00	24,30	1,90	1,00
TF685	C_2C_2 (Zn)	DOF	28,81	1,76	1,00	28,65	1,82	1,00	23,62	1,98	1,00	24,95	1,89	1,00	26,82	1,81	1,00	26,17	1,88	1,00
TF686	C3H	C3H-type 1 (Zn)	23,85	1,92	1,00	23,19	1,92	1,00	22,56	1,87	1,00	23,36	1,87	1,00	23,23	1,94	1,00	22,27	1,91	1,00

Table S1, continued

TF687	BTB/POZ		21,75	1,95	1,00	22,05	2,13	1,00	22,19	1,94	1,00	23,53	1,95	1,00	22,96	1,95	1,00	22,59	1,91	1,00
TF688	bHLH		27,11	1,93	1,00	26,94	1,92	1,00	26,71	1,80	1,00	26,66	1,81	1,00	26,43	1,77	1,00	26,38	1,89	1,00
TF689	AUX/IAA		22,47	2,69	1,00	22,56	1,73	1,00	24,67	1,83	1,00	24,72	1,86	1,00	23,24	1,81	1,00	22,59	1,90	1,00
TF690	bZIP		24,27	1,75	1,00	24,21	1,82	1,00	24,78	1,96	1,00	24,04	1,82	0,99	23,57	1,83	1,00	23,03	1,92	1,00
TF691	E2F		22,15	2,00	1,00	19,71	2,01	1,00	17,55	2,25	0,99	22,28	2,03	1,00	23,62	1,87	1,00	19,14	2,24	1,00
TF692	E2F		24,13	1,86	1,00	24,36	1,90	1,00	24,93	1,82	1,00	24,94	1,76	1,00	24,85	1,82	1,00	24,42	1,71	1,00
TF693	CCHC (Zn)		28,47	1,68	1,00	28,37	1,70	1,00	24,41	1,76	1,00	27,40	1,61	1,00	26,85	1,69	1,00	26,77	1,74	1,00
TF694	ARF		31,00	1,70	1,00	30,37	1,69	1,00	23,77	1,81	1,00	26,40	1,79	1,00	27,21	1,78	1,00	26,54	1,75	1,00
TF695	ARF		32,79	1,81	1,00	33,09	1,78	1,00	28,79	1,79	1,00	35,43	1,74	1,00	32,85	1,79	1,00	32,80	1,76	1,00
TF696	ARF		22,17	1,85	1,00	18,44	1,89	1,00	15,39	1,23	0,99	17,57	1,49	0,99	15,99	1,33	0,99	17,56	2,37	0,99
TF697	ARF		30,50	1,76	1,00	28,23	2,11	1,00	22,95	1,88	1,00	26,32	1,81	1,00	25,83	1,84	1,00	27,97	1,84	1,00
TF698	MYB		23,91	1,99	1,00	24,28	1,98	1,00	23,44	1,94	1,00	25,01	2,06	1,00	23,87	1,89	1,00	23,69	1,92	1,00
TF699	GRAS		25,05	1,88	1,00	23,22	1,95	1,00	19,38	1,99	1,00	22,87	1,97	1,00	21,86	1,84	1,00	23,29	1,98	1,00
TF700	BTB/POZ		19,99	1,87	1,00	20,09	1,94	1,00	19,88	1,82	1,00	22,91	1,93	1,00	23,19	2,02	1,00	22,67	1,89	1,00
TF701	bZIP		29,94	1,96	1,00	26,53	1,79	1,00	24,09	1,80	1,00	30,09	1,96	1,00	30,23	1,99	1,00	25,68	2,07	1,00
TF702	bZIP		29,62	1,84	1,00	29,17	1,92	1,00	23,16	1,99	1,00	25,66	2,05	1,00	27,54	1,93	1,00	26,72	1,94	1,00
TF703	HD-like		29,09	1,83	1,00	27,52	1,80	1,00	23,34	1,74	1,00	28,71	1,76	1,00	24,61	1,79	1,00	27,14	1,79	1,00
TF704	HD-like		29,35	1,80	1,00	26,80	1,79	0,99	26,00	1,91	1,00	29,19	1,72	1,00	29,66	1,62	1,00	25,90	1,95	1,00
TF705	Tc/PD		22,81	2,02	1,00	22,94	1,85	1,00	23,01	1,89	1,00	23,75	1,87	1,00	23,32	1,88	1,00	22,91	1,91	1,00
TF706	GRAS		29,03	1,80	1,00	28,97	1,84	1,00	23,72	1,88	1,00	26,14	1,86	1,00	27,46	1,76	1,00	26,31	1,73	1,00
TF707	AP2/EREBP		31,03	1,85	1,00	29,66	1,84	1,00	26,14	1,92	1,00	32,70	1,82	1,00	32,12	1,82	1,00	28,87	1,83	1,00
TF708	SNF2		27,34	1,88	1,00	27,36	1,92	1,00	21,08	1,86	1,00	23,38	1,92	1,00	26,32	1,88	1,00	24,75	1,87	1,00
TF709	bHLH		28,76	2,12	1,00	28,36	1,91	1,00	23,06	2,05	1,00	25,30	1,81	1,00	26,26	1,85	1,00	25,33	1,87	1,00
TF710	SNF2		22,26	1,88	1,00	22,42	1,96	1,00	18,87	1,99	1,00	21,10	2,01	1,00	21,79	1,91	1,00	21,19	1,89	1,00
TF711	C_2C_2 (Zn)	YABBY	22,39	1,92	1,00	22,68	1,94	1,00	23,02	1,83	1,00	23,62	1,85	1,00	23,41	1,93	1,00	22,86	1,90	1,00
TF712	CCHC (Zn)		31,21	1,84	1,00	29,04	1,88	1,00	26,10	1,86	1,00	30,13	1,81	0,98	31,44	1,90	1,00	27,59	1,98	1,00
TF713	CCHC (Zn)		35,77	1,71	1,00	31,29	1,71	1,00	27,97	1,78	1,00	36,04	1,68	1,00	n.d.	1,46	1,00	29,41	1,92	1,00
TF714	HD family	HD	23,91	1,90	1,00	24,32	1,86	1,00	21,79	1,88	1,00	22,90	1,86	1,00	23,57	1,89	1,00	22,95	1,89	1,00
TF715	C_2C_2 (Zn)	GATA	25,13	2,01	1,00	25,11	1,97	1,00	21,39	2,00	1,00	23,25	1,87	1,00	23,84	1,92	1,00	23,73	1,92	1,00
TF716	C_2C_2 (Zn)	GATA	25,65	1,83	1,00	25,53	1,83	1,00	25,66	1,87	1,00	27,65	1,91	1,00	26,87	1,87	1,00	26,84	1,84	1,00
TF717	FHA		25,16	1,79	1,00	25,96	1,80	1,00	23,61	1,95	1,00	27,62	1,72	1,00	25,41	1,86	1,00	24,59	1,79	1,00
TF718	CCHC (Zn)		31,12	1,61	1,00	29,82	1,70	1,00	26,20	1,73	1,00	27,79	1,81	1,00	27,14	1,71	1,00	26,40	1,81	1,00
TF719	GRF		30,39	1,64	1,00	29,77	1,69	1,00	27,93	1,62	1,00	31,09	1,56	1,00	30,18	1,80	1,00	28,83	1,77	1,00
TF720	CCHC (Zn)		25,90	1,84	1,00	25,89	1,94	1,00	20,72	1,91	1,00	22,27	2,10	1,00	24,26	1,97	1,00	22,50	1,89	1,00
TF721	MYB/HD-like		26,16	1,99	1,00	27,36	1,92	1,00	24,99	2,00	1,00	27,21	1,89	1,00	28,36	1,88	1,00	26,99	1,89	1,00
TF722	MYB/HD-like		30,90	1,79	1,00	27,68	1,87	1,00	22,87	2,05	1,00	30,54	1,73	1,00	32,51	1,76	1,00	26,38	1,84	1,00
TF723	MYB		34,16	1,80	1,00	25,73	1,90	1,00	21,15	1,99	1,00	25,26	2,01	1,00	23,80	1,94	1,00	26,35	2,00	1,00
TF724	MYB		32,12	1,30	1,00	28,44	1,83	1,00	23,45	2,04	1,00	26,22	1,74	1,00	26,55	1,82	1,00	28,19	1,90	1,00
TF725	AP2/EREBP		28,31	1,88	1,00	23,63	1,93	1,00	20,20	1,93	1,00	22,72	1,91	1,00	21,36	1,93	1,00	24,13	1,94	1,00
TF726	MYB/HD-like		23,54	1,88	1,00	23,60	1,95	1,00	23,92	1,83	1,00	23,75	1,82	1,00	22,79	1,86	1,00	22,64	1,87	1,00
TF727	C_2H_2 (Zn)		23,68	1,94	1,00	24,00	1,97	1,00	22,67	1,89	1,00	24,51	1,91	1,00	23,05	1,88	1,00	23,13	1,93	1,00
TF728	C_2H_2 (Zn)		31,29	1,73	1,00	27,93	1,75	1,00	23,38	1,93	1,00	25,91	1,84	1,00	24,76	1,77	1,00	27,35	1,76	1,00
TF729	C_2H_2 (Zn)		38,50	1,34	0,98	31,57	1,88	1,00	24,64	1,65	1,00	28,15	1,77	1,00	27,17	1,85	1,00	29,03	1,63	1,00

Table S1, continued

TF730	MYB/HD-like		27,06	2,00	1,00	21,40	2,13	1,00	18,94	2,17	1,00	25,01	1,96	1,00	26,06	1,94	1,00	20,41	1,93	1,00
TF731	MYB/HD-like		26,63	1,87	1,00	26,60	1,87	1,00	21,40	1,89	1,00	22,66	1,89	1,00	24,15	1,91	1,00	23,69	1,95	1,00
TF732	MYB		28,94	1,77	1,00	28,99	1,76	1,00	23,05	1,79	1,00	25,42	1,80	1,00	26,16	1,82	1,00	25,01	1,81	1,00
TF733	MYB		29,19	1,77	1,00	29,38	1,80	1,00	23,94	1,83	1,00	24,90	1,98	1,00	26,41	1,98	1,00	26,30	1,81	1,00
TF734	MYB		27,35	1,84	1,00	26,90	2,02	1,00	25,04	2,01	1,00	28,39	1,91	1,00	27,69	1,88	1,00	26,12	1,88	1,00
TF735	CCHC (Zn)		35,35	1,67	1,00	29,49	1,72	1,00	27,29	1,72	1,00	37,82	1,63	1,00	37,93	1,60	1,00	28,19	1,77	1,00
TF736	MYB		27,46	1,87	1,00	27,62	1,86	1,00	27,57	1,84	1,00	29,47	1,85	1,00	28,35	1,87	1,00	27,36	1,82	1,00
TF737	AS2		26,99	2,01	1,00	21,37	1,94	1,00	18,40	2,04	1,00	21,29	1,92	1,00	20,03	1,96	1,00	21,77	2,02	1,00
TF738	MBF		22,34	2,59	1,00	23,33	1,97	1,00	24,32	1,70	1,00	25,11	1,64	0,99	22,52	2,25	1,00	22,08	1,23	1,00
TF739	CCHC (Zn)		20,98	1,97	1,00	20,69	2,05	1,00	20,10	1,89	1,00	21,61	2,18	1,00	21,49	1,97	1,00	20,46	1,95	1,00
TF740	CCHC (Zn)		24,24	2,05	1,00	22,82	1,98	1,00	19,14	1,98	1,00	24,34	2,02	0,99	25,43	1,93	1,00	20,53	2,08	1,00
TF741	MYB/HD-like		25,75	1,91	1,00	26,18	1,94	1,00	24,50	1,75	1,00	25,97	1,75	1,00	27,03	1,81	1,00	27,12	1,82	1,00
TF742	AS2		n.d.	1,26	0,99	35,27	1,55	1,00	31,49	1,65	1,00	35,69	1,49	1,00	34,66	1,55	1,00	36,72	1,51	1,00
TF743	MYB/HD-like		30,37	1,68	1,00	32,44	1,67	1,00	28,37	1,67	1,00	30,06	1,57	1,00	30,76	1,77	1,00	29,54	1,76	1,00
TF744	MYB/HD-like		28,01	1,87	1,00	28,70	2,07	1,00	20,27	1,92	1,00	23,45	1,85	1,00	24,37	1,95	1,00	23,61	1,95	1,00
TF745	SSB protein		38,43	1,65	1,00	37,90	1,69	1,00	30,49	1,70	1,00	33,05	1,81	1,00	26,43	1,87	1,00	39,09	1,45	0,99
TF746	TUB		26,48	1,91	1,00	22,22	1,90	1,00	20,35	1,91	1,00	26,33	1,86	1,00	26,58	1,91	1,00	21,68	1,93	1,00
TF747	HD family	HD	28,73	1,61	1,00	29,77	1,63	1,00	34,76	1,53	1,00	32,65	1,58	1,00	30,69	1,62	1,00	30,28	1,63	1,00
TF748	ARF		21,69	1,89	1,00	21,63	1,86	1,00	21,59	1,82	1,00	21,54	2,02	1,00	21,32	1,84	1,00	21,10	1,91	1,00
TF749	ARF		24,81	1,94	1,00	24,32	1,92	1,00	20,60	1,98	1,00	20,72	1,87	1,00	21,38	1,90	1,00	20,87	2,07	1,00
TF750	WRKY family	WRKY	33,13	1,82	1,00	29,48	1,64	1,00	24,92	1,84	1,00	27,96	1,83	1,00	27,69	1,94	1,00	28,92	1,86	1,00
TF751	TTF-type (Zn)		27,97	1,67	1,00	27,59	1,70	1,00	25,29	1,74	1,00	26,48	1,75	1,00	26,24	1,62	1,00	25,22	1,81	1,00
TF752	MADS		33,46	1,60	1,00	30,57	1,65	1,00	23,33	1,79	1,00	32,35	1,63	1,00	32,43	1,63	1,00	27,47	1,86	1,00
TF753	CCHC (Zn)		25,07	1,91	1,00	25,98	1,86	1,00	20,23	2,00	1,00	24,45	1,91	1,00	23,53	1,91	1,00	22,91	1,92	1,00
TF754	C_2C_2 (Zn)	CO-like	21,39	1,94	1,00	21,46	1,90	1,00	21,93	1,93	1,00	19,76	2,00	1,00	19,71	2,04	1,00	19,32	1,93	1,00
TF755	C3H	C3H-type 1 (Zn)	23,90	2,30	0,98	21,19	1,83	1,00	18,89	1,83	1,00	23,47	1,99	1,00	23,67	1,99	1,00	20,44	1,92	1,00
TF756	bHLH		24,27	1,85	1,00	24,25	1,33	1,00	23,95	1,87	1,00	25,70	1,27	1,00	25,41	1,89	1,00	23,95	1,87	1,00
TF757	LIM		22,55	1,55	1,00	22,90	1,39	1,00	22,51	1,33	1,00	23,93	1,42	1,00	18,65	1,23	1,00	21,45	1,39	1,00
TF758	Euk_TF		21,64	1,89	1,00	20,98	1,86	1,00	19,36	1,86	1,00	21,86	1,90	1,00	21,86	1,89	1,00	20,31	1,92	1,00
TF759	YEATS		23,29	1,92	1,00	23,94	1,87	1,00	23,74	1,91	1,00	24,83	2,04	1,00	21,11	1,86	1,00	23,78	2,04	1,00
TF760	C3H	C3H-type 1 (Zn)	20,72	1,90	1,00	20,95	1,93	1,00	21,27	1,95	1,00	20,99	1,88	1,00	20,84	1,90	1,00	20,73	1,88	1,00
TF761	C3H	C3H-type 1 (Zn)	20,69	1,90	1,00	20,78	1,80	1,00	21,05	1,86	1,00	21,36	1,89	1,00	20,76	1,93	1,00	20,67	2,03	1,00
TF762	bHLH		23,66	1,87	1,00	23,84	1,85	1,00	20,11	1,86	1,00	21,85	1,95	1,00	22,60	1,90	1,00	21,83	1,74	1,00
TF763	CCHC (Zn)		26,80	1,89	1,00	27,10	1,87	1,00	25,75	1,87	1,00	27,62	1,78	1,00	26,72	1,84	1,00	25,94	1,91	1,00
TF764	YEATS		23,28	1,90	1,00	23,88	2,03	1,00	24,32	1,90	0,99	24,83	2,04	1,00	23,60	1,91	1,00	23,64	1,89	1,00
TF765	bZIP		22,98	1,91	1,00	22,89	1,87	1,00	22,86	1,95	1,00	23,40	1,89	1,00	23,39	1,95	1,00	22,78	1,97	1,00
TF766	C3H	C3H-type 1 (Zn)	31,75	2,01	1,00	30,28	1,43	1,00	28,03	1,93	1,00	32,56	2,14	0,99	34,86	1,89	1,00	30,61	1,86	1,00
TF767	C3H	C3H-type 1 (Zn)	27,78	1,77	1,00	26,23	1,85	1,00	22,95	1,89	1,00	23,15	1,86	1,00	24,61	1,86	1,00	24,00	1,88	1,00
TF768	AP2/EREBP		29,03	1,95	1,00	27,10	2,05	1,00	24,29	1,85	1,00	30,30	1,63	1,00	30,76	2,16	1,00	25,77	1,92	1,00
TF769	AP2/EREBP		27,00	1,89	1,00	25,94	1,90	1,00	24,27	1,88	1,00	30,41	2,13	1,00	32,21	1,91	1,00	26,19	1,84	1,00
TF770	AP2/EREBP		28,46	1,89	1,00	27,23	1,93	1,00	23,77	1,89	1,00	30,38	1,97	1,00	30,38	1,87	1,00	26,29	1,89	1,00
TF771	AP2/EREBP		29,97	1,85	1,00	28,33	1,88	1,00	24,68	1,88	1,00	31,76	1,88	1,00	31,83	1,86	1,00	27,05	1,90	1,00
TF772	CCHC (Zn)		26,14	1,88	1,00	25,08	1,84	1,00	23,25	1,87	1,00	26,49	1,91	1,00	26,94	1,90	1,00	24,84	1,93	1,00

Table S1, continued

TF773	ABI3-VP1		n.d.	1,38	0,96	37,11	3,11	0,85	33,74	1,63	1,00	39,22	1,50	1,00	35,79	1,64	1,00	37,31	1,37	1,00
TF774	ABI3-VP1		28,10	1,86	1,00	26,68	1,94	1,00	24,52	1,87	1,00	29,49	1,76	1,00	29,88	1,85	1,00	26,02	1,95	1,00
TF775	MYB/HD-like		29,75	1,85	1,00	25,42	1,92	1,00	23,14	1,92	1,00	29,45	2,12	1,00	31,75	1,79	1,00	24,69	1,95	1,00
TF776	ABI3-VP1		27,84	1,96	1,00	27,72	1,72	1,00	27,94	1,75	1,00	28,11	1,67	1,00	28,24	1,72	1,00	27,62	1,77	1,00
TF777	ABI3-VP1		37,22	1,27	1,00	24,45	1,95	1,00	24,04	1,85	1,00	24,78	1,95	1,00	24,36	1,87	1,00	24,09	1,93	1,00
TF778	ABI3-VP1		26,29	1,86	1,00	26,30	1,91	1,00	25,60	1,76	1,00	27,50	1,83	1,00	27,34	1,91	1,00	26,55	1,93	1,00
TF779	ABI3-VP1		23,49	1,89	1,00	23,68	1,90	1,00	23,99	1,93	1,00	24,43	2,04	1,00	23,69	1,93	1,00	23,46	1,92	1,00
TF780	AUX/IAA		25,63	1,87	1,00	25,16	1,82	1,00	25,03	1,75	1,00	24,94	1,91	1,00	24,72	1,99	1,00	24,11	1,91	1,00
TF781	MYB/HD-like		23,99	1,81	1,00	24,30	1,90	1,00	18,58	1,88	1,00	23,85	1,82	1,00	23,83	1,97	1,00	20,43	1,94	1,00
TF782	HTH	FIS	29,61	1,74	0,98	35,25	1,34	1,00	32,22	1,74	1,00	39,72	1,26	1,00	28,32	1,85	1,00	n.d.	1,45	0,96
TF783	CCHC (Zn)		28,88	1,61	1,00	28,91	1,75	1,00	23,44	1,86	1,00	25,66	1,84	1,00	25,52	1,83	1,00	25,31	1,86	1,00
TF784	NAC		28,69	1,76	1,00	28,35	1,86	1,00	25,65	1,80	1,00	30,35	1,91	1,00	29,65	1,99	1,00	27,47	1,87	1,00
TF785	CCHC (Zn)		30,60	1,76	1,00	31,67	1,72	1,00	26,13	1,89	1,00	28,38	1,73	1,00	29,22	1,77	1,00	28,31	1,77	1,00
TF786	MADS		23,81	2,11	1,00	23,90	1,99	1,00	24,34	1,89	1,00	23,02	1,98	1,00	22,68	1,91	1,00	22,19	1,92	1,00
TF787	MADS		23,09	1,80	1,00	23,35	1,91	1,00	23,57	1,88	1,00	22,78	1,87	1,00	21,95	1,87	1,00	21,73	1,90	1,00
TF788	bHLH		28,70	1,85	1,00	24,26	1,93	1,00	21,91	1,91	1,00	28,32	1,97	1,00	29,33	1,85	1,00	23,41	1,90	1,00
TF789	bHLH		30,30	1,75	1,00	33,44	1,77	1,00	28,14	1,82	1,00	29,04	1,81	1,00	29,02	1,92	1,00	29,55	1,69	1,00
TF790	WRKY family	WRKY	26,36	1,82	1,00	24,57	2,28	1,00	24,07	1,64	1,00	27,42	1,58	1,00	26,46	1,82	1,00	23,00	1,91	1,00
TF791	DDT		24,73	1,90	1,00	25,04	1,82	1,00	24,97	1,82	1,00	25,13	1,89	1,00	24,28	1,93	1,00	24,01	1,91	1,00
TF792	TrpR		25,72	1,98	1,00	25,52	2,02	0,99	24,14	1,91	1,00	24,70	1,91	1,00	20,94	1,91	1,00	23,80	1,89	1,00
TF793	MYB/HD-like		27,53	1,80	1,00	27,48	1,90	1,00	26,34	1,78	1,00	27,76	1,77	1,00	26,97	1,95	1,00	26,26	1,88	1,00
TF794	MYB/HD-like		29,93	1,72	1,00	30,02	1,69	1,00	28,11	1,73	1,00	29,35	1,77	1,00	28,81	1,79	1,00	27,96	1,85	1,00
TF795	bHLH		29,03	1,96	1,00	28,61	1,80	1,00	23,59	1,95	1,00	26,12	1,84	1,00	24,85	1,84	1,00	24,37	1,82	1,00
TF796	GRF		28,37	1,87	1,00	29,02	1,78	1,00	27,11	1,79	1,00	26,97	1,79	1,00	26,69	1,82	1,00	26,24	1,87	1,00
TF797	HD-like		28,00	1,87	1,00	28,50	1,93	1,00	28,04	1,78	1,00	29,39	1,77	1,00	28,98	1,81	1,00	28,10	1,82	1,00
TF798	C_2H_2 (Zn)		22,70	1,94	1,00	22,77	1,88	1,00	17,85	1,97	1,00	19,63	1,98	1,00	20,97	1,91	1,00	20,38	2,00	1,00
TF799	C_2H_2 (Zn)		23,91	1,91	1,00	23,95	1,92	1,00	22,73	1,93	1,00	24,13	1,94	1,00	24,19	2,03	1,00	23,12	1,89	1,00
TF800	CCHC (Zn)		29,93	1,92	1,00	27,79	1,87	1,00	25,45	1,79	1,00	30,16	2,04	1,00	29,33	1,83	1,00	26,81	1,94	1,00
TF801	HD-like		23,55	1,89	1,00	23,64	1,88	1,00	23,83	1,85	1,00	24,23	1,89	1,00	24,08	1,96	1,00	23,49	1,91	1,00
TF802	CCHC (Zn)		27,14	1,80	1,00	23,95	1,83	1,00	22,00	1,86	1,00	28,25	1,84	1,00	29,35	1,78	1,00	23,28	1,97	1,00
TF803	ARF		29,92	1,76	1,00	29,04	1,86	1,00	25,63	1,79	1,00	26,92	1,80	1,00	28,85	1,75	1,00	28,47	1,73	1,00
TF804	ARF		27,39	1,86	1,00	27,21	1,91	1,00	21,87	1,88	1,00	23,20	1,89	1,00	24,82	1,81	1,00	24,54	1,86	1,00
TF805	CCHC (Zn)		30,16	1,66	1,00	27,31	1,74	1,00	24,79	1,75	1,00	30,09	1,16	1,00	30,27	1,70	1,00	25,75	1,76	1,00
TF806	bZIP		25,84	1,82	1,00	23,11	2,09	1,00	20,25	2,11	1,00	25,81	1,82	1,00	26,26	1,82	1,00	22,10	1,95	1,00
TF807	bZIP		27,57	1,80	1,00	26,37	1,90	1,00	22,58	1,83	1,00	25,12	1,88	1,00	23,86	1,75	1,00	25,46	1,82	1,00
TF808	MYB/HD-like		20,76	1,90	1,00	20,60	1,92	1,00	20,54	1,96	1,00	19,91	1,91	1,00	19,87	1,92	1,00	19,38	1,99	1,00
TF809	AP2/EREBP		26,73	1,80	1,00	26,33	1,79	1,00	23,00	1,90	1,00	24,80	1,87	1,00	26,18	1,90	1,00	25,56	1,95	1,00
TF810	HD family	HD-ZIP	23,13	1,92	1,00	23,25	1,87	1,00	23,50	1,79	1,00	22,87	1,89	1,00	22,75	1,93	1,00	22,15	1,93	1,00
TF811	MYB/HD-like		22,06	1,99	1,00	22,05	1,78	1,00	21,43	1,53	1,00	21,75	1,78	1,00	21,61	1,71	1,00	21,18	1,75	1,00
TF812	bHLH		21,79	1,94	1,00	21,51	1,96	1,00	19,97	2,30	1,00	22,02	1,97	1,00	22,52	1,97	1,00	20,55	1,95	1,00
TF813	ABI3-VP1		31,25	1,72	1,00	30,54	1,76	1,00	29,59	1,74	1,00	32,24	1,74	1,00	33,20	1,70	1,00	33,09	1,70	1,00
TF814	HD-like		24,06	1,83	1,00	24,04	2,00	1,00	19,01	2,18	1,00	21,29	1,92	1,00	22,19	1,86	1,00	21,32	1,92	1,00
TF815	bZIP		23,42	1,90	1,00	23,51	1,90	1,00	20,36	2,09	1,00	22,04	2,00	1,00	23,22	1,89	1,00	22,50	1,97	1,00

Table S1, continued

TF816	MYB/HD-like		23,67	1,85	1,00	23,62	1,72	1,00	23,71	1,87	1,00	23,19	1,88	1,00	23,34	1,89	1,00	22,82	1,92	1,00
TF817	C_2C_2 (Zn)	DOF	24,32	1,98	1,00	24,29	1,86	1,00	25,37	1,75	1,00	27,47	1,81	1,00	26,52	2,18	1,00	25,75	1,83	1,00
TF818	HD-like		23,19	1,93	1,00	23,37	1,95	1,00	23,19	1,90	1,00	23,95	1,91	1,00	23,56	1,87	1,00	23,32	1,93	1,00
TF819	MYB/HD-like		22,09	1,92	1,00	22,36	1,86	1,00	18,71	1,90	1,00	20,35	1,98	1,00	21,11	2,13	1,00	21,21	1,86	1,00
TF820	AP2/EREBP		29,81	1,75	1,00	28,98	1,79	1,00	25,57	1,82	1,00	27,63	1,74	1,00	27,41	1,76	1,00	28,22	1,85	1,00
TF821	AP2/EREBP		29,58	1,85	1,00	26,57	1,76	1,00	24,58	1,72	1,00	30,31	1,76	1,00	29,66	1,73	1,00	27,41	1,80	1,00
TF822	DDT		25,09	1,97	1,00	25,11	1,88	1,00	23,75	1,94	1,00	26,15	1,85	1,00	24,88	1,82	1,00	25,08	1,95	1,00
TF823	C_2H_2 (Zn)		28,46	1,95	1,00	27,67	1,95	1,00	25,02	1,99	1,00	27,40	2,27	1,00	27,44	2,06	1,00	26,69	2,12	1,00
TF824	C_2H_2 (Zn)		29,37	1,79	1,00	29,15	1,76	1,00	27,79	1,73	1,00	28,01	1,59	1,00	26,77	1,88	1,00	26,09	1,89	1,00
TF825	CCHC (Zn)		30,57	1,78	1,00	31,23	1,79	1,00	26,35	1,82	1,00	29,56	1,88	1,00	30,13	1,84	1,00	29,30	1,88	1,00
TF826	AS2		24,32	1,82	1,00	22,47	1,95	1,00	17,69	2,06	1,00	20,94	1,93	1,00	19,56	1,98	1,00	20,95	2,09	1,00
TF827	C_2C_2 (Zn)	DOF	23,74	1,85	1,00	23,96	1,81	1,00	22,43	1,89	1,00	24,41	1,92	1,00	23,52	1,93	1,00	23,44	1,88	1,00
TF828	bHLH		30,83	1,87	1,00	34,94	1,69	1,00	27,93	1,77	1,00	30,36	1,90	1,00	31,35	2,33	1,00	29,52	2,04	1,00
TF829	bHLH		24,15	1,84	1,00	24,24	1,82	1,00	21,66	1,80	1,00	22,94	1,81	1,00	23,34	1,88	1,00	22,75	1,83	1,00
TF830	PHD		23,99	1,79	1,00	24,10	1,97	1,00	21,22	1,97	1,00	22,06	2,01	1,00	23,53	1,75	1,00	23,08	1,87	1,00
TF831	RR		20,17	1,96	1,00	20,19	2,16	1,00	20,64	2,00	1,00	23,65	1,83	1,00	23,15	1,93	1,00	22,91	1,92	1,00
TF832	bZIP		21,84	1,89	1,00	21,75	1,97	1,00	22,10	1,82	1,00	22,13	1,88	1,00	21,32	1,91	1,00	20,64	1,94	1,00
TF833	HD-like		27,74	1,89	1,00	27,63	1,94	1,00	25,10	1,90	1,00	28,18	1,93	1,00	27,97	1,92	1,00	26,39	1,89	1,00
TF834	HD family	HD	27,08	1,92	1,00	25,44	1,89	1,00	21,92	1,75	1,00	24,89	1,85	1,00	24,87	1,90	1,00	24,51	2,19	1,00
TF835	bHLH		23,24	1,75	1,00	23,34	2,10	1,00	23,63	1,72	1,00	23,30	1,92	1,00	23,02	1,86	1,00	22,35	1,84	1,00
TF836	MYB		28,11	1,91	1,00	23,16	1,99	1,00	18,09	2,31	1,00	21,02	2,42	1,00	19,97	1,98	1,00	21,95	2,03	1,00
TF837	MYB		24,20	1,88	1,00	24,55	1,90	1,00	22,89	1,79	1,00	23,67	1,86	1,00	22,53	1,87	1,00	22,33	1,87	1,00
TF838	MYB/HD-like		25,01	1,95	1,00	22,75	1,81	1,00	20,20	2,09	1,00	25,51	1,92	1,00	26,43	2,03	1,00	21,83	2,19	1,00
TF839	MYB/HD-like		23,65	1,93	1,00	21,97	1,93	1,00	19,31	1,94	1,00	22,75	1,96	1,00	22,66	1,99	1,00	20,90	2,00	1,00
TF840	HD family	HD	23,65	1,92	1,00	23,80	2,04	1,00	23,21	1,84	1,00	24,05	1,79	1,00	23,29	1,85	1,00	22,84	1,95	1,00
TF841	NAC		26,16	1,77	1,00	25,95	1,83	1,00	23,38	1,88	1,00	25,84	1,78	1,00	24,41	1,76	1,00	24,80	1,87	1,00
TF842	PHD		20,00	1,98	1,00	20,18	1,96	1,00	20,53	1,93	1,00	20,94	1,88	1,00	20,64	1,93	1,00	20,39	2,01	1,00
TF843	HD-like		26,34	1,92	1,00	25,77	1,91	1,00	22,29	1,96	1,00	24,42	1,87	1,00	24,28	1,96	1,00	24,42	1,93	1,00
TF844	MYB		22,49	1,92	1,00	23,16	2,04	1,00	22,99	1,82	1,00	23,97	1,85	1,00	23,14	1,89	1,00	22,57	1,97	1,00
TF845	bHLH		19,59	1,90	1,00	19,91	1,98	1,00	17,98	1,89	1,00	20,91	1,87	1,00	19,96	1,90	1,00	20,67	2,07	1,00
TF846	SRS		29,75	1,69	1,00	22,56	1,81	1,00	19,88	1,68	1,00	22,34	1,77	1,00	20,91	2,03	1,00	22,66	1,91	1,00
TF847	JUMONJI		26,66	1,74	1,00	27,26	1,79	1,00	26,75	1,67	1,00	27,40	1,67	1,00	27,32	1,71	1,00	26,98	1,73	1,00
TF848	MYB/HD-like		24,49	1,95	1,00	24,84	1,62	1,00	21,28	1,57	1,00	23,07	1,89	1,00	21,32	1,82	1,00	20,75	2,03	1,00
TF849	MYB		26,93	1,88	1,00	24,63	1,94	1,00	20,82	1,96	1,00	23,70	1,83	1,00	22,38	1,90	1,00	23,74	2,00	1,00
TF850	WRKY family	WRKY	21,46	1,99	1,00	21,66	2,10	1,00	21,63	2,02	1,00	21,58	1,99	1,00	21,43	1,93	1,00	20,87	2,04	1,00
TF851	HD-like		28,27	1,83	1,00	28,57	1,99	0,99	29,51	1,94	1,00	29,47	2,05	1,00	29,14	1,89	1,00	28,08	1,72	1,00
TF852	MYB/HD-like		23,64	2,01	0,99	22,96	1,85	1,00	21,82	1,82	1,00	23,09	1,87	1,00	22,97	1,93	1,00	22,09	1,96	1,00
TF853	AP2/EREBP		27,26	1,83	1,00	26,87	1,95	1,00	23,16	1,83	1,00	25,42	1,81	1,00	25,11	1,87	1,00	24,58	1,97	1,00
TF854	AP2/EREBP		26,03	1,91	1,00	26,52	1,93	1,00	22,57	1,96	1,00	24,03	1,82	1,00	24,68	1,91	1,00	24,32	1,89	1,00
TF855	AP2/EREBP		22,61	1,92	1,00	22,93	1,91	1,00	22,75	1,87	1,00	24,75	1,93	1,00	23,61	1,97	1,00	23,59	1,92	1,00
TF856	bZIP		23,01	1,73	1,00	22,70	2,37	1,00	20,68	2,06	1,00	24,62	1,66	0,99	23,02	1,89	1,00	21,36	1,73	1,00
TF857	CCAAT	CCAAT-HAP3	21,51	1,95	1,00	21,62	1,90	1,00	22,02	1,91	1,00	21,45	1,92	1,00	21,39	1,94	1,00	20,91	1,96	1,00
TF858	bHLH		29,36	1,39	1,00	28,84	1,92	1,00	27,26	2,10	1,00	28,73	1,68	1,00	27,50	1,84	1,00	26,34	1,65	1,00

Table S1, continued

TF859	HD-like		26,13	1,92	1,00	26,27	1,92	1,00	27,26	1,86	1,00	26,97	1,84	1,00	26,37	1,88	1,00	25,44	1,87	1,00
TF860	WRKY family	WRKY	34,27	1,75	1,00	32,88	1,79	1,00	29,73	1,99	1,00	33,99	1,86	1,00	n.d.	1,16	0,99	36,23	1,75	1,00
TF861	WRKY family	WRKY	33,63	1,76	1,00	32,30	1,64	1,00	26,74	1,80	1,00	29,00	1,76	1,00	30,68	1,81	1,00	29,73	1,81	1,00
TF862	HD-like		32,01	1,80	1,00	28,47	1,82	1,00	25,23	1,80	1,00	32,10	1,68	1,00	31,84	1,79	1,00	27,56	1,83	1,00
TF863	CCHC (Zn)		32,35	1,65	1,00	31,15	1,79	1,00	27,63	1,70	1,00	28,44	1,87	1,00	29,60	1,85	1,00	30,16	1,75	1,00
TF864	RR		22,41	1,96	1,00	22,50	1,94	1,00	20,93	1,84	1,00	22,98	1,78	1,00	24,96	1,84	1,00	24,66	1,89	1,00
TF865	MYB/HD-like		30,75	1,84	1,00	31,76	1,82	1,00	28,05	1,73	1,00	29,96	1,87	1,00	30,98	1,89	1,00	30,31	1,82	1,00
TF866	JUMONJI		24,38	1,88	1,00	23,39	1,91	1,00	21,95	1,92	1,00	24,41	1,95	1,00	24,42	1,95	1,00	22,67	1,88	1,00
TF867	C_2H_2 (Zn)		21,46	1,88	1,00	21,07	1,86	1,00	16,18	2,28	0,99	19,21	1,93	1,00	19,62	1,95	1,00	18,78	1,85	1,00
TF868	MYB		24,94	1,85	1,00	25,24	1,92	1,00	23,70	1,76	1,00	25,64	1,77	1,00	24,21	2,02	0,99	24,06	1,91	1,00
TF869	MADS		27,89	1,90	1,00	26,33	1,76	0,99	22,02	1,83	1,00	27,76	1,61	1,00	23,53	1,91	1,00	23,64	1,94	1,00
TF870	HD family	HD	30,39	1,82	1,00	28,66	1,83	1,00	24,33	1,87	1,00	30,94	1,74	1,00	28,63	1,76	1,00	30,01	1,76	1,00
TF871	HTH	FIS	29,68	1,91	1,00	23,90	1,91	1,00	19,90	1,89	1,00	23,15	1,94	1,00	20,69	1,89	1,00	23,81	1,91	1,00
TF872	CCHC (Zn)		33,47	1,80	1,00	30,27	1,99	1,00	27,54	1,89	1,00	31,67	1,79	1,00	32,13	1,84	1,00	28,31	1,90	1,00
TF873	HMG		22,41	1,87	1,00	22,67	2,01	1,00	22,80	2,13	1,00	24,36	1,95	1,00	23,33	1,97	1,00	22,97	2,00	1,00
TF874	HD family	HD	21,70	1,93	1,00	21,34	1,96	1,00	19,58	2,02	1,00	21,42	1,97	1,00	20,11	1,97	1,00	21,32	1,91	1,00
TF875	WRKY family	WRKY	17,60	2,19	1,00	18,12	1,94	1,00	14,22	1,37	0,96	15,34	2,08	0,99	15,06	2,20	0,99	14,78	2,03	0,98
TF876	CCHC (Zn)		28,26	1,90	1,00	27,29	1,84	1,00	24,81	1,75	1,00	30,68	1,88	1,00	28,21	1,94	1,00	25,42	1,86	1,00
TF877	CCHC (Zn)		28,95	1,80	1,00	23,63	1,87	1,00	21,03	1,90	1,00	27,81	1,84	1,00	29,77	1,87	1,00	22,24	2,00	1,00
TF878	ARF		25,01	1,90	1,00	24,66	2,03	1,00	23,09	1,92	1,00	24,15	1,90	1,00	23,20	1,89	1,00	23,37	1,97	1,00
TF879	PHD		23,15	1,96	1,00	23,58	2,34	1,00	23,48	1,90	1,00	23,82	1,89	1,00	22,89	1,89	1,00	22,44	1,90	1,00
TF880	NAC		30,56	1,91	1,00	21,05	1,93	1,00	18,24	2,10	1,00	20,86	1,93	1,00	19,54	1,95	1,00	22,09	1,93	1,00
TF881	AP2/EREBP		26,94	1,71	1,00	25,95	2,04	1,00	20,52	1,73	1,00	22,61	2,04	1,00	22,51	1,80	1,00	22,83	1,88	1,00
TF882	WRKY family	WRKY	29,58	1,56	1,00	29,23	1,75	1,00	26,26	1,79	1,00	31,88	1,54	1,00	31,45	1,69	1,00	30,04	1,58	1,00
TF883	CCHC (Zn)		32,80	1,85	1,00	26,97	1,90	1,00	24,13	1,89	1,00	32,45	1,85	1,00	32,58	1,85	1,00	25,76	1,94	1,00
TF884	ABI3-VP1		23,94	1,91	1,00	23,27	1,89	1,00	19,35	1,97	1,00	19,90	1,90	1,00	21,91	1,93	1,00	21,42	1,96	1,00
TF885	ABI3-VP1		32,08	1,76	1,00	32,40	1,72	1,00	27,67	1,90	1,00	36,50	1,75	1,00	33,96	1,77	1,00	29,82	1,93	1,00
TF886	HMG		23,12	1,84	1,00	23,61	1,86	1,00	22,46	1,79	1,00	24,59	2,07	1,00	23,71	1,69	1,00	23,29	1,86	1,00
TF887	AP2/EREBP		24,01	1,90	1,00	24,09	1,89	1,00	23,79	1,87	1,00	23,85	1,83	1,00	23,79	1,93	1,00	23,13	1,92	1,00
TF888	MYB/HD-like		23,91	1,86	1,00	24,05	1,88	1,00	24,37	2,00	1,00	27,19	1,95	1,00	28,21	1,85	1,00	28,37	1,87	1,00
TF889	C3H	C3H-type 1 (Zn)	33,43	1,67	1,00	28,24	2,07	1,00	24,87	1,94	1,00	32,77	1,69	1,00	32,32	1,78	1,00	27,34	1,93	1,00
TF890	C_2H_2 (Zn)		27,95	1,70	1,00	24,72	1,85	1,00	21,68	1,73	1,00	28,81	1,85	1,00	28,70	1,85	1,00	22,97	1,95	1,00
TF891	TUB		23,57	1,94	1,00	23,64	2,03	1,00	22,02	1,88	1,00	23,60	1,98	1,00	23,39	1,89	1,00	22,89	1,88	1,00
TF892	TUB		33,09	1,87	1,00	31,70	1,85	1,00	32,30	1,84	1,00	31,68	1,85	1,00	30,29	1,79	1,00	30,29	1,69	1,00
TF893	HMG		37,30	2,08	1,00	33,41	1,65	1,00	30,38	1,72	1,00	34,69	1,60	1,00	32,76	1,34	1,00	34,36	1,58	1,00
TF894	HMG		32,74	1,67	1,00	27,82	1,86	1,00	23,45	1,88	1,00	26,44	1,82	1,00	25,66	1,84	1,00	27,45	1,84	1,00
TF895	CCAAT	CCAAT-HAP3	31,70	1,80	1,00	30,31	1,77	1,00	29,99	1,76	1,00	33,14	1,86	1,00	32,80	1,78	1,00	31,93	1,83	1,00
TF896	CCHC (Zn)		29,87	1,40	1,00	29,58	1,75	1,00	28,99	1,82	1,00	29,83	1,80	1,00	29,96	1,74	1,00	29,37	1,80	1,00
TF897	SBP		26,82	1,82	1,00	20,86	1,93	1,00	18,10	1,94	1,00	21,16	1,90	1,00	20,08	1,90	1,00	21,86	1,93	1,00
TF898	JUMONJI		29,64	2,08	1,00	29,87	1,91	1,00	25,63	1,92	1,00	29,99	1,95	1,00	29,13	1,95	1,00	28,91	1,79	1,00
TF899	TCP		21,92	1,89	1,00	22,09	1,89	1,00	22,19	1,96	1,00	22,85	1,96	1,00	22,86	1,93	1,00	22,15	1,90	1,00
TF900	CCHC (Zn)		29,91	1,72	1,00	27,37	1,82	1,00	24,93	1,87	1,00	29,78	1,79	1,00	30,43	1,78	1,00	26,50	1,91	1,00
TF901	SBP		35,85	1,95	1,00	28,27	1,90	1,00	24,16	1,85	1,00	28,98	1,87	1,00	26,37	1,85	1,00	27,59	1,89	1,00

Table S1, continued

TF902	CCHC (Zn)		24,73	1,95	1,00	22,76	1,97	1,00	20,37	1,96	1,00	25,78	1,77	1,00	25,97	1,90	1,00	21,12	1,97	1,00
TF903	SBP		25,02	1,91	1,00	24,97	1,90	1,00	25,12	1,78	1,00	25,04	1,98	1,00	24,68	1,86	1,00	23,99	1,91	1,00
TF904	bZIP		20,29	1,89	1,00	20,66	1,99	1,00	18,35	2,06	1,00	20,54	1,95	1,00	19,64	1,95	1,00	19,99	1,87	1,00
TF905	RR		29,29	1,84	1,00	29,31	1,90	1,00	22,93	1,94	1,00	26,39	1,87	1,00	26,30	1,95	1,00	27,76	1,99	1,00
TF906	GRAS		31,84	1,78	1,00	26,78	1,75	1,00	23,72	1,98	1,00	26,58	1,84	1,00	25,32	1,83	1,00	27,32	2,16	1,00
TF907	MYB		22,78	1,95	1,00	22,98	2,08	1,00	22,27	1,81	1,00	22,98	1,93	1,00	22,57	2,00	1,00	21,91	1,91	1,00
TF908	C3H	C3H-type 1 (Zn)	27,57	1,77	1,00	26,82	1,75	1,00	21,78	1,99	1,00	27,39	1,72	1,00	23,98	1,56	1,00	26,36	1,83	1,00
TF909	C3H	C3H-type 1 (Zn)	31,37	1,80	1,00	30,16	1,79	1,00	25,81	1,88	1,00	30,29	1,77	1,00	27,53	1,75	1,00	29,58	1,85	1,00
TF910	C3H	C3H-type 1 (Zn)	30,92	1,76	1,00	22,98	1,80	1,00	18,73	1,96	1,00	21,97	1,91	1,00	20,61	1,87	1,00	22,83	1,87	1,00
TF911	C3H	C3H-type 1 (Zn)	36,71	1,75	1,00	28,81	1,87	1,00	25,48	1,86	1,00	29,24	1,78	1,00	27,56	1,86	1,00	30,05	2,01	1,00
TF912	C3H	C3H-type 1 (Zn)	33,80	1,67	0,97	37,09	1,57	1,00	32,65	1,67	1,00	33,61	1,63	1,00	n.d.	1,32	0,98	32,39	1,78	1,00
TF913	WRKY family	WRKY	22,74	1,90	1,00	22,77	1,88	1,00	22,69	1,81	1,00	23,22	1,83	1,00	22,50	1,86	1,00	22,22	1,84	1,00
TF914	ARF		22,39	2,19	1,00	22,37	1,98	1,00	22,97	1,96	1,00	21,68	1,89	1,00	20,76	1,88	1,00	20,52	2,00	1,00
TF915	PHD		22,04	1,93	1,00	19,70	1,91	1,00	16,82	1,95	0,99	21,97	1,93	1,00	22,47	1,91	1,00	19,22	2,11	1,00
TF916	CCHC (Zn)		29,00	1,85	1,00	28,17	1,94	1,00	27,19	1,95	1,00	27,94	1,80	1,00	27,56	1,75	1,00	27,63	1,81	1,00
TF917	MYB/HD-like		28,77	2,05	1,00	26,95	2,04	0,99	23,13	1,95	1,00	29,04	1,73	1,00	29,67	1,99	1,00	24,46	1,97	1,00
TF918	GRAS		26,00	1,92	1,00	26,07	1,92	1,00	24,88	1,88	1,00	25,98	1,83	1,00	26,49	1,92	1,00	26,28	1,95	1,00
TF919	GRAS		28,76	1,89	1,00	28,61	1,87	1,00	25,99	1,77	1,00	27,35	1,88	1,00	26,23	1,91	1,00	26,27	1,99	1,00
TF920	GRAS		25,50	1,91	1,00	24,99	1,89	1,00	21,34	2,00	1,00	24,16	1,85	1,00	23,87	1,91	1,00	25,42	1,92	1,00
TF921	GRAS		28,49	1,86	1,00	26,96	1,86	1,00	23,09	1,98	1,00	24,90	1,83	1,00	24,05	1,87	1,00	25,56	1,78	1,00
TF922	GRAS		30,22	1,83	1,00	29,38	1,87	1,00	30,05	1,86	1,00	30,17	1,90	1,00	29,19	1,89	1,00	30,17	1,92	1,00
TF923	HD-like		29,49	1,90	1,00	29,68	1,80	1,00	24,97	1,91	1,00	26,80	1,92	1,00	28,22	1,85	1,00	28,35	1,87	1,00
TF924	C_2H_2 (Zn)		36,90	1,74	1,00	30,26	1,80	1,00	27,31	1,82	1,00	31,62	1,89	1,00	39,19	1,45	1,00	29,73	1,84	1,00
TF925	C_2H_2 (Zn)		28,09	1,85	1,00	27,84	1,77	1,00	22,96	1,83	1,00	24,72	1,81	1,00	25,70	1,76	1,00	24,01	1,87	1,00
TF926	CCHC (Zn)		27,30	1,80	1,00	27,23	1,88	1,00	24,26	1,84	1,00	24,94	1,79	1,00	26,04	1,86	1,00	25,17	1,84	1,00
TF927	ABI3-VP1		31,26	1,19	1,00	26,94	1,66	1,00	24,54	1,74	1,00	26,84	1,67	1,00	24,36	1,57	1,00	27,40	1,66	1,00
TF928	HMG		33,78	1,91	1,00	31,66	1,82	1,00	23,01	2,29	1,00	27,36	1,81	1,00	26,20	1,93	1,00	27,96	1,98	1,00
TF929	C_2H_2 (Zn)		21,60	2,00	1,00	19,99	2,00	1,00	17,03	1,93	1,00	20,04	2,00	1,00	18,64	1,96	1,00	19,21	1,94	1,00
TF930	AP2/EREBP		23,99	2,02	1,00	22,76	1,87	1,00	19,88	1,85	1,00	21,78	1,39	0,99	21,05	1,98	1,00	22,38	1,98	1,00
TF931	bZIP		23,06	1,90	1,00	22,94	1,83	1,00	23,54	1,22	1,00	23,49	1,85	1,00	23,50	1,91	1,00	22,93	1,92	1,00
TF932	MYB		29,48	1,70	1,00	26,38	1,84	1,00	22,38	1,88	1,00	25,07	1,77	1,00	23,34	1,90	1,00	25,92	1,77	1,00
TF933	MYB/HD-like		31,88	1,84	1,00	37,07	1,68	1,00	30,81	1,75	1,00	33,61	1,65	1,00	32,98	1,86	1,00	35,23	1,78	1,00
TF934	MYB/HD-like		28,06	1,88	1,00	28,16	1,80	1,00	27,90	1,95	1,00	28,66	1,85	1,00	27,97	1,86	1,00	27,25	1,91	1,00
TF935	RR		27,69	1,93	1,00	27,09	1,95	1,00	23,43	1,88	1,00	26,55	1,83	1,00	25,67	1,94	1,00	26,61	1,75	1,00
TF936	MYB		25,76	1,91	1,00	26,26	1,91	1,00	25,97	1,80	1,00	27,30	1,81	1,00	25,64	1,86	1,00	25,63	1,88	1,00
TF937	HD-like		28,56	1,86	1,00	23,40	1,90	1,00	19,97	2,20	1,00	22,29	1,91	1,00	21,58	1,83	1,00	23,67	2,23	1,00
TF938	WRKY family	WRKY	24,47	1,93	1,00	22,82	1,97	1,00	20,14	1,95	1,00	22,18	1,97	1,00	21,44	1,91	1,00	22,39	2,00	1,00
TF939	MADS		25,72	1,95	1,00	26,44	1,92	1,00	21,23	1,89	1,00	23,89	1,90	1,00	24,75	1,96	1,00	24,07	1,93	1,00
TF940	AP2/EREBP		21,12	1,88	1,00	21,40	1,93	1,00	19,29	1,85	1,00	20,48	1,95	1,00	19,48	1,92	1,00	19,59	1,91	1,00
TF941	HD family	HD	23,13	1,90	1,00	23,26	1,89	1,00	21,71	1,98	1,00	24,00	1,27	1,00	21,97	1,90	1,00	22,14	1,97	1,00
TF942	AP2/EREBP		21,17	1,94	1,00	21,65	1,89	1,00	21,06	1,84	1,00	21,71	1,93	1,00	20,64	1,98	1,00	20,36	1,98	1,00
TF943	AP2/EREBP		24,24	1,80	1,00	25,55	1,90	1,00	24,04	1,60	1,00	24,64	1,89	1,00	23,65	2,38	1,00	23,12	1,89	1,00
TF944	A20-like		20,63	1,28	1,00	20,92	2,00	1,00	18,36	2,01	0,99	20,64	1,28	1,00	20,33	1,91	0,99	18,86	1,36	1,00

Table S1, continued

TF945	ABI3-VP1		25,58	1,88	1,00	23,47	1,94	1,00	20,87	1,96	1,00	25,35	1,91	1,00	26,32	1,93	1,00	22,90	2,55	1,00
TF946	bZIP		30,63	1,75	1,00	30,94	1,69	1,00	29,08	1,69	1,00	31,02	1,81	1,00	31,09	1,74	1,00	30,39	1,78	1,00
TF947	HD-like		25,97	1,86	1,00	24,94	1,86	1,00	23,54	1,98	1,00	26,01	1,90	1,00	25,84	1,88	1,00	24,30	2,19	1,00
TF948	ABI3-VP1		31,03	1,82	1,00	29,40	1,78	1,00	26,41	1,72	1,00	32,53	1,71	1,00	32,20	1,32	1,00	28,03	1,78	1,00
TF949	HD-like		27,44	1,64	1,00	24,55	1,92	1,00	20,49	1,99	1,00	23,74	1,87	1,00	22,49	1,97	1,00	23,85	1,96	1,00
TF950	BTB/POZ		22,78	1,85	1,00	22,90	1,90	1,00	22,90	2,09	1,00	23,35	1,90	1,00	23,79	1,79	1,00	22,92	1,94	1,00
TF951	CCHC (Zn)		28,72	1,81	1,00	26,00	1,73	1,00	24,43	1,78	1,00	29,71	1,87	1,00	29,71	1,78	1,00	25,61	1,78	1,00
TF952	CCHC (Zn)		23,09	1,92	1,00	23,40	1,88	1,00	22,49	1,82	1,00	23,40	1,95	1,00	23,00	1,91	1,00	22,54	1,95	1,00
TF953	PHD		29,15	1,78	1,00	31,59	1,72	1,00	26,37	1,81	1,00	29,01	1,86	1,00	28,74	1,75	1,00	29,22	1,74	1,00
TF954	AP2/EREBP		24,98	1,87	1,00	24,79	1,69	1,00	24,28	1,84	1,00	23,35	2,06	1,00	23,55	1,87	1,00	22,87	1,92	1,00
TF955	AP2/EREBP		23,21	1,83	1,00	23,17	1,72	1,00	23,82	1,83	1,00	23,95	1,78	1,00	23,75	1,89	1,00	23,39	1,96	1,00
TF956	C_2C_2 (Zn)	YABBY	24,10	1,86	1,00	24,60	1,96	1,00	22,95	1,96	1,00	25,60	1,85	1,00	24,65	1,86	1,00	25,51	1,97	1,00
TF957	HMG		20,34	1,87	1,00	20,86	2,00	1,00	20,47	1,93	1,00	21,05	1,98	1,00	20,13	2,17	1,00	19,92	1,97	1,00
TF958	ABI3-VP1		32,00	1,65	1,00	31,05	1,70	1,00	32,40	1,68	1,00	33,31	1,26	1,00	23,85	1,82	1,00	33,71	1,68	1,00
TF959	C_2H_2 (Zn)		24,46	1,91	1,00	25,01	1,95	1,00	24,96	1,89	1,00	25,57	1,97	1,00	24,19	2,00	1,00	24,11	1,97	1,00
TF960	C3H	C3H-type 1 (Zn)	23,05	1,89	1,00	23,53	1,92	1,00	23,16	1,92	1,00	23,34	1,90	1,00	22,72	1,85	1,00	22,41	1,92	1,00
TF961	CCHC (Zn)		36,89	1,58	0,99	n.d.	1,47	0,99	33,20	1,73	1,00	33,31	1,72	1,00	n.d.	1,37	0,96	33,34	1,71	1,00
TF962	AP2/EREBP		32,81	1,78	1,00	33,05	1,80	1,00	31,63	1,80	1,00	29,49	1,86	1,00	29,29	1,91	1,00	28,44	1,84	1,00
TF963	GRAS		23,62	1,96	1,00	24,00	1,91	1,00	23,47	1,79	1,00	25,12	1,97	1,00	23,63	1,88	1,00	23,73	1,99	1,00
TF964	AS2		32,00	1,77	1,00	24,66	1,90	1,00	19,80	1,92	1,00	23,64	1,89	1,00	23,15	1,93	1,00	25,62	1,97	1,00
TF965	WRKY family	WRKY	26,98	1,92	1,00	27,06	1,90	1,00	23,76	1,82	1,00	27,31	1,81	1,00	26,11	1,85	1,00	26,22	1,84	1,00
TF966	AP2/EREBP		33,57	1,61	1,00	30,19	1,84	1,00	25,61	1,78	1,00	29,22	1,63	1,00	27,17	1,65	1,00	30,10	1,74	1,00
TF967	MYB		27,98	1,92	1,00	25,69	1,78	1,00	21,56	1,85	1,00	26,08	1,85	1,00	23,16	1,65	1,00	24,81	1,97	1,00
TF968	C_2C_2 (Zn)	DOF	27,58	1,93	1,00	24,44	1,95	1,00	20,59	1,91	1,00	23,98	1,93	1,00	22,07	1,90	1,00	24,73	1,90	1,00
TF969	HD family	HD	30,40	1,90	1,00	27,29	1,90	1,00	23,01	1,98	1,00	26,51	1,83	1,00	25,10	1,87	1,00	27,59	1,84	1,00
TF970	C_2H_2 (Zn)		29,25	1,69	1,00	28,12	1,72	1,00	23,91	1,66	1,00	31,37	1,68	1,00	25,70	1,70	1,00	26,99	1,65	1,00
TF971	MYB		31,39	1,75	1,00	32,14	1,69	1,00	33,37	1,63	1,00	33,34	1,62	1,00	23,68	1,90	1,00	30,57	1,68	1,00
TF972	WRKY family	WRKY	31,08	1,73	1,00	24,40	2,06	1,00	20,18	1,84	1,00	24,00	1,76	1,00	22,42	1,90	1,00	23,85	2,13	1,00
TF973	MYB		32,34	1,75	1,00	32,86	1,87	1,00	27,94	2,67	0,99	31,83	2,15	1,00	29,87	1,74	1,00	30,13	1,69	1,00
TF974	MYB		26,35	1,86	1,00	26,50	1,79	1,00	24,95	1,73	1,00	28,39	1,71	1,00	26,52	1,85	1,00	27,98	1,69	1,00
TF975	MYB		n.d.	1,34	0,97	29,49	1,83	1,00	26,65	1,84	1,00	29,20	2,05	1,00	27,42	1,77	1,00	30,32	1,71	1,00
TF976	MYB		31,34	1,72	1,00	26,97	1,92	1,00	21,89	1,73	1,00	25,60	1,90	1,00	23,92	1,94	1,00	25,99	1,88	1,00
TF977	SRS		23,80	1,98	1,00	24,37	1,85	1,00	24,06	1,82	1,00	24,20	1,84	1,00	23,50	1,84	1,00	23,25	1,88	1,00
TF978	C_2C_2 (Zn)	CO-like	33,62	1,77	1,00	33,95	11,39	0,63	37,19	1,63	1,00	33,91	1,67	1,00	32,66	1,75	1,00	36,81	1,25	1,00
TF979	CCHC (Zn)		28,29	1,88	1,00	22,70	1,97	1,00	18,47	2,02	1,00	21,56	2,05	1,00	20,83	1,93	1,00	22,63	1,94	1,00
TF980	SBP		26,54	1,77	1,00	26,66	1,72	1,00	23,26	1,82	1,00	27,59	1,80	1,00	25,46	1,80	1,00	26,26	1,76	1,00
TF981	bZIP		28,86	1,89	1,00	26,87	1,86	1,00	23,32	1,90	1,00	26,18	1,86	1,00	24,73	1,89	1,00	26,15	1,96	1,00
TF982	C_2H_2 (Zn)		24,31	1,91	1,00	22,98	1,89	1,00	20,38	2,02	1,00	22,58	1,81	1,00	21,21	1,83	1,00	22,43	1,82	1,00
TF983	MYB		23,71	1,78	1,00	24,45	2,36	1,00	23,34	1,74	1,00	25,25	1,93	0,99	23,52	1,85	1,00	23,24	1,85	1,00
TF984	bHLH		27,99	1,20	1,00	28,38	1,88	1,00	22,70	1,90	1,00	27,37	1,91	1,00	25,02	1,74	1,00	26,05	1,51	1,00
TF985	C3H	C3H-type 1 (Zn)	31,22	1,80	1,00	29,46	1,88	1,00	25,98	1,43	1,00	28,63	1,91	1,00	26,81	1,88	1,00	29,28	1,84	1,00
TF986	C3H	C3H-type 1 (Zn)	33,60	1,78	1,00	31,24	1,67	1,00	24,33	1,91	1,00	28,67	1,95	1,00	27,77	1,78	1,00	29,58	1,76	1,00
TF987	C3H	C3H-type 1 (Zn)	32,73	1,68	1,00	28,48	1,78	1,00	26,41	2,04	1,00	30,36	1,89	1,00	26,29	1,91	1,00	29,19	1,76	1,00

Table S1, continued

TF988	HD-like		28,91	1,80	1,00	26,04	1,58	1,00	22,01	1,65	1,00	26,49	1,90	1,00	23,72	1,77	1,00	25,99	1,98	1,00
TF989	C3H	C3H-type 1 (Zn)	26,65	1,88	1,00	25,93	1,89	1,00	23,18	1,96	1,00	26,95	1,82	1,00	24,51	1,96	1,00	26,14	1,91	1,00
TF990	NAC		23,79	1,90	1,00	23,97	1,93	1,00	23,21	1,89	1,00	24,49	1,85	1,00	22,84	1,88	1,00	23,39	1,91	1,00
TF991	MADS		33,71	1,74	1,00	27,64	1,87	1,00	22,81	1,88	1,00	26,43	1,89	1,00	25,07	1,95	1,00	28,13	1,84	1,00
TF992	MADS		30,71	1,78	1,00	32,21	1,78	1,00	31,30	1,81	1,00	34,46	1,58	1,00	26,03	1,91	1,00	31,47	1,63	1,00
TF993	NAC		25,23	1,83	1,00	25,95	1,91	1,00	25,70	1,92	1,00	26,66	1,88	1,00	25,92	1,90	1,00	25,39	1,94	1,00
TF994	TCP		21,14	1,89	1,00	21,46	1,95	1,00	20,91	1,98	1,00	23,34	1,96	1,00	22,15	1,90	1,00	22,19	1,90	1,00
TF995	bHLH		24,95	1,95	1,00	24,94	1,89	1,00	22,44	1,95	1,00	26,81	1,79	1,00	26,18	1,92	1,00	23,60	1,89	1,00
TF996	HD-like		26,39	1,85	1,00	19,82	2,03	1,00	17,05	1,75	0,99	19,40	1,96	1,00	18,30	2,05	1,00	20,05	1,92	1,00
TF997	HD-like		29,71	1,86	1,00	29,58	1,95	1,00	25,03	1,80	1,00	28,59	1,86	1,00	27,72	1,90	1,00	29,22	1,78	1,00
TF998	CCHC (Zn)		22,43	1,87	1,00	22,54	1,92	1,00	21,70	1,88	1,00	22,52	1,93	1,00	22,51	1,89	1,00	22,23	1,90	1,00
TF999	MADS		32,80	1,60	1,00	32,25	1,26	1,00	28,52	1,61	1,00	31,34	1,61	1,00	31,72	1,50	1,00	30,50	1,64	1,00
TF1000	MADS		31,65	1,63	1,00	31,36	1,70	1,00	26,61	1,70	1,00	28,68	1,48	1,00	29,89	1,72	1,00	29,23	1,77	1,00
TF1001	C_2H_2 (Zn)		21,66	1,95	1,00	21,80	1,91	1,00	20,81	2,30	1,00	22,74	1,80	1,00	21,07	2,03	1,00	21,16	1,87	1,00
TF1002	CCAAT	CCAAT-HAP3	30,69	1,90	1,00	29,95	1,58	1,00	23,61	1,92	1,00	27,60	1,88	1,00	26,00	1,94	1,00	27,55	1,87	1,00
TF1003	MYB		30,28	1,65	1,00	26,54	1,89	1,00	22,56	1,74	1,00	26,05	1,62	1,00	24,50	1,62	1,00	26,24	1,55	1,00
TF1004	JUMONJI		22,97	1,92	1,00	23,28	1,92	1,00	22,84	1,85	1,00	23,96	1,85	1,00	22,76	2,26	1,00	22,35	1,91	1,00
TF1005	MYB		22,12	2,00	1,00	22,47	1,99	1,00	18,78	2,15	1,00	22,92	1,92	1,00	21,94	1,93	1,00	21,94	1,91	1,00
TF1006	bHLH		27,60	1,91	1,00	28,15	1,95	1,00	23,50	1,93	1,00	26,02	2,05	1,00	25,99	1,93	1,00	25,97	1,96	1,00
TF1007	bHLH		24,83	1,83	1,00	25,42	1,83	1,00	25,69	1,83	1,00	25,13	1,95	1,00	23,61	1,87	1,00	23,18	1,86	1,00
TF1008	AP2/EREBP		27,93	1,75	1,00	28,59	1,94	1,00	26,13	2,02	1,00	28,59	1,78	1,00	26,17	1,75	1,00	27,13	1,79	1,00
TF1009	JUMONJI		28,74	1,89	1,00	29,14	1,93	1,00	26,40	1,92	1,00	28,37	1,81	1,00	27,48	1,89	1,00	26,81	1,91	1,00
TF1010	PHD		26,82	2,04	1,00	27,04	1,90	1,00	25,92	1,81	1,00	26,96	2,03	1,00	26,36	2,05	1,00	25,89	1,96	1,00
TF1011	ZF-HD		23,22	1,88	1,00	23,98	1,83	1,00	22,62	1,87	1,00	24,09	1,87	1,00	23,36	1,87	1,00	23,23	1,85	1,00
TF1012	MYB		23,57	1,95	1,00	23,89	1,89	1,00	23,29	1,72	1,00	24,66	1,85	1,00	23,52	1,89	1,00	23,53	1,83	1,00
TF1013	bHLH		25,66	1,88	1,00	25,57	1,92	1,00	24,03	1,85	1,00	26,62	1,84	1,00	25,37	1,78	1,00	25,98	1,96	1,00
TF1014	C_2C_2 (Zn)	GATA	21,99	1,90	1,00	22,50	1,90	1,00	22,08	2,01	1,00	24,61	1,88	1,00	23,38	1,92	1,00	22,93	1,86	1,00
TF1015	PHD		22,23	1,23	1,00	22,52	1,94	1,00	18,80	1,96	1,00	22,16	1,89	1,00	21,56	1,89	1,00	21,55	2,01	1,00
TF1016	CCHC (Zn)		28,24	1,88	1,00	27,99	1,85	1,00	23,53	1,92	1,00	25,38	2,05	1,00	26,75	2,01	1,00	25,94	1,92	1,00
TF1017	C3H	C3H-type 1 (Zn)	23,62	1,84	1,00	23,84	1,94	1,00	23,96	1,87	1,00	23,82	1,87	1,00	23,26	1,90	1,00	22,99	1,93	1,00
TF1018	AS2		31,45	1,68	1,00	30,76	1,62	1,00	24,27	1,77	1,00	28,05	1,76	1,00	27,86	1,70	1,00	28,16	1,72	1,00
TF1019	PHD		24,96	1,89	1,00	25,54	1,82	1,00	25,31	1,90	1,00	25,92	1,81	1,00	25,36	1,84	1,00	24,97	1,91	1,00
TF1020	GRAS		29,28	1,91	1,00	23,15	2,01	1,00	18,04	2,43	1,00	21,79	1,90	1,00	21,48	1,91	1,00	22,40	1,92	1,00
TF1021	AP2/EREBP		25,15	1,93	1,00	26,32	1,98	1,00	23,20	1,88	1,00	25,99	1,83	1,00	25,31	1,91	1,00	25,29	2,04	1,00
TF1022	PHD		22,13	1,79	1,00	22,05	1,90	1,00	16,71	1,38	0,99	20,17	1,95	1,00	20,35	2,07	1,00	19,12	1,93	1,00
TF1023	PHD		28,52	1,49	1,00	31,08	1,69	1,00	26,48	1,71	1,00	28,48	1,64	1,00	30,32	1,72	1,00	28,24	1,74	1,00
TF1024	TCoAp15		21,99	2,00	1,00	22,52	2,03	1,00	21,89	1,89	1,00	23,13	1,87	1,00	22,19	2,00	1,00	22,03	1,90	1,00
TF1025	WRKY family	WRKY	31,47	1,71	1,00	27,99	1,79	1,00	22,70	1,86	1,00	25,91	1,83	1,00	26,62	1,86	1,00	28,22	1,84	1,00
TF1026	AS2		23,17	1,88	1,00	20,54	1,97	1,00	19,11	1,96	1,00	20,25	2,05	1,00	18,70	1,86	1,00	20,33	2,06	1,00
TF1027	C_2H_2 (Zn)		25,93	1,81	1,00	25,60	1,86	1,00	21,60	1,96	1,00	24,27	1,88	1,00	22,98	1,84	1,00	23,33	1,82	1,00
TF1028	MYB		24,49	1,90	1,00	23,67	1,92	1,00	20,07	1,53	0,99	23,12	2,00	1,00	21,70	1,72	1,00	23,29	1,90	1,00
TF1029	EIL		33,91	1,43	1,00	30,72	1,62	1,00	24,77	1,92	1,00	27,75	1,80	1,00	26,50	1,74	1,00	29,27	1,85	1,00
TF1030	C_2C_2 (Zn)	GATA	24,83	2,00	1,00	19,87	1,89	1,00	16,99	1,78	0,99	22,15	1,87	1,00	18,45	2,09	1,00	20,48	1,95	1,00

Table S1, continued

TF1031	MYB		25,21	1,80	1,00	22,27	1,89	1,00	18,55	1,99	1,00	21,02	1,95	1,00	20,14	2,03	1,00	21,51	1,99	1,00
TF1032	NIN-like		27,12	1,87	1,00	23,81	1,82	1,00	19,42	1,91	1,00	27,63	1,81	1,00	20,73	1,99	1,00	23,13	1,81	1,00
TF1033	HTH	FIS	23,59	1,99	1,00	19,19	1,90	1,00	16,41	1,78	0,99	18,55	2,11	1,00	17,51	1,88	1,00	18,60	2,04	1,00
TF1034	NAC		22,77	1,96	1,00	23,82	1,89	1,00	23,13	1,93	1,00	22,32	2,05	1,00	21,49	1,95	1,00	21,22	1,94	1,00
TF1035	ABI3-VP1		29,01	1,87	1,00	23,58	1,93	1,00	21,14	1,84	1,00	23,93	1,86	1,00	21,83	2,00	1,00	24,71	1,88	1,00
TF1036	ABI3-VP1		32,16	1,82	1,00	28,51	1,80	1,00	22,54	1,95	1,00	29,78	1,83	1,00	24,84	1,77	1,00	27,31	1,92	1,00
TF1037	ABI3-VP1		31,04	1,86	1,00	21,26	1,96	1,00	17,71	2,21	1,00	20,05	1,96	1,00	18,96	2,03	1,00	21,02	1,97	1,00
TF1038	ABI3-VP1		31,30	1,62	1,00	29,98	1,76	1,00	23,42	2,31	1,00	27,57	1,87	1,00	26,74	1,83	1,00	28,24	1,86	1,00
TF1039	ABI3-VP1		25,23	1,95	1,00	24,98	1,94	1,00	22,14	1,74	1,00	24,74	1,87	1,00	23,99	1,91	1,00	25,14	1,87	1,00
TF1040	MADS		28,67	1,69	1,00	21,16	1,92	1,00	17,51	2,07	1,00	20,99	1,89	1,00	18,06	2,00	1,00	20,06	1,95	1,00
TF1041	HD family	HD	21,74	1,90	1,00	22,19	1,93	1,00	22,03	1,94	1,00	23,12	1,87	1,00	21,85	1,84	1,00	21,74	1,93	1,00
TF1042	C3H	C3H-type 1 (Zn)	22,86	1,85	1,00	22,25	1,91	1,00	19,69	1,86	1,00	22,17	2,01	1,00	21,11	2,00	1,00	22,10	1,86	1,00
TF1043	GRAS		36,70	1,64	1,00	32,55	1,65	1,00	28,67	1,79	1,00	32,41	1,69	1,00	29,50	1,73	1,00	31,28	1,66	1,00
TF1044	CCAAT	CCAAT-HAP3	20,25	1,88	1,00	20,93	2,09	1,00	19,91	1,92	1,00	22,77	1,90	1,00	21,40	1,91	1,00	21,28	1,96	1,00
TF1045	C_2H_2 (Zn)		23,67	1,92	1,00	23,52	1,81	1,00	23,13	1,89	1,00	24,08	1,87	1,00	24,03	1,98	1,00	23,33	1,93	1,00

Table S2 Details of regulated TF genes clustered in groups among *Medicago truncatula* genotypes analyzed, SA1306 and Parabinga, in response to *Erysiphe pisi* infection. Relative gene expression ratios (M) are listed and sorted by cluster (Group). Genes were considered differentially expressed in response to *E. pisi* infection if to meet the prerequisites $p \leq 0.05$ and $M \leq -0.7$ or $M \geq 0.7$. ID: Identification number of TF gene. TC: *Medicago* gene Accession Numbers (TIGR). TF family: Transcription factor family. TF subfamily: Subfamily names. M: Average $\log_2$ differential expression ratios (inoculated/control) for Parabinga (PB) and SA1306 (SA) genotypes. F: Fold change expression ratios of differentially expressed genes in SA1306 compared to Parabinga, $\log_2$ expression ratio SA1306/Parabinga. Group: Heat map expression profiles clustered (Figure 3).

ID	TC	TF family	TF subfamily	M PB	M SA	F	Group
TF700	CX528154	BTB/POZ		-2,31	-3,55	-1,24	I
TF479	TC110178	NAC		-1,54	-1,12	0,42	I
TF823	-	C_2H_2 (Zn)		-1,46	-3,36	-1,89	I
TF436	TC98230	SBP		-1,16	-1,24	-0,08	I
TF855	-	AP2/EREBP		-0,87	-1,49	-0,62	I
TF303	-	AP2/EREBP		-0,86	-1,83	-0,97	I
TF485	TC109384	bHLH		-0,83	-3,51	-2,68	I
TF425	-	bHLH		-0,36	-1,98	-1,62	I
TF101	TC103429	C_2H_2 (Zn)		-0,28	-1,62	-1,34	I
TF8	TC109476	LIM		-0,28	-1,75	-1,47	I
TF388	BG448434	TTF-type (Zn)		0,61	-2,13	-2,74	I
TF244	TC108091	MYB/HD-like		0,54	-1,04	-1,58	I
TF780	-	AUX/IAA		0,49	-1,21	-1,70	I
TF691	BG450549	E2F		0,49	-1,00	-1,49	I
TF233	-	HMG		0,72	-1,43	-2,15	I
TF962	-	AP2/EREBP		-5,08	1,56	6,64	II
TF626	-	HD-like		-3,62	0,91	4,52	II
TF913	TC97332	WRKY family	WRKY	-1,48	0,77	2,25	II
TF393	TC95605	C_2C_2 (Zn)	DOF	-2,65	-2,19	0,45	II
TF265	-	C_2C_2 (Zn)	DOF	-4,31	-1,42	2,89	II
TF716	AL382911	C_2C_2 (Zn)	GATA	-2,46	-1,60	0,86	II
TF767	-	C_3H	C_3H-type 1 (Zn)	-2,42	0,44	2,86	II
TF822	-	DDT		-1,24	0,69	1,92	II
TF448	TC97611	RR		-1,23	0,06	1,29	II
TF546	AL366881	AP2/EREBP		-0,71	0,26	0,97	II
TF618	-	HD family	HD	-1,03	-0,27	0,76	II
TF598	TC95256	NAC		-0,92	-0,47	0,45	II
TF631	TC96049	HSF		-0,69	-0,47	0,22	II
TF837	-	MYB		5,96	1,87	-4,09	III
TF996	-	HD-like		4,24	3,23	-1,01	III
TF129	TC102127	MYB/HD-like		4,45	2,37	-2,08	III
TF549	TC107542	HD family	HD-ZIP	3,89	3,02	-0,87	III
TF3	-	AP2/EREBP		3,11	1,02	-2,08	III
TF934	TC109302	MYB/HD-like		4,22	0,39	-3,82	III
TF428	-	C_2H_2 (Zn)		2,88	2,17	-0,71	IV
TF879	CB066652	PHD		2,42	3,53	1,11	IV
TF333	-	bHLH		2,18	1,99	-0,19	IV
TF322	-	MADS		1,98	1,70	-0,28	IV
TF63	-	MYB		1,76	2,80	1,04	IV
TF270	-	C_2H_2 (Zn)		1,59	4,49	2,90	IV
TF258	-	HD family	HD	1,41	5,26	3,85	IV
TF563	-	MADS		1,25	3,13	1,88	IV
TF230	TC109855	HD-like		0,71	5,66	4,95	IV
TF600	TC103296	bHLH		1,44	1,72	0,29	V
TF87	TC96308	ZF DHHC		1,20	1,40	0,20	V
TF639	TC100932	bHLH		1,32	1,40	0,08	V
TF296	-	GRAS		1,68	1,66	-0,02	V
TF565	-	HTH	FIS	1,57	1,09	-0,48	V
TF386	TC110943	ARF		1,55	0,79	-0,75	V
TF473	TC107897	AP2/EREBP		2,15	1,22	-0,93	V
TF136	TC96243	NAC		2,17	1,21	-0,96	V
TF497	BF636434	HD family	HD	2,08	1,01	-1,07	V
TF276	BE249457	RR		1,71	0,65	-1,06	V

Table S2, continued

TF364	TC96319	CCAAT	CCAAT-HAP3	-0,20	-0,15	0,05	VI
TF196	TC106782	EIL		-0,05	-0,12	-0,07	VI
TF351	TC103599	bHLH		-0,21	-0,42	-0,21	VI
TF543	TC101251	BD		0,25	-0,44	-0,70	VI
TF449	-	CCHC (Zn)		0,21	-0,59	-0,80	VI
TF438	-	PHD		0,38	-0,43	-0,81	VI
TF899	-	TCP		0,39	-0,51	-0,90	VI
TF441	-	JUMONJI		0,41	-0,54	-0,95	VI
TF959	-	C_2H_2 (Zn)		0,60	-0,67	-1,28	VI
TF537	-	bZIP		1,09	0,80	-0,29	VII
TF429	TC111833	MYB/HD-like		0,99	0,59	-0,40	VII
TF140	TC107912	PHD		0,86	1,22	0,37	VII
TF97	CX534602	HD-like		0,77	1,28	0,51	VII
TF588	TC106806	HD family	HD	0,73	0,63	-0,10	VII
TF523	TC102139	MYB/HD-like		0,63	0,67	0,04	VII
TF199	-	NAC		0,58	0,55	-0,03	VII
TF464	TC109097	bZIP		0,48	1,05	0,57	VII
TF437	-	CCHC (Zn)		0,47	0,44	-0,03	VII
TF816	TC96871	MYB/HD-like		0,25	0,29	0,04	VII
TF372	TC96859	HD family	HD	0,15	0,97	0,82	VII
TF389	TC104194	C_2C_2 (Zn)	DOF	1,59	-0,06	-1,66	VIII
TF1007	-	bHLH		1,11	0,32	-0,79	VIII
TF349	TC98775	CCHC (Zn)		1,00	0,30	-0,70	VIII
TF179	CX533076	U1-type (Zn)		0,99	0,32	-0,67	VIII
TF481	TC112164	FHA		0,88	-0,03	-0,91	VIII
TF143	-	MYB/HD-like		0,80	0,21	-0,59	VIII
TF797	-	HD-like		1,26	2,47	1,21	IX
TF200	TC109833	NAC		1,10	2,23	1,13	IX
TF814	BG451025	HD-like		1,11	2,45	1,34	IX
TF552	TC107542	HD family	HD-ZIP	0,87	2,09	1,22	IX
TF666	CX541503	HD-like		0,65	2,13	1,48	IX
TF982	TC96831	C_2H_2 (Zn)		0,52	2,77	2,25	IX
TF901	-	SBP		0,48	2,71	2,23	IX
TF27	-	ARID		0,05	3,00	2,95	IX
TF1009	-	JUMONJI		0,08	1,73	1,65	X
TF726	AL375449	MYB/HD-like		0,45	1,52	1,07	X
TF158	-	HD-like		0,44	1,43	0,99	X
TF540	-	SBP		-0,38	1,31	1,69	X
TF660	-	CCHC (Zn)		-0,83	1,04	1,88	X
TF308	-	C_2C_2 (Zn)	DOF	-0,33	0,75	1,08	X
TF295	-	HD family	HD	-0,35	0,65	1,00	X
TF562	TC98196	HD family	HD	-0,08	0,48	0,55	X

Table S3 Details of regulated TF genes among *Medicago truncatula* genotypes analyzed, SA1306 and Parabinga, in response to *Erysiphe pisi* infection ($p \leq 0.05$; $-0.7 \geq M \geq 0.7$). Relative gene expression ratios (M) are listed and sorted by class and M values. ID: Identification number of TF gene. TF family: Transcription factor family. TF subfamily: Subfamily names. M: Average $\log_2$ differential expression ratios (inoculated/control) for Parabinga (PB) and SA1306 (SA) genotypes. F: Fold change expression ratios of differentially expressed genes in SA1306 compared to Parabinga, $\log_2$ expression ratio SA1306/Parabinga. Class: Genes that were specifically regulated in SA1306 (SA), Parabinga (PB) and both genotypes (Common).

ID	TF family	TF subfamily	M_PB	M_SA	F	Class
TF767	C_3H	C_3H-type 1 (Zn)	-2,42	0,44	2,86	PB
TF822	DDT		-1,24	0,69	1,92	PB
TF448	RR		-1,23	0,06	1,29	PB
TF618	HD family	HD	-1,03	-0,27	0,76	PB
TF598	NAC		-0,92	-0,47	0,45	PB
TF546	AP2/EREBP		-0,71	0,26	0,97	PB
TF934	MYB/HD-like		4,22	0,39	-3,82	PB
TF276	RR		1,71	0,65	-1,06	PB
TF389	C_2C_2 (Zn)	DOF	1,59	-0,06	-1,66	PB
TF1007	bHLH		1,11	0,32	-0,79	PB
TF349	CCHC (Zn)		1,00	0,30	-0,70	PB
TF429	MYB/HD-like		0,99	0,59	-0,40	PB
TF179	U1-type (Zn)		0,99	0,32	-0,67	PB
TF481	FHA		0,88	-0,03	-0,91	PB
TF143	MYB/HD-like		0,80	0,21	-0,59	PB
TF588	HD family	HD	0,73	0,63	-0,10	PB
TF388	TTF-type (Zn)		0,61	-2,13	-2,74	SA
TF425	bHLH		-0,36	-1,98	-1,62	SA
TF8	LIM		-0,28	-1,75	-1,47	SA
TF101	C_2H_2 (Zn)		-0,28	-1,62	-1,34	SA
TF780	AUX/IAA		0,49	-1,21	-1,70	SA
TF244	MYB/HD-like		0,54	-1,04	-1,58	SA
TF691	E2F		0,49	-1,00	-1,49	SA
TF27	ARID		0,05	3,00	2,95	SA
TF982	C_2H_2 (Zn)		0,52	2,77	2,25	SA
TF901	SBP		0,48	2,71	2,23	SA
TF666	HD-like		0,65	2,13	1,48	SA
TF1009	JUMONJI		0,08	1,73	1,65	SA
TF726	MYB/HD-like		0,45	1,52	1,07	SA
TF158	HD-like		0,44	1,43	0,99	SA
TF540	SBP		-0,38	1,31	1,69	SA
TF464	bZIP		0,48	1,05	0,57	SA
TF372	HD family	HD	0,15	0,97	0,82	SA
TF308	C_2C_2 (Zn)	DOF	-0,33	0,75	1,08	SA
TF265	C_2C_2 (Zn)	DOF	-4,31	-1,42	2,89	Common
TF303	AP2/EREBP		-0,86	-1,83	-0,97	Common
TF393	C_2C_2 (Zn)	DOF	-2,65	-2,19	0,45	Common
TF436	SBP		-1,16	-1,24	-0,08	Common
TF479	NAC		-1,54	-1,12	0,42	Common
TF485	bHLH		-0,83	-3,51	-2,68	Common
TF700	BTB/POZ		-2,31	-3,55	-1,24	Common
TF716	C_2C_2 (Zn)	GATA	-2,46	-1,60	0,86	Common
TF823	C_2H_2 (Zn)		-1,46	-3,36	-1,89	Common
TF855	AP2/EREBP		-0,87	-1,49	-0,62	Common
TF233	HMG		0,72	-1,43	-2,15	Common
TF626	HD-like		-3,62	0,91	4,52	Common
TF660	CCHC (Zn)		-0,83	1,04	1,88	Common
TF913	WRKY family	WRKY	-1,48	0,77	2,25	Common
TF962	AP2/EREBP		-5,08	1,56	6,64	Common
TF3	AP2/EREBP		3,11	1,02	-2,08	Common
TF63	MYB		1,76	2,80	1,04	Common
TF87	ZF DHHC		1,20	1,40	0,20	Common
TF97	HD-like		0,77	1,28	0,51	Common

Table S3, continued

TF129	MYB/HD-like		4,45	2,37	-2,08	Common
TF136	NAC		2,17	1,21	-0,96	Common
TF140	PHD		0,86	1,22	0,37	Common
TF200	NAC		1,10	2,23	1,13	Common
TF230	HD-like		0,71	5,66	4,95	Common
TF258	HD family	HD	1,41	5,26	3,85	Common
TF270	C_2H_2 (Zn)		1,59	4,49	2,90	Common
TF296	GRAS		1,68	1,66	-0,02	Common
TF322	MADS		1,98	1,70	-0,28	Common
TF333	bHLH		2,18	1,99	-0,19	Common
TF386	ARF		1,55	0,79	-0,75	Common
TF428	C_2H_2 (Zn)		2,88	2,17	-0,71	Common
TF473	AP2/EREBP		2,15	1,22	-0,93	Common
TF497	HD family	HD	2,08	1,01	-1,07	Common
TF537	bZIP		1,09	0,80	-0,29	Common
TF549	HD family	HD-ZIP	3,89	3,02	-0,87	Common
TF552	HD family	HD-ZIP	0,87	2,09	1,22	Common
TF563	MADS		1,25	3,13	1,88	Common
TF565	HTH	FIS	1,57	1,09	-0,48	Common
TF600	bHLH		1,44	1,72	0,29	Common
TF639	bHLH		1,32	1,40	0,08	Common
TF797	HD-like		1,26	2,47	1,21	Common
TF814	HD-like		1,11	2,45	1,34	Common
TF837	MYB		5,96	1,87	-4,09	Common
TF879	PHD		2,42	3,53	1,11	Common
TF996	HD-like		4,24	3,23	-1,01	Common

Overall results and discussion

With the advent of the "omics" techniques, genomic and post-genomic studies have allowed characterizing biological cell processes at a molecular level. However, the functional biological machinery is complex, whose network is regulated at transcriptional and post-transcriptional level. Hence, a multidisciplinary approach that integrating transcriptomics, proteomics, metabolomics, bioinformatics, statistics and mathematical modeling is necessary. In agreement with the assumed complexity of biological functions and its interactional character, we have analyzed the legume responses to phytopathogenic fungi infection by using a functional genomics approach (transcriptomics and proteomics).

Within the functional genomics approaches carried out to study the defense mechanisms in legumes to phytopathogenic fungi infection, a differential expression proteomic approach was carried out in order to unveil which resistance mechanisms are involving in the response of the *Pisum sativum* to *Erysiphe pisi* and *Mycosphaerella pinodes* infections (Chapter 1 and 2, respectively). In addition, two different transcriptomics approaches have been carried out in an attempt to elucidate which mechanisms are acting in the response of the model legume *M. truncatula* to *E. pisi* infection (Chapter 3 and 4). In the chapter 3, we studied the transcriptome profile of *M. truncatula* in response to *E. pisi* infection using a microarray platform (Curto et al. 2014). For deeper knowledge of this pathosystem, we screened more than 1000 transcription factors using a high-throughput quantitative real-time PCR (qPCR) technology (Chapter 4).

One of the objectives pursued in our current project is to study the response of *P. sativum* to *E. pisi* infection by a proteomic approach. In this study, the main used platform in comparative studies was applied, i.e., a non-targeted approach based on protein separation by 2-DE, band-cutting, protein digestion, MS peptide analyses and protein identification from mass spectra (Jorrín-Novo et al. 2007; Jorrín-Novo et al. 2009). In this work the changes in the leaf proteome of two pea genotypes differing in their resistance phenotype to *E. pisi*, was analyzed by a combination of 2-DE and MALDI-TOF/TOF MS (Curto et al. 2006). Petri dish bioassays confirmed the existence

of differences in resistance to *E. pisi* between Messire and JI2480 genotypes. Furthermore, Messire leaf tissue was completely covered by powdery mildew and collapsed by day 12 post infection, while only punctual necrotic lesions (Chapter 1, fig. 1). The protein profiles of both *P. sativum* genotypes leaf tissues were analyzed by 2-DE in healthy as well as in inoculated leaves 48 h *E. pisi* post infection. Thus, leaf proteins from control non-inoculated and inoculated susceptible (Messire) and resistant (JI2480) plants were resolved by 2-DE, with IEF in the 5–8 pH range and SDS-PAGE on 12% gels. The CBB-stained gels revealed some differences between extracts from: (i) non-inoculated leaves of both genotypes (77 spots); (ii) inoculated and non-inoculated Messire leaves (19 spots); and (iii) inoculated and non-inoculated JI2480 leaves (12 spots) (Chapter 1, fig. 3).

Protein identification was accomplished by PMF combined with PFF of selected peptides by MALDI-TOF/TOF, resulting in 67 matches out of the differences observed (Chapter 1, table 2). Out of the 67 identified proteins, 57 having an assigned function belonging to several functional categories, including photosynthesis and carbon metabolism, energy production, stress and defense, protein synthesis and degradation and signal transduction. Several spots identified as proteins of the photosynthesis-carbohydrate metabolism and Krebs cycle occurred in larger amounts in JI2480 than in Messire plants, which could indicate a greater efficiency of the former in transforming light into chemical energy, CO_2 assimilation, and obtaining intermediate metabolites from photoassimilates needed for biosynthetic pathways (Burdon and Thrall 2003; Somssich and Hahlbrock 1998). As we expected another major set of proteins differentiating genotypes, all of them unique or more abundant in the JI2480 resistant plants, corresponded to stress and defense related proteins. Between them are noteworthy three identified proteins (spots 21, 22 and 29) (Chapter 1, table 2) that encoded by members of the highly duplicated family of nucleotide binding site-leucine-rich repeats (NBS-LRR) plant resistance genes that confer resistance to many plant pathogens (Schulze-Lefert and Vogel 2000), as well as a number of the proteins identified also correspond to typical pathogenesis-related proteins (PRs) that display antimicrobial activity and accumulate to high levels in response to pathogen challenge. Some of these PRs are considered molecular markers for resistance against a broad range of pathogens including *E. pisi* (Van Loon and Van Strien 1999). In addition, several identified proteins belonged to reactive oxygen species (ROS), such as

phospholipid-hydroperoxide, glutathione peroxidase, peroxidase and superoxide dismutase (Spots 20, 72 and 42, respectively) (Chapter 1, table 2), which are involved in hydrogen peroxide detoxification and are associated with lignification and cell wall phenol deposition (Passardi et al. 2004). These results indicated that defense responses are activated in the susceptible genotype, supporting the idea that resistance is a very complex process depending not only on the activation of defenses, but more importantly, on the activation kinetics of these responses. In summary, these work provided an overview of the *P. sativum-E. pisi* interaction and shed light on the putative mechanisms involved in resistance.

The *P. sativum-M. pinodes* pathosystem was analyzed by a proteomic approach to study the responses of *P. sativum* to *M. pinodes* infection (Castillejo et al. 2010). In this study response to *M. pinodes* in *P. sativum* were analyzed by using a combination of 2-DE and MALDI-TOF/TOF MS (Chapter 2). *M. pinodes* symptoms were observed on the leaves of susceptible Messire and incomplete resistant Radley pea cultivars (Chapter 2, fig. 1). Thus, resistance to *M. pinodes* in Radley was characterized by a lower success in colony establishment, associated with the rapid death of the epidermal cell being attacked by *M. pinodes* and by a smaller colony size. Two-dimensional electrophoresis allowed comparing the leaf proteome of two pea cultivars displaying different phenotypes (susceptible and partial resistance to the fungus), as well as in response to the inoculation. The analysis of CBB staining of the gels revealed a total of 84 differential protein spots (Chapter 2, table 1, fig. 2). All of the 84 protein spots were analyzed by mass spectrometry, and 31 could be matched against the NCBI database (Chapter 2, table 2). These identified proteins were classified in the following functional categories: photosynthesis, glycolysis/glyconeogenesis, citrate cycle, glutamine biosynthetic process, metabolic process, protein binding, nucleic acid binding, transcription/translation, defense and stress related proteins, cellular processes and unknown. A high proportion of photosynthetic (4/5), metabolic (4/6) and transcriptomic/translational, as well as nucleic acid binding (7/7) proteins, were found more abundant in Messire than Radley cultivar, when both inoculated and non-inoculated plants were compared (Chapter 2, fig. 5). Moreover, stress and defense-related proteins were found in all of the pairwise comparisons of protein abundance, with a clear trend to increase in inoculated plants.

In summary, the results obtained in these work revealed that differences observed between non-inoculated cultivars could be related to efficiency in energy utilization for growth and fitness purposes. With regard to the abundance pattern from differential identified proteins under inoculation, we observed an increase of proteins involved in energetic and amino acid metabolism in the resistant cultivar. In addition, a general increase in the amounts of proteins belonging to the defense and stress related categories were detected in both cultivars at the earliest stages of infection. A clear distinction between both cultivars cannot be made based on the defense and stress-related proteins identified in this study. However, most differences observed were related to efficiency in energy utilization, probably to compensate the cost of resistance, such as has been described in previous plant-pathogen interactions (Burdon and Thrall 2003). This work could help to study molecular aspects of the defense and resistance responses of legumes to ascochyta blight, as well as being used in programs aimed at improving new crop varieties by means of plant breeding and biotechnology.

The *M. truncatula-E. pisi* system was used in the study of transcriptome profile by using a microarray platform (Chapter 3). This work reported the transcriptome profiles of two *Medicago truncatula* genotypes, the powdery mildew susceptible commercial variety Parabinga and the resistant accession SA1306, at 4 and 12 h after *E. pisi* infection (hai), using Mt16kOLI1 microarrays. Differences in the response to *E. pisi* between the two genotypes were macroscopically clearly visible 2 weeks after inoculation, with profuse sporulation in the susceptible Parabinga genotype and absence of symptoms in the resistant SA1306 genotype (Chapter 3, fig. S1c, d). In addition, the histological assessments confirmed the resistance and susceptibility to *E. pisi* in Parabinga and SA1306, respectively (Chapter 3, fig. S1, table S1). The hypersensitive response associated with epidermal cell death observed as host cell cytoplasm disorganization (Chapter 3, fig. S1f) was negligible in Parabinga but marked in SA1306. Four hundred and forty six probes out of 16,086 on the microarray were significantly regulated ($p<0.05$; $0.8 \leq M \leq -0.8$) in the two *M. truncatula* genotypes in response to *E. pisi* infection at the studied time points (Chapter 3, table S4). Two hundred and ninety five of them showed sequence similarities to genes of known functional categories described by Journet et al. (Journet et al. 2002) (Chapter 3, fig. 1). The most represented category was “Secondary metabolism and hormone metabolism” (15.25 %), followed

by “Abiotic stimuli and development”, “Cell Wall”, “Defense and cell rescue”, “Protein synthesis and processing” and “Primary metabolism” (around 10 % each).

Out of 295 genes, 76 showed sequence similarities to genes of know functional categories described by Journet et al. (Journet et al. 2002), were differentially regulated in SA1306 compared to Parabinga ($0.8 \leq F \leq -0.8$, $p \leq 0.05$). Most of them (48/76) were regulated at 4 hai, meanwhile around 30 % of sequences (24/76) were regulated at 12 hai. The four remaining sequences were regulated at both time points. The vast proportions of regulated genes at 4 hai were induced at this time point (38/48). These sequences mainly belong to categories related to defense and stress responses (Chapter 3, table 1). Moreover, a minor proportion of regulated genes were differentially expressed in SA1306 compared to Parabinga at 12 hai (24/76). The most represented categories at this time point are “Cell Wall”, “Secondary metabolism and hormone metabolism”, “Primary metabolism” and “Gene expression and RNA metabolism”, respectively. Among the regulated genes in response to *E. pisi* infection, an important number of genes belong to cell wall metabolism, as “early nodulin 12A” , “nodulin MtN3”, “nodulin MtN19”, and expansin, involved in cell wall strengthening and elongation processes (Chapter 3, table 1). These enzymes contribute to pathogen resistance playing an important role in the guard against the spore penetration by means of physical barriers as cell wall appositions (CWAs) (Chapter 3, fig. 2). These results revealed a wide variety of mechanisms and pathways were detected to be regulated in *M. truncatula* in response to *E. pisi* infection, which mainly included cell wall reinforcement, phenylpropanoids and phytoalexins biosynthesis, pathogenesis-related proteins, burst oxidative-related proteins and signaling pathways controlled by jasmonic and salicylic acids. In summary, this study provides deep and comprehensive information of the metabolic pathways involved in a new *E. pisi/M. truncatula* pathosystem, which will help to develop new genetic tools in the breeding program of this legume.

The *M. truncatula-E. pisi* pathosystem was also studied by using high-throughput quantitative real-time PCR (qPCR) technology (Chapter 4). In this work more than 1,000 *Medicago truncatula* transcription factors (TFs) gene-specific primers were analyzed in two *Medicago truncatula* genotypes, the powdery mildew susceptible Parabinga and the resistant accession SA1306, at four hours after *E. pisi* infection, using

a *M. truncatula* transcription factor platform (Kakar et al. 2008). In this study a total of 623 genes of the qPCR TF platform (59.6%) were considered detected (Cq<40; n≥2) and 95 from them showed statistically significant differences (P<0.05) (Chapter 4, fig. 3, table S2). These 95 genes were clustered into ten groups with different expression patterns (Chapter 4, fig. 3). Around eighty percent of TF genes (79/95 genes) that showed statistically significant differences (P<0.05) were regulated at least 1.6-fold changes (0.7≥M≥0.7) (Chapter 4, table S3). Out of 79 genes, 16 and 18 were specifically regulated in Parabinga and in SA1306, respectively. The remaining 45 genes were regulated in both genotypes (Chapter 4, fig. 4 and table S3). Most of these genes including genes involved in plant disease resistance belonging to AP2/EREBP, C_2H_2 (Zn), MYB, HD, MYB/HD-like, NAC and PHD TF families. Forty eight out of the 79 TFs showed significant differences in the resistant SA1306 genotype compared to the susceptible Parabinga in response to *E. pisi* infection, suggesting that they play a critical role in the resistance mechanism against pathogen infection. Hence, this study suggest a model for the regulatory network controlling the expression of the TF genes involved in *M. truncatula* resistance to *E. pisi* (Chapter 4, fig. 4).

A subset of these genes were noteworthy to be involved in known defense pathways suggesting that they act as major regulators of transcription throughout *E. pisi* defense responses in SA1306 genotype, which belong to AUX/IAA, bHLH, E2F, HD, JUMONJI, MYB and zinc finger families (C_2C_2, C_2H_2, LIM and SBP) (Chapter 4, table 1). In summary, this work reported a collection of TFs and a regulatory network that controls the expression in *M. truncatula* of genes involved in resistance to *E. pisi*. These results will help to systematically decipher the functional roles of TF genes and to develop new strategies against powdery mildew.

References

Burdon J, Thrall P (2003) The fitness costs to plants of resistance to pathogens. Genome Biol 4:227

Castillejo MA, Curto M, Fondevilla S, Rubiales D, Jorrín JV (2010) Two-dimensional electrophoresis based proteomic analysis of the pea (*Pisum sativum*) in response to *Mycosphaerella pinodes*. J Agric Food Chem 58:12822-12832

Curto M, Camafeita E, Lopez JA, Maldonado AM, Rubiales D, Jorrín JV (2006) A proteomic approach to study pea (*Pisum sativum*) responses to powdery mildew (*Erysiphe pisi*). Proteomics 6:S163-S174

Curto M, Krajinski F, Schlereth A, Rubiales D (2014) Plant defense responses in *Medicago truncatula* unveiled by microarray analysis. Plant Mol Biol Rep, in press

Jorrín-Novo JV, Maldonado AM, Castillejo MA (2007) Plant proteome analysis: A 2006 update. Proteomics 7:2947-2962

Jorrín-Novo JV, Maldonado AM, Echevarría-Zomeño S, Valledor L, Castillejo MA, Curto M, Valero J, Sghaier B, Donoso G, Redondo I (2009) Plant proteomics update (2007–2008): Second-generation proteomic techniques, an appropriate experimental design, and data analysis to fulfill MIAPE standards, increase plant proteome coverage and expand biological knowledge. J Proteomics 72:285-314

Journet EP, van Tuinen D, Gouzy J, Crespeau H, Carreau V, Farmer MJ, Niebel A, Schiex T, Jaillon O, Chatagnier O, Godiard L, Micheli F, Kahn D, Gianinazzi-Pearson V, Gamas P (2002) Exploring root symbiotic programs in the model legume *Medicago truncatula* using EST analysis. Nucleic Acids Res 30:5579-5592

Kakar K, Wandrey M, Czechowski T, Gaertner T, Scheible W-R, Stitt M, Torres-Jerez I, Xiao Y, Redman J, Wu H, Cheung F, Town C, Udvardi M (2008) A community resource for high-throughput quantitative RT-PCR analysis of transcription factor gene expression in *Medicago truncatula*. Plant Methods 4:18

Passardi F, Penel C, Dunand C (2004) Performing the paradoxical: how plant peroxidases modify the cell wall. Trends Plant Sci 9:534-540

Schulze-Lefert P, Vogel J (2000) Closing the ranks to attack by powdery mildew. Trends Plant Sci 5:343-348

Somssich IE, Hahlbrock K (1998) Pathogen defence in plants — a paradigm of biological complexity. Trends Plant Sci 3:86-90

Van Loon LC, Van Strien EA (1999) The families of pathogenesis-related proteins, their activities, and comparative analysis of PR-1 type proteins. Physiol Mol Plant Pathol 55:85-97

Conclusions

The conclusions of the work presented in this PhD thesis, related to the different objectives pursued, are the following:

- Differential expression proteomics by 2-DE revealed changes in the protein profile of two *P. sativum* genotypes in response to *E. pisi* infection. These differences were detected between extracts: (i) non-inoculated leaves of both genotypes (77 spots); (ii) inoculated and non-inoculated susceptible Messire leaves (19 spots); and (iii) inoculated and non-inoculated resistant JI2480 leaves (12 spots).

- Out of the 106 differential spots detected in the *P. sativum-E. pisi* pathosystem, 67 were identified after MALDI-TOF/TOF analysis and database searching. These spots encode proteins belonging to several functional categories, including photosynthesis and carbon metabolism, energy production, stress and defense, protein synthesis and degradation and signal transduction.

- The *M. pinodes-P. sativum* pathosystem was studied by using a combination of 2-DE and MALDI-TOF/TOF MS revealing a total of 84 differential expressed proteins. Out of the 84 spots, 31 were identified and classified in the following functional categories: photosynthesis, glycolysis/glyconeogenesis, citrate cycle, glutamine biosynthetic process, amino acid metabolism, protein and nucleic acid binding, transcription/translation, defense and stress related proteins, cellular processes and unknown.

- The *M. truncatula-E. pisi* pathosystem was analyzed by using a microarray platform revealing 446 six probes significantly regulated, in the *M. truncatula* genotypes analyzed, in response to *E. pisi* infection at the studied time points. Out of 446 sequences, 295 showed sequence similarities to genes of known functional categories.

- The microarray studies allowed identifying 76 genes that were differentially regulated in SA1306 compared to Parabinga, which showed sequence

similarities to genes of know functional categories. Out of 76 genes, 48 and 24 were regulated at 4 hai and 12 hai, respectively. Meanwhile the rest four genes were regulated at both time points.

- Among the regulated genes detected in the microarray experiments are noteworthy an important number of genes belong to cell wall metabolism, which are involved in cell wall strengthening and elongation processes. These enzymes may contribute to pathogen resistance playing an important role in the guard against the spore penetration, by means of physical barriers as cell wall appositions.

- The *M. truncatula-E. pisi* pathosystem was analyzed by using quantitative real-time PCR (qPCR). Out of 623 transcription factor genes detected, 95 showed statistically significant differences ($P<0.05$) in the *M. truncatula* genotypes analyzed in response to *E. pisi* infection.

- 95 transcription factor genes were differential expressed in the qPCR studies in the *M. truncatula-E. pisi* pathosystem. 79 of them were regulated at least 1.6-fold changes, 16 and 18 genes were specifically regulated in Parabinga and SA1306, respectively. Meanwhile, the remaining 45 genes were regulated in both genotypes. This study suggests that these genes form part of a regulatory network that controls the expression of genes involved in resistance to *E. pisi*.

Conclusiones

Las conclusiones del trabajo presentado en esta tesis doctoral, en relación con los objetivos planteados, son los siguientes:

- El estudio de proteómica diferencial mediante 2-DE mostraron cambios en el perfil proteico de dos genotipos de *P. sativum* en respuesta a la infección de *E. pisi*. Estas diferencias fueron detectadas entre los extractos: (i) hojas de ambos genotipos no infectadas (77 spots); (ii) hojas de Messire infectadas y no infectadas (19 spots); y (iii) hojas de JI2480 infectadas y no infectadas (12 spots).

- 106 spots diferencialmente expresados fueron detectados en el patosistema *P. sativum-E. pisi*, 67 de los cuales fueron identificados mediante análisis MALDI-TOF/TOF y búsqueda en bases de datos. Estos spots codifican proteínas pertenecientes a diversas categorías funcionales, incluyendo fotosíntesis y metabolismo de carbono, metabolismo energético, stress y defensa, síntesis y degradación de proteínas y transducción de señales.

- El patosistema *M. pinodes-P. sativum* fue estudiado usando una combinación de 2-DE y MALDI-TOF/TOF MS revelando un total de 84 proteínas diferencialmente expresadas. De los 84 spots, 31 fueron identificados y clasificados en las siguientes categorías funcionales: fotosíntesis, glicolisis/gluconeogénesis, ciclo del citrato, biosíntesis de glutamina, metabolismo de aminoácidos, interacción de proteínas y ácidos nucleicos, transcripción/traducción, proteínas de defensa y stress, procesos celulares y desconocidos.

- El patosistema *M. truncatula-E. pisi* fue analizado mediante una plataforma de microarray revelando 446 genes significantemente regulados, en los genotipos de *M. truncatula* evaluados, en respuesta a la infección de *E. pisi* a los tiempos analizados. De las 446 secuencias, 295 mostraron similitud con genes pertenecientes a categorías funcionales conocidas.

- Los experimentos de microarray permitieron identificar 76 genes que fueron diferencialmente regulados en SA1306 comparados con Parabinga, los cuales mostraron similitud con genes de categorías funcionales conocidas. De los 76 genes, 48 y 24 fueron regulados a las 4 y 12 hai, respectivamente. Mientras que los cuatro genes restantes fueron regulados a los dos tiempos de muestreo evaluados.

- Entre los genes regulados que fueron identificados en los experimentos de microarray son de especial interés un importante número de genes pertenecientes al metabolismo de la pared celular, los cuales participan en los procesos de fortalecimiento y elongación de la pared celular. Estas enzimas pueden contribuir a la resistencia de la infección mediante su participación en los procesos de defensa, evitando la penetración de la espora mediante barreras físicas y cutículas de la pared celular.

- El patosistema *M. truncatula-E. pisi* fue analizado mediante PCR cuantitativa en tiempo real (qPCR). De los 623 genes que codifican factores de transcripción, 95 mostraron diferencias estadísticamente significativas ($P<0.05$) en los genotipos de *M. truncatula* analizados en respuesta a la infección de *E. pisi*.

- 95 genes que codifican factores de transcripción fueron diferencialmente expresados en los estudios de qPCR realizados sobre el patosistema *M. truncatula-E. pisi*. 79 de ellos fueron regulados al menos 1,6 veces, 16 y 18 genes fueron específicamente regulados en Parabinga y SA1306, respectivamente. Mientras que los restantes 45 genes fueron regalados en ambos genotipos. Este estudio sugiere que estos genes forman parte de una red reguladora que controla la expresión de genes implicados en la resistencia de *E. pisi*.

Appendixes: other publications

Appendix 1: Proteomics: a promising approach to study biotic interaction in legumes. A review

Euphytica (2006) 147: 37–47
DOI: 10.1007/s10681-006-3061-1

Proteomics: a promising approach to study biotic interaction in legumes. A review

J.V. Jorrín[1,4,*], D. Rubiales[2], E. Dumas-Gaudot[3], G. Recorbet[3], A. Maldonado[1], M.A. Castillejo[1] & M. Curto[1,2]

[1]*Agricultural and Plant Biochemistry Research Group, Department of Biochemistry and Molecular Biology, University of Córdoba, Córdoba, Spain;* [2]*Institute for Sustainable Agriculture, CSIC, Apdo. 4084, 14080 Córdoba, Spain;* [3]*UMR 1088 INRA/CNRS 5184/UB, (Plante-Microbe-Environnement) INRA-CMSE, BP 86510, 21065 Dijon-Cedex, France;* [4]*Present address: Campus de Rabanales, Ed. Severo Ochoa, 14071 Córdoba, Spain*
*(*author for correspondence: e-mail: bf1jonoj@uco.es)*

Received 3 December 2004; accepted 1 March 2005

Key words: Aphanomyces euteiches, broomrape, legume proteomics, *Medicago truncatula*, *Orobanche crenata*, *Pisum sativum*

Summary

During the 1990s and early 2000s, the genomes of different organisms have been completely sequenced. Nowadays, biological research is directed to understand gene expression and function. Proteomics, understood as protein biochemistry on an unprecedented and high-throughput scale, is becoming a promising and active approach in this post-genomic period. However, its application to plants is still rather limited as compared to other biological systems. After having referred to the most recent plant proteomic reviews, we focused on legume proteomics including studies with the model species *Medicago truncatula*. This review is aimed at providing to non-proteomic specialists a global overview of what might be expected in entering this field.

Abbreviations: AHL: *N*-acyl homoserine lactone; 2-DE: two-dimensional electrophoresis; ESI: electrospray ionization; ESTs: Expressed Sequence Tags; MS: mass spectrometry; MS-MS: tandem mass spectrometry; MALDI-TOF: matrix-assisted laser desorption/ionization-time of flight; MudPIT: multidimensional protein identification technology; PMF: Peptide Mass Fingerprinting

Introduction: Why proteomics?

As Nature's senior editor B. Marte stated in the March 13th, 2003, Nature insight issue on Proteomics, "We are just beginning to appreciate the power and limitations of the genomics revolution, yet hard on its heels proteomics promises an even more radical transformation of biological research" (Marte, 2003). Indeed, genomics has been the most active research field in biological science since the 1990s (in October 1990, the "Apollo Project" started; Lander et al., 2001; Venter et al., 2001), generating a huge amount of information. The genome of the model plant *Arabidopsis* (AGI, 2000) has been completely sequenced, whereas several others, including the model legume *Medicago truncatula* (http://www.ncbi.nlm.nih.gov/mapview/map_search), and cereal rice (Yu et al., 2002) are in progress. Moreover, an increasing number of Expressed Sequence Tags (ESTs) of economically important crops as well as of various plant species are now publicly available, the number of nucleotide sequences reaching 10745611 (http://www.ncbi.nlm.nih.gov/).

Once genomics, and more concretely structural genomics, has partially covered, at least at the methodological level, the objectives proposed in the early 1990s, a new era, "post-genomic era", has emerged in which biological research is directed to understand

gene expression and function at a large scale (functional genomics).

Proteomics, understood in an overall sense, as "protein biochemistry on an unprecedented, high-throughput scale" is definitely required to proceed further insight into the understanding of life processes. In the same direction "metabolomics" research, out of the scope of this review, is directed towards the understanding of the metabolic consequences of gene expression and protein activity. Proteomic studies are justified first because gene function is carried out by proteins, second because a large number of genes (i.e. an important portion (85%) of about 25,000 reported in *Arabidopsis* and 32–56,000 reported for rice) have no assigned function, third because the information obtained by using a transcriptomic approach is incomplete (i.e., post-translational modifications and protein–protein interactions), and finally because the correlation between mRNA and protein levels is remarkably and unexpectedly low (Gygi et al., 1999a; Ideker et al., 2001; Jansen & Nap, 2002; Watson et al., 2003).

Advances in proteomics have been made possible due to improvements in protein separation by two dimensional-gel electrophoresis (2-DE) (Görg et al., 2000) or multidimensional liquid chromatography (MudPIT) (Washburn et al., 2001, 2002), peptide sequencing by mass spectrometry (MS) (Steen & Mann, 2004; Venable et al., 2004), and bioinformatics (Apweiler et al., 2004; Liska & Shevchenko, 2003; Morris et al., 2002). However, progress in defining proteomes is expected to proceed at a slower pace than genome sequencing. In principle, proteins are physically and chemically far more complicated than nucleic acids with protein interactions and functions depending to a great extent on their tri-dimensional structure. In addition, the number of protein species is greater than the number of genes (depending of the type of organism and its state, from 10,000 to 150,000 gene products can be expected) due to different RNA splicing and post-traductional modifications. Finally, and unfortunately, there is no amplification method for proteins and consequently the study of low copy number species is still a problematic task.

In this review, we would like to emphasise the potential of proteomics to gain knowledge in the various fields of legume research. For this purpose, a few examples among the most demonstrative plant proteomic studies have been selected. This paper is particularly aimed at providing to non-proteomic specialists a global overview on the major plant proteomic achievements to date.

Proteomics: Objectives and technological platforms

In studying biological systems by classical biochemical approaches, researchers have traditionally attempted to purify to homogeneity one of the components of a system, excluding the possibility to analyse complex mixtures at the same time. To overcome this limitation, global approaches termed "omics" (genomics, transcriptomics, proteomics, and metabolomics) have recently been developed.

Proteomics (either considered as a scientific area or a methodological approach) deals with the study and characterization of the cellular proteome defined as the set of protein species present in a biological unit (organism, organ, tissue, cell or organelle) at a specific developmental stage and under determined external biotic and abiotic conditions. Different from a genome, a proteome must be considered dynamic. Considering the objectives, four main areas of proteomics can be defined: (i) large-scale protein identification by linking structural information obtained by N-terminal sequencing or MS analyses to DNA or protein databases (descriptive proteomics) (Dubery & Grover, 2001); (ii) variations in protein profiles between samples associated to genotypes, mutants, organs, tissues, cells, developmental stages or environmental factors followed by identification of protein showing qualitative or quantitative changes (comparative proteomics); (iii) post-translational modifications (Mann & Jensen, 2003); (iv) studies of protein–protein, protein-DNA, and protein-other ligand interactions (interactomics) (Figeys, 2003). From a methodological point of view, different strategies can be used. The first one uses classical biochemical techniques for protein separation (electrophoresis and/or chromatography) coupled with MS for analysing individual proteins, the identification of which being obtained following peptide mass fingerprinting (PMF) or *de novo* sequencing by using specific algorithms to search within protein, genomic or ESTs sequence databases. This is called "classical proteomic approach." The second would implicate the generation of a set of clones that express a representative of each protein of a proteome followed by the analysis on a genome-wide basis (genomic wide approaches) (Phizicky et al., 2003).

The classical approach, including electrophoretic separation and MS analysis, has been the main, almost exclusive, approach used in plant studies. New platforms such as multidimensional protein identification technology (MudPIT) have occasionally

Table 1. List of reviews covering the different theoretical and practical aspects of proteomics

Proteomic areas	References
General opinion	Phizicky et al., 2003; Patterson & Aebersold, 2003
Sample preparation	Shaw & Riederer, 2003. Righetti et al., 2003
2-DE electrophoresis	Görg et al., 2000; Gygi et al., 2000; Rabilloud, 2002
Detection	Gygi et al., 1999b; Patton, 2002; Patton et al., 2002; Miura, 2003; Chevalier et al., 2004
Mass spectrometry	Aebersold & Mann, 2003; Chamrad et al., 2004; Newton et al., 2004
Bioinformatics and related	Apweiler et al., 2004; Mathesius et al., 2002; Liska & Shevchenko, 2003

been used with very promising results (Koller et al., 2002). Other techniques such as multiplexed/tagged proteomics, protein chips or microarrays, wide genomic approaches, *in vivo* proteomics by direct tissue profiling are far from being a reality in plant research. Numerous excellent reviews have recently been published describing developments in diverse proteomic areas. The reader is refereed to the non-exhaustive list presented in Table 1.

Proteomic studies in plants

Proteomics is expected to revolutionize plant research by bringing new opportunities to deepen our knowledge in plant biology and crop improvement (Jacobs et al., 2000). However, up to now, most of the proteomic studies were focused on humans, model prokaryotes (*Escherichia coli*) or unicellular eukaryotes (*Saccharomyces cerevisiae*) (Patterson & Aebersold, 2003). As an example, the number of plant proteomic papers published so far in specialised journals such as Proteomics, Electrophoresis or Molecular and Cellular Proteomics is about 5%, leading to the statement that "plant proteomics is still in its infancy" (Thiellement et al., 2002). These studies are mainly concerned with the model plant *Arabidopsis thaliana*, and to a lesser extent rice. Nevertheless, the number of plant proteomic articles has increased exponentially (i.e. Phytochemistry 2004, volume 65, issues 11 and 12). Plant proteomic projects and published papers cover different aspects of both basic and applied plant biology research including structural proteomics of the whole organism, organ, tissue, cells, subcellular compartments as well as comparative proteomics in relation to various processes (developmental stages, responses to environmental biotic and abiotic stresses, signal transduction pathways, post-translational protein modifications, mutational analysis, genotype characterisation, and phylogenetic studies). All this has now been covered by an important number of reviews, as summarised in Table 2. In plant interactions with other organisms and plant defence responses to biotic stresses, few studies have been carried out that have focused on signalling processes (Butt et al., 2003; Lecourieux-Ouaked et al., 2000; Martin et al., 2003; Mathesius et al., 2003b; Peck, 2003; Rakwal & Agrawal, 2003; Ramonell & Somerville, 2002; Romeis, 2001; Xing et al., 2002).

Proteomic studies in legumes

The study of economically important legume crops such as soybean, pea, alfalfa, bean or chickpea is complicated because of their large genome sizes or polyploidy. Fortunately, due to their suitability for plant genomics and with the aim of getting insight into agronomically important legume-microbe interactions, two plant species: *Medicago truncatula* and *Lotus japonicus* have emerged as model systems for legumes (www.medicago.org; Handberg & Stougaard, 1992). Both models are convenient for proteomic studies as their genome sequencing is under way and large collections of ESTs databases corresponding to various biological situations are available on line. Nevertheless, to our knowledge all proteomic papers published to date have dealt with the model system *Medicago truncatula* while few proteomics studies have been reported with other legume species (David et al., 2004; Fecht-Christoffers et al., 2003; Maruyama et al., 2003; Mooney & Thelen, 2004; Morris & Djordjevic, 2001; Repetto et al., 2003; Schiltz et al., 2004; Watson et al., 2004).

Proteomic studies in *Medicago truncatula*

The alfalfa relative *Medicago truncatula* (annual barrel medic) is gaining interest as a model plant for structural

Table 2. Plant proteomic reviews published since 1999

Thiellement et al., 1999. Proteomics for genetic and physiological studies in plants.
Santoni et al., 1999. Proteomics for genetic and physiological studies in plants.
Jacobs et al., 2000. Proteomics in plant biotechnology and secondary metabolism.
Porubleva & Chitnis, 2000. Proteomics: A powerful tool in the post-genomic era.
Zivy & de Vienne, 2000. Proteomics: A link between genomics, genetics and physiology.
Dubery & Grover, 2001. Current initiatives in proteomics research: The plant perspective.
Rossignol, 2001. Analysis of the plant proteome.
Van Wijk, 2001. Challenges and prospects of plant proteomics.
Holtorf et al., 2002. Plant functional genomics.
Kersten et al., 2002. Large-scale plant proteomics.
Thiellement et al., 2002. Combining proteomic and genetic studies in plants.
Whitelegge, 2002. Plant proteomics: BLASTing out of a MudPIT.
Xing et al., 2002. Towards genomic and proteomic studies of protein phophorilation in plant-pathogen interactions.
Yi-Ming et al., 2002. Plant Proteomics in the post-genomic era.
Heazlewood & Millar, 2003. Integrated plant proteomics-putting the green genome to work.
Kazan, 2003. Alternative splicing and proteome diversity in plants: the tip of the iceberg has just emerged.
Mathesius et al., 2003a. Proteomics as a functional genomics tool.
Rakwal & Agrawal, 2003. Proteomics: Current status and future perspectives.
Cánovas et al., 2004. Plant proteome analysis.
Park, 2004. Proteomic studies in plants.
Newton et al., 2004. Plant proteome analysis by mass spectrometry: principles, problems, pitfalls and recent developments.
Hirano et al., 2004. Technical aspects of functional proteomics in plants.
Rose et al., 2004. Tackling the plant proteome: Practical approaches, hurdles and experimental tools.

and functional genomics directed to help in the identification of agronomical important genes in crop legumes, including those for root symbioses, disease/pest resistance, plant architecture, seed quality and production of specific secondary metabolites (Frugoli & Harris, 2001). Its validation as a model system is due to the relatively high level of synteny between legume genomes and, in comparison with other members of the *Leguminosae* family, to its diploid ($2n = 16$) and smaller genome (454 to 526 Mbp) (Blondon et al., 1994). Additional advantages concern its self-fertilising nature, short regeneration time of about 3 months, together with its capacity to be regenerated from cell culture lines, and transformed by *Agrobacterium.* Numerous ecotypes of *M. truncatula*, collected throughout its center of origin in the Mediterranean basin exhibit considerable phenotypic variations for growth habit, flowering time, symbiotic specificity and disease resistance, constituting an important resource to examine the genetic basis of legume functions (Cook, 1999). A number of mutants have also been obtained (Penmetsa & Cook, 2000). In the last 3 years, as a result of initiatives and intensive research on *M. truncatula* genomics more than 190,000 expressed sequence tags (ESTs) obtained from different organs, developmental stages, beneficial and pathogen-challenged plants, have been sequenced (Bell et al., 2001; Lamblin et al., 2003) and deposited in public databases: the *Medicago* Genome Initiative (MGI) at the Noble Foundation (http://www.noble.org/medicago/index.htm), the TIGR *Medicago truncatula* gene index (http://www.tigr.org/tdb/mtgi). More genomic information is now available from the NSF/EU-sponsored *Medicago truncatula* Consortium (http://www.medicago.org/) and from the international genomic sequence project initiated in spring 2001 at the University of Oklahoma (http://www.genome.ou.edu/medicago.html) that has completed sequencing the chloroplast genome.

Projects to study the *Medicago truncatula* proteome have been initiated in different labs worldwide with a number of papers being published (Asirvatham et al., 2002; Bestel-Corre et al., 2002, 2004; Dumas-Gaudot et al., 2004; Gallardo et al., 2003; Mathesius et al., 2001; Watson et al., 2003), and 2-DE protein map databases available on line (http://www.noble.org/2dpage/search.asp; http://semele.anu.edu.au/2d/2d.html). The E. Dumas-Gaudot's group at Dijon (France), after having studied the root proteome with regards to colonisation with either the mycorrhizal fungus *Glomus mosseae* or the

bacterium *Sinorhizobium meliloti* (Bestel-Corre et al., 2002, 2004) has initiated subcellular approaches on membrane compartments to analyse the arbuscular mycorrhizal symbiosome (Valot et al., 2004 and personal communication). The L.W. Sumner's group at the Noble Foundation (Ardmore, OK, USA) is currently conducting a survey of the *Medicago truncatula* proteomes involving protein profiling of specific tissues and cell cultures (Watson et al., 2004; http://www.noble.org/PlantBio/MS/proteomics.html). The B.G. Rolfe's group, at the Australian National University (Canberra, Australia) has established the proteome reference maps of both roots and embryogenic cell cultures (Imin et al., 2004; Mathesius et al., 2001; http://semele.anu.edu.au/2d/2d.html) and has extensively studied nitrogen-fixing legume symbioses (Rolfe et al., 2003; Mathesius et al., 2003a, b). Within the EU Grain Legumes Project, Thompson's group at Dijon (France), is using proteomics to establish the time frame of diverse metabolic processes related to reserve accumulation during *M. truncatula* seed development (Gallardo et al., 2003). The role of the identified proteins will further be assessed by a combination of forward and reverse genetics such as TILLING (targeting induced local lesions in genomes) methodology (McCallum et al., 2000). Finally, and within the same EU project, the J. Jorrín's group, at the University of Córdoba (Spain) has just initiated a project in which plant responses and resistance to pathogens (*Uromyces, Erysiphe* and *Mycosphaerella*) and parasitic plants (*Orobanche crenata*) in *M. truncatula* and *P. sativum* are being studied at the proteomic level. The general strategy utilized for these experiments comprises 2-DE protein profile characterization of resistant and susceptible genotypes followed by MS analysis of differential expressed spots (MALDI-TOF or MS-MS) and identification by DNA, EST or protein database searching using specific algorithms (i.e. MASCOT) (Figure 1).

Proteomic studies of the pathogen and parasitic plant interactions in legumes

Compared to the number of proteomic publications in the field of beneficial plant–microbe interactions (nitrogen-fixing symbioses in legumes and arbuscular mycorrhizal symbioses), the use of proteomics appears rather limited in the area of plant responses to pathogens. To our knowledge, only three studies dealt with root interactions with pathogens and parasitic plants (Table 3).

Mathesius et al. (2003b) used a proteomic approach to detect the *M. truncatula* responses to the *N*-acyl homoserine lactone (AHL) signals from the pathogenic bacteria *Pseudomonas aeruginosa*. Compared to the AHL from the nitrogen-fixing bacteria *Sinorhizobium meliloti*, they established that one-third of the responsive proteins to the two AHL was distinct in terms of magnitude or direction of changes. It was suggested that the plant was able to distinguish between AHLs of fairly similar structures.

By using 2-DE, the root protein profiles of *M. truncatula* after *Aphanomyces euteiches* pathogen infection were analyzed during a time course experiment (Colditz et al., 2004). Following MALDI-TOF-MS analyses and PMF, a number of spots that were differentially expressed in response to the infection were identified. The majority of the induced proteins belonged to the family of the class 10 of Pathogenesis-Related proteins (PR10), while others corresponded to putative cell wall proteins and enzymes of the phenylpropanoid–isoflavonoid pathway.

A comparative proteomics approach is being carried out between resistant and susceptible accessions of *M. truncatula* to broomrape parasitic plants (Castillejo et al., 2004a). A similar study was conducted with *Pisum sativum*, which allowed the same group to identify a certain number of proteins belonging to the carbohydrate and nitrogen metabolisms (Castillejo et al., 2004b). The fact that two metabolic pathways

Table 3. Proteomic publications on legume-microbe and -parasitic plants interactions

Biological situation	References
Nitrogen-fixing symbioses	Winzer et al., 1999; Panter et al., 2000; Natera et al., 2000; Morris & Djordjevic, 2001; Saalbach et al., 2002; Rolfe et al., 2003; Mathesius et al., 2003b
Arbuscular mycorrhizal symbiosis	Bestel-Corre et al., 2002; Repetto et al., 2003; Bestel-Corre et al., 2004
Pathogen infection	Mathesius et al., 2003b; Colditz et al., 2004; David et al., 2004
Plant parasitic interactions	Castillejo et al., 2004a,b

42

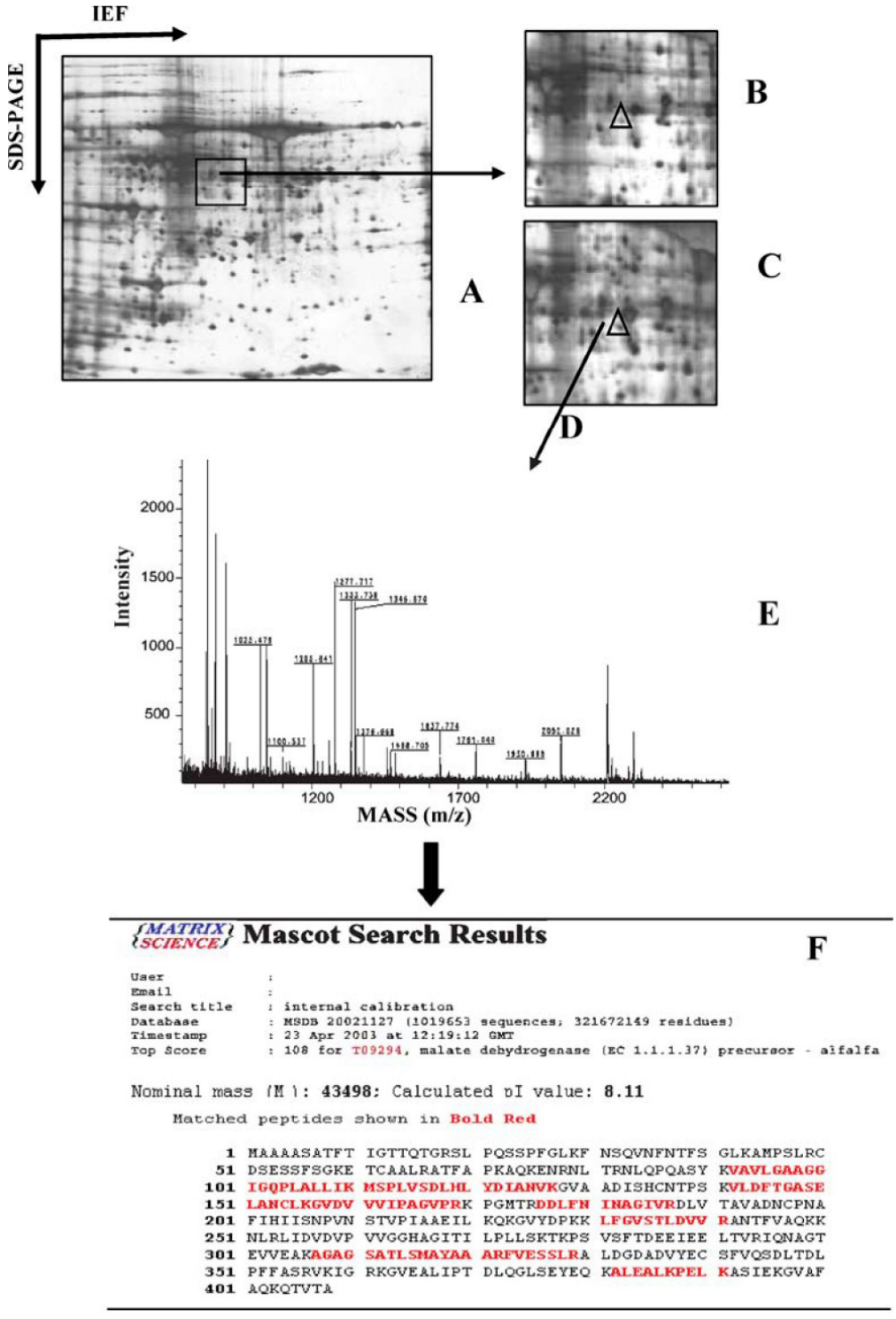

Figure 1. Schematic representation of the strategy utilized in the identification of proteins differentially expressed in leaves of *Medicago truncatula* in response to the inoculation with *Uromyces striatus.* A. 2-DE gel (pH 5–8) of infected leaf tissue. B and C correspond to gel areas showing differentially expressed spots (B: control non-infected; C: infected). D. Excised spots are subjected to trypsin digestion. E. Mass spectrometry analysis (MALDI-TOF). F. Protein spot identification by using MASCOT algorithm. PMF values allowed the identification of malate dehydrogenase precursor.

(carbon and nitrogen) seemed to be affected in relation to susceptibility/resistance of the pea genotype has opened up new possibilities to better understand the re-direction of host assimilates from host sinks to the parasite. In addition, these data have indicated that typical plant defence responses to microbial pathogens were also involved in resistance to parasitic plants.

Conclusions

As underlined above, proteomics in legumes has mainly addressed the characterisation of proteins from different tissues/organs or related to biotic interactions. However, this approach is also expected to be relevant to many additional aspects of legume biology including pathology, tolerance to abiotic stresses and genotype characterisation, allowing improvements to be made in marker-assisted selection. Such aspects have been underlined in Thiellement et al. (2002). As an example, Cabané et al. (1993) identified chilling–acclimation-related proteins in soybean, one of them being a heat shock protein. More recent papers emphasise the use of proteomics for studying basal and R-gene-mediated resistance in *Arabidopsis* (Jones et al., 2004). Similarly, a comparative proteomic analysis was carried out in two lines of *Lycopersicon hirsutum* harbouring two different quantitative trait loci (QTL) that control resistance to bacterial canker, suggesting that these two QTLs may confer resistance to bacterial infection through distinct mechanisms (Coaker et al., 2004). In a given pathologic situation, additional knowledge may also be gained when well-defined stages of the plant infection process are targeted as it was recently exemplified in the rice blast fungus interaction in which the fungal proteome was analysed during appressoria formation (Kim et al., 2004). The development of a similar approach in the case of legume resistance to parasitic plant infection could reveal new, unexpected pathways and will help to understand the specific early resistance mechanisms involved, if any. In addition, the proteomic investigation of biocontrol situations can be considered (Jie et al., 2004). Last but not least, proteomics can be employed to analyse nutritionally relevant proteins (Kvasnicka, 2003) and to study important legume seed proteins (Gallardo et al., 2003; Mooney et al., 2004; Schiltz et al., 2004). Proteomic surveys have also proved to be a useful tool to investigate food and feed sources for known allergens (Koller et al., 2002).

In summary, the combination of proteomic technology with genetics, molecular biology, plant pathology and physiology is expected to increase our knowledge of protein functions in legumes. Plant proteomics will certainly continue to benefit from the most recent technical developments, among which sub-cellular proteomics is likely to play a major role (Hoa le et al., 2004). Nevertheless, one has to keep in mind that protein expression monitoring in plants may be hampered by practical limitations such as costs and availability of required instrumentation.

Acknowledgments

JVJ acknowledges financial support from the EU (Grain Legumes Project; GL-IP, FP6-566223).

References

Aebersold, R. & M. Mann, 2003. Mass spectrometry-based proteomics. Nat Biotechnol 422: 198–207.

AGI, 2000. *Arabidopsis* genome initiative. Nature 408: 796–815.

Apweiler, R., A. Bairoch & C.H. Wu, 2004. Protein sequence databases. Curr Opin Chem Biol 8: 76–80.

Asirvatham, V.S., B.S. Watson & L.W. Sumner, 2002. Analytical and biological variances associated with proteomic studies of *Medicago truncatula* by two-dimensional polyacrylamide gel electrophoresis. Proteomics 2: 960–968.

Bell, C.J., R.A. Dixon, A.D. Farmer, R. Flores, J. Inman, R.A. Gonzales, M.J. Harrison, N.L. Paiva, A.D. Scott, J.W. Weller & G.D. May, 2001. The *Medicago* Genome Initiative: A model legume database. Nucl Acids Res 29: 114–117.

Bestel-Corre, G., E. Dumas-Gaudot, V. Poinsot, M. Dieu, J.F. Dierick, D. van Tuinen, J. Remacle, V. Gianinazzi-Pearson & S. Gianinazzi, 2002. Proteome analysis and identification of symbiosis-related proteins from *Medicago truncatula* Gaertn. by two dimensional electrophoresis and mass spectrometry. Electrophoresis 23: 122–137.

Bestel-Corre, G., S. Gianinazzi & E. Dumas-Gaudot, 2004. Impact of sewage sludge on *Medicago truncatula* symbiotic proteome. Phytochemistry 65: 1651–1659.

Blondon, F., D. Marie, S. Brown & A. Kondorosi, 1994. Genome size and base composition in *Medicago sativa* and *Medicago truncatula* species. Genome 37: 264–270.

Butt, Y.K.C., J.H.K. Lum & S.C.L. Lo, 2003. Proteomic identification of plant proteins probed by mammalian nitric oxide synthase antibodies. Planta 216: 762–771.

Cabané, M., P. Calvet, P. Vincens & A.M. Boudet, 1993. Characterization of chilling-acclimation-related proteins in soybean and identification of one as a member of the one of the heat shock (HSP70) family. Planta 190: 346–355.

Cánovas, F.M., E. Dumas-Gaudot, G. Recorbet, J. Jorrín, H.-P. Mock & M. Rossignol, 2004. Plant Proteome analysis. Proteomics 4: 285–298.

Castillejo, M.A., E. Dumas-Gaudot, D. Rubiales & J. Jorrín, 2004a. 2-DE analysis of the protein profile in healthy and broomrape (*Orobanche crenata*)-infected *Medicago truncatula* root tissue. 6th Siena Meeting (from Genome to Proteome). Abstract book, 156.

Castillejo, M.A., N. Amiour, E. Dumas-Gaudot, D. Rubiales & J. Jorrin, 2004b. A proteomic approach to studying response to crenate broomrape (*Orobanche crenata*) in pea (*Pisum sativum*). Phytochemistry 65: 1817–1828.

Chamrad, D.C., G. Körting, K. Stühler, H.E. Meyer, J. Klose & M. Blüggel, 2004. Evaluation of algorithms for protein identification from sequence databases using mass spectrometry data. Proteomics 4: 619–628.

Chevalier, F., V. Rofidal, P. Vanovz, A. Bergoin & M. Rossignol, 2004. Proteomic capacity of recent fluorescent dyes for protein staining. Phytochemistry 65: 1499–1506.

Coaker, G.L., B. Willard, M. Kinter, E.J. Stockinger & D. Francis, 2004. Proteomic analysis of resistance mediated by Rcm 2.0 and Rcm 5.1, two loci controlling resistance to bacterial canker of tomato. Mol Plant Microbe In 9: 1019–1028.

Colditz, F., O. Nyamsuren, K. Niehaus, H. Eubel, H.-P. Braun & F. Krajinski, 2004. Proteomic approach: Identification of *Medicago truncatula* proteins induced in roots after infection with the pathogenic oomycete *Aphanomyces euteiches*. Plant Mol Biol 55: 109–120.

Cook, D.R., 1999. *Medicago truncatula* – A model in the making! Curr Opin Plant Biol 2: 301–304.

David, H., N. Slaymaker & T. Keen, 2004. Syringolide elicitor-induced oxidative burst and protein phosphorylation in soybean cells, and tentative identification of two affected phosphoproteins. Plant Sci 166: 387–396.

Dubery, H. & A. Grover, 2001. Current initiatives in proteomics research: The plant perspective. Curr Sci India 80: 262–269.

Dumas-Gaudot, E., N. Amiour, S. Weidmann, G. Bestel-Corre, B. Valot, S. Lenogue, V. Gianninazzi-Pearson & S. Gianninazzi, 2004. A technical trick for studying proteomics in parallel to transcriptomics in symbiotic root-fungus interactions. Proteomics 4: 451–453.

Fecht-Christoffers, M.M., H.-P. Braun, C. Lemaitre-Guillier, A. VanDorsselaer & W.J. Horst, 2003. Effect of manganese toxicity on the proteome of the leaf apoplast in cowpea. Plant Physiol 133: 1935–1946.

Figeys, D., 2003. Novel approaches to map protein interactions. Curr Opin Biotechnol 14: 119–125.

Frugoli, J. & J. Harris, 2001. *Medicago truncatula* on the move. Plant Cell 13: 458–463.

Gallardo, K., C. Le Signor, J. Vandekerckhove, R.D. Thompson & J.Burstin, 2003. Proteomics of *Medicago truncatula* seed development establishes the time frame of diverse metabolic processes related to reserve accumulation. Plant Physiol 134: 1598–1613.

Görg, A., C. Obermaier, G. Boguth, A. Harder, B. Scheibe, R. Wildgruber & W. Weiss, 2000. The current state of two-dimensional electrophoresis with immobilized pH gradients. Electrophoresis 21: 1037–1053.

Gygi, S.P., G.L. Corthals, Y. Zhang, Y. Rochon & R. Aebersold, 2000. Evaluation of two-dimensional gel electrophoresis-based proteome analysis technology. Proc Natl Acad Sci USA 97: 9390–9395.

Gygi, S.P., Y. Rochon, B.R. Franza & R. Aebershold, 1999a. Correlation between protein and mRNA abundance in yeast. Mol Cell Biol 19: 1720–1730.

Gygi, S.P., B. Rist, S.A. Gerber, F. Turecek, M.H. Gelb & R. Aebersold, 1999b. Quantitative analysis of complex protein mixtures using isotope-coded affinity tags. Nat Biotechnol 17: 994–999.

Handberg, K. & J. Stougaard, 1992. *Lotus japonicus*, an autogamous, diploid legume species for classical and molecular genetics. Plant J 2: 487–496.

Heazlewood, J.L. & A.H. Millar, 2003. Integrated plant proteomics-putting the green genome to work. Funct Plant Biol 30: 471–482.

Hirano, H., N. Islam & H. Kawasaki, 2004. Technical aspects of functional proteomics in plants. Phytochemistry 65: 1487–1498.

Hoa le, T.P., M. Nomura, H. Kajiwara, D.A. Day & S. Tajima, 2004. Proteomic analysis on symbiotic differentiation of mitochondria in soybean nodules. Plant Cell Physiol 45: 300–308.

Holtorf, H., M.C. Guitton & R. Reski, 2002. Plant functional genomics. Naturwissenchaften 89: 235–249.

Ideker, T., V. Thorsson, J.A. Ranish, R. Christmas, J. Buhler, J.K. Eng, R. Bumgarner, D.R. Goodlett, R. Aebersold & L. Hood, 2001. Integrated genomic and proteomic analyses of a systematically perturbed metabolic network. Science 292: 929–934.

Imin, N., F. De Jong, U. Mathesius, G. van Noorden, N.A. Saeed, X.D. Wang, R.J. Rose & B.G. Rolfe, 2004. Proteome reference maps of *Medicago truncatula* embryogenic cell cultures generated from single protoplasts. Proteomics 7: 1883–1896

Jacobs, D.I., R. van der Heijden & R. Verpoorte, 2000. Proteomics in plant biotechnology and secondary metabolism. Phytochem Anal 11: 277–287.

Jansen, R.C. & J.P. Nap, 2002. Errors in genomics and proteomics. Nat Biotechnol 20: 19.

Jie, C., G.G. Harman, A. Comis, C. GenWu & L. Hainan, 2004. The change of maize plant proteome affected by *Trichoderma harzianium* and *Pithium ultimum.* Acta Phytopathol Sin 34: 319–328.

Jones, A.M.E., V. Thomas, B. Truman, K. Lilley, J. Mansfield & M. Grant, 2004. Specific changes in the *Arabidopsis* proteome in response to bacterial challenge: differentiating basal and R-gene mediated resistance. Phytochemistry 65: 1805–1816.

Kazan, K., 2003. Alternative splicing and proteome diversity in plants: The tip of the iceberg has just emerged. Trends Plant Sci 8: 468–471.

Kersten, B., L. Bürkle, E.J. Kuhn, P. Giavalisco, Z. Konthur, A. Lueking, G. Walter, H. Eickhoff & U. Schneider, 2002. Large-scale plant proteomics. Plant Mol Biol 48: 133–141.

Kim, S.T., S. Yu, S.G. Kim, H.J. Kim, S.Y. Kang, D.U. Hwang, Y.S. Jang & K.Y. Kang, 2004. Proteome analysis of rice blast fungus (*Magnaporthe grisea*) proteome during appressorium formation. Proteomics 4: 3579–3587.

Koller, A., M.P. Washburn, B.M. Lange, N.L. Andon, C. Deciu, P.A. Haynes, L. Hays, D. Schieltz, W. Ulaszek, D. Wolters & J.R. Yates III, 2002. Proteomic survey of metabolic pathways in rice. Proc Natl Acad Sci USA: 11969–11974.

Kvasnicka, F., 2003. Proteomics: General strategies and application to nutritionally relevant proteins. J Chromat B 787: 77–89.

Lamblin, A.F.J., J.A. Crow, J.E. Johnson, K.A.T. Silverstein, T.M. Kunau, A. Kilian, D. Benz, M. Stromvik, G. Endre, K.A. Van den Bosch, D.R. Cook, N.D. Young & E.F. Retzel, 2003. MtDB: a database for personalized data mining of the model legume *Medicago truncatula* transcriptome. Nucl Acids Res 31: 196–201.

Lander, E.S., L.M. Linton, B. Birren, C. Nusbaum, M.C. Zody, J. Baldwin, K. Devon, K. Dewar, M. Doyle, W. FitzHugh, R. Funke, D. Gage, K. Harris, A. Heaford, J. Howland, L. Kann, J. Lehoczky, R. LeVine, P. McEwan, K. McKernan, J. Meldrim, J.P. Mesirov, C. Miranda, W. Morris, J. Naylor, C. Raymond, M. Rosetti, R. Santos, A. Sheridan, C. Sougnez, N. Stange-Thomann, N. Stojanovic, A. Subramanian, D. Wyman, J. Rogers, J. Sulston,

R. Ainscough, S. Beck, D. Bentley, J. Burton, C. Clee, N. Carter, A. Coulson, R. Deadman, P. Deloukas, A. Dunham, I. Dunham, R. Durbin, L. French, D. Grafham, S. Gregory, T. Hubbard, S. Humphray, A. Hunt, M. Jones, C. Lloyd, A. McMurray, L. Matthews, S. Mercer, S. Milne, J.C. Mullikin, A. Mungall, R. Plumb, M. Ross, R. Shownkeen, S. Sims, R.H. Waterston, R.K. Wilson, L.W. Hillier, J.D. McPherson, M.A. Marra, E.R. Mardis, L.A. Fulton, A.T. Chinwalla, K.H. Pepin, W.R. Gish, S.L. Chissoe, M.C. Wendl, K.D. Delehaunty, T.L. Miner, A. Delehaunty, J.B. Kramer, L.L. Cook, R.S. Fulton, D.L. Johnson, P.J. Minx, S.W. Clifton, T. Hawkins, E. Branscomb, P. Predki, P. Richardson, S. Wenning, T. Slezak, N. Doggett, J.F. Cheng, A. Olsen, S. Lucas, C. Elkin, E. Uberbacher, M. Frazier, R.A. Gibbs, D.M. Muzny, S.E. Scherer, J.B. Bouck, E.J. Sodergren, K.C. Worley, C.M. Rives, J.H. Gorrell, M.L. Metzker, S.L. Naylor, R.S. Kucherlapati, D.L. Nelson, G.M. Weinstock, Y. Sakaki, A. Fujiyama, M. Hattori, T. Yada, A. Toyoda, T. Itoh, C. Kawagoe, H. Watanabe, Y. Totoki, T. Taylor, J. Weissenbach, R. Heilig, W. Saurin, F. Artiguenave, P. Brottier, T. Bruls, E. Pelletier, C. Robert, P. Wincker, D.R. Smith, L. Doucette-Stamm, M. Rubenfield, K. Weinstock, H.M. Lee, J. Dubois, A. Rosenthal, M. Platzer, G. Nyakatura, S. Taudien, A. Rump, H. Yang, J. Yu, J. Wang, G. Huang, J. Gu, L. Hood, L. Rowen, A. Madan, S. Qin, R.W. Davis, N.A. Federspiel, A.P. Abola, M.J. Proctor, R.M. Myers, J. Schmutz, M. Dickson, J. Grimwood, D.R. Cox, M.V. Olson, R. Kaul, C. Raymond, N. Shimizu, K. Kawasaki, S. Minoshima, E.G.A. Vans, M. Athanasiou, R. Schultz, B.A. Roe, F. Chen, H. Pan, J. Ramser, H. Lehrach, R. Reinhardt, W.R. McCombie, M. de la Bastide, N. Dedhia, H. Blocker, K. Hornischer, G. Nordsiek, R. Agarwala, L. Aravind, J.A. Bailey, A. Bateman, S. Batzoglou, E. Birney, P. Bork, D.G. Brown, C.B. Burge, L. Cerutti, H.C. Chen, D. Church, M. Clamp, R.R. Copley, T. Doerks, S.R. Eddy, E.E. Eichler, T.S. Furey, J. Galagan, J.G. Gilbert, C. Harmon, Y. Hayashizaki, D. Haussler, H. Hermjakob, K. Hokamp, W. Jang, L.S. Johnson, T.A. Jones, S. Kasif, A. Kaspryzk, S. Kennedy, W.J. Kent, P. Kitts, E.V. Koonin, I. Korf, D. Kulp, D. Lancet, T.M. Lowe, A. McLysaght, T. Mikkelsen, J.V. Moran, N. Mulder, V.J. Pollara, C.P. Ponting, G. Schuler, J. Schultz, G. Slater, A.F. Smit, E. Stupka, J. Szustakowski, D. Thierry-Mieg, J. Thierry-Mieg, L. Wagner, J. Wallis, R. Wheeler, A. Williams, Y.I. Wolf, K.H. Wolfe, S.P. Yang, R.F. Yeh, F. Collins, M.S. Guyer, J. Peterson, A. Felsenfeld, K.A. Wetterstrand, A. Patrinos, M.J. Morgan, P. de Jong, J.J. Catanese, K. Osoegawa, H. Shizuya, S. Choi & Y.J. Chen, 2001. Initial sequencing and analysis of the human genome. Nature 409: 860–921.

Lecourieux-Ouaked, F., A. Pugin & A. Lebrun-Garcia, 2000. Phosphoproteins involved in the signal transduction of cryptogein, an elicitor of defense reactions in tobacco. Mol Plant Microb In 8: 821–829.

Liska, A.J. & A. Shevchenko, 2003. Expanding the organismal scope of proteomics: Cross-species protein identification by mass spectrometry and its implication. Proteomics 3: 19–28.

Mann, M. & O.N. Jensen, 2003. Proteomic analysis of post-translational modifications. Nat Biotechnol 21: 255–261.

Marte, B., 2003. Proteomics editorial. Nat Biotechnol 422: 191.

Martin, G.B., A.J. Bogdanove & G. Sessa, 2003. Understanding the functions of plant disease resistance proteins. Annu Rev Plant Biol 54: 23–61.

Maruyama, M., T. Fukuda, S. Saka, N. Inui, J. Coto, M. Miyagawa, M. Hayashi, M. Sawada, T. Moriyama & S. Utsumi, 2003. Molecular and structural analysis of electrophoretic variants of soybean seed storage proteins. Phytochemistry 64: 701–708.

Mathesius, U., N. Imin, S.H.A. Natera & B.G. Rolfe, 2003a. Proteomics as a functional genomics tool. In: Plant functional genomics. Methods Protocols 236: 395–414.

Mathesius, U., S. Mulders, M.S. Gao, M. Teplitski, G. Caetano-Anolles, B.G. Rolfe & W.D. Bauer, 2003b. Extensive and specific responses of a eukaryote to bacterial quorum-sensing signals. Proc Natl Acad Sci USA 100: 1444–1449.

Mathesius, U., N. Imin, H. Chen, M.A. Djordjevic, J.J. Weinman, S.H. Natera, A.C. Morris, T. Kerim, S. Paul, C. Menzel, G.F. Weiller & B.G. Rolfe, 2002. Evaluation of proteome reference maps for cross-species identification of proteins by peptide mass fingerprinting. Proteomics 2: 1288–303.

Mathesius, U., G. Keijzers, S.H.A. Natera, J.J. Weinman, M.A. Djordjevic & B.G. Rolfe, 2001. Establishement of a root proteome reference map for the model legume *Medicago truncatula* using the expressed sequence tag database for peptide mass fingerprinting. Proteomics 1: 1424–1440.

McCallum, C., L. Comai, E.A. Greene & S. Henikoff, 2000. Targeted screening for induced mutations. Nat Biotechnol 18: 455–457.

Miura, K., 2003. Imaging technologies for the detection of multiple stains in proteomics. Proteomics 3: 1097–1108.

Morris, A.C. & M.A. Djordjevic, 2001. Proteome analysis of cultivar-specific interactions between *Rhizobium leguminosarum* biovar *trifolii* and subterranean clover cultivar Woogenellup. Electrophoresis 22: 586–598.

Morris, A.C., T. Kerim, S. Paul, C. Menzel, G.R. Weiller & B.G. Rolfe, 2002. Evaluation of proteome reference maps for cross-species identification of proteins by peptide mass fingerprinting. Proteomics 2: 1288–1303.

Mooney, B.P. & J.J. Thelen, 2004. High-throughput peptide mass fingerprinting of soybean seed proteins: Automated workflow and utility of UniGene expressed sequence tag databases. Phytochemistry 65: 1733–1744.

Natera, S.H.A., N. Guerreiro & N.A. Djordjevic, 2000. Proteome analysis of differentially displayed proteins as a tool for the investigation of symbiosis. Mol Plant. Microb In 13: 995–1009

Newton, R.P., A.G. Brenton, C.J. Smith & E. Dudley, 2004. Plant proteome analysis by mass spectrometry: Principles, problems, pitfalls and recent developments. Phytochemistry 65: 1449–1485.

Panter, S., R. Thomson, G. de Bruxelles, D. Laver, B. Trevaskis & M. Udvardi, 2000. Identification with proteomics of novel proteins associated with the peribacteroid membrane of soybean root nodules. Mol Plant Microb In 13: 325–33.

Park, O.K., 2004. Proteomic studies in plants. J Biochem Mol Biol 37: 133–138.

Patterson, S.D. & R.H. Aebersold, 2003. Proteomics: the first decade and beyond. Nat Genet 33: 311–323.

Patton, W.F., 2002. Detection technologies in proteome analysis. J Chromatogr B 771: 3–31.

Patton, W.F., B. Schulenberg & T.H. Steinberg, 2002. Two-dimensional gel electrophoresis; better than a poke in the ICAT. Curr Opin Biotech 13: 321–328.

Peck, S.C., 2003. Early phosphorylation events in biotic stress. Curr Opin Plant Biol 6: 334–338.

Peck, S.C., T.S. Nuhse, D. Hess, A. Iglesias, F. Meins & T. Boller, 2001. Directed proteomics identifies a plant-specific protein rapidly phosphorylated in response to bacterial and fungal elicitors. Plant Cell 13: 1467–1475.

Penmetsa, R.V. & D.R. Cook, 2000. Production and characterization of diverse developmental mutants of *Medicago truncatula*. Plant Physiol 123: 1387–1398.

Phizicky, E., P.I.H. Bastiaens, H. Zhu, M. Snyder & S. Fields, 2003. Protein analysis on a proteomic scale. Nat Biotechnol 422: 208–215.

Porubleva, L. & P.R. Chitnis, 2000. Proteomics: a powerful tool in the post-genomic era. Ind J Biochem Biophys 37: 360–368.

Rabilloud, T., 2002. Two-dimensional gel electrophoresis in proteomics: Old, old fashioned, but still climbs up the mountains. Proteomics 2: 3–10.

Rakwal, R. & G.K. Agrawal, 2003. Rice Proteomics: Current status and future perspectives. Electrophoresis 24, 3378–3389.

Ramonell, K.M. & S. Somerville, 2002. The genomics parade of defense responses: To infinity and beyond. Curr Opin Plant Biol 5: 291–294.

Repetto, O., G. Bestel-Corre, E. Dumas-Gaudot, G. Berta, V. Gianinazzi-Pearson & S. Gianinazzi, 2003. Targeted proteomics to identify cadmium-induced protein modifications in *Glomus mosseae*-inoculated pea roots. New Phytol 157: 555–567.

Righetti, P.-G., A. Castagna, B. Herbert, F. Reymond & J.S. Rossier, 2003. Prefractionation techniques in proteome analyses. Proteomics 3: 1397–1407.

Rolfe, B.G., U. Mathesius, M. Djordjevic, J. Weinman, C. Hocart, G. Weiller & B. Dietz, 2003. Proteomic analysis of legume-microbe Interactions. Comput Funct Genome 4: 225–228.

Romeis, T., 2001. Protein kinases in the plant defence response. Curr Opin Plant Biol 4: 407–414.

Rose, J.K., S. Bashir, J.J. Giovannoni, M.M. Jahn & R.S. Saravanan, 2004. Tackling the plant proteome: Practical approaches, hurdles and experimental tools. Plant J 39: 715–33.

Rossignol, M., 2001. Analysis of the plant proteome. Curr Opin Biotechnol 12: 131–134.

Santoni, V., D. de Vienne & M. Zivy, 1999. Proteomics for genetic and physiological studies in plants. Electrophoresis 17: 855–865.

Saalbach, G., P. Erik & S. Wienkoop, 2002. Characterisation by proteomics of peribacteroid space and peribacteroid membrane preparations from pea (*Pisum sativum*) symbiosomes. Proteomics 2: 325–337.

Schiltz, S., K. Gallardo, M. Huart, L. Negroni, N. Sommerer & J. Burstin, 2004. Proteome reference maps of vegetative tissues in pea. An investigation of nitrogen mobilization from leaves during seed filling. Plant Physiol 135: 2241–2260.

Shaw, M.M. & B.M. Riederer, 2003. Sample preparation for two-dimensional gel electrophoresis. Proteomics 3: 1408–14017.

Steen, H. & M. Mann, 2004. The ABC's (and XYZ's) of peptide sequencing. Nat Rev Mol Cell Biol 5: 699–711.

Thiellement, H., M. Zivy & C. Plomion, 2002. Combining proteomic and genetic studies in plants. J Chromat B 782: 137–149.

Thiellement, H., N. Bahrman, C. Damerval, C. Plomion, M. Rossignol, V. Santoni, D. de Vienne, & M. Zivy, 1999. Proteomics for genetic and physiological studies in plants. Electrophoresis 17: 855–865.

Van Wijk, K.J., 2001. Challenges and prospects of plant proteomics. Plant Physiol 126: 501–508.

Valot, B., S. Gianninazi & E. Dumas-Gaudot, 2004. Sub-cellular proteomic analysis of a *Medicago truncatula* root microsomal fraction. Phytochemistry 65: 1721–1732.

Venable, J.D., M.-Q. Dong, J. Wholschlegel, A. Dillin & J.R. Yates III, 2004. Automates approach for quantitative analysis of complex peptide mixtures from tandem mass spectra. Nat Methods 1: 39–45.

Venter, J.C., M.D. Adams, E.W. Myers, P.W. Li, R.J. Mural, G.G. Sutton, H.O. Smith, M. Yandell, C.A. Evans, R.A. Holt, J.D. Gocayne, P. Amanatides, R.M. Ballew, D.H. Huson, J.R. Wortman, Q. Zhang, C.D. Kodira, X.H. Zheng, L. Chen, M. Skupski, G. Subramanian, P.D. Thomas, J. Zhang, G.L.G. Miklos, C. Nelson, S. Broder, A.G. Clark, J. Nadeau, V.A. McKusick, N. Zinder, A.J. Levine, R.J. Roberts, M. Simon, C. Slayman, M. Hunkapiller, R. Bolanos, A. Delcher, I. Dew, D. Fasulo, M. Flanigan, L. Florea, A. Halpern, S. Hannenhalli, S. Kravitz, S. Levy, C. Mobarry, K. Reinert, K. Remington, J. Abu-Threideh, E. Beasley, K. Biddick, V. Bonazzi, R. Brandon, M. Cargill, I. Chandramouliswaran, R. Charlab, K. Chaturvedi, Z. Deng, V.D. Francesco, P. Dunn, K. Eilbeck, C. Evangelista, A.E. Gabrielian, W. Gan, W. Ge, F. Gong, Z. Gu, P. Guan, T.J. Heiman, M.E. Higgins, R.-R. Ji, Z. Ke, K.A. Ketchum, Z. Lai, Y. Lei, Z. Li, J. Li, Y. Liang, X. Lin, F. Lu, G.V. Merkulov, N. Milshina, H.M. Moore, A.K. Naik, V.A. Narayan, B. Neelam, D. Nusskern, D.B. Rusch, S. Salzberg, W. Shao, B. Shue, J. Sun, Z.Y. Wang, A. Wang, X. Wang, J. Wang, M.-H. Wei, R. Wides, C. Xiao, C. Yan, A. Yao, J. Ye, M. Zhan, W. Zhang, H. Zhang, Q. Zhao, L. Zheng, F. Zhong, W. Zhong, S.C. Zhu, S. Zhao, D. Gilbert, S. Baumhueter, G. Spier, C. Carter, A. Cravchik, T. Woodage, F. Ali, H. An, A. Awe, D. Baldwin, H. Baden, M. Barnstead, I. Barrow, K. Beeson, D. Busam, A. Carver, A. Center, M.L. Cheng, L. Curry, S. Danaher, L. Davenport, R. Desilets, S. Dietz, K. Dodson, L. Doup, S. Ferriera, N. Garg, A. Gluecksmann, B. Hart, J. Haynes, C. Haynes, C. Heiner, S. Hladun, D. Hostin, J. Houck, T. Howland, C. Ibegwam, J. Johnson, F. Kalush, L. Kline, S. Koduru, A. Love, F. Mann, D. May, S. McCawley, T. McIntosh, I. McMullen, M. Moy, L. Moy, B. Murphy, K. Nelson, C. Pfannkoch, E. Pratts, V. Puri, H. Qureshi, M. Reardon, R. Rodriguez, Y.-H. Rogers, D. Romblad, B. Ruhfel, R. Scott, C. Sitter, M. Smallwood, E. Stewart, R. Strong, E. Suh, R. Thomas, N.N. Tint, S. Tse, C. Vech, G. Wang, J. Wetter, S. Williams, M. Williams, S. Windsor, E. Winn-Deen, K. Wolfe, J. Zaveri, K. Zaveri, J.F. Abril, R. Guigó, M.J. Campbell, K.V. Sjolander, B. Karlak, A. Kejariwal, H. Mi, B. Lazareva, T. Hatton, A. Narechania, K. Diemer, A. Muruganujan, N. Guo, S. Sato, V. Bafna, S. Istrail, R. Lippert, R. Schwartz, B. Walenz, S. Yooseph, D. Allen, A. Basu, J. Baxendale, L. Blick, M. Caminha, J. Carnes-Stine, P. Caulk, Y.-H. Chiang, M. Coyne, C. Dahlke, A.D. Mays, M. Dombroski, M. Donnelly, D. Ely, S. Esparham, C. Fosler, H. Gire, S. Glanowski, K. Glasser, A. Glodek, M. Gorokhov, K. Graham, B. Gropman, M. Harris, J. Heil, S. Henderson, J. Hoover, D. Jennings, C. Jordan, J. Jordan, J. Kasha, L. Kagan, C. Kraft, A. Levitsky, M. Lewis, X. Liu, J. Lopez, D. Ma, W. Majoros, J. McDaniel, S. Murphy, M. Newman, T. Nguyen, N. Nguyen, M. Nodell, S. Pan, J. Peck, M. Peterson, W. Rowe, R. Sanders, J. Scott, M. Simpson, T. Smith, A. Sprague, T. Stockwell, R. Turner, E. Venter, M. Wang, M. Wen, D. Wu, M. Wu, A. Xia, A. Zandieh & X. Zhu, 2001. The sequence of the human genome. Science 291: 1304–1351.

Washburn, M.P., R. Ulaszek, C. Deciu, D.M. Schieltz & J.R. Yates III, 2002. Analysis of quatitative proteomic data via multidimensional protein identification technology. Anal Chem 74: 1650–1657.

Washburn, M.P., D. Wolters & Jr. Yates III, 2001. Large scale analysis of the yeast proteome by multidimensional protein identification technology. Nat Biotech 19: 242–247.

Watson, B.S., Z. Lei, R.A. Dixon & L.W. Sumner, 2004. Proteomics of *Medicago sativa* cell walls. Phytochemistry 65: 1709–1720.

Watson, B.S., V.S. Asirvatham, L. Wang & L.W. Summer, 2003. Mapping the proteome of barrel medic (*Medicago truncatula*). Plant Physiol 131: 1104–1123.

Whitelegge, J.P., 2002. Plant proteomics: BLASTing out of a MudPIT. Proc Natl Acad Sci USA 99: 11564–11566.

Winzer, T., A. Bairl, M. Linder, D. Linder, D. Werner & P. Muller, 1999. A novel 53 kDa nodulin of the symbiosome membrane of soybean nodules, controlled by *Bradyrhizobium japonicum*. Mol Plant Microb In 12: 218–226.

Xing, T., T. Ouellet & B.L. Miki, 2002. Towards genomic and proteomic studies of protein phosphorilation in plant–pathogen interactios. Trends Plant Sci 7: 224–230.

Yi-Ming, G., S. Shi-Hua, J. Yu-Xiang & K. Ting-Yung, 2002. Plant proteomics in the post-genomic era. Acta Bot Sin 44: 631–641.

Yu, J., S. Hu, J. Wang, G.K. Wong, S. Li, B. Liu, Y. Deng, L. Dai, Y. Zhou, X. Zhang, M. Cao, J. Liu, J. Sun, J. Tang, Y. Chen, X. Huang, W. Lin, C. Ye, W. Tong, L. Cong, J. Geng, Y. Han, L. Li, W. Li, G. Hu, X. Huang, W. Li, J. Li, Z. Liu, L. Li, J. Liu, Q. Qi, J. Liu, L. Li, T. Li, X. Wang, H. Lu, T. Wu, M. Zhu, P. Ni, H. Han, W. Dong, X. Ren, X. Feng, P. Cui, X. Li, H. Wang, X. Xu, W. Zhai, Z. Xu, J. Zhang, S. He, J. Zhang, J. Xu, K. Zhang, X. Zheng, J. Dong, W. Zeng, L. Tao, J. Ye, J. Tan, X. Ren, X. Chen, J. He, D. Liu, W. Tian, C. Tian, H. Xia, Q. Bao, G. Li, H. Gao, T. Cao, J. Wang, W. Zhao, P. Li, W. Chen, X. Wang, Y. Zhang, J. Hu, J. Wang, S. Liu, J. Yang, G. Zhang, Y. Xiong, Z. Li, L. Mao, C. Zhou, Z. Zhu, R. Chen, B. Hao, W. Zheng, S. Chen, W. Guo, G. Li, S. Liu, M. Tao, J. Wang, L. Zhu, L. Yuan & H. Yang, 2002. A draft sequence of the rice genome (*Oryza sativa* L. ssp. *Indica*). Science 296: 380–383.

Zivy, M. & D. de Vienne, 2000. Proteomics: A link between genomics, genetics and physiology. Plant Mol Biol 44: 575–580.

Appendix 2: Plant proteomics update (2007–2008): Second-generation proteomic techniques, an appropriate experimental design, and data analysis to fulfill MIAPE standards, increase plant proteome coverage and expand biological knowledge

JOURNAL OF PROTEOMICS 72 (2009) 285–314

available at www.sciencedirect.com

ScienceDirect

www.elsevier.com/locate/jprot

Review

Plant proteomics update (2007–2008): Second-generation proteomic techniques, an appropriate experimental design, and data analysis to fulfill MIAPE standards, increase plant proteome coverage and expand biological knowledge

Jesús V. Jorrín-Novo[a,*], *Ana M. Maldonado*[a], *Sira Echevarría-Zomeño*[a], *Luis Valledor*[b], *Mari A. Castillejo*[a], *Miguel Curto*[a], *José Valero*[a], *Besma Sghaier*[a], *Gabriel Donoso*[a], *Inmaculada Redondo*[a]

[a]*Agricultural and Plant Biochemistry and Proteomics Research Group, Dept. of Biochemistry and Molecular Biology, University of Córdoba, Córdoba, Spain*

[b]*EPIPHYSAGE Research Group, Área de Fisiología Vegetal, Departamento B.O.S., Universidad de Oviedo, Oviedo, Spain*

ARTICLE DATA

Keywords:
Subcellular Proteomics
Differential Expression Proteomics
Posttranslational Modifications
Interactomics

ABSTRACT

This review is the continuation of three previously published articles [Jorrin JV, Maldonado AM, Castillejo MA. Plant proteome analysis: a 2006 update. Proteomics 2007; 7: 2947–2962; Rossignol M, Peltier JB, Mock HP, Matros A, Maldonado AM, Jorrin JV. Plant proteome analysis: a 2004–2006 update. Proteomics 2006; 6: 5529–5548; Canovas FM, Dumas-Gaudot E, Recorbet G, Jorrin J, Mock HP, Rossignol M. Plant proteome analysis. Proteomics 2004; 4: 285–298] and aims to update the contribution of Proteomics to plant research between 2007 and September 2008 by reviewing most of the papers, which number approximately 250, that appeared in the Plant Proteomics field during that period. Most of the papers published deal with the proteome of *Arabidopsis thaliana* and rice (*Oryza sativa*), and focus on profiling organs, tissues, cells or subcellular proteomes, and studying developmental processes and responses to biotic and abiotic stresses using a differential expression strategy. Although the platform based on 2-DE is still the most commonly used, the use of gel-free and second-generation Quantitative Proteomic techniques has increased. Proteomic data are beginning to be validated using complementary -omics or classical biochemical or cellular biology techniques. In addition, appropriate experimental design and statistical analysis are being carried out in accordance with the required Minimal Information about a Proteomic Experiment (MIAPE) standards. As a result, the coverage of the plant cell proteome and the plant biology knowledge is increasing. Compared to human and yeast systems, however, plant biology research has yet to exploit fully the potential of proteomics, in particular its applications to PTMs and Interactomics.

* *Corresponding author*. Fax: +34957218439.
E-mail address: bf1jonoj@uco.es (J.V. Jorrín-Novo).

1874-3919/$ – see front matter © 2009 Elsevier B.V. All rights reserved.
doi:10.1016/j.jprot.2009.01.026

Contents

1. Introduction

1.1. *Where is (Plant) Proteomics and where should it be?*

"How", "where", "when", and "what for" are the several hundred thousand of individual protein species produced in a living organism? How do they interact with one another and with other molecules to construct the cellular building? How do they work in order to fit in with programmed growth and development, and to interact with their biotic and abiotic environment? To answer all of these questions is the objective, first, of Proteomics, and ultimately of Systems Biology [4].

In order to approach the above questions experimentally, continuous improvements in techniques and protocols for High-throughput Proteomics are being made at all workflow stages, starting from the laboratory (tissue and cell fractionation, protein extraction, depletion, purification, separation, MS analysis) and ending at the computer (algorithms for protein identification and bioinformatics tools for data analysis, databases and repositories). Since no single approach can fully unravel the complexity of living organisms, and experimental results need to be validated, Proteomics, like any methodology, should be considered as part of a multidisciplinary integrative analysis at different levels, extending from the gene to the phenotype through proteins. This analysis should involve -omics (Genomics, Transcriptomics, Proteomics, Metabolomics) as well as classical biochemical and cellular biology techniques [5–7]. Integrative transcriptomic and proteomic studies, and depending on the biological system, may or may not show good correlationship between the level of protein and mRNA. Biological or methodological explanations are normally forwarded to explain such discrepancies [8–11].

Despite the technological achievements in Proteomics, only a tiny fraction of the cell proteome has been characterized so far, and only for a few biological systems (human, fruit fly, *Arabidopsis*, rice). Even for these organisms, the function of quite a number of proteins remains to be investigated [12]. Proteomic techniques have a number of limitations, such as sensitivity, resolution and speed of data capture. They also face a number of

challenges, such as deeper proteome coverage, Proteomics of unsequenced "orphan" organisms [13], Top-down Proteomics [14], protein quantitation [15], PTMs and Interactomics. Most of these limitations and challenges reflect the difficulty of working with the biological diversity of proteins and their range of physicochemical properties.

One of the unanswered biological questions is to determine the number of protein species that can be translated from a single gene as a result of alternative splicing or PTMs, and the biological meaning of each one [16,17]. The percentage of plant genes with at least one alternative transcript [18] is estimated to be 20%, and while this figure is likely to be an underestimate [19], it is lower than that estimated for humans. An example of alternative splicing in plants is represented by the pre-mRNAs of *Arabidopsis thaliana* genes that encode serine/arginine-rich proteins, a conserved family of splicing regulators in eukaryotes [20]. Remarkably, up to 95 transcripts are produced from only 15 genes, resulting in a six-fold increase of the transcriptome. Sequence analysis of the splice variants reveals that the proteins predicted for most of these variants either lack one or more modular domains or contain truncated domains. The alternative splicing of Ser/Arg-rich genes is controlled in a developmental and tissue-specific manner, and is affected by various hormones and abiotic stresses.

Alternative transcripts arise with the use of multiple transcription start sites that produce in frame protein species differing only in their N-terminal sequence. This phenomenon has been observed for *A. thaliana* glutathione S-transferase GSTF8 [21]. Analysis of GSTF8-L and GSTF8-S proteins showed that the former is targeted to plastids, whereas the latter is cytoplasmic. *In silico* analyses revealed that GSTF8-S is conserved across a wide range of plants, while GSTF8-L is confined to the Brassicaceae. These studies support the fact that alternative translation start sites of the GSTF8 promoter are used to create tissue-specific and stress-responsive expression patterns as well as target the same protein to two different subcellular localisations. Another example of multiple transcription start sites is represented by two genes of *Arabidopsis* encoding the L-isoaspartate methyltransferase enzymes PIMT1 and 2 (EC 2.1.1.77). PIMT2 produces at least eight transcripts depending on which of the four potential start sites is used; this results in three different initiating methionines, and two possibilities, 5′ and 3′, for alternative splice site selection of the first intron [22]. The entire array of transcripts produces mature proteins capable of converting L-isoaspartate to L-aspartate using small peptide substrates. However, the location of each of the corresponding protein forms–nucleus, cytoplasm, endo-membrane system, chloroplasts, or mitochondria–depends on the transcript from which they are produced.

Proteomics has experienced an explosion of new protocols, platforms and workflows; some of them are quite complex and require sophisticated equipment and expertise, with each technique has its own features, advantages and limitations. A huge amount of data is being generated, and some of it is being deposited and organised in several databases available to the scientific community: the PPDB, http://ppdb.tc.cornell.edu [23]; the PODB, http://proteome.dc.affrc.go.jp/Soybean/; the Organellome, http://podb.nibb.ac.jp/Organellome [24]; the UniProt knowledgebase reported in this issue by Schneider et al.; and others mentioned throughout the manuscript (Table 1).

Exploiting the full potential of Proteomics surpasses the possibilities of individual laboratories and requires large-scale open collaborations [25,26] such as the Human Proteome Organization (HUPO) (http://www.hupo.org/). Along these lines, the multinational coordinated project called the "Green Proteome" is one of the major challenges for Plant Proteomics in the near future. In this respect, the Proteomics Subcommittee of the Multinational *Arabidopsis* Steering Committee has begun to operate; this subcommittee was created to help to coordinate International Proteomics Research in *Arabidopsis* (http://www.masc-Proteomics.org/) [27]. One of its most important benefits has been the establishment of a searchable database of MS/MS reference spectra derived from *Arabidopsis*, *Chlamydomonas reinhardtii*, *Medicago truncatula*, *Solanum tuberosum* (potato), *Solanum lycopersicum* (tomato) and other plants (ProMEX; http://promex.mpimp-golm.mpg.de/home.shtml) [28]. This database allows reliable protein identification through a genome-independent approach, since newly generated MS/MS spectra can be matched against previous experimental MS/MS spectra. This approach allows semiquantitative analysis at the same time as spectrum matching. Other initiatives that deserve to be mentioned is the Plant Proteomics in Europe" (COST Action FA0603).

After nearly 10 years of Proteomics research [29], it is possible to look back at previous research and publications, identifying errors, which also allows us to avoid repeating them in new studies. These errors come from the experimental design, the analysis and the interpretation of the data [30]. In addition, data validation should always aspire to more than merely description or speculation. It is not uncommon to find low-confidence protein identification in the literature, especially in the case of unsequenced organisms; and inappropriate statistical analyses of results have often been performed. It is interesting to see how many manuscripts contain the term "Proteome" when probably only a tiny fraction of the total proteome has been analysed. Along these lines, HUPO's Proteomic Standard Initiative has developed guidance modules [31] that have been translated into Minimal Information about a Proteomic Experiment (MIAPE) documents. The MIAPE documents recommend proteomic techniques that should be considered and followed when conducting a proteomic experiment. Proteomics journals should be, and in fact are, extremely strict when recommending that investigators follow the MIAPE standards for publishing a proteomic experiment.

The huge amount of data generated in a proteomic experiment has led many journals to recommend, and some to require, that original data be submitted to public repositories. The repository options available and analysis of the data in the pipeline are presented in the review by Mead et al. [32], which discusses recent papers in greater detail [33]. A shift in the protein identification paradigm is currently underway, moving from sequencing and database searching to spectrum searching in spectral libraries. This underscores the importance of repositories for Proteomics [28,34,35].

Different areas within Proteomics can be defined: i) Descriptive Proteomics, including Subcellular Proteomics; ii) Differential Expression Proteomics; iii) Posttranslational

Table 1 – Useful online resources and Plant Proteome Databases.

Web site	Name/description
Genome databases	
[a]http://www.ncbi.nlm.nih.gov/	National Center for Biotechnology Information
[a]http://www.ncbi.nlm.nih.gov/Genbank	NIH genetic sequence database
[a]http://compbio.dfci.harvard.edu/tgi/plant.html	The gene index project. The Computational Biology and Functional Genomics Laboratory, and the Dana-Farber Institute and Public School of Public Health
http://www.arabidopsis.org/	TAIR, The *Arabidopsis* Information Resource
[a]http://www.legoo.org/	Legoo, a bioinformatics gateway towards integrative legume biology
[a]http://medicago.toulouse.inra.fr/Mt/EST/	MENS, *Medicago* EST Navigation System
[a]http://www.medicago.org/genome/	*Medicago truncatula* sequencing project
[a]http://www.sgn.cornell.edu/about/tomato_sequencing.pl	International Tomato Sequencing Project
[a]http://www.maizesequence.org/index.html	Maize Genomes Sequencing Project
[a]http://www.potatogenome.net	The Potato Genome Sequencing Consortium
[a]http://www.phytozome.net/sorghum	The Sorghum bicolor Genome Project
http://pgrc.ipk-gatersleben.de/cr-est/index.php	The IPK Crop EST Database
http://chloroplast.cbio.psu.edu/	A database for fully sequenced plastid genomes
http://genomics.msu.edu/plant_specific/	Plant Specific Database
http://www.plantgdb.org/	The Plant Genome Database (GDB)
http://rice.plantbiology.msu.edu	The Rice Genome Annotation Project
http://mips.gsf.de/proj/plant/jsf/rice/index.jsp	MosDB, the MIPS *Oryza sativa* database
http://ricegaas.dna.affrc.go.jp/	RiceGAAS, Rice Genome Automated Annotation System
http://cgf.ucdavis.edu/home/	CGF, College of Agricultural and Environmental Sciences. Genomics Facilities
http://harvest.ucr.edu/	HarvEST, EST database-viewing software. Oriented to comparative genomics
Proteome databases	
http://ca.expasy.org/	The ExPASy (Expert Protein Analysis System) proteomics server of the Swiss Institute of Bioinformatics (SIB) Analysis of protein sequences, structures and 2-D PAGE
[a]http://www.hupo.org/	HUPO, Human Proteome Organization
http://mips.gsf.de/	MIPS, Munich Information Center for Protein Sequences
http://www.ebi.ac.uk/pride/	The PRIDE, PRoteomics IDEntifications Database. EMBL-EBI (European Bioinformatic Institute)
http://www.ebi.ac.uk/integr8/EBI-Integr8-HomePage.do	Integr8, Integrated information about deciphered genomes and their corresponding proteomes. EMBL-EBI (European Bioinformatic Institute)
http://organelledb.lsi.umich.edu/	Organelle DB, A database of organelle proteins, and subcellular structures/complexes
http://www.compbio.dundee.ac.uk/SNAPPI/downloads.jsp	SNAPPIVIEW (Structures,iNterfaces and Alignments for Protein–Protein Interactions)
http://cbm.bio.uniroma2.it/phospho3d/	Phospho3.Database of three-dimensional structures of phosphorylation sites
http://www.cs.ualberta.ca/~bioinfo/PA/GOSUB/	Proteome Analyst PA-GOSUB 2.5. Sequences, predicted GO molecular functions and subcellular localisations
http://www.rcsb.org/pdb/home/home.do	RCSB, The Research Collaboratory for Structural Bioinformatics. Protein Database (PDB)
http://wwwmgs.bionet.nsc.ru/mgs/gnw/pdbsite/	PDB-Site. Comprehensive structural and functional information on PTMs, catalytic active sites, ligand binding, protein–protein, protein–DNA and protein–RNA interactions) in the Protein Data Bank (PDB)
http://wolfpsort.org/	WoLF PSORT, Protein Subcellular Localization Prediction
http://www.rostlab.org/db/NMPdb/	NMPdb, Nuclear Matrix Associated Proteins

JOURNAL OF PROTEOMICS 72 (2009) 285–314

http://www.cbs.dtu.dk/services/TargetP/	TargetP, predicts the subcellular location of eukaryotic proteins, based on the predicted presence of the N-terminal presequences
http://www.cbs.dtu.dk/services/SecretomeP/	The SecretomeP, Predictions of protein secretion and information on various PTMs and localizational localisational aspects of the protein
http://www.yass.sdu.dk/	VEMS, Virtual Expert Mass Spectrometrist. Program for integrated proteome analysis.
http://www.cbs.dtu.dk/services/NetPhos/	The NetPhos server produces neural network predictions for serine, threonine and tyrosine phosphorylation sites in eukaryotic proteins
Plant Proteome Databases	
[a]http://ca.expasy.org/sprot/ppap/ppap_stat.html	PPAP, the UniProtKB/Swiss-Prot Plant Proteome Annotation Program
[a]http://www.costfa0603.com/index.php	Plant Proteomics in Europe, COST F0603
[a]http://www.masc-proteomics.org/	The Multinational *Arabidopsis* Steering Committee, Proteomics Subcommittee
Standard for sample handling and data interpretation	
[a]http://fgcz-atproteome.unizh.ch/index.php	*Arabidopsis* proteome database
http://proteomics.arabidopsis.info/	NASC Proteomics database for *Arabidopsis* data. Proteomics experiments and their related data
http://gabi.rzpd.de/projects/Arabidopsis_Proteomics/	Gabipd, Proteomic data. *Arabidopsis thaliana* and *Brassica napus*
[a]http://ppdb.tc.cornell.edu	The PPDB (Plant Proteome DataBase) for *Arabidopsis thaliana* and maize
[a]http://proteome.dc.affrc.go.jp/Soybean/	Soybean proteome Database (2-DE)
http://www.noble.org/medicago/proteomics.html	Center for *Medicago* Genomics Research: Proteomics
http://gene64.dna.affrc.go.jp/RPD/	Rice Proteome Database (2-DE)
Plant Proteome Specialized databases	
[a]http://promex.mpimp-golm.mpg.de/home.shtml	ProMEX (Protein Mass spectra Extraction) MSMS spectral database
[a]http://podb.nibb.ac.jp/Organellome	PODB2, The Plant Organelles Database, 2
[a]www.suba.bcs.uwa.edu.au	SUBA, Subcelllular location of *Arabidopsis* proteins
http://www.araperox.uni-goettingen.de/	AraPerox, Database of Putative Proteins of *Arabidopsis* Peroxisomes
http://andrewschein.com/pclr/index.html	PCLR, Chloroplast Localization Prediction
http://www.cbs.dtu.dk/services/ChloroP/	The ChloroP server predicts the presence of chloroplast transit peptides (cTP) in and the location of potential cTP cleavage sites
http://www.gartenbau.uni-hannover.de/genetik/AMPP	The *Arabidopsis* Mitochondrial Proteome Project
http://www.plantenergy.uwa.edu.au/ampdb/	*Arabidopsis* Mitochondrial Protein Database
http://www.plprot.ethz.ch/	plprot — a plastid protein database
http://www.seed-proteome.com/	*Arabidopsis* Seed proteome
http://aramemnon.botanik.uni-koeln.de/	Aramemnon, Plant membrane protein databases
http://plantrbp.uoregon.edu/	Putative Orthologous Groups and Plant RNA Binding Protein Database
http://www.coiled-coil.org/arabidopsis/index.html	ARABI-COIL, *Arabidopsis* Coiled-Coil Protein Database
http://bioinf.scri.sari.ac.uk/cgi-bin/atnopdb/home	AtNoPDB, *Arabidopsis* Nucleolar Protein Database
[a]http://phosphat.mpimp-golm.mpg.de/	*Arabidopsis* phosphoproteome database
http://digbio.missouri.edu/p3db/	P3DB, Plant protein phosphorilation phosphorylation database

[a] Cited in the text.

Modifications; iv) Interactomics; and v) Proteinomics (targeted or hypothesis-driven Proteomics). In plants, PTMs–with the exception of the phosphoproteome [36]–and Interactomics remain the main challenges.

Deeper proteome coverage has become possible by combining electrophoresis and liquid chromatography techniques, resulting in the report of nearly 50% of all *Arabidopsis* predicted gene models, including some not represented in The *Arabidopsis* Information Resource (TAIR) (AtProteome; http://fgcz-atproteome.unizh.ch/index.php) [37]. The combination of subcellular fractionation techniques with the use of modern mass spectrometry equipment has allowed extensive characterization of the plant subcellular proteome, which has led to the discovery of new metabolic pathways [38]. An expanded update of the subcellular localisation of *Arabidopsis* proteins has been carried out (SUBA; www.suba.bcs.uwa.edu.au) [39], and the most comprehensive study on the *Arabidopsis* chloroplast proteome has been published, including information on sorting signals, PTMs and protein abundance. This information is accessible at the PPDB (http://ppdb.tc.cornell.edu) [40]. Despite these advances, some recalcitrant proteomes, as is the case with membrane proteins or other highly hydrophobic proteins, remain elusive, and protein trafficking is still an important unresolved issue [41,42]. In fact, some proteins have been identified at the "apparently wrong" location [43].

Plant Proteomics is beginning to make some practical contributions to applied fields including biomedicine, through the identification and characterization of allergens [44; Fasoli et al., this issue]; agronomy, through studies of the equivalence of transgenic crops [45], genotyping [46,47], studies of heterosis [48] and the environment [45]; and food science, through studies of food quality control and traceability [49].

Knowledge at the molecular level on relevant plant-derived food allergens is scanty, and their detailed and comprehensive characterization can be carried out using proteomics. This is the case of three papers that appeared during the period reviewed; these papers analyse allergens from wheat flour [50], maize pollen [51] and olive tree pollen [52].

The proteomic and transcriptomic analysis of seeds from wheat transgenic plants overexpressing a low-molecular-weight glutenin subunit by Scossa et al. [53] revealed that an increase in the amount of transgenic protein is accompanied by a reduction in the endogenous levels of the glutenin subunit, all subclasses of gliadins and metabolic enzymes, as well as chloroform/methanol-soluble proteins. These results support the hypothesis that a global compensatory metabolic response is occurring. Similarly, at least three additional papers have reported changes in the protein profile as a result of transgenesis, including maize [54], grape [55] and tobacco [56].

Proteomics could be a good complementary approach to molecular breeding, as shown for *Brassica napus* [57], grape [58], sunflower [47] and strawberry [46]. The genetic diversity among 10 Iranian bread wheat (*Triticum aestivum*) genotypes has been analysed by testing 12 quality traits, 320 amplified fragment length polymorphisms (AFLP), 491 simple sequence repeat (SSR) alleles and 294 proteome markers. The average genetic diversity based on quality traits (0.684 with a range of 0.266–0.997) is higher than that based on AFLP (0.502 with a range of 0.328–0.717), SSR (0.503 with a range of 0.409–0.595) and proteome markers (0.464 with a range of 0.264–0.870) [59].

This review is a continuation of three ones previously published [1–3] and aims to update the contribution of Proteomics to plant research during 2007–September 2008 by reviewing most of the papers that appeared on this field throughout this period. We have tried not to be repetitive with recently published reviews (Table 2), and instead we have sought to emphasise new contributions or improvements published since the three previous review periods. Two Plant Proteomics books have recently appeared covering the literature up to 2006, with chapters devoted to technologies, including bioinformatics tools, as well as discussions of Descriptive/Expression Proteomics studies in *Arabidopsis*, rice, legumes, cereals, oilseed crops, Subcellular Proteomics, PTMs, Interactomics, responses to stresses and Structural Proteomics [60,61]. In addition, an excellent and extensive review on Rice Proteomics by Agrawal, Jwa, and Rakwal has recently appeared in Proteomics [62]. In this issue two reviews on Crop Proteomics appear, by Komatsu and Ashan on soybean, and by Finnie and Svensson on barley. Because of their novelty and originality, the reviews by Weckerth [5] and Farrokhi et al. [63] should be mentioned. The former covers methodological aspects of Metabolomics and Proteomics, including statistical analysis and data integration. It reports a strategy combining metabolic and protein profiling with multivariate exploratory data mining. The latter review introduces the field of peptidomics and its application to the study of plant peptides. This field, developed in the last few years, has been used primarily to study neuropeptides in animals and protease degradation products. A number of plant peptides that are both extracellular and intracellular and that involve a number of functions, including signalling and defence, have been identified and characterized through biochemical and genetic studies. Nevertheless, a systematic throughput analysis using Proteomics has so far not been reported.

2. Publications for period from 2007 to September 2008

2.1. *Plant Proteomics: still trailing behind Human and Yeast Proteomics*

The use of Proteomics in plant biology research has increased significantly in the period from 2007 to September 2008, becoming a routine methodology in a number of plant laboratories worldwide. During this period, both qualitative and quantitative improvements in Plant Proteomics have occurred, ushering in a new phase of "Second-Generation Plant Proteomics". During this period, research has moved towards the use of new platforms (DIGE and other Quantitative Proteomic approaches such as iTRAQ, SILAC and gel-free), the performance of suitable experimental designs and data analyses and the use of complementary approaches for data validation, such as Western blotting, transcriptomics, enzyme activity, reverse genetics, and those of Cell Biology. MIAPE requirements are being observed in most of the papers

Table 2 – Plant Proteomics reviews that have appeared in the 2007–September 2008 period [a].

Weckwerth W. Integration of metabolomics and proteomics in molecular plant physiology—coping with the complexity by data-dimensionality reduction. Physiol Plant 2008; 132: 176–189 [5].	Commented in the text
Salekdeh GH and Komatsu S. Crop proteomics: aim at sustainable agriculture of tomorrow. Proteomics 2007; 7:2976–2996 [45].	Review of proteomics of agricultural crops (rice, soybean, wheat, barley, maize), with emphasis on the use of the technique in food trazeability, substantial equivalence, allergen characterization, genotype cataloguing, assisting plant breeding. Proteomics of plant responses to stress. The omnipresent proteins: RubisCO, and other photosynthetic proteins, stress-responsive
Agrawal GK, Jwa N-S and Rakwal R. Rice proteomics: ending phase I and the beginning of phase II. Proteomics 2009; (in press) [62].	Excellent review on rice proteomics
Komatsu S, Toorchi M and Yukawa K. Soybean Proteomics. Curr Proteomics 2007; 4:182–186 [256].	Discuss the strength and weaknesses of proteomics technologies and limitations of current techniques for soybean biology studies.
Carpentier SC, Panis B, Vertommen A, Swennen R, Sergeant K, Renaut J, Laukens K, Witters E, Samyn B and Devreese B. Proteome analysis of non-model plants: a challenging but powerful approach. Mass Spectrom Rev 2008; 27: 354–377 [13].	Excellent review on proteomics of "orphan", non-model, non-sequenced plant species, but of interest from an agricultural point of view. Methodological considerations. Emphasis on protein identification. Banana as the species the authors work with.
Farrokhi N, Whitelegge JP and Brusslan JA. Plant peptides and peptidomics. Plant Biotechnol J 2008; 6:105–134 [63].	Commented in the text
Thelen JJ and Peck SC. Quantitative proteomics in plants: choices in abundance. Plant Cell 2007; 19: 3339–3346 [149].	Overview of the methodological options for Quantitative Proteomics, including label-free approaches, *in vivo* and *in vitro* isotopic labeling, iTRAQ and AQUA
Haynes PA and Roberts TH. Subcellular shotgun proteomics in plants: looking beyond the usual suspects. Proteomics 2007;7: 2963–2975 [185].	Subcellular Proteomics, assigning (bioinformatics) and determining (microscopy) subcellular location of proteins. Methodology: organelle purification, sample preparation, 2-DE, MudPIT, SDS/IEF-LC
Ito J, Heazlewood JL and Millar AH. The plant mitochondrial proteome and the challenge of defining the Posttranslational Modifications responsible for signalling and stress effects on respiratory functions. Physiol Plant 2007; 129: 207–224 [187].	Plant mitochondrial proteins and PTMs (phosphorylation, oxidation). Comparative study between plants (*Arabidopsis*), yeast and mammals (human).
Komatsu S, Konishi H and Hashimoto M. The proteomics of plant cell membranes. J Exp Bot 2007; 58: 103–112 [181].	Characterization of membrane proteins is still challenging. Proteomics of membrane proteins in *Arabidopsis* and rice.
Jamet E, Albenne C, Boudart G, Irshad M, Canut H and Pont-Lezica R. Recent advances in plant cell wall proteomics. Proteomics 2008; 8: 893–908 [186].	Methodology employed to study plant cell wall proteome. Around 400 cell wall proteins (CWPs) of *Arabidopsis*, representing about one fourth of its estimated cell wall proteome, have been described. From the proteins identified the biology of the cell wall can be reconstructed.
Qureshi MI, Qadir S and Zolla L. Proteomics-based dissection of stress-responsive pathways in plants. J Plant Physiol 2007; 164: 1239–1260 [257].	Comparison of the proteins that are induced or overexpressed under abiotic stress, including those identified by classical biochemical approaches and high throughput proteomics. Classical approaches: antioxidant enzymes, signalling proteins (salt-overly sensitive, jasmonate, abscisic acid pathways, MAPK, calcium, GABA). Proteomics of water, temperature, heavy metals, ozone, light, nutrient, stresses.
De la Fuente van Bentem S and Hirt H. Using phosphoproteomics to reveal signalling dynamics in plants. Trends Plant Sci 2007; 12:404–411 [221].	Research on plant signalling network through mass spectrometry and protein and peptide microrrays for identifying and characterizing phophorylated proteins and sites and to identify kinase activities. Specific reference to flagellin signalling in *Arabidopsis*.
Mehta A, Magalhaes BS, Souza DS, Vasconcelos EA, Silva LP, Grossi-de-Sa MF, Franco OL, da Costa PH and Rocha TL. Rooteomics: the challenge of discovering plant defence-related proteins in roots. Curr Protein Pept Sci 2008; 9:108–116 [258].	A new term coined: rooteomics. Root, probably the most recalcitrant organ. Recent developments, limitations of the current techniques, and technological perspectives for root proteomics aiming at the identification of resistance-related proteins are discussed.
Zhang Q and Riechers DE. Proteomics: An Emerging Technology for Weed Science Research Weed Science 2008;56: 306–313 [259].	Proteomics can be used to understand mechanisms of herbicide tolerance and weed resistance

(continued on next page)

Table 2 (*continued*)

Mehta A, Brasileiro AC, Souza DS, Romano E, Campos MA, Grossi-de-Sa MF, Silva MS, Franco OL, Fragoso RR, Bevitori R and Rocha TL. Plant–pathogen interactions: what is proteomics telling us? Febs J 2008;275:3731–3746 [260].	A review of papers covering plant–pathogen (virus, bacteria, fungi, nematodes) interactions with list of pathogen responsive proteins identified.
Nesatyy VJ and Suter MJ. Analysis of environmental stress response on the proteome level. Mass Spectrom Rev 2008. 27:556–574 [261].	Potential of proteomics to the analysis of environmental stress, defining a new field: environmental proteomics, mainly directed at studying the effect of toxic chemicals, on living organisms. General remarks on proteomics, experimental methods and technologies. released to the environment

[a] The books "Plant Proteomics. Technologies, strategies, and applications", edited by G.K. Agrawal and R. Rakwal, and "Plant Proteomics", edited by J. Samaj and J.J. Thelen, have not been included. A number of reviews, no listed, appear in this issue of the Journal of Proteomics: barley seed proteomics (Finnie and Svenson), soybean proteomics (Komatsu and Ahsan), root–microbe interactions (Mathesius), abiotic environmental stress in *Arabidopsis thaliana* (Taylor et al.), disulfide proteome, thioredoxin targets (Montrichard et al., and Lindahl1 and Kieselbach).

published most recently. However, plant biology research is far from fully exploiting the potential of Proteomics and, as is a general rule for plant biology research, progress in Plant Proteomics continues to lag behind that of Human and Yeast Proteomics (Fig. 1). Advances in Plant Genomics facilitate proteomic research, increasing confidence in protein identification and characterization. For example, among the 6,212,793 entries in the UniProtKB/TrEMBL (Release 39.1 of 02-Sep-2008), only 488,400 (7.86%) correspond to plants (Fig. 1A) (also see Schneider et al., in this issue). During this period, the complete genome sequences of grape [64], *Populus trichocarpa* [65] and the seedless plant *Physcomitrella patens* [66] have been reported [67], and genome sequencing projects for several important agricultural crops are in progress: barrel medic (http://www.medicago.org/, http://www.legoo.org/), tomato (http://www.sgn.cornell.edu/about/tomato_sequencing.pl), maize (http://www.maizesequence.org/index.html), potato (http://www.potatogenome.net), sorghum (http://www.jgi.doe.gov/sequencing/why/CSP2006/sorghum.html), and soybean (http://www.ncbi.nlm.nih.gov/Genbank). The number of ESTs reported at the Dana Farber (http://compbio.dfci.harvard.edu/tgi/plant.html) is indicated in Table 3. In all, at least 1.8 million plant-derived ESTs exist in the public domain. Sputnik (The Sputnik Exhaustive and Comprehensive Analysis of Plant-derived EST Sequences Database, http://www.plant-genomic-papers.com) has been implemented as a largely automated pipeline for processing, clustering and annotating large numbers of EST

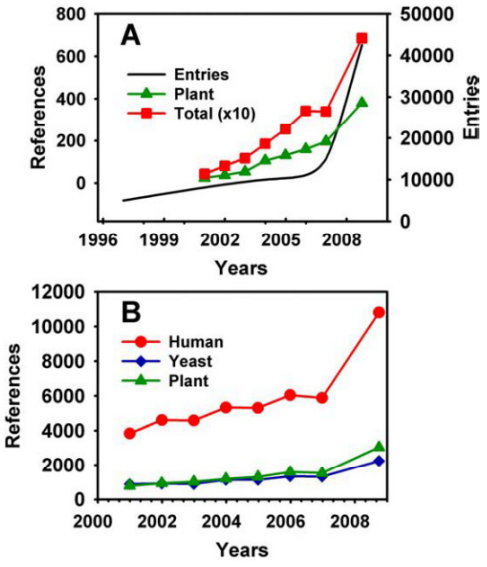

Fig. 1 – Number of references reported in the ISI Web of Knowledge during the 2000–2008 (up to September 19th) period. The search was performed with the key words: "proteomic(s)" or "proteome(s)" and "proteomic(s)" or "proteome(s)"plus "plant", "human" or yeast (A); "genomic (s)" or "genome (s)" plus "plant", "human" or "yeast" (B). In A, the number of entries reported at the UniProtKB/TrEMBL is also shown (http://us.expasy.org/sprot/ppap_stat.htm1).

Table 3 – Number of ESTs entries for some plant spp. by September 2008 [a].

Plant spp.	Dana Faber/NCBI
Apple (*Malus domestica*)	251 233/263 977
*Arabidopsis thaliana**	619 908/1 788 657
Barley (*Hordeum vulgare*)	479 742/517 057
Grape (*Vitis vinifera*)	347 879/209 596
Letuce (*Lactuca sativa*)	80 598/80854
Lotus (*Lotus japonicus*)	148 338/1581 37
Maize (*Zea mays*)	1 151 181/1 466 402
*Medicago truncatula**	259 642/262 363
Nicotiana benthamiana	41 922/43 668
Pine (*Pinus*)	355 326/509 731
Popplar (*Populus*)	411 781/417 092
Rice (*Oryza sativa*)	1 163 134/1 400 741
Soybean (*Glycine max*)	381 524/906 215
Sunflower (*Helianthus annuus*)*	93 283/94 562
Tobacco (*Nicotiana tabacum*)	163 524/244 400
Tomato (*Solanum lycopersicum*)	330 396/260 951
Wheat (*Triticum aestivum*)	1 034 368/1 067 423
Pea (*Pisum sativum*)*	No entries/6327
Holm oak (*Quercus ilex*)*	No entries/no entries
Radiate pine (*Pinus radiata*)*	No entries/151
Aleppo pine (*Pinus halepensis*)*	No entries/no entries
Pineaple (*Ananas comosus*)*	No entries/5649
Date palm (*Phoenix dactylifera*)*	No entries/4
Notro (*Embothrium coccineum*)*	No entries/no entries
Pteris vitata fern*	No entries/no entries

[a] Taken from The Gene Index Project at the Dana Farber Cancer Institute (http://compbio.dfci.harvard.edu/tgi/plant.html) and NCBI (http://www.ncbi.nlm.nih.gov/). With asterisk the plant systems our group is/has working/worked with.

sequences. Peptide sequences can be derived from the non-redundant cluster set, allowing large-scale genomic analyses on the basis of the partially reconstructed proteome. In fact, the term "Genomeless Genomics" has been coined to describe the application of complete-genomic analyses to these reconstructed genomes.

A total of 380 reports were found in the 'ISI Web of Knowledge' during this period by entering "Plant" and "Proteome(s)" or "Proteomic(s)" as keywords. This figure represents just a small proportion of the 6855 references on Proteomic(s) or Proteome(s) found in ISI; most of these references in ISI are devoted to Yeast and Human Proteomes (Fig. 1).

During this period there have not been large differences with respect to the previously revised ones (Table 1 of Rossignol et al., 2006, Jorrin et al., 2007 [1,2]) concerning the plant species under investigation, with *Arabidopsis* and rice, being the subject of around 75% of the original papers published. Nevertheless, proteomic papers have recently appeared on new species which include several herbaceous non-crops and woody plants (fruit and forest trees, these last ones being the species least addressed): wheatgrass *Elymus elongatum* [68], jasmine tobacco *Nicotiana alata* [69], the resurrection plants *Boea hygrometrica* [70] and *Xerophyta viscosa* [71], chaco potato *Solanum chacoense* [72], wild watermelon *Citrullus lanatus* [73], citrus *Citrus sinensis* [74], Austrian pine *Pinus nigra* [75], rose gum eucalyptus *Eucalyptus grandis* [76], sitka spruce *Picea sitchensis* [77], California pine *Pinus radiata* [78], and conference pears *Pyrus communis* [79].

As has been discussed before [1,2], proteomic analyses have been carried out with different individuals, plant developmental stages, organs, tissues, cells, and subcellular fractions. With the exception of the use of cell suspensions, protoplasts [80], pollen [81], and xylem/phloem saps [82], most Differential Expression Proteomics papers have used plant organs. It is important to note that organs contain a mixture of different cell types; each one with its own proteome signature, and only a small fraction of the cell types are likely to respond to chemical or biological stimuli. The use of laser microdissection techniques [83] for plant cell sampling has been reported in the transcriptomic and proteomic analysis of non-dividing pericycle cells of primary root of maize (*Zea mays*) [84]. The protein profile of these cells is compared with that of the rest of the transverse nonpericycle cells. In this study, approximately 30 μg of protein were extracted from 200,000 cells in 2-DE sample buffer, then separated by 2-DE (small gels, pH 4–7, silver staining). Altogether 20 proteins were identified after n-HPLC-ESI-Q-TOF and after searching through the nrNCBI database using MASCOT.

The proteome, by definition, is quite dynamic, and this is true even for clonal cells, as shown by Sigal et al. [85] using the non-small cell lung carcinoma line Hl299. They studied the variability of protein levels as well as the temporal dynamics of this variability using *in silico* synchronised cells. They used time-lapse fluorescence microscopy to follow the fluctuations in the level of 20 endogenous YFP-tagged proteins in individual cells over multiple cell cycles under controlled conditions. They found that the average coefficient of variation of the total fluorescence depended on the protein measured and ranged from 0.12 to 0.28, and that it remained nearly constant for a given protein throughout the cell cycle. Little is known about the genetic basis of variation in protein levels in genetically diverse populations. Using a label-free, mass spectrometry-based approach to measure protein levels in total, unfractionated cellular proteins, the genetic basis of variation in protein abundance was studied in a cross between two diverse strains of yeast [86]. Loci that influenced protein abundance differed from those that influenced transcript levels, a finding that highlights the importance of analysing the proteome directly to understand fluctuations in protein levels. Plants respond to small changes in the environment by adapting their metabolism, and this response is part of their survival strategy. Consistent with this idea, we found in our analysis of the *Quercus ilex* leaf proteome from mature trees in the field that the 2-DE protein profile depended on leaf orientation (North, South, East and West), position (top, bottom), and the time of day when the leaves were collected [87]. What originally was considered to be homogeneous material, since all the leaves came from the same tree, turned out to be far from true. As a consequence, it has been almost impossible to use the leaf protein profile in cataloguing trees or populations, since the intrapopulation variability can be greater than the interpopulation variability. Thus we changed the focus of our analyses to an organ with a more stable proteome, namely the seed (Valero et al., unpublished results).

In the present update, a total of 152 original papers have been reviewed. Descriptive Proteomics papers (13) deal with the proteome of whole plants; the proteome of major organs, leaves, roots, seeds, fruit, or pollen; or the proteome of extracellular xylem and phloem sap. Subcellular Proteomic papers (11) are devoted primarily to characterizing the proteomes of the chloroplast/plastid, mitochondria, and membrane fraction. A Differential Expression Proteomics strategy has been used to study developmental processes (18), responses to biotic (19) and abiotic stresses (31), and hormones (6). A number of papers deal with cataloguing plant genotypes or populations, comparative analysis of mutant/transgenic plants and their wild parental, and the characterization of allergens (14). PTM studies have characterized the phosphoproteome (9), and to a lesser extent the redox proteome (disulfide, nitrosylation, glutathionylation; 5), with only one paper each published on ubiquitination [88], glycosylation [89], acetylation [90], N-terminal modification, and protein sorting [91]. Only five papers deal with Interactomics block, and they have sought to identify Trx [92], calmodulin [93], 14-3-3 protein [94], and rice OsG1 (an ortholog of GIGANTEA that regulates photoperiod flowering in *Arabidopsis*) targets [95], and photosystem II light-harvesting complexes [96]. A number of papers appearing in the Proteinomics or Targeted Proteomics approach group study seed proteins and proteases, among others (16).

3. Methodology

3.1. *Second-generation techniques and appropriate experimental design and data analysis*

The workflow of a standard proteomic experiment includes all or most of the following steps: experimental design, sampling,

tissue/cell or organelle preparation, protein extraction/fractionation/purification, labelling/modification, separation, MS analysis, protein identification, and statistical analysis of data and validation. New insights and advances in the different steps of the workflow in the literature reviewed are discussed below. The most appropriate protocols to be used depends on and must be optimised for the biological system (i.e. plant species, organ, tissue, cells), as well as the objectives of the research (descriptive, comparative, PTMs, interactions, targeted Proteomics).

3.2. *Experimental design*

A good experimental design is crucial for the success of any proteomic experiment. Erykson and Fenyo [97] have developed a simulation tool for evaluating the success of current designs and for predicting the performance of future, better-designed proteomics experiments [96]. The simulation gives a holistic view of a general analytical experiment and attempts to identify the factors that affect the success rate. It has been used to predict the success of proteome analyses of Human tissue and body fluids that use various experimental design principles. Several parameters are required to simulate the steps of a proteome analysis: i) the distribution of protein amounts in the sample analysed; ii) the loss of analyte material and the maximal limit of the amount loaded at each step of sample manipulation (e.g. separation, digestion, and chemical modification); iii) the dynamic range, the detection limit and the losses associated with MS analysis. Depending on what experiment is being modelled, the detection limit used in a simulation can represent either protein identification only (lower identification limit) or protein identification with quantification (lower quantification limit).

The establishment of an adequate number of replicates is essential for any Differential Expression Proteomics experiment. This number should be set up while taking into account the dynamic nature of the proteome, and a good number will allow correct interpretation of the results and the confident assignment of any protein to the group of variable ones. This makes sense when searching for proteins that can be used as markers of disease or when looking for protein markers to develop plant breeding programmes. In our work to characterize the *P. radiata* needle proteome [78], we previously determined the analytical and biological variability. Tests of the analytical variability examined both the experimental procedures (protein extraction, IEF, SDS-PAGE, gel staining-destaining) and the accuracy of the hardware and software in acquiring and analysing images. Tests of the biological variability looked at several different samples from different trees. Tests performed using 10 and 12 analytical and biological replicates from a representative set of 250 spots gave values for the analytical and biological variability, respectively, of 31% and 42%. This is in contrast to the analytical and biological variability reported for other systems, which is as low as 16% and 24%, respectively. In our work using *P. radiata*, we found differences in the standard error of mean spot quantity, depending on the number of replicates; the error ranged from 111 and 115 ng for two analytical and biological replicates, to 58 and 59 ng for 10 analytical and 12 biological gel replicates. Using more than six biological replicates did not significantly reduce the standard error, so this figure should be optimal for comparative proteomic experiments. Since normally this is not feasible, most of papers in our literature review used only three biological replicates. Given the susceptibility of the data to variation, we were restrictive in our study of *P. radiata* when deciding whether a spot showed variation. First, all the spots considered had to be consistent, i.e., present or absent in all the biological replicates of the particular stage in question; second, when not qualitative (presence vs. absence), differences had to be statistically significant ($p \leq 0.05$, ANOVA); finally, the variance with respect to a control (in this case, embryos from mature seeds) had to be higher than the average biological coefficient of variance determined for a representative set of 150 spots.

3.3. *Sample preparation*

The importance of the extraction protocol in a proteomic experiment can be summarised in the following statement: only if you can extract and solubilise a protein you have the chance to detect and identify it. This sentence summarises the importance of the extraction protocol in a proteomic experiment. This is even more important in the case of plant tissues, due to the low protein content relative to other systems, the presence of the cell wall and vacuoles that account for the majority of the cell mass, the presence of proteases and oxidative enzymes, and the accumulation of large quantities of polysaccharides, lipids, phenolics and other secondary metabolites [98]. Two main types of protocols have been used with plant material. The first type involves tissue homogenisation in buffer-based media, while the second one uses organic solvent media (TCA-acetone, phenol, precipitation protocols), although both protocols can be combined. Since no single protein extraction protocol can capture the full proteome, the chosen protocol should be optimised for the particular plant tissue and research objective. The ideal method should be highly reproducible and should extract the greatest number of protein species, while at the same time reducing the level of contaminants and minimising artifactual protein degradation and modification. Advantages and limitations of each extraction media have been evaluated and discussed in recent publications [99–104]. Now, hydrophobic proteins require specific protocols. Thus, for example, n-dodecyl β-D-maltoside favours the capturing and analysis of hydrophobic proteins, and in contrast to SDS, it can be removed prior to MS analysis. Recently, Toorchi et al. have reported the use of acoustic technology for tissue and protein pellet homogenisation, which stands as an alternative to the classic mortar and pestle or sonic baths [105]. This technology performs far better than water bath sonication at producing high-quality 2D gels and minimising the processing time required for High-throughput Proteomics research.

In order to evaluate the effectiveness of a given extraction protocol, protein quantification is needed. This makes the total absence of such data from some recent papers all the more striking. When using standard colorimetric methods for protein quantitation, namely the Bradford, Lowry and BCA assays, we must consider that some of the components of the solubilisation media may interfere with the colour development reaction [106].

Another issue to consider is the extreme complexity of the proteome and the large dynamic range in protein abundance, which overwhelm the capability of all currently available analytical platforms. Sample prefractionation is a good approach to reduce the complexity of the proteome sample and decrease the dynamic range. Jiang et al. [107] reviewed different protein fractionation technologies and methods based on structural and functional characteristics of the proteins, including the isolation of peptides containing rare amino acids, terminal peptides, PTM peptides and endogenous peptides. Recently, a number of papers have reported the applicability of ribulose-1,5-bisphosphate carboxylase/oxygenase depletion columns for leaf proteomic analysis [108]. In our hands, the method has given excellent results. Polyethylene glycol fractionation has also proven to be valuable for depleting RubisCO from samples [109,110]. Another possibility is the EQUALIZER technology, based on a combinatorial library of hexameric peptide (combinatorial peptide ligand libraries or CPLL) ligands bound to porous beads. Each bead contains billions of copies of a unique hexapeptide ligand distributed throughout its porous structure, and each bead potentially has a ligand different from that of every other bead. With a population of millions of individual peptide ligands obtained by combinatorial chemistry, any protein present in the starting material could theoretically interact with one or a few particular beads [111]. This technology has not yet been reported in studies on plants.

3.4. *One and two-dimensional electrophoresis*

One-dimensional electrophoresis, SDS-PAGE, in combination with appropriate software, is a simple and reliable technique for finger-printing crude plant extracts [112], and is especially useful in the case of hydrophobic and low-molecular-weight proteins. We are using it to characterize and catalogue populations of holm oak (Valero et al., unpublished results). It can also be used to quantify changes in the abundance of a specific protein or changes in specific modifications of a protein using in-gel stable isotope labelling. The combination of SDS-PAGE, band cutting, trypsin digestion and LC separation of the resulting peptides remains the proteomic technique capable of providing the greatest protein coverage [113,114]. Electrophoretic methods can be made compatible with chemical labelling in order to allow Quantitative Proteomics using such techniques as iTRAQ [115].

2-DE is by far the predominant separation technology, and it is continuously being evaluated and improved in the areas of separation of hydrophobic proteins [116], gel staining [117–121], image capture and analysis [122–126] and automation [127]. One of the major criticisms of 2-DE is its low precision, with relative standard deviations reported to fall in the range of 15–70%. Major sources of variability for this technique may include the transfer between the first and the second dimension, the analyst's expertise and the detection of separated proteins [128,129]. One of the main error sources can be attributed to the irregular changes in the background signal from gel to gel, which can be solved using fluorescence labelling.

To compare 2-DE maps between samples, which could be analytical or biological replicates, cells, tissues, organs or treatments, plant proteomic papers prior to the reviewed period used arbitrary criteria (fold ratios) or univariate parametric and non-parametric statistical tests, namely Student's *t*-test or Mann–Whitney *U*-test to compare two groups and ANOVA or Kruskal–Wallis to compare more than two groups. These tests analyse individual spots instead of the complete set, omitting information about correlated variables. Multivariate data analysis methods, such as principal component analysis (PCA), are now used to pinpoint spots that differ between samples. These multivariate methods focus not only on differences in individual spots, but also on the covariance structure between proteins [122]. However, the results of these methods are sensitive to data scaling, and they may fail to produce valid multivariate models due to the high number of spots in the gels that do not contribute to the discrimination process [130]. One of the limitations of PCA analysis is that it does not allow missing values, a problem that can be avoided by imputing them when possible (if enough replicates are available) [131]. In contrast to these multivariate methods, univariate tests increase the number of false positives, and for each species, a measure of significance reflecting rates of false discovery should be calculated. This measure of significance is called a *q* value, and it has been described by Karp et al. [132].

Blue native polyacrylamide gel electrophoresis (BN-PAGE) has become very popular for analysing membrane proteins and protein complexes, but in some cases, as in the analysis of chloroplast light-harvesting complexes (LHC), it shows poor resolution, especially for proteins in the range of 22–25 kDa [133]. In order to preserve the advantages of the technique and use it with in-gel fluorescent detection and in-gel catalytic activity assays, Coomassie dye in the cathode buffer can be replaced with non-coloured mixtures of anionic and neutral detergents [134]. D'Amici et al. have reported a new protocol for native 3-D electrophoresis that allows exhaustive separation and identification of membrane proteins [135]. The method was applied first to the thylakoid membrane of spinach, which contains four large protein complexes. The protocol includes native liquid phase isoelectrofocusing (N-LP-IEF) of protein complexes in the first dimension, followed by blue native polyacrylamide gel electrophoresis (BN-PAGE) in the second dimension. Finally, the individual components of the complex are resolved using denaturing electrophoresis (SDS-PAGE).

3.5. *Second-generation techniques*

The use of differential 2-DE (DIGE) for comparative studies is reported in a significant number of papers published during the reviewed period (Heinemeyer et al., this issue). Problems can arise with this methodology when two different species for a given protein, one labelled and the other unlabeled, differ in masses. As a consequence, in the case of automated spot picking according to CyDye coordinates, the exact positions of the maximum amounts of the proteins under study are not accurate, resulting in a loss of sensitivity in the subsequent MS analyses. To solve this, differences in the migration of labelled and unlabelled species should be quantified in order to obtain more reliable protein identification [136].

The use of gel-free, LC-based approaches [137; Stevenson et al., this issue], including MudPIT [138,139] still remains anecdotal in Plant Proteomics studies [140].

Second-generation MS technologies for Quantitative Proteomics [141,142] have begun to be applied to Plant Proteomics research. These technologies include stable isotope labelling, ICAT [143], iTRAQ [144,145], SILAC [146,147], or label-free methods (peak integration, spectral counting). The latest trends and applications of the technique, as well as its potential, have been previously reviewed [148–150; Oeljeklaus et al., this issue). Combining different approaches increases the proteome coverage. In this way, Hebeler et al. [151] carried out a quantitative analysis of changes in protein abundance related to early leaf senescence in *Arabidopsis* using a double reverse labelling strategy, DIGE and ^{15}N-labeling of buffer extracted proteins followed by HPLC/ESI-MS/MS (Q STAR XL) and protein identification based on the *Arabidopsis* EBI protein sequence database (SEQUEST). The combination of gel and gel-free techniques allowed identification of different sets of variable spots.

3.6. *Mass spectrometry*

Mass spectrometry of proteins is constantly evolving, with protocols, machines and software continuously improving, such that the technology is approaching the limit of its capabilities. In the past few years, the development of Orbitrap and new dissociation methods such as electron-transfer dissociation, have opened up new possibilities in proteome analysis. Although Bottom-up Proteomics (analysis of proteolytic peptide mixtures) remains the predominant platform, top-down strategies (analysis of intact proteins) should allow a more complete characterization of the proteome, including protein isoforms and post-translational modifications. All these aspects have been discussed in detail in recent reviews [12,152–155].

Using classical quadrupole and ion trap mass analysers, intact protein masses can be determined with standard deviations in the range of 2–5 kDa. In some cases, these approaches, based on nonisotopically resolved related ion deconvolution using average masses from protein spectra, show differences between measured and calculated masses that exceed the standard deviations. This occurs due to the complexity of mixtures of protein isoforms and the presence of post-translational modifications. These limitations can be overcome by using highly accurate mass determinations from Fourier transform ion cyclotron resonance mass spectrometry [156,157]. The use of a hybrid ion trap Fourier transform mass spectrometer has been reported in the analysis of the citrus fruit proteome [158] and of the chloroplast envelope of pea and maize [148].

3.7. *Different techniques are complementary*

The literature makes clear that the different techniques, platforms, and workflows are complementary, and all of them are necessary for more complete coverage of the proteome. This is clearly shown in the paper by Lee et al. [159], which analysed several different *Arabidopsis* leaf protein fractions: i) TCA–acetone precipitates solubilised in urea, urea–SDS and urea-n-dodecyl β-D-maltoside buffer; ii) membrane proteins; iii) hydrophobic proteins; and iv) organellar proteins (nuclei, microsomal membranes, plastids, and mitochondria). They analysed these fractions using two shotgun approaches, MudPIT and 1-D SDS-PAGE-LC-MS, with a quadrupole IT mass spectrometer. In all, 2342 nonredundant proteins were identified, and 68–545 proteins were identified by only one of the two methods. For example, in the case of whole-leaf extract solubilised by SDS buffer, 70 proteins were identified only by MudPIT and 109 only by 1-D LC-MS. For both approaches, the number of transmembrane proteins ranged from 57 to 77. One disadvantage of 1-D gel-LC-MS/MS may be that the limits of protein discovery are reached after a few replicate experiments. This is not the case for MudPIT, which requires multiple analyses in order to survey all the proteins in a sample.

3.8. *Algorithms*

Proteomic investigation is facilitated, and the proteomic scientist's life is complicated, by the increasing number of protein databases containing protocols, search and quantification algorithms, protein sequences, predicted and verified functional information, structural and functional classifications, phylogeny and ontology [159]. It is outside the scope of this review to discuss all of these aspects in detail, and we refer the reader to recent key reviews or original papers [30,160–167]. Of special relevance to the community is the characterization of proteomes using homology-driven proteomics, since the genomes of most plant species of interest have not been sequenced and in fact databases lack any entries for some of them [168,169].

4. Descriptive Proteomics

4.1. *Increasing proteome coverage, at least in Arabidopsis and rice*

Within the Descriptive Proteomics area, the work by Baerenfaller et al. should be highlighted [37], since it represents the most exhaustive proteome map reported for plants. This study supports that a combination of SDS-PAGE, band cutting, trypsin digestion and LC separation of the resulting peptides constitutes the most powerful technique in terms of protein coverage [113,114]. In all, 1354 linear ion trap runs were conducted with protein extracts from six different organs and cell suspensions. The outcome was 13,029 proteins identified, comprising 10,902 from plant organs and 8698 from cell suspensions, using PeptideProphet and PepSplice algorithms, with 86,456 unique peptides originating from 790,181 tandem MS peaks, with a rate of false discoveries below 1%. This figure corresponds to nearly 50% of all predicted *Arabidopsis* gene products, not including protein variants. Despite its success, this work is a clear example of the limitations of the proteomic approach. Proteins involved in transcriptional regulation and signalling are underrepresented, while housekeeping proteins, involved in primary metabolism (mainly carbohydrate metabolisms), are overrepresented. This analysis preferentially detected large proteins and proteins for which the transcripts are expressed at high levels. Major modifications of peptides that were detected included Met or Trp oxidation and Cys carbamidomethylation, all of which supposedly took place during *in vitro* manipulation.

When protein and transcript levels were compared, values were found to range from 0.52 (seeds) to 0.68 (leaves). Comparing the MS/MS spectra with the TAIR7 genome database identified peptides from genomic regions with no annotated protein-coding capacity. Such comparison also identified organ-specific biomarkers, allowing the compilation of an organ-specific set of peptides corresponding to 4105 proteins that will facilitate targeted, Quantitative Proteomic surveys in the future.

Using a (descriptive) proteomic approach, Catusse et al. reported a 2-DE reference map of sugarbeet seeds, root, stem, cotyledons and perisperm tissues. Some of the proteins identified were not reported previously in seeds, and the results allowed the proposal of novel mechanisms for translation initiation based on both cap-independent and dependent processes. Seed metabolism could be reconstructed from the proteins identified, which corresponded to 121 biochemical functions, and some pathways such as glycolysis were thoroughly represented [170]. In a similar work, Katz et al. studied the metabolism of the citrus fruit, with a focus on citrate and sugar metabolism, as well as vesicular trafficking [158].

Due to their simple proteome, some plant samples are very good candidates for proteomic analysis, with their low protein content posing the major difficulty to complete coverage. Aki et al. [171] reported a shotgun analysis of the proteome of phloem and xylem saps from rice. In that work, they took advantage of the complete genomic information available for this plant. Xylem sap was prepared using the root pressure method, whereas phloem sap was prepared using the insect laser method. The technical difficulties caused by the limited amount of protein in these samples were overcome by the use of nano-flow liquid chromatography linked to a mass spectrometer. Two alternative methods were used: i) SDS-PAGE, band cutting and digestion with the tryptic peptides subjected to an integrated microfluidic device (HPLC-Chip for a nano scale LC) coupled to an ion trap MS; and ii) 2-D LC of the sample tryptic peptides (SCX-HPLC-chip), with the chip coupled to the IT. The number of proteins identified using both strategies was high: 118 different proteins and eight different peptides in xylem sap, 107 different proteins and five different peptides in phloem sap. The identified proteins included signal transduction proteins, putative transcription factors, stress response factors, and metabolic enzymes. In phloem sap, three of the proteins identified showed significant similarity to the *Arabidopsis* TFL1 and FT proteins that play important roles in controlling the inflorescence architecture and the transition from the vegetative phase to the reproductive phase. The expression pattern of genes coding for the FT-like proteins identified was examined by qRT-PCR, revealing a tissue-specific protein pattern. The existence of peptide signals that act over long distances by moving through the phloem or xylem is a matter of controversy and speculation. Consequently, this study also carried out MS analysis of peptides, but no known plant peptide hormones were detected, such as systemin, phytosulfokine or CLAVATA3.

In addition to these studies, the proteomes of several other plants were analysed in the papers published during the review period: *Arabidopsis* leaves, roots, and flowers [172], *P. radiata* needles [78], wheat roots [173], tomato pollen [174], maritime pine xylem [6], soybean xylem/apoplast [140], maize root pericycle cells from primary roots [84] and *M. truncatula* protoplasts [80].

5. Subcellular Proteomics

5.1. *Imminent completion of the chloroplast and mitochondrial proteomes*

Proteomics provides a powerful tool for characterizing the biochemistry of organelles. However, information obtained through proteomics can only be valid if the organelle sample is not heavily cross-contaminated. Hence, although proteomic analysis can give an indication of possible cross-contamination, biochemical analyses comprising tests of enzyme activity, Western blotting, and metabolite analysis must always be performed [7,175]. Significant effort has been devoted to the development of protocols for isolating highly purified preparations of organelles and sub-organellar compartments for protein profiling. These organelles and compartments include: chloroplasts [176,177], mitochondria [178], vacuoles [179], cell wall [180], membranes [181,182], and embryoplasts [139].

The technique known as LOPIT, which stands for localisation of organelle proteins by isotope tagging, assesses the distribution patterns of organelles by measuring the relative abundance of proteins between fractions along density gradients using stable isotopic tags, and has been used to assign proteins to different endomembrane organelles [183].

Subcellular Proteomics in plants has been extensively reviewed [38,181,184–187]. In this issue, H. Millar and coworkers review a collection of papers in which plant responses to abiotic stresses were evaluated in *Arabidopsis* using whole-tissue and Subcellular Proteomics approaches. Therefore, we will comment on just some of the papers that have appeared on this topic during the review period.

A detailed analysis and characterization of the *Arabidopsis* ribosomal proteome, both cytosolic and mitochondrial, has been reported by Carroll et al. [188]. They performed *in silico* digestion of the complete ribosomal proteome using an in-house, modified version of Proteogest in order to define targets for data acquisition and to establish a strategy for data collection that maximises recognition of peptides derived from ribosomal proteins. Approximately 13,000 unique peptide sequences were obtained, with 9400 predicted to come from only one of the 409 protein sequences (gene-specific peptides) corresponding to 80–249 proteins. Ribosomal proteins were separated by SDS-PAGE, and bands (21) or ribosomal extracts containing low-molecular-weight proteins were digested with trypsin, or with both chymotrypsin and pepsin in order to increase the coverage. Peptide match information from MASCOT files was extracted and filtered, and only the highest quality unambiguous spectra that matched exclusively certain *in silico* predicted gene-specific peptides were accepted. This procedure, based on high confidence criteria, allows what are called gene-specific identifications. A total of 1446 high-quality MS/MS spectra matching 795 peptide sequences was reported, allowing the identification of peptides from five gene families previously unidentified, and providing experimental data on 79 of the 80

different types of ribosomal subunits. The analysis identified 31 small subunit proteins, 46 large subunit proteins, and seven P-proteins, all of them gene-specific. Several PTMs were identified using chemically mild sample preparation conditions, electrophoretic prefractionation and phosphoprotein/phosphopeptide enrichment, including initiator methionine removal, N-terminal acetylation, N-terminal methylation, lysine N-methylation and phosphorylation.

Several studies have provided new insights into the role of sphingolipid/sterol-rich domains, detergent-insoluble membranes (DIM), and so-called "lipid rafts" of the plasma membrane (PM) in mammalian cells and in leaves, cell cultures and seedlings of higher plants [189]). Lipid rafts are defined as a Triton X-100-insoluble, low-density membrane fraction. DIM fractions prepared from *M. truncatula* root PMs [190] were characterized by structure-electron microscopy and the levels of lipid, sterol, sphingolipid and protein analysed. They were found to be enriched in sphingolipids and Delta (7)-sterols, with spinasterol being the main component, although steryl glycosides and acyl-steryl glycosides were also present. A total of 270 proteins were identified following SDS-PAGE, gel slice digestion, Q-TRAP nLC-MS/MS, and MASCOT searches of the nonredundant NCBI subdatabase *M. truncatula*, the *M. truncatula* local EST database (http://medicago.toulouse.inra.fr/Mt/EST/) and the *M. truncatula* genomic database (http://www.medicago.org/genome/). Among the proteins identified, receptor kinases and other proteins related to signalling, cellular trafficking and cell wall functioning were well represented, whereas those involved in transport and metabolism were poorly represented. The results also showed evidence for the existence of a complete PM redox system in lipid rafts.

Other subcellular proteomic studies, which are not mentioned in detail here, deal with chloroplast envelope membranes from pea and maize [148], stroma lamellae from 10 different plant species [191], potato tuber amyloplasts [192], soybean peroxisomes [193] and plasma membrane and tonoplast from rice [194,195] and *Arabidopsis* [196].

6. Differential Expression Proteomics

6.1. *The first option to get into Proteomics and dominated by 2-DE*

The biological meaning of a protein can be inferred from its differential presence in specific genotypes (i.e. wild, transgenic, mutant), cell type, developmental stage and external conditions. Half of the original plant proteomic papers published during this review period used this strategy to identify and characterize proteins or genes involved in growth, development and plant responses to hormones, stresses, and other events including pollen germination, embryo formation, seed development and germination, fruit development and ripening, leaf senescence, programmed cell death, wood formation, the effect of auxins, giberellins, abscisic and jasmonic acids, mineral nutrition, symbioses, biotic stress (pathogen, insects), abiotic stress (drought, osmotic shock, temperature, UV light, ozone, heavy metals, waterlogging), and oxidative stress (Table 4).

Although 2-DE coupled to MS is by far the most frequently used platform for Differential Expression Proteomics, there are some exceptions. For example, Larson et al. [197] and Wen et al. [198] used MudPIT to study the reaction of sugar beet to *Fusarium oxysporum* and the reaction of root pea to *Nectria haematococca*, respectively. Other exceptions are the works of Palmblad et al. and Patterson et al. The former reported the use of metabolic stable isotope ^{15}N-labelling to identify heat-responsive proteins in *Arabidopsis* [146]. The latter used the iTRAQ approach to identify boron-responsive proteins in barley roots [199].

6.2. *Stress responses*

Proteomics has been used widely during the review period to gain a deeper knowledge of the processes that take place in an organism subjected to stress. The type of stress most studied is pathogenesis, followed by drought stress, metal toxicity, and salt-osmotic stress. Although diversity is the rule, most studies examining these stresses have focused on *Oryza sativa* (rice). The plant tissues used in these papers have been as diverse as leaves and cotyledons, roots, fruits, phloem and xylem saps, apoplastic fluid, entire seedlings, shoots, stem segments, seeds, nuclear fractions, gametophores and meristematic tissue. Among the proteins observed to respond to stress are those involved in detoxifying reactive oxygen species (ROS), which makes sense considering that most stressors increase production of ROS in plants. Hajheidari et al. [200] studied the effect of drought stress in the seeds of three wheat genotypes that differ in their tolerance of water shortage. Soluble proteins were buffer-extracted and separated by 2-DE, and significant differences were assessed by two-way ANOVA. A total of 121 drought-responsive spots were analysed by MALDI TOF/TOF, and 57 proteins were identified. Of these, 38 have been identified as putative Trx targets, indicating a link between drought tolerance and redox homeostasis.

Kang et al. [201] carried out an interesting research aimed at characterizing the phenotype of the lesion-mimic mutant *spotted leaf 6* (*spl6*) rice. Proteins present at different levels in the leaf blades of wild-type and mutant plants were identified by MALDI-TOF using ProFound. Northern blot assays were performed to correlate protein expression with the levels of the corresponding transcripts. Microscopy observations allowed the detection of degradation of the thylakoid membrane in the nonspotted sections of the mutant, which explained the absence of ATP synthase, RuBisCO large subunit, and RuBisCO activase in this genotype. The authors propose the absence of TPX and PDI as the reason why the cells cannot resist the oxidative burst that results in the degradation of the thylakoid membranes, programmed cell death and lesion development.

Other proteins that are often found in response to stress are the pathogenesis-related proteins (PRs). Many papers that were published before the present review period and that examine plant development and responses to stresses limit their proteomic analysis to one time point. As a consequence, information on multiple quantitative plant responses and the sequential events that mediate them is missing. Time-course analysis can provide this missing information, and has been useful, for example, in showing that plant resistance

Table 4 – Differential Expression Proteomics papers appeared during the reviewed period.

Topic	Biological system	Ref.
Seed development	*Medicago truncatula* seeds (seed coat, endosperm and embryo) at five developmental stages	[205]
	Zea mays kernel or endosperm	[206]
Seed germination	*Fagus sylvatica* seeds imbibed in water or treated with ABA or GA_3	[207]
	Oryza sativa seeds sampled at different germination times	[203]
	Arabidopsis thaliana seeds with a controlled deterioration treatment	[204]
De-etiolation	*Oryza sativa* etiolated seedlings	[262]
Fruit development and ripening	*Solanum lycopersicum* var. *cerasiforme* fruits collected from anthesis to maturity	[263]
	Vitis vinifera L. cv. Cabernet Sauvignon grape skin collected at different days after anthesis	[264]
	Vitis vinifera cv. Nebbiolo Lampia grapes sampled from 1 month after flowering to complete ripe stage	[265]
Tillering	*Oryza sativa* basal nodes sampled from two cultivars with different numbers of tillers	[266]
Senescence (leaves)	*Arabidopsis thaliana* mutant plants displaying advanced leaf senescence	[151]
Pollen germination	*Oryza sativa* mature and germinated pollen grains	[81]
Microspore derived embryo	*Brassica napus* microscospore-derived embryos in two different culture systems	[10]
Juvenile wood formation	*Eucalyptus grandis* stems cambial region sampled at different ages	[76]
Chloroplast differentiation	*Oryza sativa* seedling-derived plastids with different periods of light exposure	[267]
	Pisum sativum L. protein complexes from etioplasts, etio-chloroplast and chloroplasts	[268]
Callus differentiation	*Oryza sativa* seed-derived callus at different differentiation stages	[269]
Plant hormones	*Oryza sativa* seeds treated with gibberellins GA and ABA	[270]
	Oryza sativa leaf sheats treated with gibberellin GA_3	[271]
	Oryza sativa leaves with different ABA treatments	[272]
	Oryza sativa leaf sheaths treated with auxin 2,4-D or auxin repressor PCIB	[273]
	Oryza sativa seedling-derived shoots and roots with different concentrations of jasmonic acid	[274]
Signal transduction	Brassinosteroid response in *Arabidopsis thaliana*. BR-deficient mutant *det2*-1 and BR-insensitive mutant *bri*1-116. brassinolide	[208,209, 275]
Nitrogen source	Roots from *Lolium perenne* plants grown in liquid medium with different N supplies (ammonium, nitrate, glycine)	[276]
Mineral nutrition: Fe	Roots from tomato plants (*fer* mutant, wild-type and overexpressing transgenic line) grown with different amounts of Fe	[277]
Programmed cell death	Rice seedlings (wild and lesion mimic mutants) inoculated with *Magnaporthe grisea*.	[278]
Symbiosis: *Sinorhizobium meliloti*	*Medicago truncatula* roots (wild type and supernodulation mutant) inoculated with the *Sinorhizobium meliloti*.	[279]
	Nodules from 10-weeks old *Medicago truncatula* inoculated with *Sinorhizobium meliloti* (control and drought stressed)	[280]
Pathogens	Leaves of blackleg-susceptible *Brassica napus* and blackleg-resistant *Brassica carinata* inoculated with *Leptosphaeria maculans*.	[281]
	Leaves of canola (*Brassica napus* L.) plants infected with *Sclerotinia sclerotiorum*	[282]
	Roots of *Brassica napus* infected by *Plasmodiophora brassicae*	[283]
	Leaves of *Capsicum chinense* plants harbouring the L^3 gene infected by two strains (compatible, incompatible) of pepper mild mottle virus	[202]
	Spikelets of six barley genotypes of varying resistance inoculated with *Fusarium graminearum*.	[284]
	Leaves of *Populus euramericana* inoculated with *Marssonina brunnea* f. sp. *multigermtubi* at different after inoculation times	[285]
	Leaves of *Arabidopsis* wild-type and *CaHIR1*-overexpressing transgenic plants inoculated with *P. syringae* pv. *tomato*, *Hyaloperonospora parasitica* and *Botrytis cinerea*.	[286]
	Peach fruit inoculated with *Penicillium expansum* and treated with SA or *Pichia membranefaciens*.	[287]
	Sugar beet genotypes resistant (R) and susceptible (S) inoculated with *Fusarium oxysporum* (F-19)	[197]
	Roots of pea inoculated with *Nectria haematococca*.	[198]
	Xylem sap of tomato plants infected with *Fusarium oxysporum*	[82]
	Phloem of Austrian pine inoculated with *Diplodia scrobiculata* and *Sphaeropsis sapinea*	[75]
	Leaves of *spl6* mutant and wild-type rice plants were used	[201]
	Apoplastic fluid of *Arabidopsis* seedlings, control or treated with oligogalacturonids.	[288]
	Seedlings of *O. sativa* subsp. *japonica* treated with probenazole and inoculated with bacteria	[289]
Trichoderma induced resistance	Cotiledons of *Cucumis sativus* L. plants inoculated with *T. asperellum* strain T34+ and *Pseudomonas syringae* pv. *lachrymans* (Psl).	[290]
	Root and shoot tissues of maize (*Zea mays*) treated with *Trichoderma harzianum* T22	[291]
Insects	Stem segments of Sitka spruce (*P. sitchensis*) seedlings mechanically wounded and weevils inoculated	[77]

(continued on next page)

Table 4 (*continued*)

Topic	Biological system	Ref.
Drought	Droughted seeds of three spring wheat genotypes differing in its drought tolerance.	[200]
	Roots of *Zea mays* water stressed	[292]
	Xylem sap of water stressed *Zea mays* plants	[293]
	Nuclear fraction of chickpea seedlings subjected to progressive dehydration	[294]
	Extracellular matrix (ECM) of eight chickpea (*Cicer arietinum* L.) cultivars subjected to dehydration.	[295]
	Dried and rehydrated leaves from *Boea hygrometrica* plants.	[70]
	Leaves of droughted tall wheatgrass (*Elymus elongatum* Host) plants	[68]
Salt stress	Roots of NaCl treated *Triticum aestivum* plants.	[296]
	Gametophores of *Physcomitrella patens* were exposed to high-salinity (250, 300, and 350 mM NaCl).	[67]
	Roots of *Arabidopsis* plants treated with NaCl.	[297]
Osmoticum stress:	Meristematic tissue of Cachaco (ABB cooking banana) and Mbwazirume (AAA highland banana) cultured in high-sucrose medium.	[298]
	Rice leaf sheath treated with mannitol, drought and cold	[299]
Heat	Leaves of *Arabidopsis*	[146]
	Leaves of rice	[300]
Cold	Rice leaf and roots	[109,110]
Shadow avoidance	Leaves of shadowed tomato plants	[301]
UV light	Leaves of soybean lines differing in flavonoid contents	[302]
Ozone	Rice leaves	[303]
Heavy metals	Leaves of poplar clones treated with cadmium	[304]
	Roots of *Cannabis sativa* treated with cupper	[305]
	Second oldest trifoliate leaf of cowpea treated with manganese	[306]
	Roots and leaves of B-tolerant barley plants treated with boron	[307]
	Roots of Al-resistant and susceptible plants	[308]
	Roots of rice treated with Al	[309]
Nutritional limitation	Roots tomato wild and mutant plants	[310]
Agrochemicals: safeners	Root, leaf, and coleoptile of *Triticum tauschii* seedlings treated with herbicide and/or safener	[311]
Waterlogging	Leaves of tomato plants subjected to waterlogging	[312]
Oxidative stress	Roots of rice treated with GSH, DPI or ascorbate	[313]
	Leaves of rice treated with different concentrations of H_2O_2	[314]

to pathogens is associated with rapid induction of the expression of specific genes. As an example, Yoshimura et al. [73] reported changes in the proteome (2-DE) of root watermelon (*C. lanatus* L.), a xerophyte species, in response to water withholding. Comparative analysis revealed that many proteins induced in the early stage of drought stress are involved in root morphogenesis and carbon/nitrogen metabolism, which may contribute to drought avoidance by enhancing root growth. In contrast, the majority of lignin synthesis-related proteins, which enhance tolerance of physical desiccation, and molecular chaperones, which maintain protein integrity were induced at a later stage of drought stress. These data suggest that this xerophyte switches survival strategies from drought avoidance to drought tolerance during progression through drought stress, and this switch involves temporal regulation of the root proteome.

Using pepper plants harbouring the *L3* gene, which confers resistance to pepper mild motle virus (PMMoV), Elvira et al. [202] analysed the PRs induced in response to virus inoculation using either a virulent (PMMoV-I) or avirulent (PMMoV-S) strain. Acid-soluble proteins from leaves and apoplastic fluid proteins were buffer-extracted and separated by 2-DE. Proteins were analysed by Western blots and identified by Edman sequencing and BLAST searching. Northern blot analysis of RNA coding for PR proteins was also performed. From their results, they concluded that, although a few PR proteins are specifically induced in the incompatible interaction, both reactions are qualitatively similar, differing only in the degree and timing of the response. Thus, the earlier and higher accumulation of PR proteins and mRNA was detected when plants were inoculated with the avirulent strain.

6.3. *Embryogenesis, seed maturation and germination*

Embryogenesis, seed maturation and germination are the developmental processes most often studied by proteomics, with reports published on rice [203], *Arabidopsis* [204], *M. truncatula* [205], maize [206], rapeseed [10] and *Fagus sylvatica* [207]. Using a comparative proteomic approach we analysed changes in the protein profile in date palm zygotic embryos during development, maturation, and germination (Sghaier et al., 2008, Proteomics, in press). The workflow used consisted of protein extraction, 2-DE, image analysis, and differential spot identification by MS. At the analysed stages (7), up to 194 spots showed qualitative or quantitative differences. By performing a multivariate analysis such as PCA, we were able to group samples and determine the most discriminant spots, and we recommend this approach for other proteomic studies. In addition, hierarchical clustering analyses can be performed to reveal the existence of groups of proteins showing similar evolution patterns [206].

6.4. Signalling

The series of papers by Wang and coworkers on brassinosteroid (BR) responses and signalling in *Arabidopsis* is an excellent example of the use of different approaches to validate data and gain a better understanding of key biological processes. Also, they cover different proteomic areas: descriptive, PTM and Interactomics. The proteomic study of BR-regulated proteins was performed using DIGE and LC-MS/MS [208]. A total of 42 BR-regulated proteins were identified. Analyses of the BR-insensitive mutant *bri1-116* and BR-hypersensitive mutant *bzr1-1D* led to the identification of five proteins (PATL1, PATL2, THI1, AtMDAR3 and NADP-ME2) affected by BR treatment in the mutants, suggesting their importance in BR action. Selected proteins were further studied using insertion knockout mutants or immunoblotting assays. Interestingly, approximately 80% of the BR-responsive proteins had not been identified in previous microarray studies, and direct comparison of protein and RNA changes in BR mutants revealed extremely weak correlation. RT-PCR analysis of selected genes revealed gene-specific kinetic relationships between changes in RNA and protein levels. Furthermore, BR-regulated Posttranslational Modifications of BiP2 protein were detected based on spot shifts in 2-D DIGE.

Proteomics has also been used to identify elements of the brassinosteroid signal transduction cascade that interact with BRl1, the major membrane receptor-like kinase of BRs [209]. Seedlings of the BR-deficient mutant *det-21* were treated with brassinolide and total or plasma membrane protein preparations were subjected to DIGE. Mass spectrometry analysis of differential abundant control- and brassinolide-treated seedling proteins allowed the identification of two BR-signalling kinases, BSK1 and 2, which are members of the receptor-like cytoplasmic kinase subfamily RLCK-XII. In response to BR, these two proteins are phosphorylated and shift in position from the basic to the acidic part of the gel. Proteomic data in that study were validated using transgenic plants expressing a fusion protein of BSK1 with yellow fluorescent protein (YFP). The analysis of the *bri1-5* mutant showed that BSK phosphorylation is BRl1-dependent. A sequence analysis revealed the existence of putative N-terminal myristoylation sites that target them to the membrane, as shown by confocal microscopy of BSK1-YFP. MS analysis revealed Ser^{230} to be the phosphorylation site, both *in vitro* and *in vivo*. *In vivo* interaction of BRI1 and BSK1 was demonstrated using bimolecular fluorescence complementation and co-immunoprecipitation assays. T-DNA insertion mutants and transgenic plants overexpressing BSK3 were used to determine the function of BSKs.

7. PTMs

7.1. Phospho and, to some extent, the redox proteomes

Mass spectrometry is the key technology for detecting, mapping and quantifying the great array of Posttranslational Modifications occurring on proteins, with as many as 300 being reported [17]. Such chemical modifications determine the activity status, localisation, turnover and interactions of proteins. The biological motivation for studying these modifications is their relevance for modulating and determining nearly all aspects of cell biology. MS strategies developed and successfully used for large-scale analysis of PTMs in other biological systems laid the foundation for plant biology studies, but only a few of the available protocols have been used to explore PTMs in plant systems, and most of these modifications remain unexplored.

In this section we discuss the recent advances done in this area, focusing on protein phosphorylation, the most extensively studied PTM, as well as on redox modifications. Some reviews on these topics have appeared recently [187]. Except for two papers using maize and *S. chacoense* [72], a relative of tomato, all the published works deal with model systems: *Arabidopsis* (15), rice (3) and *M. truncatula* (1). Most of the papers are descriptive, while some of them study changes in the PTM pattern in response to environmental stress [210,211].

7.2. Phosphoproteome

The current challenges in Phosphoproteomics can be summarised as the following three. First, efficient enrichment of phosphoproteins/phosphopeptides is needed due to the low abundance of such regulatory phosphoproteins, which is too low for the sensitivity of most mass spectrometers. Second, quantitative analysis is necessary because reversible protein phosphorylation/dephosphorylation events control many physiological processes. Third, plant phosphoprotein databases are needed in order to integrate current knowledge on plant phosphoproteins and bioinformatic tools to predict phosphorylation motifs. The papers described below address some of these issues using a wide variety of biochemical and analytical chemical approaches to enrich, detect and characterize protein and peptide phosphorylation on a proteome-scale. These techniques have advantages and drawbacks, but the overall conclusion is that a combination of all of them would increase the coverage of the proteome studied and the knowledge of its dynamics and implications for plant physiology.

Large-scale identification of *in vivo* phosphorylation sites by MS is possible as a result of the development of different techniques for the enrichment of phosphopeptides and phosphoproteins [212–215]. This achievement, together with the use of highly sensitive and accurate mass spectrometers, has led to the identification and mapping of thousands of phosphopeptides. Using Fe-IMAC and HAMMOC prior to the nLC-MS analysis, Sugiyama et al. [212] made possible the identification of 2172 phosphorylation sites in 1346 *Arabidopsis* proteins, stressing the relevance of tyrosine phosphorylation in plant physiology. Tan et al. [214] use SCX-RP coupled with ESI IT to identify 269 phosphoproteins in rice that are associated with chromatin, including transcription factors and histone modification proteins. Organelle purification [215,216] and prefractionation of protein or peptide samples are necessary in order to increase the coverage of the phosphoproteome. In addition, a number of chemical derivatisation strategies, in which the phosphate group can be replaced by a more stable moiety, have been developed. Using a Ser- and Thr-biotin-tagged approach, Kwon et al. [217] identified 31 protein spots from RuBisCO-depleted fractions from *Arabidopsis* seedlings.

The work by Meimoun et al. [218] describes the use of a commercial phosphoprotein affinity matrix (Qiagen), and this was tested on sorghum and *Arabidopsis* extracts. Phosphoenolpyruvate carboxylase (PEPC) enzymatic assays and Western blots, as well as 3-D mass spectrometry analysis of immunoprecipitated PEPC showed that the column efficiently binds P-PEPC with no contamination by non-P-PEPC. In fact, the column captured 80% of the proteins labelled *in vivo* using ^{32}P-phosphate, and the majority were subsequently found in the elution fraction (88%). This was also visualised by SDS-PAGE (1D and 2D gels), followed by Pro-Q diamond staining. Analysis of the P-protein fraction by 1-D gels and liquid chromatography/tandem mass spectrometry allowed the identification of 250 proteins with a variety of functions.

One of the papers reviewed analyses the proteome and phosphoproteome during ovule fertilisation in *S. chacoense*. It compares the efficiency and sensitivity of different methods for detection and purification of phosphopeptides and proteins: immunodetection, *in vivo* labelling and phosphoprotein-specific staining [72]. That study concludes that there is a small overlap among the three methods, which is in agreement with the idea that different methods must be combined to achieve complete coverage of the proteome.

Phospho Proteomics in plants is moving from being descriptive to quantitative. Concerning mass spectrometry-based quantitative Phospho Proteomics, we highlight two recent papers, both of which study the dynamics of *Arabidopsis* protein phosphorylation in response to the microbial elicitor fla22, but they use different quantitative strategies [215,219]. Benschop et al. used ^{14}N/^{15}N metabolic labelling to compare phosphorylation levels of plasma membrane proteins from treated and control cells, and the quantitative information is acquired at the MS stage, while Nushe et al. obtain quantitative data at the MS2 stage using iTRAQ labelling. Interestingly, both studies show excellent agreement in the proteins they identify as being involved in the regulation of many of the flagellin-induced phosphorylation sites, including kinases and regulatory proteins potentially involved in defence. The differences in the number of identifications may reflect the different equipment used and the statistical analyses performed. These two papers are an encouraging example of how different approaches to Quantitative Phospho Proteomics can lead to similar results. In addition, these results emphasise the potential of proteomic technology in quantifying the dynamics of phosphorylation, in which case it would join other large-scale genomic approaches that serve as valuable tools in determining regulatory mechanisms.

Recently, Kruger et al. [220] presented an alternative label-free method for Quantitative Phospho Proteomics studies that allows the determination of phosphorylation sites and phosphorylation stoichiometries. The method couples capillary liquid chromatography (capLC) with inductively coupled plasma-mass spectrometry (ICP-MS) to perform quantitative phosphodetermination of protein extracts based on their phosphorus content. As an internal control for protein amount, the sulphur content is also determined. The protein phosphorylation stoichiometry can be determined via the phosphorus to sulphur ratio, given that the number of amino acids containing sulphur (cysteine and methionine) is known. Applying this method to *Arabidopsis* and *C. reinhardtii* has enabled description of their global phosphorylation states, indicating differences in the average protein phosphorylation levels between organisms. In addition, it shows differences in the proteomic phosphorylation patterns and stoichiometry of *Arabidopsis* in a tissue- and development-dependent manner, indicating a different adjustment of the kinase/phosphatase system in each specific situation.

A recent review has summarised the large-scale mapping of *in vivo* phosphorylation sites using a combination of mass spectrometry-based techniques and protein chip-based methods, and their potential to unravel plant signal transduction pathways [221]. De la Fuente van Bentem et al. [213] used this methodology to unravel phosphoproteome dynamics in control and H_2O_2 treated-*Arabidopsis* cells by examining cytoplasmic and nuclear fractions. This analysis led to the identification of 303 *in vivo* phosphorylation sites, including 21 different protein kinases. Validation of some of these results was based on immunoblotting and mutational analysis. In addition, quantitative analysis of the phosphorylation status of proteins (kinome profiling) was estimated using peptide arrays generated using peptides corresponding to *in vivo* phosphorylation sites. The investigators concluded that different protein kinases operate in cytosolic and nuclear compartments.

These protein/peptide array experiments provide a large-scale inventory of the site specificity of multiple protein kinases, revealing specific phosphomotifs for different kinases [213]. To facilitate the experimental validation of kinase-substrate pairs identified by MS, it would be useful to have software applications that integrate all the information available and enable prediction of upstream kinases for substrate phosphorylation sites based on data from plant systems. Along these lines, Heazlewood et al. [36] have developed a method for the prediction of phosphorylation sites in *Arabidopsis*. They describe the *Arabidopsis* Protein Phosphorylation Site Database (PhosPhAt) (http://phosphat.mpimpgolm.mpg.de) as a valuable resource for plant researchers since it integrates current knowledge of MS-based identified phosphorylation sites in *Arabidopsis* and site prediction based on phosphorylation motifs. They used 802 experimentally validated serine phosphorylation sites to develop prediction software for serine phosphorylation, resulting in 27,782 predicted sites in 17,035 proteins. This information is accessible for each peptide, together with the experimental conditions such as tissue sampled and the phosphopeptide enrichment method. An integrative approach combining large-scale mass spectrometry-based mapping of phosphorylation sites with protein and peptide chip analysis and bioinformatic predictive tools, will reveal protein kinases and phosphatases, their substrates and their positions within signalling webs.

7.3. *Redox proteome*

Although it has not been studied nearly so extensively as the phosphoproteome, the number of plant redox proteome studies has increased over the past few years. This is due mainly to the continuous development of new, more sensitive chemical derivatisation reactions, affinity purification media, specific detection reagents and the use of highly sensitive mass spectrometers that allow direct detection of such modifications [222–225]. A recent review [226] summarises the progress made on the study of redox regulation from a systems biology

perspective, and it illustrates the central role of redox regulation in plant networks. We discuss below some of the recent progress made in describing the thiol/disulfide proteome, the redox-dependent and cross-talking signalling pathways, and the target genes/proteins of redox regulation. The specificity of these modifications is an intriguing issue that is still far from being understood.

Two studies use 2-DE oxidant/reductant diagonal-SDS-PAGE to analyse the dynamics of the thiol–disulphide redox proteome from mitochondrial [227] and chloroplast fractions [228]. The mitochondrial analysis resulted in the identification of 18 proteins, from both the soluble and membrane fractions, among them known glutaredoxin/thioredoxin targets. In addition, comparison of the identified protein sequences with homologues from other species identified specific Cys residues that may be responsible for plant-specific redox modulations of mitochondrial proteins [227]. The analysis of the chloroplast fractions (thylakoid, luminal and RuBisCO-depleted stroma) resulted in the identification of 22 novel proteins, not previously reported as being part of the redox proteome [228].

For several years Buchanan and coworkers have investigated the central role of the regulatory disulfide protein thioredoxin (Trx) in various aspects of cereal physiology, allowing them to identify potential Trx targets [229]. They have extended such studies to dicot species, and they have analysed the redox state of seed proteins during germination in *M. truncatula* [92].

After one decade of investigating nitric oxide (NO) functions in plant physiology, it is well established that NO modulates the activity of proteins through nitrosylation and probably tyrosine nitration (reviewed in Besson-Bard et al. [230]) [229]. Lindermayr et al. (2005) reported in *Arabidopsis* the first study and catalogue of nitrosylated proteins in plants, using the "biotin switch" combined with LC-MS, and this paper was singled out as "high impact" in Plant Physiology Journal. Using this approach, Romero-Puertas et al. [231] analysed changes in S-nitrosylated proteins in *Arabidopsis* during the hypersensitive disease resistance response. This analysis identified 16 proteins belonging to different functional categories such as metabolic enzymes, signalling and antioxidant defence. We have used biotin switch-affinity chromatography but we have coupled it to a nano-HPLC-LTQ mass spectrometer to identify protein targets of S-nitrosylation in both *Arabidopsis* leaves and cell suspension cultures during compatible and incompatible interaction with the bacteria *Pseudomonas syringae*. This analysis resulted in the identification of nearly 200 candidate proteins, some of which had already been described in *Arabidopsis* and in animal systems in the context of redox regulation. Among the proteins identified, we found some involved in defence and stress-related responses, redox-related proteins, cytoskeleton proteins, metabolic enzymes and signalling/regulating proteins (Maldonado et al., unpublished).

The experimental evidence for protein functional regulation and the identification of the residues involved are critical to understanding the molecular mechanisms by which NO exerts its action. This should be approached in a step-by-step manner [231,232]. For example, the molecular mechanism for S-nitrosylation of peroxiredoxin II was investigated using biochemical and reverse genetics, revealing a novel regulatory mechanism for peroxiredoxins in which NO modification inhibits the hydroperoxide-reducing peroxidase activity and the $ONOO^-$ detoxification activity of PrxII E. This system regulates the effects of its own radicals through the S-nitrosylation of crucial components of the antioxidant defence [231]. Reported studies evidenced the need for sufficiently sensitive methods for detecting and identifying low levels of S-nitrosylated proteins in complex protein mixtures in order to fully appreciate the range, extent and selectivity of this modification under both physiological and pathological conditions. However this has been limited by the lack of rapid and accurate methods for the detection of these S-nitrosylated proteins and the exact modification sites. In fact, the identification of the Cys residue involved is critical to understanding the biological significance of such modification on modulating protein function, and it will give clues into NO signal specificity. Recent papers have reviewed the methodology available for the proteomic analysis of protein S-nitrosylation, and they have described new chemical approaches to detect and purify S-nitrosothiols [222–224,233]. These advances have been developed in other biological systems, and we hope it is only a matter of time before they can be used in plants. For example, Han and Chen [223] describe an improvement in the classical biotin switch method using a urea-based, detergent-free protocol combined with LC-MS/MS that allows simultaneous identification of S-nitrosylated sites and their cognate proteins in S-nitrosoglutathione(GSNO)-treated HeLa cell extracts. This considerably reduces the amount of starting material needed. The use of extracted ion chromatography (XIC) enables quantitative comparison of S-nitrosylation levels between control and treated samples [223]. Camerini et al. [222] reported the "His-tag switch", a novel strategy for the purification and identification of S-nitrosylated proteins that has the added advantage that it identifies the cysteine residues undergoing S-nitrosylation. Pursuing the same objective, Han et al. [233] developed the "AMCA switch method" that involves labelling the S-nitrosylated cysteines with the fluorophore 7-amino-4-methylcoumarin-3-acetic acid (AMCA). This label allows in-gel detection of S-nitrosylated proteins after UV exposure, and identification of modified residues by liquid chromatography-tandem mass spectrometry (LC-MS/MS) using the AMCA tag signal in the MS spectra.

Even though S-glutathionylation, the reversible formation of mixed disulfides between glutathione and cysteinyl residues, constitutes an important redox-mechanism for dynamic, posttranslational regulation of a broad range of proteins, no high-throughput analysis of this modification has appeared during the review period. Dalle-Donne et al. have summarised the current knowledge on S-glutathionylation, providing a list of S-glutathionylated proteins in both animal and plant systems, as well as the proteomic and analytical methods available for its study [234]. We are using a similar approach to that used for S-nitrosothiols to identify proteins that can be glutathionylated in *Arabidopsis* leaves, using the biotin moiety GSSG-biotin to tag the proteins followed by streptavidin-agarose capture.

Proteomic technology has led to an understanding of how key enzymes are regulated at the molecular level and has

allowed the assignment of novel additional functions to well-known enzymes. A good example is the glycolytic enzyme glyceraldehyde 3-P dehydrogenase (GAPDH). The presence of two critical Cys residues in the active site of the enzyme makes it susceptible to reversible modulation by glutathionylation and nitrosylation. Combining MS analysis and analyses of mutant and GFP-recombinant proteins, Holtgrefe et al. [235] reported the occurrence of such modifications in purified GADPH, its translocation to the nucleus and its DNA-binding properties. Based on the data obtained the authors suggest that this enzyme is part of the system that protects the cell against ROS and RNS.

7.4. *Other PTMs*

Most of the other PTMs have yet to be studied so far, despite the existence of well-established protocols [236,237]. The study of ubiquitination has emerged as one of the most active areas in proteomic research. The development of a GST-tagged approach for affinity purification of ubiquitinated proteins has allowed the large-scale analysis of the ubiquitinated proteome in *Arabidopsis* cell suspension culture and its identification using MudPIT technology. In all, 294 proteins have been identified, and 85 ubiquitinated lysine residues have been confirmed in 56 proteins [88]. This will mean a significant advance in understanding the role of ubiquitination in the functional regulation and degradation of many classes of proteins. A variety of mass spectrometric methods has been described for the identification of ubiquitination sites and of ubiquitin substrates, although they still have not been tested on plant systems [238–240].

Minic et al. [89] reported a global view of *Arabidopsis* cell wall N-glycosylated proteins by combining affinity chromatography on Concanavalin A Sepharose, 2-DE and nanoHPLC/MS/MS and MALDI-TOF/MS. These analyses resulted in the identification of 102 glycoproteins and, interestingly, *in silico* predictions that they localise to the secretory pathway.

Casati et al. [90] have studied changes in the maize nuclear proteome induced by UV using genotypes with a different UV tolerance. Differential accumulation of chromatin proteins, particularly histones, constituted the largest class identified among the responsive proteins. UV-B-tolerant lines showed a greater acetylation on the N-terminal tails of histones H3 and H4 after irradiation. These acetylated histones are enriched in the promoter and transcribed regions of the two UV-B-upregulated genes examined.

Most proteins in all organisms undergo crucial N-terminal modifications involving N-terminal methionine excision, N-α-acetylation, N-myristoylation, or S-palmitoylation. The occurrence of these poorly annotated modifications has been investigated in *Arabidopsis*. In the past, experimental data for the N-terminal sequences of animal, fungi, and archaeal proteins were used to build predictive tools, and *in vitro* N-myristoylation was performed using both plant and animal N-myristoyltransferases. N-terminal modifications from the sequenced genome of *Arabidopsis* were determined by MS, resulting in the identification of 105 new modified protein N-termini. Proteins that had undergone both N-terminal methionine (Met) cleavage and N-acetylation were found to be strongly overrepresented among the most abundant proteins, in contrast to those retaining their original, unblocked Met [241].

Since all PTMs regulate signalling events, data for each of these studies, whether phosphoproteomic, redox proteomic, or others, should be integrated in order to achieve a comprehensive view of systems biology that makes experimentally testable predictions. Finally, protein–protein interaction screens, gene expression profiling, and mutant screens and analyses, are still necessary to validate those data unequivocally.

8. Interactomics

8.1. *The major challenge of Plant Proteomics*

A key step in the advance from genomics through functional genomics towards systems biology is the definition of protein interactions in living cells [242], which is one of the main challenges in plant research for the next few years [243]. Berggard et al. [244] and Miernyk and Thelen [245] have recently reviewed methods for studying protein interactions. Five biochemical approaches can be used for isolating and characterizing *in vitro* protein complexes: co-immunoprecipitation, blue native gel electrophoresis, *in vitro* binding assays, protein cross-linking, microarrays, and rate-zonal centrifugation. These techniques have been rarely used in plant research, with only four reports found during the past 18 months.

Analysis of thioredoxin (Trx) targets is a classic in Interactomic studies. In cereals, seed germination is accompanied by extensive changes in the redox state of seed proteins, with a conversion of oxidised proteins of dry seeds to a reduced form after imbibition; Trx appears to play a key role in this process [246]. Trx targets have been characterized in *M. truncatula* seeds [92] using two complementary gel-based approaches. Proteins were (1) labelled with a thiol-specific probe, monobromobimane (mBBr), following *in vitro* reduction by an NADP/Trx system, or (2) isolated on a mutant Trx affinity column. Altogether, 111 Trx-linked proteins were identified after 1- or 2-DE/ESI-Q-TOF. The X! TANDEM software was used to match MS/MS spectra against all plant proteins in the transcript assembly of *M. truncatula* (MtGI), all plant sequences in the NCBI database, and the common Repository of Adventitious Proteins known to occur as unavoidable contamination. Identified proteins function in major processes of the seed, including metabolism, cell structure, protein biogenesis and degradation, storage proteins, binding proteins, response to stress, signal transduction, as well as unknown processes.

Calmodulin (CaM) is one of the best-studied calcium sensors, which react by binding free Ca and initiating multiple physiological responses. Popescu et al. reported the use of protein microarrays to detect calmodulin targets [93]. *Arabidopsis* clones were generated containing 1133 ORFs fused to a tandem affinity purification (9xMYC epitope, His-6, a rhinovirus 3C protease cleavage site, and the 2× IgG binding domain of protein A). Clones were transformed into *Agrobacterium tumefaciens*, and transformants were used to infiltrate *Nicotiana benthamiana*. The 1133 proteins represented putative and known protein kinases (404), transcription factors (291), protein degradation-related proteins (113), heat-shock proteins (63), cytochrome P-450 (58), CaMs and CMs like (51), RNA-

binding proteins (35), ATP/GTP binding proteins (10), and proteins with unknown functions (108). Each protein was arrayed onto FAST slides (Schleicher & Schuell, Keene, NH), and arrays incubated with three CaMs and four CMs-like antibodies, scanned. Images were processed and analysed with Matlab, to obtain protein–protein interaction data. The array proved the existence of more than 173 novel *in vitro* binding partners. Analysis of these targets revealed remarkable divergence in the binding of many of the CaMs/CMs-like, with each protein binding to unique targets. This study demonstrates the feasibility of the array technology for characterization of the interactome.

Over 150 target proteins of five 14-3-3 isoforms have been described in barley using yeast two-hybrid screens and proteomics, with 10% of the identified genes having been previously reported [94]. Protein targets were affinity-purified using His-tagged 14-3-3 recombinant proteins, separated by SDS-PAGE, and gel slices were digested with trypsin. Peptides were subjected to nLC-ESI-MS/MS (Q-TOF) and spectral data were used to search against nrNCBI using MASCOT. Both approaches showed differences in the identified proteins: the two-hybrid and affinity purification strategies identified 132 and 30 interactors, respectively, with an overlap of only 10 proteins. More than one-third of the proteins identified in the two-hybrid system belonged to the signalling functional group, while it represented only 10% of the proteins identified using proteomics, with metabolic enzymes the most abundant (42%). Carbonic anhydrase and six enzymes of the Calvin cycle, as well as enzymes of the sucrose-glycolysis pathway, were shown to be 14-3-3 targets. A number of proteins with a well-described function in hormonal signalling were identified using the two-hybrid system, but not by affinity purification.

Abe et al. [95] reported the use of tandem affinity purification to isolate proteins that interact with rice OsG1, which is an ortholog of GIGANTEA that regulates photoperiod flowering in *Arabidopsis*. Seven proteins, including dynamin, were identified as OsGI-interacting proteins. The interaction of OsGI with dynamin was verified by co-immunoprecipitation using a myc-tagged version of OsGI.

Finally, the paper by Luthje et al. included in this issue, is one more example of the use of Proteomics to characterize protein complexes-in this case, the plant plasma membrane redox complex.

9. Proteinomics

9.1. *Proteomics is more than high throughput*

Proteomic techniques are used to characterize a specific protein or a structural or functional group of proteins. This is what we can call "Hypothesis-driven Proteomics", "Targeted Proteomics", or "Proteinomics." This type of study, in which Proteomics is merely part of a multiapproach strategy in combination with microscopy, Genomics, Transcriptomics, Metabolomics, and classical biochemical techniques, provides relevant information on protein structure and function, isoforms, organs, cells and subcellular location and trafficking, processing, signal peptides, PTMs, expression kinetics and correlation with RNA and metabolites. At the same time it is a method to validate data obtained using one specific approach. Proteomic platforms have been used to investigate specific proteins: seed storage [11,122], chlorophyllase [247], glucanase [248], α-amylases [249], vacuolar sorting receptors [250], esterase [251], xylanase-inhibitors [252], and peroxidases [253]. Such platforms have also been used to investigate processes, such as mRNA processing and degradation [254], and proteolysis [255]. The stability and degradation of mRNA have been studied in chloroplasts from light-grown and dark-adapted spinach plants using biochemical approaches, including RNA processing/degradation, UV-crosslinking, TLC and polyribonucleotide phosphorylase assays; as well as proteomic approaches [254]. Soluble protein extracts that correctly reproduced *in vitro* the differential mRNA stability observed *in vivo* were prepared from chloroplasts and separated by DEAE and Mono Q ion exchange chromatography. This purification strategy was designed to enrich proteins that bind nucleic acids, including those involved in transcription and translation. Protein fractions were subjected to SDS-PAGE and MS analysis after tryptic digestion (LC-ESI-MS/MS). Tandem mass spectra were used to search the non-redundant NCBI database using the SEQUEST algorithm and a QUALSCORE tool developed in-house. In total, 234 proteins were identified, a number of which had not previously been reported in other plastid proteome studies. The 234 proteins included proteins involved in RNA stability, such as nucleases, RNA-binding proteins, and ATP-dependent RNA helicase. They also included proteins involved in transcription and translation, and in metabolism (photosynthesis, energy, amino acid, redox). On the basis of the proteins identified and the *in vitro* characterization of the RNA degradation, the investigators proposed the existence of two different pathways that determine the fate of mRNA: a processing and stabilisation pathway and a degradation pathway. Shifting light-grown spinach plants to darkness for 48 h induces the mRNA degradation pathway, which is inactive or less active under normal light conditions [254].

10. Concluding remarks

In the current scientific scenery Proteomics must be understood as part of a multidisciplinary approach. A combination of high throughput -omics, and classical biochemical and cellular biology techniques should be used for data validation and to deepen in the knowledge of living organisms.

Despite the continuous development and improvement of powerful proteomic techniques, protocols, equipments and bioinformatic tools, just a minimal fraction of the cell proteome, and for only a few organisms, has been characterized so far. This is mainly related to the enormous diversity and complexity of proteomes, and to technical limitations in quantitation, sensitivity, resolution, speed of data capture and analysis. Some recalcitrant proteomes, for example membrane proteins or other highly hydrophobic proteins, remain elusive. Nevertheless, some questions are starting to be answered, including the potential number of protein species per gene as a result of Postranscriptional and Posttranslational Modifications, protein trafficking and interactions events.

Exploiting the full potential of Proteomics surpasses the possibilities of individual laboratories and any "Green

Proteome Initiative" will require large-scale transnational collaborations. In this respect, the Proteomics Subcommittee of the Multinational *Arabidopsis* Steering Committee has begun to operate in an attempt to coordinate International Proteomics Research in *Arabidopsis*.

After nearly 10 years of Proteomics research, looking back at previous publications it is possible to identify errors derived from incorrect experimental design, data analysis and interpretation. In addition to that, proteomic data should be validated in order to go beyond description or speculation. It is not uncommon to find in the literature low-confidence protein identification (especially in the case of unsequenced organisms, one of the main challenges of Proteomics), and inappropriate statistical analyses of the results. At this respect HUPO's Proteomic Standard Initiative has developed the MIAPE documents. The establishment of repositories containing MS/MS reference spectra will be very useful and will contribute to facilitate protein identification and quantification via a genome-independent approach, especially in the case of orphan species.

The use of Proteomics in plant biology research has increased significantly in the period from 2007 to September 2008 (380 reports at the ISI Web of Knowledge), becoming a routine methodology in a number of plant laboratories worldwide. During this period, both qualitative and quantitative improvements in Plant Proteomics have occurred, ushering in a new phase, namely "Second-Generation Plant Proteomics", in which quantitative and gel-free, proteomic techniques have started to be used. However, following the general rule for plant biology research, progress in Plant Proteomics continues to lag behind that of Human and Yeast Proteomics. During the revised period there have not been large differences with respect to the previously revised ones concerning the plant species under investigation, being *Arabidopsis* and rice the subject of 75% of the original papers published.

In the present update, a total of 152 original papers have been reviewed, distributed in the following areas: Descriptive Proteomics (13), Subcellular Proteomic (11), Differential Expression Proteomics of developmental processes (18), responses to biotic (19) and abiotic stresses (31), hormones (6), plant genotypes or populations, (14), PTMs- phosphoproteome (9), -redox proteome (5), -ubiquitination (1), -glycosylation (1), -acetylation (1), -N-terminal modification, and protein sorting (1), Interactomics (5). The last two areas constitute the main challenge of Plant Proteomics in the near future. Plant Proteomics is beginning to make some practical contributions to applied fields including biomedicine, through the identification and characterization of allergens agronomy, through studies of the equivalence of transgenic crops, genotyping, studies of heterosis and food science and through studies of food quality control and traceability.

Acknowledgements

Thanks to the Spanish "Ministerio de Ciencia e Innovacion" (Project BIO-2006-14790), a la "Junta de Andalucía" y "Universidad de Córdoba" for financial support.

REFERENCES

[1] Jorrin JV, Maldonado AM, Castillejo MA. Plant proteome analysis: a 2006 update. Proteomics 2007;7:2947–62.
[2] Rossignol M, Peltier JB, Mock HP, Matros A, Maldonado AM, Jorrin JV. Plant proteome analysis: a 2004–2006 update. Proteomics 2006;6:5529–48.
[3] Canovas FM, Dumas-Gaudot E, Recorbet G, Jorrin J, Mock HP, Rossignol M. Plant proteome analysis. Proteomics 2004;4:285–98.
[4] Bruggeman FJ, Westerhoff HV. The nature of systems biology. Trends Microbiol 2007;15:45–50.
[5] Weckwerth W. Integration of metabolomics and proteomics in molecular plant physiology—coping with the complexity by data-dimensionality reduction. Physiol Plant 2008;132:176–89.
[6] Paiva JA, Garces M, Alves A, Garnier-Gere P, Rodrigues JC, Lalanne C, et al. Molecular and phenotypic profiling from the base to the crown in maritime pine wood-forming tissue. New Phytol 2008;178:283–301.
[7] Jaquinod M, Villiers F, Kieffer-Jaquinod S, Hugouvieux V, Bruley C, Garin J, et al. A Proteomics dissection of *Arabidopsis thaliana* vacuoles isolated from cell culture. Mol Cell Proteomics 2007;6:394–412.
[8] Lu P, Vogel C, Wang R, Yao X, Marcotte EM. Absolute protein expression profiling estimates the relative contributions of transcriptional and translational regulation. Nat Biotechnol 2007;25:117–24.
[9] Nie L, Wu G, Culley DE, Scholten JC, Zhang W. Integrative analysis of transcriptomic and proteomic data: challenges, solutions and applications. Crit Rev Biotechnol 2007;27:63–75.
[10] Joosen R, Cordewener J, Supena ED, Vorst O, Lammers M, Maliepaard C, et al. Combined transcriptome and proteome analysis identifies pathways and markers associated with the establishment of rapeseed microspore-derived embryo development. Plant Physiol 2007;144:155–72.
[11] Li Q, Wang BC, Xu Y, Zhu YX. Systematic studies of 12S seed storage protein accumulation and degradation patterns during *Arabidopsis* seed maturation and early seedling germination stages. J Biochem Mol Biol 2007;40:373–81.
[12] Cravatt BF, Simon GM, Yates III JR. The biological impact of mass-spectrometry-based proteomics. Nature 2007;450:991–1000.
[13] Carpentier SC, Panis B, Vertommen A, Swennen R, Sergeant K, Renaut J, et al. Proteome analysis of non-model plants: a challenging but powerful approach. Mass Spectrom Rev 2008;27:354–77.
[14] Han X, Jin M, Breuker K, McLafferty FW. Extending top-down mass spectrometry to proteins with masses greater than 200 kilodaltons. Science 2006;314:109–12.
[15] Cox J, Mann M. Is proteomics the new genomics? Cell 2007;130:395–8.
[16] Kim E, Magen A, Ast G. Different levels of alternative splicing among eukaryotes. Nucl Acids Res 2007;35:125–31.
[17] Witze ES, Old WM, Resing KA, Ahn NG. Mapping protein post-translational modifications with mass spectrometry. Nat Methods 2007;4:798–806.
[18] Barbazuk WB, Fu Y, McGinnis KM. Genome-wide analyses of alternative splicing in plants: opportunities and challenges. Genome Res 2008;18:1381–92.
[19] Simpson CG, Lewandowska D, Fuller J, Maronova M, Kalyna M, Davidson D, et al. Alternative splicing in plants. Biochem Soc Trans 2008;036:508–10.
[20] Palusa SG, Ali GS, Reddy ASN. Alternative splicing of pre-mRNAs of *Arabidopsis* serine/arginine-rich proteins:

regulation by hormones and stresses. Plant J 2007;49:1091–107.
[21] Thatcher LF, Carrie C, Andersson CR, Sivasithamparam K, Whelan J, Singh KB. Differential gene expression and subcellular targeting of *Arabidopsis* glutathione S-transferase F8 is achieved through alternative transcription start sites. J Biol Chem 2007;282:28915–28.
[22] Dinkins RD, Majee SM, Nayak NR, Martin D, Xu Q, Belcastro MP, et al. Changing transcriptional initiation sites and alternative 5- and 3-splice site selection of the first intron deploys *Arabidopsis* protein isoaspartyl methyltransferase2 variants to different subcellular compartments. Plant J 2008;55:1–13.
[23] Sun Q, Zybailov B, Majeran W, Friso G, Olinares PD, van Wijk KJ. PPDB, the database at Cornell. Nucleic Acids Res 2009;37: D969–74.
[24] Mano S, Miwa T, Nishikawa S, Mimura T, Nishimura M. The plant organelles database (PODB): a collection of visualized plant organelles and protocols for plant organelle research. Nucleic Acids Res 2008;36:D929–937.
[25] Dowsey AW, Guang-Zhong Y. The future of large-scale collaborative Proteomics. Proc IEEE 2008;96:1292–309.
[26] Brunner E, Ahrens CH, Mohanty S, Baetschmann H, Loevenich S, Potthast F, et al. A high-quality catalog of the *Drosophila melanogaster* proteome. Nat Biotechnol 2007;25:576–83.
[27] Weckwerth W, Baginsky S, van Wijk K, Heazlewood JL, Millar H. The multinational *Arabidopsis* steering subcommittee for Proteomics assembles the largest proteome database resource for plant systems biology. J Proteome Res 2008;7:4209–10.
[28] Hummel J, Niemann M, Wienkoop S, Schulze W, Steinhauser D, Selbig J, et al. ProMEX: a mass spectral reference database for proteins and protein phosphorylation sites. BMC Bioinformatics 2007;8:216.
[29] Bini L, Pallini V, Hochstrasser DF, Sanchez J-C. From genome to proteome: back to the future. Proteomics 2007;7:1561–3.
[30] Nesvizhskii AI, Vitek O, Aebersold R. Analysis and validation of proteomic data generated by tandem mass spectrometry. Nat Methods 2007;4:787–97.
[31] Taylor CF, Paton NW, Lilley KS, Binz PA, Julian Jr RK, Jones AR, et al. The minimum information about a proteomics experiment (MIAPE). Nat Biotechnol 2007;25:887–93.
[32] Mead JA, Shadforth IP, Bessant C. Public proteomic MS repositories and pipelines: available tools and biological applications. Proteomics 2007;7:2769–86.
[33] Deutsch EW, Lam H, Aebersold R. PeptideAtlas: a resource for target selection for emerging targeted proteomics workflows. EMBO Rep 2008;9:429–34.
[34] Lam H, Deutsch EW, Eddes JS, Eng JK, Stein SE, Aebersold R. Building consensus spectral libraries for peptide identification in proteomics. Nat Methods 2008;5:873–5.
[35] Falth M, Savitski MM, Nielsen ML, Kjeldsen F, Andren PE, Zubarev RA. SwedCAD, a database of annotated high-mass accuracy MS/MS spectra of tryptic peptides. J Proteome Res 2007;6:4063–7.
[36] Heazlewood JL, Durek P, Hummel J, Selbig J, Weckwerth W, Walther D, et al. PhosPhAt: a database of phosphorylation sites in *Arabidopsis thaliana* and a plant-specific phosphorylation site predictor. Nucleic Acids Res 2008;36:D1015–1021.
[37] Baerenfaller K, Grossmann J, Grobei MA, Hull R, Hirsch-Hoffmann M, Yalovsky S, et al. Genome-scale proteomics reveals *Arabidopsis thaliana* gene models and proteome dynamics. Science 2008;320:938–41.
[38] Dunkley TPJ, Hester S, Shadforth IP, Runions J, Weimar T, Hanton SL, Griffin JL, Bessant C, Brandizzi F, Hawes C, Watson RB, Dupree P and Lilley KS. Mapping the *Arabidopsis* organelle proteome. Proc Natl Acad Sci USA 2006;103:6518-6523.
[39] Heazlewood JL, Verboom RE, Tonti-Filippini J, Small I, Millar AH. SUBA: the *Arabidopsis* Subcellular Database. Nucleic Acids Res 2007;35:D213–218.
[40] Zybailov B, Rutschow H, Friso G, Rudella A, Emanuelsson O, Sun Q, et al. Sorting signals, N-terminal modifications and abundance of the chloroplast proteome. PLoS ONE 2008;3: e1994.
[41] Lunn JE. Compartmentation in plant metabolism. J Exp Bot 2007;58:35–47.
[42] Jarvis P. Targeting of nucleus-encoded proteins to chloroplasts in plants. New Phytol 2008;179:257–85.
[43] Millar AH, Whelan J, Small I. Recent surprises in protein targeting to mitochondria and plastids. Curr Opin Plant Biol 2006;9:610–5.
[44] Gonzalez-Buitrago JM, Ferreira L, Isidoro-Garcia M, Sanz C, Lorente F, Davila I. Proteomic approaches for identifying new allergens and diagnosing allergic diseases. Clin Chim Acta 2007;385:21–7.
[45] Salekdeh GH, Komatsu S. Crop proteomics: aim at sustainable agriculture of tomorrow. Proteomics 2007;7:2976–96.
[46] Alm R, Ekefjard A, Krogh M, Hakkinen J, Emanuelsson C. Proteomic variation is as large within as between strawberry varieties. J Proteome Res 2007;6:3011–20.
[47] Hajduch M, Casteel JE, Tang S, Hearne LB, Knapp S, Thelen JJ. Proteomic analysis of near-isogenic sunflower varieties differing in seed oil traits. J Proteome Res 2007;6:3232–41.
[48] Hoecker N, Lamkemeyer T, Sarholz B, Paschold A, Fladerer C, Madlung J, et al. Analysis of nonadditive protein accumulation in young primary roots of a maize (*Zea mays* L.) F(1)-hybrid compared to its parental inbred lines. Proteomics 2008;8:3882–94.
[49] Saz JM, Marina ML. High performance liquid chromatography and capillary electrophoresis in the analysis of soybean proteins and peptides in foodstuffs. J Sep Sci 2007;30:431–51.
[50] Sotkovsky P, Hubalek M, Hernychova L, Novak P, Havranova M, Setinova I, et al. Proteomic analysis of wheat proteins recognized by IgE antibodies of allergic patients. Proteomics 2008;8:1677–91.
[51] Petersen A, Dresselhaus T, Grobe K, Becker WM. Proteome analysis of maize pollen for allergy-relevant components. Proteomics 2006;6:6317–25.
[52] Napoli A, Aiello D, Di Donna L, Moschidis P, Sindona G. Vegetable proteomics: the detection of Ole e 1 isoallergens by peptide matching of MALDI MS/MS spectra of underivatized and dansylated glycopeptides. J Proteome Res 2008;7:2723–32.
[53] Scossa F, Laudencia-Chingcuanco D, Anderson OD, Vensel WH, Lafiandra D, D'Ovidio R, et al. Comparative proteomic and transcriptional profiling of a bread wheat cultivar and its derived transgenic line overexpressing a low molecular weight glutenin subunit gene in the endosperm. Proteomics 2008;8:2948–66.
[54] Zolla L, Rinalducci S, Antonioli P, Righetti PG. Proteomics as a complementary tool for identifying unintended side effects occurring in transgenic maize seeds as a result of genetic modifications. J Proteome Res 2008;7:1850–61.
[55] Sauvage FX, Pradal M, Chatelet P, Tesniere C. Proteome changes in leaves from grapevine (*Vitis vinifera* L.) transformed for alcohol dehydrogenase activity. J Agric Food Chem 2007;55:2597–603.
[56] Prins A, van Heerden PD, Olmos E, Kunert KJ, Foyer CH. Cysteine proteinases regulate chloroplast protein content and composition in tobacco leaves: a model for dynamic interactions with ribulose-1,5-bisphosphate carboxylase/

oxygenase (Rubisco) vesicular bodies. J Exp Bot 2008;59:1935–50.
[57] Devouge V, Rogniaux H, Nesi N, Tessier D, Gueguen J, Larre C. Differential proteomic analysis of four near-isogenic *Brassica napus* varieties bred for their erucic acid and glucosinolate contents. J Proteome Res 2007;6:1342–53.
[58] Vincent D, Ergul A, Bohlman MC, Tattersall EA, Tillett RL, Wheatley MD, et al. Proteomic analysis reveals differences between *Vitis vinifera* L. cv. Chardonnay and cv. Cabernet Sauvignon and their responses to water deficit and salinity. J Exp Bot 2007;58:1873–92.
[59] Eivazi, Naghavi, Hajheidari, Pirseyedi, Ghaffari, Mohammadi, et al. Assessing wheat (*Triticum aestivum* L.) genetic diversity using quality traits, amplified fragment length polymorphisms, simple sequence repeats and proteome analysis. Ann Appl Biol 2008;152:81–91.
[60] Agrawal GK, Rakwal R. Technologies, strategies, and applications. New Jersey: John Wiley & Sons Inc.; 2008.
[61] Samaj J, Thelen JJ. Plant Proteomics. Germany: Springer-Verlag; 2007.
[62] Agrawal GK, Jwa N-S and Rakwal R. Rice Proteomics: ending phase I and the beginning of phase II. Proteomics 2009;9:935–63.
[63] Farrokhi N, Whitelegge JP, Brusslan JA. Plant peptides and peptidomics. Plant Biotechnol J 2008;6:105–34.
[64] The grapevine genome sequence suggests ancestral hexaploidization in major angiosperm phyla. Nature 2007;449:463–7.
[65] Tuskan GA, DiFazio S, Jansson S, Bohlmann J, Grigoriev I, Hellsten U. The genome of black cottonwood, *Populus trichocarpa* (Torr. & Gray). Science 2006;313:1596–604.
[66] Rensing SA, Lang D, Zimmer AD, Terry A, Salamov A, Lucas S, et al. The physcomitrella genome reveals evolutionary insights into the conquest of land by plants. Science 2008;319:64–9.
[67] Wang X, Yang P, Gao Q, Liu X, Kuang T, Shen S, et al. Proteomic analysis of the response to high-salinity stress in *Physcomitrella patens*. Planta 2008;228:167–77.
[68] Gazanchian A, Hajheidari M, Sima NK, Salekdeh GH. Proteome response of *Elymus elongatum* to severe water stress and recovery. J Exp Bot 2007;58:291–300.
[69] Brownfield L, Ford K, Doblin MS, Newbigin E, Read S, Bacic A. Proteomic and biochemical evidence links the callose synthase in *Nicotiana alata* pollen tubes to the product of the NaGSL1 gene. Plant J 2007;52:147–56.
[70] Jiang G, Wang Z, Shang H, Yang W, Hu Z, Phillips J, et al. Proteome analysis of leaves from the resurrection plant *Boea hygrometrica* in response to dehydration and rehydration. Planta 2007;225:1405–20.
[71] Ingle RA, Schmidt UG, Farrant JM, Thomson JA, Mundree SG. Proteomic analysis of leaf proteins during dehydration of the resurrection plant *Xerophyta viscosa*. Plant Cell Environ 2007;30:435–46.
[72] Vyetrogon K, Tebbji F, Olson DJ, Ross AR, Matton DP. A comparative proteome and phosphoproteome analysis of differentially regulated proteins during fertilization in the self-incompatible species *Solanum chacoense* Bitt. Proteomics 2007;7:232–47.
[73] Yoshimura K, Masuda A, Kuwano M, Yokota A, Akashi K. Programmed proteome response for drought avoidance/tolerance in the root of a C3 xerophyte (wild watermelon) under water deficits. Plant Cell Physiol 2008;49:226–41.
[74] Lliso I, Tadeo FR, Phinney BS, Wilkerson CG, Talón M. Protein changes in the albedo of citrus fruits on postharvesting storage. J Agric Food Chem 2007;55:9047–53.
[75] Wang D, Eyles A, Mandich D, Bonello P. Systemic aspects of host–pathogen interactions in Austrian pine (*Pinus nigra*): a Proteomics approach. Physiol Mol Plant Pathol 2006;68:149–57.
[76] Fiorani Celedon PA, de Andrade A, Meireles KG, Gallo de Carvalho MC, Caldas DG, Moon DH, et al. Proteomic analysis of the cambial region in juvenile *Eucalyptus grandis* at three ages. Proteomics 2007;7:2258–74.
[77] Lippert D, Chowrira S, Ralph SG, Zhuang J, Aeschliman D, Ritland C, et al. Conifer defense against insects: proteome analysis of Sitka spruce (*Picea sitchensis*) bark induced by mechanical wounding or feeding by white pine weevils (*Pissodes strobi*). Proteomics 2007;7:248–70.
[78] Valledor L, Castillejo MA, Lenz C, Rodríguez R, Cañal MJ, Jorrín J. Proteomic analysis of *Pinus radiata* needles: 2-DE map and protein identification by LC/MS/MS and substitution-tolerant database searching. J Proteome Res 2008;7:2616–31.
[79] Pedreschi R, Vanstreels E, Carpentier S, Hertog M, Lammertyn J, Robben J, et al. Proteomic analysis of core breakdown disorder in conference pears (*Pyrus communis* L.). Proteomics 2007;7:2083–99.
[80] de Jong F, Mathesius U, Imin N, Rolfe BG. A proteome study of the proliferation of cultured *Medicago truncatula* protoplasts. Proteomics 2007;7:722–36.
[81] Dai S, Chen T, Chong K, Xue Y, Liu S, Wang T. Proteomics identification of differentially expressed proteins associated with pollen germination and tube growth reveals characteristics of germinated *Oryza sativa* pollen. Mol Cell Proteomics 2007;6:207–30.
[82] Houterman PM, Speijer D, Dekker HL, De Koster CG, Cornelissen BJC, Rep M. The mixed xylem sap proteome of *Fusarium oxysporum*-infected tomato plants. Mol Plant Pathol 2007;8:215–21.
[83] Gutstein HB, Morris JS. Laser capture sampling and analytical issues in Proteomics. Expert Rev Proteomics 2007;4:627–37.
[84] Dembinsky D, Woll K, Saleem M, Liu Y, Fu Y, Borsuk LA, et al. Transcriptomic and proteomic analyses of pericycle cells of the maize primary root. Plant Physiol 2007;145:575–88.
[85] Sigal A, Milo R, Cohen A, geva-Zatorsky N, Klein Y, Liron Y, et al. Variability and memory of protein levels in human cells. Nature 2006;444:643–5.
[86] Foss EJ, Radulovic D, Shaffer SA, Ruderfer DM, Bedalov AM, Goodlett DR, et al. Genetic basis of protein variation in yeast. Nat Genetics 2007;39:1369–75.
[87] Jorge I, Navarro RM, Lenz C, Ariza D, Porras C, Jorrin J. The holm oak leaf proteome: analytical and biological variability in the protein expression level assessed by 2-DE and protein identification tandem mass spectrometry de novo sequencing and sequence similarity searching. Proteomics 2005;5:222–34.
[88] Maor R, Jones A, Nuhse TS, Studholme DJ, Peck SC, Shirasu K. Multidimensional protein identification technology (MudPIT) analysis of ubiquitinated proteins in plants. Mol Cell Proteomics 2007;6:601–10.
[89] Minic Z, Jamet E, Negroni L, Arsene der Garabedian P, Zivy M, Jouanin L. A sub-proteome of *Arabidopsis thaliana* mature stems trapped on Concanavalin A is enriched in cell wall glycoside hydrolases. J Exp Bot 2007;58:2503–12.
[90] Casati P, Campi M, Chu F, Suzuki N, Maltby D, Guan S, et al. Histone acetylation and chromatin remodeling are required for UV-B-dependent transcriptional activation of regulated genes in maize. Plant Cell 2008;20:827–42.
[91] Rutschow H, Ytterberg AJ, Friso G, Nilsson R, van Wijk KJ. Quantitative proteomics of a chloroplast SRP54 sorting

mutant and its genetic interactions with CLPC1 in *Arabidopsis*. Plant Physiol 2008;148:156–75.
[92] Alkhalfioui F, Renard M, Vensel WH, Wong J, Tanaka CK, Hurkman WJ, et al. Thioredoxin-linked proteins are reduced during germination of *Medicago truncatula* seeds. Plant Physiol 2007;144:1559–79.
[93] Popescu SC, Popescu GV, Bachan S, Zhang Z, Seay M, Gerstein M, et al. Differential binding of calmodulin-related proteins to their targets revealed through high-density *Arabidopsis* protein microarrays. Proc Natl Acad Sci USA 2007;104:4730–5.
[94] Schoonheim PJ, Veiga H, Pereira Dda C, Friso G, van Wijk KJ, de Boer AH. A comprehensive analysis of the 14-3-3 interactome in barley leaves using a complementary proteomics and two-hybrid approach. Plant Physiol 2007;143:670–83.
[95] Abe M, Fujiwara M, Kurotani K, Yokoi S, Shimamoto K. Identification of dynamin as an interactor of rice GIGANTEA by tandem affinity purification (TAP). Plant Cell Physiol 2008;49:420–32.
[96] Galetskiy D, Susnea I, Reiser V, Adamska I, Przybylski M. Structure and dynamics of photosystem II light-harvesting complex revealed by high-resolution FTICR mass spectrometric proteome analysis. J Am Soc Mass Spectrom 2008;19:1004–13.
[97] Eriksson J, Fenyo D. Improving the success rate of proteome analysis by modeling protein-abundance distributions and experimental designs. Nat Biotechnol 2007;25:651–5.
[98] Isaacson T, Damasceno CM, Saravanan RS, He Y, Catala C, Saladie M, et al. Sample extraction techniques for enhanced proteomic analysis of plant tissues. Nat Protoc 2006;1:769–74.
[99] Maldonado AM, Echevarria-Zomeno S, Jean-Baptiste S, Hernandez M, Jorrin-Novo JV. Evaluation of three different protocols of protein extraction for *Arabidopsis thaliana* leaf proteome analysis by two-dimensional electrophoresis. J Proteomics 2008;71:461–72.
[100] Zheng Q, Song J, Doncaster K, Rowland E, Byers DM. Qualitative and quantitative evaluation of protein extraction protocols for apple and strawberry fruit suitable for two-dimensional electrophoresis and mass spectrometry analysis. J Agric Food Chem 2007;55:1663–73.
[101] Canas B, Pineiro C, Calvo E, Lopez-Ferrer D, Gallardo JM. Trends in sample preparation for classical and second generation proteomics. J Chromatogr A 2007;1153:235–58.
[102] Sarma AD, Oehrle NW, Emerich DW. Plant protein isolation and stabilization for enhanced resolution of two-dimensional polyacrylamide gel electrophoresis. Anal Biochem 2008;379:192–5.
[103] Wang W, Tai F, Chen S. Optimizing protein extraction from plant tissues for enhanced proteomics analysis. J Sep Sci 2008;31:2032–9.
[104] Pirovani CP, Carvalho HA, Machado RC, Gomes DS, Alvim FC, Pomella AW, et al. Protein extraction for proteome analysis from cacao leaves and meristems, organs infected by *Moniliophthora perniciosa*, the causal agent of the witches' broom disease. Electrophoresis 2008;29:2391–401.
[105] Toorchi M, Nouri M-Z, Tsumura M, Komatsu S. Acoustic technology for high-performance disruption and extraction of plant proteins. J Proteome Res 2008;7:3035–41.
[106] Kao SH, Wong HK, Chiang CY, Chen HM. Evaluating the compatibility of three colorimetric protein assays for two-dimensional electrophoresis experiments. Proteomics 2008;8:2178–84.
[107] Jiang X, Ye M, Zou H. Technologies and methods for sample pretreatment in efficient proteome and peptidome analysis. Proteomics 2008;8:686–705.
[108] Cellar NA, Kuppannan K, Langhorst ML, Ni W, Xu P, Young SA. Cross species applicability of abundant protein depletion columns for ribulose-1,5-bisphosphate carboxylase/oxygenase. J Chromatogr B Analyt Technol Biomed Life Sci 2008;861:29–39.
[109] Lee DG, Ahsan N, Lee SH, Kang KY, Lee JJ, Lee BH. An approach to identify cold-induced low-abundant proteins in rice leaf. C R Biol 2007;330:215–25.
[110] Hashimoto M, Komatsu S. Proteomic analysis of rice seedlings during cold stress. Proteomics 2007;7:1293–302.
[111] Righetti PG, Boschetti E. Sherlock Holmes and the proteome—a detective story. FEBS J 2007;274:897–905.
[112] Supek F, Peharec P, Krsnik-Rasol M, Smuc T. Enhanced analytical power of SDS-PAGE using machine learning algorithms. Proteomics 2008;8:28–31.
[113] de Godoy LM, Olsen JV, de Souza GA, Li G, Mortensen P, Mann M. Status of complete proteome analysis by mass spectrometry: SILAC labeled yeast as a model system. Genome Biol 2006;7:R50.
[114] Tribl F, Lohaus C, Dombert T, Langenfeld E, Piechura H, Warscheid B, et al. Towards multidimensional liquid chromatography separation of proteins using fluorescence and isotope-coded protein labelling for quantitative proteomics. Proteomics 2008;8:1204–11.
[115] Lengqvist J, Uhlen K, Lehtio J. iTRAQ compatibility of peptide immobilized pH gradient isoelectric focusing. Proteomics 2007;7:1746–52.
[116] Braun RJ, Kinkl N, Beer M, Ueffing M. Two-dimensional electrophoresis of membrane proteins. Anal Bioanal Chem 2007;389:1033–45.
[117] van den Broeck HC, America AH, Smulders MJ, Gilissen LJ, van der Meer IM. Staining efficiency of specific proteins depends on the staining method: wheat gluten proteins. Proteomics 2008;8:1880–4.
[118] Witzel K, Surabhi GK, Jyothsnakumari G, Sudhakar C, Matros A, Mock HP. Quantitative proteome analysis of barley seeds using ruthenium(II)-tris-(bathophenanthroline-disulphonate) staining. J Proteome Res 2007;6:1325–33.
[119] Harris LR, Churchward MA, Butt RH, Coorssen JR. Assessing detection methods for gel-based proteomic analyses. J Proteome Res 2007;6:1418–25.
[120] Wang X, Li X, Li Y. A modified Coomassie Brilliant Blue staining method at nanogram sensitivity compatible with proteomic analysis. Biotechnol Lett 2007;29:1599–603.
[121] Chakravarti B, Ratanaprayul W, Dalal N, Chakravarti DN. Comparison of SYPRO Ruby and Deep Purple using commonly available UV transilluminator: wide-scale application in proteomic research. J Proteome Res 2008;7:2797–802.
[122] Jacobsen S, Grove H, Jensen KN, Sorensen HA, Jessen F, Hollung K, et al. Multivariate analysis of 2-DE protein patterns—practical approaches. Electrophoresis 2007;28:1289–99.
[123] Berth M, Moser FM, Kolbe M, Bernhardt J. The state of the art in the analysis of two-dimensional gel electrophoresis images. Appl Microbiol Biotechnol 2007;76:1223–43.
[124] Daszykowski M, Stanimirova I, Bodzon-Kulakowska A, Silberring J, Lubec G, Walczak B. Start-to-end processing of two-dimensional gel electrophoretic images. J Chromatogr A 2007;1158:306–17.
[125] Maurer MH. Software analysis of two-dimensional electrophoretic gels in proteomic experiments. Current Bioinformatics 2006;1:255–62.
[126] Yang Y, Thannhauser TW, Li L, Zhang S. Development of an integrated approach for evaluation of 2-D gel image analysis: impact of multiple proteins in single spots on comparative proteomics in conventional 2-D gel/MALDI workflow. Electrophoresis 2007;28:2080–94.

[127] Demianova Z, Shimmo M, Poysa E, Franssila S, Baumann M. Toward an integrated microchip sized 2-D polyacrylamide slab gel electrophoresis device for proteomic analysis. Electrophoresis 2007;28:422–8.
[128] Schroder S, Zhang H, Yeung ES, Jansch L, Zabel C, Watzig H. Quantitative gel electrophoresis: sources of variation. J Proteome Res 2008;7:1226–34.
[129] Valcu CM, Valcu M. Reproducibility of two-dimensional gel electrophoresis at different replication levels. J Proteome Res 2007;6:4677–83.
[130] Jensen KN, Jessen F, Jorgensen BM. Multivariate data analysis of two-dimensional gel electrophoresis protein patterns from few samples. J Proteome Res 2008;7:1288–96.
[131] Pedreschi R, Hertog ML, Carpentier SC, Lammertyn J, Robben J, Noben JP, et al. Treatment of missing values for multivariate statistical analysis of gel-based proteomics data. Proteomics 2008;8:1371–83.
[132] Karp NA, McCormick PS, Russell MR, Lilley KS. Experimental and statistical considerations to avoid false conclusions in proteomics studies using differential in-gel electrophoresis. Mol Cell Proteomics 2007;6:1354–64.
[133] Gomez SM, Nishio JN, Faull KF, Whitelegge JP. The chloroplast grana proteome defined by intact mass measurements from liquid chromatography mass spectrometry. Mol Cell Proteomics 2002;1:46–59.
[134] Van Leene J, Stals H, Eeckhout D, Persiau G, Van De Slijke E, Van Isterdael G, et al. A tandem affinity purification-based technology platform to study the cell cycle interactome in *Arabidopsis thaliana*. Mol Cell Proteomics 2007;6:1226–38.
[135] D'Amici GM, Timperio AM, Zolla L. Coupling of native liquid phase isoelectrofocusing and blue native polyacrylamide gel electrophoresis: a potent tool for native membrane multiprotein complex separation. J Proteome Res 2008;7:1326–40.
[136] Hrebicek T, Durrschmid K, Auer N, Bayer K, Rizzi A. Effect of CyDye minimum labeling in differential gel electrophoresis on the reliability of protein identification. Electrophoresis 2007;28:1161–9.
[137] Gevaert K, Van Damme P, Ghesquiere B, Impens F, Martens L, Helsens K, et al. A la carte proteomics with an emphasis on gel-free techniques. Proteomics 2007;7:2698–718.
[138] Ye ML, Jiang XG, Feng S, Tian RJ, Zou HF. Advances in chromatographic techniques and methods in shotgun proteome analysis. Trends Analyt Chem 2007;26:80–4.
[139] Jain R, Katavic V, Agrawal GK, Guzov VM, Thelen JJ. Purification and proteomic characterization of plastids from *Brassica napus* developing embryos. Proteomics 2008;8:3397–405.
[140] Djordjevic MA, Oakes M, Li DX, Hwang CH, Hocart CH, Gresshoff PM. The glycine max xylem sap and apoplast proteome. J Proteome Res 2007;6:3771–9.
[141] Lau KW, Jones AR, Swainston N, Siepen JA, Hubbard SJ. Capture and analysis of quantitative proteomic data. Proteomics 2007;7:2787–99.
[142] Bantscheff M, Schirle M, Sweetman G, Rick J, Kuster B. Quantitative mass spectrometry in proteomics: a critical review. Anal Bioanal Chem 2007;389:1017–31.
[143] Shiio Y, Aebersold R. Quantitative proteome analysis using isotope-coded affinity tags and mass spectrometry. Nat Protoc 2006;1:139–45.
[144] Wiese S, Reidegeld KA, Meyer HE, Warscheid B. Protein labeling by iTRAQ: a new tool for quantitative mass spectrometry in proteome research. Proteomics 2007;7:340–50.
[145] Gan CS, Chong PK, Pham TK, Wright PC. Technical, experimental, and biological variations in isobaric tags for relative and absolute quantitation (iTRAQ). J Proteome Res 2007;6:821–7.
[146] Palmblad M, Mills DJ, Bindschedler LV. Heat-shock response in *Arabidopsis thaliana* explored by multiplexed quantitative proteomics using differential metabolic labeling. J Proteome Res 2008;7:780–5.
[147] Nelson CJ, Huttlin EL, Hegeman AD, Harms AC, Sussman MR. Implications of ^{15}N-metabolic labeling for automated peptide identification in *Arabidopsis thaliana*. Proteomics 2007;7:1279–92.
[148] Brautigam A, Hofmann-Benning S, Weber AP. Comparative Proteomics of chloroplast envelopes from c3 and c4 plants reveals specific adaptations of the plastid envelope to c4 photosynthesis and candidate proteins required for maintaining c4 metabolite fluxes. Plant Physiol 2008;148:568–79.
[149] Thelen JJ, Peck SC. Quantitative Proteomics in plants: choices in abundance. Plant Cell 2007;19:3339–46.
[150] America AH, Cordewener JH. Comparative LC-MS: a landscape of peaks and valleys. Proteomics 2008;8:731–49.
[151] Hebeler R, Oeljeklaus S, Reidegeld KA, Eisenacher M, Stephan C, Sitek B, et al. Study of early leaf senescence in *Arabidopsis thaliana* by quantitative proteomics using reciprocal ^{14}N/^{15}N labeling and difference gel electrophoresis. Mol Cell Proteomics 2008;7:108–20.
[152] Han X, Aslanian A, Yates III JR. Mass spectrometry for proteomics. Curr Opin Chem Biol 2008;12:483–90.
[153] Zubarev R, Mann M. On the proper use of mass accuracy in Proteomics. Mol Cell Proteomics 2007;6:377–81.
[154] Molina H, Horn DM, Tang N, Mathivanan S, Pandey A. Global proteomic profiling of phosphopeptides using electron transfer dissociation tandem mass spectrometry. Proc Natl Acad Sci USA 2007;104:2199–204.
[155] Good DM, Wirtala M, McAlister GC, Coon JJ. Performance characteristics of electron transfer dissociation mass spectrometry. Mol Cell Proteomics 2007;6:1942–51.
[156] Marshall AG, Hendrickson CL, Emmett MR, Rodgers RP, Blakney GT, Nilsson CL. Fourier transform ion cyclotron resonance: state of the art. Eur J Mass Spectrom 2007;13:57–9.
[157] Meng F, Wiener MC, Sachs JR, Burns C, Verma P, Paweletz CP, et al. Quantitative analysis of complex peptide mixtures using FTMS and differential mass spectrometry. J Am Soc Mass Spectrom 2007;18:226–33.
[158] Katz E, Fon M, Lee Y, Phinney B, Sadka A, Blumwald E. The citrus fruit proteome: insights into citrus fruit metabolism. Planta 2007;226:989–1005.
[159] Lee J, Garrett WM, Cooper B. Shotgun proteomic analysis of *Arabidopsis thaliana* leaves. J Sep Sci 2007;30:2225–30.
[160] Mulder NJ, Kersey P, Pruess M, Apweiler R. In silico characterization of proteins: UniProt, InterPro and Integr8. Mol Biotechnol 2008;38:165–77.
[161] Matthiesen R. Methods, algorithms and tools in computational Proteomics: a practical point of view. Proteomics 2007;7:2815–32.
[162] Song Z, Chen L, Ganapathy A, Wan XF, Brechenmacher L, Tao N, et al. Development and assessment of scoring functions for protein identification using PMF data. Electrophoresis 2007;28:864–70.
[163] Balgley BM, Laudeman T, Yang L, Song T, Lee CS. Comparative evaluation of tandem MS search algorithms using a target-decoy search strategy. Mol Cell Proteomics 2007;6:1599–608.
[164] Edwards NJ. Novel peptide identification from tandem mass spectra using ESTs and sequence database compression. Mol Syst Biol 2007;3:102.
[165] Higgs RE, Knierman MD, Freeman AB, Gelbert LM, Patil ST, Hale JE. Estimating the statistical significance of peptide identifications from shotgun proteomics experiments. J Proteome Res 2007;6:1758–67.
[166] Brosch M, Swamy S, Hubbard T, Choudhary J. Comparison of Mascot and X!Tandem performance for low and high

accuracy mass spectrometry and the development of an adjusted Mascot threshold. Mol Cell Proteomics 2008;7:962–70.
[167] Joo WA, Lee JB, Park M, Lee JW, Kim HJ, Kim CW. Comparison of search engine contributions in protein mass fingerprinting for protein identification. Biotechnol Bioproc E 2007;12:125–30.
[168] Waridel P, Frank A, Thomas H, Surendranath V, Sunyaev S, Pevzner P, et al. Sequence similarity-driven proteomics in organisms with unknown genomes by LC-MS/MS and automated de novo sequencing. Proteomics 2007;7:2318–29.
[169] Junqueira M, Spirin V, Balbuena TS, Thomas H, Adzhubei I, Sunyaev S, et al. Protein identification pipeline for the homology-driven proteomics. J Proteomics 2008;71:346–56.
[170] Catusse J, Strub J-M, Job C, Van Dorsselaer A, Job D. Proteome-wide characterization of sugarbeet seed vigor and its tissue specific expression. Proc Natl Acad Sci USA 2008;105:10262–7.
[171] Aki T, Shigyo M, Nakano R, Yoneyama T, Yanagisawa S. Nano scale proteomics revealed the presence of regulatory proteins including three FT-like proteins in phloem and xylem saps from rice. Plant Cell Physiol 2008;49:767–90.
[172] Espagne C, Martinez A, Valot B, Meinnel T, Giglione C. Alternative and effective proteomic analysis in *Arabidopsis*. Proteomics 2007;7:3788–99.
[173] Song X, Ni Z, Yao Y, Xie C, Li Z, Wu H, et al. Wheat (*Triticum aestivum* L.) root proteome and differentially expressed root proteins between hybrid and parents. Proteomics 2007;7:3538–57.
[174] Sheoran IS, Ross AR, Olson DJ, Sawhney VK. Proteomic analysis of tomato (*Lycopersicon esculentum*) pollen. J Exp Bot 2007;58:3525–35.
[175] Salvi D, Rolland N, Joyard J, Ferro M. Assessment of organelle purity using antibodies and specific assays: the example of the chloroplast envelope. Methods Mol Biol 2008;432:345–56.
[176] Block M, Douce R, Joyard J, Rolland N. Chloroplast envelope membranes: a dynamic interface between plastids and the cytosol. Photosynthesis Res 2007;92:225–44.
[177] Salvi D, Rolland N, Joyard J, Ferro M. Purification and proteomic analysis of chloroplasts and their sub-organellar compartments. Methods Mol Biol 2008;432:19–36.
[178] Lee CP, Eubel H, O'Toole N, Millar AH. Heterogeneity of the mitochondrial proteome for photosynthetic and non-photosynthetic *Arabidopsis* metabolism. Mol Cell Proteomics 2008;7:1297–316.
[179] Robert S, Zouhar J, Carter C, Raikhel N. Isolation of intact vacuoles from *Arabidopsis* rosette leaf-derived protoplasts. Nat Protocols 2007;2:259–62.
[180] Jamet E, Boudart G, Borderies G, Charmont S, Lafitte C, Rossignol M, et al. Isolation of plant cell wall proteins. Methods Mol Biol 2008;425:187–201.
[181] Komatsu S, Konishi H, Hashimoto M. The Proteomics of plant cell membranes. J Exp Bot 2007;58:103–12.
[182] Mitra SK, Gantt JA, Ruby JF, Clouse SD, Goshe MB. Membrane proteomic analysis of *Arabidopsis thaliana* using alternative solubilization techniques. J Proteome Res 2007;6:1933–50.
[183] Lilley KS, Dunkley TP. Determination of genuine residents of plant endomembrane organelles using isotope tagging and multivariate statistics. Methods Mol Biol 2008;432:373–87.
[184] Andersen JS, Mann M. Organellar proteomics: turning inventories into insights. EMBO Rep 2006;7:874–9.
[185] Haynes PA, Roberts TH. Subcellular shotgun proteomics in plants: looking beyond the usual suspects. Proteomics 2007;7:2963–75.
[186] Jamet E, Albenne C, Boudart G, Irshad M, Canut H, Pont-Lezica R. Recent advances in plant cell wall Proteomics. Proteomics 2008;8:893–908.
[187] Ito J, Heazlewood JL, Millar AH. The plant mitochondrial proteome and the challenge of defining the posttranslational modifications responsible for signalling and stress effects on respiratory functions. Physiol Plant 2007;129:207–24.
[188] Carroll AJ, Heazlewood JL, Ito J, Millar AH. Analysis of the *Arabidopsis* cytosolic ribosome proteome provides detailed insights into its components and their post-translational modification. Mol Cell Proteomics 2008;7:347–69.
[189] Mongrand S, Morel J, Laroche J, Claverol S, Carde J-P, Hartmann M-A, et al. Lipid rafts in higher plant cells: purification and characterization of Triton X-100-insoluble microdomains from tobacco plasma membrane. J Biol Chem 2004;279:36277–86.
[190] Lefebvre B, Furt F, Hartmann MA, Michaelson LV, Carde JP, Sargueil-Boiron F, et al. Characterization of lipid rafts from *Medicago truncatula* root plasma membranes: a proteomic study reveals the presence of a raft-associated redox system. Plant Physiol 2007;144:402–18.
[191] Zolla L, Rinalducci S, Timperio AM. Proteomic analysis of photosystem I components from different plant species. Proteomics 2007;7:1866–76.
[192] Stensballe A, Hald S, Bauw G, Blennow A, Welinder KG. The amyloplast proteome of potato tuber. FEBS J 2008;275:1723–41.
[193] Arai Y, Hayashi M, Nishimura M. Proteomic analysis of highly purified peroxisomes from etiolated soybean cotyledons. Plant Cell Physiol 2008;49:526–39.
[194] Natera SH, Ford KL, Cassin AM, Patterson JH, Newbigin EJ, Bacic A. Analysis of the *Oryza sativa* plasma membrane proteome using combined protein and peptide fractionation approaches in conjunction with mass spectrometry. J Proteome Res 2008;7:1159–87.
[195] Whiteman SA, Nuhse TS, Ashford DA, Sanders D, Maathuis FJ. A proteomic and phosphoproteomic analysis of *Oryza sativa* plasma membrane and vacuolar membrane. Plant J 2008;56:146–56.
[196] Whiteman SA, Serazetdinova L, Jones AM, Sanders D, Rathjen J, Peck SC, et al. Identification of novel proteins and phosphorylation sites in a tonoplast enriched membrane fraction of *Arabidopsis thaliana*. Proteomics 2008;8:3536–47.
[197] Larson RL, Hill AL, Nunez A. Characterization of protein changes associated with sugar beet (*Beta vulgaris*) resistance and susceptibility to *Fusarium oxysporum*. J Agric Food Chem 2007;55:7905–15.
[198] Wen F, VanEtten HD, Tsaprailis G, Hawes MC. Extracellular proteins in pea root tip and border cell exudates. Plant Physiol 2007;143:773–83.
[199] Patterson J, Ford K, Cassin A, Natera S, Bacic A. Increased abundance of proteins involved in phytosiderophore production in boron-tolerant barley. Plant Physiol 2007;144:1612–31.
[200] Hajheidari M, Eivazi A, Buchanan BB, Wong JH, Majidi I, Salekdeh GH. Proteomics uncovers a role for redox in drought tolerance in wheat. J Proteome Res 2007;6:1451–60.
[201] Kang SG, Matin MN, Bae H, Natarajan S. Proteome analysis and characterization of phenotypes of lesion mimic mutant spotted leaf 6 in rice. Proteomics 2007;7:2447–58.
[202] Elvira MI, Galdeano MM, Gilardi P, Garcia-Luque I, Serra MT. Proteomic analysis of pathogenesis-related proteins (PRs) induced by compatible and incompatible interactions of pepper mild mottle virus (PMMoV) in *Capsicum chinense* L3 plants. J Exp Bot 2008;59:1253–65.
[203] Yang P, Li X, Wang X, Chen H, Chen F, Shen S. Proteomic analysis of rice (*Oryza sativa*) seeds during germination. Proteomics 2007;7:3358–68.
[204] Rajjou L, Lovigny Y, Groot SP, Belghazi M, Job C, Job D. Proteome-wide characterization of seed aging in *Arabidopsis*: a comparison between artificial and natural aging protocols. Plant Physiol 2008;148:620–41.

[205] Gallardo K, Firnhaber C, Zuber H, Hericher D, Belghazi M, Henry C, et al. A combined proteome and transcriptome analysis of developing *Medicago truncatula* seeds: evidence for metabolic specialization of maternal and filial tissues. Mol Cell Proteomics 2007;6:2165–79.
[206] Mechin V, Thevenot C, Le Guilloux M, Prioul J-L, Damerval C. Developmental analysis of maize endosperm proteome suggests a pivotal role for pyruvate orthophosphate dikinase. Plant Physiol 2007;143:1203–19.
[207] Pawlowski TA. Proteomics of European beech (*Fagus sylvatica* L.) seed dormancy breaking: influence of abscisic and gibberellic acids. Proteomics 2007;7:2246–57.
[208] Deng Z, Zhang X, Tang W, Oses-Prieto JA, Suzuki N, Gendron JM, et al. A proteomic study of brassinosteroid response in *Arabidopsis*. Mol Cell Proteomics 2007;6:2058–71.
[209] Tang W, Kim TW, Oses-Prieto JA, Sun Y, Deng Z, Zhu S, et al. BSKs mediate signal transduction from the receptor kinase BRI1 in *Arabidopsis*. Science 2008;321:557–60.
[210] Chitteti BR, Peng Z. Proteome and phosphoproteome differential expression under salinity stress in rice (*Oryza sativa*) roots. J Proteome Res 2007;6:1718–27.
[211] El-Khatib RT, Good AG, Muench DG. Analysis of the *Arabidopsis* cell suspension phosphoproteome in response to short-term low temperature and abscisic acid treatment. Physiol Plant 2007;129:687–97.
[212] Sugiyama N, Nakagami H, Mochida K, Daudi A, Tomita M, Shirasu K, et al. Large-scale phosphorylation mapping reveals the extent of tyrosine phosphorylation in *Arabidopsis*. Mol Syst Biol 2008;4:193.
[213] de la Fuente van Bentem S, Anrather D, Dohnal I, Roitinger E, Csaszar E, Joore J, et al. Site-specific phosphorylation profiling of *Arabidopsis* proteins by mass spectrometry and peptide chip analysis. J Proteome Res 2008;7:2458–70.
[214] Tan F, Li G, Chitteti BR, Peng Z. Proteome and phosphoproteome analysis of chromatin associated proteins in rice (*Oryza sativa*). Proteomics 2007;7:4511–27.
[215] Benschop JJ, Mohammed S, O'Flaherty M, Heck AJ, Slijper M, Menke FL. Quantitative phospho proteomics of early elicitor signaling in *Arabidopsis*. Mol Cell Proteomics 2007;6:1198–214.
[216] Lee J, Xu Y, Chen Y, Sprung R, Kim SC, Xie S, et al. Mitochondrial phosphoproteome revealed by an improved IMAC method and MS/MS/MS. Mol Cell Proteomics 2007;6:669–76.
[217] Kwon SJ, Choi EY, Seo JB, Park OK. Isolation of the *Arabidopsis* phosphoproteome using a biotin-tagging approach. Mol Cells 2007;24:268–75.
[218] Meimoun P, Ambard-Bretteville F, Colas-des Francs-Small C, Valot B, Vidal J. Analysis of plant phosphoproteins. Anal Biochem 2007;371:238–46.
[219] Nuhse TS, Bottrill AR, Jones AM, Peck SC. Quantitative phosphoproteomic analysis of plasma membrane proteins reveals regulatory mechanisms of plant innate immune responses. Plant J 2007;51:931–40.
[220] Kruger R, Wolschin F, Weckwerth W, Bettmer J, Lehmann WD. Plant protein phosphorylation monitored by capillary liquid chromatography-element mass spectrometry. Biochem Biophys Res Commun 2007;355:89–96.
[221] de la Fuente van Bentem S, Hirt H. Using phospho proteomics to reveal signalling dynamics in plants. Trends Plant Sci 2007;1(2):404–11.
[222] Camerini S, Polci ML, Restuccia U, Usuelli V, Malgaroli A, Bachi A. A novel approach to identify proteins modified by nitric oxide: the HIS-TAG switch method. J Proteome Res 2007;6:3224–31.
[223] Han P, Chen C. Detergent-free biotin switch combined with liquid chromatography/tandem mass spectrometry in the analysis of S-nitrosylated proteins. Rapid Commun Mass Spectrom 2008;22:1137–45.
[224] Kettenhofen NJ, Broniowska KA, Keszler A, Zhang Y, Hogg N. Proteomic methods for analysis of S-nitrosation. J Chromatogr B Analyt Technol Biomed Life Sci 2007;851:152–9.
[225] Xu H, Zhang L, Freitas MA. Identification and characterization of disulfide bonds in proteins and peptides from tandem MS data by use of the MassMatrix MS/MS search engine. J Proteome Res 2008;7:138–44.
[226] Wormuth D, Heiber I, Shaikali J, Kandlbinder A, Baier M, Dietz KJ. Redox regulation and antioxidative defence in *Arabidopsis* leaves viewed from a systems biology perspective. J Biotechnol 2007;129:229–48.
[227] Winger AM, Taylor NL, Heazlewood JL, Day DA, Millar AH. Identification of intra- and intermolecular disulphide bonding in the plant mitochondrial proteome by diagonal gel electrophoresis. Proteomics 2007;7:4158–70.
[228] Ströher E, Dietz K-J. The dynamic thioldisulphide redox proteome of the *Arabidopsis thaliana* chloroplast as revealed by differential electrophoretic mobility. Physiologia Plantarum 2008;133:566–83.
[229] Balmer Y, Vensel WH, Cai N, Manieri W, Schurmann P, Hurkman WJ, et al. A complete ferredoxin/thioredoxin system regulates fundamental processes in amyloplasts. Proc Natl Acad Sci USA 2006;103:2988–93.
[230] Besson-Bard A, Pugin A, Wendehenne D. New insights into nitric oxide signaling in plants. Annu Rev Plant Biol 2008;59:21–39.
[231] Romero-Puertas MC, Laxa M, Matte A, Zaninotto F, Finkemeier I, Jones AM, et al. S-nitrosylation of peroxiredoxin II E promotes peroxynitrite-mediated tyrosine nitration. Plant Cell 2007;19:4120–30.
[232] Belenghi B, Romero-Puertas MC, Vercammen D, Brackenier A, Inze D, Delledonne M, et al. Metacaspase activity of *Arabidopsis thaliana* is regulated by S-nitrosylation of a critical cysteine residue. J Biol Chem 2007;282:1352–8.
[233] Han P, Zhou X, Huang B, Zhang X, Chen C. On-gel fluorescent visualization and the site identification of S-nitrosylated proteins. Anal Biochem 2008;377:150–5.
[234] Dalle-Donne I, Rossi R, Giustarini D, Colombo R, Milzani A. S-glutathionylation in protein redox regulation. Free Radical Bio Med 2007;43:883–98.
[235] Holtgrefe S, Gohlke J, Starmann J, Druce S, Klocke S, Altmann B, et al. Regulation of plant cytosolic glyceraldehyde 3-phosphate dehydrogenase isoforms by thiol modifications. Physiol Plant 2008;133:211–28.
[236] Wan J, Roth AF, Bailey AO, Davis NG. Palmitoylated proteins: purification and identification. Nat Protoc 2007;2:1573–84.
[237] Gamblin DP, van Kasteren SI, Chalker JM, Davis BG. Chemical approaches to mapping the function of post-translational modifications. FEBS J 2008;275:1949–59.
[238] Denis NJ, Vasilescu J, Lambert JP, Smith JC, Figeys D. Tryptic digestion of ubiquitin standards reveals an improved strategy for identifying ubiquitinated proteins by mass spectrometry. Proteomics 2007;7:868–74.
[239] Tomlinson E, Palaniyappan N, Tooth D, Layfield R. Methods for the purification of ubiquitinated proteins. Proteomics 2007;7:1016–22.
[240] Mollah S, Wertz IE, Phung Q, Arnott D, Dixit VM, Lill JR. Targeted mass spectrometric strategy for global mapping of ubiquitination on proteins. Rapid Commun Mass Spectrom 2007;21:3357–64.
[241] Martinez A, Traverso JA, Valot B, Ferro M, Espagne C, Ephritikhine G, et al. Extent of N-terminal modifications in

cytosolic proteins from eukaryotes. Proteomics 2008;8:2809–31.
[242] Kocher T, Superti-Furga G. Mass spectrometry-based functional Proteomics: from molecular machines to protein networks. Nat Methods 2007;4:807–15.
[243] Gingras AC, Gstaiger M, Raught B, Aebersold R. Analysis of protein complexes using mass spectrometry. Nat Rev Mol Cell Biol 2007;8:645–54.
[244] Berggard T, Linse S, James P. Methods for the detection and analysis of protein–protein interactions. Proteomics 2007;7:2833–42.
[245] Miernyk JA, Thelen JJ. Biochemical approaches for discovering protein–protein interactions. Plant J 2008;53:597–609.
[246] Lemaire SD, Michelet L, Zaffagnini M, Massot V, Issakidis-Bourguet E. Thioredoxins in chloroplasts. Curr Genet 2007;51:343–65.
[247] Shemer TA, Harpaz-Saad S, Belausov E, Lovat N, Krokhin O, Spicer V, et al. Citrus chlorophyllase dynamics at ethylene-induced fruit color-break: a study of chlorophyllase expression, posttranslational processing kinetics, and in situ intracellular localization. Plant Physiol 2008;148:108–18.
[248] Levy A, Erlanger M, Rosenthal M, Epel BL. A plasmodesmata-associated beta-1,3-glucanase in *Arabidopsis*. Plant J 2007;49:669–82.
[249] Bak-Jensen KS, Laugesen S, Ostergaard O, Finnie C, Roepstorff P, Svensson B. Spatio-temporal profiling and degradation of alpha-amylase isozymes during barley seed germination. FEBS J 2007;274:2552–65.
[250] Avila EL, Brown M, Pan S, Desikan R, Neill SJ, Girke T, et al. Expression analysis of *Arabidopsis* vacuolar sorting receptor 3 reveals a putative function in guard cells. J Exp Bot 2008;59:1149–61.
[251] Gershater MC, Cummins I, Edwards R. Role of a carboxylesterase in herbicide bioactivation in *Arabidopsis thaliana*. J Biol Chem 2007;282:21460–6.
[252] Croes E, Gebruers K, Robben J, Noben JP, Samyn B, Debyser G, et al. Variability of polymorphic families of three types of xylanase inhibitors in the wheat grain proteome. Proteomics 2008;8:1692–705.
[253] Gabaldón C, Gómez-Ros L, Núñez-Flores M, Esteban-Carrasco A, Barceló A. Post-translational modifications of the basic peroxidase isoenzyme from *Zinnia elegans*. Plant Molr Biol 2007;65:43–61.
[254] Baginsky S, Grossmann J, Gruissem W. Proteome analysis of chloroplast mRNA processing and degradation. J Proteome Res 2007;6:809–20.
[255] Schilling O, Overall CM. Proteomic discovery of protease substrates. Curr Opin Chem Biol 2007;11:36–45.
[256] Komatsu S, Toorchi M, Yukawa K. Soybean Proteomics. Curr Proteomics 2007;4:182–6.
[257] Qureshi MI, Qadir S, Zolla L. Proteomics-based dissection of stress-responsive pathways in plants. J Plant Physiol 2007;164:1239–60.
[258] Mehta A, Magalhaes BS, Souza DS, Vasconcelos EA, Silva LP, Grossi-de-Sa MF, et al. Rooteomics: the challenge of discovering plant defense-related proteins in roots. Curr Protein Pept Sci 2008;9:108–16.
[259] Zhang Q, Riechers DE. Proteomics: an emerging technology for Weed Sci Research. Weed Sci 2008;56:306–13.
[260] Mehta A, Brasileiro AC, Souza DS, Romano E, Campos MA, Grossi-de-Sa MF, et al. Plant–pathogen interactions: what is Proteomics telling us? Febs J 2008;275:3731–46.
[261] Nesatyy VJ, Suter MJ. Analysis of environmental stress response on the proteome level. Mass Spectrom Rev 2008;27:556–74.
[262] Yang P, Chen H, Liang Y, Shen S. Proteomic analysis of de-etiolated rice seedlings upon exposure to light. Proteomics 2007;7:2459–68.
[263] Faurobert M, Mihr C, Bertin N, Pawlowski T, Negroni L, Sommerer N, et al. Major proteome variations associated with cherry tomato pericarp development and ripening. Plant Physiol 2007;143:1327–46.
[264] Deytieux C, Geny L, Lapaillerie D, Claverol S, Bonneu M, Doneche B. Proteome analysis of grape skins during ripening. J Exp Bot 2007;58:1851–62.
[265] Giribaldi M, Perugini I, Sauvage FX, Schubert A. Analysis of protein changes during grape berry ripening by 2-DE and MALDI-TOF. Proteomics 2007;7:3154–70.
[266] Yeu S-Y, Park B-S, Sang W-G, Choi Y-D, Kim M-C, Song J-T, et al. The serine proteinase inhibitor OsSerpin is a potent tillering regulator in rice. J Plant Biol 2007;50:600–4.
[267] Kleffmann T, von Zychlinski A, Russenberger D, Hirsch-Hoffmann M, Gehrig P, Gruissem W, et al. Proteome dynamics during plastid differentiation in rice. Plant Physiol 2007;143:912–23.
[268] Kanervo E, Singh M, Suorsa M, Paakkarinen V, Aro E-M, Battchikova N, et al. Expression of protein complexes and individual proteins upon transition of etioplasts to chloroplasts in pea (*Pisum sativum*). Plant Cell Physiol 2008;49:396–410.
[269] Yin L, Tao Y, Zhao K, Shao J, Li X, Liu G, et al. Proteomic and transcriptomic analysis of rice mature seed-derived callus differentiation. Proteomics 2007;7:755–68.
[270] Kim ST, Kang SY, Wang Y, Kim SG, Hwang du H, Kang KY. Analysis of embryonic proteome modulation by GA and ABA from germinating rice seeds. Proteomics 2008;8:3577–87.
[271] Takasaki H, Mahmood T, Matsuoka M, Matsumoto H, Komatsu S. Identification and characterization of a gibberellin-regulated protein, which is ASR5, in the basal region of rice leaf sheaths. Mol Genet Genomics 2008;2 (79):359–70.
[272] He H, Li J. Proteomic analysis of phosphoproteins regulated by abscisic acid in rice leaves. Biochem Biophys Res Commun 2008;371:883–8.
[273] Shi F, Takasaki H, Komatsu S. Quantitative analysis of auxin-regulated proteins from basal part of leaf sheaths in rice by two-dimensional difference gel electrophoresis. Phytochemistry 2008;69:637–46.
[274] Cho K, Agrawal GK, Shibato J, Jung YH, Kim YK, Nahm BH, et al. Survey of differentially expressed proteins and genes in jasmonic acid treated rice seedling shoot and root at the proteomics and transcriptomics levels. J Proteome Res 2007;6:3581–603.
[275] Tang W, Deng Z, Oses-Prieto JA, Suzuki N, Zhu S, Zhang X, et al. Proteomics studies of brassinosteroid signal transduction using prefractionation and two-dimensional DIGE. Mol Cell Proteomics 2008;7:728–38.
[276] Thornton B, Osborne SM, Paterson E, Cash P. A proteomic and targeted metabolomic approach to investigate change in Lolium perenne roots when challenged with glycine. J Exp Bot 2007;5(8):1581–90.
[277] Brumbarova T, Matros A, Mock HP, Bauer P. A proteomic study showing differential regulation of stress, redox regulation and peroxidase proteins by iron supply and the transcription factor FER. Plant J 2008;54:321–34.
[278] Kim ST, Kim SG, Kang YH, Wang Y, Kim JY, Yi N, et al. Proteomics analysis of rice lesion mimic mutant (spl1) reveals tightly localized probenazole-induced protein (PBZ1) in cells undergoing programmed cell death. J Proteome Res 2008;7:1750–60.
[279] van Noorden GE, Kerim T, Goffard N, Wiblin R, Pellerone FI, Rolfe BG, et al. Overlap of proteome changes in *Medicago truncatula* in response to auxin and *Sinorhizobium meliloti*. Plant Physiol 2007;144:1115–31.
[280] Larrainzar E, Wienkoop S, Weckwerth W, Ladrera R, Arrese-Igor C, Gonzalez EM. *Medicago truncatula* root nodule

proteome analysis reveals differential plant and bacteroid responses to drought stress. Plant Physiol 2007;144:1495–507.
[281] Sharma N, Hotte N, Rahman MH, Mohammadi M, Deyholos MK, Kav NN. Towards identifying *Brassica* proteins involved in mediating resistance to *Leptosphaeria* maculans: a proteomics-based approach. Proteomics 2008;8:3516–35.
[282] Liang Y, Srivastava S, Rahman MH, Strelkov SE, Kav NN. Proteome changes in leaves of *Brassica napus* L. as a result of *Sclerotinia sclerotiorum* challenge. J Agric Food Chem 2008;56:1963–76.
[283] Cao T, Srivastava S, Rahman MH, Kav NNV, Hotte N, Deyholos MK, et al. Proteome-level changes in the roots of *Brassica napus* as a result of *Plasmodiophora brassicae* infection. Plant Sci 2008;174:97–115.
[284] Geddes J, Eudes F, Laroche A, Selinger LB. Differential expression of proteins in response to the interaction between the pathogen *Fusarium graminearum* and its host, *Hordeum vulgare*. Proteomics 2008;8:545–54.
[285] Yuan K, Zhang B, Zhang Y, Cheng Q, Wang M, Huang M. Identification of differentially expressed proteins in poplar leaves induced by *Marssonina brunnea* f. sp. Multigermtubi. J Genet Genomics 2008;35:49–60.
[286] Jung HW, Lim CW, Lee SC, Choi HW, Hwang CH, Hwang BK. Distinct roles of the pepper hypersensitive induced reaction protein gene CaHIR1 in disease and osmotic stress, as determined by comparative transcriptome and proteome analyses. Planta 2008;227:409–25.
[287] Chan Z, Qin G, Xu X, Li B, Tian S. Proteome approach to characterize proteins induced by antagonist yeast and salicylic acid in peach fruit. J Proteome Res 2007;6:1677–88.
[288] Casasoli M, Spadoni S, Lilley KS, Cervone F, De Lorenzo G, Mattei B. Identification by 2-D DIGE of apoplastic proteins regulated by oligogalacturonides in *Arabidopsis thaliana*. Proteomics 2008;8:1042–54.
[289] Lin YZ, Chen HY, Kao R, Chang SP, Chang SJ, Lai EM. Proteomic analysis of rice defense response induced by probenazole. Phytochemistry 2008;69:715–28.
[290] Segarra G, Casanova E, Bellido D, Odena MA, Oliveira E, Trillas I. Proteome, salicylic acid, and jasmonic acid changes in cucumber plants inoculated with *Trichoderma asperellum* strain T34. Proteomics 2007;7:3943–52.
[291] Shoresh M, Harman GE. The molecular basis of shoot responses of maize seedlings to *Trichoderma harzianum* T22 inoculation of the root: a proteomic approach. Plant Physiol 2008;147:2147–63.
[292] Zhu J, Alvarez S, Marsh EL, Lenoble ME, Cho IJ, Sivaguru M, et al. Cell wall proteome in the maize primary root elongation zone. II. Region-specific changes in water soluble and lightly ionically bound proteins under water deficit. Plant Physiol 2007;145:1533–48.
[293] Alvarez S, Marsh EL, Schroeder SG, Schachtman DP. Metabolomic and proteomic changes in the xylem sap of maize under drought. Plant Cell Environ 2008;31:325–40.
[294] Pandey A, Chakraborty S, Datta A, Chakraborty N. Proteomics approach to identify dehydration responsive nuclear proteins from chickpea (*Cicer arietinum* L.). Mol Cell Proteomics 2008;7:88–107.
[295] Bhushan D, Pandey A, Choudhary MK, Datta A, Chakraborty S, Chakraborty N. Comparative Proteomics analysis of differentially expressed proteins in chickpea extracellular matrix during dehydration stress. Mol Cell Proteomics 2007;6:1868–84.
[296] Wang MC, Peng ZY, Li CL, Li F, Liu C, Xia GM. Proteomic analysis on a high salt tolerance introgression strain of *Triticum aestivum/Thinopyrum ponticum*. Proteomics 2008;8:1470–89.
[297] Jiang Y, Yang B, Harris NS, Deyholos MK. Comparative proteomic analysis of NaCl stress-responsive proteins in *Arabidopsis* roots. J Exp Bot 2007;58:3591–607.
[298] Carpentier SC, Witters E, Laukens K, Van Onckelen H, Swennen R, Panis B. Banana (*Musa* spp.) as a model to study the meristem proteome: acclimation to osmotic stress. Proteomics 2007;7:92–105.
[299] Zang X, Komatsu S. A Proteomics approach for identifying osmotic-stress-related proteins in rice. Phytochemistry 2007;68:426–37.
[300] Lee DG, Ahsan N, Lee SH, Kang KY, Bahk JD, Lee IJ, et al. A proteomic approach in analyzing heat-responsive proteins in rice leaves. Proteomics 2007;7:3369–83.
[301] Hattrup E, Neilson KA, Breci L, Haynes PA. Proteomic analysis of shade-avoidance response in tomato leaves. J Agric Food Chem 2007;55:8310–8.
[302] Xu C, Sullivan JH, Garrett WM, Caperna TJ, Natarajan S. Impact of solar Ultraviolet-B on the proteome in soybean lines differing in flavonoid contents. Phytochemistry 2008;69:38–48.
[303] Cho K, Shibato J, Agrawal GK, Jung YH, Kubo A, Jwa NS, et al. Integrated transcriptomics, Proteomics, and metabolomics analyses to survey ozone responses in the leaves of rice seedling. J Proteome Res 2008;7:2980–98.
[304] Kieffer P, Dommes J, Hoffmann L, Hausman JF, Renaut J. Quantitative changes in protein expression of cadmium-exposed poplar plants. Proteomics 2008;8:2514–30.
[305] Bona E, Marsano F, Cavaletto M, Berta G. Proteomic characterization of copper stress response in *Cannabis sativa* roots. Proteomics 2007;7:1121–30.
[306] Führs H, Hartwig M, Molina LE, Heintz D, Van Dorsselaer A, Braun HP, et al. Early manganese-toxicity response in *Vigna unguiculata* L.—a proteomic and transcriptomic study. Proteomics 2008;8:149–59.
[307] Patterson J, Ford K, Cassin A, Natera S, Bacic A. Increased abundance of proteins involved in phytosiderophore production in boron-tolerant barley. Plant Physiol 2007;144:1612–31.
[308] Zhen Y, Qi JL, Wang SS, Su J, Xu GH, Zhang MS, et al. Comparative proteome analysis of differentially expressed proteins induced by Al toxicity in soybean. Physiol Plant 2007;131:542–54.
[309] Yang Q, Wang Y, Zhang J, Shi W, Qian C, Peng X. Identification of aluminum-responsive proteins in rice roots by a proteomic approach: cysteine synthase as a key player in Al response. Proteomics 2007;7:737–49.
[310] Li J, Wu XD, Hao ST, Wang XJ, Ling HQ. Proteomic response to iron deficiency in tomato root. Proteomics 2008;8:2299–311.
[311] Zhang Q, Xu F, Lambert KN, Riechers DE. Safeners coordinately induce the expression of multiple proteins and MRP transcripts involved in herbicide metabolism and detoxification in *Triticum tauschii* seedling tissues. Proteomics 2007;7:1261–78.
[312] Ahsan N, Lee DG, Lee SH, Kang KY, Bahk JD, Choi MS, et al. A comparative proteomic analysis of tomato leaves in response to waterlogging stress. Physiol Plant 2007;131:555–70.
[313] Kim SG, Kim ST, Kang SY, Wang Y, Kim W, Kang KY. Proteomic analysis of reactive oxygen species (ROS)-related proteins in rice roots. Plant Cell Rep 2008;27:363–75.
[314] Wan XY, Liu JY. Comparative Proteomics analysis reveals an intimate protein network provoked by hydrogen peroxide stress in rice seedling leaves. Mol Cell Proteomics 2008;7:1469–88.

Appendix 3: 2-DE based proteomic analysis of *Saccharomyces cerevisiae* wild and K^+ transport-affected mutant (*trk1,2*) strains at the growth exponential and stationary phases

JOURNAL OF PROTEOMICS 73 (2010) 2316–2335

available at www.sciencedirect.com

ScienceDirect

www.elsevier.com/locate/jprot

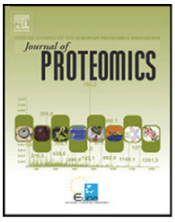

2-DE based proteomic analysis of *Saccharomyces cerevisiae* wild and K^+ transport-affected mutant (*trk1,2*) strains at the growth exponential and stationary phases

Miguel Curto[a], *Luis Valledor*[b], *Clara Navarrete*[c], *Dolores Gutiérrez*[d], *Hana Sychrova*[e], *José Ramos*[c], *Jesús Jorrin*[a,*]

[a]*Agricultural and Plant Biochemistry and Proteomics Research Group, Department of Biochemistry and Molecular Biology, University of Córdoba, Córdoba, Spain*
[b]*EPIPHYSAGE Research Group, Plant Physiology Area, Department of B.O.S., University of Oviedo, Oviedo, Spain*
[c]*Department of Microbiology, University of Córdoba, Córdoba, Spain*
[d]*Department of Microbiology II, Faculty of Pharmacy, Universidad Complutense de Madrid-Parque Científico de Madrid (UCM-PCM). Madrid, Spain*
[e]*Department of Membrane Transport, Institute of Physiology Academy of Sciences of the Czech Republic, Prague, Czech Republic*

ARTICLE INFO

Article history:
Received 27 May 2010
Accepted 6 July 2010

Keywords:
Yeast 2-DE proteomics
Potassium homeostasis
Potassium transport
trk1,2

ABSTRACT

By using a 2-DE based workflow, the proteome of wild and potassium transport mutant *trk1,2* under optimal growth potassium concentration (50 mM) has been analyzed. At the exponential and stationary phases, both strains showed similar growth, morphology potassium content, and Vmax of rubidium transport, the only difference found being the Km values for this potassium analogue transport, higher for the mutant (20 mM) than for the wild (3–6 mM) cells.

Proteins were buffer-extracted, precipitated, solubilized, quantified, and subjected to 2-DE analysis in the 5–8 pH range. More differences in protein content (37–64 mg g^{-1} cell dry weight) and number of resolved spots (178–307) were found between growth phases than between strains. In all, 164 spots showed no differences between samples and a total of 105 were considered to be differential after ANOVA test. 171 proteins, corresponding to 71 unique gene products have been identified, this set being dominated by cytosolic species and glycolitic enzymes. The ranking of the more abundant spots revealed no differences between samples and indicated fermentative metabolism, and active cell wall biosynthesis, redox homeostasis, biosynthesis of amino acids, coenzymes, nucleotides, and RNA, and protein turnover, apart from cell division and growth. PCA analysis allowed the separation of growth phases (PC1 and 2) and strains at the stationary phase (PC3 and 4), but not at the exponential one. These results are also supported by clustering analysis. As a general tendency, a number of spots newly appeared at the stationary phase in wild type, and to a lesser extent, in the mutant. These up-accumulated spots corresponded to glycolitic enzymes, indicating a more active glucose catabolism, accompanied by an accumulation of methylglyoxal detoxification, and redox-homeostasis enzymes. Also, more extensive proteolysis was observed at the stationary phase with this resulting in an accumulation of low Mr protein species.

* *Corresponding author.*
E-mail address: bf1jonoj@uco.es (J. Jorrin).

1874-3919/$ – see front matter © 2010 Elsevier B.V. All rights reserved.
doi:10.1016/j.jprot.2010.07.003

1. Introduction

Inorganic ions such as potassium and sodium play critical roles in cell biology and metabolism [1]. In yeast cells, intracellular concentration of Na^+ and K^+ are around 10–20 and 200–300 mM respectively, the former being lower and the latter higher than the present in the extracellular space, thus contributing to the potential gradient across the cell membrane [2,3]. Regulation and maintenance of intracellular cation concentration is a multicomponent critical process that affects physiological parameters such as membrane potential, intracellular pH, cell volume and that directly influence nutrient uptake, metabolism and growth [2,3]. The study of these regulatory processes will be of relevance for biomedicine and agriculture [4–10].

The budding yeast *Saccharomyces cerevisiae* is a remarkably versatile model system with a myriad of scientific and biotechnological applications that fulfils all the criteria essential for a Systems Biology approach [11]. Its applications range from the study of cellular mechanisms of cancer to neurological diseases and, particularly within the post genomics era, as biological tool from gene expression profiling to protein–protein interaction mapping [12–15]. Yeast has been the experimental system in which most of the different MS-based proteomic platforms have been developed. Such opportunities accrue from the already known functional annotation of the majority of genes, their cultivation in defined laboratory conditions, the relative ease of genetic modifications and a very reasonable background of microbiological and biochemical data [16]. Genomic, transcriptomic and metabolomic data are accessible via a number of public available databases (SGD, MIPS, GIMS, and KEGG) and literature reports [17].

Potassium and sodium homeostasis are fundamental processes in yeast. *S. cerevisiae* cells are able to grow in a broad external concentration of K^+ (10 μM–2.5 M) and Na^+ (<1.5 M) [3]. In this species, most key elements mediating influx and efflux of the major alkali cations have been identified and functionally characterized [2,3,18]. However, there are still many uncertainties concerning the quantitative contribution of each component, their regulation, the interaction between cation fluxes at the cell membrane and subcellular compartment distribution, and connection to metabolism and other biological processes. Such studies are facilitated by the relatively easy genetic manipulation of *S. cerevisiae*. The use of mutants will enable the identification and characterization of genes and proteins mediating the complex system responses to cation stress, finally leading to a deeper understanding of sensing, transport, signalling and response/detoxification mechanisms. Such studies can be performed by using classical biochemical, and cellular biology techniques as well as the holistic — omic approaches, including transcriptomics, proteomics and metabolomics [19].

In the present study, a 2-DE based comparative proteomics analysis was used to characterize a mutant lacking the two main K^+ transporters [20] and to identify differences in protein species abundance with respect to the wild strain at two stages of the growth curve, the exponential and the stationary ones. This study is justified as possible differences could be directly related to differences in intracellular K^+ content, and, indirectly, to the mutation itself, being the differences dependent on the growth phase. A similar strategy has been used to characterize other yeast mutants [21,22], growth phase and conditions [23–25], stress conditions [26], and different 2-DE reference maps are available [27]. The *TRK1* and *TRK2* loci encode major plasma membrane K^+ uptake systems. K^+ accumulation in the cytosol via these systems is driven by the electrochemical proton gradient across the plasma membrane generated by H^+-ATPase Pma1 [28]. Deletion of both *TRK* genes produces increased K^+ requirements for growth and defective high affinity potassium transport. While understanding of the role of Trk1p in cellular processes is relatively well developed, data on the function and regulation of Trk2p are incomplete [3,29]. By using a proteomics approach it was aimed to obtain information about possible involvement of potassium transport in other cellular processes and to go deeper into the knowledge of key aspects of the eukaryotic cell biology as it is cell proliferation, stress responses and long-term survival which characterize and differentiate exponential from stationary phases [30,31].

Under the growth conditions used (rich YNB-F medium), with high glucose (2%) and potassium (50 mM KCl) concentration similar growth, morphology, K^+ content and Rb^+ transport, protein content and 2-DE profile have been found in between wild and mutant cells. On the contrary, differences mainly corresponded to between growth stages. Spot intensity values were subjected to ANOVA uni- and multivariate and clustering tests. Major and variable spots were MS analyzed with 171 protein species, corresponding to 71 unique gene products identified. The proteome was dominated by cytosolic, glicolytic enzymes. On the bases of the differences identified the biological and metabolic status of the cells is discussed.

2. Material and methods

2.1. Yeast strains and growth conditions

S. cerevisiae wild type BY4741 (MATa *his3Δ1 leu2Δ met15Δ ura3Δ*; EUROSCARF, Germany) and the isogenic potassium transport double mutant (*trk1*$^-$,*2*$^-$) (BYT12, *trk1Δ::loxP trk2Δ::loxP*) (developed by Dr. Sychrova) strains were grown, in 250 ml Erlenmeyer flasks, with 100 ml YNB-F medium: 1.63 g/L Yeast Nitrogen Base (FORMEDIUM), 2% glucose, 4 g/L ammonium sulphate, enriched with 50 mM potassium chloride, 20 mg/L methionine, adenine, tryptophan and arginine; 30 mg/L tyrosine, leucine, isoleucine, and lysine; 40 mg/L uracyl, histidine; 50 mg/L phenylalanine, 100 mg/L glutamic and aspartic acid; 150 mg/L valine; 200 mg/L threonine and 400 mg/L serine. The cultures were grown at 28 °C (initial OD_{600} 0.05) in a shaker to allow good aeration (180 rpm), until OD_{600} of about 1.5 and 3.0, for exponential and stationary cultures, respectively.

2.2. Cation content and rubidium transport experiments

Exponential and stationary growing cells were collected on Millipore filters, which were rapidly washed with 20 mM $MgCl_2$. The cells were then extracted with HCl and the K^+ content of the extracts was analyzed by atomic emission spectrometry [32].

In order to study the time course of Rb^+ uptake, cells were washed and resuspended in MES buffer (2% glucose) at OD_{600} values of 0.3. The required amount of RbCl was added to the buffer at zero time and samples of cells were withdrawn at various times. Cells were treated as described for determining the K^+ content. The velocity values were expressed in nmol min^{-1} mg^{-1} of dry weight of cells. The experiments were repeated at least three times each corresponding to independent batches and the standard deviations calculated.

2.3. Microscope assay

Cells were taken at the exponential or stationary phases. Yeast preparations were observed with a phase contrast microscope (Leica, DF300 FX) with 100× magnification.

2.4. Protein extraction

Cells were sampled at the exponential and stationary phases, the growth medium being eliminated by centrifugation. The cell pellet, about 300 (exponential phase) and 800 mg (stationary phase) of fresh weight per ml of culture medium, was suspended in 600 μL homogenization (50 mM TRIS buffer, pH 7.6, containing 1 mM PMSF, 1 mM EDTA, 2 mM DTT, and a tablet of protease inhibitor cocktail (Roche-11697498001) per 50 ml of homogenization buffer) and broken by vortexing (15 to 20 times, 30 s) in the presence of glass beads (Sigma-G9268) (a volume equivalent to that of the cell pellet). Glass beads and insoluble material were eliminated by centrifugation (10,000 *g*, 5 min). To the supernatant (about 500 μL) 1.5 mL of 10% (w/v) trichloroacetic acid (TCA)/acetone solution containing 0.07% (w/v) dithiothreitol (DTT) was added. Proteins were allowed to precipitate at −20 °C for 1 h; and the precipitate was recovered after centrifugation at 10,000 *g* for 15 min. The pellet was washed with 1.5 mL of cold (−20 °C) acetone containing 0.07% (w/v) DTT, repeating this operation twice. The protein pellet was recovered after centrifugation. The final pellet was air-dried and solubilized in 250 μL of 8 M urea, 2% (w/v) 3-[(3-cholamidopropyl)dimethylammonio]propanesulfonate (CHAPS), 20 mM DTT, 0.5% (v/v) Biolytes pH range 3–10 (Bio-Rad), and 0.0001% (w/v) bromophenol blue. Insoluble material was removed by centrifugation. The protein concentration was determined by Bradford, with ovoalbumin as a standard.

2.5. 2-DE

Immobilized pH gradients (IPG) strips (17 cm, 5–8 pH linear gradient; Bio-Rad) were passively rehydrated for 2 h with 500 μg of protein in 300 μL of IEF solubilization buffer (7 M Urea; 2 M Thiourea; 4% [w/v] CHAPS; 0.5% [v/v] IPG buffer 5–8, 20 mM DTT; and 0.01% [w/v] bromophenol blue). The strips were loaded onto a Bio-Rad Protean IEF Cell system and proteins were electrofocused at 20 °C with a first step of a gradual increase in the voltage (50–8000 V) and then reaching 60,000 Vh. Strips were immediately equilibrated according to Görg et al. [33]. Second dimension SDS-PAGE was performed on 12% polyacrylamide gels using Protean Dodeca Cell system (Bio-Rad). Gels were run first at 30 mA/gel for 15 min, and second at 50 mA/gel until the dye front reached the bottom of the gel.

2.6. Staining and image analysis

Gels were stained twice with CBB G-250 (Bio-Rad) for 20 h following the method described by Mathesius et al. [34]. Images were acquired with a GS-800 calibrated densitometer (Bio-Rad) and analyzed with PDQuest 8.0.1 software (Bio-Rad) using 10-fold over background as a minimum criterion for presence/absence for the guided protein spot detection method. This criterion includes almost all spots of the gels and some staining artefacts and noise. A Spot-by-spot visual validation of automated analysis was done thereafter to increase the reliability of the matching. Experimental pI was determined using a 5–8 linear scale over the total length of the IPG strip. Mr values were calculated by mobility comparisons with protein standards markers (SDS Molecular weight standards, Broad range, Bio-Rad) run in a separate lane in the gel.

2.7. Statistics

After image analysis, normalized spot volumes were obtained for each gel and SD and CV calculated. Since raw proteomic data are known to be highly disturbing for multivariate statistics and clustering algorithms [35], because of the high rate of missing spot values and the known dependence between the volume and variance for individual spots [36,37], spot volumes were pre-processed before statistical analyses. Spot volumes were first normalized as a proportion of the total spot intensities per gel (spot volume $\times 10^5 / \sum$gel spot volumes), and then the normalized volumes were Log transformed to reduce the volume-variance dependency. These steps also reduced the coefficient of variation of each spot, increasing the reliability of the analyses.

Differentially-abundant spots were defined after applying a one-way ANOVA test. Spot values passed the Levene's homoscedasticity and Kolmogorov–Smirnov normality tests. False discovery rates (FDR) were controlled at level 0.05 employing a RFDR adjusted to 313 independent steps (adjusted p-value = 0.02508).

A multivariate analysis was performed over the whole set of spots and on those showing differences. PCA was applied to the correlation matrix to reduce its dimensionality. Using un-rotated principal component (PC) scores, the relation between the different sampling times was studied by determining the spots with the highest load on the variance. Once the PCs were determined, an independent component analysis (ICA) was applied employing the FastICA algorithm. All statistical analyses were performed under R environment (version 2.11.0 pre-release × 64).

Samples were clustered employing Cluster 3.0 using the Correlation or Euclidean distance method over an average linkage dissimilarity matrix and plotted with Java Treeview 1.1.3 software.

2.8. MS analysis and protein identification

Spots were manually excised and transferred to Multiwell 96 plates. Spots were digested with bovine trypsin (sequencing grade Roche Molecular Biochemicals) using an Ettan™ digester station (GE Healthcare Life Sciences). The digestion protocol

used was that of Schevchenko et al. [38], with minor variations. Briefly, spots were washed twice with water, and destained by twice 10 min incubation with 100% acetonitrile and dried in a Savant SpeedVac for 30 min. Then the samples were reduced with 10 mM dithioerytritol in 25 mM ammonium bicarbonate for 30 min at 56 °C and subsequently alkylated with 55 mM iodoacetamide in 25 mM ammonium bicarbonate for 15 min in the dark. Finally, samples were digested with 12 μL of trypsin (12.5 ng/μL) in 25 mM ammonium bicarbonate (pH 8.5) overnight at 37 °C. After digestion, the supernatant was collected and 1 μl was spotted onto a MALDI target plate using the dry droplet method and 0.4 μl of a 3 mg/ml of α-cyano-4-hydroxy-transcinnamic acid matrix in 50% ACN, 0.1% TFA. Samples were analyzed in a 4800 Proteomics Analyzer MALDI-TOF/TOF mass spectrometer (Applied Biosystems, Framingham, MA), in the *m/z* range 850–4000, with an accelerating voltage of 20 kV, in reflectron mode and with a delayed extraction set to 120 ns. All MS spectra were internally calibrated with peptides from trypsin autolysis. The MS analysis by MALDI-TOF/TOF mass spectrometry produces peptide mass fingerprints and the peptides observed with a Signal to Noise greater than 20 can be collated and represented as a list of monoisotopic molecular weights. Proteins ambiguously identified by peptide mass fingerprints, were subjected to MS/MS sequencing analysis. So, from the MS spectra suitable precursors were selected for MS/MS analysis with CID on (atmospheric gas was used) 1 Kv ion reflector mode and precursor mass Windows ±5 Da. The plate model and default calibration were optimized for the MS–MS spectra processing. For protein identification, the UniProt Knowledgebase Release 14.6 (UniProtKB/Swiss-Prot Release 56.6 of 16-Dec-2008, UniProtKB/TrEMBL Release 39.6 of 16-Dec-2008) was searched using MASCOT search engine v.2.1 (Matrix Science, London; http://www.matrixscience.com) through the Global Protein Server Explorer software v3.6 from Applied Biosystems.

The following parameters were allowed: taxonomy restrictions to *S. cerevisiae*, one missed cleavage, 50 80–100 and 50 80–100 ppm mass tolerance for PMF and MS–MS searches respectively, 0.3 Da for MS–MS fragments tolerance, carbamidomethylation cysteine as a fixed modification and methionine oxidation as a variable modification. The parameters for the combined search (peptide mass fingerprint plus MS–MS spectra) were the same described above.

In all protein identified, the probability scores were greater than the score fixed by Mascot as significant with a *p*-value minor than 0.05.

3. Results

3.1. *Cell growth, potassium content, and transport kinetics*

In order to characterize the general behaviour of the yeasts under our conditions, cell growth, potassium content and rubidium transport were analysed. When grown in YNB-F medium in the presence of 50 mM KCl, and 5 to 20 h after transferring to fresh medium, the *trk1,2* double mutant reached slightly lower OD_{600} values, with no statistically significant differences, than its wild relative strain BY4741 (Fig. 1). The

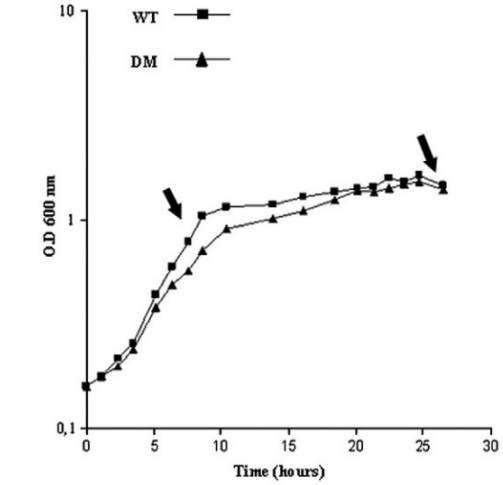

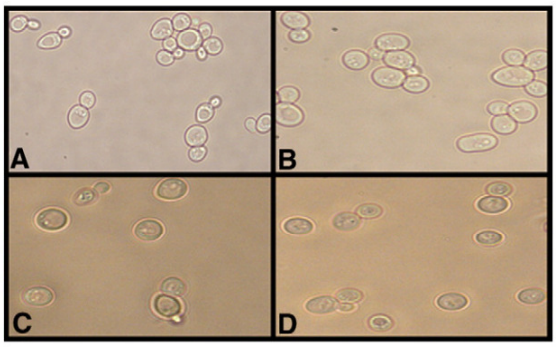

Fig. 1 – Growth curve (top) and optic microscope images (bottom). *Saccharomyces cerevisiae* BY4741 wild and mutant cells were grown in liquid medium supplemented with 50 mM KCl. Top. WT (——■——); double mutant (*trk1,2*) (——▲——). Arrows indicate sampling times. Y axes on a logarithmic scale. Bottom. Wild type (A–C) and double mutant (B–D) growing in exponential (A–B) and stationary phase (C–D).

optical density increased logarithmically in between 1 and 10 h, reaching the early stationary phase by about 20 h. Microscopic analysis indicated similar morphological characteristics although higher bud abundance during exponential phase of growth was observed (Fig. 1). Cells were sampled at the exponential (OD_{600} values of about 1.5) and stationary (OD_{600} values of about 3.0) phases for ulterior analysis.

Values of internal potassium for the exponential and stationary phases were of 380 (wild)–410 (double mutant), and 310 (wild)–350 (double mutant) nmol $K^+ mg^{-1}$ cell fresh weight (Fig. 2). The potassium transport processes were characterized by determining the kinetic constants (Vmax and Km) of rubidium transport (rubidium was used as a potassium transport analogue) (Table 1). Values of 5.1 and 5.2 nmol mg^{-1} cell fresh weight at the exponential phase were obtained for, respectively, the wild and double mutant strains. These values increased to 6.2 and 6.0 nmol mg^{-1} cell fresh weight at the stationary phase. Higher Km values were obtained for the double mutant than the wild cells, this

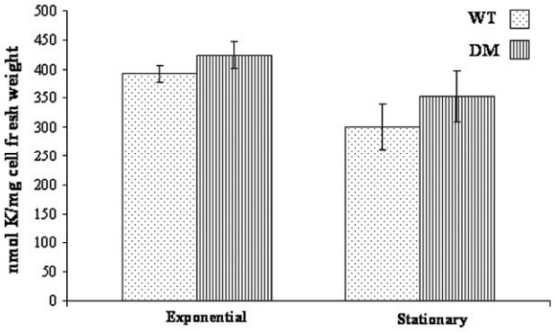

Fig. 2 – Intracellular potassium content in wild type and double mutant cells growing in exponential or stationary phases. Cells were grown in liquid medium supplemented with 50 mM KCl. WT (▨) and double mutant (*trk1,2*) (▨).

value decreasing at the stationary phase for the wild (6.2 versus 3.8 mM) but not for the mutant (20 mM) strain.

3.2. *2-DE protein profiles*

The protein yield of the protocol employed for protein extraction (buffer plus TCA-acetone precipitation) and solubilization was of 37.9–63.6 μg eq. SAB mg^{-1} cell dry weight, with higher levels at the stationary phase and in wild that in mutant cells, although these last differences were not statistically significant (ANOVA, $p<0.05$) (Table 2). After 2-D electrophoresis and Coomassie staining of the gels, from 178 to 307 consistent spots (present in the tree replicates performed per sample) could be resolved in the 5–8 pH (where most of the spots were concentrated, Supplementary Fig. 1) and 10–90 kDa Mr ranges. (Fig. 3; Supplementary Fig. 2). 2-DE gel image analysis by using PDQuest software and visual confirmation revealed the existence of qualitative and quantitative differences in spot intensity between strains and/or growth phase (Supplementary Table A). The pre-processing of the data decreased the CV% and the dependence between spot intensity and SD without a significant alteration of the original data structure (Supplementary Fig. 3; Supplementary Table C). Out of the total number of spots detected (178–307), 164 were present in all the samples, with no statistically significance differences between them (Table 2). A total of 105 spots were considered differential after ANOVA analysis (error controlled for a 5% rough false discovery rate). When comparing the 2-DE profiles to the wild exponential cells, only 2 spots are qualitatively characteristic of double mutants in logarithmic stage (312 and 313), whereas wild type showed 6 characteristic spots (191, 192, 197, 198, 200 and 311). The stationary stage, in both strains, was characterized by 96 spots, out of which 35 were exclusive to wild type. Only one differential spot (165) was common to the two stages and growth stages (Supplementary Table D).

3.3. *MS analysis and protein identification*

The most abundant and the 105 variable spots, on the basis of the one-way ANOVA, 255 in all, were subjected to MALDI-TOF–TOF MS analysis after tryptic digestion and MS and MS–MS spectra used for protein identification by searching in the UniProt database, with 171 being identified (Table 3). Proteins were grouped according to their function with indications on location, number of molecules per cell, oligomeric subunit structure, PTMs, and processing of the displayed sequence, as annotated at the UniProt database. For the majority of the identified spots a good correlationship between experimental and theoretical Mr and pI was found. For some spots, the estimated experimental Mr differed from the theoretical one by more than 15%, this probably being due to errors in Mr estimation or that the displayed sequence at the UniProt database is further processed into a mature form. There are identified proteins with almost double experimental than theoretical Mr, including spot 169 (fructose-bisphosphate aldolase, reported as homodimer) and 124 (uracil phosphoribosyltransferase). On the other hand, there is a group of spots with a much lower experimental than theoretical Mr. This is the case of the fructose-bisphosphate aldolase (11 and 25), phosphoglycerate kinase (40–94), enolase 1 (21 and 61), enolase 2 (4, 59, 84 and 89). Finally, the existence of protein species corresponding to the same gene and differing in pI better than Mr has been observed. This is the case of hexokinase 2 (164, 166 and 167), fructose-bisphosphate aldolase (96, 101 and 106), triose phosphate isomerase (39, 41, 42, 43 and 44), gliceraldehyde-3-phosphate dehydrogenase 3 (67, 68, 73, 76, 77 and 83), phosphoglycerate kinases (100–138), and enolases 1 (135–156) and 2 (104–149).

Looking at the ranking of the more abundant proteins, we found a similar pattern among samples, with enzymes of the glycolysis (enolase, PGK, TPI, aldolase, and GA3PDH) and stress-related (peroxiredoxin type-2 and SOD) plus peptidyl-prolyl cis-trans isomerase, S-adenosylmethionine synthetase 2, and FK506-binding protein 1 being the most abundant (Supplementary Table B).

Table 1 – Kinetic parameters of rubidium transport in wild type and double mutant strains at the exponential and stationary phases. Cells were grown in YNB-F + 50 mM KCl, then cells were suspended in fresh free-potassium medium containing rubidium.

Kinetic parameters	Exponential growth phase		Stationary growth phase	
	Wild strain	*trk1,2* mutant strain	Wild strain	*trk1,2* mutant strain
Vmax (nmol mg^{-1} cell dry weight min^{-1})	5.1±0.2	5.2±0.5	6.2±0.2	6.0±0.3
Km (mM)	6.2±0.3	20.1±0.8	3.8±0.2	20.0±0.4

Table 2 – Optical density, protein yield and number of spots resolved on 2-DE, with indication of common and variable ones. Values are mean ± S.E. of three biological replicates.

Strain	Growth phases	OD_{600} [a]	Protein yield (μg eq SAB mg^{-1} cell dry weight)	Spots detected	Common [b] variable spots
Wild	Exponential	1.50±0.10	40.1±3.2	195±8	164
				(186–201) [c]/185 [d]	22
trk1,2 mutant		1.50±0.11	37.9±2.7	178±6	164
				(174–185)/169	3
Wild	Stationary	2.96±0.15	63.6±4.2	307±6	164
				(302–313)/302	138
trk1,2 mutant		2.80±0.10	50.3±3.1	261±7	164
				(256–269)/256	92

[a] The number of cells and dry weight can be calculated as follow: $O.D_{600}$=1 corresponds to 8×10^7 cells/ ml of culture medium; D.W = [0.51×$O.D_{600}$] mg/ml medium.
[b] Consistent spots common to all the samples, with no statistical significant differences (ANOVA test, $p>0.05$).
[c] Maximum and minimum number of spots.
[d] Consistent spots (present in all the three replicates).

3.4. *Differences between strains and growth phases*

PCA analysis was applied to the data set. Out of the potential 313 principal components (PC) extracted, the first 11 accounted for 100% of the variance (Table 4). When PCs were tested for differences between groups, PCs 1–4 were significant in the two data sets studied (one-way ANOVA, for $p<0.1$). The employment of these components in a 2-D representation (plotting PC1 and PC2, Fig 4) allowed the effective separation of samples into the growth stage time in which were sampled. Furthermore, the representation of PC3 and PC4 allowed the separation of double mutant stationary samples, from which no characteristic spots were defined by univariate analyses (figure not shown). The spots showing a high correlation, above 0.7, with each PC were summarized in Supplementary Table E.

Differential spots were clustered employing correlation distance (Fig. 5). There was a very short distance between strains at the exponential phase, this being lower than the intra group

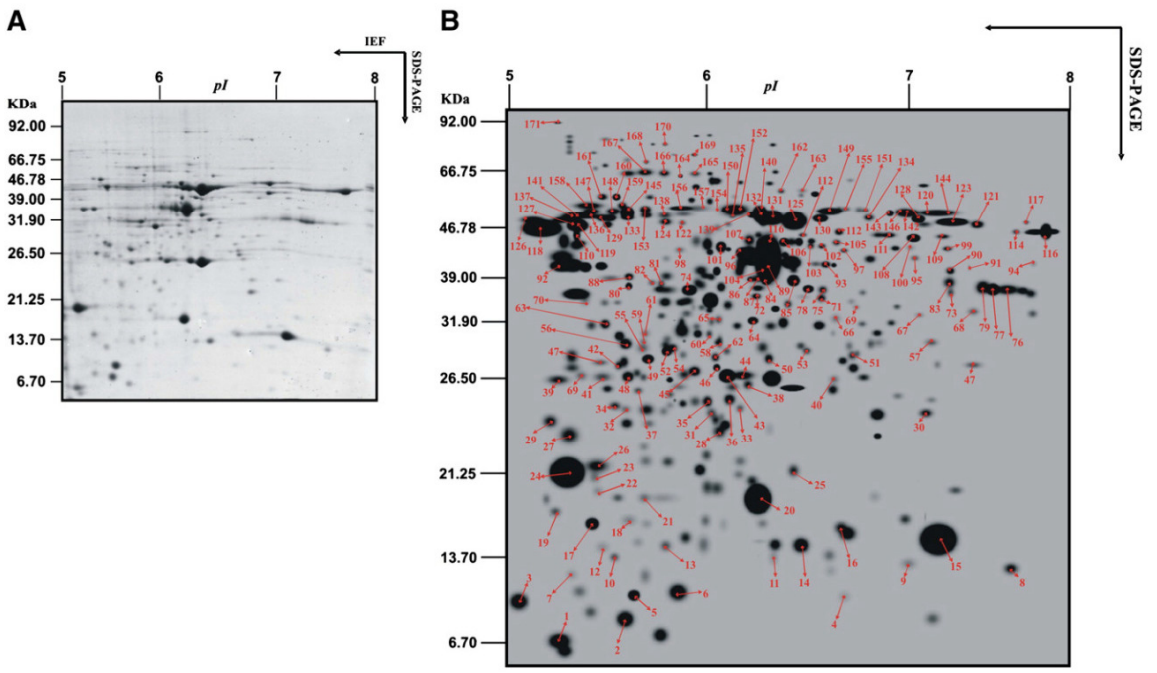

Fig. 3 – Representative 2-D gel corresponding to extracts from wild cells at the exponential phase (A), and master gel, with arrows pointing at variable spots (B). Molecular mass (on the left) and pI (on the top) were calculated using standard molecular weight markers and the PD-Quest software.

Table 3 – List of identified proteins. Information from UniProtKB (http://www.uniprot.org/) is included: i) location (cyt: cytoplas, mit: mitochondrion, nuc: nucleus, mef: membrane enriched fraction; pm: plasma membrane; er: endoplasmic reticulum; Go: Golgi); ii) number of molecules/cell in log phase SD medium (figure); iii) if so, oligomer subunit structure (homd homodimer; homt: homotetramer; hetd: heterodimer; hett: heterotetramer); iv) PTM (P: phosphoprotein; Ac: acetylation; Glyc: glycoprotein; Ub: ubiquitinated; Lip: lipoprotein; v) if so, the displayed sequence is further processed into a mature form (SP).

Number [a]	Mr/pI exp. [b]	Mr/pI theor. [c]	Name	Accession numbers [d]	Mascot scores/Matched peptides (%Coverage)/MS–MS ions (score) [e]
Metabolism					
Glycolysis					
164	65.25/5.80	54.13/5.16	Hexokinase-2	P04807/	120/15(55)
166	66.40/5.69		Cyt	YGL253W	128/16(43)
167	66.75/5.57		114,000		94/13(33)
			P		
			SP		
82	36.92/5.61	39.88/5.51	Fructose-bisphosphate	P14540/	58/8(25)
98	41.61/5.80		aldolase	YKL060C	57/6(20)/K.SLETFRTTNTL.-(32)
11	12.70/6.31		Cyt		162/8(19)/K.GISNEGQNASIK.G (62)/
			120,000		K.GAIAAAHYIR.S (38)/
			Homd		R.SIAPAYGIPVVLHSDHCAK.K (37)
25	21.32/6.41		P		122/7(18)/K.GISNEGQNASIK.G (66)/
			SP		R.SIAPAYGIPVVLHSDHCAK.K
					(23)/K.TGVIVGEDVHNLFTYAK.E (9)
92	39.23/5.02				79/10(41)
96	41.14/6.16				75/11(32)
101	42.05/6.05				88/13(39)
106	42.86/6.36				79/10(37)
107	43.38/6.19				76/12(33)
169	74.46/5.89				106/9(26)/K.GAIAAAHYIR.S
					(42)/K.SLETFRTTNTL. (24)
37	25.79/5.52	26.89/5.74	Triosephosphate isomerase	P00942/	140/4(13)/K.KPQVTVGAQNAYLK.A
			Cyt	YDR050C	(94)/K.ASGAFTGENSVDQIKDVGAK.
			207,000		W(37)
39	26.45/5.05		Homd		99/11(43)
41	26.63/5.28		SP		92/10(46)
42	26.65/5.45				65/8(35)
43	26.69/6.08				109/12(38)
44	26.74/6.16				200/7(21)/K.ASGAFTGENSVDQIK.D (77)/
					K.ASGAFTGENSVDQIKDVGAK.W (60)/
					R.SYFHEDDKFIADK.T (39)
66	32.46/6.62	35.93/6.46	Glyceraldehyde-3-phosphate	P00358/	99/4(7)/K.LVSWYDNEYGYSTR.V (59)/
			dehydrogenase 2	YJR009C	K.TVDGPSHKDWR.G (33)
			Cyt		
			207,000		
			Homt		
			SP		
67	32.86/7.04	35.83/6.46	Glyceraldehyde-3-phosphate	P00359/	292/26(87)
68	33.28/7.45		dehydrogenase 3	YJL052W	67/9(35)
73	35.63/7.28		Cyt		244/24(83)
76	35.99/7.71		169,000		278/25(83)
77	36.02/7.60		Homt		224/21(80)
83	36.93/7.27		P		203/22(57)
			SP		
32	24.69/5.44	44.76/7.11	Phosphoglycerate	P00560/	239/12(26)/K.GVEVVLPVDFIIADAFSAD
			kinase	YCR012W	ANTK.T(60)/K.EGIPAGWQGLDNGPES
			Cyt		R.K (79)/K.TIVWNGPPGVFEFEK.F(37)
40	26.47/6.61		314,000		97/12(36)
50	28.20/6.29		P, Ac		143/17(39)
53	28.99/6.48		SP		119/15(41)
57	29.84/7.13				131/16(42)
79	36.28/7.53				100/14(36)
90	38.53/7.28				205/67(54)
91	39.00/7.42				325/80(74)
93	39.43/6.57				118/14(41)
94	39.56/7.91				60/9(28)
95	40.38/7.01				80/12(33)

Table 3 (*continued*)

Number[a]	Mr/pI exp.[b]	Mr/pI theor.[c]	Name	Accession numbers[d]	Mascot scores/Matched peptides (%Coverage)/MS–MS ions (score)[e]
Glycolysis					
100	41.95/6.98				230/23(64)
114	45.73/7.78				104/14(41)
116	45.80/8.00				213/21(60)
117	46.77/7.83				237/23(67)
118	46.78/5.00				184/20(55)
119	47.63/5.12				276/25(70)
120	47.94/7.08				277/26(70)
121	47.95/7.48				294/27(67)
122	48.37/5.81				248/24(68)
123	48.64/7.29				292/27(70)
127	49.43/5.12				297/27(70)
129	49.95/5.28				84/13(35)
133	50.12/5.45				171/19(56)
134	50.16/6.78				59/9(26)
136	50.44/5.19				81/11(35)
138	50.86/5.70	388/32(77)			
47	27.58/7.45	27.59/8.81	Phosphoglycerate mutase 1 Cyt 172,000 Homt P SP	P00950/ YKL152C	182/19(62)
69	33.80/6.72	36.33/6.15	Phosphoglycerate mutase 2 Cyt 2020 P	Q12008/ YKL152C	189/10(25)/R.HSAELIEQYCK.A (76)/R.DYEGKPPPVDLDR.E (38)/K.GSSTGYEFKEPNR.Q (33)/R.TQQTIETMCEEFK.L (9)
21	20.01/5.56	46.83/6.16	Enolase 1	P00924/	85/5(10)/R.SGETEDTFIADLVVGLR.T (70)
61	30.83/5.57		Cyt	YGR254W	86/2(3)/R.SGETEDTFIADLVVGLR.T (86)
97	41.49/6.66		76,700 Homd P		117/7(13)/R.SGETEDTFIADLVVGLR.T (92)/R.SGETEDTFIADLVVGLR.T (73)/R.SGETEDTFIADLVVGLR.T (9)
109	44.40/7.22		SP		112/15(38)
128	49.65/7.04				275/28(67)
135	50.27/6.11				136/6(13)/R.SGETEDTFIADLVVGLR.T (102)/K.VNQIGTLSESIK.A (19)
142	51.61/6.97				273/28(60)
143	51.62/6.88				R.SGETEDTFIADLVVGLR.T (83)
144	51.65/7.18				278/28(67)
146	51.84/6.95				69/10(24)
147	52.07/5.21				116/3(8)/R.SGETEDTFIADLVVGLR.T (107)
151	52.54/6.76				225/25(56)
155	52.97/6.67				321/13(29)/K.AVDDFLISLDGTANK.S (110)/R.SGETEDTFIADLVVGLR.T (105)/R.GNPTVEVELTTEK.G (39)
156	53.23/5.80				137/17(43)
4	9.44/6.64	46.94/5.67	Enolase 2 Cyt 2610	P00925/ YHR174W	314/10(20)/K.AVYAGENFHHGDKL.-(85)/R.SGETEDTFIADLVVGLR.T (114)/K.VNQIGTLSESIK.A (79)
59	30.00/5.55		Homd P		192/6()/R.SGETEDTFIADLVVGLR.T (95)/K.TAGIQIVADDLTVTNPAR.I (81)
84	37.16/6.28		SP		192/20(44)
89	38.40/6.28				157/20(51)
102	42.15/6.55				220/10(23)/R.SGETEDTFIADLVVGLR.T (90)/K.TAGIQIVADDLTVTNPAR.I (69)/K.VNQIGTLSESIK.A (25)
104	42.70/6.24				134/17(45)
112	44.85/6.46				100/13(38)
113	44.87/6.24				56/9(27)
115	45.75/6.63				190/16(38)/R.VLGIDGGEGKEELFR.S (52)

(*continued on next page*)

Table 3 (*continued*)

Number [a]	Mr/pI exp. [b]	Mr/pI theor. [c]	Name	Accession numbers [d]	Mascot scores/Matched peptides (%Coverage)/MS–MS ions (score) [e]
Glycolysis					
125	49.16/6.41				272/29(61)
126	49.37/5.00				154/9(32)
130	49.96/6.54				221/24(55)
131	50.06/6.30				214/25(56)
132	50.07/6.26				199/24(56)
137	50.52/5.08				69/7(24)
139	50.97/6.20				76/7(17)/R.SGETEDTFIADLVVGLR.T (55)
141	51.38/5.12				102/14(42)
149	52.19/6.59				253/26(59)
150	52.31/6.10				192/9(20)/R.SGETEDTFIADLVVGLR.T (83)/K.AVDDFLLSLDGTANK.S (51)/ K.TAGIQIVADDLTVTNPAR.I (30)
154	52.72/6.07	192/4(20)/R.	SGETEDTFIADLVVGLR.T (83)/K.AVDDFLLSLDGTANK.S (51)/K. TAGIQIVADDLTVTNPAR.I (30)		
Ethanol fermentation					
108	44.00/7.00	37.25/6.26	Alcohol dehydrogenase 1 Cyt Homt P, Ac SP	P00330/ YOL086C	173/21(61)
Pentose phosphate pathway					
52	28.93/5.71	31.78/6.01	Probable 6-phosphogluconolactonase 3 Cyt, Nuc 3420	P38858/ YDR071C	161/16(60) Cytoplasm, nucleus
Methylglyoxal pathway					
71	34.88/6.55	31.76/5.82	Hydroxyacyl glutathione hydrolase (glyoxalase II) Cyt 13,700 P	Q05584/ YDR272W	124/14(57)
75	35.94/6.55				111/13(50)
Nucleotide-sugar pathways					
140	51.30/6.24	48.44/5.66	Mannose-6-phosphate isomerase Cyt 5220 P, Ac SP	P29952/ YER003C	112/17 (39)
152	52.61/6.12	48.44/5.66			125/16(38)
48	27.83/5.27	29.21/5.14	Phosphomannomutase Cyt3500 Homd P	P07283/ YFL045C	230/21(77)
105	42.77/6.62	39.71/5.95	Mannose-1-phosphate guanyltransferase Cyt 97,100 P	P41940/ YDL055C	140/7(18)/K.IGPDVVIGPNVTIGDGVR.I (94)/K.ETFPILVEEK.Q (21)
Oxidoreductases/redox balancing					
162	59.31/6.35	51.09/5.93	Fumarate reductase Cyt, mit, mef 7620	P32614/ YEL047C	78/12(25)
163	59.47/6.45				65/10(26)

Table 3 (*continued*)

Number [a]	Mr/pI exp. [b]	Mr/pI theor. [c]	Name	Accession numbers [d]	Mascot scores/Matched peptides (%Coverage)/MS–MS ions (score) [e]
Oxidoreductases/redox balancing					
111	44.81/6.88	44.98/6.13	NADPH dehydrogenase 2 Mit, nuc 15,100 Homd/Hetd P SP	Q03558/ YHR179W	116/14(35)
85	37.19/6.41	35.59/5.84	NADPH-dependent alpha-keto amide reductase Cyt, nuc 4030 P	Q07551/ YDL124W	145/15(42)
86	37.37/6.20				78/10(27)
87	37.42/6.22				116/14(42)
Phosphate					
74	35.93/5.86	32.33/5.36	Inorganic pyrophosphatase Cyt 68,400 Homd P	P00817/ YBR011C	128/13(53)
171	91.24/5.00	53.19/4.43	Constitutive acid phosphatase precursor CW 952 Glyc SP	P24031/ YBR092C	100/5(9)/R.GYSDVCDIFTEDELVR.Y (66)/K.SWYVPQGAR.V (20)
Glycerol					
81	36.76/5.68	28.10/5.35	(DL)-glycerol-3-phosphatase 1 Cyt 193,000 P, Ub SP	P41277/ YIL053W	98/11(36)
168	71.23/5.57	62.45/5.25	Dihydroxyacetone kinase 1 Cyt 23,600 P	P54838/ YML070W	115/15(35)
Pyrimidine					
78	36.08/6.48	34.95/5.80	Dihydroorotate dehydrogenase Cyt 264,000 homd	P28272/ YKL216W	89/12(49)/R. QKNYPDAPAIFFSVAG MSIDENLNLLR.K (5)
35	25.14/5.98	24.86/5.58	Uracil phosphoribosyltransferase P	P18562/ YHR128W	80/7(28)/K.LFYEKLPEDISER.Y (22)/ R.LLVEEGLNHLPVQK.Q (21)
45	27.00/5.89				227/21(79)
124	48.73/5.70				62/8(39)
Amino acid biosynthesis					
80	36.44/5.46	36.98/5.11	Homocysteine S-methyltransferase 2 Cyt, nuc 60,300 P	Q08985/ YPL273W	205/19(57)
88	37.72/5.46				93/11(45)
153	52.67/5.57	42.07/5.04	S-adenosylmethionine synthetase 1 Cyt 103,000 Hett	P10659/ YLR180W	93/12(29)
160	57.14/5.38				377/34(78)
161	57.22/5.28				80/6(11)/R.FVIGGPQGDAGLTGR.K (50)/K. NFDLRPGVLVK.E (15)

(*continued on next page*)

Table 3 (*continued*)

Number[a]	Mr/pI exp.[b]	Mr/pI theor.[c]	Name	Accession numbers[d]	Mascot scores/Matched peptides (%Coverage)/MS–MS ions (score)[e]
Amino acid biosynthesis					
145 148 158	51.67/5.45 52.13/5.36 54.17/5.19	42.51/5.18	S-adenosylmethionine synthetase 2 Cyt 22,000 Hett	P19358/ YDR502C	285/26(69) 133/15(41) 52/6(9)/R.FVIGGPQGDAGLTGR.K (19)/K.NFDLRPGVLVK.E(16)
165	66.14/5.90	57.55/5.46	Threonine synthase Cyt, nuc 26,000 P	P16120/ YCR053W	143/15(36)
159	54.18/5.41	49.11/5.10	Saccharopine dehydrogenase [NADP+, L-glutamate-forming] Cyt 57,500 Ketol-acid reductoisomerase	P38999/ YNR050C	251/10(15)/R.TKTDVVTSSYISPALR.E (90)/K.DLYHIPEAETVIR.G (64)/K.FGIEWADGTTETR.T (63)
99	41.78/7.26	44.51/9.10	Mit 883,000 P	P06168/ YLR355C	147/18(47)
Cofactor					
33 36	24.75/6.15 25.26/6.09	20.50/5.50	3-hydroxyanthranilate 3,4-dioxygenase Cyt, nuc 2330	P47096/ YJR025C	77/8(47) 89/9(53)
46	27.33/6.03	22.89/5.46	3,4-dihydroxy -2-butanone 4-phosphate synthase Cyt, mit 5460 Homd P	Q99258/ YDR487C	138/14(66)
9	12.09/6.97	17.78/6.44	Hit family protein 1 Cyt, nuc 5410	Q04344/ YDL125C	79/8(50)
Polyamine					
31	24.47/6.00	22.04/5.58	Polyamine N-acetyltransferase 1 Cyt 8680	Q12447/ YDR071C	124/12(60)
Transcription, RNA maturation and transport					
60	30.75/5.99	73.55/5.11	RNA polymerase III transcription initiation factor complex (TFIIIC) Nuc 15,800 P	P32367/ YBR123C	52/15(19)
58	29.96/6.05	561.18/4.90	Midasin Nuc, mit 538 P	Q12019/ YLR106C	54/37(7)

Table 3 (*continued*)

Number[a]	Mr/pI exp.[b]	Mr/pI theor.[c]	Name	Accession numbers[d]	Mascot scores/Matched peptides (%Coverage)/MS–MS ions (score)[e]
Protein fate					
18 23 27 29	16.87/5.46 21.00/5.23 23.20/5.06 23.99/5.02	24.12/4.46	Co-chaperone protein SBA1 Cyt, nuc 33,700 SP	P28707/ YKL117W	66/3(8)/K.DLESEYWPR.L (57) 62/3(7)/K.DLESEYWPR.L (54) 78/5(12)/K.DLESEYWPR.L (64) 86/7(22)/K.DLESEYWPR.L (57)
8 15	11.65/7.74 14.56/7.19	17.49/6.90	Peptidyl-prolyl cis-trans isomerase Cyt, mit 86,000 SP	P14832/ YDR155C	105/10(57) 136/13(67)
5	9.49/5.49	12.20/5.72	FK506-binding protein 1 Cyt 43,300 P	P20081/ YNL135C	195/14(91)
13	13.85/5.70	14.59/5.34	FK506-binding protein 2 Er 5400	P32472/ YDR519W	84/8(54)
6	9.72/5.79	20.57/6.75	ADP-ribosylation factor 1 Go 19,300 Lip	P11076/ YDL192W	73/7(26)/R.NTEGVIFVVDSNDR.S (34)/ K.NISFTVWDVGGQDRIR.S (8)
3	8.97/5.00	14.44/4.50	Nuclear transport factor 2 cyt	P33331/ YER009W	101/5(52)/NESMLTFETSQLQGAK.D (66)
64	32.23/6.21	34.89/5.8	Guanine nucleotide-binding protein subunit beta-like protein Cyt 333,112 P, Ac SP	P38011/ YMR116C	65/10(29)
14	13.93/6.45	16.61/6.04	Ubiquitin -conjugating enzyme E2 4 13,500 P	P15731/ YBR082C	K.DQWSPALTLSK.V (37)
16	15.96/6.64	15.70/6.30	Ubiquitin -conjugating enzyme variant MMS2 Cyt, nuc 2760 P	P53152/ YGL087C	85/10(76)
51	28.52/6.70	27.37/5.93	Family of serine hydrolases 1 Cyt, nuc 14,600	P38777/ YHR049W	130/15(51)
Cytoskeleton					
17 22	16.42/5.22 20.32/5.25	15.94/5.05	Cofilin Cyt 19,600 P	Q03048/ YLL050C	133/11(73) 115/7(36)/R.SKIVFFTWSPDT APVR.S (41)/K.IVFFTWSPDTAPVR.S (23)
2	7.91/5.44	13.72/5.47	Profilin Cyt	P07274/ YOR122C	86/9(53)

(*continued on next page*)

Table 3 (*continued*)

Number[a]	Mr/pI exp.[b]	Mr/pI theor.[c]	Name	Accession numbers[d]	Mascot scores/Matched peptides (%Coverage)/MS–MS ions (score)[e]
Signalling					
7	10.89/5.07	85.70/8.57	Protein SOK2 Nuc 314 P	P53438/ YMR016C	M.PIGNPINTNDIKSNR.M(31)
157	53.27/5.90	127.26/8.90	Inhibitory regulator protein BUD2/CLA2 1230	P33314/ YKL092C	56/18(18)/K.KLLTCLIWWSSMK.T (1)
62	31.65/6.13	121.87/9.65	Probable serine/ threonine-protein kinase Nuc P	Q12236/ YOL100W	55/18(16)
12	13.70/5.29	22.86/5.52	Synaptobrevin homolog YKT6 Pm Lip	P36015/ YKL196C	185/10(41)/R.QSIEEGNYIGHVYAR.S (72)/K.DLSQFGFFER.S (43)/R.IYYIGVFR.S (22)
Stress-related					
20	19.82/6.23	15.95/5.62	Superoxide dismutase Cyt, mit, nuc 519,000 P, Ub SP	P00445/ YJR104C	109/10(71)
63	31.83/5.30	40.38/5.95	Cytochrome c peroxidase Mit 6730 P	P00431/ YKR066C	67/9(28)
1	6.70/5.00	11.31/4.79	Thioredoxin-2 Cyt, Go, mem, nuc 17,237 P	P22803/ YGR209C	95/8(90)
72	35.13/6.23	34.44/5.69	Thioredoxin reductase 1 Cyt 292,000 Homd P SP	P29509/ YDR353W	61/5(8)/K.IVAGQVDTDEAGYIK.T (49)
10	12.70/5.36	12.48/4.98	Glutaredoxin-1 Cyt 6730 P SP	P25373/ YCL035C	163/9(70)/K.HIGGNDDLQELR.E (57)/K.TYCPYCHAALNTLFEK.L(31)
34	24.88/5.37	21.69/5.03	Peroxiredoxin TSA1 Cyt 378,000 Homd P SP	P34760/ YML028W	102/5(23)/R.DYGVLIEEEGVALR.G (77)
24	21.24/5.05	19.27/5.01	Peroxiredoxin	P38013/	221/19(92)
26	21.56/5.25		type-2 Cyt, mef	YLR109W	58/3(15)/K.SIGFELAVGDGVYWSGR.W (47)
110	44.79/5.11		Homd P, Ac, Ub		161/5(27)/K.SIGFELAVGDGVYWSGR.W (97)/K.FASDPGCAFTK.S (43)
30	24.46/7.09	21.43/6.51	Peptide methionine sulfoxide reductase Cyt, nuc 3070 P	P40029/ YER042W	108/11(58)

Table 3 (*continued*)

Number[a]	Mr/pI exp.[b]	Mr/pI theor.[c]	Name	Accession numbers[d]	Mascot scores/Matched peptides (%Coverage)/MS–MS ions (score)[e]
Stress-related					
170	79.60/5.70	66.66/5.37	Heat shock protein SSB2 Cyt 104,000 SP	P40150/ YNL209W	91/14(25)
49	28.17/5.59	23.86/5.31	HSP26 Cyt, nuc 19,300 P SP	P15992/ YBR072W	R.VITLPDYPGVDADNIK.A (27)
No well defined functional category/unknown					
103	42.22/6.49	39.46/5.78	3′(2′),5′ -bisphosphate nucleotidase Cyt 7330	P32179/ YOL064C	133/15(39)
19	18.00/5.05	11.59/4.92	Ubiquitin-like protein SMT3 precursor Nuc 2940 P SP	Q12306/ YDR510W	66/4(19)/K.VSDGSSEIFFKIK.K (17)/K.VSDGSSEIFFK.I (30)
28	23.42/6.04	21.01/5.46	Protoplast secreted protein 2 2330 SP	Q12335/ YDR032C	61/7(35)
70	34.81/5.17	35.17/7.75	Protein GCY Cyt, Nuc	P14065/ YOR120W	68/9(35)
54	29.24/5.75	27.69/5.28	Uncharacterized phosphatase Cyt, nuc 12,600	P53981/ YNL010W	131/14(57)
55	29.30/5.55	27.54/5.10	Uncharacterized protein YLR301W Cyt, nuc 15,400 P	Q05905/ YLR301W	123/6(19)/K.VTDEAYDGLVIVIGR.W (92)
56	29.72/5.44				177/16(65)
38	26.15/6.19	24.98/5.63	UPF0659 protein YMR090W Cyt 704	Q04304/ YMR090W	136/11(33)/K.ANDSFSTPLAIVR.T (48)/K.AEDRDFWYNIK.G (30)/K.AEDRDFWYNIK.G (29)
65	32.35/6.04	26.86/5.45	UPF0717 protein YJL055W Cyt, nuc 6440 P	P47044/ YJL055W	149/6(27)/K.SVCVYCGSSFGAK.A (65)/K.SVCVYCGSSFGAK.A (62)

[a] Numbers correspond to Fig. 3.
[b] Molecular weight (KDa) and isoelectric point calculated by using molecular weight standards and the PD-Quest Advanced (8.0.1) software.
[c] Molecular weight (KDa) and isoelectric point annotated in the UniProt database.
[d] UniProt and Saccharomyces genome database (SGD) accession numbers.
[e] Mascot score ($S=-10*\mathrm{Log}(P)$; where P is the probability that the observed match is a random event, peptide matched in MS analysis, percentage of sequence coverage (into the brackets), and ions sequence matched (ions score into the brackets) from MS–MS analysis.

distances of samples at the stationary phase. Stationary 2-DE maps showed more heterogeneity, even in intra-strain samples. When employing all of the spots based on the Euclidean distance the plot obtained is similar (Supplementary Fig. 4).

Spots in the same tree were compared, employing a clustering method and a representation of quantitative variations between strains and growth stages. This comparison permitted the determination of three main groups. The different expression dynamics of each spot could be distinguished in the heat map, allowing a definition of some expression groups, the presence or absence of some of them being a characteristic of a particular stage or strain: group I, only present in wild stationary, group II present in stationary wild and mutant, and group III, only present in wild.

Table 4 – Principal components (PCs) calculated from dataset.

Total variance explained			
Initial eigenvalues			
	All spots		
Component	Total	% of variance	Cumulative%
1	163.560	52.423	52.423
2	69.323	22.219	74.642
3	30.332	9.722	84.364
4	15.538	4.980	89.344
5	14.059	4.506	93.850
6	5.371	1.721	95.571
7	5.028	1.612	97.183
8	3.493	1.120	98.302
9	2.411	0.773	99.075
10	1.793	0.575	99.650
11	1.092	0.350	100.00

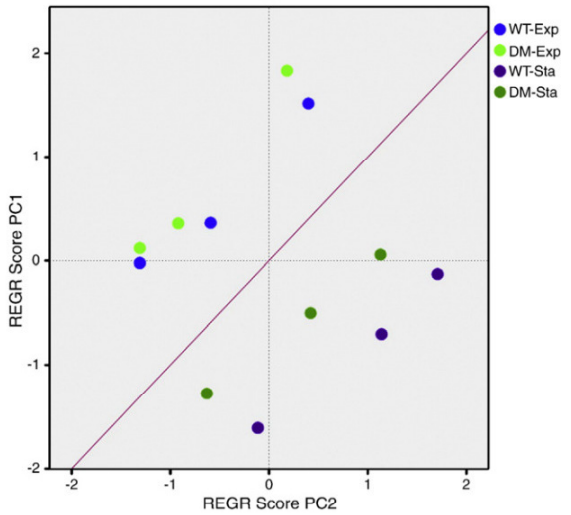

Fig. 4 – Representation of the samples based on main principal components found after PCA by 2-D plotting of the main principal components (PC1 and PC2).

4. Discussion

4.1. *Cell growth, potassium content, and transport kinetics*

The mutation in the *TRK* genes did not significantly affected cells growth when cultured in 50 mM KCl, as shown by similar OD_{600} and morphological characteristics (Fig. 1). Microscopic observations revealed cell division in both lines at the two sampling times, 8 (exponential phase, OD_{600} values of about 1.5) and 28 (stationary phase, OD_{600} values of about 3.0) h, with higher bud abundance during the exponential phase. Intracellular potassium measurements confirmed a similar status in wild type and *trk1,2* cells (Fig. 2). Interestingly, stationary cells of both strains kept less intracellular potassium than exponential cells suggesting that changes in the growth phase somehow affected cation homeostasis. An extensive study on genomic expression programs in yeast cells reported that *TRK1* seems to be less expressed at stationary phase [39] but no additional information reporting regulation of TRK1 at expression level has been published.

The process mediating potassium transport was analyzed by determining the kinetic constants of rubidium transport. While in wild type the TRk1/Trk2 system is active, in the mutant nonspecific transporter/s must be cooperating in the transport process [40]. Both processes seem to work at similar velocity (identical Vmax obtained). Significant differences between strains and phases were found when the affinity of the transport was determined. On the one hand, wild type cells showed higher affinity for potassium than *trk1,2* cells, and on the other, they adapted to changes in growth phase by increasing their affinity for the cation. Changes in the affinity (Km) were not observed in the double mutant showing that the residual non-specific potassium transport process working in these cells is poorly regulated, and cannot adapt to changing environmental conditions. Differences in intracellular potassium content between strains were not observed, as under high cation concentration in the medium is Vmax, which determines the rate of uptake. All together, the results of growth, potassium content and rubidium transport indicate that, at non limiting potassium, no important differences between wild type and mutant strains were found.

4.2. *2-DE protein profiles*

The protein yield of the extraction protocol (37.9–63.6 μg eq. SAB mg^{-1} cell dry weight; Table 2) was much lower, at about 10%, than the total protein content reported for yeast as determined by the Kjeldahl method (around 50% of the dry weight; http://www.cofalec.com; [41]), that used to happen with standard protein extraction protocols (reported 5×10^{-12} g protein per cell for high efficient protocols; [42]). In between 178 and 307 consistent spots were resolved after 2-DE (Table 2). This figure is within the range found in the literature when using 2-DE ([23]; Yeast protein map http://www.ibgc.u-bordeaux2.fr/YPM/index.html), and represents just a small fraction of the total yeast proteome. The total number of genes in yeast is of 6600 and that of verified ORFs 4857 (http://www.yeastgenome.org/cache/genomeSnapshot.html). By using epitope-tagged yeast fusion libraries with 6234 ORFs, 4251 protein products were observed [43], a similar figure to the set of GFP-fused proteins detected by fluorescence microscopy [44],

Fig. 5 – Two-way hierarchical cluster of differentially accumulated spots. A heat map representation of the clustered spots shows the protein value according to the standardized spot percent in each replicate, with red intensity indicating up-accumulation and black absence. Samples were grouped employing a correlation-based distance. Original plot was divided for a better presentation and reading. A, miniature of the original heatmap, B and C magnified upper and lower parts, respectively, including the names of the identified proteins.

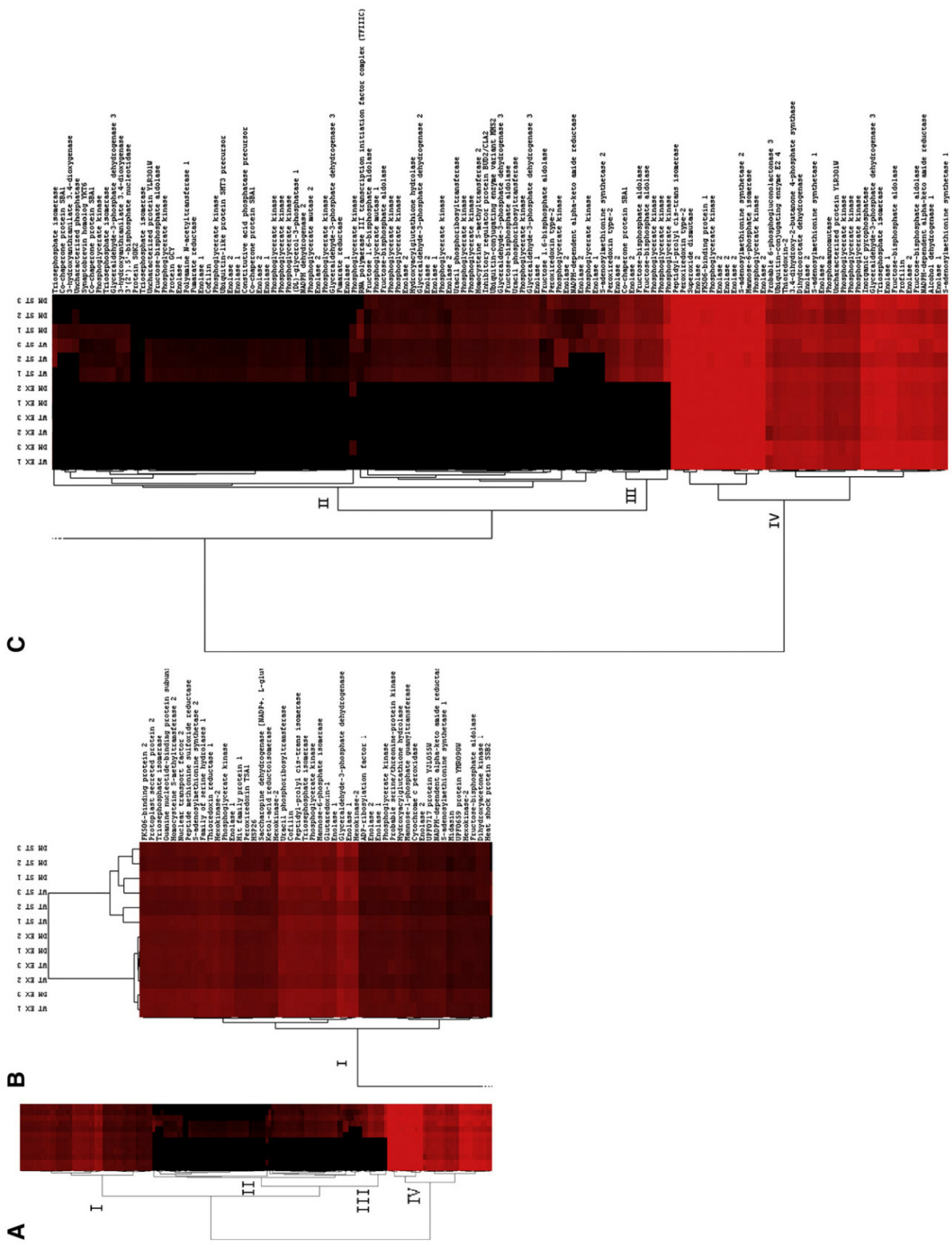
A
B
C
I
II
III
IV
DM ST 3
DM ST 2
DM ST 1
VT ST 3
VT ST 2
VT ST 1
DM EX 2
DM EX 1
VT EX 3
VT EX 2
DM EX 3
VT EX 1
Triosephosphate isomerase
Co-Chaperone protein SBA1
Uncharacterized protein YLR301W
Synaptobrevin homolog YKT6
Phosphoglycerate kinase
Triosephosphate isomerase
Fructose-bisphosphate aldolase
3-hydroxyanthranilate 3,4-dioxygenase
3'(2'),5'-bisphosphate nucleotidase
Enolase 2
Phosphoglycerate kinase
Protein SCY
Enolase 1
Polyamine N-acetyltransferase 1
Flavastatin reductase
Cofilin
Uncharacterized protein YKR043C
Constitutive acid phosphatase precursor
Co-Chaperone protein SBA1
Enolase 2
Enolase 1
Phosphoglycerate kinase
Phosphoglycerate kinase
Phosphoglycerate kinase
Phosphoglycerate kinase
IDH1-glycerol-3-phosphatase 1
Aldehyde reductase
Phosphoglycerate mutase 1
Phosphoglycerate mutase 2
Enolase 2
Phosphoglycerate kinase
Glyceraldehyde-3-phosphate dehydrogenase 3
Flavastatin reductase
Enolase 2
Enolase 1
Phosphoglycerate kinase
RNA polymerase III transcription initiation factor complex (TFIIIC)
Fructose-bisphosphate aldolase
Phosphoglycerate mutase 1
Fructose-bisphosphate aldolase
Phosphoglycerate kinase
Hydroxyacylglutathione hydrolase
Glyceraldehyde-3-phosphate dehydrogenase 2
Enolase 2
Enolase 1
Phosphoglycerate kinase
Uracil phosphoribosyltransferase
Phosphoglycerate kinase
Phosphoglycerate kinase
Homocysteine S-methyltransferase 2
Inhibitory regulator protein BUD2/CLA2
Glyceraldehyde-3-phosphate dehydrogenase 3
Fructose-bisphosphate aldolase
Phosphoglycerate kinase
Glyceraldehyde-3-phosphate dehydrogenase 3
Fructose 1,6-bisphosphate aldolase
Peroxiredoxin type-2
Peroxiredoxin type-2
Enolase 2
S-adenosylmethionine synthetase 2
Peroxiredoxin type-2
Co-Chaperone protein SBA1
Enolase 2
Fructose-bisphosphate aldolase
Fructose-bisphosphate aldolase
Phosphoglycerate kinase
Phosphoglycerate kinase
Phosphoglycerate kinase
Peptidyl-prolyl cis-trans isomerase
Phosphoglycerate kinase
Superoxide dismutase
Enolase 2
PDZ domain protein
Enolase 2
Enolase 2
S-adenosylmethionine synthetase 2
Mannose-6-phosphate isomerase
Phosphoglycerate kinase
Enolase 2
Probable 6-phosphogluconolactonase 3
Ubiquitin-conjugating enzyme E2 4
3,4-dihydroxy-2-butanone 4-phosphate synthase
Dihydrotoxicate dehydrogenase
Enolase 2
S-adenosylmethionine synthetase 1
Enolase 2
Phosphoglucomutase
Uncharacterized protein YLR301W
Phosphoglycerate kinase
Phosphoglycerate kinase
Phosphoglycerate kinase
Inosamic pyrophosphatase
Glyceraldehyde-3-phosphate dehydrogenase 3
Triosephosphate isomerase
Enolase 2
Fructose-bisphosphate aldolase
Profilin
Enolase 1
Fructose-bisphosphate aldolase
NADPH-dependent alpha-keto amide reductase
Aldose reductase
Enolase 1
S-adenosylmethionine synthetase 1
PKS06-binding protein 2
Protoplast secreted protein 2
Ribosomal protein L3-beta
Guanine nucleotide-binding protein subunit
Homocysteine S-methyltransferase 2
Aldose reductase-related protein 2
Peptide methionine sulfoxide reductase
S-adenosylmethionine synthetase 2
Flavastatin reductase 1
Thioredoxin reductase 1
Hexokinase-2
Phosphoglycerate kinase
Enolase 1
Hit family protein 1
Peptidoprolin ?ib1
HSP26
Saccharopine dehydrogenase (NADP+, L-glu
Aldose reductase
Hexokinase-2
Uracil phosphoribosyltransferase
Cofilin 1
Peptidyl-prolyl cis-trans isomerase
Triosephosphate isomerase
Phosphoglycerate kinase
Mannose-6-phosphate isomerase
Enolase-phosphatase-1
Glyceraldehyde-3-phosphate dehydrogenase
Enolase 1
Hexokinase-2
ADP-ribosylation factor 1
Enolase 1
Enolase 1
Phosphoglycerate kinase
Serine/threonine-protein kinase
Hydroxyacylglutathione hydrolase
Mannose-1-phosphate guanyltransferase
Cytosolic 5'-nucleotidase
Enolase 2
UPF0071 protein YJL053W
Probable 2-hydroxy-3-oxo-4-keto amide reductase
S-adenosylmethionine synthetase 1
Enolase 2
UPF0213 protein YMR090W
Hexokinase-2
Fructose-bisphosphate aldolase
Phosphoglycerate kinase
Heat shock protein SSB2

corresponding to about 80% of the ORFs with assigned gene names. Out of the detected proteins at least 4500 are expressed during log-phase growth in rich media. Combined results from different experiments have been used to construct the *Saccharomyces cerevisiae* PeptideAtlas with 4063 proteins matching ORFs [45]. In single proteomics experiments around 500 (2-DE approaches) and 2000 (LC based approach) protein species are identified [22,27]. As a characteristic of the 2-DE technique, minor as well as hydrophobic and extreme pI Mr proteins are missed [46]. Protein yield, number of resolved and variable spots, as it happened with cell growth estimations and potassium content, revealed more differences in between growth phases than strains, and with higher and slightly lower values for, respectively, the stationary phase and double mutant strain.

4.3. *MS analysis and protein identification*

From mass spectra and by searching the UniProt database, 171 proteins, including major and variable spots, were identified (Table 3). In general, those proteins corresponded to those present at high number of copies per cell (in the 2000–300,000 copies/cell range; [43,44]). When comparing experimental and theoretical Mr and p*I* we found that some spots could correspond to protein aggregates, degradation products, and PTM (phosphorylation) variants, thus justifying the multiple spot identification of the same protein. This conclusion is supported by published papers and information provided at the UniProt database (http://www.uniprot.org/). Thus, identified low molecular weight species corresponded to proteins reported to belong to the group of those with high turnover in glucose grown yeast cells at steady state [47]. On the other hand, and by using proteome chip technology, over 4000 phosphorylation events involving 1325 different proteins have been reported [48]. As annotated at the UniProt database, hexokinase, triose phosphate isomerase, glyceraldehyde-3-phosphate dehydrogenase, and enolase belong to the group of phosphoproteins. The highest level of hexokinase phosphorylation occurs in a medium with a low glucose concentration [49]. In any case, these conclusions need to be experimentally supported.

In all, matched proteins belonged to 71 different unique gene products. The set of identified proteins was predominantly cytosolic, and to a lesser extent mitochondrial or nuclear (Table 2). Curiously, none of the mitochondrial ones corresponded to enzymes of the Krebs cycle, but to redox enzymes, this indicating fermentative rather than respiratory metabolism in both strains and growth phases. Almost half the identified proteins are enzymes of the carbohydrate metabolism, the glycolitic ones being those most represented (seven enzymes out of the 10 from glucose to pyruvate). The rest were related to defense (stress-related, including antioxidants and HSP), amino acid (Met, Thr, Lys, and aliphatic), glycerol, pyrimidine, and cofactor metabolism, redox balancing, transcription, RNA maturation and transport, protein fate, cytoskeleton, and signalling. Eight proteins were unknown or with no well defined functional category. Looking at the more abundant proteins (Supplementary Table B), we found a similar ranking among samples, with enzymes of the glycolysis (enolase, PGK, TPI, aldolase, and GA3PDH) and stress-related (peroxiredoxin type-2, SOD) plus peptidyl-prolyl cis-trans isomerase, S-adenosylmethionine synthetase 2, and FK506-binding protein 1 being the most abundant, this indicating no large differences in status and metabolism between strains and sampling times. Similar figures and identified proteins have been reported by Bruckmann et al. [24] when comparing the proteome of aerobically and anaerobically grown cells. The biological or metabolic characteristics can be inferred from the identified proteins, thus active fermentation rather than respiration, cell wall biosynthesis, redox homeostasis, biosynthesis of aminoacids, coenzymes, nucleotides, and RNA, and protein turnover can be concluded. In glucose rich media, the main pathway of glucose utilization is the glycolitic chain leading to ethanol as almost the only end-product, independently of the presence of oxygen, with practically absent TCA cycle, and with this glucose repression primarily mediated by hexokinase-2 [41,50]. This is even true while the glucose is not below a certain limit. Assuming the growth yield of 1 mg yeast 46 μmol^{-1} glucose in enriched medium [41], initial 11 mmol glucose would be reduced to around 4 mmol at the second sampled time, this being enough to repress respiration. Other indicative proteins are mannose-1-phosphate guanyltransferase (involved in cell cycle progression through cell-size checkpoint; [43]) NADPH-dependent alpha-keto amide reductase (transiently induced shortly after the switch from aerobic to anaerobic growth at protein level; [51]), cofilin (has a role in the mitotic reorganization of the actin cytoskeleton; [52]), profilin (bipolar cellular bud site selection, http://www.uniprot.org/uniprot/P07274), protein SOK2 (regulates the expression of genes important to growth and development; may inhibit the switch from unicellular to filamentous growth; [53] Ward et al. 1995), HSP26 (expressed during the entry into stationary phase resulting from glucose limitation; http://www.uniprot.org/uniprot/P15992).

4.4. *Differences between strains and growth phases*

PCA analysis was performed with the whole (313) spots. PC1 and PC2 allowed the separation of growth phases but not of strains, with PC3 and PC4 being necessary to discriminate strains at the stationary phase, but not at the exponential one. This support indicated hypothesis in terms of close similarities in between strains, especially at the exponential phase. The selection of the spots with higher loadings over PCs1–4 allowed us to define growth stage biomarkers that could be of great interest. Out of the identified functional catalogued proteins, those with the highest correlation in PC1 corresponded to enzymes of the glycolisis and redox homeostasis. In comparative proteomics studies of *S. cerevisiae* cells grown in chemostat cultures limited for carbon sources, it has been shown that out of 400 proteins analyzed only enzymes involved in central carbon metabolism showed a significant change [54].

Differential spots were clustered employing correlation distance (Fig. 5). As stated above, there were almost no differences between strains at the exponential phase, but at the stationary one. In any case, more differences in between phases than strains have been found. As a general tendency, quite a number of proteins were absent in samples from exponential phase, but were detected in stationary wild, and to a lesser extent, mutant. They constitute the cluster group

II (wild and mutant), and group III (wild). Within the latter, protein species of the glycolisis, have been found. The exact meaning of each species in terms of glucose catabolism regulation remains to be investigated, but, as a whole, our data could suggest a more active glycolitic pathway at the stationary phase in order to satisfy a higher energy demand or intermediate metabolites for biosynthetic routes. Daran-Lapujade et al. [55] have developed a method to dissect hierarchical regulation into contributions by transcription, translation, protein degradation, and PTM contributions to glycolytic fluxes in *S. cerevisiae*. Up to 10-fold changes in flux through the glycolytic enzymes can be found, with each enzyme contribution depending on the conditions and enzyme. Regulation of protein synthesis or degradation was the most important factor, with transcription playing a minor role [55]. In parallel to the glycolysis rate increase, an overproduction of subproducts could be expected, such as methylglyoxal that would request the activation of enzymes of its detoxification pathway, as has been observed with glyoxalase II (spot 75). The up-accumulation of fumarate reductase and NADPH dehydrogenase observed in stationary wild but not mutant cells, would help to balance NADH/NAD as a consequence of higher consumption of NAD in the glycolytic pathway and to supply reducing equivalents for biosynthesis, and also indicates some imbalance in the mutant. Curiously, no differences were observed for alcohol dehydrogenase (spot 108), this not contributing to redox imbalance. Higher oxidative stress conditions at the stationary phase, corresponding to a more active catabolism, could be deduced from the up-accumulation in both strains of peroxdiredoxin type 2 (spots 26 and 110). BUD2/CLA 2, which participates in the regulation of bud-site selection was newly detected at the stationary phase in both type of cells. The same, but only in wild, was observed with SOK 2 (spot 7), involved in the inhibition of the switch from unicellular to filamentous growth, and cofilin (which has a role in the mitotic reorganization of the actin cytoskeleton.

As commented above, a number of the identified spots corresponded to low experimental molecular weight protein species, speculating those being degradation products. These appeared newly in stationary wild and double mutants, indicating more intense proteolysis at this stage. I was the case of spots 11, 25 (fructose bis-phosphate aldolase, 40, 50, 53, 90, 93, 94 (phosophoglycerate kinase), and 21, 59, 61, 84 (enolase). More proteolysis is supported by the new detection of the ubiquitin-conjugating enzyme variant MMs2 (spot 16).

Observed changes could be more related to cell density, with growth rate changes than to nutritional conditions. Castrillo et al. [56] have reported a first comprehensive system biology study on growth rate control in eukaryotes, using *S. cerevisiae* as model system. Among the group of proteins whose levels were modified with growth, irrespective of the specific nutrient limitation are some identified here, such as enzymes of the glycolisis, methionine biosynthesis and metabolism, ubiquitin-dependent protein catabolism, and purine nucleotide biosynthesis. While comparing the proteome of different *S. cerevisiae* strains, including wild and mutants, Kummel et al. [50] have observed higher abundance in glycolityc enzyme proteins in those with lower growth rates. Cheng et al. [57] have published on changes in the 2-DE protein profile in yeast as a consequence of inoculum density, with increases in glycolytic, methionine and redox enzymes, and heat shock proteins up-accumulated in high density inoculation.

5. Conclusions

Despite the limitations of the used protein extraction protocols and separation by 2-D electrophoresis in terms of protein yield and proteome coverage, this platform has provided information on the features of the proteome of wild and potassium transport-affected mutant *trk1,2* at the exponential and stationary phases of the growth curve and under optimal growth potassium concentration (50 mM). From 178 to 306 spots were resolved, with 171 identified, these corresponding to 71 unique gene products. The proteome is dominated by high abundant, cytosolic species and glycolitic enzymes. This set provided information on glycolysis, cell wall biosynthesis, redox homeostasis, biosynthesis of aminoacids, coenzymes, nucleotides, and RNA, and protein turnover, apart from cell division and growth. Differences found were more associated with the growth phase (exponential versus stationary) than to the strains (wild versus mutant), the letter being more related to the cell density than to the nutritional conditions. As a general tendency, a number of spots newly appeared at the stationary phase in the wild, and to a lesser extent, in the mutant, has been observed. These up-accumulated spots corresponded to glycolitic enzymes, indicating a more active glucose catabolism, accompanied by an accumulation of methylglyoxal detoxification, and redox-homeostasis enzymes. Also, more extensive proteolisis was observed at the stationary phase, this resulting in an accumulation of low Mr protein species.

Acknowledgements

This work is part of the research projects GEN2006-27748-C2-2-E/SYS (SysMo ERA-NET) and BFU2008-04188-C03-03 (FEDER co-financed). Financial support from the Spanish Ministry of Science and Education, Junta de Andalucía and University of Cordoba is acknowledged.

Appendix A. Supplementary Data

Supplementary data associated with this article can be found, in the online version, at doi:10.1016/j.jprot.2010.07.003.

REFERENCES

[1] Gouaux E, MacKinnon R. Principles of selective ion transport in channels and pumps. Science 2005;310:1461–5.
[2] Rodriguez-Navarro A. Potassium transport in fungi and plants. Biochim Biophys Acta 2000;1469:1–30.
[3] Ariño J, Ramos J, Sychrova H. Alkali-metal cation transport and homeostasis in yeasts. Microbiol Mol Biol Rev 2010;74:95–120.

[4] Clark R, Proks P. ATP-sensitive potassium channels in health and disease. Adv Exp Med Biol 2010;654:165–92.
[5] Flourakis M, Prevarskaya N. Insights into Ca^{2+} homeostasis of advanced prostate cancer cells. Biochim Biophys Acta 2009;1793:1105–9.
[6] Edwards A. Modeling transport in the kidney: investigating function and dysfunction. Am J Physiol Renal Physiol 2010;298:475–84.
[7] Váli L, Stefanovits-Bányai E, Szentmihályi K, Drahos A, Sardy M, Febel H, et al. Alterations in the content of metal elements and fatty acids in hepatic ischaemia-reperfusion: induction of apoptotic and necrotic cell death. Dig Dis Sci 2008;53:1325–33.
[8] Wolfs JLN, Comfurius P, Bekers O, Zwaal RFA1, Balasubramanian K, Schroit AJ, et al. Direct inhibition of phospholipid scrambling activity in erythrocytes by potassium ions. Cell Mol Life Sci 2009;66:314–23.
[9] Krumschnabel G, Maehr T, Nawaz M, Schwarzbaum PJ, Manzl C. Staurosporine-induced cell death in salmonid cells: the role of apoptotic volume decrease, ion fluxes and MAP kinase signaling. Apoptosis 2007;12:1755–68.
[10] Blumwald E. Sodium transport and salt tolerance in plants. Curr Opin Cell Biol 2000;12:431–4.
[11] Petranovic D, Vemuri GN. Impact of yeast systems biology on industrial biotechnology. J Biotechnol 2009;144:204–11.
[12] Diaz-Ruiz R, Uribe-Carvajal S, Devin A, Rigoulet M. Tumor cell energy metabolism and its common features with yeast metabolism. Biochim Biophys Acta-Rev Cancer 2009;1796:252–65.
[13] Braun RJ, Buttner S, Ring J, Kroemer G, Madeo F. Nervous yeast: modeling neurotoxic cell death. Trends Bioch Sci 2010;35:135–44.
[14] Abreu RD, Penalva LO, Marcotte EM, Vogel C. Global signatures of protein and mRNA expression levels. Mol Biosys 2009;5:1512–26.
[15] Krogan NJ, Cagney G, Yu HY, Zhong GQ, Guo XH, Ignatchenko A, et al. Global landscape of protein complexes in the yeast *Saccharomyces cerevisiae*. Nature 2006;440:637–43.
[16] Goffeau A, Barrell BG, Bussey H, Davis RW, Dujon B, Feldmann H, et al. Life with 6000 genes. Science 1996;274:546–67.
[17] Snyder M, Gallagher JEG. Systems biology from a yeast omics perspective. FEBS Lett 2009;583:3895–9.
[18] Ruiz A, Ariño J. Function and regulation of the *Saccharomyces cerevisiae* ENA sodium ATPase system. Eukaryot Cell 2007;6: 2175–83.
[19] Hohmann S, Pim WH, editors. Yeast stress responses. Topics in current genetics. Berlin: Springer; 2003.
[20] Navarrete C, Petrezsélyová S, Barreto L, Martínez JL, Zahrádka J, Ariño J, et al. Lack of main K^+ uptake systems in *Saccharomyces cerevisiae* cells affects yeast performance both in potassium sufficient and potassium limiting conditions. FEMS Yeast Res 2010;10:508–17.
[21] Karhumaa K, Pahlman A-K, Hahn-Hagerda B, Levander F. Proteome analysis of the xylose-fermenting mutant yeast strain TMB 3400. Yeast 2009;26:371–82.
[22] Usaite R, Wohlschlegel J, Venable JD, Park SK, Nielsen J, Olsson L, et al. Characterization of global yeast quantitative proteome data generated from the wild-type and glucose repression *Saccharomyces cerevisiae* strains: the comparison of two quantitative methods. J Prot Res 2009;7:266–75.
[23] Massoni A, Moes S, Perrot M, Jenoe P, Boucherie H. Exploring the dynamics of the yeast proteome by means of 2-DE. Proteomics 2009;9:4674–85.
[24] Bruckmann A, hensbergen PJ, Balog CIA, Deelder AM. Proteome análisis of aerobically and anaerobically grown *Saccharomyces cerevisiae* cells. J Prot 2009;71:662–9.
[25] Cheng JS, Ding MZ, Tian HC, Yuan YJ. Inoculation-density-dependent responses and pathway shifts in *Saccharomyces cerevisiae*. Proteomics 2009;9:4704–13.
[26] Braconi D, Bernardini G, Possenti S, Laschi M, Arena S, Scaloni A, et al. Proteomics and redox-proteomics of the effects of herbicides on a wild-type wine *Saccharomyces cerevisiae* Strain. J Proteome Res 2009;8:256–67.
[27] Perrot M, Moes S, Massoni A, Jenoe P, Boucherie H. Yeast proteome map (last update). Proteomics 2009;9:4669–73.
[28] Serrano R, Kielland-Brandt MC, Fink GR. Yeast plasma membrane ATPase is essentials for growth and has homology with $(Na^+ + K^+)$, K^+- and Ca^{2+}-ATPases. Nature 1986;319:689–93.
[29] Bertl A, Ramos J, Ludwig J, Lichtenberg-Frate H, Reid J, Bihler H, et al. Characterization of potassium transport in wild-type and isogenic yeast strains carrying all combinations of *trk1*, *trk2* and *tok1* null mutations. Mol Microbiol 2003;47:767–80.
[30] Gray JV, Petsko GA, Johnston GC, Ringe D, Singer RA, Werner-Washburne M. "Sleeping beauty": quiescence in *Saccharomyces cerevisiae*. Microbiol Mol Biol Rev 2004;68: 187–206.
[31] Herman PK. Stationary phase in yeast. Curr Opin Microbiol 2002;5:602–7.
[32] Ramos J, Haro R, Rodriguez-Navarro A. Regulation of potassium fluxes in *Saccharomyces cerevisiae*. Biochim Biophys Acta 1990;1029:211–7.
[33] Görg A, Postel W, Weser J, Günther S, Strahler J, Hanash SM, et al. Horizontal two-dimensional electrophoresis with immobilized pH gradients in the 1st-dimension in the presence of nonionic detergent. Electrophoresis 1987;8:45–51.
[34] Mathesius U, Keijzers G, Natera SHA, Weinman JJ, Djordjevic MA, Rolfe BG. Establishment of a root proteome reference map for the model legume *Medicago truncatula* using the expressed sequence tag database for peptide mass fingerprinting. Proteomics 2001;1:1424–40.
[35] Meunier B, Dumas E, Piec I, Béchet D, ebraud M, Hocquette JF. Assessment of hierarchical clustering methodologies for proteomic data mining. J Prot Res 2007;6:358–66.
[36] Valledor L, Castillejo MA, Lenz C, Rodriguez R, Canal MJ, Jorrin J. Proteomic analysis of *Pinus radiata* needles: 2-DE map and protein identification by LC/MS/MS and substitution-tolerant database searching. J Prot Res 2008;7: 2616–31.
[37] Sghaier-Hammami B, Valledor L, Noureddine D, Jorrin J. Proteomic analysis of the development and germination of date palm (*Phoenix dactylifera* L.) zygotic embryos. Proteomics 2009;9:2543–54.
[38] Schevchenko A, Wilm M, Vorm O, Mann M. Mass spectrometric sequencing of proteins from silver stained polyacrylamide gels. Anal Chem 1996;68:850–8.
[39] Gasch AP, Spellman PT, Kao CM, Carmel-Harel O, Eisen MB, Storz G, et al. Genomic expression programs in the response of yeast cells to environmental changes. Mol Biol Cell 2000;11: 4241–57.
[40] Madrid R, Gomez MJ, Ramos J, Rodriguez-Navarro A. Ectopic potassium uptake in trk1 trk2 mutants of *Saccharomyces cerevisiae* correlates with a highly hyperpolarized membrane potential. J Biol Chem 1998;273:14838–44.
[41] Lagunas R, Gancedo JM. Reduced pyridine-nucleotides balance in glucose-growing *Saccharomyces cerevisiae*. Eur J Biochem 1973;37:90–4.
[42] Von der Haar T. Optimized protein extraction for quantitative proteomics of yeast. PLoS ONE 2007;10:e1078.
[43] Ghaemmaghami S, Huh W, Bower K, Howson RW, Belle A, Dephoure N, et al. Global analysis of protein expression in yeast. Nature 2003;425:737–41.
[44] Huh WK, Falvo JV, Gerke LC, Carroll AS, Howson RW, Weissman JS, et al. Global analysis of protein localization in budding yeast. Nature 2003;425:686–91.
[45] King NL, Deutsch EW, Ranish JA, Nesvizhskii AI, Eddes JS, Mallick P, et al. Analysis of the *saccharomyces cerevisiae* proteome with PeptideAtlas. Genome Biol 2006;7:R106.
[46] Gorg A, Drews O, Luck C, Weiland F, Weiss W. 2-DE with IPGs. Electrophoresis 2009;30:S122–32.

[47] Pratt JM, Petty J, Riba-Garcia I, Robertson DHL, Gaskell SJ, Oliver SG, et al. Dynamics of protein turnover, a missing dimension in proteomics. Mol Cel Prot 2002;1:579–91.
[48] Ptacek J, Devgan G, Michaud G, Zhu H, Zhu XW, Fasolo J, et al. Global analysis of protein phosphorylation in yeast. Nature 2005;438:679–84.
[49] Vojtek AB, Fraenkel G. Phosphorylation of yeast hexokinases. Eur J Biochem 1990;190:371–5.
[50] Kummel A, Ewald JC, Fendt SM, Jol SJ, Picotti P, Aebersold R, et al. Differential glucose repression in common yeast strains in response to HXK2 deletion. FEMS Yeast Res 2010;10:322–32.
[51] Salusjaervi L, Poutanen M, Pitkaenen J-P, Koivistoinen H, Aristidou A, Kalkkinen N, et al. Proteome analysis of recombinant xylose-fermenting Saccharomyces cerevisiae. Yeast 2003;20:295–314.
[52] Ojala PJ, Paavilainen V, Lappalainen P. Identification of yeast cofilin residues specific for actin monomer and PIP2 binding. Biochemistry 2001;40:15562–9.
[53] Ward MP, Gimeno CJ, Fink GR, Garrett S. SOK2 may regulate cyclic AMP-dependent protein kinase-stimulated growth and pseudohyphal development by repressing transcription. Mol Cell Biol 1995;15:6854–63.
[54] Kolkman A, Olsthoorn MA, Heeremans CEM, Heck AJR, Slijper M. Comparative proteomic analysis of *Saccharomyces cerevisiae* grown in chemostat cultures limited for glucose or ethanol. Mol Cell Prot 2005;4:1–11.
[55] Daran-Lapujade P, Rossell S, van Gulik WM, de Groot MJL, Slijper M, et al. The fluxes through glycolytic enzymes in *Saccharomyces cerevisiae* are predominantly regulated at postrancriptional levels. Proc Natl Acad Sci USA 2007;104: 15753–8.
[56] Castrillo JI, Zeef LA, Hoyle DC, Zhang N, Hayes A, Gardner DCJ, et al. Growth control of the eukaryote cell: a systems biology study in yeast. J Biol 2007;6:4.
[57] Cheng J-S, Ding M-Z, Tian H-Ch, Yuan Y-J. Inoculation-density-dependent responses and pathway shift in *Saccharomyces cerevisiae*. Proteomics 2009;9:4704–13.

Appendix 4: Adaptation to potassium starvation of wild-type and K^+-transport mutant (*trk1,2*) of *Saccharomyces cerevisiae*: 2-dimensional gel electrophoresis-based proteomic approach

MicrobiologyOpen

Open Access

Adaptation to potassium starvation of wild-type and K^+-transport mutant (*trk1,2*) of *Saccharomyces cerevisiae*: 2-dimensional gel electrophoresis-based proteomic approach

Samuel Gelis[1], Miguel Curto[2], Luis Valledor[3], Asier González[4], Joaquín Ariño[4], Jesús Jorrín[2] & José Ramos[1]

[1]Department of Microbiology, University of Córdoba, Córdoba, Spain
[2]Department of Biochemistry and Molecular Biology, Agricultural and Plant Biochemistry and Proteomics Research Group, University of Córdoba, Córdoba, Spain
[3]Molecular Systems Biology, University of Vienna, Vienna, Austria
[4]Institut de Biotecnologia i Biomedicina and Departament de Bioquímica i Biologia Molecular, Universitat Autònoma de Barcelona, Bellaterra 08193, Barcelona, Spain

Keywords
2D-gels, potassium homeostasis, *Saccharomyces cerevisiae*, *TRK1*, *TRK2*.

Correspondence
José Ramos, Departamento de Microbiología, Edificio Severo Ochoa, Campus de Rabanales, Universidad de Córdoba, E14071 Córdoba, Spain. Tel: +34 957 212 527; Fax: +34 957 218 650; E-mail: mi1raruj@uco.es

Funded by the Ministry of Science and Innovation, Spain, and FEDER.
Received: 30 November 2011; Revised: 29 March 2012; Accepted: 3 May 2012

***MicrobiologyOpen* 2012; 1(2): 182–193**

doi: 10.1002/mbo3.23

Abstract

Saccharomyces cerevisiae wild-type (BY4741) and the corresponding mutant lacking the plasma membrane main potassium uptake systems (*trk1,trk2*) were used to analyze the consequences of K^+ starvation following a proteomic approach. In order to trigger high-affinity mode of potassium transport, cells were transferred to potassium-free medium. Protein profile was followed by two-dimensional (2-D) gels in samples taken at 0, 30, 60, 120, 180, and 300 min during starvation. We observed a general decrease of protein content during starvation that was especially drastic in the mutant strain as it was the case of an important number of proteins involved in glycolysis. On the contrary, we identified proteins related to stress response and alternative energetic metabolism that remained clearly present. Neural network-based analysis indicated that wild type was able to adapt much faster than the mutant to the stress process. We conclude that complete potassium starvation is a stressful process for yeast cells, especially for potassium transport mutants, and we propose that less stressing conditions should be used in order to study potassium homeostasis in yeast.

Introduction

Alkali metal cations, especially potassium and sodium play an important role in cell physiology and metabolism. Among organisms studied, the yeast *Saccharomyces cerevisiae* is still chosen as a model to elucidate homeostasis in eukaryotic cells because of the availability of the complete genome sequence (Goffeau et al. 1996), an in silico prediction of all transporters (Nelissen et al. 1997), a wide range of genetic tools to generate mutants, and availability of postgenomic tools such as proteomic databases.

In yeasts cells, intracellular concentrations of Na^+ and K^+ are around 10–20 and 200–300 mM, respectively. K^+ is required for many physiological functions, such as cell volume and intracellular pH regulation, maintenance of stable potential across the plasma membrane, protein synthesis, and enzyme activation (Hoffman 1964; Ariño et al. 2010). *Saccharomyces cerevisiae* cells are able to grow in media containing a large range of K^+, from 2 μM to 2 M, in all conditions internal K^+ remains quite constant that allows normal cell growth and division (Ramos et al. 1994; Haro and Rodríguez-Navarro 2002).

Two different systems of K^+ uptake have been described in *S. cerevisiae* (Ramos and Rodriguez-Navarro 1986). A low-affinity mode of transport with a Km in the millimolar range, observed in cells cultured without K^+ limitation, and a high-affinity transport with a Km in the micromolar range observed in either K^+-starved cells or cells growing in the presence of Na^+. Full activity of the high-affinity K^+ transport is usually observed after growing the cells without K^+ limitation in minimal medium and then starving the cells during 4–5 h in the same medium lacking added K^+ (i.e., arginine phosphate medium; Rodriguez-Navarro and Ramos

Table 1. Optical density, protein yield, and number of spots resolved in 2-DE, with indication of qualitative and quantitative differences of spots regarding the wild-type strain at time 0.

						Variable spots (with respect to WT 0)			
						Qualitative		Quantitative 1.5-fold	
Yeast strain	Time (min)	OD_{600nm} mean SD	DW* (mg)	Protein yield μg eq. SAB/mg DW	Total of consistent spots	Appear	Disappear	Up	Down
BY4741 (WT)	0	1.89 ± 0.04	96.54	37.55	271				
	30	2.02 ± 0.068	103.17	37.34	264	0	15	6	10
	60	2.17 ± 0.076	110.52	37.15	253	0	25	5	15
	180	2.25 ± 0.05	114.75	36.17	248	0	32	2	32
	300	2.28 ± 0.093	116.13	34.20	239	0	33	1	48
BYT12 (*trk1,2*)	0	1.86 ± 0.032	95.01	31.08	208	0	69	11	47
	30	1.80 ± 0.05	91.95	29.23	193	0	95	13	31
	60	1.81 ± 0.051	92.16	16.84	170	0	110	11	21
	180	1.73 ± 0.042	88.38	8.44	138	0	142	9	16
	300	1.67 ± 0.059	85.02	5.28	106	0	162	6	20

*$DW - [0.51 \times OD_{600nm}]$ mg·mL^{-1} medium.

1984). Active K^+ uptake is mediated by two membrane transporters, Trk1 and Trk2, Trk1 being the most important (Ko et al. 1990; Ramos et al. 1994). Deletion of both genes leads to a growth inhibition at low K^+ concentrations, hyperpolarization of plasma membrane, and observation of residual ectopic potassium transport (Madrid et al. 1998; Navarrete et al. 2010). Those phenotypes appear to be due mainly to *TRK1* deletion as the effect of *TRK2* absence is almost negligible in most experimental conditions (Madrid et al. 1998).

Two-dimensional (2-D) gel-based comparative proteomics analyses have been widely used to characterize yeast strains (Usaite et al. 2008; Karhumaa et al. 2009), growth phase (Bruckmann et al. 2009; Cheng et al. 2009; Massoni et al. 2009), or stress responses (Braconi et al. 2009). In our laboratory, we previously focused our proteomic analysis on the double mutant (DM) *trk1,trk2* mutant growing without potassium limitation in exponential and stationary phase (Curto et al. 2010). It was observed that there were almost no differences between wild-type and DM strains at the exponential phase of growth. However, significant differences related mainly to glycolytic enzymes were found at stationary phase.

In this study, a similar kind of analysis was used to characterize the same wild-type and DM *trk1,trk2* in the extreme condition of potassium starvation. Statistically significant differences were observed in the protein 2-D profile, corresponding both to the mutations and/or potassium starvation. Spot intensity values were subjected to uni- and multivariant statistical analyses and a clustering test. Major and variable spots were mass spectrometry (MS) analyzed, and 73 protein species, corresponding to 49 unique gene products were identified. We conclude that potassium starvation is a very stressful condition to study potassium homeostasis, especially in the case of double *trk1,2* mutant strain.

Results

2-D protein profiles

Strains were grown in translucent YNB-F media with no limiting potassium (50 mM KCl) until they reach an OD_{600nm} of around 1.9 in order to obtain high cell biomass but still in exponential phase (Navarrete et al. 2010). Parental strain BY4741 and DM *trk1,trk2* were then transferred to medium without added potassium, samples of cells were taken during 5 h and proteins were extracted. Protein yield obtained after extraction plus TCA–acetone precipitation was evaluated. Cells of both strains kept full viable as monitored by colony forming units counts ($9.3 \times 10^6 \pm 0.2$ and $9.5 \times 10^6 \pm 0.3$ at time zero in wild-type and DM strains, respectively, and $2.1 \times 10^7 \pm 0.3$ and $1.1 \times 10^7 \pm 0.4$ after 5-h starvation), but total protein yield decreased in function of starvation time from 37.55 to 34.20 μg eq. serum albumin bovine mg^{-1} dry weight for the parental strain and from 31.08 to 5.28 μg eq. SAB mg^{-1} dry weight for the mutant strain were obtained (Table 1).

After 2-D electrophoresis and Coomassie staining of the gels, 106–271 consistent spots (present in the three replicates) were resolved in the 5–8 pH range and 10–90 kDa molecular weight (Mr) range (Fig. 1). A 2-D gel image analysis was performed using PDQuest software v 8.01 and, at all times studied, quantitative and qualitative differences in spot intensity were observed between parental and mutant strains. During potassium starvation and comparing to the parental strain at time 0, we observed an increased number of missing spots; thus, 33 spots were missed after 5-h starvation

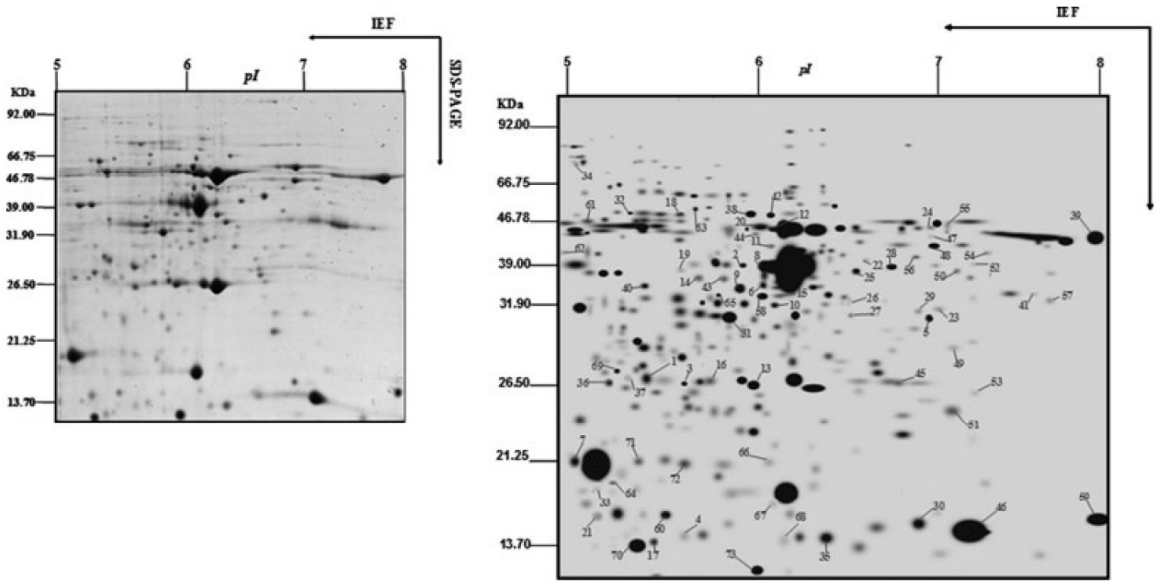

Figure 1. Representative 2-D gel corresponding to extracts from wild cells in control conditions (A), and master gel, with arrows pointing at variable spots (B). Molecular mass (on the left) and p*I* (on the top) were calculated using standard molecular weight markers and the PD-Quest software.

in the case of the parental strain and 162 spots in the case of the *trk1,2* DM (Table 1). Interestingly, new additional spots were not found either in the wild type or in the mutant during the starvation process. Quantitatively, the same behavior was observed in both strains, most spots intensity tends to decrease and just few of them were increased during starvation.

After applying a two-way analysis of variance (ANOVA), 231 spots were assumed to be differentially accumulated between strains and 209 spots between the different sampling times (Fig. 2). A total of 61 spots were variable between strains, but not between sampling times, reflecting those proteins not affected by the experimental environment but by the mutation. On the other hand, 39 spots showed differences only between the different sampling times, reflecting those common responses to the treatment in wild-type and mutant strains. Most of the gel spots (170) presented significant differences between strains and time, showing that the experimental environment affects both wild-type and mutant strains, but in a different way. Moreover, 20 spots were invariable across strains and sampling times (Table S1).

To obtain further information, different and additional statistical approaches were performed. First of all, a data reduction to the whole dataset by means of principal component analysis (PCA) analysis was applied. Of the potential 290 principal components (PC) extracted, the first six PCs accounted for 94.18% of the biological variability (Table 2). The use of these components in a 2-D representation (plotting PC1 and PC2) allowed the effective separation of samples into the different strains and sampling times (Fig. 3). In the DM, duration from 0 to 60 min were closely grouped in both plots, indicating similarity in the spot map. The correlation of each particular spot to PC 1 and 2 was determined from the loading matrix generated during the PCA (Tables S2 and S3). The five spots showing the highest correlation with each PC were determined. Of these spots, five (7, 9, 21, 62, and 68) were identified after MS analysis, corresponding to a co-chaperone protein, dihydrooronate dehydrogenase, glutaredoxin-1, S-adenosylmethyonine synthase, and ubiquitin-conjugating enzyme, respectively (see Discussion).

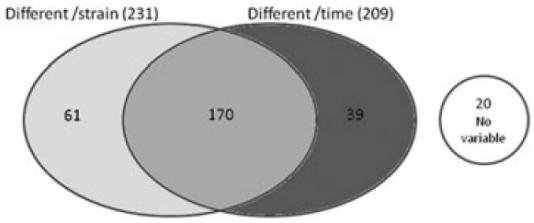

Figure 2. Graphical representation of spots statistically different during potassium starvation in function of strains and/or time after two-way ANOVA and also the 20 spots always present in both strains at any sampled time.

Neural network-based analysis was performed employing Kohonen's Self Organizing Maps (SOM), known to be a

Table 2. Proportion of the explained variance and standard deviation of the principal components obtained after performing a principal component analysis, employing whole dataset and the normalized spot intensities of each spot.

	PC1	PC2	PC3	PC4	PC5	PC6	PC7	PC8	PC9
Standard deviation	131.319	64.175	409.411	35.391	27.224	211.077	157.055	147.692	136.269
Proportion of variance	0.6375	0.1522	0.06196	0.0463	0.0274	0.01647	0.00912	0.00806	0.00686
Cumulative proportion	0.6375	0.7897	0.85172	0.898	0.9254	0.94189	0.95101	0.95907	0.96594

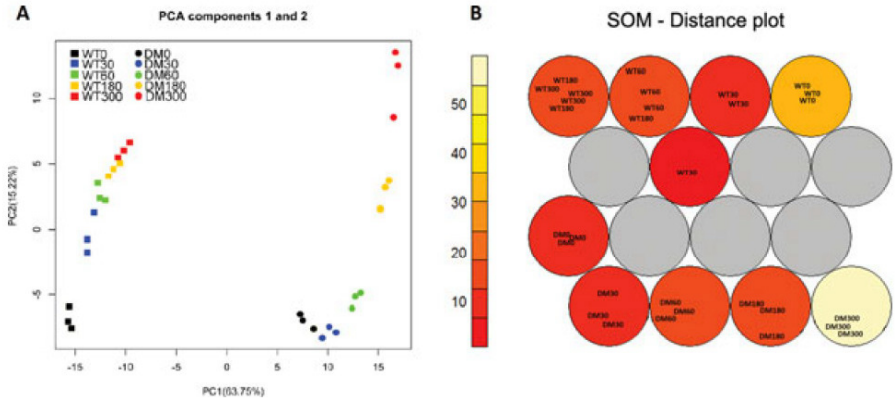

Figure 3. (A) Representation of the samples based on main principal components found after PCA by 2-D plotting of the main principal components (PC1 and PC2). (B) SOM analysis representation. The samples are grouped in nodes based on the scores obtained after applying Kohonen's self-organizing map algorithms. The topology of the grid was set to hexagonal and 4 × 4 and the distances are indicated in left-side bar.

powerful multivariate analysis method, with a mathematical basis completely different than PCA. Wild-type and DM strains were completely differentiated (Fig. 3). In the case of the wild type, samples coming from time 180 min (WT180) and 300 min (WT300) were in the same node, being this node closer to WT60 while WT30 and WT0 were more distant. In the case of DM, nodes grouping samples DM0, DM30, and DM60 were closer together while DM180 and DM300 were clearly more distant.

MS analysis and protein identification

Seventy-three variable spots from the most abundant were excised and analyzed by MALDI-TOF-TOF MS after trypsin digestion. Results obtained were compared to the UniProt database allowing the identification of 49 unique proteins. Resulting proteins were classified in functional categories and are presented in Table 3; complementary information including indications on location, number of molecules per cell, and the identified peptide sequence is available in Table S4. A good correlation between theoretical and experimental pI was obtained whereas some differences in Mr were observed. For some spots, a higher Mr was observed maybe due to the absence of mature form in UniProt database. We identified proteins with double experimental Mr, including spots 63 (superoxide dismutase, reported as homodimer), spot 16 (FK506 binding protein 1), and spot 38 (hydroxyacylglutathione hydrolase). On the other hand, there were spots with a much lower Mr experimental than theoretical, probably due to degraded proteins. This was the case for the spot 30 (glyceraldehyde-3-phosphate dehydrogenase 3), spot 70 (protein YLR301W), spot 73 (uracil phosphoribosyltransferase), spot 39 (inhibitory regulator protein Bud2), and spot 59 (Sok2). Finally, there was a group of spots corresponding to the same proteins but with different Mr, possibly due to the presence of isoforms. We identified in this group the glyceraldehyde-3-phosphate dehydrogenase 2 (spots 22–24), the glyceraldehyde-3-phosphate dehydrogenase 3 (spots 25–30), the hexokinase 2 (spots 33 and 34), the phosphoglycerate kinase (spots 47–56), and the uracil phosphoribosyltransferase (spots 71 and 72).

Within the proteins identified, we found proteins related to metabolism (28 proteins), mainly involved in the glycolytic pathway (nine proteins), to stress response (nine proteins), protein fate (seven proteins), signaling (two proteins), or other functions (three proteins). The different pathways related to energy production were not altered equally during potassium starvation in the two yeast strains. The level of the nine proteins of the glycolysis tend to decrease radically in the mutant *trk1,2* while their level remained constant in the parental strain, except in the case of two proteins (Hxk2

Table 3. List of identified proteins.

Proteins*	Accession number†	Spots‡
Glycolysis		
Enolase 1	P00924/YGR254W/Eno1	10–11–12
Enolase 2	P00925/YHR174W/Eno2	13–14
Fructose-bisphosphate aldolase	P14540/YKL060C/Fba1	18–19
Glyceraldehyde-3-phosphate dehydrogenase 2	P00358/YJR009C/Tdh2	22–23–24
Glyceraldehyde-3-phosphate dehydrogenase 3	P00359/YJL052W/Tdh1	25–26–27–28–29–30
Hexokinase-2	P04807/YGL253W/Hxk2	33–34
Phosphoglycerate kinase	P00560/YCR012W/Pgk1	47–48–49–50–51–52 53–54–55–56
Phosphoglycerate mutase 1	P00950/YKL152C/Gpm1	57
Triosephosphate isomerase	P00942/YDR050C/Tpi1	65–66
Ethanol fermentation		
Alcohol dehydrogenase 1	P00330/YOL086C/Adh1	6
Pentose phosphate pathway		
6-phosphogluconolactonase 3	P38858/YHR163W/Sol3	58
Methylglyoxal pathway		
Hydroxyacylglutathione hydrolase	Q05584/YDR272W/Glo2	38
Cell wall biogenesis		
Mannose-1-phosphate guanyltransferase	P41940/YDL055C/Psa1	42
Mannose-6-phosphate isomerase	P29952/YER003C/Pmi40	43
Oxidoreductases/redox balancing		
Fumarate reductase	P32614/YEL047C/Frd1	20
NADPH dehydrogenase 2	Q03558/YHR179W/Oye2	44
Phosphate		
Inorganic pyrophosphatase	P00817/YBR011C/Ipp1	40
Glycerol		
(DL)-glycerol-3-phosphatase 1	P41277/YIL053W/Rhr2	1
Pyrimidine		
Dihydroorotate dehydrogenase	P28272/YKL216W/Ura1	9
Uracil phosphoribosyltransferase	P18562/YHR128W/Fur1	72–73
Amino acid biosynthesis		
3′(2′),5′-bisphosphate nucleotidase	P32179/YOL064C/Met22	2
Homocysteine S-methyltransferase 2	Q08985/YPL273W/Sam4	36
Ketol-acid reductoisomerase	P06168/YLR355C/Ilv5	41
Saccharopine dehydrogenase	P38999/YNR050C/Lys9	61
S-adenosylmethionine synthetase	P10659/YLR180W/Sam1	62
Cofactor production		
3,4-dihydroxy-2-butanone 4-phosphate synthase	Q99258/YDR487C/Rib3	3
3-hydroxyanthranilate 3,4-dioxygenase	P47096/YJR025C/Had1	4
Hit family protein 1	Q04344/YDL125C/Hnt1	35
Protein fate		
ADP-ribosylation factor 1	P11076/YDL192W/Arf1	5
Co-chaperone protein Sba1	P28707/YKL117W/Sba1	7
Family of serine hydrolases 1	P38777/YHR049W/Fsh1	15
FK506-binding protein 1	P20081/YNL135C/Fpr1	16
Peptidyl-prolyl cis-trans isomerase	P32472/YDR519W/Fpr2	17
G-protein beta subunit	P38011/YMR116C/Asc1	31
Peptidyl-prolyl cis-trans isomerase	P14832/YDR155C/Cpr1	46
Signaling		
Inhibitory regulator protein Bud2/Cla2	P33314/YKL092C/Bud2	39
Protein Sok2	P53438/YMR016C/Sok2	59
Stress related		
Cytochrome c peroxidase	P00431/YKR066C/Ccp1	8
Glutaredoxin-1	P25373/YCL035C/Grx1	21

Table 3. Continued.

Proteins*	Accession number†	Spots‡
Heat shock protein Ssb2	P40150/YNL209W/Ssb2	32
Heat shock protein 26	P15992/YBR072W/Hsp26	37
Peptide methionine sulfoxide reductase	P40029/YER042W/Mxr1	45
Superoxide dismutase	P00445/YJR104C/Sod1	63
Thioredoxin-2	P22803/YGR209C/Trx2	64
Ubiquitin-conjugating enzyme Ubc2	P15731/YBR082C/Ubc2	67
Ubiquitin-conjugating enzyme variant	P53152/YGL087C/Mms2	68
No well-defined functional category/unknown		
Protoplast secreted protein 2	Q12335/YDR032C/Pst2	60
Uncharacterized phosphatase	P53981/YNL010W	69
Uncharacterized protein YLR301W	Q05905/YLR301W/Hri1	70–71

*Functionally related proteins.
†Swiss-Prot and Saccharomyces Genome Database (SGD) accession numbers and common name.
‡Numbers corresponded to Figure 1.

and Tdh2). On the contrary, proteins of the pentose phosphate pathway (Sol3) and the methylglyoxal pathway (Glo2) remained present during the starvation process although a tendency to smoothly decrease was observed in the methylglyoxal pathway in the case of the mutant strain. Interestingly, some biosynthetic pathways seem to remain active during potassium starvation, like the pyrimidine pathway (Ura1 and Fur1) that keeps a relative good level of proteins, and the amino acid biosynthesis-related proteins (Met22, Sam4, Sam1, and Lys9) that present a higher amount of proteins in the mutant strains during potassium starvation. Proteins related with DNA-repair system are found in both strain (Ubc2 and Mms2). In the case of the mutant, they were present with a two-fold factor increase. Proteins related with stress, especially with oxidative stress, presented the same behavior, Sod1 and Ccp1 were expressed in both strains, being more important the amount in the mutant strain. Other proteins such as Trx2 and Grx2 were only detectable in the mutant strain after 30–60 min of potassium starvation. Finally, other proteins showed a pattern difficult to explain with no homogenous behavior within a same functional category or between spots corresponding to the same single proteins (Hri1).

In order to better understand the behavior of the different groups of proteins identified, differential spots were clustered employing Ward's minimum variance method over a Pearson distance-based dissimilarity matrix (Fig. 4), which has proved to be an accurate procedure for proteomics data (Meunier et al. 2007). Spots in the same tree were compared, employing a clustering method and a representation of quantitative variations between strains and times. While wild-type samples showed bigger distance between time 0 and the several starvation times, DM samples were closely grouped from 0 to 60 min suggesting a slower response of the mutant to the potassium starvation process. These results are in agreement with the PCA and SOM analyses shown above.

Evaluation of hexokinase and alcohol dehydrogenase activity in wild-type and *trk1,2* cells upon potassium starvation

To complement the data obtained by our proteomic analysis, we selected two examples of glycolytic activities corresponding to proteins identified above, the first one is hexokinase, which is an example of activity likely to decrease (due to the loss of Hxk2), and the second is alcohol dehydrogenase (Adh), which is a possible example of unaltered activity. As observed in Figure 5, the hexokinase activity versus glucose or fructose is very similar for wild-type and *trk1,2* cells in the presence of potassium. Interestingly, deprivation of potassium did not decrease the amount of glucose phosphorylation activity, but it resulted in a relative increase in the preference for fructose in wild-type and, even more markedly, in Trk-deficient cells. Although apparently surprising, this result is compatible with the disappearance of Hxk2. There are three glucose-phosphorylating enzymes in yeast: Hxk1, Hxk2, and Glk1. They differ in their V_{max} for fructose and glucose, being the fructose/glucose ratio of 3 for Hxk1 and 1.2 for Hxk2 (Barnar 1975). Glk1 barely phosphorylates fructose (Lobo and Maitra 1977). We observe that after 240 min, there is an increase in the fructose/glucose phosphorylation ratio from 0.60 $\pm$ 0.03 to 0.73 $\pm$ 0.06 in wild-type cells, and 0.52 $\pm$ 0.04 to 0.82 $\pm$ 0.09 in the *trk1,2* mutant (in which the disappearance of Hxk2 is more prominent; see Table S4). The transcriptomic profile shown in Figure 5 indicates that *HXK1*, encoding the most effective fructose-phosphorylating isoform, is greatly induced by potassium starvation, whereas *HXK2* is not. The emergence of Hxk1 and the disappearance of Hxk2 would explain the increase in the ratio of phosphorylation—fructose/glucose. This increase is probably less drastic than expected because Glk1, whose activity levels are normally lower, is also significantly induced.

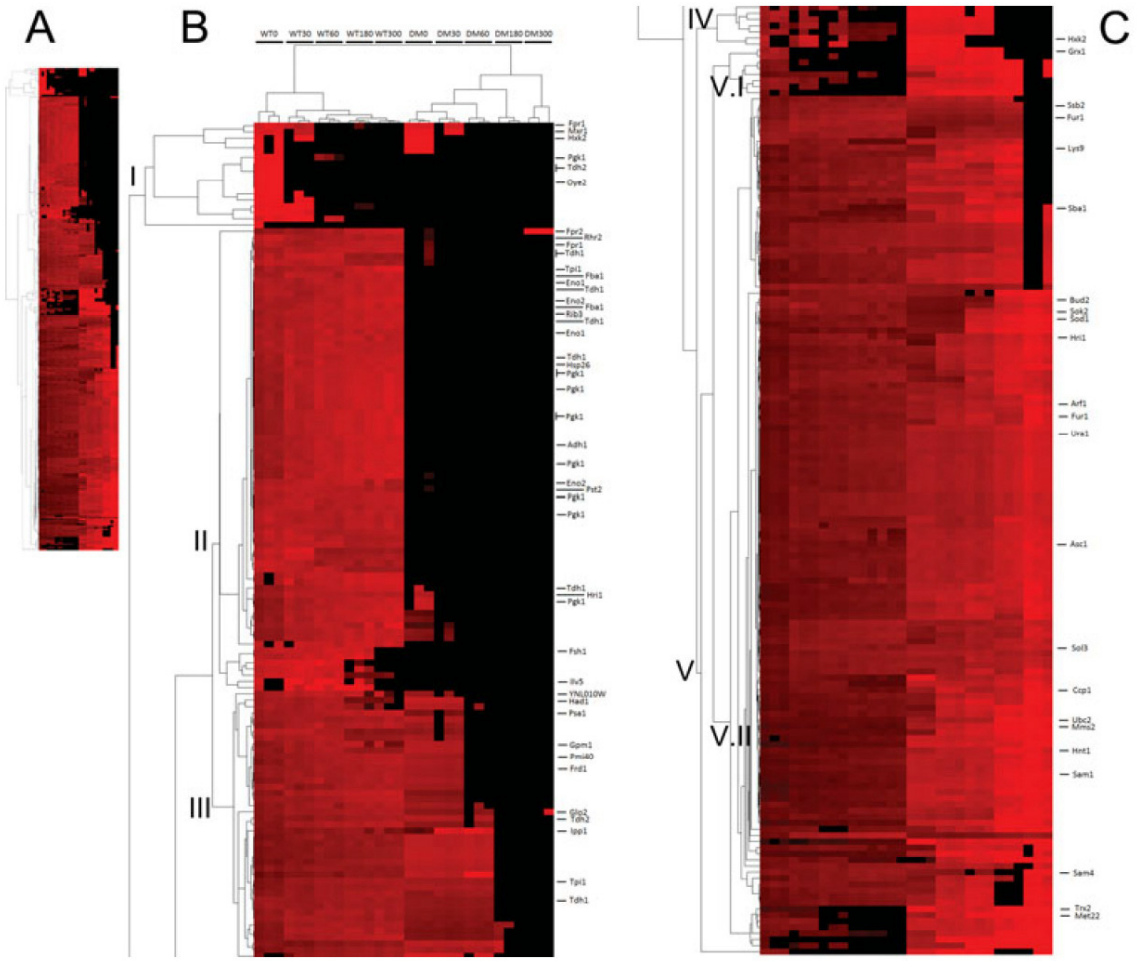

Figure 4. Two-way hierarchical cluster of differentially accumulated spots. A heat map representation of the clustered spots shows the protein value according to the standardized spot percent in each replicate, with red intensity indicating accumulation and black absence. Samples were grouped employing a correlation-based distance. Original plot was divided for a better presentation and reading. (A) Miniature of the original heat map, (B and C) magnified upper and lower parts, respectively, including the names of the identified proteins.

In contrast, the amount of alcohol dehydrogenase activity is not decreased by lack of potassium (see Fig. 5), in agreement with the stability of Adh1, the major Adh isoform in exponentially growing yeast (Leskovac et al. 2002).

Discussion

Saccharomyces cerevisiae is endowed with two genes coding for the main plasma membrane potassium transporters. These proteins are essential for the cell to grow at limiting potassium concentrations and mutants lacking the corresponding genes (*TRK1* and *TRK2*) show defective growth and transport at low potassium. However, at high potassium (in the mM range) other no specific systems can transport enough amounts of the cation, thus allowing mutant cells to grow at rates similar to those in the wild type (Navarrete et al. 2010). A first proteomic study of *trk1,2* mutants was recently published (Curto et al. 2010). It is important to notice that in that paper both wild-type and mutant cells were grown under nonlimiting potassium concentrations (50 mM KCl) and the authors concluded that most of the differences observed between parental and DM strains corresponded to proteins related to glycolysis and redox-homeostasis enzymes.

Considering that full activity of the so-called high-affinity/high-velocity potassium transport process dependent upon the Trk1/2 system is usually observed after obtaining K^+-starved cells by incubation in media without added potassium during 4–5 h (Rodríguez-Navarro and Ramos 1984; Bertl et al. 2003), we decided to study changes in the proteome of the wild type and DM during the starva-

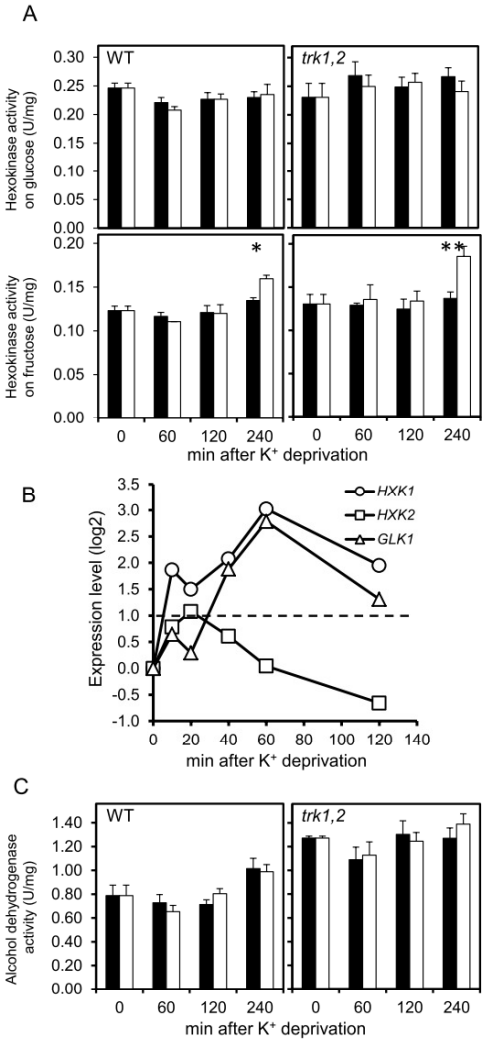

Figure 5. Changes in enzymatic activities triggered by potassium starvation. (A) Determination of hexokinase activity in wild-type and *trk1,2* strains in cells growing in 50 mM K^+ (closed bars) or in the absence of the cation, (open bars). Substrates are glucose (upper panel) or fructose (lower panel). Data are mean ± SEM from four to eight experiments. $*P < 0.05$; $**P < 0.01$. (B) Profile of expression pattern for genes encoding glucose phosphorylation enzymes in response to potassium starvation (no K^+ vs. 50 mM K^+). Data were obtained by DNA microarray analysis (Barreto et al., unpubl. ms.) and correspond to the mean from four biological replicates. Values above the discontinuous line are considered significant gene inductions. (C) Determination of alcohol dehydrogenase activity in wild-type and *trk1,2* strains in the presence of absence of external potassium (see A). Data are mean ± SEM from three experiments.

tion process. The most important observation was the extraordinary decay in protein content and number of spots, observed during the 5 h of starvation with special relevance in the case of the mutant strain. It has to be considered that in 2D gels, only a fraction of the total proteome can be observed, mainly proteins that are the most abundant such as the housekeeping proteins (Buxbaum 2010). Previous work reported that K^+ deprivation during 24 h produced, in *S. cerevisiae*, a decrease in cell viability by inducing a programmed cell death process (Lauff and Santa-María 2010). Although this is a very important observation, in our conditions and after 5-h starvation we observed high decrease in protein content but no changes in cell viability. From these results, we conclude that potassium starvation is a very stressing process for the cells and it looks like 5-h incubation without potassium is excessive since it provokes a very important and general decay in many cellular processes. As mentioned above, 4–5 h K^+-starvation is a general method used to induce full activity of the Trk1/2 system. However, we have recently shown that in the newly designed medium YNB translucent (Navarrete et al. 2010), used also in this work, adaptation to the high-affinity/high-velocity state is much faster. In fact, the higher affinity for Rb^+ (K^+) is observed after 30-min starvation and higher V_{max} is reached after 2-h starvation. Therefore, we propose that this would be a much more rational way to obtain yeast cells expressing the high-affinity/high-velocity mode of transport.

PCA analysis allowed a clear classification of samples. The plot of PC1 (50.7%) and PC2 (22.2%) shows differences between mutant and wild type and also between the different sampling times. This supports the above-indicated hypothesis in terms of the differences found between strains behavior during the adaptation to the lack of potassium. This idea was confirmed after the application of a SOM neural network, a methodology for the classification of the samples more powerful than PCA analyses. Wild-type strain adapted quicker to the new conditions, since samples taken at 0, 30, and 60 min were already separated. Adaptation seems to be already completed after 3 h since samples taken at 180 and 300 min group together. On the other hand, the DM needed more time to try to adapt to the new environmental condition, that is, samples at time 0, 30, and 60 min grouped together. In conclusion, the wild-type strain adapted and got stabilized faster to the stress condition while the mutant seems to have problems to sense or adapt to the absence of potassium.

It is relevant that in the 2D gels we have identified most of the enzymes involved in glycolysis. During the starvation process, most of them enzymes were present in the wild type but in the mutant there was a fast decay. Our biochemical results on hexokinase activities are in agreement with this observation. The strong reduction in Hxk2 protein levels during starvation was not completely reflected in drastic changes in hexokinase activity. This apparent discrepancy could be explained by the induction of *HXK1* and *GLK1*. The corresponding Hxk1 and Glk1 proteins, which would keep the capacity to phosphorylate glucose, are less abundant than

Hxk2 and we did not identify them by proteomics; however, our transcriptomic results support that possibility.

On the other hand enzymes involved in two other important energetic pathways were detected: pentose phosphate and methylglyoxal pathways; in general, proteins from both pathways remained present during the starvation process. In fact, the transcriptomic profile of *GLO1* and *GLO2*, the two genes involved in detoxification of methylglyoxal, shows induction during starvation (not shown). It is tempting to speculate that the glycolysis pathway is more sensitive to low K^+ than the alternative pathways and for that reason it is more inhibited in the mutant. It has been reported that, on the one hand, potassium plays a crucial role in the activation of the glycolytic enzyme pyruvate kinase (see Page and Di Cera (2006) for a review) and, on the other hand, the mutant shows defective potassium transport. These facts may be related to the higher sensitivity of the glycolysis in the mutant.

We have mentioned the importance of the stress induced by potassium starvation, especially in mutant cells. The fact that two ubiquitin enzymes related with DNA-repair system (Ubc2 and Mms2) were identified along the 5 h of the experiment is in agreement with this observation (Broomfield et al. 1998; Game and Chernikova 2009). Even more in the mutant, the amount of the two ubiquitin proteins was not only present, but significantly increased during potassium starvation. On the other hand, some important pathways seem to be unaffected by starvation. Two examples are the metabolism of some amino acids (methionine, lysine) and bases (pyrimidine ribonucleotides). The application of two different algorithms for sample classification, one of them based on recent algorithms based on neural networks, lead to the obtaining of complementary results increasing the discriminatory power of this analysis (Valledor and Jorrín 2011). Cluster analysis allowed a distance-based classification of the samples and spots reinforcing that idea. Five major groups of spots could be distinguished in the plot being relevant that most of the glycolytic proteins appear in groups I and II and show a completely different behavior in wild-type and mutant strain.

It is conceivable to pose the question about how *TRK* mutation affects these metabolic processes. We have no definitive answer to this question but our results indicating a defective metabolic adaptation to the lack of potassium in the mutant may be taken as a clue on the relevant role of potassium fluxes and/or levels triggering adaptation. Unpublished results of our group show that wild-type and *trk1,2* cells grown under nonlimiting KCl are able to adapt and reach a new internal K^+ stationary state when suspended in lower K^+ concentrations, requiring mutant cells higher external K^+ to keep similar internal amounts of the cation. In conclusion, the DM *trk1,2* is still able to sense a decrease in external potassium but lacks the mechanism to properly adapt to this stress. A similar behavior may explain the defective metabolic adaptation during starvation.

In summary, the decrease in protein content during potassium starvation experiments lead to a global decrease of the basic cellular functions such as the cell energy production pathways, with a radical decrease of the glycolytic proteins that was more evident in the mutant. In the context of a general decrease of proteins, it is relevant that some cellular processes such as the pentose phosphate and methylglyoxal pathways were kept. These results indicate that conditions commonly used in the past to characterize adaptation to potassium (4–5 h in the absence of the cation) are too stressful for the cells and this should be considered in future studies on potassium homeostasis. In fact, the study of the proteome under less extreme potassium limitation is under way. This would allow to analyze differences between parental and mutant strains under more physiological conditions.

Experimental Procedures

Strains and growth conditions

Saccharomyces cerevisiae wild-type BY4741 (MATa*his3*Δ*1leu2*Δ *met15*Δ *ura3*Δ; EUROSCARF, Germany) and the derivative isogenic potassium transport DM (*trk1*,*trk2*) (BYT12, *trk1*Δ*::loxPtrk2*Δ*::loxP*) (Petrezselyova et al. 2010) strains were grown, in 250-mL Erlenmeyer flasks, with 100-mL K^+-free translucent YNB medium: 1.63 g/L Yeast Nitrogen Base (ForMedium™ UK, CYN7505), 2% glucose, 4 g/L ammonium sulphate, enriched with 50mM potassium chloride, 20 mg/L methionine, adenine, tryptophan, and arginine; 30 mg/L tyrosine, leucine, isoleucine, and lysine; 40 mg/L uracyl, histidine; 50 mg/L phenylalanine, 100 mg/L glutamic and aspartic acid; 150 mg/L valine; 200 mg/L threonine and 400 mg/L serine. The cultures were grown at 28°C (initial $OD_{600nm} = 0.05$) in a shaker to allow good aeration (180 rpm), until they reach $OD_{600nm} = 1.9$. K^+ starvation was induced by washing the cells twice with milli-Q water, and then resuspending in YNB medium without KCl. At indicated times, cell samples were withdrawn and used for protein extraction.

Protein extraction

Cells were recovered by centrifugation. The cell pellet was suspended in 600 μL homogenization buffer (50 mM TRIS buffer, pH 7.6, containing 1 mM PMSF, 1 mM EDTA, 2 mM DTT, and a tablet of protease inhibitor cocktail [Roche-11697498001] per 50 mL of homogenization buffer). Cells were broken by vortexing (15–20 times, 30 sec) in the presence of glass beads (Sigma-G9268) (ratio v/v of 1). Glass beads and insoluble material were eliminated by centrifugation (10,000 *g*, 5 min). To the supernatant (about 500 μL), 1.5 mL of 10% (w/v) trichloroacetic acid (TCA)/acetone solu-

tion containing 0.07% (w/v) dithiothreitol (DTT) was added. Proteins were allowed to precipitate at –20°C for 1 h; then, the precipitate was recovered after centrifugation at 10,000 *g* for 15 min. The pellet was washed twice with 1.5 mL of cold (–20°C) acetone containing 0.07% (w/v) DTT. The protein pellet was recovered after centrifugation. The final pellet was air-dried and solubilized in 250 μL of 8 M urea, 2% (w/v) 3-[(3-cholamidopropyl)dimethylammonio]propanesulfonate (CHAPS), 20 mM DTT, 0.5% (v/v) Biolytes pH range 3–10 (Bio-Rad), and 0.0001% (w/v) bromophenol blue. Insoluble material was removed by centrifugation. The protein concentration was determined by Bradford, with ovoalbumin as a standard.

2-DE

Immobilized pH gradients (IPG) strips (17 cm, 5–8 pH linear gradient; Bio-Rad) were passively rehydrated for 2 h with 500 μg of protein in 300 μL of IEF solubilization buffer (7 M urea; 2 M thiourea; 4% [w/v] CHAPS; 0.5% [v/v] IPG buffer 5–8, 20 mM DTT; and 0.01% [w/v] bromophenol blue). The strips were loaded onto a Bio-Rad Protean IEF Cell System and proteins were electrofocused at 20°C with a first step of a gradual increase in the voltage (50–8000 V) and then reaching 60,000 Vh. Strips were immediately equilibrated according to Görg et al. (1987). Second dimension SDS-PAGE was performed on 12% polyacrylamide gels using Protean Dodeca Cell System (Bio-Rad). Gels were run first at 30 mA per gel for 15 min and then at 50 mA per gel until the dye front reached the bottom of the gel.

Staining and image analysis

Gels were stained twice with CBB G-250 (Bio-Rad) for 20 h following the method described by Mathesius et al. (2001). Images were acquired with a GS-800 calibrated densitometer (Bio-Rad) and analyzed with PDQuest 8.0.1 software (Bio-Rad) using 10-fold over background as a minimum criterion for presence/absence for the guided protein spot detection method. This criterion includes almost all spots of the gels and some staining artifacts and noise. A spot-by-spot visual validation of automated analysis was done thereafter to increase the reliability of the matching. Experimental pI was determined using a 5–8 linear scale over the total length of the IPG strip. Mr values were calculated by mobility comparisons with protein standards markers (SDS molecular weight standards, Broad range, Bio-Rad) run in a separate lane in the gel.

Statistics

Statistical analysis was performed following the recommendations proposed by Valledor and Jorrín (2011). In brief, spot volumes were preprocessed before statistical analyses. Spot volumes were first normalized as a proportion of the total spot intensities per gel (spot volume $\times$ $10^5/\Sigma$ gel spot volumes), and then the normalized volumes were log transformed to reduce the volume-variance dependency. Spot values passed the Levene's homoscedasticity and Kolmogorov–Smirnov normality tests. Differentially abundant spots were defined after applying a two-way ANOVA considering strain and sampling time as factors. False discovery rate (FDR) *q*-values were calculated with FDRtool package. Cut-off *q*-value was set to allow less than one false positive in this study. The joint spot analysis was performed following three different multivariate approaches: PCA (centered normalized spot values, unrotated solution), heat map clustering (employing Euclidean distance and Ward's aggregation method), and a neural-network based SOM (centered values, 4 $\times$ 4, hexagonal topology).

Three biological and one technical replicates were done for each time and strain. All of the statistical analyses were performed in R Environment v 2.12 (R Development Core Team 2011) employing its core functions and the packages gplots2, Kohonen, and FDRtool.

MS analysis and protein identification

Spots were manually excised and transferred to multiwell 96 plates. Spots were digested with bovine trypsin (sequencing grade Roche Molecular Biochemicals) using an Ettan^{TM} digester station (GE Healthcare Life Sciences). The digestion protocol used was that of Schevchenko et al. (1996), with minor variations. Briefly, spots were washed twice with water and distained by twice 10-min incubation with 100% acetonitrile and dried in vacuum (Savant SpeedVac) for 30 min. Then the samples were reduced with 10 mM dithiotreitol in 25 mM ammonium bicarbonate for 30 min at 56°C and subsequently alkylated with 55 mM iodoacetamide in 25 mM ammonium bicarbonate for 15 min in the dark. Finally, samples were digested with 12 μL of trypsin (12.5 ng/μL) in 25 mM ammonium bicarbonate (pH 8.5) overnight at 37°C. After digestion, the supernatant was collected and 1 μL was spotted onto a MALDI target plate using the dry droplet method and 0.4 μL of a 3 mg/mL of α-cyano-4-hydroxy-transcinnamic acid matrix in 50% acetonitrile (ACN) and 0.1% trifluoroacetic acid (TFA). Samples were analyzed in a 4800 Proteomics Analyzer MALDI-TOF/TOF mass spectrometer (Applied Biosystems, Framingham, MA), in the *m/z* range 850–4000, with an accelerating voltage of 20 kV, in reflectron mode and with a delayed extraction set to 120 nsec. All MS spectra were internally calibrated with peptides from trypsin autolysis. The MS analysis by MALDI-TOF/TOF mass spectrometry produces peptide mass fingerprints and the peptides observed with a signal to noise greater than 20 can be collated and represented as a list of monoisotopic molecular weights. Proteins ambiguously identified by peptide mass fingerprints were subjected to MS–MS sequencing analysis. So, from the MS

spectra suitable precursors were selected for MS–MS analysis with collision-induced dissociation (CID) on (atmospheric gas was used) 1 kV ion reflector mode and precursor mass Windows ± 5 Da. The plate model and default calibration were optimized for the MS–MS spectra processing. For protein identification, the UniProt Knowledgebase Release 14.6 (UniProtKB/Swiss-Prot Release 56.6 of 16 December 2008, Uni-ProtKB/TrEMBL Release 39.6 of 16 December 2008) was searched using MASCOT search engine v.2.1 (Matrix Science; http://www.matrixscience.com) through the Global Protein Server Explorer software v3.6 from Applied Biosystems.

The following parameters were allowed: taxonomy restrictions to *S. cerevisiae*, one missed cleavage, 50 80–100 and 50 80–100 ppm mass tolerance for peptide mass fingerprinting (PMF) and MS–MS searches, respectively, 0.3 Da for MS-MS fragments tolerance, carbamidomethylation cysteine as a fixed modification, and methionine oxidation as a variable modification. The parameters for the combined search (peptide mass fingerprint plus MS–MS spectra) were the same described above.

In all protein identified, the probability scores were greater than the score fixed by Mascot as significant with a *P*-value less than 0.05.

Enzymatic activity determinations

Growth of cultures was as above, except that cells were washed in K^+-free translucent medium instead of milliQ water. Whole-cell lysates (25 mL of culture) were prepared by resuspending the cells in 500 μL of homogenization buffer (20 mM imidazole, pH 7.0). One volume of 0.5-mm zirconia/silica beads (Biospec Products, Inc.) was added and cells were broken at 4°C by vigorous shaking in a Fastprep-24 cell breaker (MP Biomedicals) for five times (30 sec each, setting 5), with intervals of 1 min on ice. After sedimentation at 1000 × *g* for 15 min at 4°C, the cleared lysate was recovered and the protein concentration was determined by the Bradford assay.

The hexokinase activity was determined as described in Gancedo et al. (1977) adding either 10 mM glucose or 25 mM fructose as substrate. The alcohol dehydrogenase activity was determined essentially as described in Ganzhorn et al. (1987) using 0.5 mM NAD^+ and 100 mM ethanol. All the enzymatic activity measurements were performed on 96-well microplates, with a final volume of 300 μL. The reactions were monitored by following the changes in absorbance at 340 nm using a microplate-based UV spectrophotometer (Multiskan Ascent, ThermoLabsystems).

Acknowledgments

We are grateful to J. M. Gancedo, C. Gancedo, and J. A. Biosca for fruitful discussions. Supported by grants GEN2006-27748-C2-2-E/SYS, EUI2009-04153 (SysMo ERA-NET), and BFU2008-04188-C03-03 to J. R. and EUI2009–04147 to J. A. (Ministry of Science and Innovation, Spain and FEDER). We thank all members of the Translucent Consortium for fruitful discussions.

References

Ariño, J., J. Ramos, and H. Sychrová. 2010. Alkali metal cation transport and homeostasis in yeasts. Microbiol. Mol. Biol. Rev. 74:95–120.

Barnar, E. A. 1975. Hexokinases from yeast. Methods Enzymol. 42:6–20.

Bertl, A., J. Ramos, J. Ludwig, H. Lichtenberg-Fraté, J. Reid, H. Bihler, F. Calero, P. Martínez, and P. O. Ljungdahl. 2003. Characterization of potassium transport in wild-type and isogenic yeast strains carrying all combinations of trk1, trk2 and tok1 null mutations. Mol. Microbiol. 47:767–780.

Braconi, D., G. Bernardini, S. Possenti, M. Laschi, S. Arena, A. Scaloni, M. Geminiani, M. Sotgiu, and A. Santucci. 2009. Proteomics and redox-proteomics of the effects of herbicides on a wild-type wine *Saccharomyces cerevisiae* strain. J. Proteome Res. 8:256–267.

Broomfield, S., B. L. Chow, and W. Xiao. 1998. MMS2, encoding a ubiquitin-conjugating-enzyme-like protein, is a member of the yeast error-free postreplication repair pathway. Proc. Natl. Acad. Sci. U.S.A. 95:5678–5683.

Bruckmann, A., P. J. Hensbergen, C. I. Balog, A. M. Deelder, R. Brandt, I. S. Snoek, H. Y. Steensma, and G. P. van Heusden. 2009. Proteome analysis of aerobically and anaerobically grown *Saccharomyces cerevisiae* cells. J. Proteomics 71:662–669.

Buxbaum, E. 2010. Biophysical chemistry of proteins: an introduction to laboratory methods. Springer, New York.

Cheng, J. S., M. Z. Ding, H. C. Tian, and Y. J. Yuan. 2009. Inoculation-density-dependent responses and pathway shifts in *Saccharomyces cerevisiae*. Proteomics 9:4704–4713.

Curto, M., L. Valledor, C. Navarrete, D. Guitiérrez, H. Sychrova, J. Ramos, and J. Jorrin. 2010. 2-DE based proteomic analysis of *Saccharomyces cerevisiae* wild and K^+ transport-affected mutant (*trk1,2*) strains at the growth exponential and stationary phases. J. Proteomics 73:2316–2335.

Game, J. C., and S. B. Chernikova. 2009. The role of *RAD6* in recombinational repair, checkpoints and meiosis via histone modification. DNA Repair (Amst). 8:470–482.

Gancedo, J. M., D. Clifton, and D. G. Fraenkel. 1977. Yeast hexokinase mutants. J. Biol. Chem. 252:4443–4444.

Ganzhorn, A. J., D. W. Green, A. D. Hershey, R. M. Gould, and B. V. Plapp. 1987. Kinetic characterization of yeast alcohol dehydrogenases. Amino acid residue 294 and substrate specificity. J. Biol. Chem. 262:3754–3761.

Goffeau, A., B. G. Barrell, H. Bussey, R. W. Davis, B. Dujon, H. Feldmann, F. Galibert, J. D. Hoheisel, C. Jacq, M. Johnston, et al. 1996. Life with 6000 genes. Science 274:546–567.

Görg, A., W. Postel, J. Weser, S. Günther, J. R. Strahler, S. M. Hanash, and L. Somerlot. 1987. Horizontal two-dimensional electrophoresis with immobilized pH gradients in the 1st-dimension in the presence of nonionic detergent. Electrophoresis 8:45–51.

Haro, R., and Rodriguez-Navarro, A. 2002. Molecular analysis of the mechanism of potassium uptake through the *TRK1* transporter of *Saccharomyces cerevisiae*. Biochim. Biophys. Acta. 1564:114–122.

Hoffman, J. F. 1964. The cellular functions of membrane transport. Prentice-Hall, Englewood Cliffs, NJ.

Karhumaa, K., A. K. Påhlman, B. Hahn-Hägerdal, F. Levander, and M. F. Gorwa-Grauslund. 2009. Proteome analysis of the xylose-fermenting mutant yeast strain TMB 3400. Yeast 26:371–382.

Ko, C. H., A. M. Buckley, and R. F. Gaber. 1990. *TRK2* is required for low affinity K^+ transport in *Saccharomyces cerevisiae*. Genetics 125:305–312.

Lauff, D. B., and G. E. Santa-María. 2010. Potassium deprivation is sufficient to induce a cell death program in *Saccharomyces cerevisiae*. FEMS Yeast Res. 10:497–507.

Leskovac, V., S. Trivić, and D. Pericin. 2002. The three zinc-containing alcohol dehydrogenases from baker's yeast, *Saccharomyces cerevisiae*. FEMS Yeast Res. 2:481–494.

Lobo, Z., and P. K. Maitra. 1977. Physiological role of glucose-phosphorylating enzymes in *Saccharomyces cerevisiae*. Arch. Biochem. Biophys. 182:639–645.

Madrid, R., M. J. Gómez, J. Ramos, and A. Rodríguez-Navarro. 1998. Ectopic potassium uptake in *trk1 trk2* mutants of *Saccharomyces cerevisiae* correlates with a highly hyperpolarized membrane potential. J. Biol. Chem. 273:14838–14844.

Mathesius, U., G. Keijzers, S. H. Natera, J. J. Weinman, M. A. Djordjevic, and B. G. Rolfe. 2001. Establishment of a root proteome reference map for the model legume *Medicago truncatula* using the expressed sequence tag database for peptide mass fingerprinting. Proteomics 1:1424–1440.

Massoni, A., S. Moes, M. Perrot, P. Jenoe, and H. Boucherie. 2009. Exploring the dynamics of the yeast proteome by means of 2-DE. Proteomics 9:4674–4685.

Meunier, B., E. Dumas, I. Piec, D. Béchet, M. Hébraud, and J. F. Hocquette. 2007. Assessment of hierarchical clustering methodologies for proteomic data mining. J. Proteome Res. 6:358–366.

Navarrete, C., S. Petrezsélyová, L. Barreto, J. L. Martínez, J. Zahrádka, J. Ariño, H. Sychrová, and J. Ramos. 2010. Lack of main K^+ uptake systems in *Saccharomyces cerevisiae* cells affects yeast performance in both potassium-sufficient and potassium-limiting conditions. FEMS Yeast Res. 10:508–517.

Nelissen, B., R. De Wachter, and A. Goffeau. 1997. Classification of all putative permeases and other membrane plurispanners of the major facilitator superfamily encoded by the complete genome of *Saccharomyces cerevisiae*. FEMS Microbiol. Rev. 21:113–134.

Page, M. J., and E. Di Cera. 2006. Role of Na^+ and K^+ in enzyme function. Physiol. Rev. 86:1049–1092.

Petrezselyova, S., J. Zahradka, and H. Sychrova. 2010. Saccharomyces cerevisiae BY4741 and W303–1A laboratory strains differ in salt tolerance. Fungal Biol. 114:144–150.

R Development Core Team. 2011. R: a language and environment for statistical computing. R Foundation for Statistical Computing, Vienna, Austria. ISBN 3-900051-07-0.

Ramos, J., and A. Rodriguez-Navarro. 1986. Regulation and interconversion of the potassium transport system of *Saccharomyces cerevisiae* as revealed by rubidium transport. Eur. J. Biochem. 154:307–311.

Ramos, J., R. Alijo, R. Haro, and A. Rodríguez-Navarro. 1994. *TRK2* is not a low-affinity potassium transporter in *Saccharomyces cerevisiae*. J. Bacteriol. 176:249–252.

Rodríguez-Navarro, A., and J. Ramos. 1984. Dual system for potassium transport in *Saccharomyces cerevisiae*. J. Bacteriol. 159:940–945.

Schevchenko, A., M. Wilm, O. Vorm, and M. Mann. 1996. Mass spectrometric sequencing of proteins from silver stained polyacrylamide gels. Anal. Chem. 68:850–858.

Usaite, R., J. Wohlschlegel, J. D. Venable, S. K. Park, J. Nielsen, L. Olsson, and J. R. Yates, Iii. 2008. Characterization of global yeast quantitative proteome data generated from the wild-type and glucose repression *Saccharomyces cerevisiae* strains: the comparison of two quantitative methods. J. Proteome Res. 7:266–275.

Valledor, L., and J. Jorrin. 2011. Back to the basics: maximizing the information obtained by quantitative two dimensional gel electrophoresis analyses by an appropriate experimental design and statistical analyses. J. Proteomics. 74:1–18.

Supporting Information

Additional Supporting Information may be found online on Wiley Online Library.

Table S1. Quantitation, univariate statistics, and identification table.

Table S2. PCA loading matrix.

Table S3. PCA score matrix.

Table S4. Detailed list of identified proteins.

Please note: Wiley-Blackwell is not responsible for the content or functionality of any supporting materials supplied by the authors. Any queries (other than missing material) should be directed to the corresponding author for the article.

Appendix 5: Communications in congresses and conferences

Proteómica • Número 5 • Febrero 2010

Estudio comparativo del perfil proteico de cepas silvestre (BY4741) y mutante (trk1,2) de *Saccharomyces cerevisiae* en condiciones de ayuno en K^+

Miguel Curto[1], Clara Navarrete[2], Luis Valledor[3], María Luisa Hernández[4], José Ramos[2], Jesús Jorrín[1]

[1] Departamento de Bioquímica y Biología Molecular, Universidad de Córdoba, 14071 Córdoba, España. [2]Departamento de Microbiología, Universidad de Córdoba, Córdoba, España. [3] Departamento de Biología de Organismos y Sistemas, Área de fisiología vegetal, Universidad de Oviedo, Oviedo, España. [4]Departamento de Microbiología II, Facultad de farmacia, Universidad Complutense de Madrid- Parque Científico de Madrid (UCM-PCM). Madrid, España.

Resumen

Se ha llevado a cabo el estudio comparativo del proteoma de las cepas silvestre (BY4741) y mutante (trk1,2) de *Saccharomyces cerevisiae* en condiciones limitantes de K^+, utilizando electroforesis bidimensional acoplada a MS. En respuesta al ayuno en K^+ se observó un marcado descenso del contenido en proteínas en extractos celulares y del número de spots en geles bidimensionales, tanto en la variedad silvestre como la mutante. Los spots que presentaron diferencias cualitativas o cuantitativas, estadísticamente significativas, entre cepas se analizaron por espectrometría de masas (MALDI-TOF-TOF). Tras la identificación mediante búsqueda en base de datos (UniProtKB-SwissProt; limitada a la taxonomía de *Saccharomyces cerevisiae* (Baker's yeast)) las proteínas se agruparon de acuerdo a su función. El ayuno en potasio causó una disminución en enzimas del metabolismo energético y del metabolismo de aminoácidos, así como a proteínas de respuesta a estrés.

Este trabajo forma parte del proyecto TRANSLUCENT (http://www.translucent-network.org/),

cuyo objetivo es analizar los mecanismos implicados en la homeostasis catiónica [1] usando como sistema modelo *S. cerevisiae*. Mediante una aproximación de proteómica de expresión diferencial basada en electroforesis bidimensional, se ha intentado identificar cambios en el contenido en proteínas como resultado de la doble mutación en los genes que codifican proteínas transportadoras de K^+ (TRK1 y TRK2) [1], y en condiciones de ayuno en K^+. En un trabajo preliminar, el proteoma de las dos cepas (silvestre y doble mutante) se comparó en las fases exponencial y estacionaria de la curva de crecimiento, con concentraciones óptimas (50 mM ClK) de K^+ en el medio [2]. Se realizaron extracciones de proteínas [3] y geles bidimensionales (IEF en el rango de pH 5-8; SDS-PAGE 12 %; tinción con Coomassie coloidal) [4] de WT y *trk1,2* a 0 (control), 30, 60, 180 y 300 tras la eliminación del K^+. Se detecto un descenso progresivo con el tiempo de ayuno tanto en el contenido en proteínas del extracto como en el número de spots resueltos, siendo este efecto más acusado en la cepa mutante que en la silvestre (Figura 1). Se picaron los spots que mostraron diferencias cualitativas o cuantitativas, estadísticamente significativas, 303 en total, se sometieron a digestión tríptica, analizándose los péptidos resultantes por MS (MALDI-TOF-TOF). Tras la búsqueda en bases de datos (UniProtKB-SwissProt; limitada a la taxonomía de *Saccharomyces cerevisiae* (Baker's yeast)) utilizando el software MASCOT [5], se identificaron 171 proteínas, que se agruparon según su función (Figura 2). El ayuno en potasio causó una disminución en enzimas del metabolismo energético y del metabolismo de aminoácidos, así como a proteínas de respuesta a estrés. Entre las proteínas identificadas, las relacionadas con el estrés y/o reacciones de defensa, metabolismo de nucleótidos y transcripción, fueron las que presentaron mayores cambios entre cepas, siendo más abundantes en la cepa silvestre.

Agradecimientos

Agradecemos el trabajo desarrollado, por la Dra. Hanna Sychrova (Departamento del transporte de membrana, Instituto de fisiología, Republica Checa, Praga), con las cepas de *S. cerevisiae* usadas en este trabajo. Así como al proyecto "Gene interaction networks and models of cation homeostasis in *Saccharomyces cerevisiae* –TRANSLUCENT" por financiar este trabajo.

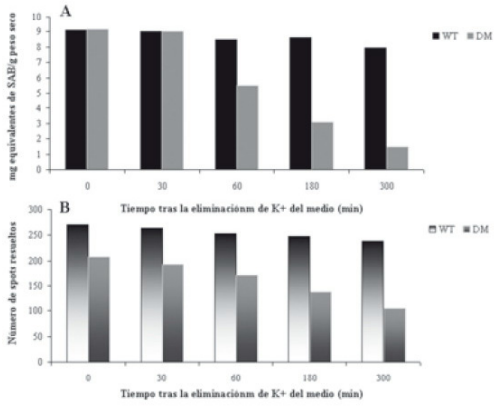

Figura 1. *A. Contenido en proteínas en extractos de la cepa silvestre y doble mutante a distintos tiempos tras la eliminación de K+ del medio. B. Número de spots resueltos en dichos extractos, en el rango de pH 5-8 y Mr 6-95 KDa.*

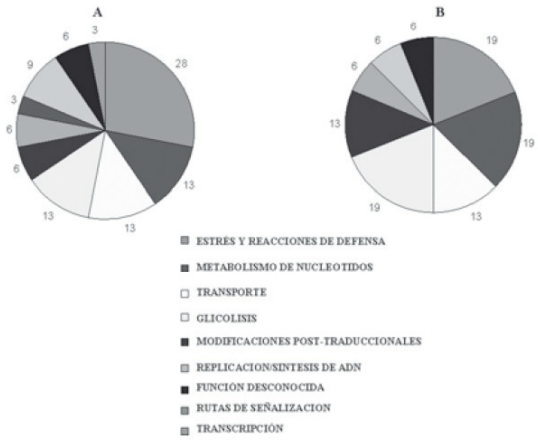

Figura 2. *Agrupación funcional de las proteínas afectadas por el ayuno en potasio. A. Cepa silvestre; B. Doble mutante. Datos expresados en porcentaje.*

Referencias

[1] Rodríguez-Navarro A y Ramos J. Dual system for potassium transport in *Saccharomyces cerevisiae*. Journal of bacteriology, 1984; 159: 940-45.

[2] Curto M, Ramos J, Gutierrez L, Gil C, Jorrin J, Proteome analysis of Saccharomyces cerevisiae wild and potassium transport-affected mutant strains. Joint congreess of the spanish society and the latin american human proteome organization. 2009 ; Pamplona.

[3] Damerval C, De Vienne D, Zivy M, Thiellement H. Technical improvements in two-dimensional electrophoresis increase the level of genetic variation detected in wheat-seedling proteins. Electrophoresis, 1986; 7: 52–54.

[4] Mathesius U, Keijzers G, Natera SHA, Weinman JJ, Djordjevic MA, Rolfe BG. Establishment of a root proteome reference map for the model legume *Medicago truncatula* using the expressed sequence tag database for peptide mass fingerprinting. Proteomics 2001; 1: 1424–40.

[5] Perkins DN, Pappin DJC, Creasy DM, Cottrell JS. Probability-based protein identification by searching sequence databases using mass spectrometry data. Electrophoresis, 1999; 20: 3551-67.

Jorrín J, Rubiales D. (2007). *New Phytologist* 173, 703-712

35. *Medicago truncatula* resistance to powdery mildew (*Erysiphe pisi*): a proteomic study

Curto, M.[1], Gil, C.[3], Gutiérrez, M.[3], Rubiales, D.[2], Maldonado, A.[1] , Jorrín, J.V[1].

[1]Agricultural and Plant Biochemistry Research Group, Dpt. of Biochemistry and Molecular Biology, University of Córdoba, Campus de Rabanales, Edificio Severo Ochoa (C6), 14071 Córdoba, Spain, b72curum@uco.es. [2] Institute for Sustainable Agriculture, CSIC, Apdo 4084, 14080 Córdoba, Spain. [3] Centro de Genómica y Proteómica, Unidad de Proteómica, Facultad de Farmacia, Pza. Ramón y Cajal, s/n, 28040, Madrid, Spain.

In order to characterize the mechanisms of resistance of *M. truncatula* to powdery mildew (*E. pisi*), we had carried out a proteomic approach, in which the classical platform 2-DE/MS (MALDI-TOF/TOF) has been utilized. We have compared the leaf proteome of either control (non-inoculated) and inoculated plants from susceptible (Parabinga) and resistant (SA 1306) genotypes. Proteins were extracted by using the TCA-acetone precipitation protocol and resolved by 2-DE, with IEF in the 5-8 pH range. Gels were Coomassie stained, images captured by using a densitometer (GS-800, Bio-Rad) and analyzed with the PD-Quest software. Around 380 resolved spots were detected in the 7–98-kDa range. Forty five spots showed differential protein expression between genotypes in non-inoculated plants. 41 and 61 spots were differentially expressed between control and inoculated leaf extracts from Parabinga and SA1306 plants, respectively. Proteins were identified from PMF or MS/MS spectra by interrogating NCBI and *M. truncatula.*

(ftp://ftp.tigr.org/pub/data/m_truncatula/OLD/) databases. From the 147 differential spots 60 proteins were identified, being them grouped in the following categories: a) enzymes of the photosynthesis and carbohydrate metabolism: i.e. RubisCO activase (gi|23320705); b) stress and defence related proteins: i.e. chaperonin (gi|806808); HSP70 (gi|20835); L-ascorbate peroxidase (gi|7484752); c) enzymes of the secondary metabolism: i.e. S-adenosylmethionine synthetase (gi|21593291); isoflavone reductase (gi|19620), d) signal transduction: i.e. villin (gi|4938492); e) protein synthesis and degradation: i.e. endopeptidase (gi|419773).

36. Comparison of 2D patterns of mild and lethal pathotypes of *Verticillium albo-atrum*

Stanislav, M., Javornik, B.

University of Ljubljana, Biotechnical Faculty, Dept. of Agronomy, Ljubljana, Slovenia

Verticillium wilt, caused by the phytopathogenic fungus *Verticillium albo-atrum*, is a serious threat to hop production in Slovenia since 1997, when a new, more virulent pathotype of *V. albo-atrum* was first observed. Before Slovenia, the lethal pathotype of *V. albo-atrum* was known only in England. 2D patterns of the two Slovenian and two English pathotypes were analyzed and compared. Major differences were observed and identified by LC-MS/MS. Our results indicate that the main differences between mild and lethal pathotypes include proteins involved in interfering with plant defence like peroxiredoxine and proteins which are the building blocks and regulating factors of the cytoskeleton. The cytoskeleton is thought to be of great importance concerning fungal ability to penetrate the plant surface, hyphal growth inside the xylem vessels and especially conidiation rate at trapping sites. Some proteins from carbohydrate and protein metabolism pathways were also up-regulated in lethal pathotypes. These results reveal some of the differences between the two pathotypes at molecular level, which could explain a considerable portion of the difference in virulence.

37. Proteomic and genomic approaches for the study of in-root interaction between nematode (*Meloidogyne artiellia*) and fungal (*Fusarium oxysporum* f. sp. *ciceris* race 5) chickpea pathogens

Palomares Rius, J.E.[1],Tena, M.[2], Jiménez-Díaz, R.M[1,3], Castillo, P[1].

[1]Instituto de Agricultura Sostenible, CSIC, Apdo. 4084, 14080 Córdoba, Spain. [2]ETSIAM-(UCO), Edificio C6- "Severo Ochoa", Carretera N-IVa (Km 396), Campus de Rabanales, 14071 Córdoba, Spain. [3]ETSIAM-UCO, Edificio C4- "Celestino Mutis", Carretera N-IVa (Km 396), Campus de Rabanales, 14071 Córdoba, Spain.

Chickpea, the most important food legume in the Mediterranean Basin and the Indian subcontinent, can be severely affected by more than 50 diseases of diverse aetiology that occur worldwide. Fusarium wilt, caused by *Fusarium oxysporum* f. sp. *ciceris* (*Foc*), is the most important soil borne disease of chickpeas and ranks as the major yield-limiting factor for the crop. Control of the disease is primarily by the use of chickpea cultivars with resistance to specific races of the pathogen. However, valuable *Foc*-resistance can be annulled by joint infections of resistant roots with *Foc* and the root-knot nematode *Meloidogyne artiellia*. Infections by the nematode begins with penetration of root tissues by second-stage juveniles (J2) at the zone of root elongation; thereafter, the J2s individuals establish a permanent feeding site and induce formation of several (usually 4-6) multinucleate giant cells that support growth and reproduction of the sedentary reproductive females.

Co-infections of chickpea by *M. artiellia* and race 5 of *F. oxysporum* f. sp. *ciceris* (*Foc* 5) increased the severity of Fusarium wilt in genotypes partially resistant

MODEL LEGUMES CONGRESS, 24-28 March 2007, Tunis, Tunisia

Real-time RT-PCR profiling of transcription factors in *Medicago truncatula* in response to powdery mildew (*Erysiphe pisi*)

Curto, M, [1] **Ferro, N**[2]**, Krajinski, F**[2,3]**, Schlereth, A**[3]**, Udvardi, M**[3]**, Rubiales, D**[1]

[1] Institute for Sustainable Agriculture-CSIC. Córdoba, Spain; [2] Institute for Plant Genetics- University of Hannover. Hanover, Germany; [3] Nobel institute, Ardmore, Oklahoma, USA

b72curum@uco.es

Transcription factors (TF) are key elements in the regulation of gene transcription [1]. They (TF) are involved in the regulation of many biological processes, including responses to pathogens.

Powdery mildew is an important plant disease caused by *Erysiphe pisi*. The obligate biotrophic ascomycete infects different parts of the plant and causes noteworthy losses, especially in semiarid regions [2]. We analyzed the transcriptional response of two *Medicago truncatula* lines (Parabinga and Line 5) displaying different levels of susceptibility against *E. pisi* to an infection with this pathogen. The aim was to detect differences in mRNA accumulation of genes encoding TFs.

RNA was harvested from leaves at 4h after inoculation. We analysed the mRNA accumulation of 1084 predicted transcription factors [3] in the two genotypes in infected and non-infected leaves by Real time RT-PCR including three biological repetitions. Data are statistically analysed by descriptive and decisional analyses like Discriminant Analysis using with different programs software like SPSS, MATLAB and R. Preliminarily results indicate that some putative TFs display different mRNA accumulation in infected and non-infetced tissue of both genotypes.

1.- Chen,W., Provart, N.J., Glazebrook, J. et al., (2002). Plant Cell, 14, 559-574.

2.- Smith, P. H., Foster, E. M., Boyd, L. A. and Brown, J. K. M. (1996). Plant Pathol. 45: 302-309.

3.- Czechowski, T., Bari, R.P., Stitt, M. Scheible, W.R. Udvardi, M.K., (2004) Plant Journal. 38(2): 366-379.

MODEL LEGUMES CONGRESS, 24-28 March 2007, Tunis, Tunisia

Medicago truncatula as a model plant to boost progress for disease resistance in grain legumes

Rubiales[1] D, E Prats[1], M Fernández-Aparicio[1], MD Lozano[1], M Curto[1], E Madrid[2], J Gil[2], N Rispail[2], A.M. Maldonado[3], M.A. Castillejo[3], J.V. Jorrín[3], M.A. Dita[4], S. Fondevilla[5], J. Die[5], B. Román[5], A. Pérez-de-Luque[5]

[1]CSIC, Institute Sustainable Agriculture, Apdo 4084, 14080 Córdoba, Spain, [2]Department Genetics, University Córdoba, Campus Rabanales, 14071 Córdoba, Spain; [3]Department of Biochemistry and Molecular Biology, University of Córdoba, 14071 Córdoba, Spain; [4]Laboratorio Central de Biologia Molecular, Universidade Federal de Lavras, Minas Gerais, Brasil; [5]IFAPA-CICE (Junta de Andalucía), CIFA Alameda del Obispo, Apdo. 3092, 14080 Córdoba, Spain

ge2ruozd@uco.es

Grain legumes are challenged by a large number of pathogens that are often major constraints for its cultivation. Genetic resistance is acknowledged as the most desirable type of control. Significant progresses in resistance breeding were obtained by classical breeding after huge efforts. Genetic maps have been produced for most legumes and resistance genes or QTLs have been identified. However, we still face severe limitations for an efficient use of these markers in breeding. Confidence intervals of QTLs and marker-gene distances are still too large and we need a deeper knowledge on mechanisms of resistance.

Studies about the interaction between pathogens and their legume hosts are yet under preliminary development. However the use of model plants is leading to a further understanding of the plant-pathogen interaction biology. The development of new techniques and their transference from other fields of research will certainly increase and in a few years we will learn more about this pathosystem than in the past fifty years. *M. truncatula* offers the basis needed for developing the tools for marker-assisted breeding and to understand the molecular basis of plant resistance.

Examples on recent achievements on cytochemistry, genomics and proteomics will be briefly presented and discussed on three groups of pathogens: the necrotrophic *Mycosphaerella pinodes*, the biotrophic *Erysiphe pisi* and the parasitic plant *Orobanche crenata*.

COST ACTION 849: Parasitic plant management in sustainable agriculture
Thematic meeting "GENETIC DIVERSITY OF PARASITIC PLANTS"
19-21 February 2004, Córdoba, Spain

Two-dimensional gel electrophoresis as a tool to identify and characterize the protein profile of *Orobanche* spp. seeds.

M. Curto[1], M.M. Castillejo[2], D. Rubiales[1], J.V. Jorrín[2]
[1]*Institute for Sustainable Agriculture, IAS-CSIC, Córdoba*
[2]*Departament of Biochemistry and Molecular Biology, University of Córdoba.*

Proteomics is becoming a powerful tool in plant biology studies (Cánovas et al., 2004). Defined as a scientific discipline or experimental approach, deals with the cellular proteome characterization, considered in the most ample sense, from individual structural and functional protein identification, to postraductional modifications and interaction studies. Differently from the genome, the cellular proteoma is quite dynamic, depending on the specie, individual, organ, tissue, developmental stage and environmetal conditions. A typical proteomic experiment includes the following steps: protein extraction, protein separation by using mainly two-dimensional gel electrophoresis (2-DE), analysis of peptide digests by mass spectrometry and identification through genomic or protein database searching by using specific algorithms.

Our groups have just initiated a proteomics research programme for studying plant-parasitic plant interactions (Castillejo et al., 2004). We pretend to evaluate if 2-DE can be used to discriminate and identify *Orobanche* spp. populations or races. 2-DE have been used, with success, to detect genetic diversity (Thiellement et al., 1999).

Broomrape species, populations and races characterization and identification is still a key unsolved problem that has been approached by using morphological, biochemical, and the most recent molecular biology techniques.

In a preliminary step we are optimising a protocol for protein extraction and electrophoresis by using seeds of different *Orobanche* spp., including *O. cumana, O. ramose, O. crenata,* and *O. foetida.* Seeds were abundantly washed with 1:3 bleach water diluted, dried, homogenized with liquid nitrogen by using a mortar, and proteins extracted by using the TCA-acetone protocol. Proteins were resolved by 2-DE, IEF as first dimension (7 cm, 3-10 pH linear gradient), and SDS-PAGE (13% polyacrilamide gel) as second dimension. Gels were Coomassie or silver stained, captured and analysed by using the PD-Quest (Bio-Rad) software.

References

Cánovas *et al.* (2004). Proteomics 4: 285-298.
Castillejo *et al.*. Submitted.
Thiellement *et al.* (1999). Electrophoresis 20: 2013-2026.

Potassium homeostasis in yeast. A biochemical and proteomic approach

Navarrete C [(1)]; Curto M [(2)]; Martínez JL [(1)] ;Jorrín J [(2)]; Ramos J [(1)*]

[(1)] Departamento de Microbiología [(2)] Departamento de Bioquímica y Biología Molecular.
Edificio Severo Ochoa, Campus de Rabanales, Universidad de Córdoba, Spain.
*mi1raruj@uco.es

Introduction

Potassium homeostasis is a fundamental process in living cells. In the context of Translucent, the group in Córdoba is characterising a wild type *Saccharomyces cerevisiae* and the corresponding double potassium transport mutant (*trk1,trk2*) by using biochemical and proteomic approaches.

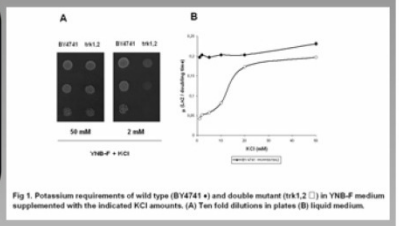

Fig 1. Potassium requirements of wild type (BY4741 •) and double mutant (trk1,2 □) in YNB-F medium supplemented with the indicated KCl amounts. (A) Ten fold dilutions in plates (B) liquid medium.

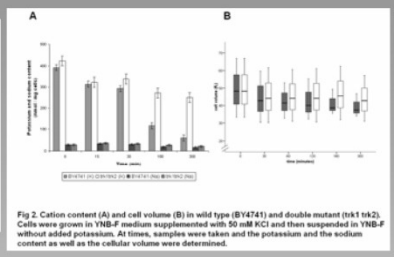

Fig 2. Cation content (A) and cell volume (B) in wild type (BY4741) and double mutant (trk1 trk2). Cells were grown in YNB-F medium supplemented with 50 mM KCl and then suspended in YNB-F without added potassium. At times, samples were taken and the potassium and the sodium content as well as the cellular volume were determined.

Results and Discussion

In order to better understand cation homeostasis, we are analysing cation requirements (Fig 1), contents and fluxes as well as changes in the 2-DE map, in response to potassium starvation.

Changes in cation content and cell volume of the wild type and double mutant have been studied in detail. During potassium starvation both parameters diminished in both strains, being this change more accused in the wild type than in the mutant (Fig 2).

Kinetics of rubidium (potassium) transport has been determined under potassium non limiting and starvation conditions (Table I). Differently from what has been reported with other synthetic media, the high affinity systems is manifested minutes, instead of hours, after potassium deprivation.

Comparative analysis of the 2-DE protein map of wild and double mutant strains grown under non limiting potassium concentrations (exponential and stationary phases), reveals the existence of at least 20 differential spots between samples of both yeasts (Figs 3 and 4), in a visual inspection.

Changes in the 2-DE protein profile in response to potassium starvation were also studied. Cells were grown at high potassium and then starved and harvested at different times. Proteins were extracted and quantified (Table II). 2-DE gels are now running.

Kinetic constants at different starvation times

	Km (mM)							Vmax (nmol/mg/min)						
Strain	0min	15min	30min	60min	120min	180min	300min	0min	15min	30min	60min	120min	180min	300min
BY4741	6.21	0.31	0.14	0.13	0.13	0.14	0.16	5.12	8.91	9.64	15.4	26.8	24.9	27.2
trk1trk2	20.1	-	20.1	-	-	20.4	-	5.23	-	6.03	-	-	5.27	-

Table I. Kinetic parameters of rubidium (potassium) transport in wild type (BY4741) and double mutant (trk1 trk2). Cells were grown in YNB-F medium supplemented with 50 mM KCl and then suspended in YNB-F without added potassium. At times, samples were taken and the characteristics of rubidium transport were determined.

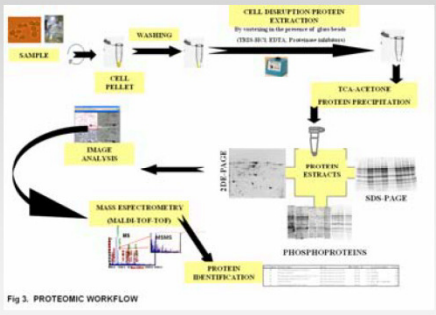

Fig 3. PROTEOMIC WORKFLOW

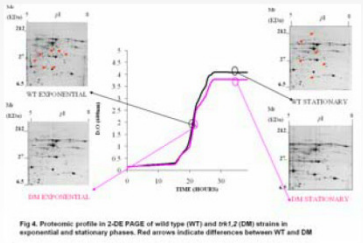

Fig 4. Proteomic profile in 2-DE PAGE of wild type (WT) and trk1,2 (DM) strains in exponential and stationary phases. Red arrows indicate differences between WT and DM

Table II. Protein content in extracts subjected to electrophoresis analysis. Cells (0.2–0.5 g fresh weight, corresponding to 0.1–0.12 dry weight) were homogenized and proteins extracted as indicated in Figure 3. Values are mean of three biological replicates

Strain/stage		Protein concentration/yield (μg/μl^{-1} in the final extract) / (mg gl^{-1} fresh weight)
Experiment1. Cells harvested at different growth stages (exponential and stationary)		
Wild type	Exponential	18.0 / 33.8
	Stationary	19.0 /36. 0
Double mutant	Exponential	19.0 / 37.0
	Stationary	8.0 / 17.0
Experiment 2. Cells harvested at different times after potassium starvation (30, 60, 18, and 300 min)		
Wild type	30	18.0 / 38.0
	60	17.0 / 30.0
	180	18.0 / 26.0
	300	14.0 / 20.0
Double mutant	30	17.0 / 38.0
	60	9.0 / 20.8
	180	5.0 / 9.1
	300	2.0 / 4.2

Funded by Ministerio de Educación y Ciencia. Spain (GEN2006-27748-C2-2-E)

A PROTEOMIC APPROACH TO STUDY PEA (*PISUM SATIVUM*) RESPONSES TO POWDERY MILDEW (*ERYSIPHE PISI*)

M. Curto[1,2], E. Camafeita[3] , J. A. Lopez[3], A. Maldonado[2] , D. Rubiales[1] and J.V. Jorrín[1]

[1] Agricultural and Plant Biochemistry Research Group, Dpt. of Biochemistry and Molecular Biology, University of Córdoba, Campus de Rabanales, Edificio Severo Ochoa (C6), 14071 Córdoba, Spain. b72curum@uco.es.
[2] Instituto de Agricultura Sostenible-CSIC, Apdo 4084, 14080 Córdoba, Spain.
[3] Unidad de Proteómica, Centro Nacional de Investigaciones Cardiovasculares, Ronda de Poniente 5, E-28760 Tres Cantos, Madrid, Spain.

Summary

Pea (*Pisum sativun*) is the highest yielding grain legume grown for vegetable and grain purposes and pea powdery mildew (*Erysiphe pisi*) causes important crop damage and yield losses [1]. We had applied Proteomics as a global approach to identify proteins involved in pea powdery mildew resistance. For that purpose, changes in the leaf proteome of two pea genotypes displaying different behavior against *E. pisi,*, suceptible Messire and resistant JI2480, have been analyzed by a combination of 2-DE and MALDI-TOF/TOF mass spectrometry [2]. Results are presented and discussed in terms of the fuctional implications of the proteins identified.

Results

Differences in resistance between pea genotypes

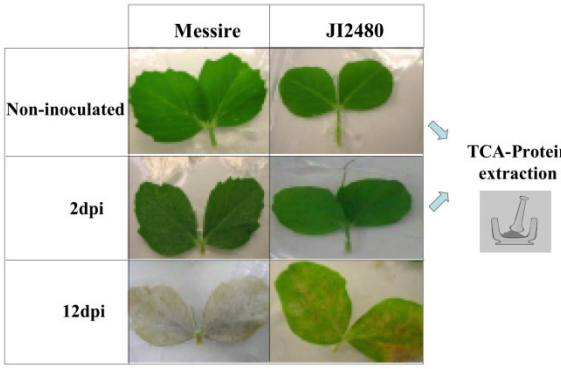

Figure 1. Development of *E. pisi* on leaves from Messire and JI2480 genotypes. The phenotypic differences between genotypes appeared at 2 days post-inoculation (dpi). At 12 dpi Messire leaves were covered by powdery mildew, while JI2480 leaves showed punctual necrotic lesions.

Two dimensional electrophoresis and spot analysis

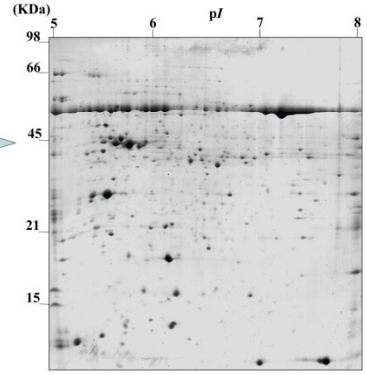

Figure 2. 2-DE profile of Coomassie-stained leaf proteins from pea. The gel correspond to leaf extracts from non-infected JI2480 plants.

About 450 resolved spots could be detected in Coomassie stained gels (Fig.2). Quantitative as well as qualitative differences in the 2-DE maps were observed between non-inoculated genotypes and between non-inoculated and inoculated plants (Table 1).

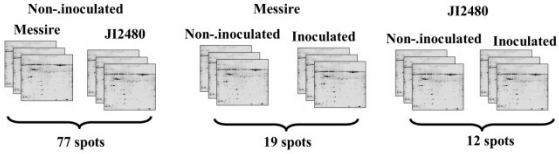

Some of the differential spots were identified after a combination of MALDI-TOF/TOF analysis and *de novo* sequencing and database searching. Proteins identified were grouped in functional categories (Table 1).

Table 1 : Identified protein.

Functional categories	JI 2480/ Messire	JI 2480 inoculated/ control	Messire inoculated/ control
Photosynthesis and carbohydrate metabolism	Rubisco activase Rubisco Ribosomal protein Flavoenzyme reductose Carbonic anhydrase	Rubisco activase Fructose bisphospahte aldolase Cloroplast elongation factor	Rubisco Fructoquinase Aldolase Triose phosphate isomerase
Krebs cycle	Isocitrate dehydrogenase Malato dehydrogenase		Dehydrogenase Malato dehydrogenase
Stress and defence responses	Exopolygalacturonase Resistance protein Gluatation peroxidase Disease resistance Superoxide dismutase ABA-response protein Pathogenesis related	Disease resistance Exopolygalacturonase	HSP70
Synthesis and degradation protein	E2 Proteasome		DEG protease
Signal transduction	G protein		
Vesicle trafficking	Rab-2-B		
Secondary metabolism	strictosidine synthase		Adenosyl methionine synthase Acetyil serine lyase

A number of proteins, 77, were present at higher amount or only detected in leaves from the resistant variety, being functionally grouped as enzymes of the photosynthesis and carbohydrate catabolism pathways and as stress and defence related proteins.
A much lower number of proteins were modified after pathogen challenge, being mainly increased in infected tissue. Changes affected to enzymes of the photosynthesis and carbohydrate catabolism and to some defense related proteins,

Conclusions

Our results support the hypothesis of:

i) Resistance to *E. pisi* in JI2480 plants is based on constitutive rather than inducible defense responses.

ii) An increased activity of the energetic metabolism could be priming defence responses in JI2480 plants.

iii) Defese responses are also activated in the susceptible genotype, support the idea that resistance is a very complex process depending on the activation of defenses, and on the kinetics of activation of such responses, based on early recognition of the pathogen.

References

1. Smith, P. H., Foster, E. M., Boyd, L. A., Brown, J. K. M., Plant Pathol. 1996, 45, 302–309.

2. Curto, M., Camafeita, L. E., Lopez, J. A., Maldonado, A. M., Rubiales, D., Jorrin, J. V., A proteomic approach to study pea (Pisum sativum) responses to powdery mildew (Erysiphe pisi). *Proteomics* 6, S163–S174, 2006.